UNIVERSITAT
POLITÈCNICA
DE VALÈNCIA

PROGRAMA DE DOCTORADO EN RECURSOS Y TECNOLOGÍAS AGRÍCOLAS

TESIS DOCTORAL

Study of the physiological, metabolomic and transcriptional changes mediated by rootstocks to explain the water stress tolerance of grafted pepper plants

Presentada por:
Yaiza Gara Padilla Herrero

Dirigida por:
Dra. Ángeles Calatayud Chover
Dr. Salvador López Galarza

Valencia, septiembre 2023

Abstract

Since the 20th century, pepper production and consumption have increased all around the world. Particularly, Spain is the first pepper producer in Europe and the fifth producer in the world with more than 1.5 million tonnes in 2021. However, pepper harvested area decreases every year, which is partly associated with climate change effects such as drought, salinity and extreme temperatures. Drought affects pepper plants by limiting photosynthesis, plant growth, increasing reactive oxygen species, among others, leading to reduced production and fruit quality. Grafting has raised as an effective technique to cultivate in unfavorable environmental conditions, because crops yields increase when tolerant rootstocks are employed due to vanish the stress perception in the scion.

In previous studies, the Horticulture Department at the Valencian Institute of Agricultural Research (IVIA) and the Vegetable Production Department at the Polytechnic University of Valencia (UPV) research groups evaluated the water stress responses in grafted pepper plants to obtain tolerant pepper rootstocks that make the grafted variety able to overcome water stress conditions. The best rootstocks are then studied in the field under long-term water stress conditions. In this way, the NIBER® pepper hybrid rootstock was obtained and patented as water stress-tolerant rootstock, because plants grafted onto NIBER® had a lower impact on biomass and yield under long-term deficit irrigation conditions. NIBER® tolerance response was attributed to sustained photosynthetic activity and improved root biomass distribution under long-term water stress. However, the sustained tolerance response observed in plants grafted onto NIBER® may be linked to prompt responses in the early phase of water stress conditions, but the short-term modulation and behavior of NIBER® water stress response has not been studied. Hence, studying the contribution of the NIBER® short-term water stress responses to tolerance in the grafted variety would shed light into tolerance mechanisms in grafted pepper plants. Moreover, understanding the modulation of the gene expression, phytohormones balance and metabolic profile will also broad the knowledge on the molecular mechanisms implicated in water stress response. For these reasons, the main objectives in this doctoral thesis are: i) characterize pepper hybrid rootstocks through the physiological parameters involved in the water stress response to study the relation between photosynthesis maintenance and antioxidant systems in grafted pepper plants and to obtain biomarkers for water stress-tolerant pepper rootstocks selection purposes; ii) study the transcriptome profile of the tolerant pepper hybrid rootstock NIBER® and the pepper-sensitive accession A10 under short-term water stress to identify prompt responses that constitute master regulators in water stress tolerance achievement; iii) identify early responses in the phytohormones network of leaves and roots in the self-grafted variety and grafted onto NIBER® under short-term water stress to address the contribution of NIBER® hormonal regulation to confer the variety tolerance; iv) analyze the prompt metabolic responses of leaves and roots in the self-grafted pepper plants and grafted onto NIBER® under short-term water stress to elucidate the biochemical bases that lead to metabolic profiles modulation toward water stress tolerance.

In the present doctoral thesis, we stated that the constitutive mechanisms taking place under non-water stress conditions dispose the response to water stress in grafted pepper plants, and NIBER® constitutive strategies include an enhanced ROS detoxification system and maintained ABA induction. When the water stress comes into play, its impact was minor in NIBER® roots in relation to A10 roots, which is reflected in lesser GSSG content from lower oxidative damage. NIBER® promotes the synthesis of osmolytes in roots and vitamin B6 in the grafted variety leaves to protect the plants from the oxidative damage resulting from water stress. Moreover, proline has a role in photosynthetic apparatus protection, because it is accumulated in plants grafted onto pepper hybrid H92, which showed sustained photosynthetic activity under long-term water stress conditions. The proline role in water stress tolerance is not observed under short-term water stress and may constitute a late strategy in grafted pepper plants. Short-term responses to water stress include stomatal movements in NIBER® during early phases (5h) of water stress, starting with the avoidance of stomatal closure up to 48 h by gene expression changes in ABA negative regulators and aquaporins, and followed by stomatal closure at 48 h associated with previous ABA synthesis in roots and transport to leaves. JA is also increased in the leaves of the variety grafted onto NIBER® at 48 h under water stress, and is regulated by long-distance signals from roots that promote its synthesis on leaves and transport to roots and resynthesis. JA is involved in stomatal closure and stress signaling, which leads to dehydration-responsive transcription factors activation. The auxins/cytokinins ratio is also fine-tuned by NIBER® roots during the early water stress response, beginning with promotion of root over shoot growth at 5 h, then increases the cytokinins and reduces the auxins content at 24 h, and finally increases the auxins and reduces the cytokinins content to obtain higher root biomass and greater water exploring ability. In the leaves of the grafted variety, NIBER® increases protective metabolites as chlorophyll a, stearic acid, anthocyanins and suberin and cutin biosynthesis-related metabolites, being the latter also increased in the roots. The mentioned metabolites have an antioxidant role or act as cellular barrier constituents that can control fluxes of water, gases and solutes. Lastly, siroheme increases in roots and it is possibly linked to a more effective nitrogen assimilation.

Resumen

Desde el siglo XX, la producción y el consumo de pimiento han aumentado en todo el mundo. Particularmente, España es el primer productor de pimiento en Europa y el quinto en el mundo con más de 1.5 millones de toneladas en 2021. Sin embargo, el área de pimiento cosechada disminuye cada año, lo que se asocia en parte a los efectos del cambio climático como es la sequía, la salinidad y las temperaturas extremas. La sequía afecta a las plantas de pimiento limitando la fotosíntesis, el crecimiento, aumentando las especies reactivas de oxígeno, entre otros efectos, lo que resulta en una reducción de la producción y la calidad del fruto. El injerto se ha posicionado como una técnica efectiva para cultivar en condiciones ambientales desfavorables, dado que el rendimiento de los cultivos aumenta cuando se utilizan patrones tolerantes para disminuir la percepción del estrés en la variedad.

En estudios previos, los grupos de investigación del Departamento de Horticultura del Instituto Valenciano de Investigaciones Agrarias (IVIA) y del Departamento de Producción Vegetal de la Universidad Politécnica de Valencia (UPV) evaluaron la respuesta a estrés hídrico en plantas de pimiento injertadas para obtener patrones de pimiento tolerantes que confieran tolerancia a la variedad injertada en condiciones de estrés hídrico. Los mejores patrones se estudian posteriormente en el campo bajo condiciones de estrés hídrico a largo plazo. En este sentido, se obtuvo y se patentó el patrón híbrido de pimiento NIBER® como patrón tolerante a estrés hídrico, dado que las plantas injertadas sobre NIBER® mostraron un menor impacto sobre la biomasa y el rendimiento bajo condiciones de déficit hídrico a largo plazo. La tolerancia de NIBER® se atribuyó al mantenimiento de la actividad fotosintética y la mejora de la distribución de la biomasa radicular bajo estrés hídrico a largo plazo. Además, la respuesta sostenida de tolerancia observada en las plantas injertadas sobre NIBER® podría estar relacionada con la respuesta rápida en la fase inicial en condiciones de estrés hídrico, pero la respuesta de NIBER® no se ha estudiado a corto plazo. Así, estudiar la contribución de las respuestas al estrés hídrico de NIBER® a corto plazo sobre la tolerancia de la variedad injertada arrojaría luz sobre los mecanismos de tolerancia en plantas injertadas de pimiento. Del mismo modo, entender la modulación de la expresión génica, el balance hormonal y el perfil metabólico también ampliará el conocimiento existente sobre los mecanismos moleculares implicados en la respuesta a estrés hídrico. En consecuencia, los objetivos principales de la presente tesis doctoral son: i) caracterizar patrones híbridos de pimiento con parámetros fisiológicos implicados en la respuesta a estrés hídrico para estudiar la relación entre la fotosíntesis mantenida y los sistemas antioxidantes en plantas de pimiento injertadas y obtener biomarcadores para la selección de patrones de pimiento tolerantes a estrés hídrico; ii) estudiar el perfil transcriptómico del patrón híbrido tolerante de pimiento NIBER® y la accesión de pimiento sensible A10 bajo condiciones de estrés hídrico a corto plazo para identificar respuestas rápidas que constituyen reguladores principales en la tolerancia a estrés hídrico; iii) identificar respuestas tempranas en la red de fitohormonas de hojas y raíces en la variedad autoinjertada y la variedad injertada sobre NIBER® en condiciones de estrés hídrico a corto plazo para conocer la contribución de la regulación hormonal de NIBER® para conferir tolerancia a

la variedad; iv) analizar las respuestas tempranas de hojas y raíces en plantas de pimiento autoinjertadas e injertadas sobre NIBER® bajo estrés hídrico a corto plazo para elucidar las bases bioquímicas que conducen a la modulación de los perfiles metabólicos para lograr tolerancia a estrés hídrico.

En la presente tesis doctoral, constatamos que los mecanismos constitutivos que tienen lugar en ausencia de estrés hídrico influyen en la respuesta a estrés hídrico en plantas injertadas de pimiento, y que las estrategias constitutivas de NIBER® incluyen la estimulación del sistema de detoxificación de ROS y una inducción de ABA sostenida. Con la presencia de estrés hídrico, las raíces de NIBER® mostraron un menor impacto en comparación con las raíces de A10, lo que se refleja en un menor contenido en GSSG debido a un menor daño oxidativo. NIBER® promueve la síntesis de osmolitos en la raíz y de vitamina B6 en las hojas de la variedad injertada para proteger al aparato fotosintético de las plantas del daño oxidativo producido por el estrés hídrico. Además, la prolina está implicada en la protección del aparato fotosintético, ya que se acumula en las plantas injertadas sobre el híbrido de pimiento H92, mostrando un mantenimiento de la actividad fotosintética bajo condiciones de estrés hídrico a largo plazo. El papel de la prolina en la tolerancia a estrés hídrico no se observó en condiciones de estrés hídrico a corto plazo y podría tratarse de una estrategia tardía en plantas de pimiento injertadas. Las respuestas al estrés hídrico a corto plazo incluyen la regulación del movimiento estomático en NIBER® en la fase inicial de estrés hídrico (5 h), primero evitando el cierre estomático hasta las 48 h mediante cambios en la expresión génica de reguladores negativos de ABA y acuaporinas, seguido de un cierre estomático a las 48 h asociado a una síntesis previa de ABA en las raíces y su transporte a las hojas. El JA también aumentó en las hojas de la variedad injertada sobre NIBER® a las 48 h bajo estrés hídrico, y está regulado por señales a larga distancia desde las raíces que promueven la síntesis en las hojas y el transporte a las raíces y su resíntesis. El JA está implicado en el cierre estomático y la señalización en condiciones de estrés, lo que deriva en la activación de factores de transcripción de respuesta a la deshidratación. El ratio auxinas/citoquininas también se regula en las raíces de NIBER® en la respuesta inicial al estrés hídrico, primeramente favoreciendo el crecimiento de la raíz sobre el crecimiento del tallo a las 5 h, posteriormente aumentando las citoquininas y disminuyendo las auxinas a 24 h y finalmente aumentando las auxinas y reduciendo las citoquininas para obtener una mayor biomasa radicular y una mayor capacidad exploratoria. En las hojas de la variedad injertada, NIBER® aumenta el contenido de metabolitos protectores como la clorofila a, el ácido esteárico, las antocianinas y metabolitos relacionados con la síntesis de suberina y cutina, estos últimos también aumentan en las raíces. Los metabolitos mencionados tienen un papel antioxidante o bien actúan como constituyentes de barreras celulares controlando los flujos de agua, gases y solutos. Finalmente, el contenido en sirohemo aumenta en las raíces y posiblemente está relacionado con una asimilación del nitrógeno más eficiente.

Resum

Des del segle XX, la producció i el consum de pebrera han augmentat a tot el món. Particularment, Espanya és el primer productor de pebrera d'Europa i el cinqué del món amb més de 1.5 milions de tones en 2021. Però, l'àrea de collita de pebrera disminueix cada any, el què s'associa en part als efectes de canvi climàtic com són la sequera, la salinitat i les temperatures extremes. La sequera afecta a les plantes de pebrera limitant la fotosíntesi, el creixement, augmentant les espècies reactives d'oxigen, entre altres efectes, el què resulta en una reducció de la producció i la qualitat del fruit. L'empelt s'ha posicionat com a tècnica efectiva per a cultivar en condicions ambientals desfavorables, ja que el rendiment dels cultius s'incrementa quan s'utilitzen patrons tolerants per disminuir la percepció de l'estrés a la varietat.

En estudis previs, els grups d'investigació del Departament d'Horticultura de l'Institut Valencià d'Investigacions Agràries (IVIA) i del Departament de Producció Vegetal de la Universitat Politècnica de València (UPV) van avaluar la resposta a estrés hídric en plantes de pebrera empeltades per obtenir patrons de pebrera tolerants que conferisquen tolerància a la varietat empeltada en condicions d'estrés hídric. Els millors patrons s'estudien posteriorment al camp en condicions d'estrés hídric a llarg termini. Així, es va obtenir i patentar el patró híbrid de pebrera NIBER® com a patró tolerant a estrés hídric, ja que les plants empeltades sobre NIBER® van mostrar un menor impacte sobre la biomassa i el rendiment en condicions de dèficit hídric a llarg termini. La tolerància de NIBER® es va atribuir al manteniment de l'activitat fotosintètica i a la millora de la distribució de la biomassa radicular en estrés hídric a llarg termini. A més a més, la resposta sostinguda de tolerància que es va observar a les plantes empeltades sobre NIBER® podria estar relacionada amb la resposta ràpida a la fase inicial en condicions d'estrés hídric, però la resposta de NIBER® no s'ha estudiat a curt termini. En conseqüència, estudiar la contribució de les respostes al estrés hídric de NIBER® a curt termini sobre la tolerància de la varietat empeltada ajudaria a entendre els mecanismes de tolerància en plantes empeltades de pebrera. En aquest sentit, comprendre la modulació de l'expressió gènica, el balanç hormonal i el perfil metabòlic també ampliaria el coneixement existent sobre els mecanismes moleculars implicats en la resposta a estrés hídric. D'aquesta manera, els objectius principals de la tesi doctoral són: i) caracteritzar patrons híbrids de pebrera amb paràmetres fisiològics implicats en la resposta a estrés hídric per estudiar la relació entre la fotosíntesis mantinguda i els sistemes antioxidants en plantes de pebrera empeltades i per a obtenir biomarcadors per a la selecció de patrons de pebrera tolerants a estrés hídric; ii) estudiar el perfil transcriptòmic del patró híbrid tolerant de pebrera NIBER® i la accessió de pebrera sensible A10 en condicions d'estrés hídric a curt termini per a identificar respostes ràpides que constituïsquen reguladors principals en la tolerància a estrés hídric; iii) identificar respostes primerenques en la xarxa de fitohormones de fulles i arrels en la varietat auto-empeltada i la varietat empeltada sobre NIBER® en condicions d'estrés hídric a curt termini per conèixer la contribució de la regulació hormonal de NIBER per a conferir tolerància a la varietat; iv) analitzar les respostes inicials de fulles i arrels en plantes de pebrera auto-empeltades i empeltades sobre NIBER® en condicions d'estrés hídric a curt termini per elucidar les

bases bioquímiques que condueixen a la modulació dels perfils metabòlics per a aconseguir tolerància a estrés hídric.

En aquesta tesi doctoral vam comprovar que els mecanismes constitutius que es donen en absència d'estrés hídric influeixen en la resposta a estrés hídric en plantes empeltades de pebrera i que les estratègies constitutives de NIBER® inclouen l'estimulació del sistema de detoxificació de ROS i una inducció sostinguda d'ABA. En presència d'estrés hídric, les arrels de NIBER® van mostrar un menor impacte en comparació amb les arrels de A10, el què es reflecteix en un menor contingut de GSSG degut a un menor dany oxidatiu. NIBER® promou la síntesis d'osmòlits a les arrels i de vitamina B6 a les fulles de la varietat empeltada per a protegir a l'aparell fotosintètic de les plantes del dany oxidatiu produït per l'estrés hídric. A més a més, la prolina està implicada en la protecció de l'aparell fotosintètic, ja que s'acumula a les plantes empeltades sobre l'híbrid de pebrera H92, les quals mantenen l'activitat fotosintètica en condicions d'estrés hídric a llarg termini. El paper de la prolina en la tolerància a estrés hídric no es va observar en condicions d'estrés hídric a curt termini i podria tractar-se d'una estratègia tardana en plantes de pebrera empeltades. Les respostes a l'estrés hídric a curt termini inclouen la regulació del moviment estomàtic en NIBER® a la fase inicial d'estrés hídric (5 h), primer evitant el tancament estomàtic fins a les 48 h mitjançant canvis a l'expressió gènica de reguladors negatius d'ABA i acuaporines, seguit d'un tancament estomàtic a les 48 h associat a una síntesis prèvia d'ABA a les arrels i transport a les fulles. L'àcid jasmònic també va augmentar a les fulles de la varietat empeltada sobre NIBER® a les 48 h en estrés hídric i està regulat per senyals a llarga distància des de les arrels que promouen la síntesis a les fulles i el transport a les arrels i resíntesi. L'àcid jasmònic està implicat al tancament estomàtic i la senyalització en condicions d'estrés, el què deriva en l'activació de factors de transcripció de resposta a la deshidratació. El rati auxines/citoquinines també es regula a les arrels de NIBER® a la resposta inicial a l'estrés hídric, primerament afavorint el creixement de l'arrel sobre el creixement de la part aèria a les 5 h, posteriorment augmentant les citoquininas i disminuint les auxines a les 24 h i finalment augmentant les auxines i reduint les citoquininas per obtenir una major biomassa radicular i una major capacitat exploratòria. A les fulles de la varietat empeltada, NIBER® augmenta el contingut de metabòlits protectors com la clorofil·la a, l'àcid esteàric, les antocianines i metabòlits relacionats amb la síntesi de suberina i cutina, aquests últims també augmenten a les arrels. Els metabòlits mencionats tenen un paper antioxidant o actuen com a constituents de barreres cel·lulars controlant els fluxos d'aigua, gasos i soluts. Finalment, el contingut en siroheme augmenta a les arrels i possiblement està relacionat amb una assimilació de nitrogen més eficient.

Index

1. Introduction

1.1. Pepper taxonomy, distribution and botany

1.1.1. Pepper taxonomy, origin and distribution

Capsicum genus taxonomy is complex to define, and has been discussed for its high varietal, morphological and physiological diversity (CABI, 2022). It is estimated that the genus contains up to 20 species, of which the five main species are *C. annuum* L., *C. chinense* Jacq., *C. baccatum* L., *C. frutescens* L. and *C. pubescens* Ruiz & Pav. (Basu & De, 2003).

The *Capsicum* genus origin is hypothesized to lie in the west and northwest of South America, in Peru, Ecuador and Colombia next to the Andes mountains (Carrizo-García et al., 2016). *Capsicum* genus distribution started next to the Amazon area in Colombia and extended to the central-east and then southeast of Brazil by following a clockwise direction to arrive in central-north America in Mexico (Carrizo-García et al., 2016). It is speculated that the above-mentioned five major *Capsicum* species were independently domesticated: on the one hand *C. baccatum*, *C. chinense* and *C. pubescens* in South America; on the other hand *C. annuum* and *C. frutescens* in Mesoamerica (Figure 1) (Pickersgill, 2007).

Later in the late 15th century, as the Europeans who arrived at the Americas found out that the natives used *Capsicum* species, they introduced the so-called “ají/axí” into Europe (Chiou & Hastorf, 2014; Powis et al., 2013). It was in the 17th century when *Capsicum* was broadly cultivated in Europe and introduced for cultivation in colonies like Japan and India to be used as a spice and for its medical applications (Basu & De, 2003).

From there on, *Capsicum* has been introduced and grown in a temperate climate, and Mediterranean and tropical regions all around the world, which has been favored by the trade routes connecting Europe, the Middle East and Asia. Of all the *Capsicum* spp., *C. baccatum* and *C. pubescens* failed outside the Andes basin, *C. chinense* and *C. frutescens* were well-received in Asia and Africa, whereas *C. annuum* is now the winning species by being extensively cultivated worldwide (Nicolaï et al., 2013). Hence the *C. annuum* genetic pool contains many landraces, cultivars, breeding lines, and artificial and natural hybrids (Barchenger et al., 2019), including the most important commercial pepper varieties like bell pepper. For all these reasons, the present thesis focuses on *C. annuum*.

Figure 1. *Capsicum* species distribution in 1530 (AD). From Chiou and Hastorf (2014).

1.1.2. *C. annuum* L. botany

C. annuum varieties are compact, annual or short-lived, herbaceous or subshrub, and are 1 to 1.5 m tall, with a main steam branched at the base where the diameter is 0.5-1 cm. Young stems are fragile, with 3-4 angles and glabrescent to moderately pubescent, and not usually densely pubescent. These young stems are green-colored, and even brownish-green, and may have purple lines. They include simple, eglandular and uniseriate trichomes that are 0.5-2 mm long. Nods are green and can be purple-spotted. Older stem bark is brown, from glabrescent to scarcely pubescent with hardly any lenticels or without. The leaf pairs that derive from difoliated sympodial units are size and shape analogous, and their leaves are glabrescent to slightly pubescent on both faces, with trichomes as in stems, and green-colored within a spectrum from pale to dark green. Leaf size ranges from 2.5 to 8 cm wide and from 3 to 15.5 cm long, ovately to elliptically shaped with a base that can be truncated, cordated, cuneated or attenuated. Petiole size ranges from 0.5 to 10 cm, has equal pubescence to stems, and the apex is acuminated or long-acuminated.

***C. annuum* inflorescences** are axillary and contain mainly one flower, sometimes two, but no more. Flower pedicels are erect upon anthesis or pendent, up to 40 mm long and green- or purple-colored. The corolla is usually white, almost never pale yellow or purple. Its diameter is 8 to 22 mm and its length ranges from 8 to 15 mm. The corolla is predominantly campanulate and contains 5-7 flower lobes. The flower calyx is green, cupped-shape, 1 to 4 mm long and 3 to 5 mm wide, with trichomes resembling those in stems. Stamens are normally inserted into the corolla, and filaments are white and occasionally purple, up to 3 mm long. There are usually 5-7 stamens per flower, which are equal. They contain pale blue to purplish anthers, connivent or not connivent upon anthesis, which are ellipsoidal or ovoidal, and whose size is 2-3 mm. The gynoecium can be classified into three types depending on the style: a short style if it does not surpass anthers (2.2-2.5 mm long); a medium style if it reaches approximately the same height and long style by exceeding anthers (3-5.1 mm long). In all cases, the style is white or purple and cylindrically-shaped. The stigma is pale green or yellow, of a discorded or capitated shape. Its length goes up to 0.2 mm and it is 0.4 mm wide. The ovary has 2-4 locules. It is ovoidal or globosal, green-colored, its diameter ranges from 1.2 to 2.5 mm and it is 1.5 to 3 mm long. The nectary is approximately 0.5 mm long. *C. annuum* can be cross-pollinated by insects, but is generally self-compatible like most *Capsicum* spp., although interspecific crosses are not always viable (Barboza et al., 2022).

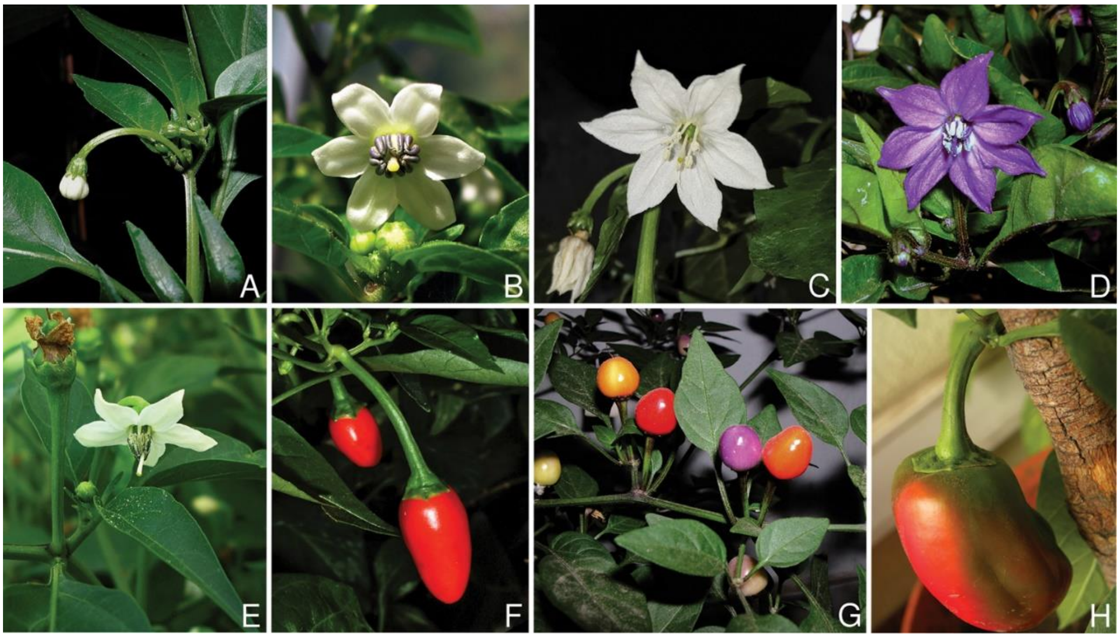

Figure 2. *Capsicum annuum* var. *annuum.* A) Flower bud on pendent pedicel. B) Flower with connivent anthers. C) Flower with hexamerous corolla (note the nectar droplets on the limb) and style almost the same length as anthers. D) Flower with heptamerous purple corolla. E) Flower with pentamerous corolla and style exceeding anthers. F, H) Mature fruit on pendent pedicels. G) Mature fruit on upright pedicels. From Barboza et al. (2022).

***C. annuum* fruit** are scarcely pulped persistent berries of variable size, color and shape. Fruit length can be up to 30 cm, with a diameter from 6 to 65 mm. Immature fruit can be green, cream, yellow or purple, and change to yellow, red, orange, brown, purple or purple-black after maturing. Fruit shape is normally elongate or blocky, and can sometimes be globose or conical. The fruit pedicel can be erect or pendent, from 25 to 70 mm long and green-colored, with a constant width and usually angled. The fruit calyx is green, cupped or disc-shaped, and its size ranges from 15 to 25 mm in diameter. Pungency is a distinctive fruit trait in *Capsicum,* and it is also widely variable in *C. annuum*. It includes many degrees starting from non pungent fruit. Fruit are sclereid-free. The pericarp is opaque and thick, and comprised of giant cells and an alveolated endocarp. Each fruit can contain up to 50 seeds, which are pale yellow-colored and C-shaped. Seed size is 3.2 to 3.6 mm wide, 3.8 to 4.4 mm long and approximately 1 mm thick. Seeds are covered with a smooth to barely reticulate seed coat, which is cerebelloid and its cells are not uniformly shaped. The embryo is imbricate in shape.

1.2. Pepper's socio-economic impact

1.2.1. The economic importance of pepper

Bell pepper is the common name given to the plants belonging to the *Capsicum annuum* L. species. According to (FAO, 2023a), in 2021 the harvested pepper area in the world was 2.055.310 ha and world pepper production was 36.286.643 tonnes.

The pepper trade in the world corresponded to 6.62 billion US dollars in 2021 (OEC, 2023). In the same year (2021), the top five pepper exporters were Mexico (1.64 billion US dollars), Spain (1.59 billion US dollars), the Netherlands (1.07 billion US dollars), Canada and Turkey, respectively with 477 and 204 million US dollars (OEC, 2023). Regarding imports, in 2021 the top five pepper importers were the United States (2.1 billion US dollars), Germany (1.07 billion US dollars), the United Kingdom, France and Canada respectively with 523, 313 and 309 million US dollars (OEC, 2023).

Particularly in Europe, the pepper area harvested in 2021 was 105.131 ha and pepper production was 3.916.870 tonnes (FAO, 2023a). Pepper production has increased in Europe in the last few decades, but the harvested pepper area decreases every year because it covered 144.963 ha in 2000 and dropped to 101.403 ha in 2020 (FAO, 2023a). This loss in croplands can be attributed partly to climate change, which accelerates land degradation by means of extreme temperatures, drought, desertification and other environmental and social constraints (UN, 2023).

Of European countries, Spain is the top pepper producer and the fifth pepper producer in the world. In 2021, its production was 1.511.560 tonnes over 22.240 ha of harvested area (FAO, 2023a). The Valencian Community (east Spain) was the third pepper producer of all Spanish regions in 2021 (Table 1), preceded by Andalusia and the Murcia Region (MAPA, 2023).

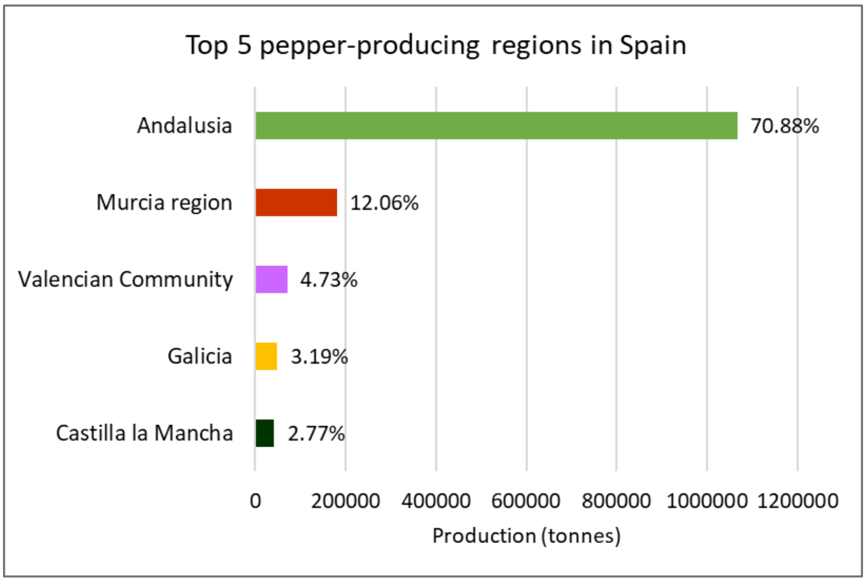

Figure 3. The top five pepper-producing regions in Spain in 2021. Bars represent production in tonnes and the percentages are calculated in relation to the total production tonnes in Spain in 2021 (MAPA, 2023).

1.2.2. Pepper in society

Pepper is usually consumed as a vegetable or spice, either fresh or processed. It is also employed for the medical and cosmetic applications of its extract, and has an ornamental purpose (Morris & Taylor, 2017).

In the 20th century, pepper consumption and production increased all over the world, and pepper has become a main ingredient in the cuisines of many countries of the globe for its dual role as a spice and vegetable (Delelegn, 2011). In Spain, from 2020 to 2021 fresh pepper spending and consumption per capita increased 13.5% and 11%, respectively (MAPA, 2022). Moreover, if fruit contains a notable amount of capsaicin, it is typically employed in cooking to add flavor and pungency to dishes (Bhattacharya, 2023).

Pepper global success is, in part, attributed to its nutritional composition, which comprises minerals, fiber, carotenoids, flavonoids, tocopherols like vitamin E, ascorbic acid (vitamin C), with the concentration of the last high enough to be available for consumers (Olatunji & Afolayan, 2018). These compounds, and other phytochemicals found in pepper, play a role in improving human health for their antioxidant, antimicrobial, antiviral, anti-inflammatory and anticancer activity (Khan et al., 2014), and can also be employed to correct micronutrient deficiencies (Olatunji & Afolayan, 2018).

In addition, pepper is very appropriate as an ornamental plant because it is quite diverse in shape, its leaves and fruit can be composed of many different colors, which also change during and after ripening. It can be easily propagated by seeds and does not take a long time to grow (Stommel & Bosland, 2007).

1.3. Environmental constraints in pepper cultivation

1.3.1. Biotic stress

The FAO (2021) predicts on a global scale that up to 40 % of crop production is anually destroyed by pests, which corresponds to 220 billion US dollar losses for the world economy. Moreover, the climate change scenario damages not only ecosystems, but also crop systems worldwide, which aggravates biotic stress effects by altering infection, distribution and severity pest patterns (IPPC, 2021).

Pepper is harmed by many pathogens, from viruses (i.e., *Cucumoviruses*, *Potyviruses*, *Tobamoviruses*, *Tospoviruses*) to fungi (i.e., *Fusarium* spp., *Leveillula taurica, Verticillium dahliae*, *Colletotrichum* spp., *Phytophthora capsici*), and also including bacteria (i.e., *Xanthomonas* spp.), nematodes (i.e., *Meloidogyne* spp.) and insects (i.e., thrips, aphids, mites, *Lepidoptera*) (Parisi et al., 2020).

1.3.1.1. Viral diseases

Of ***Cucumoviruses***, the dominant virus is the *Cucumber mosaic virus* (CMV), and it is also one of the most widespread viruses all over the world (Kenyon et al., 2014). It is transmitted through plant sap mechanical inoculation, which is mainly performed naturally by aphids (Li et al., 2020). CMV symptoms are strain-, cultivar-, infection time- and growing conditions-dependent, and comprise necrotic rings on leaves (Figure 4A), which can also be matte-colored (Figure 4B) and chlorotic (Figure 4C). In addition, flower formation and set can be made difficult and can be ring-spotted fruit (Figure 4D), and also discolored and misshapen (Kenyon et al., 2014; Tóbiás et al., 2017).

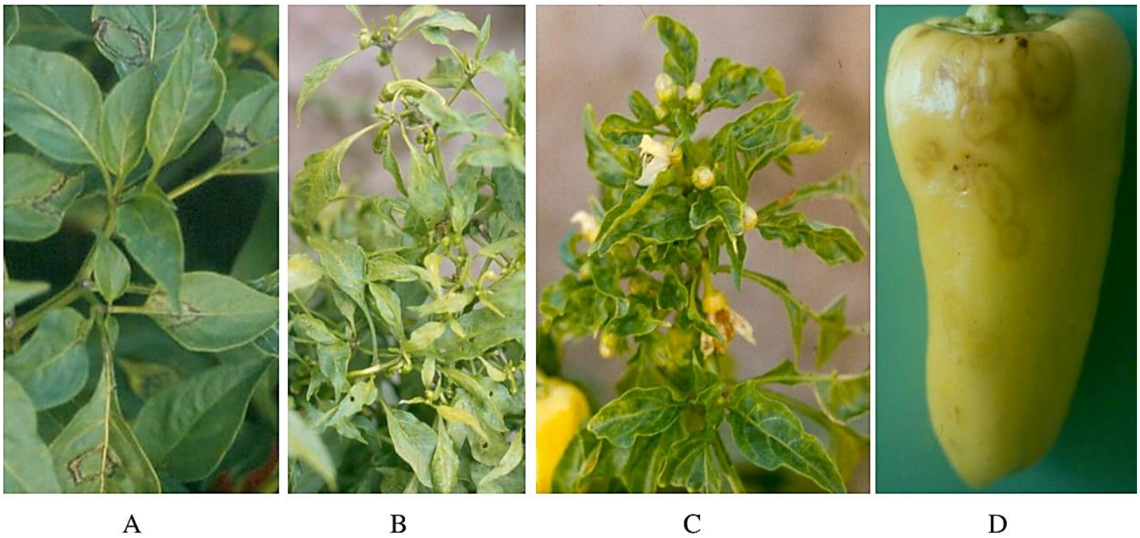

Figure 4. *Cucumber mosaic virus* symptoms on pepper plants. A. Necrotic rings and pattern. B. Chlorosis and chlorotic mosaic with several degrees of leaf deformation and protruding primary veins. C. Chlorosis and chlorotic mosaic with stunting. D. Ring spotting on fruit. From Tóbiás et al. (2017).

Potyviruses are transmitted by aphids and the worldwide disseminated *Potato virus Y* (PVY) is the prevalent pepper-damaging potyvirus in Europe (Moury et al., 2005). PVY symptoms include stunted plants, with mosaic or mottling on leaves, which can have clearer veins and green vein banding. Fruit might exhibit necrotic spots and necrosis may also be found on stems and apical buds (Pernezny et al., 2003).

Tobamoviruses are the most pepper-harming viruses in protected cultivation because they are very persistent and their transmission is mechanical, which means that they can remain in seeds, plant debris, on tools, and in soil and water, and be easily transmitted by contact (Parisi et al., 2020). The most frequent tobamoviruses in Southern Europe are *Tobacco mosaic virus* (TMV), *Tomato mosaic virus* (ToMV), *Tobacco mild green mosaic virus* (TMGMV) and *Pepper mild mottle virus* (PMMoV) (Moury & Verdin, 2012). Symptoms are strain- and cultivar-dependent, and can be resumed in leaves with mottle-chlorotic or mosaic patterns, usually distorted. Fruit can be discolored, small and misshapen. Necrotic stains can appear on both leaves and fruit (Kenyon et al., 2014).

Tospoviruses are usually transmitted by thrips in a propagative and persistent way. *Tomato spotted wilt virus* (TSWV) is the prevalent tospovirus, although other tospoviruses have been described (Kenyon et al., 2014). Symptoms are stems with necrotic stripe, which can reach the upper part of shoots and fruit, with chlorotic and necrotic spots and stripes showing mosaic and concentric rings (Figure 5A), and chlorotic leaves may have chlorotic rings (Figure 5B) (Kenyon et al., 2014).

Figure 5. Symptoms caused by TSWV in plants photographed by Gerald Holmes, California Polytechnic State University at San Luis Obispo. A. Pepper fruit. B. Pepper leaf. From Pappu et al. (2021).

1.3.1.2. Fungal diseases

Vascular diseases are provoked by both ***Fusarium*** and ***Verticillium***, mainly by *F. oxysporum* and *Verticillium dahliae*, respectively. They enter planta naturally or through wounds, and spread acropetally to stems, and cause plant wilting, chlorosis, stunted growth, discolored stems with *Fusarium* and vascular tissue browning with *Verticillium* (Parisi et al., 2020; UF, 2021).

Leveillula taurica is responsible for powdery mildew disease, which especially affects peppers growing in warm areas. It first causes light-yellow patches to leaf uppersides and gray-white patches to leaf undersides (Sabaratnam, 2021).

Anthracnose can be produced by several ***Colletotrichum*** spp. (i.e., *C. scovillei*, *C. truncatum*, *C. siamense*) and is the most widespread fruit rot in pepper. It usually affects fruit, particularly ripe fruit, but can damage non ripe fruit, which show symptoms when maturation starts. These symptoms are circular spots that grow over time until fruit softens and rots, which causes major pre- and post-harvest damage (McGrath, 2023).

Root Rot and Foliar Blight are caused by ***Phytophthora capsica*** (Figure 6), which is an oomycete that infests in roots and the crown near the soil line, but can be transported from infested soil to plants by water splashes, usually from irrigation or raining events. It causes crown and fruit rot, with dark brown lesions that grow acropetally on stems and can result in plant death (Quesada-Ocampo, 2020).

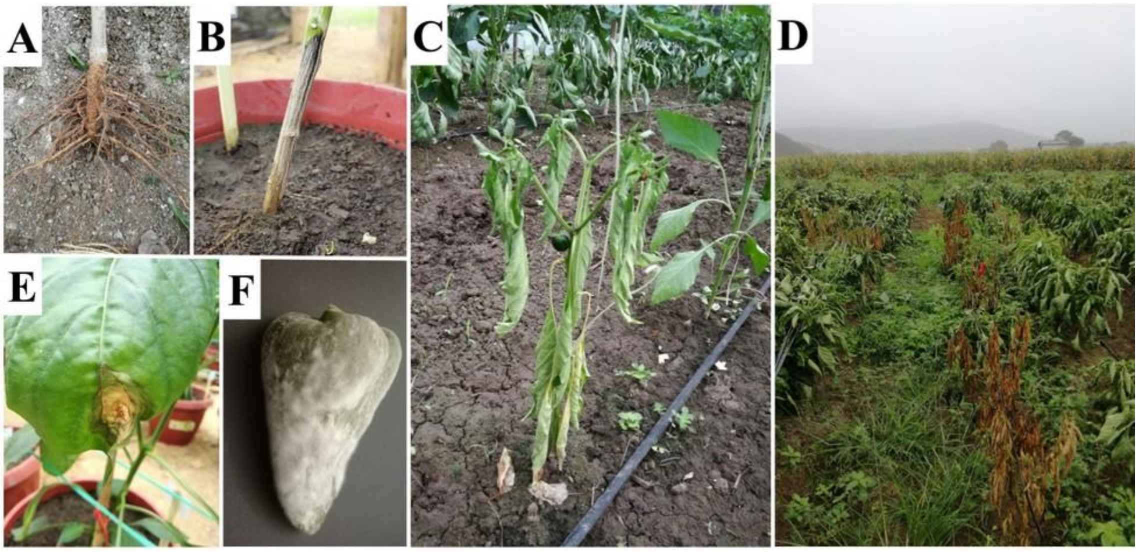

Figure 6. Rot symptoms on roots (A) and stems (B), wilting (C) and death (D) in plants, leaf blight (E) and fruit rot (F) in *Capsicum* spp. caused by *Phytophthora capsici*. From Gaibor-Vaca et al. (2021).

1.3.1.3. Bacterial diseases

Bacterial spot is the most usual leaf disease in pepper, and is provoked mainly by ***Xanthomonas*** spp. It affects plant aerial parts. On leaves, it causes dark spots to grow and necrosis develops. Leaves can become yellow and fall, which diminishes productivity. There can be long cankers on stems. On fruit, pale-green spots first appear and then become brown, which makes fruit unmarketable (Li, 2015).

1.3.1.4. Nematodes

Nematodes infestation is produced by microscopic roundworms from *Meloidogyne* spp., mostly by *M. incognita*, *M. arenaria* and *M. javanica*. They affect plant roots by feeding from them and limiting their function, and also cause chlorosis, wilt, necrosis and stunted growth in plant aerial parts (Ploeg & Kodira, 2016).

1.3.1.5. Insects

Insects themselves can damage plants and are also the vectors for many pathogens, which they transmit to plants as mentioned in **3.1.1.** *Cucumoviruses* and *Potyviruses* are transmitted by **aphids**, which can also cause chlorosis, leaf abscission, poorer photosynthetic activity and flower and fruit abortion. **Thrips** transmit *Tospoviruses* and harm leaves, flowers and fruit because they feed from them (Parisi et al., 2020).

The **Lepidoptera** *Helicoverpa armigera* seriously damages pepper in Europe, specifically in Spain and Portugal. Its larvae harm leaves, flowers and fruit by feeding on them (Parisi et al., 2020). Of **mites**, *Polyphagotarsonemus latus* is quite important and can lead to plant death if infestation occurs. It usually feeds from leaf sap, a process that particularly affects the outer layer of the cells in leaves, which appear deformed and rigid, and their color changes to bronze (Parisi et al., 2020).

1.3.2. Abiotic stress

Abiotic stress is a serious threat to agriculture worldwide. In fact it is the first source of crop productivity losses, which can be as high as 50% for major crops (Sah et al., 2016; Wang et al., 2003). Abiotic stresses include drought, salinity, extreme temperatures, among others, and their severity and prevalence are only increasing under current and expected climate change conditions (Figure 6) (IMF, 2022). Specifically drought and salinity are expected to transform more than 50% of the arable land on the globe into salinized land by 2050 (Wang et al., 2003).

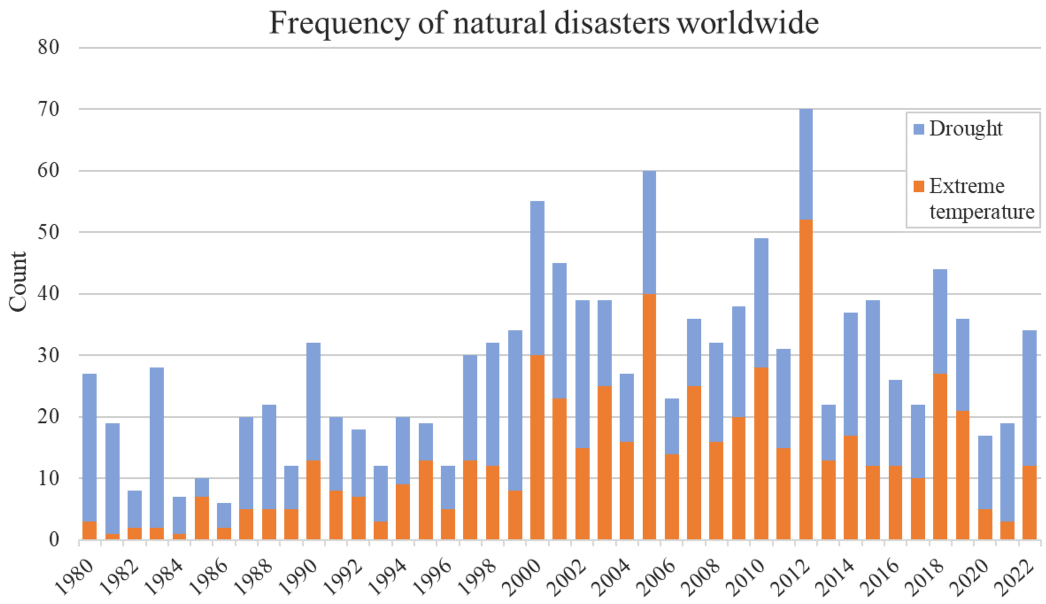

Figure 6. Frequency of natural disasters worldwide from 1980 to 2022. Dataset from the International Monetary Fund Indicators: Climate-related Disasters Frequency (2022). Blue bars depict drought events and orange bars refer to extreme temperature events.

1.3.2.1. Salinity

Salinity stress is a major limitation for plant growth and productivity, and also impacts soil erosion, soil biodiversity and water quality (FAO, 2023b). Salinity can be classified into primary and secondary salinity depending on the origin of stress. Primary salinity occurs when the salts in soil or groundwater appear in excess, and these salts accumulate naturally for a long time. Secondary salinity is a consequence of human activity, which undoes the hydrologic balance between the amount of irrigated or rainfall water and the amount of water used by crops (Parihar et al., 2015). Of all the salt types that induce salinity stress, sodium chloride (NaCl) is the most ubiquitous and soluble that plants must cope with (Munns & Tester, 2008).

Salt stress affects all developmental stages, from germination to the reproductive phase. So it causes a wide range of symptoms: leaves are smaller, but thicker and more succulent, are abscissed, with necrosis on shoots and roots. There is a consequence on several physiological processes, such as photosynthesis and transpiration. It interferes with phytohormones metabolism and other metabolic pathways, and even disturbs genes and protein functions are affected (Murad et al., 2020).

Salinity response usually has detrimental effects on plant growth. First there is a quick response that starts minutes after salinity exposure and lasts for some days (the osmotic phase) to inhibit young leaf growth and to promote stomatal closure. Then there is a delayed response that can last for days or weeks (the ionic phase) to induce mature leaf senescence, stop metabolic processes, and even cause cell death (Isayenkov & Maathuis, 2019; Munns & Tester, 2008).

The **osmotic stress** phase driven by salinity ruins water potential homeostasis because of the excess concentration of solutes in water and/or soil outside roots (Munns, 2002). To overcome **osmotic stress**, plants perform osmotic adjustment to reduce the osmotic potential in the cytosol, and then they synthesize compatible solutes and activate water transport systems, which imply less energy for plant growth to survive under stress (Munns, 2011; Zhao et al., 2021). The compatible solutes are also called osmolytes or osmoprotectants, and include metabolites like sugars (sucrose, trehalose, fructans), polyols (sorbitol, mannitol), amino acids (proline), etc. (Gupta & Huang, 2014).

The **ionic stress** phase involves the imbalance of ionic distribution and ionic homeostasis due to the cellular toxicity of sodium and chloride ions, which is much higher for Na^+, and also to the unbalanced K^+/Na^+ ratio inside plants (Miura & Tada, 2014; Murad et al., 2020; Navarro et al., 2003). To counteract **ionic stress,** plants attempt to prevent high Na^+ and Cl^- concentrations in the cytoplasm by two different mechanisms: avoiding salt uptake in roots and the following transport across plants (exclusion and/or transferring salt from the cytoplasm to vacuoles (sequestration) (Munns, 2011).

Salt stress also triggers the production of secondary stresses, mostly **oxidative stress**, and plants develop detoxification strategies to restore osmotic, ionic and reactive oxygen species (ROS) balance (Yang & Guo, 2018). These strategies promote antioxidants synthesis and antioxidant enzymes activities to scavenge ROS, along with the regulation of ROS-responsive genes expression, to balance ROS production (Yang & Guo, 2018; Zhao et al., 2021).

Besides, there is a molecular response to overcome salinity that implicates salt-responsive genes that perform many functions, such as transcription factors (*DREB*s), molecular chaperones (*HSP*s), ion homeostasis or transport (*SOS*, *NHX1*, *H^+-ATPase*), among others (Gupta & Huang, 2014). This response is often mediated by Ca^{2+} accumulation sensing, which starts complex signal transduction pathways, and/or ABA, because these genes may contain ABA-responsive elements (Chaudhry et al., 2021).

In pepper under salt stress, Navarro et al. (2003) observed decreased growth with salinity due to the toxic effect of ions and the poor ability to perform osmotic adjustment. Suarez et al. (2021) stated that all the tested pepper cultivars limited the root-to-shoot Na^+ flux in salinity, with lower Na concentrations and lesser gene expression of ion transporters in the leaves of tolerant pepper cultivars. Hence they concluded that Na^+ exclusion is a crucial trait in pepper plants' response to salt stress, and there is wide variability among genotypes in relation to salt tolerance (Suarez et al., 2021). Penella et al. (2013) determined that net photosynthetic rate maintenance is a reliable trait to select pepper cultivars for their tolerance to salt stress. To acquire more-in-depth knowledge of tolerance mechanisms in pepper, Aktas et al. (2012) studied the response of two pepper genotypes with differing salt tolerance, and observed that the decrease in relative water content (RWC) in the tolerant genotype was lesser than the sensitive genotype. Moreover, the tolerant genotype maintained chlorophyll concentration, lipid peroxidation increase was less severe, and glutathione content and superoxide dismutase activity increases were higher than in the sensitive genotype (Aktas et al., 2012). Similarly, López-Serrano et al. (2021) observed that a tolerant pepper cultivar showed a higher leaf and root biomass, higher proline content and less disturbed photosynthesis than the sensitive genotype under salinity conditions.

1.3.2.2. Heat stress

The frequency of extreme temperature events is increasing because of climate change, as depicted in Figure 6. **Heat stress** is a complex stress of variable duration, and is commonly considered to be heat shock when temperatures rise 10-15 °C above the usual crop development range for long enough to irreversibly harm plants (Wahid et al., 2007). Thus increases in temperature can be transitory (heat shock or heat wave) or constant (prolonged heat stress), which lead to detrimental effects on plant growth and development, yield losses, and can even cause plant death in a drastic scenario (Kotak et al., 2007; Raza et al., 2023). Therefore, heat stress affects plants at morpho-anatomical, physiological, reproductive and biochemical levels (Nadeem et al., 2018).

High temperatures provoke cellular damage in exposed plants, such as alterations to lipid membranes integrity by changing their fluidity, or interference with enzymes function by modifying proteins activity (Hu et al., 2020). Besides, high temperature incidence on plant development depends on the growth stage, i.e., seed germination is delayed, which could end in total germination inhibition, but it is determined by both heat stress intensity and plant species (Wahid et al., 2007). In succeeding stages, chloroplasts are extremely vulnerable to temperature increases. Thus damage to chloroplasts results in disturbed chlorophyll biosynthesis, electron transport among both photosystems, CO_2 assimilation, and other photosynthesis-associated processes (Hu et al., 2020). Other important processes, such as respiration, water relations and primary and secondary metabolisms, are also interfered with by heat stress, which triggers changes in gene expression and protein regulation to achieve plant tolerance (Hu et al., 2020; Wahid et al., 2007).

Plant strategies to overcome heat stress include promoting cooling using transpiration, changing leaf orientation to avoid direct solar radiation, preserving plant membranes stability through alteration to its lipid composition, ROS scavenging by means of antioxidants synthesis, production of compatible osmolytes, activation of heat response-related factors and genes, including heat shock factors (HSFs) and heat shock proteins (HSPs), and several signaling strategies, such as chaperones, mitogen-activated protein kinase (MAPK) and calcium-dependent protein kinase (CDPK) cascades (Nadeem et al., 2018; Panikulangara et al., 2004; Wahid et al., 2007).

In HSPs terms, pepper heat stress response has been studied by Guo et al. (2014), who proposed a main role for the *Hsp70-1* gene in thermotolerance. This gene was induced by calcium ion (Ca^{2+}), hydrogen peroxide (H_2O_2) and putrescine, and this induction was stronger under heat stress. So the authors suggested that it is implicated in a signaling pathway for heat stress tolerance (Guo et al., 2014). Later, Guo et al. (2016) confirmed the implication of HSP70s in pepper heat stress response, and also *via* the regulation of stress-related genes expression, and their connection with plant growth and development. The glutathione metabolism has also been associated with thermotolerance in pepper because, under heat stress, the increase in the genes and metabolites implicated in this pathway in the tolerant pepper genotype was greater than in the sensitive genotype (Wang et al., 2019). Rajametov et al. (2021) proposed that the photosynthetic rate maintained *via* enhanced transpiration, together with an increased proline concentration, is an effective strategy in thermotolerant pepper for overcoming heat stress in the seedling stage. Regarding the reproductive stage, Aloni et al. (1994) suggested a relation between flower abscission under heat stress and ethylene production; that is, flower abscission depends on flowers' susceptibility to the ethylene produced under these stress conditions. In relation to pollen, under heat stress germination reduces, the concentration of sugars and starch lowers due to decreased pollen metabolism, and these result in fewer seeds (Aloni et al., 2001; Gisbert-Mullor et al., 2021). In pepper fruit, Liu et al. (2022) performed a multi-omic analysis (transcriptomics, proteomics and metabolomics) to find that heat stress inhibits secondary metabolite synthesis, i.e., capsaicin and ascorbic acid. They identified three TFs involved in capsaicin synthesis regulation under heat stress.

1.3.2.3. Drought

Water is an essential resource that is being threatened by a growing population and the development of urban areas, particularly in arid regions, which also suffer climate change conditions that, in turn, increase the prevalence, span and frequency of droughts (FAO, 2023b). According to the FAO (2023c), agriculture is the most and first affected sector by drought, and drought impact on crops can be a consequence of many factors, such as scarce rainfall, salinity, extreme (high and low) temperatures or high light intensity (Salehi-Lisar & Bakhshayeshan-Agdam, 2016).

Drought incidence on plants triggers several adverse effects that have an impact at all plant levels: molecular, cellular, biochemical, physiological and morphological levels. It ultimately leads to reduced crop yields (Anjum et al., 2011). Morphological alterations due to drought are observed mainly as delayed growth and reduced plant height, which are consequences of slower cell expansion on stems and roots and senescing leaves, whose size and number decrease (Anjum et al., 2011; Yang et al., 2021).

Due to physiological perturbations, photosynthesis, which is an essential process for plant survival, diminishes or is even inhibited under drought conditions. The CO_2 assimilation rate lowers, which can be accompanied by reduced transpiration (Anjum et al., 2011; Flexas et al., 2004; Yang et al., 2021). Here phytohormones play a role in drought response, especially abscisic acid (ABA), whose synthesis is promoted under drought conditions in roots, and is transported to shoots and leaves to mainly induce stomatal closure and to avoid water losses by transpiration (Salehi-Lisar & Bakhshayeshan-Agdam, 2016).

Moreover, the changes in water relations favor root growth over shoot growth by means of quick decreases in the water potential (Ψ_w) in roots, which promote water uptake, while Ψ_w in leaves decreases at a slower rate (Hsiao & Xu, 2000). In connection with Ψ_w rapid decline to allow water to enter, osmotic adjustment is usually performed by osmoprotectant synthesis and accumulation, which increase the concentration of the solutes inside the cell (Ozturk et al., 2021). Osmoprotectants or osmolytes comprise a considerable amount of compounds, such as sugars (trehalose, raffinose), sugar alcohols (myo-inositol), amino acids (proline) and quaternary ammonium compounds (glycine betaine), which also function by reducing oxidative damage from drought stress (Ejaz et al., 2020; Jogawat, 2019).

Oxidative damage is generated by drought exposure and is produced by excess ROS, which results in detrimental effects like lipid peroxidation, protein denaturation, DNA nicking and photosynthesis restriction (Yang et al., 2021). Plants attempt to counteract oxidative damage by the activation of antioxidant systems, which involve enzymatic activities (i.e., superoxide dismutase (SOD), catalase (CAT), ascorbate peroxidase (APX), monodehydroascorbate reductase (MDHAR), dehydroascorbate reductase (DHAR), glutathione reductase (GR), glutathione peroxidase (GPX), glutathione S-transferase (GST), ferritin, thioredoxins, glutaredoxins) and antioxidant compounds (i.e., ascorbic acid, glutathione, carotenoids, flavonoids, phenolic acids, α-tocopherol) (Hasanuzzaman et al., 2020; Reddy et al., 2004).

In addition, ROS can act as secondary messengers in drought signaling, along with other secondary messengers like Ca^{2+} and ABA, to regulate the expression of the drought-responsive genes and drought-induced proteins involved in signaling pathways (Kaur & Asthir, 2017). Transcription factors, such as dehydration responsive element binding (*DREB*), *HSFs*, *MYB*, *NAC*, basic leucine zipper (*bZIP*), and *WRKY* are key regulators of the downstream genes implicated in the drought molecular response (Manna et al., 2021). Moreover, some drought-responsive proteins are aquaporins (water channels that also transport small solutes, gases and metal ions), dehydrins (promote water retention, photosynthetic activity, ROS scavenging and osmolyte accumulation) and LEA proteins (protect plant membranes to avoid water losses, among other actions) (Afzal et al., 2016; Aslam et al., 2015; Riyazuddin et al., 2021).

Drought effects on pepper plants have been studied by Delfine et al. (2002), who observed photosynthetic limitations through lower stomatal conductance and decreased leaf Ψ_w and ion accumulation in leaves, which resulted in lesser plant growth, productivity and fruit quality in relation to well-irrigated control plants. Hu et al. (2010) obtained similar results in two pepper cultivars left under drought conditions; that is, a lower photosynthetic rate accompanied by increases in ROS and then the activation of antioxidant enzymes SOD and APX. Moreover, Anjum et al. (2012) studied the behavior of two pepper cultivars with different tolerance degrees, and noted opposite responses to progressive drought stress. Cultivar Shanshu-2001 was more tolerant to drought with higher growth and yield values, which were probably the result of higher relative water content in leaves, a prolonged increase in proline concentration, lower lipid peroxidation and electrolyte leakage than cultivar Nongchengjiao-2, which seemed to show a sensitivity response (Anjum et al., 2012). It is interesting to note that the more tolerant cultivar displayed greater constitutive activity of SOD, CAT and peroxidase activities than the more sensitive cultivar, which may confer a better ability to resist drought (Anjum et al., 2012). Sahitya et al. (2019) also studied the response of two pepper genotypes (one tolerant and one sensitive) under water stress and obtained comparable results: the tolerant genotype had a higher photosynthetic rate, RWC, lower g_s and differential gene expression regulation; that is, aquaporin genes were up-regulated in the tolerant genotype and down-regulated in the sensitive one. Park et al. (2003) studied the transcriptomic response of water-stressed pepper plants and identified seven rapidly induced cDNAs, of which one (*Ca-LEAL1*) encoded for a LEA-like protein and was also induced by ABA application. Similarly, Hong & Kim (2005) identified and described a DREB-like gene that was rapidly induced in pepper roots by water stress. They suggested a role in transcription activation. Pepper fruits are affected by drought in terms of reduced production, delayed ripening and modified bioactive and volatile compounds, and these alterations depend on the plant stage because they are the mechanisms needed to adapt to drought conditions (Borràs et al., 2021).

1.4. Grafting technique to overcome abiotic stresses

1.4.1. Grafting uses and importance

Grafting is a technique used in agriculture. It consists of joining together two parts of different plants: the scion, which brings the shoot, and the rootstock, which supplies the root system (Figure 7). Both the rootstock and scion are connected through their vascular systems union, which become a single plant after they have been joined (Hu & Beartrack, 2021).

Figure 7. Grafted pepper seedlings by Lidia López-Serrano.

Grafting is a very ancient technique that has been applied to fruit trees for more than 2000 years. This practice was expanded to vegetable crops in the last century (Bie et al., 2017). Grafting in vegetables started in Japan and Korea to restore crop losses due to the soil-borne pathogens that caused severe diseases, which were intensified through serial cropping (Lee et al., 2010). Later on in 1950s, greenhouses and tunnels became popular, and most farmers adopted protected cultivation to extend the crop season and left behind the rotating crop system. Thus grafting then became a necessity to control soil-borne infections and other diseases (Bie et al., 2017).

Apart from soil disease mitigation applications, grafting has many other uses, of which cultivation under adverse environmental conditions (both biotic and abiotic stresses) stands out, as well as enhanced crop yields that result from employing vigorous rootstocks (Kyriacou et al., 2017; Lee et al., 2010). Nowadays, most research focuses on vegetable grafting physiology and biotic stress resistance, and on two families, i.e., Cucurbitaceae and Solanaceae, whose cultivation as grafted plants extends to Europe, Asia and North America (Gaion et al., 2018; Goldschmidt, 2014).

1.4.2. Grafting in horticultural crops

Grafting for cultivation under biotic and abiotic stress conditions in horticultural crops is based on the rootstock's ability to survive undesirable stressors; that is, its resistance (Rivero et al., 2003a). Grafted plants show various traits that modify scion stress perception of the unfavorable environment, such as a robust and big root system from the rootstock, which allows better ability for water and nutrients uptake related to the latter, greater photosynthetic activity and a better water relations balance, enhanced antioxidant system, activation of the hormonal signaling network, and long-distance signal transmission by proteins, mRNAs and small RNAs (Rouphael et al., 2018. It is well-accepted that a bidirectional genetic exchange between the scion and rootstock takes place in grafting plants by means of the grafting union (Tsaballa et al., 2021). Particularly, long-distance signals lately appear as a promising strategy to regulate rootstock-scion relations and to modify physiological functions (Goldschmidt, 2014; Lu et al., 2020).

1.4.3. Grafting in Solanaceae to overcome abiotic stress

Abiotic stress amelioration by grafting on Solanaceae crops has been proven to be an effective strategy, mainly under salinity, heat stress and drought conditions. Regarding **salinity**, He et al. (2009) stated that grafted plants mitigate growth reduction under salt stress thanks to improved photosynthesis and the increased activity of antioxidant enzymes. In pepper under salt stress. Penella et al. (2015) attributed grafted plants' tolerance to the rootstock's ability to maintain ion homeostasis in the scion, which results in less disrupted photosynthesis, nitrate reductase and lipid peroxidation on leaves. Similarly, López-Serrano et al. (2020) observed a lesser impact of salinity on the biomass of the plants grafted onto the NIBER® rootstock (F1 hybrid obtained by IVIA-UPV), probably due to a less reduced photosynthetic rate, stomatal conductance and nitrate reductase compared to self-grafted and ungrafted plants. Besides, these authors proposed a signaling role to H_2O_2, which activates antioxidant mechanisms because it is reflected by increased phenols and proline content (López-Serrano et al., 2020). Lastly, Gálvez et al. (2021) found that grafted pepper plants' response to salinity was rootstock-dependent and they described three different strategies: i) the Atlante rootstock had an invigorating effect that resulted from an improved cytokinins/ABA balance; ii) Creonte increased fruit yield and the reproductive to vegetative ratio was undisturbed, thanks to better biomass distribution, and opposite cytokinins and ethylene precursor regulation; iii) Terrano decreased plant height by means of non gibberellins accumulation and induced ABA to maintain the reproductive and vegetative biomass.

When focusing on **heat stress**, the impact of this stress on grafted tomato plants is less severe than the effect on non grafted tomato, and grafted plants showed higher biomass and improved development, which were related to lesser phenolic compounds accumulation as a resistance response (Rivero et al., 2003b). With pepper, Gisbert-Mullor et al. (2021, 2023) studied the response to high temperatures in a controlled environment, and verified that pepper yields are higher when using a thermotolerant rootstock under greenhouse conditions. These higher yields are dependent on mechanisms in the vegetative stage (i.e., less electrolyte leakage, more ascorbic acid, undisturbed chlorophyll and carotenoids) and in the reproductive stage (enhanced anthers proline content, improved pollen germination and fruit set).

In relation to **drought**, tomato-grafted seedlings tolerance has been attributed to enhanced root growth produced by better osmotic adjustment, which may facilitate water uptake and nutrients (Zhang et al., 2020). Fullana-Pericàs et al. (2020) studied the grafted tomato response to drought in plant growth and yield terms. The grafting plants showed higher growth and production rates not only under drought stress, but also under well-watered conditions. The grafted pepper responses under water stress induced by PEG were studied by Penella et al. (2014), who observed decreased photosynthetic activity and NO_3^- uptake and transport to leaves in all the grafted plants. However, the photosynthesis of the plants grafted onto tolerant accessions was less disturbed. These authors suggested a protective role of proline accumulation and osmotic adjustment (Penella et al. 2014). López-Serrano et al. (2019) reported a protective role for the tolerant pepper rootstock they tested under short-term water stress because it was able to alleviate oxidative stress in the scion and could balance the biomass distribution of C and N, which resulted in bigger crop yields. Lastly, the NIBER® pepper tolerant rootstock has been tested under deficit irrigation conditions for consecutive years. The authors stated that both plant biomass and fruit production had less impact on the plants grafted onto the NIBER® rootstock (Gisbert-Mullor et al., 2020). They also suggested that better NIBER® performance under water stress was associated with less affected shoot biomass and photosynthesis. However, the physiological, biochemical and molecular mechanisms of NIBER® tolerance have not yet been explored.

1.5. Thesis Objectives

The research groups from the Horticulture Department at the Valencian Institute of Agricultural Research (IVIA) and the Vegetable Production Department at the Polytechnic University of Valencia (UPV) study and develop tolerant pepper rootstocks to confer water stress tolerance in grafted plants and to minimize the yield losses produced by water stress. To do so, the research groups conducted experiments to evaluate physiological responses to water stress in pepper accessions when used as rootstocks. The outstanding accessions are crossed to obtain hybrids. After a selection process, the best hybrids are then studied in the field in a growing cycle under water stress conditions to assess their agronomical behavior.

In this context, both the aforementioned research groups obtained the pepper F1 hybrid rootstock NIBER®, which is patented as a water- and salt stress-tolerant pepper rootstock. When NIBER® was used as a rootstock with sustained deficit irrigation in the field, the variety obtained bigger yields compared to the ungrafted variety (Gisbert-Mullor et al., 2020). In addition, NIBER® physiological adaptation and root biomass contribution to long-term water stress tolerance have been studied by Gisbert-Mullor et al. (2023). However, it is not known if the tolerance to sustained water stress observed in the variety grafted onto NIBER® is related to differential responses in the early water stress phase. Moreover, as far as know, there is no published research into the molecular mechanisms involved in water stress response in pepper grafted plants, and their tolerance to drought has not been addressed from the transcriptomic and/or the metabolomic perspective. Understanding the short-term modulation of water stress responses with the analysis of gene expression changes, phytohormonal balance and metabolic signatures will broaden knowledge about tolerance achievement and will make tolerant pepper rootstocks development more effective.

The main objectives of the present doctoral dissertation are to:

1. Characterize pepper hybrid rootstocks through the physiological parameters involved in the water stress response to i) study the relation between photosynthesis maintenance and antioxidant systems in grafted pepper plants and to ii) obtain biomarkers for water stress-tolerant pepper rootstocks selection purposes (Chapter 1).
2. Study the transcriptome profile of the tolerant pepper hybrid rootstock NIBER® and the pepper-sensitive accession A10 under short-term water stress to identify prompt responses that constitute master regulators in water stress tolerance achievement (Chapter 2).
3. Identify early responses in the phytohormones network of leaves and roots in the self-grafted variety and grafted onto NIBER® under short-term water stress to address the contribution of NIBER® hormonal regulation to confer the variety tolerance (Chapter 3).
4. Analyze the prompt metabolic responses of leaves and roots in the self-grafted pepper plants and grafted onto NIBER® under short-term water stress to elucidate the biochemical bases that lead to metabolic profiles modulation toward water stress tolerance (Chapter 4).

1.6. References

Afzal, Z., Howton, T. C., Sun, Y., & Mukhtar, M. S. (2016). The Roles of Aquaporins in Plant Stress Responses. *Journal of Developmental Biology 2016, Vol. 4, Page 9*, *4*(1), 9. https://doi.org/10.3390/JDB4010009

Aktas, H., Abak, K., & Eker, S. (2012). Anti-oxidative responses of salt-tolerant and salt-sensitive pepper (*Capsicum annuum* L.) genotypes grown under salt stress. *The Journal of Horticultural Science and Biotechnology*, *87*(4), 360–366. https://doi.org/10.1080/14620316.2012.11512877

Aloni, B., Karni, L., Zaidman, Z., Riov, Y., Huberman, M., & Goren, R. (1994). The susceptibility of pepper (*Capsicum annuum*) to heat induced flower abscission: Possible involvement of ethylene. *Journal of Horticultural Science*, *69*(5), 923–928. https://doi.org/10.1080/14620316.1994.11516528

Aloni, B., Peet, M., Pharr, M., & Karni, L. (2001). The effect of high temperature and high atmospheric CO_2 on carbohydrate changes in bell pepper (*Capsicum annuum*) pollen in relation to its germination. *Physiologia Plantarum*, *112*(4), 505–512. https://doi.org/10.1034/j.1399-3054.2001.1120407.x

Anjum, S. A., Farooq, M., Xie, X. yu, Liu, X. jian, & Ijaz, M. F. (2012). Antioxidant defense system and proline accumulation enables hot pepper to perform better under drought. *Scientia Horticulturae*, *140*, 66–73. https://doi.org/10.1016/j.scienta.2012.03.028

Anjum, S. A., Xie, X.-Y., Wang, L.-C., Saleem, M. F., Man, C., & Lei, W. (2011). Morphological, physiological and biochemical responses of plants to drought stress. *African Journal of Agricultural Research*, *6*(9), 2026–2032. https://doi.org/10.5897/AJAR10.027

Aslam, M., Maqbool, M. A., & Cengiz, R. (2015). *Mechanisms of Drought Resistance*. 19–36. https://doi.org/10.1007/978-3-319-25442-5_3

Barboza, G. E., García, C. C., de Bem Bianchetti, L., Romero, M. V., & Scaldaferro, M. (2022). Monograph of wild and cultivated chili peppers (*Capsicum* L., Solanaceae). *PhytoKeys 200: 1-423*, *200*, 1–423. https://doi.org/10.3897/PHYTOKEYS.200.71667

Barchenger, D. W., Naresh, P., & Kumar, S. (2019). *Genetic Resources of Capsicum* (pp. 9–23). Springer, Cham. https://doi.org/10.1007/978-3-319-97217-6_2

Basu, S. K., & De, A. K. (2003). *Capsicum*: historical and botanical perspectives. In A. K. De (Ed.), *Capsicum - The genus Capsicum* (Vol. 33, pp. 21–35). Taylor & Francis. https://doi.org/10.1201/9780203381151-8

Bhattacharya, S. (2023). Fruits and vegetables. *Snack Foods*, 95–116. https://doi.org/10.1016/B978-0-12-819759-2.00013-6

Bie Z, Nawaz, M. A., Huang Yuan, H. Y., Lee JungMyung, L. J., & Colla, G. (2017). Introduction to vegetable grafting. In G. Colla, F. Pérez-Alfocea, & D. Schwarz (Eds.), *Vegetable grafting: principles and practices* (pp. 1–21). CABI. https://doi.org/10.1079/9781780648972.0001

Borràs, D., Plazas, M., Moglia, A., & Lanteri, S. (2021). The influence of acute water stresses on the biochemical composition of bell pepper (*Capsicum annuum* L.) berries. *Journal of the Science of Food and Agriculture*, *101*(11), 4724–4734. https://doi.org/10.1002/JSFA.11118

CABI. (2022). *Capsicum annuum* (bell pepper). *CABI Compendium*, *CABI Compendium*. https://doi.org/10.1079/cabicompendium.15784

Carrizo García, C., Barfuss, M. H. J., Sehr, E. M., Barboza, G. E., Samuel, R., Moscone, E. A., & Ehrendorfer, F. (2016). Phylogenetic relationships, diversification and expansion of chili peppers (*Capsicum*, Solanaceae). *Annals of Botany*, *118*(1), 35–51. https://doi.org/10.1093/AOB/MCW079

Chaudhry, U. K., Gökçe, Z. N. Ö., & Gökçe, A. F. (2021). The Influence of Salinity Stress on Plants and Their Molecular Mechanisms. *IECPS 2021*, *11*(1), 31. https://doi.org/10.3390/IECPS2021-12017

Chiou, K. L., & Hastorf, C. A. (2014). A Systematic Approach to Species–Level Identification of Chile Pepper (*Capsicum* spp.) Seeds: Establishing the Groundwork for Tracking the Domestication and Movement of Chile Peppers through the Americas and Beyond. *Economic Botany*, *68*(3), 316–336. https://doi.org/10.1007/S12231-014-9279-2/FIGURES/13

Delelegn, S. (2011). *Evaluation of Elite hot pepper varieties (Capsicum species) for growth, dry pod yield and quality under Jimma condition, South West Ethiopia* [Jimma University]. https://cgspace.cgiar.org/handle/10568/3613

Delfine, S., Tognetti, R., Loreto, F., & Alvino, A. (2002). Physiological and growth responses to water stress in field-grown bell pepper (*Capsicum annuum* L.). *Journal of Horticultural Science and Biotechnology*, *77*(6), 697–704. https://doi.org/10.1080/14620316.2002.11511559

Ejaz, S., Fahad, S., Anjum, M. A., Nawaz, A., Naz, S., Hussain, S., & Ahmad, S. (2020). *Role of Osmolytes in the Mechanisms of Antioxidant Defense of Plants* (pp. 95–117). Springer, Cham. https://doi.org/10.1007/978-3-030-38881-2_4

FAO. (2021). *FAO publications*. Climate Change Fans Spread of Pests and Threatens Plants and Crops, New FAO Study.

FAO. (2023a). *Drought and Agriculture*. Food and Agriculture Organization. https://www.fao.org/land-water/water/drought/droughtandag/en/

FAO. (2023b). *Soil salinity | Global Soil Partnership*. https://www.fao.org/global-soil-partnership/areas-of-work/soil-salinity/en/

FAO. (2023c, April 3). *FAOSTAT-Crops and livestock products*. https://www.fao.org/Faostat/En/#data/QCL/Visualize. https://www.fao.org/faostat/en/#data/QCL/visualize

Flexas, J., Bota, J., Cifre, J., Escalona, J., Galmes, J., Gulias, J., Lefi, E.-K., Martinez-Canellas, S., Moreno, M., Ribas-Carbo, M., Riera, D., Sampol, B., & Medrano, H. (2004). Understanding down-regulation of photosynthesis under water stress: future prospects and searching for physiological tools for irrigation management. *Annals of Applied Biology*, *144*(3), 273–283. https://doi.org/10.1111/j.1744-7348.2004.tb00343.x

Fullana-Pericàs, M., Conesa, M., Pérez-Alfocea, F., & Galmés, J. (2020). The influence of grafting on crops' photosynthetic performance. *Plant Science*, *295*, 110250. https://doi.org/10.1016/j.plantsci.2019.110250

Gaion, L. A., Braz, L. T., & Carvalho, R. F. (2018). Grafting in Vegetable Crops: A Great Technique for Agriculture. *International Journal of Vegetable Science*, *24*(1), 85–102. https://doi.org/10.1080/19315260.2017.1357062

Gálvez, A., Albacete, A., Martínez-Andújar, C., Del Amor, F. M., & López-Marín, J. (2021). Contrasting Rootstock-Mediated Growth and Yield Responses in Salinized Pepper Plants (*Capsicum annuum* L.) Are Associated with Changes in the Hormonal Balance. *International Journal of Molecular Sciences 2021, Vol. 22, Page 3297*, *22*(7), 3297. https://doi.org/10.3390/IJMS22073297

Gisbert-Mullor, R., Padilla, Y. G., Martínez-Cuenca, M.-R., López-Galarza, S., & Calatayud, Á. (2021). Suitable rootstocks can alleviate the effects of heat stress on pepper plants. *Scientia Horticulturae*, *290*, 110529. https://doi.org/10.1016/j.scienta.2021.110529

Gisbert-Mullor, R., Pascual-Seva, N., Martínez-Gimeno, M. A., López-Serrano, L., Badal Marín, E., Pérez-Pérez, J. G., Bonet, L., Padilla, Y. G., Calatayud, Á., Pascual, B., & López-Galarza, S. (2020). Grafting onto an Appropriate Rootstock Reduces the Impact on Yield and Quality of Controlled Deficit Irrigated Pepper Crops. *Agronomy*, *10*(10), 1529. https://doi.org/10.3390/agronomy10101529

Goldschmidt, E. E. (2014). Plant grafting: New mechanisms, evolutionary implications. *Frontiers in Plant Science*, *5*(DEC), 727. https://doi.org/10.3389/fpls.2014.00727

Guo, M., Liu, J.-H., Ma, X., Zhai, Y.-F., Gong, Z.-H., & Lu, M.-H. (2016). Genome-wide analysis of the Hsp70 family genes in pepper (*Capsicum annuum* L.) and functional identification of *CaHsp70-2* involvement in heat stress. *Plant Science*, *252*, 246–256. https://doi.org/10.1016/j.plantsci.2016.07.001

Guo, M., Zhai, Y.-F., Lu, J.-P., Chai, L., Chai, W.-G., Gong, Z.-H., & Lu, M.-H. (2014). Characterization of *CaHsp70-1*, a Pepper Heat-Shock Protein Gene in Response to Heat Stress and Some Regulation Exogenous Substances in *Capsicum annuum* L. *International Journal of Molecular Sciences*, *15*(11), 19741–19759. https://doi.org/10.3390/ijms151119741

Gupta, B., & Huang, B. (2014). Mechanism of salinity tolerance in plants: Physiological, biochemical, and molecular characterization. *International Journal of Genomics*, *2014*. https://doi.org/10.1155/2014/701596

Hasanuzzaman, M., Bhuyan, M. H. M. B., Zulfiqar, F., Raza, A., Mohsin, S. M., Mahmud, J. Al, Fujita, M., & Fotopoulos, V. (2020). Reactive Oxygen Species and Antioxidant Defense in Plants under Abiotic Stress: Revisiting the Crucial Role of a Universal Defense Regulator. *Antioxidants*, *9*(8), 681. https://doi.org/10.3390/antiox9080681

He, Y., Zhu, Z., Yang, J., Ni, X., & Zhu, B. (2009). Grafting increases the salt tolerance of tomato by improvement of photosynthesis and enhancement of antioxidant enzymes activity. *Environmental and Experimental Botany*, *66*(2), 270–278. https://doi.org/10.1016/j.envexpbot.2009.02.007

Hong, J.-P., & Kim, W. T. (2005). Isolation and functional characterization of the *Ca-DREBLP1* gene encoding a dehydration-responsive element binding-factor-like protein 1 in hot pepper (*Capsicum annuum* L. cv. Pukang). *Planta*, *220*(6), 875–888. https://doi.org/10.1007/s00425-004-1412-5

Hsiao, T. C., & Xu, L. (2000). Sensitivity of growth of roots versus leaves to water stress: biophysical analysis and relation to water transport. *Journal of Experimental Botany*, *51*(350), 1595–1616. https://doi.org/10.1093/jexbot/51.350.1595

Hu, B., & Beartrack, M. (2021, April). *Ferguson College of Agriculture*. Introduction to Vegetable Grafting. https://extension.okstate.edu/fact-sheets/introduction-to-vegetable-grafting.html

Hu, S., Ding, Y., & Zhu, C. (2020). Sensitivity and Responses of Chloroplasts to Heat Stress in Plants. *Frontiers in Plant Science*, *11*, 375. https://doi.org/10.3389/fpls.2020.00375

Hu, W. H., Xiao, Y. A., Zeng, J. J., & Hu, X. H. (2010). Photosynthesis, respiration and antioxidant enzymes in pepper leaves under drought and heat stresses. *Biologia Plantarum*, *54*(4), 761–765. https://doi.org/10.1007/s10535-010-0137-5

IMF. (2022). *Climate Change Indicators Dashboard*. https://climatedata.imf.org/

IPPC. (2021). Scientific review of the impact of climate change on plant pests. *Scientific Review of the Impact of Climate Change on Plant Pests*. https://doi.org/10.4060/CB4769EN

Isayenkov, S. V., & Maathuis, F. J. M. (2019). Plant salinity stress: Many unanswered questions remain. *Frontiers in Plant Science*, *10*, 435515. https://doi.org/10.3389/FPLS.2019.00080/BIBTEX

Jogawat, A. (2019). Osmolytes and their Role in Abiotic Stress Tolerance in Plants. In *Molecular Plant Abiotic Stress* (pp. 91–104). Wiley. https://doi.org/10.1002/9781119463665.ch5

Kaur, G., & Asthir, B. (2017). Molecular responses to drought stress in plants. *Biologia Plantarum*, *61*(2), 201–209. https://doi.org/10.1007/s10535-016-0700-9

Kenyon, L., Kumar, S., Tsai, W. S., & Hughes, J. d. A. (2014). Virus Diseases of Peppers (*Capsicum* spp.) and Their Control. *Advances in Virus Research*, *90*, 297–354. https://doi.org/10.1016/B978-0-12-801246-8.00006-8

Khan, F. A., Mahmood, T., Ali, M., Saeed, A., & Maalik, A. (2014). Pharmacological importance of an ethnobotanical plant: *Capsicum annuum* L. *Natural Product Research*, *28*(16), 1267–1274. https://doi.org/10.1080/14786419.2014.895723

Kotak, S., Larkindale, J., Lee, U., von Koskull-Döring, P., Vierling, E., & Scharf, K.-D. (2007). Complexity of the heat stress response in plants. *Current Opinion in Plant Biology*, *10*(3), 310–316. https://doi.org/10.1016/j.pbi.2007.04.011

Kyriacou, M. C., Rouphael, Y., Colla, G., Zrenner, R., & Schwarz, D. (2017). Vegetable Grafting: The Implications of a Growing Agronomic Imperative for Vegetable Fruit Quality and Nutritive Value. *Frontiers in Plant Science*, *8*. https://doi.org/10.3389/fpls.2017.00741

Lee, J.-M., Kubota, C., Tsao, S. J., Bie, Z., Echevarria, P. H., Morra, L., & Oda, M. (2010). Current status of vegetable grafting: Diffusion, grafting techniques, automation. *Scientia Horticulturae*, *127*(2), 93–105. https://doi.org/10.1016/j.scienta.2010.08.003

Li, N., Yu, C., Yin, Y., Gao, S., Wang, F., Jiao, C., & Yao, M. (2020). Pepper Crop Improvement Against *Cucumber Mosaic Virus* (CMV): A Review. *Frontiers in Plant Science*, *11*, 1932. https://doi.org/10.3389/FPLS.2020.598798/BIBTEX

Li, Y. (2015). *The Connecticut Agricultural Experiment Station*. Bacterial Spot on Pepper. www.ct.gov/caes

Liu, C., Luo, S., Zhao, Y., Miao, Y., Wang, Q., Ye, L., Gao, L., Ahammed, G. J., & Cheng, Y. (2022). Multiomics analyses reveal high temperature-induced molecular regulation of ascorbic acid and capsaicin biosynthesis in pepper fruits. *Environmental and Experimental Botany*, *201*, 104941. https://doi.org/10.1016/J.ENVEXPBOT.2022.104941

López-Serrano, L., Calatayud, Á., López-Galarza, S., Serrano, R., & Bueso, E. (2021). Uncovering salt tolerance mechanisms in pepper plants: a physiological and transcriptomic approach. *BMC Plant Biology*, *21*(1), 169. https://doi.org/10.1186/s12870-021-02938-2

López-Serrano, L., Canet-Sanchis, G., Selak, G. V., Penella, C., San Bautista, A., López-Galarza, S., & Calatayud, Á. (2020). Physiological characterization of a pepper hybrid rootstock designed to cope with salinity stress. *Plant Physiology and Biochemistry*, *148*, 207–219. https://doi.org/10.1016/j.plaphy.2020.01.016

López-Serrano, L., Canet-Sanchis, G., Vuletin Selak, G., Penella, C., San Bautista, A., López-Galarza, S., & Calatayud, Á. (2019). Pepper Rootstock and Scion Physiological Responses Under Drought Stress. *Frontiers in Plant Science*, *10*, 38. https://doi.org/10.3389/fpls.2019.00038

Manna, M., Thakur, T., Chirom, O., Mandlik, R., Deshmukh, R., & Salvi, P. (2021). Transcription factors as key molecular target to strengthen the drought stress tolerance in plants. *Physiologia Plantarum*, *172*(2), 847–868. https://doi.org/10.1111/PPL.13268

MAPA. (2022). *Informe del consumo de alimentación en España 2021*. https://www.fepex.es/Info/Documentos/pdf/Consumo/Informe_anual_MAPA_2021_consumo_Extracto_FyH.pdf

MAPA. (2023). *Anuario de Estadística 2021 - Superficies y producciones de cultivos*.

McGrath, M. (2023). *Vegetable Pathology – Long Island Horticultural Research & Extension Center*. Anthracnose or Ripe Rot of Pepper. https://blogs.cornell.edu/livegpath/gallery/peppers/anthracnose-on-pepper/

Miura, K., & Tada, Y. (2014). Regulation of water, salinity, and cold stress responses by salicylic acid. *Frontiers in Plant Science*, *5*. https://doi.org/10.3389/fpls.2014.00004

Morris, W. L., & Taylor, M. A. (2017). The Solanaceous Vegetable Crops: Potato, Tomato, Pepper, and Eggplant. *Encyclopedia of Applied Plant Sciences*, *3*, 55–58. https://doi.org/10.1016/B978-0-12-394807-6.00129-5

Moury, B., Palloix, A., Caranta, C., Gognalons, P., Souche, S., Gebre Selassie, K., & Marchoux, G. (2005). Serological, Molecular, and Pathotype Diversity of Pepper veinal mottle virus and Chili veinal mottle virus. *Phytopathology*, *95*(3), 227. https://doi.org/10.1094/PHYTO-95-0227

Moury, B., & Verdin, E. (2012). Viruses of Pepper Crops in the Mediterranean Basin: A Remarkable Stasis. *Advances in Virus Research*, *84*, 127–162. https://doi.org/10.1016/B978-0-12-394314-9.00004-X

Munns, R. (2002). Comparative physiology of salt and water stress. *Plant, Cell & Environment*, *25*(2), 239–250. https://doi.org/10.1046/j.0016-8025.2001.00808.x

Munns, R. (2011). Plant Adaptations to Salt and Water Stress. In *Advances in Botanical Research* (Vol. 57, pp. 1–32). Academic Press. https://doi.org/10.1016/B978-0-12-387692-8.00001-1

Munns, R., & Tester, M. (2008). Mechanisms of Salinity Tolerance. *Annual Review of Plant Biology*, *59*(1), 651–681. https://doi.org/10.1146/annurev.arplant.59.032607.092911

Murad, M. Al, Khan, A. L., & Muneer, S. (2020). Silicon in Horticultural Crops: Cross-talk, Signaling, and Tolerance Mechanism under Salinity Stress. *Plants 2020, Vol. 9, Page 460*, *9*(4), 460. https://doi.org/10.3390/PLANTS9040460

Nadeem, M., Li, J., Wang, M., Shah, L., Lu, S., Wang, X., & Ma, C. (2018). Unraveling Field Crops Sensitivity to Heat Stress: Mechanisms, Approaches, and Future Prospects. *Agronomy*, *8*(7), 128. https://doi.org/10.3390/agronomy8070128

Navarro, J. M., Garrido, C., Martínez, V., & Carvajal, M. (2003). Water relations and xylem transport of nutrients in pepper plants grown under two different salts stress regimes. *Plant Growth Regulation*, *41*(3), 237–245. https://doi.org/10.1023/B:GROW.0000007515.72795.c5

Nicolaï, M., Cantet, M., Lefebvre, V., Sage-Palloix, A. M., & Palloix, A. (2013). Genotyping a large collection of pepper (*Capsicum* spp.) with SSR loci brings new evidence for the wild origin of cultivated *C. annuum* and the structuring of genetic diversity by human selection of cultivar types. *Genetic Resources and Crop Evolution*, *60*(8), 2375–2390. https://doi.org/10.1007/S10722-013-0006-0/FIGURES/6

OEC. (2023). *Peppers fresh or chilled*. https://oec.world/en/profile/hs/peppers-capsicum-pimenta-fresh-or-chilled

Olatunji, T. L., & Afolayan, A. J. (2018). The suitability of chili pepper (*Capsicum annuum* L.) for alleviating human micronutrient dietary deficiencies: A review. *Food Science & Nutrition*, *6*(8), 2239–2251. https://doi.org/10.1002/FSN3.790

Ozturk, M., Turkyilmaz Unal, B., García-Caparrós, P., Khursheed, A., Gul, A., & Hasanuzzaman, M. (2021). Osmoregulation and its actions during the drought stress in plants. *Physiologia Plantarum*, *172*(2), 1321–1335. https://doi.org/10.1111/PPL.13297

Panikulangara, T. J., Eggers-Schumacher, G., Wunderlich, M., Stransky, H., & Schöffl, F. (2004). *Galactinol synthase1*. A novel heat shock factor target gene responsible for heat-induced synthesis of raffinose family oligosaccharides in Arabidopsis. *Plant Physiology*, *136*(2), 3148–3158. https://doi.org/10.1104/pp.104.042606

Pappu, H. R., Whitfield, A. E., & de Oliveira, A. S. (2021). *Tomato Spotted Wilt Virus* (Tospoviridae). *Encyclopedia of Virology: Volume 1-5, Fourth Edition*, *1–5*, 761–767. https://doi.org/10.1016/B978-0-12-809633-8.21329-0

Parihar, P., Singh, S., Singh, R., Singh, V. P., & Prasad, S. M. (2015). Effect of salinity stress on plants and its tolerance strategies: a review. *Environmental Science and Pollution Research*, *22*(6), 4056–4075. https://doi.org/10.1007/S11356-014-3739-1/FIGURES/4

Parisi, M., Alioto, D., & Tripodi, P. (2020). Overview of Biotic Stresses in Pepper (*Capsicum* spp.): Sources of Genetic Resistance, Molecular Breeding and Genomics. *International Journal of Molecular Sciences*, *21*(7). https://doi.org/10.3390/IJMS21072587

Park, J. A., Cho, S. K., Kim, J. E., Chung, H. S., Hong, J. P., Hwang, B., Hong, C. B., & Kim, W. T. (2003). Isolation of cDNAs differentially expressed in response to drought stress and characterization of the *Ca-LEAL1* gene encoding a new family of atypical LEA-like protein homologue in hot pepper (*Capsicum annuum* L. cv. Pukang). *Plant Science*, *165*(3), 471–481. https://doi.org/10.1016/S0168-9452(03)00165-1

Penella, C., Nebauer, S. G., Bautista, A. S., López-Galarza, S., & Calatayud, Á. (2014). Rootstock alleviates PEG-induced water stress in grafted pepper seedlings: Physiological responses. *Journal of Plant Physiology*, *171*(10), 842–851. https://doi.org/10.1016/j.jplph.2014.01.013

Penella, C., Nebauer, S. G., Lopéz-Galarza, S., San Bautista, A., Gorbe, E., & Calatayud, A. (2013). Evaluation for salt stress tolerance of pepper genotypes to be used as rootstocks. *Journal of Food, Agriculture and Environment*, *11*(3–4), 1101–1107.

Penella, C., Nebauer, S. G., Quiñones, A., San Bautista, A., López-Galarza, S., & Calatayud, A. (2015). Some rootstocks improve pepper tolerance to mild salinity through ionic regulation. *Plant Science*, *230*, 12–22. https://doi.org/10.1016/j.plantsci.2014.10.007

Pernezny, K., Roberts, P., Murphy, J., & Goldberg, N. (2003). *Compendium of pepper diseases: Vol. No. 633.8493/P452*. APS press. ISBN: 0890543003.

Pickersgill, B. (2007). Domestication of Plants in the Americas: Insights from Mendelian and Molecular Genetics. *Annals of Botany*, *100*(5), 925–940. https://doi.org/10.1093/AOB/MCM193

Ploeg, A. T., & Kodira, U. C. (2016). *UC IPM Pest Management Guidelines: Peppers*. Nematodes. https://ipm.ucanr.edu/agriculture/peppers/nematodes/

Powis, T. G., Murrieta, E. G., Lesure, R., Bravo, R. L., Grivetti, L., Kucera, H., & Gaikwad, N. W. (2013). Prehispanic Use of Chili Peppers in Chiapas, Mexico. *PLOS ONE*, *8*(11), e79013. https://doi.org/10.1371/JOURNAL.PONE.0079013

Quesada-Ocampo, L. (2020). *Vegetable Pathology Factsheets*. Phytophthora Blight of Peppers. https://content.ces.ncsu.edu/phytophthora-blight-of-peppers

Rajametov, S. N., Yang, E. Y., Cho, M. C., Chae, S. Y., Jeong, H. B., & Chae, W. B. (2021). Heat-tolerant hot pepper exhibits constant photosynthesis via increased transpiration rate, high proline content and fast recovery in heat stress condition. *Scientific Reports*, *11*(1), 14328. https://doi.org/10.1038/s41598-021-93697-5

Raza, A., Charagh, S., Abbas, S., Hassan, M. U., Saeed, F., Haider, S., Sharif, R., Anand, A., Corpas, F. J., Jin, W., & Varshney, R. K. (2023). Assessment of proline function in higher plants under extreme temperatures. *Plant Biology*, *25*(3), 379–395. https://doi.org/10.1111/plb.13510

Reddy, A. R., Chaitanya, K. V., & Vivekanandan, M. (2004). Drought-induced responses of photosynthesis and antioxidant metabolism in higher plants. *Journal of Plant Physiology*, *161*(11), 1189–1202. https://doi.org/10.1016/j.jplph.2004.01.013

Rivero, R. M., Ruiz, J. M., & Romero, L. (2003a). Can grafting in tomato plants strengthen resistance to thermal stress? *Journal of the Science of Food and Agriculture*, *83*(13), 1315–1319. https://doi.org/10.1002/jsfa.1541

Rivero, R. M., Ruiz, J., & Romero, L. (2003b). Role of grafting in horticultural plants under stress conditions. *Journal of Food Agriculture & Environment*, *1*(1), 70–74. www.world-food.net

Riyazuddin, R., Nisha, N., Singh, K., Verma, R., & Gupta, R. (2021). Involvement of dehydrin proteins in mitigating the negative effects of drought stress in plants. *Plant Cell Reports 2021 41:3*, *41*(3), 519–533. https://doi.org/10.1007/S00299-021-02720-6

Rouphael, Y., Kyriacou, M. C., & Colla, G. (2018). Vegetable Grafting: A Toolbox for Securing Yield Stability under Multiple Stress Conditions. *Frontiers in Plant Science*, *8*, 2255. https://doi.org/10.3389/fpls.2017.02255

Sabaratnam, S. (2021). Powdery Mildew of Greenhouse Peppers. *British Columbia Ministry of Agriculture, Food and Fisheries*.

Sah, S. K., Reddy, K. R., & Li, J. (2016). Abscisic acid and abiotic stress tolerance in crop plants. *Frontiers in Plant Science*, *7*, 571. https://doi.org/10.3389/fpls.2016.00571

Sahitya, U. L., Krishna, M. S. R., & Suneetha, P. (2019). Integrated approaches to study the drought tolerance mechanism in hot pepper (*Capsicum annuum* L.). *Physiology and Molecular Biology of Plants*, *25*(3), 637–647. https://doi.org/10.1007/S12298-019-00655-7

Salehi-Lisar, S. Y., & Bakhshayeshan-Agdam, H. (2016). Drought Stress in Plants: Causes, Consequences, and Tolerance. In *Drought Stress Tolerance in Plants, Vol 1* (Vol. 1, pp. 1–16). Springer International Publishing. https://doi.org/10.1007/978-3-319-28899-4_1

Stommel, J. R., & Bosland, P. W. (2007). Ornamental pepper. *Flower Breeding and Genetics*, 561–599. https://doi.org/10.1007/978-1-4020-4428-1_21

Suarez, D. L., Celis, N., Ferreira, J. F. S., Reynolds, T., & Sandhu, D. (2021). Linking genetic determinants with salinity tolerance and ion relationships in eggplant, tomato and pepper. *Scientific Reports*, *11*(1), 16298. https://doi.org/10.1038/s41598-021-95506-5

Tóbiás, I., Almási, A., Csilléry, G., Nemes, K., & Salánki, K. (2017). Virus Diseases of Pepper (*Capsicum annuum* L.) in Hungary. *Agriculture and Food*.

Tsaballa, A., Xanthopoulou, A., Madesis, P., Tsaftaris, A., & Nianiou-Obeidat, I. (2021). Vegetable Grafting From a Molecular Point of View: The Involvement of Epigenetics in Rootstock-Scion Interactions. *Frontiers in Plant Science*, *11*, 621999. https://doi.org/10.3389/FPLS.2020.621999/BIBTEX

UF. (2021). *Pepper diseases*. Fusarium Wilt. https://plantpath.ifas.ufl.edu/u-scout/pepper/fusarium-wilt.html

UN. (2023). Land - the planet's carbon sink. *United Nations*. https://www.un.org/en/climatechange/science/climate-issues/land

Wahid, A., Gelani, S., Ashraf, M., & Foolad, M. (2007). Heat tolerance in plants: An overview. *Environmental and Experimental Botany*, *61*(3), 199–223. https://doi.org/10.1016/j.envexpbot.2007.05.011

Wang, J., Lv, J., Liu, Z., Liu, Y., Song, J., Ma, Y., Ou, L., Zhang, X., Liang, C., Wang, F., Juntawong, N., Jiao, C., Chen, W., & Zou, X. (2019). Integration of Transcriptomics and Metabolomics for Pepper (*Capsicum annuum* L.) in Response to Heat Stress. *International Journal of Molecular Sciences*, *20*(20), 5042. https://doi.org/10.3390/ijms20205042

Wang, W., Vinocur, B., & Altman, A. (2003). Plant responses to drought, salinity and extreme temperatures: Towards genetic engineering for stress tolerance. *Planta*, *218*(1), 1–14. https://doi.org/10.1007/s00425-003-1105-5

Yang, X., Lu, M., Wang, Y., Wang, Y., Liu, Z., & Chen, S. (2021). Response Mechanism of Plants to Drought Stress. *Horticulturae*, *7*(3), 50. https://doi.org/10.3390/horticulturae7030050

Yang, Y., & Guo, Y. (2018). Unraveling salt stress signaling in plants. *Journal of Integrative Plant Biology*, *60*(9), 796–804. https://doi.org/10.1111/JIPB.12689

Zhang, Z., Liu, Y., Cao, B., Chen, Z., & Xu, K. (2020). The effectiveness of grafting to improve drought tolerance in tomato. *Plant Growth Regulation*, *91*(1), 157–167. https://doi.org/10.1007/s10725-020-00596-2

Zhao, S., Zhang, Q., Liu, M., Zhou, H., Ma, C., & Wang, P. (2021). Regulation of Plant Responses to Salt Stress. *International Journal of Molecular Sciences*, *22*(9), 4609. https://doi.org/10.3390/ijms22094609

CHAPTER I

Grafting Enhances Pepper Water Stress Tolerance by Improving Photosynthesis and Antioxidant Defense Systems

Yaiza Gara Padilla[1], Ramón Gisbert-Mullor[2], Lidia López-Serrano[1], Salvador López-Galarza[2] and Ángeles Calatayud[1]

1 Departamento de Horticultura, Centro de Citricultura y Producción Vegetal, Instituto Valenciano de Investigaciones Agrarias (IVIA), CV-315, Km 10,7, Moncada, 46113 Valencia, Spain.

2 Departamento de Producción Vegetal, Centro Valenciano de Estudios sobre el Riego, Universitat Politècnica de València (UPV), Camí de Vera s/n, 46022 Valencia, Spain.

Antioxidants **2021**, 10, 576.
doi.org/10.3390/antiox10040576

2.1. Abstract

Currently, limited water supply is a major problem in many parts of the world. Grafting peppers onto adequate rootstocks is a sustainable technique used to cope with water scarcity in plants. For 1 month, this work compared grafted peppers by employing two rootstocks (H92 and H90), with different sensitivities to water stress, and ungrafted plants in biomass, photosynthesis, and antioxidant response terms to identify physiological–antioxidant pathways of water stress tolerance. Water stress significantly stunted growth in all the plant types, although tolerant grafted plants (variety grafted onto H92, Var/H92) had higher leaf area and fresh weight values. Var/H92 showed photosynthesis and stomata conductance maintenance, compared to sensitive grafted plants (Var/H90) and ungrafted plants under water stress, linked with greater instantaneous water use efficiency. The antioxidant system was effective in removing reactive oxygen species (ROS) that could damage photosynthesis; a significant positive and negative linear correlation was observed between the rate of CO2 uptake and ascorbic acid (AsA)/total AsA (AsAt) and proline, respectively. Moreover, in Var/H92 under water stress, both higher proline and ascorbate concentration were observed. Consequently, less membrane lipid peroxidation was quantified in Var/H92.

2.2. Introduction

Abiotic stresses pose a huge threat for crops by limiting their growth and development, which eventually leads to poor productivity and low yields [1–3]. One abiotic stress is water limitation, which is considered a major problem because of its high intensity and time span, and because it causes significant crop losses worldwide every year [4–7]. Besides, many crops are now cultivated in areas where climate conditions are not always ideal, and precipitation may periodically go below optimal levels and lead to water scarcity [8].

Many kinds of approaches have been tested to deal with this threat, including agricultural practices focused on irrigation management, but also the introgression of drought resistance traits by molecular breeding. On the one hand, agricultural practices are not always suitable, given the peculiarities of each growing area and the unpredictability of drought periods. On the other hand, molecular and conventional breeding strategies have faced many difficulties when assessing drought tolerance because it is achieved by combining quantitative characters. These, in turn, are controlled by many minor genes with additive effects [2,4–6,9]. Alternatively, Genetically Modified plants have been developed, but these organisms are closely regulated and, like molecular breeding findings, they need to be validated in the field to prove their usefulness [10].

Given all these different approaches, vegetable grafting emerges as a sustainable effective technique, particularly in Solanaceae and Cucurbitaceae species, to overcome water deficit and other abiotic stresses by preventing harmful impacts on shoots [5,11–14]; because rootstock (root) performance stands out over scion (shoot) behavior when stress affects soil [15].

Several studies have confirmed positive physiological traits when employing tolerant rootstocks under water starvation conditions compared to ungrafted, self-grafted or plants grafted on susceptible rootstocks [16–20]. Photosynthesis is one of the first metabolic processes to be affected by drought [21,22]. Grafting has been identified as an effective tool for increasing CO_2 assimilation and intrinsic water use efficiency (A_N/E, WUE) [12,13] when tolerant rootstocks are employed. The increased WUE in tolerant grafted plants, compared to ungrafted plants or using sensitive rootstocks, is often related to a higher net CO_2 assimilation rate and less transpiration, and is joined with stomata regulation [23–25]. However, a drop in WUE has also been observed in two tomato landraces grafted onto commercial tomato rootstocks, which has been associated with a more marked increase in stomatal conductance, linked with minor increases in net photosynthesis [26,27]. These differential WUE patterns indicate that WUE performance can depend not only on the rootstock, but also on the scion used, and mainly on water stress severity [28,29]. Generally with mild and moderate water stress, the decline in A_N can be less severe than the drop in g_s, which causes WUE to increase. These results imply that stomatal limitations are responsible for reducing A_N under drought stress, which is associated with a down-regulated photosynthetic metabolism [22,25,30]. Nevertheless, with severe water stress A_N values drop more than g_s values and, consequently, WUE usually lowers. This situation implies the existence of stomatal, but mainly non-stomatal limitations (inhibition of metabolic processes) connected with photosynthesis damage, which thus affects physiological adaptation to water stress [18,22].

Maintaining photosynthesis under water limitation levels is essential because its suppression could increase excitation energy excess and electron flux to O_2; which would result in photo-oxidative stress by reactive oxygen species (ROS) overproduction **[31,32]**. ROS damage proteins and nucleic acids by causing membrane dysfunction, followed by lipid peroxidation and enzymes inactivation **[33]**. ROS detoxification is most important in any defense mechanism, this is why plants possess a complex antioxidant system that includes non-enzymatic molecules (e.g., ascorbate, proline, phenols, tocopherols **[34]**), but also antioxidant enzymatic components (e.g., catalase, superoxide dismutase, peroxidase, and components of the ascorbate–glutathione cycle **[35]**).

Increasing antioxidant system activities is necessary to enhance plant protection and for reaching tolerance below non optimal water levels **[8]**. In recent years, more attention has been paid to understand the antioxidative system in plants under water deficit **[36]**, but less research has been performed in grafted plants to identify potential antioxidative mechanisms of drought tolerance. These studies have been performed mainly in tomato, watermelon and cucumber grafted plants **[5]**, with very few reports available on antioxidants regulation in pepper-grafted plants **[16,20]**.

Pepper is one of the most important crops grown in the Mediterranean climate, where water scarcity is a relevant constraint **[16]**. Nevertheless, commercial rootstocks are not usually employed in pepper plants as they do not provide enough benefits **[37,38]**.

Our previous studies performed classical breeding assays with pepper accessions (*C. annuum* x *C. annuum*) that resulted in hybrids with more uniform germination, vigor, and growth. These hybrids were tested and screened under water stress conditions based on photosynthetic parameters, leading to identify both tolerant and sensitive hybrids under water stress (unpublished data). Of these, one tolerant rootstock (H92) with higher CO_2 assimilation and one sensitive rootstock (H90) were chosen to test the hypothesis herein posed.

The aim of the present study is to determine whether the maintenance of photosynthesis observed in the tolerant hybrid rootstock (H92) under water stress is associated with the protection of the photosynthetic apparatus, mediated by the activation of the antioxidant system components. For this purpose, several parameters, such as biomass, photosynthetic parameters, ascorbate, proline, catalase activity, and lipid peroxidation were determined in grafted plants using tolerant and sensitive rootstocks and ungrafted plants, grown both in water stress and control conditions.

2.3. Materials and Methods

2.3.1. Plant Material

Two Capsicum annuum hybrids (codes H92 and H90, tolerant and sensitive to water stress, respectively), obtained through traditional breeding by crossing pepper accessions in previous studies **[39–41]**, were selected from a pool of 11 hybrids to be used as rootstocks in the present study. Pepper landrace "Sueca" (Var) was employed as scion and as ungrafted plants. Seeds were sown in March 2020 in 104-hole trays with enriched substrate under greenhouse conditions. Two months after germination, Var was grafted by the tube-grafting method onto the studied hybrid rootstocks. Three weeks after grafting, plants were transplanted in 6-L pots with coconut coir fiber (Cocopeat, Projar Co., Valencia, Spain) in a polyethylene greenhouse at the Valencian Institute of Agriculture Research (IVIA; Valencia, Spain). During the experimental period, temperature ranged from 20 °C to 30 °C, with 40–80% relative humidity. Twelve plants per plant combination were used.

After allowing pepper plants to adapt to the greenhouse for 1 week, they were distributed for two treatments (six plants per treatment). Under the water stress conditions, water irrigation was lowered to 55% of total irrigation under the control conditions, which was calculated based on the weekly crop evapotranspiration (ETc). The number of irrigations was scheduled to maintain drainage between 20% and 30%. Plants were irrigated with Hoagland's no. 2 nutrient solution containing (all in mM): 14 NO_3^-, 1.0 $H_2PO_4^-$, 2.0 SO_4^{2-}, 1.0 NH4$^+$, 6.0 K^+, 4.0 Ca^{2+}, and 2.0 Mg^{2+}. Micronutrients were also provided (all in μM): 15 Fe^{2+}, 10 Mn^{2+}, 5 Zn^{2+}, 30 B^{3+}, 0.75 Cu^{2+}, and 0.6 Mo^{6+}) **[42]**. Electrical conductivity was 1.9 dSm^{-1} and pH was 6.7. To apply the same fertilizer doses in the control and water stress treatments, nutrient solution was applied to both treatments when irrigation to stressed plants was administered. To meet irrigation water requirements, only water was applied to the other irrigation events in the non-stressed treatment.

All of the measurements were taken 10 days after treatment (10 DAT) started, 20 DAT, and 30 DAT. During each measurement event, four measurements (one plant/replication) per plant type and treatment combination were taken. Photosynthetic parameters and physiological analyses were measured on the third or fourth leaves from the apex. For the physiological analysis, leaves were previously frozen with liquid nitrogen and stored at -80 °C. Samples were ground by a mixer mill (MM400, Retsch, Hann, Germany) with liquid nitrogen to prevent melting.

2.3.2. Water Relations

Osmotic potential of leaf sap (Ψ_s, in MPa) and relative water content (RWC) were measured at 30 DAT in leaves. RWC was determined by weighing leaves before and after a 24 h rehydration process performed with distilled water, obtaining the fresh weigh (FW) and turgid weight (TW), respectively. To obtain the dry weight (DW), leaves were dried at 65 °C for 72 h and then weighed. RWC was determined as: RWC (%) = (FW-DW)/(TW-DW) x 100.

The Ψ_s was measured by an osmometer (Digital Osmometer,Wescor, Logan, UT, USA). Leaves were detached, placed inside 1 mL tubes, and quickly frozen at -20 °C. After melting, sap was collected by centrifugation for 1 min at 9.000 rpm in 1.5 mL tubes. Osmolyte content of leaf sap (mmol kg^{-1}) was converted into MPa by the Van't Hoff equation **[18]**.

2.3.3. Gas Exchange Measurements

The CO_2 assimilation rate (A_N, μmol CO_2 m^{-2} s^{-1}), stomatal conductance to water vapor (g_s, mol H_2O m^{-2} s^{-1}), substomatal CO_2 concentration (C_i, μmol CO_2 mol^{-1} air) and transpiration rate (E, mmol H_2O m^{-2} s^{-1}) were measured by a portable LI-COR 6400 infrared gas analyzer (Li-Cor Inc., Lincoln, NE, USA). The A_N/E parameter was calculated as instantaneous WUE. Measurements were taken under saturating light conditions (1000 μmol quanta m^{-2} s^{-1}), 400 μmol CO_2 mol^{-1} of reference CO_2, at 27 °C (27 ± 2 °C) and 75% RH. For each measurement time, data were collected on two consecutive days from 09:00 h to 11:00 h (UT + 01:00 h).

2.3.4. Ascorbate Metabolism

Ascorbic acid (AsA), dehydroascorbate (DHA) and total AsA (AsA_t = AsA + DHA) were determined in parallel according to **[43]** with some variations. First 0.4 g of sample was mixed with 80% (w/v) trichloroacetic acid (TCA) and centrifuged for 5 min at 15,000 x *g* and 4 °C. Then 50 μL of the supernatant were mixed with 150 μL of 0.2M phosphate buffer (pH 7.4) and 50 μL of distilled H_2O_2 for the AsA determination. For AsA_t, 50 μL of the supernatant were mixed with 50 μL of 10 mM dithiothreitol (DTT) and 100 μL of 0.2 M phosphate buffer (pH 7.4), and incubated in a water bath at 42 °C for 15 min. Then 50 μL of 0.5% (w/v) N-ethylmaleimide (NEM) were added and samples were incubated for 1 min at room temperature. Both AsA and AsA_t tubes were mixed with 250 μL of 10% (w/v) TCA, 200 μL of 42% (v/v) H_3PO_4, 200 μL of 4% (w/v) 2,2'-dipyridyl and 100 μL of 3% (w/v) $FeCl_3$, and incubated in a water bath for 40 min at 42 °C. Absorbance was recorded at 525 nm in both cases. The DHA concentration was determined as: AsA_t - AsA.

2.3.5. Catalase Activity

Catalase enzyme activity (EC 1.11.1.6) was measured as in **[44]**, but with modifications: 0.5 g of the sample was mixed with 2.5 mL of 10 mM potassium phosphate buffer (with 1.27 mM EDTA and pH 7) and 2.5% (w/v) polyvinylpolypyrrolidone (PVPP), and was centrifuged for 30 min at 10,000 x *g* and 4 °C. The supernatant was conserved under ice conditions until measurements were taken. To start the reaction, 1960 μL of 50 mM potassium phosphate (pH 7) were mixed with 20 μL of sample and 20 μL of H_2O_2. Reduction of H_2O_2 by catalase activity was monitored spectrophotometrically at 240 nm for 4 min at room temperature. U (μmol/min) g^{-1} FW was calculated using the Lambert–Beer equation with the H_2O_2 extinction coefficient ($\varepsilon = 39.4$ mM^{-1} cm^{-1}).

2.3.6. Lipid Peroxidation Analysis

Lipid peroxidation was determined by the malondialdehyde (MDA) procedure using the thiobarbituric acid (TBA) reaction according to **[45]**, and modified by **[46]**: 0.1 g of sample was mixed with 2 mL of 0.1% (w/v) TCA and centrifuged for 5 min at 10,000 x *g* and 4 °C. Later, 1 mL of supernatant was mixed with 2 mL of reaction buffer (20% TCA + 0.5% TBA) and samples were incubated for 30 min at 95

°C in a water bath. The non-specific background absorbance reading at 600 nm was subtracted from the specific absorbance reading at 532 nm.

2.3.7. Proline Determination

Proline quantification was performed as reported in **[47]** with slight differences: 0.2 g of the sample was mixed with 1.5 mL of 3% sulfosalicylic acid and centrifuged for 5 min at 14,000 rpm and room temperature. Next, 0.6 mL of glacial acetic acid and 0.7 mL of ninhydrin reagent (40 mL of 6 M phosphoric acid mixed with 2.5 g ninhydrin previously blended in 600 mL of glacial acetic acid) were added to 70 µL of the supernatant, and samples were heated for 1 h at 100 °C. Absorbance measures were taken at 520 nm and interpolated on a standard curve performed with proline.

2.3.8. Plant Biomass and Leaf Area Determination

The biomass parameters were measured at the end of the experiment (30 DAT). Leaves and stems were weighed and the number of leaves per plant was recorded. The total leaf area was measured with a LI-3100 Area Meter (Li-COR Inc., Lincoln, NE, USA). Later leaves and stems were exposed to dry heat (for 72 h at 70 °C) in a laboratory oven and dry weight (DW) was recorded.

2.3.9. Statistical Analysis

The results of all the parameters were subjected to a two-way analysis of variance (ANOVA) with Statgraphics Centurion 18 (Statgraphics Technologies Inc., The Plains, VA, USA) after including two factors, namely plant type (PT) and treatment (T), and by considering their interaction. The physiological parameters were analyzed separately for each measurement time (10, 20, and 30 DAT). The means of all the parameters were compared by Fisher's least significance difference (LSD test) at $p < 0.05$. No significant differences were found in the replicates for each measured parameter. The correlation analyses between A_N and AsA/AsA$_t$ and A^N and proline were performed with the abovementioned Statgraphics software and the correlation coefficient (r) was obtained.

2.4. Results

2.4.1. Water Relations

Leaf RWC values (Figure 1A) showed significant interaction between PT and T ($p < 0.01$). Plants under control conditions maintained RWC between 90 and 100% at the end of the experiment without significant differences among them. Water stress reduced significantly the RWC in all PT. Var plants were the most sensitive (77% RWC) followed by Var/H90 (83%) and Var/H92 (86%).

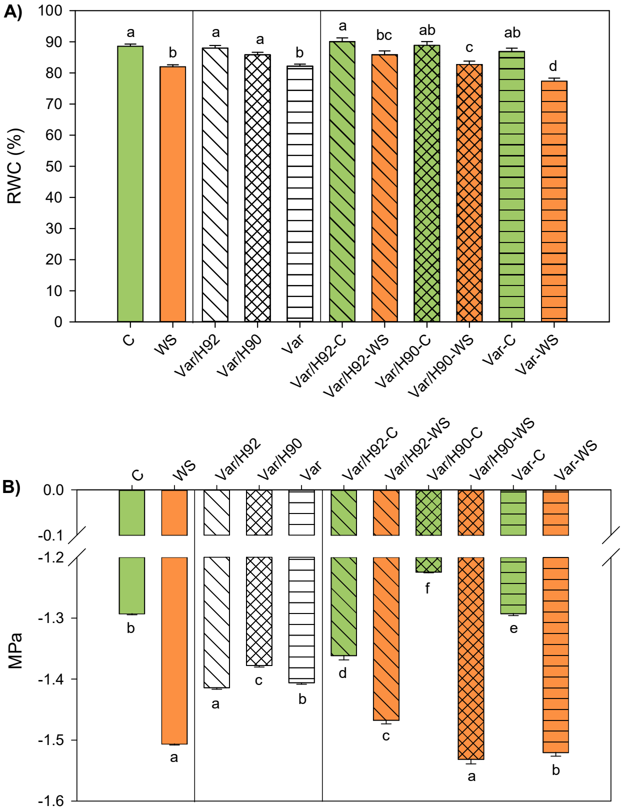

Figure 1. (A) Relative water content (RWC) and **(B)** osmotic potential (Ψ_s) in leaves for the ungrafted plants (Var, variety "Sueca") and Var grafted onto H92 or H90 (Var/H92 and Var/H90, respectively) under the water stress (WS) or control conditions (C). Measurements were taken at 30 DAT (days after treatment). Data are the mean of four replicates and the error bars belong to the standard deviation for each plant type and treatment combination. Different letters indicate significant differences at $p < 0.05$ (least significance difference (LSD) test).

Leaf osmotic potential (Ψ_s) values at 30 DAT are showed in Figure 1B. Significant interaction was observed (PT x T) with $p < 0.01$. Under WS, all PT showed significant lower values compared to control conditions; Var/H90 displayed the largest decrease and Var/H92 the lowest drop in Ψ_s with significant differences among them.

2.4.2. Gas Exchange Measurements

All the measured photosynthetic parameters (except g_s at 30 DAT and A_N/E at 20 DAT) exhibited a statistically significant interaction between treatment (T) and plant type (PT). For this interaction, A_N at 30 DAT, and g_s at 10 DAT presented $p < 0.05$, with $p < 0.01$ for the remaining photosynthetic parameters and DAT. The leaf CO_2 assimilation rate (A_N, Figure 2A) significantly lowered under water stress for the variety grafted onto H90 (Var/H90) and the ungrafted variety (Var) throughout the experiment. The variety grafted onto H92 (Var/H92) only displayed significant differences when comparing the control and water stress plants at the end of the experiment (30 DAT).

Leaf stomatal conductance (g_s, Figure 2B) reduced in all the plant types during the experiment in the WS treatment compared to the control conditions. Only Var/H92 at 20 DAT did not show any significant differences between the control and stressed plants. Instantaneous WUE (A_N/E) did not reveal any significant differences at 20 DAT when the control and WS plants were compared for all the plant types (Figure 2C). At 30 DAT, all the plant types showed significant differences between treatments, Var/H92 increased A_N/E, while Var/H90 and Var diminished A_N/E under the WS conditions. Var also showed significant differences between treatments at the beginning of the experiment (10 DAT).

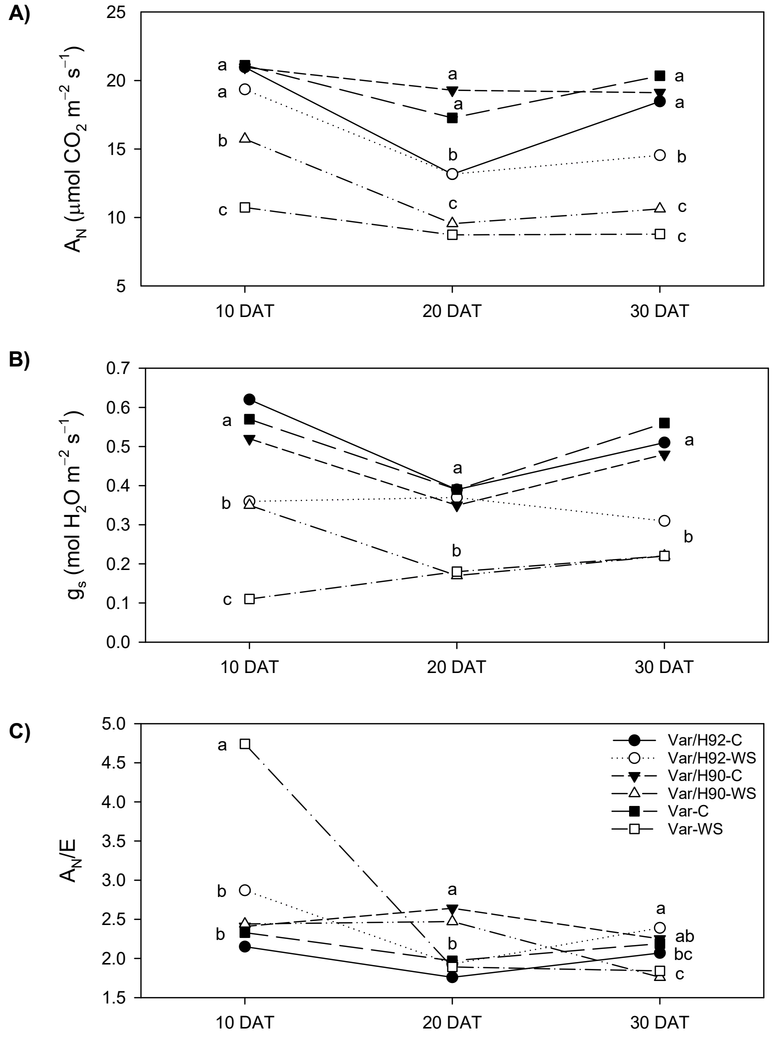

Figure 2. (A) CO_2 assimilation rate (A_N, µmol CO_2 m^{-2} s^{-1}), **(B)** stomatal conductance to water vapor (g_s, µmol H_2O_2 m^{-2} s^{-1}), and (C) instantaneous water use efficiency (A_N/E) in the ungrafted plants (Var, variety "Sueca") and Var grafted onto H92 or H90 (Var/H92 and Var/H90, respectively) under the water stress (WS) or control conditions (C). Measurements were taken at 10, 20, and 30 DAT (days after treatment). Data are the mean value for n = 4 for each plant type and treatment combination. Different letters indicate significant differences at $p < 0.05$ (LSD test) for each measurement time separately.

2.4.3. Ascorbic Acid Metabolism

For both the evaluated parameters, AsA (reduced ascorbate) and the AsA/AsA_t ratio, statistically significant interactions (PT x T) were observed throughout the experiment. AsA presented $p < 0.01$, while AsA/AsA_t showed $p < 0.05$ at 10 DAT and $p < 0.01$ at 20 DAT and 30 DAT.

At 10 DAT, the AsA values under the WS conditions significantly differed from the C conditions for all the plant types (Figure 3A), with higher Var/H92 and Var/H90 values, and lower Var values. AsA/AsAt only differed statistically in Var, with a lower ratio under the WS conditions (Figure 3D).

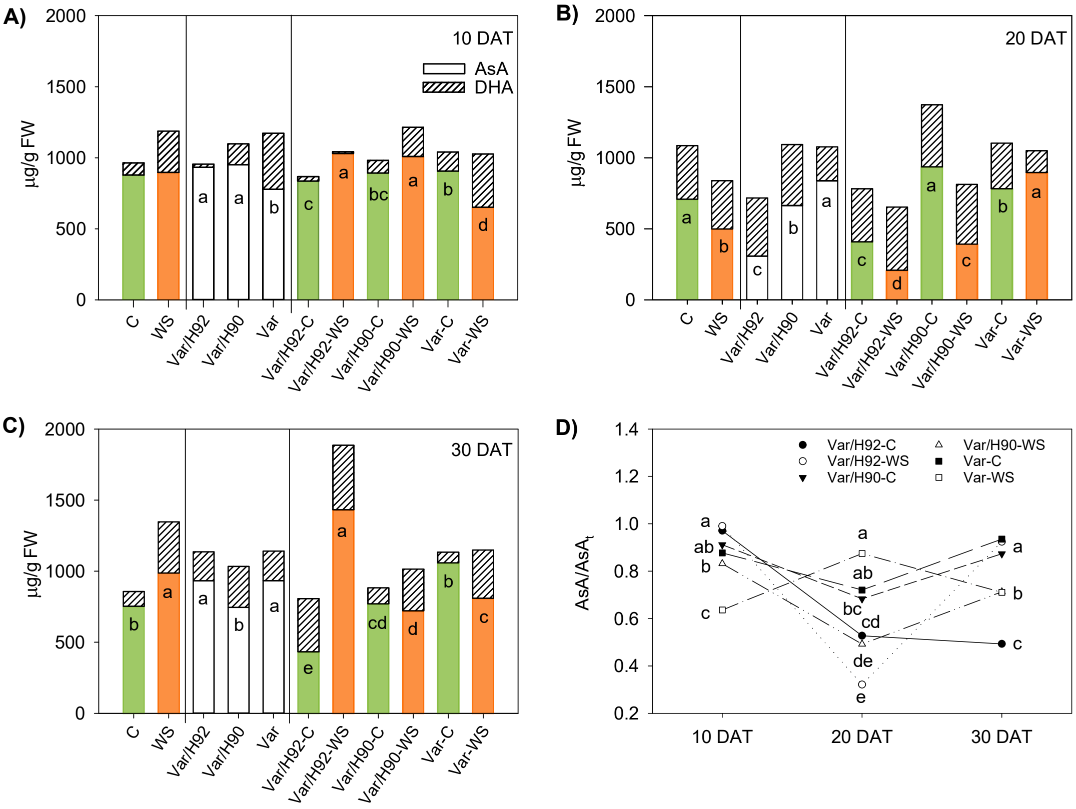

Figure 3. (A–C) Concentration of the different forms of ascorbate (AsA and DHA) in the leaves of the ungrafted plants (Var, variety "Sueca") and Var grafted onto H92 or H90 (Var/H92 and Var/H90) under the water stress (WS) or control conditions (C) at 10, 20, and 30 DAT (days after treatment), respectively. Different letters indicate significant differences at $p < 0.05$ (LSD test) for the AsA parameter. No letters in **3A** indicate no significant differences. **(D)** The AsA/AsA_t ratio for the aforementioned combinations and time measurements. Different letters indicate significant differences at $p < 0.05$ (LSD test) for each measurement time separately. Data are the mean value for n = 4 for each plant type and treatment combination.

At 20 DAT, AsA showed significant differences for each plant type between treatments (Figure 3B). Var/H92 and Var/H90 dropped under water starvation, while Var rose. AsA/AsA_t (Figure 3D) also lowered in Var/H92 and Var/H90 under the WS conditions, while no significant differences appeared between treatments in Var.

Finally, at 30 DAT, AsA and AsA/AsA_t presented significant differences between treatments in Var/H92 and Var, whose values grew and fell, respectively, under WS (Figure 3C,D). Var/H90 only displayed differences for AsA/AsA_t, which lowered under water starvation compared to the control plants (Figure 3D).

2.4.4. Catalase Activity

For this parameter, statistically significant interactions (PT x T) were found during the experiment ($p < 0.01$). All plant types showed significant differences between treatments while testing (Figure 4A–C).

Var/H92 significantly increased catalase activity during the experiment under WS (Figure 4A–C). In contrast, Var/H90 only boosted enzyme activity at the end of the experiment (30 DAT) under the water stress conditions, with reduced activity at 10 DAT and 20 DAT (Figure 4A–C). Lastly, Var obtained higher values when WS was applied at 10 DAT and 30 DAT, but lower ones at 20 DAT (Figure 4A–C).

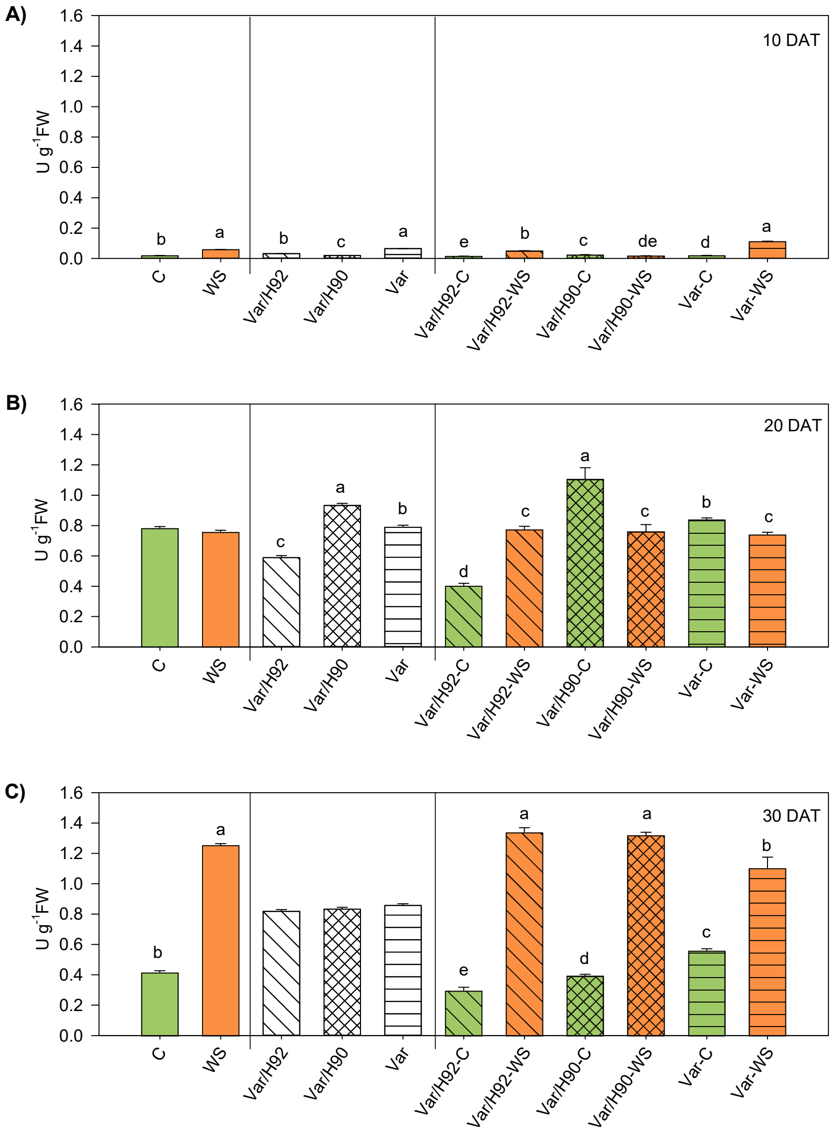

Figure 4. Catalase activity (as H_2O_2 reduction, U g^{-1} FW) in the leaves of the ungrafted plants (Var, variety "Sueca") and Var grafted onto H92 or H90 (Var/H92 and Var/H90) under the water stress (WS) or control conditions (C) at 10 **(A)**, 20 **(B)**, and 30 **(C)** days after treatment (DAT). Different letters indicate significant differences at $p < 0.05$ (LSD test) for each measurement time separately. No letters in **(B)** an **(C)** indicate no significant differences. Data are the mean of four replicates and the error bars belong to the standard deviation for each plant type and treatment combination.

2.4.5. Lipid Peroxidation

Interactions for MDA content ($p < 0.01$) were found between T and PT throughout the experiment. Var/H92 appeared to be undisturbed when subjected to WS all along the experiment. At 10 DAT, only Var showed significant differences and the lowest MDA content for the stress conditions (Figure 5A). At 30 DAT, the MDA content of Var/H90 and Var rose significantly under WS (Figure 5B).

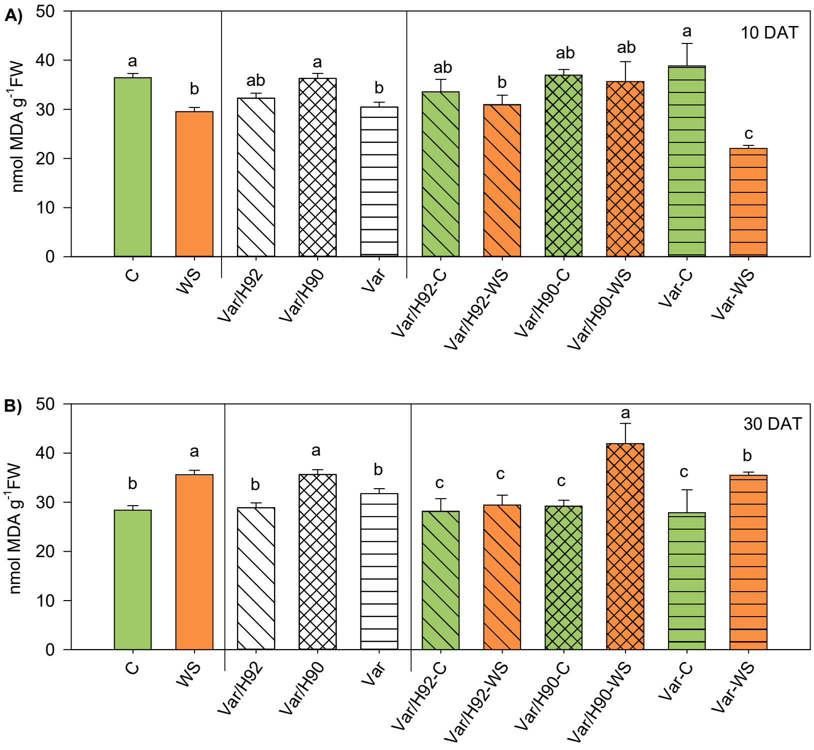

Figure 5. Lipid peroxidation (as malondialdehyde content, MDA) in the leaves of the ungrafted plants (Var, variety "Sueca") and Var grafted onto H92 or H90 (Var/H92 and Var/H90) under the water stress (WS) or control conditions (C) at 10 **(A)** and 30 **(B)** days after treatment (DAT). Different letters indicate significant differences at $p < 0.05$ (LSD test) for each measurement time separately. Data are the mean of four replicates and the error bars belong to the standard deviation for each plant type and treatment combination.

2.4.6. Proline Quantification

Proline content showed interactions ($p < 0.01$) between PT and T while testing. The whole set of plants had a significantly higher proline content when water stress was applied throughout the experiment (Figure 6A–C). Notwithstanding, more marked increases took place for Var/H90 and Var at 10 DAT (Figure 6A), and also for Var/H92 and Var at 30 DAT (Figure 6B,C).

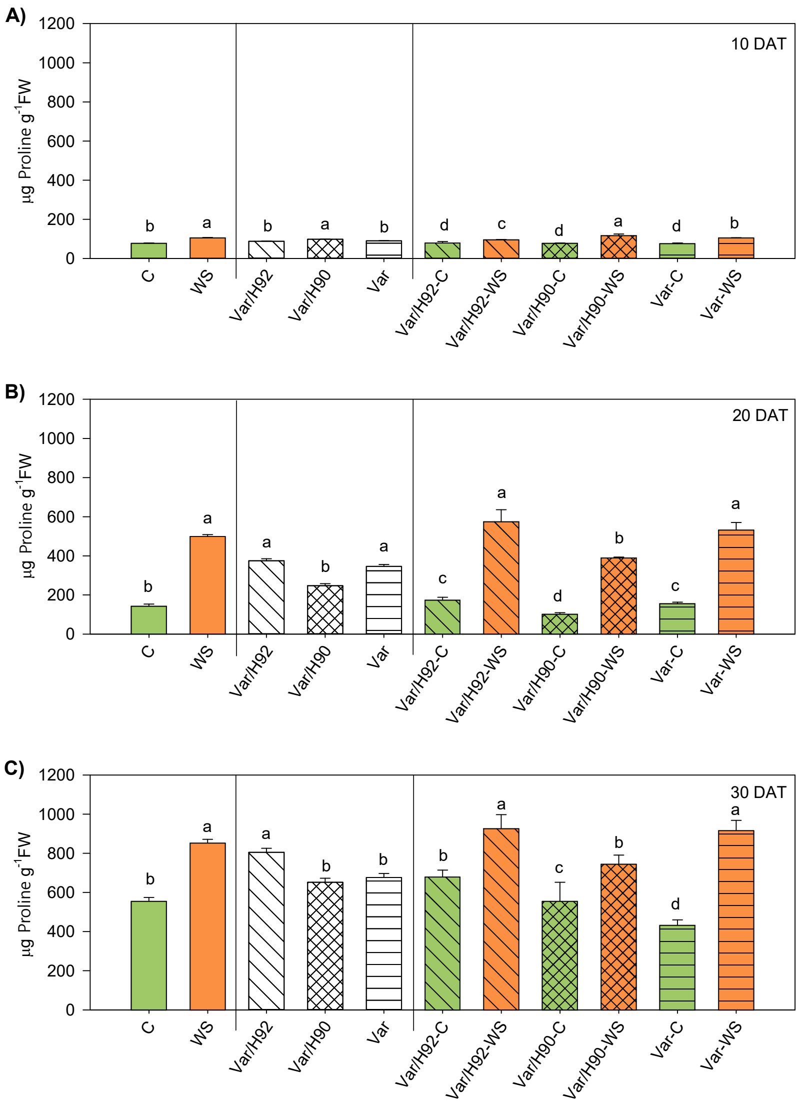

Figure 6. Proline content in the leaves of the ungrafted plants (Var, variety "Sueca") and Var grafted onto H92 or H90 (Var/H92 and Var/H90) under the water stress (WS) or control conditions (C) at 10 **(A)**, 20 **(B)**, and 30 **(C)** days after treatment (DAT). Different letters indicate significant differences at $p < 0.05$ (LSD test) for each measurement time separately. Data are the mean of four replicates and the error bars belong to the standard deviation for each plant type and treatment combination.

2.4.7. Biomass Determination

No significant interactions between T and PT were recorded for the measured biomass parameters (fresh and dry weight, leaf area, and number of leaves) (Table 1).

The fresh weight of the plant aerial parts showed significant differences for both T and PT, with $p < 0.01$ and $p < 0.05$, respectively (Table 1). Aerial fresh weight reduced by 43% in the stressed plants vs. the control ones. The highest FW mean PT value was for Var/H92, followed by Var/H90 and Var (Table 1).

Table 1. Effect of factors treatment (T) and plant type (PT) on the fresh weight (FW) of aerial parts expressed as mean values and ANOVA. Different letters following the mean values indicate significant differences at $p < 0.05$ with the LSD test. An asterisk * indicates significant differences at $p < 0.05$ with the LSD test, while two asterisks ** indicate significant differences at $p \leq 0.01$. (+) Calculated as the square root of the residual sum of squares. df degrees of freedom.

	FW (g plant^{-1})	**DW** (g plant^{-1})	**Leaf area** (cm^2)	**Number of leaves**
Treatment (T)				
C	335.27 a	50.27 a	6095.12 a	161.73 a
WS	191.43 b	28.88 b	3602.26 b	138.94 b
Plant Type (PT)				
Var/H92	277.57 a	41.15 a	5265.11 a	153.42 a
Var/H90	267.59 ab	36.48 a	4469.27 b	143.26 a
Var	244.91 b	41.09 a	4811.69 ab	154.33 a
ANOVA (df)	% Sum of squares			
T (1)	82.36 **	76.94 **	77.12 **	17.89 **
PT (2)	3.04 *	3.41	5.27 *	3.56
T * PT (2)	2.09	1.64	4.45	10.07
Residuals (30)	12.51	18.01	13.16	68.48
Standard Deviation (+)	30.58	5.64	594.64	24.31

For the dry weight of plant aerial parts, only T exhibited significant differences with $p < 0.01$. The plants under water stress had lower dry weight values than those under the control conditions (Table 1).

Leaf area exhibited significant differences for T and PT, with $p < 0.01$ and $p < 0.05$, respectively. Stressed plants reduced leaf area vs. the control plants. For PT, the biggest leaf area was for Var/H92, followed by Var and Var/H90 (Table 1).

Significant differences were recorded only for number of leaves for T ($p < 0.01$). The plants under water stress had a smaller number of leaves than the plants under the control conditions (Table 1).

2.5. Discussion

As expected, leaf RWC decreased under WS in all PT, but the highest reduction was in Var (22%) following Var/H90 (16%) and Var/H92 (12%), which showed the better RWC conservation. According to Hsiao **[48]**, the decrease in RWC might indicate that Var/H90 and Var/H92 suffered a moderate WS while Var was affected by severe WS. The greater RWC in Var/H92 indicated higher capacity of water retention **[49]**. To maintain water uptake under the osmotic stress provoked by water scarcity, plants tend to decrease leaf Ψ_s. In our conditions, under WS, a fall in leaf Ψ_s was observed in all PT, and Ψ_s decrease was not enough to maintain RWC mainly in Var and Var/H90 plants. This drop in Ψ_s could be a consequence of a reduction in the leaf water content (dehydration) and/or due to active solute accumulation. Free proline is one of the most important osmolytes whose accumulation provokes a fall in Ψ_s **[50]**. Nevertheless, in our experimental conditions, the proline role contributing to lower Ψ_s was negligible, with mean values of 0.015 MPa and a 1.1% of contribution to Ψ_s, without ruling out that other components can be implicated in the reduction of osmotic potential **[51]**.

Alterations in water relations under WS affected photosynthesis process in all PT. However, differential behavior was observed among them. After 10 DAT, A_N decreased in Var/H90 and Var, but not in Var/H92, which showed no significant differences with control plants. At the end of the experiment, A_N significantly decreased in all PT respect to their control, despite Var/H92 got the highest values under WS. These results agree with the ones obtained in grafted plants using tolerant rootstocks, which improved photosynthesis under WS (see reviews in **[5,12]**). In our experiment, the decrease in A_N showed linear correlation ($p < 0.0001$) with g_s in all PT at 10, 20 and 30 DAT ($r = 0.886$, 0.742 and 0.937, respectively), which could mean that A_N reduction was mainly due to stomata limitations **[25,30]**.

Grafting has been identified as an effective tool for increasing WUE in water stress situations **[13,27]**. A significant increase in WUE under water stress took place in Var/H92 at the end of experiment compared to the other PTs, which could result from the improvement in CO_2 assimilation rate and the amelioration of stomata performance. In Var and Var/H90 in response to water stress, higher RWC reduction and Ψ_s can be related with stomatal closure and lower WUE, according to **[52]**. This result suggests fewer water requirements in Var/H92 combination, which is interesting because its water use should be lower. Similar results have been obtained by López-Marín et al. **[17]** in pepper plants grafted onto the "Terrano" rootstock, in cucumber grafted onto luffa **[24]** or in mini-watermelon grafted onto *Cucurbita maxima* x *C. moschata* **[25]**. It is noteworthy that our results showed how H92 rootstock could influence the scion-plant response to water stress in photosynthesis, stomatal conductance and WUE terms, which suggests that this plant combination performs better under water stress in gas exchange terms.

Despite the benefits of vegetable grafting on photosynthesis maintenance, and the antioxidant system role under water stress are both widely described in the scientific bibliography **[5,12,53]**, few research has established a link between both plant mechanisms, especially in pepper grafted plants. Indeed, enhanced proline biosynthesis and proline degradation inactivation have been described to be involved in sustaining the electron flow between both photosystems by reducing photoinhibition and protecting the photosynthetic apparatus **[54–56]**. Accumulated proline also acts as a low-molecular-weight cellular antioxidant that protects plants from WS **[57]**. An improvement in proline accumulation under WS has been observed in grafted plants compared to ungrafted plants, and has been demonstrated in pepper **[16]** or tomato plants **[49]**. The increase in proline could be related to its protective role acting as a free radical scavenger, and also protecting thylakoids membrane and photosynthetic activity **[56]**; as it plays an important role in overcoming abiotic stress **[50,56]**. Indeed, a significant negative linear correlation between A_N and proline concentration ($p < 0.01$) was measured at 10 DAT, 20 DAT, and 30 DAT ($r = -0.65$, -0.72, and -0.52, respectively). This implies that while A_N decreased, proline increased with the same trend. This relation constituted a coupled response to water stress by minimizing its impact on plant performance, and it has been observed in pepper grafted plants under salt stress **[58]** and sunflower **[59]**. The highest proline concentration herein observed was detected in Var/H92 and Var under WS from 20 DAT to 30 DAT. Nevertheless, a significantly lower photosynthesis rate was observed for the Var plants under WS, similarly to the Var/H90 plants. This finding indicates that other processes or antioxidant molecules apart from proline can be activated in Var/H92 plants to sustain photosynthesis under stress. A positive linear correlation ($p < 0.01$) was found at 10 and 30 DAT between A_N and AsA/AsA_t ($r = 0.84$ for 10 DAT and $r = 0.55$ for 30 DAT). Indeed, a marked significant increase in AsA and the AsA/AsA_t ratio was measured in Var/H92 at the end of experiment, when WS pressure on plants was higher. Higher AsA levels have been observed in tolerant tomato- and pepper-grafted plants under both salinity and water stress **[8,60,61]**. With stress, AsA is involved in protecting against ROS and photooxidative stress, that linked with sustained photosynthesis provides protection through the zeaxanthin interaction and subsequent thermal dissipation regulation **[62,63]**. No AsA increase was observed in the Var/H90 and Var plants under WS at 30 DAT.

Plants under water stress overproduce ROS, one of them is H_2O_2, which is detoxified by catalase enzyme **[64]**. In our conditions, catalase activity significantly increased in all PT in response to WS, mainly at the end of the experiment. This increase was not consistent with the changes in lipid peroxidation, given that an important increase in lipid peroxidation was measured in Var/H90 and Var, but not in Var/H92. These results can indicate that other types of ROS could be implicated in the MDA production in Var and Var/H90, and the catalase activity was enough to eliminate H_2O_2 in Var/H92.

Water-limiting conditions result in impaired growth, and reduce both the number of leaves and individual leaf size **[65]**. According to our results obtained under water stress, the fresh and dry weights of aerial plant parts, leaf area, and number of leaves decreased in all the plants respect to control conditions. In addition, DW values in aerial part did not show any significant differences between PT, probably because root biomass, which could be significant for total biomass, has not been quantified as the culture characteristics of potted plants with substrate made it difficult to obtain roots.

Nonetheless, FW considering PT factor was higher in the Var/H92 plants, associated with higher water conservation or acquisition capacity. Leaf expansion normally depends on turgor pressure and assimilates supply. Thus, slow CO_2 fixation could limit this process in Var/H90 and Var, and to a lesser extent in Var/H92 **[65]**. Nevertheless, our biomass values reflected the performance of whole plant net photosynthesis throughout the growth period, and not through the effect on the instantaneous net assimilation rate of CO_2 by single-leaf measurements.

2.6. Conclusions

In conclusion, the higher maintained rate of CO_2 uptake observed using the tolerant rootstock H92 seems to involve minor oxidative stress, as observed by lesser membrane lipid peroxidation related to higher proline content and AsA concentration. Nonetheless, to validate these results, rootstock H92 should be tested under long-term experiments to evaluate its effects in terms of productivity and biomass under water stress.

2.7. References

1. Sah, S.K.; Reddy, K.R.; Li, J. Abscisic acid and abiotic stress tolerance in crop plants. *Front. Plant Sci.* **2016**, 7, 571. doi.org/10.3389/fpls.2016.00571
2. Athar, H.R.; Ashraf, M. Strategies for Crop Improvement Against Salinity and Drought Stress: An Overview. In *Salinity and Water Stress*; Springer: Dordrecht, The Netherlands, 2009; pp. 1–16. ISBN 978-1-4020-9065-3.
3. Wang, W.; Vinocur, B.; Altman, A. Plant responses to drought, salinity and extreme temperatures: Towards genetic engineering for stress tolerance. *Planta* **2003**, 218, 1–14. doi.org/10.1007/s00425-003-1105-5
4. Ashraf, M. Inducing drought tolerance in plants: Recent advances. *Biotechnol. Adv.* **2010**, 28, 169–183. doi.org/10.1016/j.biotechadv.2009.11.005
5. Kumar, P.; Rouphael, Y.; Cardarelli, M.; Colla, G. Vegetable Grafting as a Tool to Improve Drought Resistance and Water Use Efficiency. Front. Plant Sci. **2017**, 8, 1130. doi.org/10.3389/fpls.2017.01130
6. Mastrangelo, A.M.; Mazzucotelli, E.; Guerra, D.; De Vita, P.; Cattivelli, L. Improvement of drought resistance in crops: From conventional breeding to genomic selection. In *Crop Stress and Its Management: Perspectives and Strategies*; Springer: Dordrecht, The Netherlands, 2012; pp. 225–259. ISBN 9789400722200.
7. Farooq, M.; Wahid, A.; Kobayashi, N.; Fujita, D.; Basra, S.M.A. Plant drought stress: Effects, mechanisms and management. *Agron. Sustain. Dev.* **2009**, 29, 185–212. doi.org/10.1051/agro:2008021
8. Sánchez-Rodríguez, E.; del Rubio-Wilhelmi, M.; Blasco, B.; Leyva, R.; Romero, L.; Ruiz, J.M. Antioxidant response resides in the shoot in reciprocal grafts of drought-tolerant and drought-sensitive cultivars in tomato under water stress. *Plant Sci.* **2012**, 188-189, 89–96. doi.org/10.1016/j.plantsci.2011.12.019
9. Bourzac, K. Water: The flow of technology. *Nature* **2013**, 501, S4–S6. doi.org/10.1038/501S4a
10. Eisenstein, M. Plant breeding: Discovery in a dry spell. *Nature* **2013**, 501. doi.org/10.1038/501S7a
11. Rouphael, Y.; Kyriacou, M.C.; Colla, G. Vegetable Grafting: A Toolbox for Securing Yield Stability under Multiple Stress Conditions. *Front. Plant Sci.* **2018**, 8, 2255. doi.org/10.3389/fpls.2017.02255
12. Schwarz, D.; Rouphael, Y.; Colla, G.; Venema, J.H. Grafting as a tool to improve tolerance of vegetables to abiotic stresses: Thermal stress, water stress and organic pollutants. *Sci. Hortic.* **2010**, 127, 162–171. doi.org/10.1016/j.scienta.2010.09.016
13. Fullana-Pericàs, M.; Conesa, M.; Pérez-Alfocea, F.; Galmés, J. The influence of grafting on crops' photosynthetic performance. *Plant Sci.* **2020**, 295, 110250. doi.org/10.1016/j.plantsci.2019.110250
14. Goldschmidt, E.E. Plant grafting: New mechanisms, evolutionary implications. *Front. Plant Sci.* **2014**, 5, 727. doi.org/10.3389/fpls.2014.00727
15. Koevoets, I.T.; Venema, J.H.; Elzenga, J.T.M.; Testerink, C. Roots withstanding their environment: Exploiting root system architecture responses to abiotic stress to improve crop tolerance. *Front. Plant Sci.* **2016**, 7, 1335. doi.org/10.3389/fpls.2016.01335
16. Penella, C.; Nebauer, S.G.; Bautista, A.S.; López-Galarza, S.; Calatayud, Á. Rootstock alleviates PEG-induced water stress in grafted pepper seedlings: Physiological responses. *J. Plant Physiol.* **2014**, 171, 842–851. doi.org/10.1016/j.jplph.2014.01.013
17. López-Marín, J.; Gálvez, A.; del Amor, F.M.; Albacete, A.; Fernández, J.A.; Egea-Gilabert, C.; Pérez-Alfocea, F. Selecting vegetative/generative/dwarfing rootstocks for improving fruit yield and quality in water stressed sweet peppers. *Sci. Hortic.* **2017**, 214, 9–17. doi.org/10.1016/j.scienta.2016.11.012
18. López-Serrano, L.; Canet-Sanchis, G.; Vuletin Selak, G.; Penella, C.; San Bautista, A.; López-Galarza, S.; Calatayud, Á. Pepper Rootstock and Scion Physiological Responses Under Drought Stress. Front. *Plant Sci.* **2019**, 10, 38. doi.org/10.3389/fpls.2019.00038
19. Zhang, Z.; Cao, B.; Gao, S.; Xu, K. Grafting improves tomato drought tolerance through enhancing photosynthetic capacity and reducing ROS accumulation. *Protoplasma* **2019**, 256, 1013–1024. doi.org/10.1007/s00709-019-01357-3
20. Penella, C.; Nebauer, S.G.; López-Galarza, S.; Quiñones, A.; San Bautista, A.; Calatayud, Á. Grafting pepper onto tolerant rootstocks: An environmental-friendly technique overcome water and salt stress. *Sci. Hortic.* **2017**, 226, 33–41. doi.org/10.1016/j.scienta.2017.08.020
21. Chaves, M.M. Effects of Water Deficits on Carbon Assimilation. *J. Exp. Bot.* **1991**, 42, 1–16. doi.org/10.1093/jxb/42.1.1
22. Flexas, J.; Bota, J.; Cifre, J.; Escalona, J.; Galmes, J.; Gulias, J.; Lefi, E.-K.; Martinez-Canellas, S.; Moreno, M.; Ribas-Carbo, M.; et al. Understanding down-regulation of photosynthesis under water stress: Future prospects and searching for physiological tools for irrigation management. *Ann. Appl. Biol.* **2004**, 144, 273–283. doi.org/10.1111/j.1744-7348.2004.tb00343.x
23. Khah, E.M.; Katsoulas, N.; Tchamitchian, M.; Kittas, C. Effect of grafting on eggplant leaf gas exchanges under Mediterranean greenhouse conditions. *Int. J. Plant Prod.* **2011**, 5, 121–134. doi.org/10.22069/ijpp.2012.726
24. Liu, S.; Li, H.; Lv, X.; Ahammed, G.J.; Xia, X.; Zhou, J.; Shi, K.; Asami, T.; Yu, J.; Zhou, Y. Grafting cucumber onto luffa improves drought tolerance by increasing ABA biosynthesis and sensitivity. *Sci. Rep.* **2016**, 6, 1–14. doi.org/10.1038/srep20212
25. Rouphael, Y.; Cardarelli, M.; Colla, G.; Rea, E. Yield, mineral composition, water relations, and water use efficiency of grafted mini-watermelon plants under deficit irrigation. *HortScience* **2008**, 43, 730–736. doi.org/10.21273/HORTSCI.43.3.730

26. Fullana-Pericàs, M.; Ponce, J.; Conesa, M.; Juan, A.; Ribas-Carbó, M.; Galmés, J. Changes in yield, growth and photosynthesis in a drought-adapted Mediterranean tomato landrace (*Solanum lycopersicum* 'Ramellet') when grafted onto commercial rootstocks and *Solanum pimpinellifolium*. *Sci. Hortic.* **2018**, 233, 70–77. doi.org/10.1016/j.scienta.2018.01.045

27. Fullana-Pericàs, M.; Conesa, M.À.; Ribas-Carbó, M.; Galmés, J. The Use of a Tomato Landrace as Rootstock Improves the Response of Commercial Tomato under Water Deficit Conditions. *Agronomy* **2020**, 10, 748. doi.org/10.3390/agronomy10050748

28. Galmés, J.; Conesa, M.À.; Ochogavía, J.M.; Perdomo, J.A.; Francis, D.M.; Ribas-Carbó, M.; Savé, R.; Flexas, J.; Medrano, H.; Cifre, J. Physiological and morphological adaptations in relation to water use efficiency in Mediterranean accessions of *Solanum lycopersicum*. *Plant. Cell Environ.* **2011**, 34, 245–260. doi.org/10.1111/j.1365-3040.2010.02239.x

29. Galmés, J.; Ochogavía, J.M.; Gago, J.; Roldán, E.J.; Cifre, J.; Conesa, M.À. Leaf responses to drought stress in Mediterranean accessions of *Solanum lycopersicum*: Anatomical adaptations in relation to gas exchange parameters. *Plant. Cell Environ.* **2013**, 36, 920–935. doi.org/10.1111/pce.12022

30. Delfine, S.; Tognetti, R.; Loreto, F.; Alvino, A. Physiological and growth responses to water stress in field-grown bell pepper (*Capsicum annuum* L.). *J. Hortic. Sci. Biotechnol.* **2002**, 77, 697–704. doi.org/10.1080/14620316.2002.11511559

31. Zhou, Y.; Zhou, J.; Huang, L.; Ding, X.; Shi, K.; Yu, J. Grafting of *Cucumis sativus* onto *Cucurbita ficifolia* leads to improved plant growth, increased light utilization and reduced accumulation of reactive oxygen species in chilled plants. *J. Plant Res.* **2009**, 122, 529–540. doi.org/10.1007/s10265-009-0247-3

32. Pinheiro, H.A.; DaMatta, F.M.; Chaves, A.R.M.; Fontes, E.P.B.; Loureiro, M.E. Drought tolerance in relation to protection against oxidative stress in clones of *Coffea canephora* subjected to long-term drought. *Plant Sci.* **2004**, 167, 1307–1314. doi.org/10.1016/j.plantsci.2004.06.027

33. Blokhina, O. Antioxidants, Oxidative Damage and Oxygen Deprivation Stress: A Review. *Ann. Bot.* **2003**, 91, 179–194. doi.org/10.1093/aob/mcf118

34. Apel, K.; Hirt, H. Reactive Oxygen Species: Metabolism, Oxidative Stress, and Signal Transduction. *Annu. Rev. Plant Biol.* **2004**, 55, 373–399. doi.org/10.1146/annurev.arplant.55.031903.141701

35. Foyer, C.H.; Halliwell, B. The presence of glutathione and glutathione reductase in chloroplasts: A proposed role in ascorbic acid metabolism. *Planta* **1976**, 133, 21–25. doi.org/10.1007/BF00386001

36. Kaur, K.; Kaur, N.; Gupta, A.K.; Singh, I. Exploration of the antioxidative defense system to characterize chickpea genotypes showing differential response towards water deficit conditions. *Plant Growth Regul.* **2013**, 70, 49–60. doi.org/10.1007/s10725-012-9777-0

37. Lee, J.M.; Kubota, C.; Tsao, S.J.; Bie, Z.; Echevarria, P.H.; Morra, L.; Oda, M. Current status of vegetable grafting: Diffusion, grafting techniques, automation. *Sci. Hortic.* **2010**, 127, 93–105. doi.org/10.1016/j.scienta.2010.08.003

38. Kyriacou, M.C.; Rouphael, Y.; Colla, G.; Zrenner, R.; Schwarz, D. Vegetable grafting: The implications of a growing agronomic imperative for vegetable fruit quality and nutritive value. *Front. Plant Sci.* **2017**, 8, 741. doi.org/10.3389/fpls.2017.00741

39. Penella, C.; Nebauer, S.G.; Lopéz-Galarza, S.; San Bautista, A.; Gorbe, E.; Calatayud, A. Evaluation for salt stress tolerance of pepper genotypes to be used as rootstocks. *J. Food Agric. Environ.* **2013**, 11, 1101–1107.

40. Penella, C.; Nebauer, S.G.; López-Galarza, S.; San Bautista, A.; Rodríguez-Burruezo, A.; Calatayud, A. Evaluation of some pepper genotypes as rootstocks in water stress conditions. *Hortic. Sci.* **2014**, 41, 192–200. doi.org/10.17221/163/2013-HORTSCI

41. López-Serrano, L.; Penella, C.; San-Bautista, A.; López-Galarza, S.; Calatayud, A. Physiological changes of pepper accessions in response to salinity and water stress. *Span. J. Agric. Res.* **2017**, 15, 1–10. doi.org/10.5424/sjar/2017153-11147

42. Maynard, D.N.; Hochmuth, G.J. *Knott's Handbook for Vegetable Growers*, 5th ed.; JohnWiley & Sons Inc: Hoboken, NJ, USA, 2006; ISBN 9780470121474.

43. Kampfenkel, K.; Vanmontagu, M.; Inze, D. Extraction and Determination of Ascorbate and Dehydroascorbate from Plant Tissue. *Anal. Biochem.* **1995**, 225, 165–167. doi.org/10.1006/abio.1995.1127

44. Martinez-Cuenca, M.-R.; Primo-Capella, A.; Quiñones, A.; Bermejo, A.; Forner-Giner, M.A. Rootstock influence on iron uptake responses in Citrus leaves and their regulation under the Fe paradox effect. *PeerJ* **2017**, 5, e3553. doi.org/10.7717/peerj.3553

45. Heath, R.L.; Packer, L. Photoperoxidation in isolated chloroplasts. *Arch. Biochem. Biophys.* **1968**, 125, 189–198. doi.org/10.1016/0003-9861(68)90654-1

46. Dhindsa, R.S.; Plumb-Dhindsa, P.; Thorpe, T.A. Leaf Senescence: Correlated with Increased Levels of Membrane Permeability and Lipid Peroxidation, and Decreased Levels of Superoxide Dismutase and Catalase. *J. Exp. Bot.* **1981**, 32, 93–101. doi.org/10.1093/jxb/32.1.93

47. Bates, L.S.; Waldren, R.P.; Teare, I.D. Rapid determination of free proline for water-stress studies. *Plant Soil* **1973**, 39, 205–207. doi.org/10.1007/BF00018060

48. Hsiao, T.C. Plant Responses to Water Stress. *Annu. Rev. Plant Physiol.* **1973**, 24, 519–570. doi.org/10.1146/annurev.pp.24.060173.002511

49. Yao, X.; Yang, R.; Zhao, F.; Wang, S.; Li, C.; Zhao, W. An analysis of physiological index of differences in drought tolerance of tomato rootstock seedlings. *J. Plant Biol.* **2016**, 59, 311–321. doi.org/10.1007/s12374-016-0071-y

50. Gill, S.S.; Tuteja, N. Reactive oxygen species and antioxidant machinery in abiotic stress tolerance in crop plants. *Plant Physiol. Biochem.* **2010**, 48, 909–930. doi.org/10.1016/j.plaphy.2010.08.016

51. Navarro, J.M.; Garrido, C.; Martínez, V.; Carvajal, M. Water relations and xylem transport of nutrients in pepper plants grown under two different salts stress regimes. *Plant Growth Regul.* **2003**, 41, 237–245. doi.org/10.1023/B:GROW.0000007515.72795.c5

52. Gaion, L.A.; Monteiro, C.C.; Cruz, F.J.R.; Rossatto, D.R.; López-Díaz, I.; Carrera, E.; Lima, J.E.; Peres, L.E.P.; Carvalho, R.F. Constitutive gibberellin response in grafted tomato modulates root-to-shoot signaling under drought stress. *J. Plant Physiol.* **2018**, 221, 11–21. doi.org/10.1016/j.jplph.2017.12.003

53. Rivero, R.M.; Ruiz, J.; Romero, L. Role of grafting in horticultural plants under stress conditions. *J. Food Agric. Environ.* **2003**, 1, 70–74.

54. Szabados, L.; Savouré, A. Proline: A multifunctional amino acid. *Trends Plant Sci.* **2010**, 15, 89–97. doi.org/10.1016/j.tplants.2009.11.009

55. Ashraf, M.; Foolad, M.R. Roles of glycine betaine and proline in improving plant abiotic stress resistance. *Environ. Exp. Bot.* **2007**, 59, 206–216. doi.org/10.1016/j.envexpbot.2005.12.006

56. Reddy, A.R.; Chaitanya, K.V.; Vivekanandan, M. Drought-induced responses of photosynthesis and antioxidant metabolism in higher plants. *J. Plant Physiol.* **2004**, 161, 1189–1202. doi.org/10.1016/j.jplph.2004.01.013

57. Anjum, S.A.; Farooq, M.; Xie, X.-Y.; Liu, X.-J.; Ijaz, M.F. Antioxidant defense system and proline accumulation enables hot pepper to perform better under drought. *Sci. Hortic.* **2012**, 140, 66–73. doi.org/10.1016/j.scienta.2012.03.028

58. Penella, C.; Nebauer, S.G.; Quiñones, A.; San Bautista, A.; López-Galarza, S.; Calatayud, A. Some rootstocks improve pepper tolerance to mild salinity through ionic regulation. *Plant Sci.* **2015**, 230, 12–22. doi.org/10.1016/j.plantsci.2014.10.007

59. Ghobadi, M.; Taherabadi, S.; Ghobadi, M.E.; Mohammadi, G.R.; Jalali-Honarmand, S. Antioxidant capacity, photosynthetic characteristics and water relations of sunflower (*Helianthus annuus* L.) cultivars in response to drought stress. *Ind. Crops Prod.* **2013**, 50, 29–38. doi.org/10.1016/j.indcrop.2013.07.009

60. He, Y.; Zhu, Z.; Yang, J.; Ni, X.; Zhu, B. Grafting increases the salt tolerance of tomato by improvement of photosynthesis and enhancement of antioxidant enzymes activity. *Environ. Exp. Bot.* **2009**, 66, 270–278. doi.org/10.1016/j.envexpbot.2009.02.007

61. Penella, C.; Landi, M.; Guidi, L.; Nebauer, S.G.; Pellegrini, E.; Bautista, A.S.; Remorini, D.; Nali, C.; López-Galarza, S.; Calatayud, Salt-tolerant rootstock increases yield of pepper under salinity through maintenance of photosynthetic performance and sinks strength. J. *Plant Physiol.* **2016**, 193, 1–11. doi.org/10.1016/j.jplph.2016.02.007

62. Foyer, C.H. Redox homeostasis: Opening up ascorbate transport. *Nat. Plants* **2015**, 1, 1–2. doi.org/10.1038/nplants.2014.12

63. Horton, P.; Ruban, A. Molecular design of the photosystem II light-harvesting antenna: Photosynthesis and photoprotection. *J. Exp. Bot.* **2004**, 56, 365–373. doi.org/10.1093/jxb/eri023

64. Hasanuzzaman, M.; Bhuyan, M.H.M.B.; Zulfiqar, F.; Raza, A.; Mohsin, S.M.; Mahmud, J.A.; Fujita, M.; Fotopoulos, V. Reactive Oxygen Species and Antioxidant Defense in Plants under Abiotic Stress: Revisiting the Crucial Role of a Universal Defense Regulator. *Antioxidants* **2020**, 9, 681. doi.org/10.3390/antiox9080681

65. Fahad, S.; Bajwa, A.; Anjum, S.A. Crop Production under Drought and Heat Stress: Plant Responses and Management Options. *Front. Plant Sci.* **2017**, 8, 1147. doi.org/10.3389/fpls.2017.01147

CHAPTER II

New insights into short-term water stress tolerance through transcriptomic and metabolomic analyses on pepper roots

Yaiza Gara Padilla[1], Ramón Gisbert-Mullor[2], Eduardo Bueso[3], Leilei Zhang[4], Javier Forment[3], Luigi Lucini[4], Salvador López-Galarza[2] and Ángeles Calatayud[1]

1 Departamento de Horticultura, Centro de Citricultura y Producción Vegetal, Instituto Valenciano de Investigaciones Agrarias (IVIA), CV-315, Km 10,7, Moncada, 46113 Valencia, Spain.

2 Departamento de Producción Vegetal, Centro Valenciano de Estudios sobre el Riego, Universitat Politècnica de València (UPV), Camí de Vera s/n, 46022 Valencia, Spain.

3 Instituto de Biología Molecular y Celular de Plantas (IBMCP), Universitat Politècnica de València-C.S.I.C., Valencia, Spain.

4 Department for Sustainable Food Process, Research Centre for Nutrigenomics and Proteomics, Università Cattolica del Sacro Cuore, 29122 Piacenza, Italy.

Plant Science **2023**, 333, 111731.
doi.org/10.1016/J.PLANTSCI.2023.111731

3.1. Abstract

In the current climate change scenario, water stress is a serious threat to limit crop growth and yields. It is necessary to develop tolerant plants that cope with water stress and, for this purpose, tolerance mechanisms should be studied. NIBER® is a proven water stress- and salt-tolerant pepper hybrid rootstock (Gisbert-Mullor et al., 2020; López-Serrano et al., 2020), but tolerance mechanisms remain unclear. In this experiment, NIBER® and A10 (a sensitive pepper accession (Penella et al., 2014)) response to short-term water stress at 5 h and 24 h was studied in terms of gene expression and metabolites content in roots. GO terms and gene expression analyses evidenced constitutive differences in the transcriptomic profile of NIBER® and A10, associated with detoxification systems of reactive oxygen species (ROS). Upon water stress, transcription factors like *DREB*s and *MYC* are upregulated and the levels of auxins, abscisic acid and jasmonic acid are increased in NIBER®. NIBER® tolerance mechanisms involve an increase in osmoprotectant sugars (*i.e.*, trehalose, raffinose) and in antioxidants (spermidine), but lower contents of oxidized glutathione compared to A10, which indicates less oxidative damage. Moreover, the gene expression for aquaporins and chaperones is enhanced. These results show the main NIBER® strategies to overcome water stress.

3.2. Introduction

Crop yields are being limited by climate change *via* many direct and not so direct effectors, such as droughts, fluctuating rainfall, floods and the dissemination of diseases and pests to new locations (FAO, 2022). Of abiotic stressors, water stress is one of the main factors to affect vegetative growth, successful reproduction and, in the end, plant survival (Arbona et al., 2013). According to the FAO (2022), water stress has become the severest natural hazard for the population all over the world in the last 40 years, but has also to the increased affected land. Hence, the need to act and improve plant tolerance to the severe water stress, that takes part in the global warming scenario (Ozturk et al., 2021).

Water stress is a multidimensional stress that provokes several diverse plant responses by affecting physiological, morphological and molecular levels (Salehi-Lisar and Bakhshayeshan-Agdam, 2016). Among others, water stress impacts major physiological processes, such as photosynthesis, respiration and stomatal movement, which lead to plant growth restrictions (Yang et al., 2021). In addition, leaf size becomes smaller, which appear cutinized, have a thicker surface and premature induced senescence. This comes with decreased total biomass, which extends to lower plant development (Anjum et al., 2011). The onset of all plant processes affected by water stress involves multiple signals, which are transmitted through signaling pathways to drive the expression of water stress-responsive genes such as transcription factors, heat shock proteins, dehydrins, aquaporins, late embryogenesis abundant proteins, among others (Kaur and Asthir, 2017).

To overcome water stress effects, plants have developed different strategies that range from improving water uptake in roots to minimizing transpiration water loss on leaves (Farooq et al., 2009). Roots are the first organs to sense the presence of water stress and preserving root growth is an indicator of water stress tolerance (Mia et al., 2020). Furthermore, there are more specific mechanisms available to cope with water stress, for instance synthesis of organic compatible solutes and antioxidants and antioxidant enzymes, hormonal regulation, leaf rolling, epicuticular wax accumulation and a higher root/shoot ratio (Athar and Ashraf, 2009; Seleiman et al., 2021). These strategies are part of a reprogramming process at the whole plant level, triggered by gene expression changes that enable plants to survive under water stress conditions. Thus understanding plants modulation at the ‘omics’ level when they face water stress could help to achieve water stress-resilient plants.

The increasing number of molecular biotechnology studies is helping to untangle the molecular mechanisms involved in water stress response by gene expression approaches (You et al., 2019). Plant gene expression strategies have been conducted to study water stress tolerance on several crops, such as maize (Song et al., 2017; Zenda et al., 2019; Zheng et al., 2020; Li et al., 2021) sorghum (Fracasso et al., 2016; Varoquaux et al., 2019; Zhang et al., 2019; Kumari et al., 2021) and soybean (Xu et al., 2018; Tamang et al., 2021; Wang et al., 2022). With Solanaceae plants, the transcriptomics approach has been mostly applied to tobacco and tomato as model plants. In tobacco, Yang et al. (2017) showed upregulation of genes related to alpha-linolenic acid, arginine and proline metabolisms when stress was applied, while Khan et al. (2019) observed an enhanced expression for the genes involved in plant hormone signal transduction, starch and sucrose metabolism, and arginine and proline metabolism in the water stress-tolerant tobacco cultivar. In tomato, Lee et al. (2018) reported the down-regulation of the gene expression for the signaling pathways associated with abiotic stress responses, lignification, cell wall development and hormones in the sensitive genotype. In tomato, Iovieno et al. (2016) observed the down-regulation of the genes implicated in photosynthesis, cell proliferation and cell cycle after two water stress cycles and final rewatering. However, there have been very few studies to date on pepper plants transcriptomic responses under water stress. Borràs et al. (2021) described the complex role of *NAC* transcription factors when facing water stress on *Capsicum annuum*, because one *NAC* gene usually responds to the different stress agents that participate in multiple signaling pathways as a positive or negative regulator. Kang et al. (2020) provided the transcriptomic data of pepper exposed to different abiotic stresses to be used as information in other studies, including the expression pattern of top differentially expressed genes (DEGs) (*i.e.*, *ABI2*, *PP2CA*, *GLP3*) and representative stress-related GO terms.

In the present study, a transcriptomic experiment was performed to broaden knowledge about water stress response mechanisms on *Capsicum annuum* and understand how tolerance could be achieved through the analysis of gene expression changes. To do so, we used two *C. annuum* genotypes: NIBER® and A10. A10 is a pepper accession that has been characterized as sensitive to water stress (Penella et al., 2014). NIBER® is a hybrid pepper rootstock that has been proven tolerant to water stress (Gisbert-Mullor et al., 2020) and salt (López-Serrano et al., 2020). It was obtained and has been patented by our research team. NIBER® was able to confer the grafted variety tolerance to deficit irrigation when used as a rootstock (Gisbert-Mullor et al., 2020) due to sustained photosynthesis and lesser reduction in both biomass and fruit yield. However, there is no information to date on the short-term molecular mechanisms involved in NIBER® performance under water stress conditions that lead to its resilience. The transcriptome profile of NIBER® roots under water stress conditions could provide useful information about the hybrid's prompt responses that constitute master regulators in tolerance achievement. For this purpose, changes in gene expression and primary and secondary metabolisms were studied for NIBER® and A10 in a short-term water stress experiment.

3.3. Material and methods

3.3.1. Plant material and greenhouse conditions

Two *C. annuum* genotypes were selected as plant material according to previous studies: A10 (Habanero accession) for being sensitive to water stress (Penella et al., 2014) and the NIBER® hybrid for being tolerant to water stress conditions (Gisbert-Mullor et al., 2020). Seeds were sown in 104-hole seed trays filled with enriched substrate for germination. When plants had 6–8 real leaves, roots were cleaned to remove substrate and plants were placed in 2 L polyethylene pots covered with aluminium to block light. Pots were filled with a nutrient solution containing (mmol L^{-1}): 12.3 NO^{3-}, 1.02 H_2PO_4, 2.45 SO_4^{2-}, 3.24 Cl^-, 5.05 K^+, 0.6 NH_4^+, 4.23 Ca^{2+}, 2.2 Na^+, 2.55 Mg^{2+}; micronutrients (μmol L^{-1}): 15.8 Fe^{2+}, 10.3 Mn^{2+}, 4.2 Zn^{2+}, 43.5 B^+ and 2.14 Cu^{2+} with artificial aeration. The electrical conductivity (EC) and pH of this nutrient solution were 2.15 dS m^{-1} and 6.6, respectively. The nutrient solution was refilled daily to compensate for absorption. After 14 days of plant acclimation, water stress was induced by replacing nutrient solution with 4% polyethylene glycol (PEG) nutrient solution in the pots corresponding to the water stress treatment, whereas the pots for the control conditions were refilled with nutrient solution. Osmotic potential was -0.55 MPa for the water stress pots (4% PEG) and -0.05 MPa for the control pots (0% PEG), measured by a vapor osmometer (Digital osmometer, Wescor, Logan, USA). The layout design was completely randomized with 20 plants per genotype and treatment. During the culture and experiment, plants were grown in a greenhouse at the Polytechnic University of Valencia (UPV, Valencia, Spain) under natural light conditions (800–1000 μmol m^{-2} s^{-1}), with a temperature range of 21–25 ºC and 50–70% relative humidity (RH). Root samples were taken immediately before stress induction (T0), 5 h after stress induction (T1) and 24 h after stress induction (T2), and were immediately frozen in liquid nitrogen to be stored at -80 ºC.

3.3.2. RNA sequencing and data processing for the gene expression analysis

Four root samples per treatment, genotype and sampling time (T0, T1 and T2) were ground in liquid nitrogen with a mortar for RNA extraction. Total RNA was extracted using the Rneasy Plant Mini Kit (Qiagen, Germantown, MD, USA) following the manufacturer's instructions and treated to remove the remaining genomic DNA with the Rnase-Free Dnase Set (Qiagen, USA). RNA concentration and purity were measured by a NanoDrop ND-1000 spectrophotometer (ThermoFisher Scientific, Waltham, MA, USA) to select the samples with a proper RNA concentration and appropriate A260/A280 and A260/A230 absorption ratios. Twenty-million 100 nt reads (pair ends) per library were sequenced by DNBseq™ eukaryotic transcriptome resequencing by BGI Genomics (Cambridge, MA, USA). Three replicates were used per treatment and genotype. After adapter removal and the quality trimming of raw reads with cutadapt (Martin, 2011), a quality analysis of clean reads was done with FastQC (Andrews, 2010). Clean read pairs longer than 20 nt were then mapped to the *Capsicum annuum* genome assembly ASM51225v2 from EnsemblPlants (Capsicum_annuum - Ensembl Genomes (n.d.); Yates et al., 2022) using HISAT2 (Kim et al., 2019) with default parameters. The number of read counts mapped to one and only one of the annotated genes of the genome (uniquely mapped) were obtained with htseq-count (Anders et al., 2015). A differential expression analysis was done with DESeq2 (Love et al., 2014). The differential expression analysis was performed between both genotypes under the control conditions (NIBER®/A10) to study the constitutive differences. Another differential expression analysis was performed between water stress and the control conditions in each genotype to study the water stress-associated differences.

3.3.3. Gene Ontology analysis and functional annotation of DEGs

The Protein Analysis Through Evolutionary Relationships (PANTHER) classification system (Mi et al., 2019) was employed to perform a Statistical Overrepresentation Test against the *Capsicum annuum* genome to find statistically over- and under-represented GO terms among the differentially expressed genes. GO terms belong to the Gene Ontology Consortium and include the "Biological Process", "Molecular Function" and "Cellular Component" categories. GO terms are included in a hierarchical classification, where an *Ancestor* term occupies a higher position and is followed by *Child* terms. The functional annotation of DEGs was performed with the UniProt Consortium (Bateman et al., 2021) and The Arabidopsis Information Resource (TAIR) (Berardini et al., 2015).

3.3.4. Metabolites quantification

Four root samples per treatment and genotype were used for metabolites quantification.

For hormones quantification, ground root samples from sampling times T1 and T2 (5 h and 24 h) were suspended in 80% methanol and 1% acetic acid containing internal standards and mixed by shaking for 1 h at 4 °C. The extract was kept at -20 ºC overnight and then centrifuged. The supernatant was dried in a vacuum evaporator. The dry residue was dissolved in 1% acetic acid and passed through an Oasis HLB (reverse-phase) column, as described in (Seo et al., 2011). The dried eluate was dissolved in 5% acetonitrile-1% acetic acid, and hormones were separated using an autosampler and reverse phase UPHL chromatography (2.6 μm Accucore RP-MS column, 100-mm length 2.1-mm inner diameter; ThermoFisher Scientific) with a 5–50% acetonitrile gradient containing 0.05% acetic acid at 400 μL min-1 for 21 min. Hormones were analyzed in a Q-Exactive mass spectrometer (Orbitrap detector; ThermoFisher Scientific) by targeted Selected Ion Monitoring (SIM). The concentrations of hormones in extracts were determined using embedded calibration curves and XCALIBUR 2.2 SP1 build 48 and TRACEFINDER. The internal standards for the quantification of each different plant hormones were the deuterium-labeled hormones.

For the other metabolites, the samples from sampling time T2 (24 h) were lyophilized in a vacuum evaporator (Labconco Corporation, Kansas City, USA) and extracted by the ultrasound method in a mixture of 20% (v/v) methanol + 2 mM EDTA and acidified with 1% (v/v) formic acid at a ratio of 1:40. Extracts were than centrifuged at 8000 g for 10 min at 4 ºC (Eppendorf 5810R, Hamburg, Germany). Next, supernatants were collected, syringe-filtered (0.22 μm pore size), and transferred to vials for the subsequent analysis.

The trehalose, galactinol, raffinose, and stachyose oligosaccharides quantification on root samples was performed by a high-performance anion exchange chromatography coupled with a pulsed amperometric detection approach (HPAEC-PAD). Equipment consisted in a Dionex ICS- 5000 + (Thermo Fisher Scientific, Waltham, USA), containing an electrochemical cell with a gold working electrode combined with a pH-Ag/ AgCl reference electrode as the detection system. The separation method applied for the

HPAEC-PAD analysis was optimized for all four oligosaccharides through a Dionex CarboPac PA200 column (3 x 250 mm) coupled to a guard column (3 x 50 mm) as the stationary phase (both purchased from Thermo Scientific), which confers high-resolution separation of monosaccharides and linear oligosaccharides (Rocchetti et al., 2022). Specifically for trehalose and raffinose, the mobile phase was a binary solvent system composed by H_2O milliQ (eluent A) and 30 mM NaOH (eluent B). An isocratic separation method was applied with a total run time of 30 min, the flow rate was adjusted at 0.4 mL/min and the temperatures for both the column and detector compartments were set at 300 ºC. Second, the stachyose oligosaccharide was separated using a binary solvent system composed of H_2O milliQ (eluent A) and 25 mM NaOH (eluent B). An isocratic separation method was applied with a total run time of 30 min, the flow rate was adjusted at 0.25 mL/min and the temperatures for both the column and detector compartments were set at 30 ºC. Finally, the galactinol oligosaccharide was separated by a binary solvent system comprising H_2O milliQ (eluent A) and 500 mM NaOH (eluent B). An isocratic separation method was applied with a total run time of 30 min, the flow rate was adjusted at 0.4 mL/min and the temperatures for both the column and detector compartments were set at 30 ºC. Quantification of oligosaccharides was achieved according to the standard curves of trehalose dihydrate, galactinol dihydrate, raffinose pentahydrate (Merck KGaA, Darmstadt, Germany), and stachyose hydrate (Cayman Chemical, Michigan, USA), designed with five concentration points.

The target analysis for polyamines and oxidized glutathione was performed using a Q Exactive Focus Hybrid Ultra-High Pressure Liquid Chromatography Quadrupole-Orbitrap Mass Spectrometer (UHPLC-HRMS; Thermo Scientific) coupled to a Vanquish UHPLC pump and equipped with a heated electrospray ionization-II probe (Thermo Scientific; (Rocchetti et al., 2021)). Chromatographic separation was based on a water-acetonitrile (LC-MS grade, Sigma-Aldrich) gradient elution (6–94% acetonitrile in 35 min), employing 0.1% formic acid as the phase modifier and an Agilent Zorbax Eclipse Plus C18 column (50 × 2.1 mm, 1.8 µm) at a flow rate of 200 µL/min and an injection volume of 6 µL.

Data acquisition was performed in the data-dependent (Top N = 3) MS/MS mode, in a full scan mass resolution of 17500 at *m/z* 200 using positive ionization for spermine, spermidine and putrescine, and negative ionization for oxidized L-glutathione. Identification was performed with an AGC target value of 1 × 105, a maximum injection time of 100 ms and an isolation window of 1.0 *m/z*. The Top N ions were fragmented employing a stepped Normalized Collisional Energy (*i.e.*, 10, 20, 40 eV). The heated electrospray ionization parameters were the following: sheath gas flow 40 arbitrary units, auxiliary gas flow 20 arbitrary units, spray voltage 3.5 kV, capillary temperature 320 °C. Specifically, quantification of polyamines and glutathione was performed with the standard calibration curves of spermine, spermidine, putrescine and oxidized L-glutathione (Merck KGaA, Darmstadt, Germany).

3.3.5. Statistical analysis

As mentioned in 2.1., the layout design of the experiment was completely randomised and included 20 plants per treatment and genotype combination. The samples for metabolites quantification (2.4.) were tested by a one-way ANalysis Of VAriance (ANOVA) with Statgraphics Centurion XVIII (Statgraphics Technologies, Inc., The Plains, Virginia, USA). Fisher's Least Significant Difference test (LSD) was performed at $p < 0.05$. For oligosaccharides, data were expressed as the difference between the oligosaccharide content under the water stress and control conditions for each genotype.

3.4. Results

3.4.1. Gene expression constitutive differences between NIBER® and A10 roots

The transcriptome comparison between genotypes NIBER® and A10 under the control conditions showed 1597 up-regulated and 1430 down-regulated DEGs. The Gene Ontology Overrepresentation test on DEGs was performed for Biological Process (Fig. 1), Molecular Function (Fig. S1) and Cellular Component (Fig. S2).

The GO test on Biological Process showed statistically over-represented categories (Fig. 1) for NIBER® *versus* A10, classified by an increasing Gene Ratio to include “response to stimulus” and “response to chemical” with more genes (222 and 115 genes, respectively) and a lower p-value ($p < 0.01$), followed by “response to oxidative stress”, “response to inorganic substance” and “photosynthesis, light harvesting in photosystem I” with the highest Gene Ratio and fewer genes (32, 25 and 10 genes, respectively). All the over-represented categories were statistically significant ($p < 0.05$).

The GO test on Biological Process also showed statistically under-represented categories (Fig. 1) for NIBER® *versus* A10, classified by a lowering Gene Ratio, including “primary metabolic process”, “protein metabolic process”, “nitrogen compound metabolic process” and “macromolecule metabolic process” with more genes (393, 198, 326 and 288 genes, respectively), followed by “nucleobase-containing compound metabolic process”, “RNA metabolic process”, “gene expression” and “RNA processing” with the lowest Gene Ratio and fewer genes (82, 39, 46 and 16 genes, respectively). All the under-represented categories were statistically significant ($p < 0.01$).

The GO test on Molecular Function (Fig. S1) showed statistically over- and under-represented categories with $p < 0.01$. The over-represented categories included “oxidoreductase activity” (188 genes), “heme binding” (68 genes) and “tetrapyrrole binding” (79 genes), classified by an increasing Gene Ratio. The under-represented categories included “RNA binding” (32 genes) and “cysteine-type peptidase activity” (7 genes), classified by a lowering Gene Ratio.

The GO test on Cellular Component (Fig. S2) showed statistically over- and under-represented categories with $p < 0.05$. The over-represented categories included “extracellular region” (69 genes), “chloroplast thylakoid” (25 genes) and “photosystem I” (16 genes), classified by an increasing Gene Ratio. The under-represented categories included “intracellular organelle” (396 genes), “protein-containing complex” (113 genes), “intracellular non-membrane-bounded organelle” (43 genes) and “ribonucleoprotein complex” (13 genes), classified by a lowering Gene Ratio.

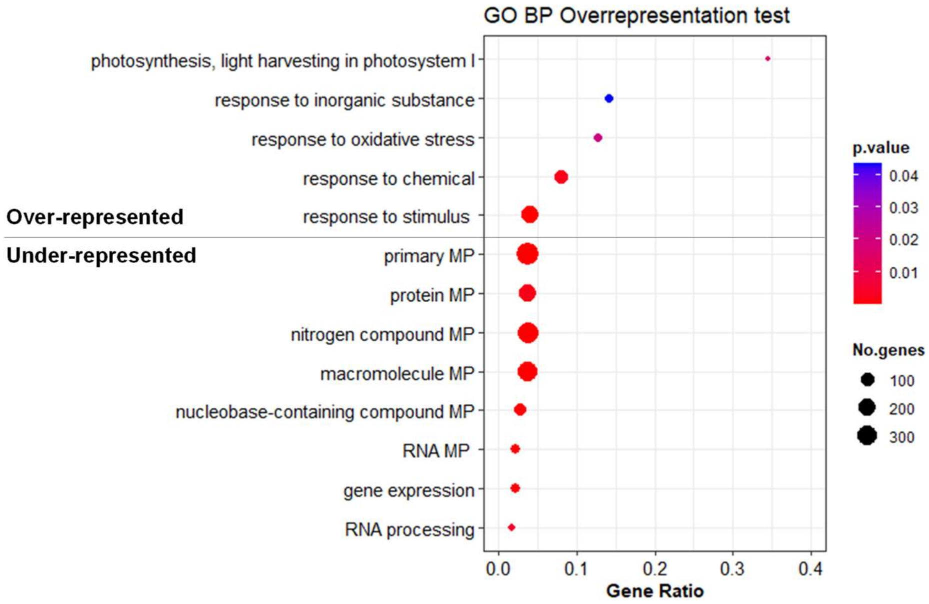

Fig. 1. GO Overrepresentation test for the DEGs resulting from NIBER® in relation to A10 comparison under the control conditions showing the statistically over-and under-represented categories for Biological Process. The Gene Ratio is the percentage of DEGs in relation to the total number of genes associated with the GO term in the Capsicum annuum genome. MP means Metabolic Process.

The DEGs under the control conditions suggested constitutive differences in the stress-related processes between NIBER® and A10 (Table S1). NIBER® is a hybrid pepper rootstock with the feature that overcomes water stress situations (Gisbert-Mullor et al., 2020). However, the gene signaling network involved in its tolerance remains unclear.

In this analysis we were able to find DEGs related to **osmoprotection**, specifically for trehalose synthesis. Genes such as *TPS1* (trehalose-phosphate synthase 1, T459_35236, (Fichtner et al., 2020)) and *TPP* (trehalose 6-phosphate phosphatase, T459_05222, (Vogel et al., 1998)) were down-regulated in NIBER®. In addition, sugar transporters like *SWEET* (T459_11884) and other genes related to glucose transport (T459_19291 and T459_08278; Dyson et al., 2014) were also down-regulated in NIBER®. This up-regulation of the sugar-related genes in A10 is in accordance with the *SS1* (soluble starch synthase 1, T459_09622) down-regulation in A10.

Regarding **hormones**, auxin synthesis and signaling are key for explaining differences in plant growth. We confirmed that two important genes, *i.e.*, *TIR1* (auxin receptor, T459_15901; Dharmasiri et al., 2005) and *ILR1* (an amidohydrolase that releases active indole-3-acetic acid from conjugates, T459_25791; Bartel and Fink, 1995) were up-regulated in NIBER®. Similarly, four genes encoding putative indole-3-acetic acid-amido synthetase *GH3* (T459_33260, T459_24904, T459_20103, T459_33259; Staswick et al., 2005) to, thus favour indole-3-acetic acid (IAA) inactivation, were down-regulated in NIBER®. Abscisic acid (ABA) is also crucial for overcoming abiotic stress. *NCED1* (a main enzyme involved in ABA synthesis, T459_20461; Schwartz et al., 2001) was up-regulated in NIBER®, but *PYL1*, one of the receptors of this hormone, was down-regulated (T459_17022; Hao et al., 2011). Finally, we found five putative *ACO* genes (1-aminocyclopropane-1-carboxylate oxidase, T459_24052, T459_14026, T459_07834, T459_22421, T459_07844) coding for a key enzyme in the ethylene synthesis (Jafari et al., 2013) and down-regulated in NIBER®.

Photosynthetic performance is one of the main processes with a differential response to stress when comparing tolerant and sensitive plants (Padilla et al., 2021). In agreement with this, we were able to find that *APO1* (T459_00386) was up-regulated in NIBER®, a protein required for the accumulation of Photosystem I and NADH dehydrogenase complexes in the chloroplast (Amann et al., 2004). *CYP89A9* (T459_09773) is a cytochrome involved in the formation of major chlorophyll catabolites during leaf senescence in Arabidopsis (Christ et al., 2013) and was up-regulated in NIBER®, together with *TGD1*, a permease involved in lipid transfer from the endoplasmic reticulum (ER) to the chloroplast (T459_33667; Xu et al., 2003). However, we found down-regulated genes coding for Photosystem II subunit P-2 (T459_26094; Kochhar et al., 1996), two subunits of the cytochrome b6-f complex (T459_23921 and T459_31770; Munekage et al., 2001), two genes coding for protein gradient regulation (*PGR5*, T459_04004 and *PGRL1A*, T459_07652; DalCorso et al., 2008), subunit K of the Photosystem I reaction center (T459_03540; Varotto et al., 2002) and a protein required for anchoring the FNR flavoenzyme to the thylakoid membrane (T459_21968; Jurić et al., 2009).

We also observed changes in important genes for **membrane homeostasis**. Calcium is one of the most significant cations for stress signaling (Edel et al., 2017). Two calcineurin-binding proteins, *i.e.*, *CBL7* and *CBL9* (T459_08611, T459_16980; Batistič et al., 2009), and *CIPK20* (T459_05348, a CBL-interacting protein kinase) were up-regulated in NIBER®. Nevertheless, calcium-dependent protein kinase *CPK4* (T459_17188; Zhu et al., 2007) and calmodulin *CML11* (T459_07898; McCormack and Braam, 2003) were down-regulated. Other down-regulated genes in this rootstock were aquaporin *PIP2–4* (T459_26048; Quigley et al., 2001) and vacuolar proton pump *AVP1* (T459_34590; Gaxiola et al., 2001).

Reactive oxygen species (ROS) formation is also a consequence of stress exposure in plants (Gill and Tuteja, 2010). Constitutive differences in **detoxification systems** are key for overcoming future stress (Landi et al., 2017). Based on this, the analysis showed the DEGs involved in the scavenging of these toxic compounds. Formate and malate dehydrogenase (T459_06869, T459_31834) are enzymes involved in coping with oxidative stress, which were up-regulated in NIBER® (Heyno et al., 2014; Thomas et al., 2016). *HIRD11* was also up-regulated in NIBER® and is a dehydrin that can reduce ROS formation (T459_15197; Hara et al., 2013). In contrast, we found up-regulation in A10 of two glutathione transferases, enzymes that are involved in detoxification (T459_27445, T459_31012), and *RbohB* was up-regulated, which is one of the main isozymes responsible for superoxide anion production (T459_34097; Sagi and Fluhr, 2006). It has been demonstrated that polyamines function in stress tolerance by modulating ROS homeostasis (Alcázar et al., 2006). We found that *PAO4* was up-regulated in NIBER®, which is a flavoprotein that catalyzes the oxidative conversion of spermine into spermidine in *Arabidopsis thaliana* (T459_24048; Kamada-Nobusada et al., 2008), as well as *PUT4*, a polyamine uptake transporter (T459_06454; Mulangi et al., 2012). Finally, T459_03483, coding for spermidine synthase, was up-regulated in the sensitive rootstock (Hanzawa et al., 2002).

Chaperones are crucial in preventing protein denaturation (Wang et al., 2004). This analysis displayed *BAG4* as being up-regulated in NIBER® (T459_16041; Yan et al., 2003), but also the downregulation of one isoform of a heat shock protein (HSP) 90 co-chaperone (T459_26371; D'Alessandro et al., 2015) and the small HSP (sHSP) 18.2KDa (T459_25314).

3.4.2. Water stress impact on gene expression and associated GO categories

The comparison of the response under water stress (simulated by PEG addition) and the control conditions 5 h after treatment (T1) resulted in 437 specific DEGs for A10, 168 DEGs in NIBER®, and 222 DEGs were shared by both genotypes (Fig. 2A, Table S1). However, at 24 h after treatment (T2), the number of DEGs of NIBER® and A10 dropped in relation to T1, and only 68 DEGs were specific for A10, 108 DEGs for NIBER®, and 22 DEGs in both genotypes (Fig. 2B, Table S1).

The GO Overrepresentation test for the aforementioned DEGs showed that several BP categories were shared by both genotypes involved in the response to water stress at T1 and T2 (Fig. 3), but there were also some categories only present in either A10 (Fig. 4) or NIBER® (Fig. 5).

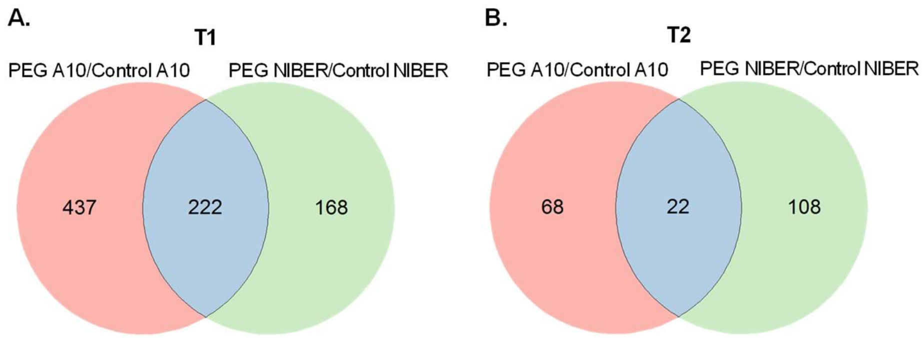

Fig. 2. Venn diagram for the DEGs under water stress/control conditions at T1 **(A)** and T2 **(B)** for each genotype. Red depicts the DEGs exclusive for A10, green the DEGs specific for NIBER® and blue the DEGs shared by both genotypes.

The BP shared by both genotypes (Fig. 3) belong to the *ancestor* categories "response to stimulus", "biological regulation", "primary metabolism", "other metabolic processes" and "CC organization or biogenesis" (the last one for T2). For "response to stimulus" the *child* terms were "response to oxygen-containing compound", "oxidant detoxification" and "auxin-activated signaling pathway" for T1 and T2; "hydrotropism" and "response to abscisic acid" for T1; "response to oxidative stress" and "response to auxin" for T2. The "Biological regulation" *child* terms were "cellular ion and lipid homeostasis" and "regulation of stomatal closure" for T1, and "negative regulation of proteolysis" for T2. "Cellular component organization or biogenesis", which appeared at T2, was associated with cell wall. The "Primary metabolism" at T1 included the carbohydrate metabolic processes for trehalose biosynthesis, L-arabinose and galacturonan; the lipid processes for steroids, fatty acids and lipid oxidation; several protein processes related to ubiquitination, retrograde transport and catabolism of misfolded proteins. However, the primary metabolism in T2 could be summarized in lipid catabolism. Lastly, "other metabolic processes" comprised glutathione biosynthesis and hydrogen peroxide catabolism for T1 and T2; the polyamine biosynthesis and photosynthesis-related processes involving the electron transport chain and PSI for T1.

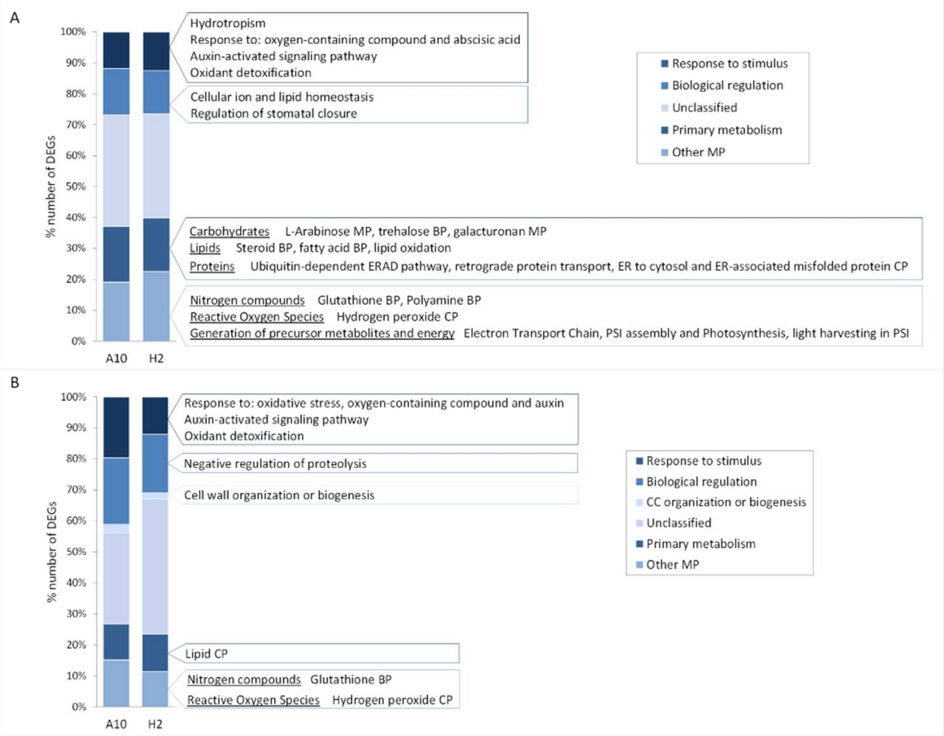

Fig. 3. *Ancestor* and *Child* BP categories shared by NIBER® and A10 for the water stress/control conditions at T1 **(A)** and T2 **(B)**. MP is Metabolic Process, BP is Biological Process, ER is Endoplasmic Reticulum, CP is Catabolic Process, PSI is Photosystem I and CC is Cellular Component.

The BP exclusive for A10 under water stress in relation to control conditions (Fig. 4) belong to the *ancestor* categories "response to stimulus", "transport", "biological regulation", "primary metabolism", "organelle organization" (for T1) and "other metabolic processes" (for T2). The "Response to stimulus" *child* terms were "abscisic acid-activated signaling pathway" for T1 and T2; "response to water deprivation" for T1; response to abscisic acid and ethylene, and "ethylene-activated signaling pathway" for T2. The "Transport" associated categories were "phospholipid translocation" and vesicle-mediated transport including docking, budding from membrane and fusion for T1; "protein import into nucleus" for T2. "Organelle organization", which appeared at T1, was related to the vacuole and chloroplast accumulation and avoidance movements. For "biological regulation" the *child* terms were auxin homeostasis and catabolism, "regulation of brassinosteroid-mediated signaling pathway" and "protein stabilization" for T1; "regulation of protein dephosphorylation" for T2. The "Primary metabolism" at T1 comprised the carbohydrate biosynthesis processes for glucose, sucrose and cell wall cellulose; lipid processes, such as abscisic and jasmonic acid metabolism and phospholipid biosynthesis; protein metabolism, with some catabolism processes involving ubiquitination and/or the proteasome, but also proline catabolism and arabinogalactan protein metabolism. At T2, the "primary metabolism" included galacturonan metabolism for carbohydrates and protein autophosphorylation, but also a common process at T1 and T2, which was the "SFC-dependent proteasomal ubiquitin-dependent protein catabolic process". Lastly, "other metabolic processes" was present at T2 and was associated with oxoacid metabolism.

The specific BP in NIBER® under water stress in relation to the control conditions (Fig. 5) belong to the *ancestor* categories "response to stimulus", "transport", "biological regulation", "protein folding", "primary metabolism” and “other metabolic processes”. The “Response to stimulus” *child* terms were “response to hydrogen peroxide” for T1 and T2, response to salicylic acid and unfolded protein for T1, response to osmotic stress and ER-unfolded protein for T2. “Transport” at T1 was related to “plasmodesmata-mediated intercellular transport”, while T2 included lipid, water and vesicle-mediated transport. For “biological regulation” the *child* terms were “brassinosteroid homeostasis”, “regulation of jasmonic acid-mediated signaling pathway”, “regulation of proteolysis” and “regulation of photosynthesis, light reaction” for T1; hormone biosynthesis and regulation of hormone levels and cellular response to hypoxia for T2. “Protein folding” can be summarized in “chaperone cofactor-dependent protein folding” for T1 and T2. The “Primary metabolism” common process at T1 and T2 was cellulose catabolism; at T1 there were lipid processes, such as “fatty acid alpha-oxidation” and biosynthesis of brassinosteroid and unsaturated fatty acid. At T2 there was hemicellulose metabolism for carbohydrate-related processes and ubiquitination and dephosphorylation for protein-related processes. Lastly, “other metabolic processes” was associated with polyamine biosynthesis, which was a common *child* term at T1 and T2, but could be identified as spermine and spermidine biosynthesis at T1.

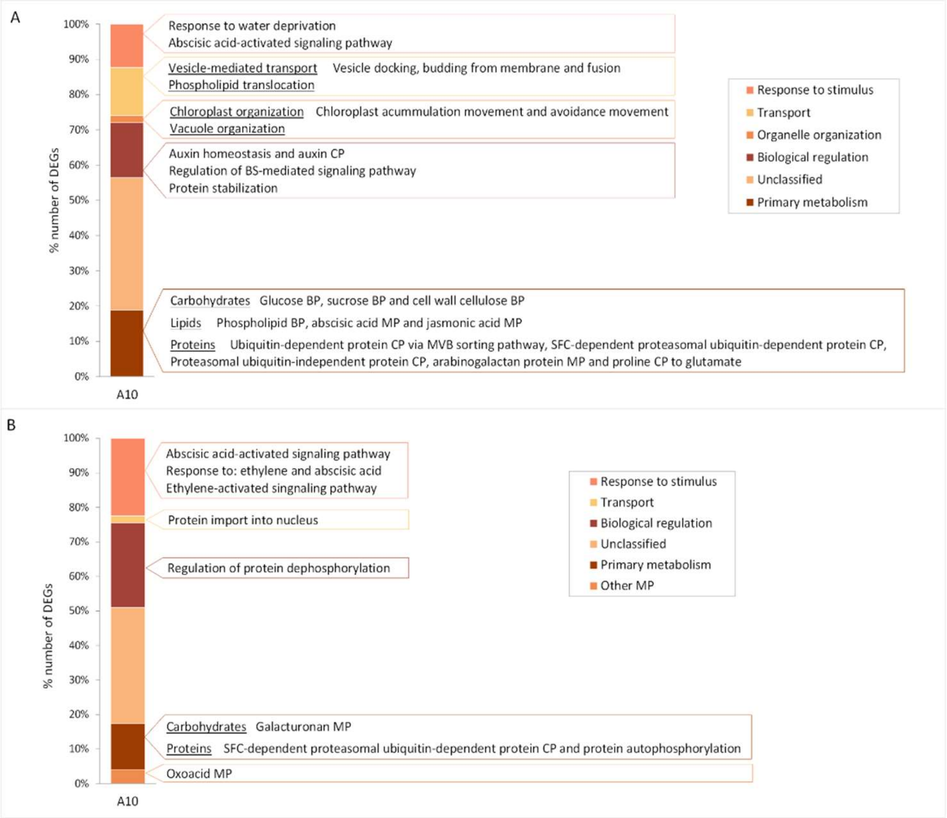

Fig. 4. *Ancestor* and *Child* BP specific categories in A10 for the water stress/control conditions at T1 **(A)** and T2 **(B)**. CP is Catabolic Process, BS is brassinosteroid, BP is Biological Process, MP is Metabolic Process and MVB is multivesicular body.

Fig. 5. *Ancestor* and *Child* BP categories found only in NIBER® for the water stress/control conditions at T1 **(A)** and T2 **(B)**. CP is Catabolic Process, BP is Biological Process, ER is Endoplasmic Reticulum and MP is Metabolic Process.

3.4.3. Outstanding genes with differential expression under water stress

NIBER® and A10 have a common response after water stress, but also a specific one for each genotype (Table S1). Both genotypes respond to water stress with the deregulation of the genes involved in **carbohydrates** synthesis. For instance, the genes involved in raffinose synthesis (Nishizawa et al., 2008) were upregulated as T459_10139 in NIBER® and T459_06047 in A10. We specifically found *GolS2* (galactinol synthase 2, T459_06371; Taji et al., 2002) was up-regulated in NIBER® and a trehalose-phosphate synthase (T459_18743) in A10. However, the analysis also displayed down-regulated genes in both genotypes; for instance T459_16904 (a trehalose-phosphate phosphatase).

We also detected the deregulation of other **osmoprotectant**-related genes in A10. By way of example, the genes involved in proline catabolism (T459_06801; Funck et al., 2010) and transport (T459_23231; Rentsch et al., 1996) were up-regulated, while a glycine betaine biosynthesis gene (T459_17755; Missihoun et al., 2015) was down-regulated.

The genes coding for **hormone** signaling or synthesis are commonly deregulated after stress. Lower synthesis, inactivation or degradation of **auxins** usually happen in all plant species after stress exposure. We found two auxin-related genes that are down-regulated in both genotypes, *i.e.*, *MIZ1* (T459_12756, plays a role in maintaining auxin levels; Moriwaki et al., 2011) and *ABCG37* (T459_33922, transporter of indole-3-butyric acid and probably other auxin metabolites; Růžička et al., 2010). In A10 we found that the genes involved in the synthesis of IAA amino-acid conjugates (putative indole-3-acetic acid-amido synthetase *GH3.8*, T459_06630) were up-regulated and a gene homolog, which irreversibly inactivates this hormone in rice (2-oxoglutarate-dependent dioxygenase *DAO*, T459_04872: Zhao et al., 2013)).

Cell division in plants typically slows down after stress. **Cytokinin** (CK) synthesis is blocked, and hormone degradation starts. In this experiment in A10 there were several genes related to CK biosynthesis that were down-regulated (*IPT* genes, T459_23598 and T459_26831; Takei et al., 2001), but only the last one was also down-regulated in NIBER®. Besides, in A10, we also found the up-regulation of a gene that regulates the degradation of this hormone (cytokinin dehydrogenase, T459_24347; Werner et al., 2003). Curiously, a gene involved in CK activation (*LOG1*, T459_13377; Kuroha et al., 2009) was up-regulated in both genotypes.

Regarding **ABA**-related gene expression, we noted differences between the two rootstocks. For instance, a protein phosphatase 2C (T459_14080; Schweighofer et al., 2004) was down-regulated in A10, but up-regulated in NIBER®. In A10, we also observed the down-regulation of a gene involved in ABA catabolism (abscisic acid 8’-hydroxylase 1, T459_03838; Kushiro et al., 2004) and the up-regulation of another gene involved in protein trafficking and sorting (*NHL6*, T459_04332; Bao et al., 2016).

Ethylene is another hormone involved in stress. We found the deregulation of several genes related to ethylene biosynthesis (1-aminocyclopropane-1-carboxylate oxidase genes). However, there was no clear regulation trend in this case because genes indistinctively appeared up- and down-regulated.

Photosynthesis, as a general indicator of plant performance under stress, can provide information about tolerance mechanisms through the deregulation of associated genes. In this experiment, several photosynthetic chain components were down-regulated for A10, *i.e.*, NAD(P)H- quinone oxidoreductase subunit T (it acts as an electron shuttle in the photosynthetic chain and probably in the chloroplast respiratory chain, T459_08381; Yamamoto et al., 2011) and chlorophyll a-b binding protein (Light Harvesting Complex, T459_05321). However, some chlorophyll synthesis genes were up-regulated for NIBER®, *i.e.*, magnesium-chelatase subunit *ChlH* (plastid-to-nucleus retrograde signaling and ABA perception, T459_13633; Mochizuki et al., 2001; Tsuzuki et al., 2011) and geranylgeranyl diphosphate reductase (it provides phytol for both tocopherol and chlorophyll synthesis, T459_10457; Keller et al., 1998), but also an early light-induced protein that modulates chlorophyll synthesis to prevent photooxidative stress (T459_07967; Tzvetkova-Chevolleau et al., 2007).

Chaperones’ transcription deregulation after water stress treatment took place because chaperone gene dnaJ 20 was down-regulated for both genotypes (T459_20966; Pulido et al., 2013). Besides, we observed many different chaperone genes up-regulated in NIBER®, such as heat shock cognate 70 kDa (T459_18252; Zhang et al., 2018), dnaJ 8 (T459_17550; Chen et al., 2011) and sHSP 22.0 kDa class IV (T459_13892; Li et al., 2018).

Calcium signaling was also affected after water stress. So, calcium-binding protein *CP1* (T459_22923; Jang et al., 1998) was up-regulated, while calcineurin T459_14199 was down-regulated for both genotypes. Specifically, calcineurin *CBL4* was down-regulated in A10 (T459_09604; Halfter et al., 2000).

Some gene **transporters** were also regulated. Aquaporin *TIP1–3* (T459_28400) was down-regulated for both genotypes, while putative aquaporin *TIP-2-like* (T459_16939) was down-regulated in A10 and up-regulated in NIBER®. Other aquaporins were down-regulated and specific for A10, such as aquaporin *PIP1–5* (T459_03898) and aquaporin *TIP1-like* (T459_26097). Curiously, the genes coding for vacuolar iron transporters (T459_14318, T459_32063, T459_32062, T459_32064 and T459_12384; Kim et al., 2006; Gollhofer et al., 2014) were down-regulated for both genotypes. For A10 S-type anion channel *SLAH1* (involved in anion homeostasis maintenance, T459_22888; Negi et al., 2008) was down-regulated. For NIBER®, vacuolar proton pump *AVP1* (T459_34590) was also down-regulated.

Transcription factors regulate gene expression and constitute the starting point in several signaling pathways in plants exposed to biotic and abiotic stresses. The regulation of transcription factors after water stress differed depending on the genotype. In NIBER®, the response was more robust because *WRKY70* (T459_25223, involved in preventing stomatal closure; Li et al., 2013), *MYC2* (T459_04029, a master regulator in jasmonic acid (JA) signaling; Fernández-Calvo et al., 2011) and many *DREB*s (T459_09275, T459_09274, T459_15138; Sakuma et al., 2002) were up-regulated. In A10, the response was weaker because only *JUB1* (T459_21054; Wu et al., 2012) was specifically down-regulated.

As previously mentioned, plants under stress produce **ROS** and its ability to eliminate these compounds is related to plant tolerance. Glutathione is an important player in oxidative stress metabolism. Indeed, both genotypes show up-regulated glutathione-related genes, like the glutathione biosynthesis gene (glutamate-cysteine ligase, T459_00299; Vernoux et al., 2000), glutathione peroxidase (T459_00315), glutaredoxin C9 (T459_24935; Huang et al., 2016) and many glutathione transferase genes. However, the glutaredoxin C6 gene (T459_21376) was down-regulated in both genotypes.

In this experiment, the glycolate oxidase 2 gene, which encodes an enzyme that produces H_2O_2 from glycolate oxidation (T459_24757; Dellero et al., 2015) was specifically down-regulated in NIBER® and, consequently, the catalase gene (T459_31096) was also down-regulated. Nevertheless, we were unable to find any marked trend in peroxidase genes because there were more than 20 differentially expressed genes, and some were up- and some were down-regulated in both genotypes. However in A10, we noted two up-regulated genes that code for suberization associated anionic peroxidases (T459_31642 and T459_05761), and root suberization a common response to oxidative stress, together with lignification. Accordingly in A10, the up-regulation of four laccase genes (T459_19889, T459_15127, T459_16504, T459_19890; Cai et al., 2006) involved in lignin formation was observed.

Other genes involved in the **oxidative stress response** were up-regulated in A10, such as formate dehydrogenase (T459_06869; Olson et al., 2000) and mitochondrial uncoupling protein 6 (T459_29341), the latter of which functions in decreasing oxidative phosphorylation and increasing heat production (Borecký et al., 2006). Conversely in A10, we detected the down-regulation of NADP-dependent glyceraldehyde-3-phosphate dehydrogenase (T459_18879), which generates NADPH that is essential for antioxidant systems (Kirch et al., 2004). Lastly for polyamines, we observed the up-regulation in NIBER® for the spermidine synthase-coding gene (T459_03483).

3.4.4. Water stress-related metabolite responses

The targeted metabolomics performed in the root samples for various metabolic families showed differential regulation when plants were exposed to water stress in relation to the control conditions.

The **oligosaccharides** quantification at T2 (24 h) (Fig. 6) revealed an increase in trehalose content after stress for both genotypes, but with a greater increase in NIBER® than in A10. Galactinol was also affected by stress because both genotypes significantly decreased its content compared to the control conditions, but there was no significant difference between genotypes. With raffinose, A10 and NIBER® showed an opposite effect for its content. The A10 raffinose content dropped and NIBER® raffinose content rose after 24 h under water stress. Stachyose content lowered for both genotypes under water stress compared to the control conditions, and was significantly higher in A10.

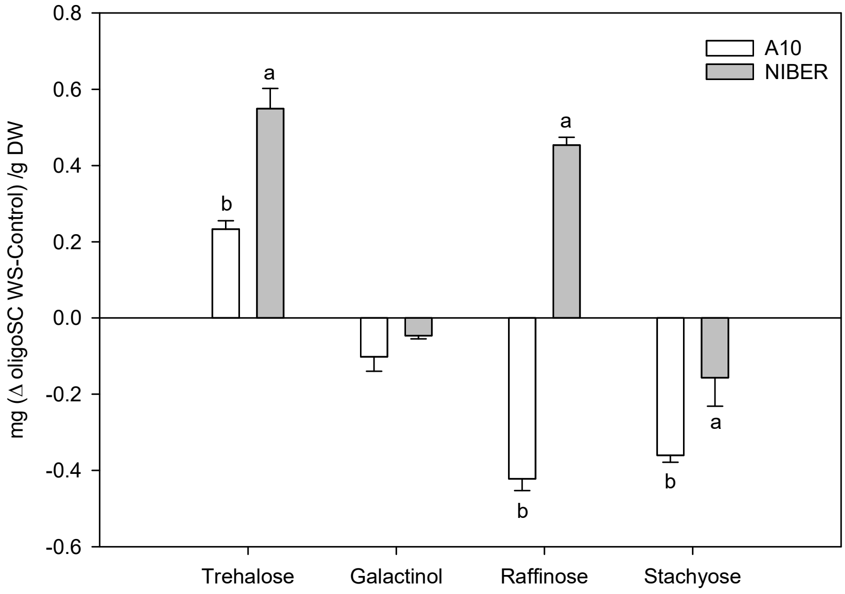

Fig. 6. Oligosaccharides quantification (trehalose, galactinol, raffinose, stachyose) as a difference between water stress and the control conditions (mg)/g DW (dry weight) in the A10 and NIBER® roots. Different letters indicate statistical differences for the LSD test with a p-value of < 0.05 for n = 4. OligoSC means oligosaccharide.

The **hormones** quantification in roots at T1 (5 h) and T2 (24 h) is shown in Fig. 7. IAA increased significantly at T1 for both genotypes under stress *versus* the control conditions (Fig. 7A). At T2, IAA decreased for A10 in relation to the control, while there were no significant differences for IAA content in NIBER® under the stress conditions (Fig. 7A). ABA content significantly decreased at T1, but only for A10 under the stress *vs.* the control conditions (Fig. 7B). At T2, significant differences were noted for ABA content under the stress *vs.* the control conditions, where ABA increased for both genotypes (Fig. 7B). There was a difference for JA at both T1 and T2 because NIBER® JA content significantly increased, and A10 JA content was not affected by stress compared to the control conditions during both events (Fig. 7C).

The **polyamines** quantification in roots at T2 (24 h) (Fig. 8) exhibited significant differences for spermine content in both genotypes because it decreased under the stress conditions, but this decrease was greater in NIBER®. Spermidine content increased significantly under stress *vs.* the control conditions for both genotypes, and the A10 increase was greater. However, there were no significant differences in putrescine content between genotypes and when comparing the stress and control conditions.

The **glutathione** quantification for the oxidized form in roots at T2 (Fig. 9) revealed a significant increase in GSSG content for both genotypes when stress was applied, but the increase in GSSG content in A10 was greater (68%) than in NIBER® (23%) *versus* the control conditions.

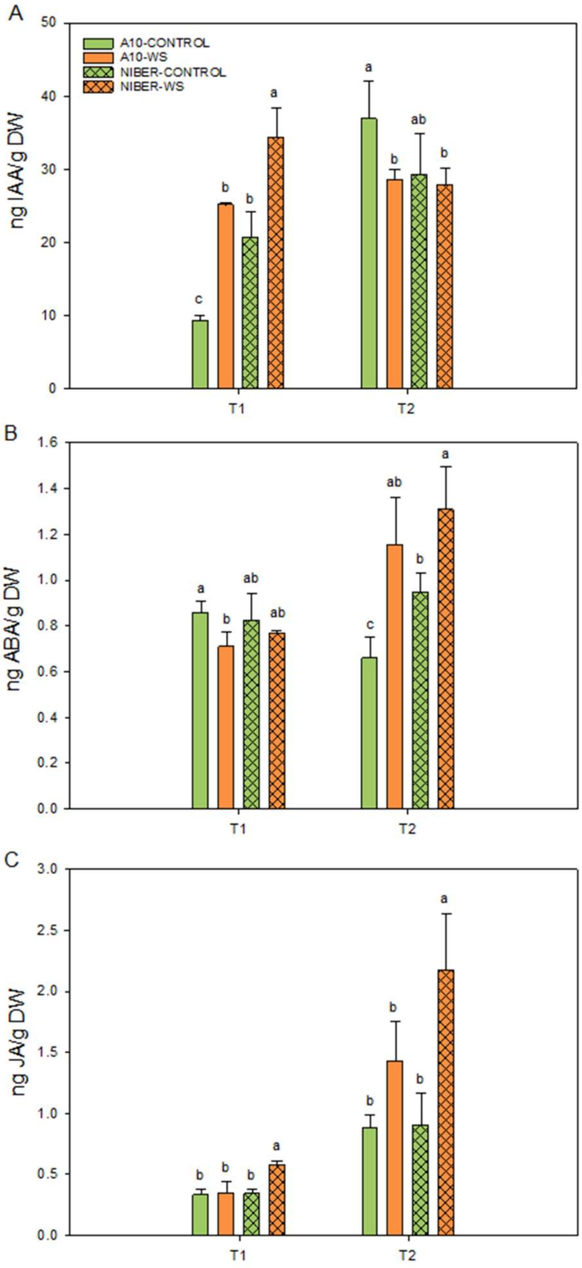

Fig. 7. Hormones quantification for IAA **(A)**, ABA **(B)** and JA **(C)** as ng of hormone/g DW (dry weight) in the A10 and NIBER® roots. Different letters indicate statistical differences for the LSD test with a p-value of < 0.05 for n = 4. IAA is indoleacetic acid, ABA is abscisic acid and JA is jasmonic acid.

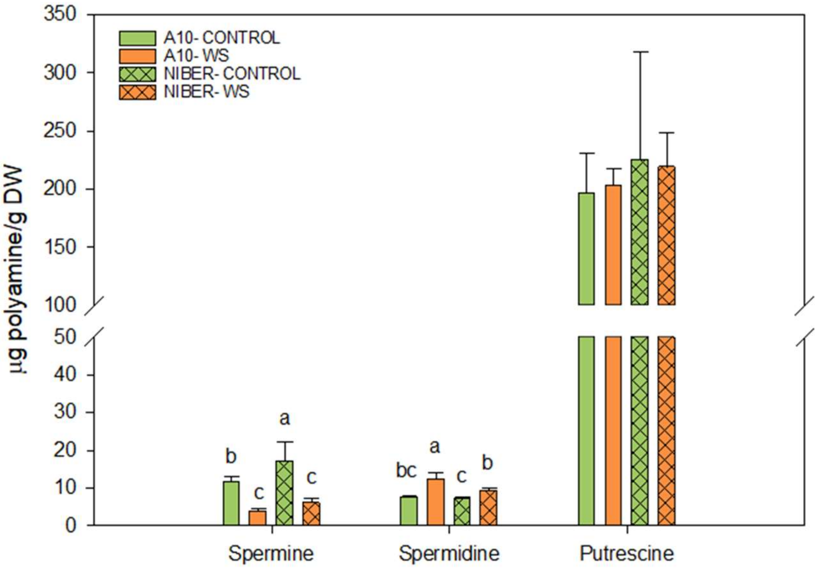

Fig. 8. Polyamines quantification (spermine, spermidine, putrescine) as µg of polyamine/g of DW (dry weight) in the A10 and NIBER® roots. Different letters indicate statistical differences for the LSD test with a p-value of < 0.05 for n = 4.

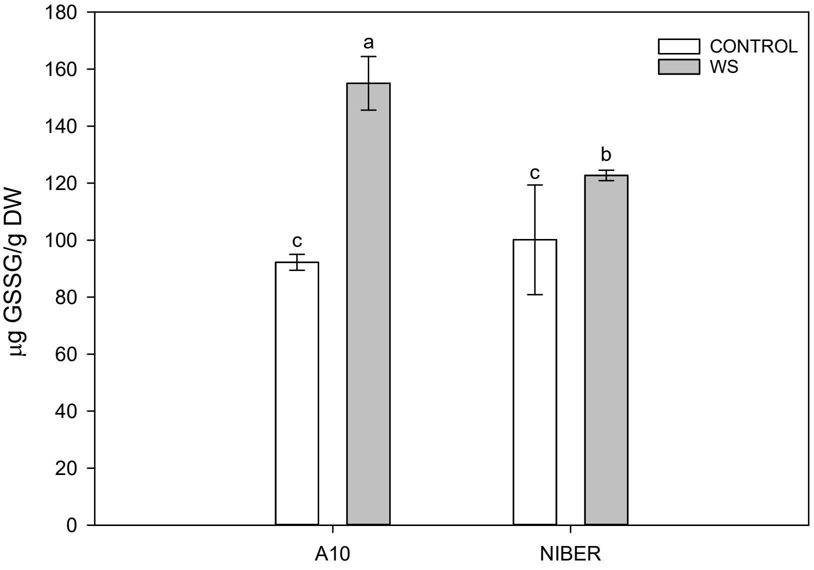

Fig. 9. Oxidized glutathione quantification as µg of GSSG/g of DW (dry weight) in A10 and NIBER®. Different letters indicate statistical differences for the LSD test with a p-value of < 0.05.

3.5. Discussion

In this experiment, a water stress-tolerant hybrid rootstock (NIBER®; Gisbert-Mullor et al., 2020) was studied under water stress conditions together with the A10 accession, which is considered sensitive to this stress (Penella et al., 2014). Both genotypes were analyzed for changes in transcriptome and different metabolites to address the differential patterns related to the short-term water stress response. The results uncovered some essential gene signaling pathways and metabolites to cope water stress. Some of these mechanisms are genotype-constitutive, while others are regulated after stress exposure.

3.5.1. Constitutive differences in gene expression

Under the non-water stress conditions, we observed differences between genotypes in gene expression terms, which could influence plant performance once stress has been applied. Up to 3000 genes were differentially expressed between NIBER® and A10 when water stress was absent. This constitutive difference between accessions has been observed by Fracasso et al. (2016) in sorghum genotypes with contrasting water use efficiency, where the tolerant genotype showed an up-regulation in the genes associated with the “secondary metabolic process” and “glutathione transferase activity” GO terms under well-watered conditions. Similarly, López-Serrano et al. (2021) stated advantageous characteristics in salt-tolerant pepper accession A25 under control conditions compared to sensitive accession A6, with a marked abundance of genes related to GO terms such as “response to stress”, “response to abiotic or biotic stimulus”, “transport”, among others. Similarly, in this study, NIBER® showed an over-representation of the “response to stimulus”, “response to chemical”, “response to oxidative stress” and “response to inorganic substance” GO terms compared to A10 under the control conditions (Fig. 1).

The genes related to these over-represented GO terms in NIBER® (Table S1) could be associated with the constitutive tolerance that this rootstock manifests under water stress. Hence, several of the genes involved in ROS detoxification were up-regulated in NIBER®/A10 under the control conditions (formate and malate dehydrogenases), while superoxide anion production gene *RbohB* was down-regulated. ROS production could be promoted in a hormonal-dependent way (Mori and Schroeder, 2004), and frequently by the activation of NADPH oxidases, which are encoded by *Rboh* genes (Sagi and Fluhr, 2006). Accordingly, ethylene has been proven to manage ROS production by regulating *Rboh* genes transcription through MAPK cascades and by triggering cell death under stress conditions (Xia et al., 2015). We found five down-regulated putative *ACO* genes in NIBER®/A10 under the control conditions. The ACO enzyme catalyses the final step in the ethylene biosynthesis pathway (Houben and van de Poel, 2019) and is encoded by *ACO* genes. Ethylene has been described to act in an antagonistic manner to ABA, because the presence of high ABA and ethylene levels results in the inhibition of the production of both hormones (Müller and Hasanuzzaman, 2021). The main enzyme responsible for ABA synthesis, *NCED1*, was up-regulated in NIBER®/A10 under the control conditions, but ABA receptor *PYL1* was down-regulated. High ABA levels cause the down-regulation of PYR/PYL receptors to prevent detrimental ABA accumulation effects (Ruiz-partida et al., (2021)). Moreover, PYL receptors have been linked with ABA-induced stomatal closure regulation, and also under optimal conditions (Gonzalez-Guzman et al., 2012). *PYL1* down-regulation in NIBER® could avoid

ABA-dependent stomatal closure and reduce undesirable growth effects from enhanced ABA synthesis (*NCED1*).

Besides the role of these stress-related hormones, oscillations in the levels of other plant hormones take place in the initial stress response phases by bringing about several metabolic changes that lead to modifications in the growth pattern to help to adapt to stress conditions (Verma et al., 2016). For instance, auxin homeostasis is achieved by several strategies, one of which is conjugation and de-conjugation (Hayashi et al., 2021). In this experiment, auxin receptor *TIR1* and amidohydrolase *ILR1* that releases free IAA from conjugates were up-regulated in NIBER®/A10, while four putative *GH3* genes that inactivate IAA by forming conjugates were down-regulated under the control conditions. Therefore, NIBER® constitutively showed an active IAA regulation pattern in relation to A10 that could help to achieve its better performance when the stress comes into play.

An increase in IAA levels has been related to improved survival to water stress because of the auxin-dependent protective effect on photosynthesis (Tognetti et al., 2010). It has been suggested that IAA protection to photooxidative inhibition exists by altering the chloroplast structure and pigments composition given that photosynthesis is one of the earliest affected processes when abiotic stress like water stress is present (Tognetti et al., 2012). Accordingly, we found several DEGs that encode for photosynthetic components and pigments, which were up-regulated (*APO1*, *CYP89A9*, *TGD1*) and down-regulated (*PSBP1*, cytochrome b6-f subunits, *PSI-K*, *PGRL1A, PGR5*, among others) when comparing NIBER® and A10 under the control conditions. However, the NIBER® down-regulated genes *PGRL1A* and *PGR5* have been associated with cyclic electron flow (CEF) around Photosystem I, which constitutes an alternative electron transfer pathway to achieve photoprotection under stress conditions (Nawrocki et al., 2019). These results suggest that A10 may already be performing CEF under the control conditions, and NIBER® mainly performs the linear electron flow (LEF).

Calcium is involved in the regulation of the genes related to chloroplast components and it is known as a major signaling cation when plants sense an external stimulus (Wang et al., 2019). Several calcium-associated genes, such as calcineurin-binding proteins (*CBL7* and *CBL9*) and CBL-interacting kinase *CIPK20,* were up-regulated in NIBER®/A10, but calcium-dependent protein kinase *CPK4* and calmodulin *CML11* were down-regulated in NIBER®/A10 under the control conditions. Unlike CDPKs, CBLs and CIPKs interact in a very specific way by conducting calcium signaling in certain locations, *i.e.*, vacuole membrane, where calcium can be sensed only by the CBL-CIPK interaction (Edel et al., 2017). Nevertheless, calcium is a wide-range and complex component of many signaling transduction pathways, and it is present as a ubiquitous second messenger in many biological processes (Batistič et al., 2009), including the response to environmental stresses and developmental processes (Pirayesh et al., 2021).

Calcium signaling, together with phytohormones and MAP kinases, regulates the expression of the genes included in osmolytes synthesis pathways in the presence of abiotic stress (Jogawat, 2019). Osmolytes synthesis and accumulation are key for plant survival under stress conditions because osmolytes diminish the detrimental effects of water starvation by preserving the water potential (Ozturk et al., 2021). However, several genes related to osmoprotectant sugars synthesis and transport were downregulated in NIBER®/A10 under the control conditions, such as trehalose synthase genes (*TPS1* and *TPP*) and a *SWEET* transporter.

Notwithstanding, some authors have reported negative trehalose overproduction effects under control conditions that have resulted in penalty growth and, thus, suggest employing tissue-specific promoters or those induced by stress conditions (Iqbal and Nazar, 2016).

Polyamines are molecules involved in osmoprotection, but are also considered for their ability to detoxify excess ROS and to avoid oxidative damage by acting as antioxidants themselves or by promoting the action of other antioxidant enzymes and molecules (Zulfiqar et al., 2019). Two genes related to polyamines were up-regulated in NIBER®/A10 under the control conditions (*PAO,* that catalyzes spermine to spermidine conversion, and *PUT4*, a polyamine transporter), and one spermidine synthase gene was down-regulated. Additionally, dehydrins are soluble proteins whose expression is modified in the presence of abiotic stress, and are associated with the protection of other proteins, but also with osmotic adjustment with water stress (Ozturk et al., 2021). Thus, dehydrin *HIRD11* was up-regulated in NIBER®/A10 under the control conditions. Furthermore, this dehydrin has been proven to reduce ROS formation, including H_2O_2 and hydroxyl radicals (Hara et al., 2013).

Lastly, molecular chaperones usually present an enhanced expression under stress conditions, and they are in charge of rearranging protein conformation when it has been altered due to stress (Wang et al., 2004). Despite the role of chaperones being essential in protein homeostasis, an HSP90 co-chaperone and *sHSP 18.2KDa* genes were down-regulated in NIBER®/A10 under the control conditions. These results could be supported by the minimal expression of sHSPs, which is typically found when abiotic stress is absent, except for specific reproductive developmental stages, such as embryogenesis, germination, among others (Sun et al., 2002). Besides, *BAG4* was up-regulated in NIBER®/A10 under the control conditions, and this chaperone has been linked with stomatal movement regulation through the interaction with potassium channels (Locascio et al., 2019).

3.5.2. Transcriptomic and metabolomic changes under water stress conditions

Under water stress conditions, the number of DEGs was 4-fold bigger at 5 h (T1) than at 24 h (T2) (Fig. 2), which indicates that short-term gene transcription is crucial for water stress responses. Similarly to the control conditions, the water stress that impacted both genotypes was different in gene expression regulation terms because A10 showed more than double the amount of specifically DEGs compared to NIBER® at 5 h (T1) (Fig. 2A). Nevertheless, there are common pathways in the stress response for both genotypes, notably mechanisms that counteract oxidant compounds effects, such as peroxidases, calcium signaling and glutathione regulation (glutathione synthase, peroxidases, transferases and glutaredoxins). Regarding glutathione, it is well-known that GSH is oxidized to GSSG under stress conditions for redox homeostasis (Dorion et al., 2021), and lower GSSG content has been associated with water stress tolerance (Hasanuzzaman and Fujita, 2011). In this experiment, the GSSG content under stress was higher in A10 than in NIBER® (Fig. 9). Moreover, in A10 the regulation of the genes related to oxidants detoxification (formate dehydrogenase, suberization associated anionic peroxidases, *JUG1*) occurred, while the down-regulation of H_2O_2-related genes (*CAT*, glicolate oxidase) took place in NIBER®, which suggests a stronger impact of stress in A10. Fracasso et al. (2016) reported a significantly larger amount of DEGs, especially ROS detoxification genes, in the sensitive genotype in relation to the tolerant genotype, for sorghum water-stressed plants.

Photosynthetic activity triggers oxidants production in the chloroplast, and ROS should be scavenged to avoid oxidative damage. A10 showed the down-regulation of chlorophyll a-b binding protein (*LHC*) and NAD(P)H-quinone oxidoreductase subunit T (*ndhT*), both of which are photosynthetic chain elements, as well as the up-regulation of mitochondrial uncoupling protein 6 (*PUMP6*), which helps to avoid oxidative damage by increasing heat production (Borecký et al., 2006). Rivero et al. (2010) associated photosynthetic apparatus degradation in sensitive plants under water stress with increased non-photochemical quenching, plus a diminished electron transfer, while the photosynthesis of tolerant plants was not affected. NIBER® showed the up-regulation of chlorophyll synthesis genes and early light-induced protein (*ELIP*) (which prevents free chlorophyll accumulation to protect from photooxidative stress) and showed no inhibition of photorespiration in gene expression terms.

Furthermore, a common response to abiotic stress in plants is higher polyamines content (Hussain et al., 2011), which was higher for spermidine in both genotypes when stress was applied (Fig. 8). Several reports suggest an antagonistic role for polyamines and ethylene because they have a common precursor (S-adenosylmethione, SAM) (Imai et al., 2004). In this experiment, the down-regulation of *SAMDC* was noted in NIBER® at 5 h after water stress, as was the up-regulation of *SPDS1* at 24 h, which may counteract and result in the above-mentioned increased spermidine after the stress treatment. In addition, the changes in gene expression for the *ACO* genes did not follow a specific trend, but there were several ethylene-related GO terms in A10, and ethylene contribution should be further studied (Fig. 4). Polyamines have also been linked with ABA and *DREBs* because the promoters of polyamines synthesis genes, such as *SPDS1*, contain DRE and ABA-responsive elements (Alcázar et al., 2006). Accordingly, the up-regulation of three *DREBs* occurred in NIBER® with water stress compared to the control conditions, which showed the ability to develop a quick response to water stress because increases in *DREBs* expression have been observed at 5 h from water and osmotic stress exposure (Sakuma et al., 2002). *MYC2* is also a transcription regulator which has been associated with the ABA-dependent signaling pathway for water stress tolerance (Abe et al., 2003) and, to a greater extent, with dehydration resistance through JA signaling (Li et al., 2019). NIBER® JA content increased after 5 h of water stress and doubled after 24 h compared to the control conditions, while A10 JA content did not change (Fig. 7C). *MYC2* was upregulated in NIBER® 24 h after water stress treatment and Li et al. (2019) linked the accumulation of the JA that derived from water stress exposure with the activation of *MYC2*, which promotes the gene expression of the downstream genes associated with dehydration resistance.

ABA content increased under water stress in both A10 and NIBER® at 24 h (Fig. 7B). However, we were able to find different transcriptomic response in the genes related to the signaling and synthesis of this hormone. In NIBER®, the up-regulation of *CHLH* took place after 5 h of water stress, which is involved in both chlorophyll synthesis and the ABA signaling pathway for stomatal movements (Tsuzuki et al., 2011), together with the up-regulation of *WRKY70*, which is a negative regulator of stomatal closure (Li et al., 2013). In A10, the down-regulation of ABA catabolism gene (*ABA 8-hydroxylase 1*) at 5 h after water stress and up-regulation of an ABA signaling and synthesis gene (*NHL6*) occurred at 24 h, *NHL6* overexpression has been linked with sensitivity to salt and osmotic stress due to excess ABA and hypersensitivity (Bao et al., 2016). These results suggest that in early water stress exposure stages, NIBER® could avoid stomatal closure, whereas A10 could promote its closure, which agrees with *PP2C72* differential expression under water stress (down-regulated in A10 at 5 h and up-regulated in NIBER® at 24 h). PP2C-type protein phosphatases are negative regulators of ABA signaling that prevent stomatal closure (Lee et al., 2009). Besides, A10 showed related GO terms, such as "chloroplast accumulation and avoidance movements", "ABA metabolic process", "ABA-activated signaling pathway" and "response to water deprivation" for stress compared to the control conditions (Fig. 4), that were not found in NIBER®. Accordingly, many of the genes coding for aquaporins (*PIP1–2, TIP1–1, TIP1–2, TIP-type RB7–5A*) were down-regulated in A10, which could result in weaker water transport and slight uncharged molecules transport (Takano et al., 2017). NIBER® showed GO terms such as "water transport" and "plasmodesmata-mediated intercellular transport" (Fig. 5), together with the up-regulation of aquaporin *TIP-type RB7–5A*. Moreover, stomatal closure as a water-saving strategy leads to decreased photosynthetic activity from CO_2 unavailability, and aquaporins function to achieve CO_2 homeostasis (Afzal et al., 2016). Sade et al. (2009) observed more growth and bigger yields in tomato plants with the constitutive expression of *SlTIP2–2* that derived from the maintenance of transpiration and CO_2 uptake under water stress conditions. In previous experiments, the photosynthetic balance in plants grafted onto NIBER® under high salt stress conditions was better, compared to self-grated and ungrafted plants (López-Serrano et al., 2020). This improvement was attributed to the sustained stomatal opening that resulted in more growth.

Changes in the shoot/root growth ratio under water stress are regulated by auxins and cytokinins because auxin promotes root growth and inhibits shoot growth, whereas cytokinin could act as antagonist (Kurepa and Smalle, 2022). A10 and NIBER® showed increased IAA 5 h after the stress treatment (Fig. 7A), along with a down-regulation of an auxin polar transporter (*ABCG37*) and an auxin homeostasis regulator (*MIZ1*). These results are related to the "Hydrotropism" GO term, which is common for both genotypes (Fig. 3) because it is defined as growth or movement toward or away from water. For CKs, the up-regulation of CKs activation gene (*LOG1*) and the down-regulation of CKs synthesis (*IPT1*) occurred in both NIBER® and A10 at 5 h after water stress treatment. The transcriptomic results suggested that both genotypes avoid negative feedback and auxin export in roots, while stimulating CKs activation but inhibiting CKs synthesis. Furthermore, A10 showed the down-regulation of a second *IPT* gene and the up-regulation of cytokinine dehydrogenase gene at 5 h after water stress, which suggest a decrease in CKs to promote root growth over shoot growth. Despite this, A10 displayed the up-regulation of an auxin inactivation gene (*DAO*) and an auxin conjugation gene (*GH3.8*) at 5 h after water stress, which is consistent with the "auxin homeostasis" and "auxin catabolic process" GO terms (Fig. 4). These results agree with the drop in the IAA content observed in A10 at 24 h under water stress compared to the control conditions, which was not observed in NIBER® (Fig. 7A). While A10 seems to downregulate auxins activation and CKs synthesis, NIBER® apparently maintains the levels for both phytohormones.

Osmolytes accumulate in plants to protect them from oxidative damage, but also counteract existing harm, and include sugars (trehalose, RFOs), amino acids (proline), quaternary ammonium compounds (glycine betaine) and sugar alcohols (Jogawat, 2019; Ejaz et al., 2020).

Trehalose is speculated to be an osmoprotectant sugar given the tolerant genotype observed in transgenic plants for trehalose biosynthesis genes (van Houtte et al., 2013). In this experiment, trehalose content increased for both genotypes under stress *vs.* the control conditions (Fig. 6). Notwithstanding, the *TPP* gene was down-regulated for both genotypes 5 h after water stress, and it is involved in the conversion of trehalose-6-phosphate into free trehalose, which should end with lower trehalose content. Moreover, *TPS* gene expression in A10 under water stress increased at 24 h, and TPS is the enzyme responsible for trehalose-6-phosphate synthesis. These results suggest that A10 promoted trehalose-6-phosphate synthesis, probably due to its role as a signaling molecule in regulating photosynthesis and starch synthesis in plastids (Iturriaga et al., 2009). For NIBER® there were no expression changes in *TPS*, but trehalose content was higher compared to the control conditions.

Nishizawa et. al (2008) proposed an additional role for galactinol and raffinose sugars as direct ROS scavengers, apart from osmoprotectants and membrane stabilizers, by ensuring photosynthesis protection under adverse conditions like water stress. A10 and NIBER® showed higher galactinol-sucrose galactosyltransferase gene expression at 5 h after water stress, the enzyme responsible for raffinose synthesis from galactinol. This is consistent with the drop in galactinol content under stress compared to the control conditions in both genotypes (Fig. 6). However, the matching increase in raffinose content was observed only for NIBER® (Fig. 6), which also showed the up-regulation of the galactinol synthase gene (*GolS2*) at 24 h after the stress treatment. It would seem that NIBER® could provide galactinol for raffinose synthesis, as reflected in oligosaccharides quantification. Conversely, raffinose content in A10 could not be associated with the observed gene expression changes, regulation mechanisms could act at the post-translational level, and/or the processes affecting the metabolome could be delayed in relation to gene expression changes (Feussner and Polle, 2015). Moreover, oligosaccharides quantification was performed in roots and sugars could accumulate in leaves because they would be required for ROS scavenging and osmoprotection, as it has been previously mentioned.

Accumulation of glycine betaine (GB) and proline has been widely reported in multiple plant species under abiotic stresses, and these compounds are considered main organic osmolytes (Ashraf and Foolad, 2007). Proline functions like osmolyte include cell turgor maintenance and cellular homeostasis, but it also functions like an antioxidant in scavenging ROS (Hayat et al., 2012). In the A10 genotype, the up-regulation of the proline dehydrogenase gene, together with the up-regulation of a proline transporter and the GO term "proline catabolism", occurred at 5 h after water stress. Proline degradation has been observed as a strategy to favor polyamine synthesis because they have a common precursor (Ejaz et al., 2020). However, no marked increase in polyamines content in A10 other than that observed in NIBER® was noted. Thus, we cannot confirm this strategy, plus proline content should also be studied. Regarding GB, the betaine aldehyde dehydrogenase gene in A10 was down-regulated, which is responsible for the last GB synthesis step in chloroplasts. GB accumulates mainly under water stress conditions to protect chloroplasts through osmoregulation by avoiding damage to thylakoid membranes and preserving the photosynthetic yield (Dikilitas et al., 2020). Both proline and GB are capable of stabilizing membranes and proteins, and the high concentrations of these and/or other osmolytes could be an effective strategy to recover from the protein unfolding that derives from stress exposure (Ortbauer, 2013).

Protein stability and conformations are strongly affected by internal and external stimuli, including unexpected environmental changes that lead to protein unfolding and misfolding (Ha and Loh, 2012). HSPs are chaperones that assist in protein folding, and in the refolding of unfolded or misfolded proteins under abiotic stress conditions (Wang et al., 2004). With water stress *versus* the control conditions, NIBER® showed GO terms such as "response to unfolded protein", "endoplasmic reticulum unfolded protein response" and "chaperone cofactor-dependent protein folding". Accordingly, chaperone dnaJ 8 was upregulated in NIBER®, as were heat shock cognate 70 kDa and *22 kDa sHSP*. As described for the control conditions, the expression of HSPs typically increases when plants are exposed to stress conditions, which is consistent with the results obtained for NIBER®, which seems to promote chaperones as a tolerance strategy that was not observed in A10.

3.6. Conclusions

Briefly, NIBER® displays multiple mechanisms to cope with water stress (Fig. 10). The transcriptomic results suggest constitutive mechanisms, mainly involved in detoxification, which are amplified under stress conditions.

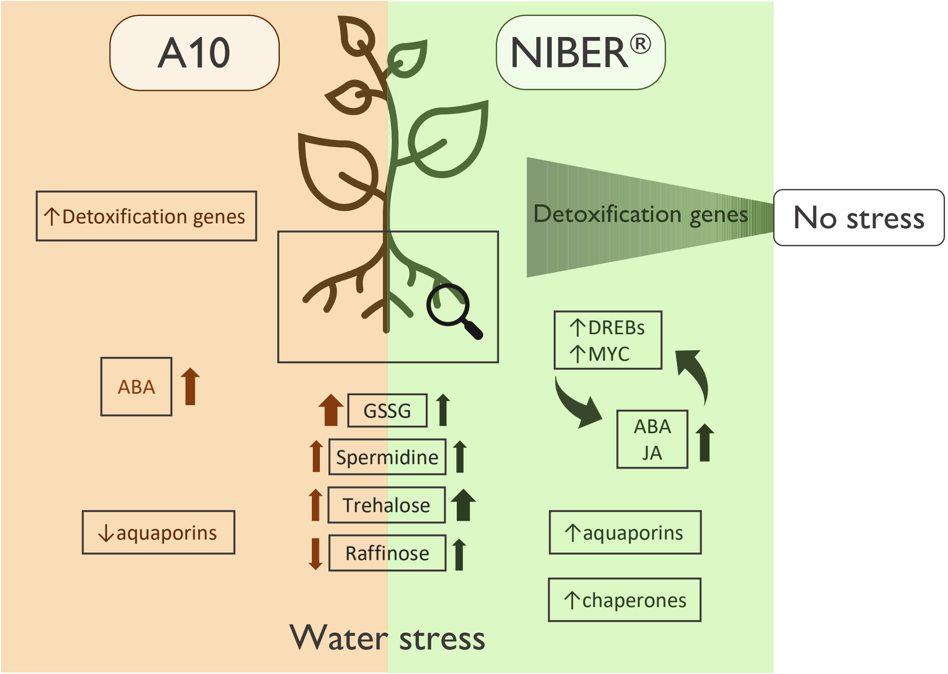

Fig. 10. Water stress response mechanisms in the NIBER® and A10 roots. Framed arrows depict a higher or lower expression level for the corresponding genes. Nonframed arrows denote higher or lower metabolite content. The wider the arrow, the higher the content.

These results also evidence the important role of transcription factors like *DREBs* and *MYC* at the beginning of the stress response. Hormones regulation under water stress in NIBER® comprises the up-regulation of auxins, ABA and JA, which might benefit the rootstock in growth and development terms. These changes are accompanied by the regulation of osmoprotectants in terms of gene expression and metabolites content. The gene expression of raffinose, galactinol and spermidine synthesis genes increases under water stress, together with enhanced trehalose, raffinose and spermidine content. For glutathione, its synthesis gene has a higher expression under water stress, and NIBER® has lower oxidised glutathione content compared to A10. All these osmoprotectant-antioxidant components contribute to NIBER® tolerance under water stress, together with aquaporins and chaperones, which display an increased gene expression for NIBER®. This study provides useful insights into rootstock (NIBER®) tolerance mechanisms, but further studies should be performed to move forward.

3.7. References

Abe, H., Urao, T., Ito, T., Seki, M., Shinozaki, K., & Yamaguchi-Shinozaki, K. (2003). Arabidopsis AtMYC2 (*bHLH*) and AtMYB2 (*MYB*) function as transcriptional activators in abscisic acid signaling. *The Plant Cell*, *15*(1), 63–78. https://doi.org/10.1105/TPC.006130

Afzal, Z., Howton, T. C., Sun, Y., & Mukhtar, M. S. (2016). The Roles of Aquaporins in Plant Stress Responses. *Journal of Developmental Biology 2016, Vol. 4, Page 9*, *4*(1), 9. https://doi.org/10.3390/JDB4010009

Alcázar, R., Marco, F., Cuevas, J. C., Patron, M., Ferrando, A., Carrasco, P., Tiburcio, A. F., & Altabella, T. (2006). Involvement of polyamines in plant response to abiotic stress. *Biotechnology Letters*, *28*(23), 1867–1876. https://doi.org/10.1007/S10529-006-9179-3

Amann, K., Lezhneva, L., Wanner, G., Herrmann, R. G., & Meurer, J. (2004). *ACCUMULATION OF PHOTOSYSTEM ONE1*, a member of a novel gene family, is required for accumulation of [4Fe-4S] cluster-containing chloroplast complexes and antenna proteins. *The Plant Cell*, *16*(11), 3084–3097. https://doi.org/10.1105/TPC.104.024935

Anders, S., Pyl, P. T., & Huber, W. (2015). HTSeq—a Python framework to work with high-throughput sequencing data. *Bioinformatics*, *31*(2), 166. https://doi.org/10.1093/BIOINFORMATICS/BTU638

Andrews, S. (2010). *FastQC: A Quality Control Tool for High Throughput Sequence Data*. https://www.bioinformatics.babraham.ac.uk/projects/fastqc/

Anjum, S. A., Xie, X.-Y., Wang, L.-C., Saleem, M. F., Man, C., & Lei, W. (2011). Morphological, physiological and biochemical responses of plants to drought stress. *African Journal of Agricultural Research*, *6*(9), 2026–2032. https://doi.org/10.5897/AJAR10.027

Arbona, V., Manzi, M., de Ollas, C., & Gómez-Cadenas, A. (2013). Metabolomics as a Tool to Investigate Abiotic Stress Tolerance in Plants. *International Journal of Molecular Sciences 2013, Vol. 14, Pages 4885-4911*, *14*(3), 4885–4911. https://doi.org/10.3390/IJMS14034885

Ashraf, M., & Foolad, M. R. (2007). Roles of glycine betaine and proline in improving plant abiotic stress resistance. *Environmental and Experimental Botany*, *59*(2), 206–216. https://doi.org/10.1016/j.envexpbot.2005.12.006

Athar, H. R., & Ashraf, M. (2009). Strategies for Crop Improvement Against Salinity and Drought Stress: An Overview. In *Salinity and Water Stress* (pp. 1–16). Springer, Dordrecht. https://doi.org/10.1007/978-1-4020-9065-3_1

Bao, Y., Song, W. M., Pan, J., Jiang, C. M., Srivastava, R., Li, B., Zhu, L. Y., Su, H. Y., Gao, X. S., Liu, H., Yu, X., Yang, L., Cheng, X. H., & Zhang, H. X. (2016). Overexpression of the NDR1/HIN1-Like gene *NHL6* modifies seed germination in response to abscisic acid and abiotic stresses in Arabidopsis. *PLoS ONE*, *11*(2). https://doi.org/10.1371/JOURNAL.PONE.0148572

Bartel, B., & Fink, G. R. (1995). *ILR1*, an amidohydrolase that releases active indole-3-acetic acid from conjugates. *Science (New York, N.Y.)*, *268*(5218), 1745–1748. https://doi.org/10.1126/SCIENCE.7792599

Bateman, A., Martin, M. J., Orchard, S., Magrane, M., Agivetova, R., Ahmad, S., Alpi, E., Bowler-Barnett, E. H., Britto, R., Bursteinas, B., Bye-A-Jee, H., Coetzee, R., Cukura, A., da Silva, A., Denny, P., Dogan, T., Ebenezer, T. G., Fan, J., Castro, L. G., … Teodoro, D. (2021). UniProt: the universal protein knowledgebase in 2021. *Nucleic Acids Research*, *49*(D1), D480–D489. https://doi.org/10.1093/NAR/GKAA1100

Batistič, O., Waadt, R., Steinhorst, L., Held, K., & Kudla, J. (2009). CBL-mediated targeting of CIPKs facilitates the decoding of calcium signals emanating from distinct cellular stores. *The Plant Journal*, *61*(2), 211–222. https://doi.org/10.1111/j.1365-313X.2009.04045.x

Berardini, T. Z., Reiser, L., Li, D., Mezheritsky, Y., Muller, R., Strait, E., & Huala, E. (2015). The Arabidopsis Information Resource: Making and mining the "gold standard" annotated reference plant genome. *Genesis*, *53*(8), 474–485. https://doi.org/10.1002/DVG.22877

Borecký, J., Nogueira, F. T. S., de Oliveira, K. A. P., Maia, I. G., Vercesi, A. E., & Arruda, P. (2006). The plant energy-dissipating mitochondrial systems: depicting the genomic structure and the expression profiles of the gene families of uncoupling protein and alternative oxidase in monocots and dicots. *Journal of Experimental Botany*, *57*(4), 849–864. https://doi.org/10.1093/jxb/erj070

Borràs, D., Barchi, L., Schulz, K., Moglia, A., Acquadro, A., Kamranfar, I., Balazadeh, S., & Lanteri, S. (2021). Transcriptome-Based Identification and Functional Characterization of NAC Transcription Factors Responsive to Drought Stress in *Capsicum annuum* L. *Frontiers in Genetics*, *12*. https://doi.org/10.3389/FGENE.2021.743902

Cai, X., Davis, E. J., Ballif, J., Liang, M., Bushman, E., Haroldsen, V., Torabinejad, J., & Wu, Y. (2006). Mutant identification and characterization of the laccase gene family in Arabidopsis. *Journal of Experimental Botany*, *57*(11), 2563–2569. https://doi.org/10.1093/JXB/ERL022

Capsicum_annuum - Ensembl Genomes. (n.d.). Retrieved November 22, 2022, from https://plants.ensembl.org/Capsicum_annuum/Info/Index

Chen, K. M., Piippo, M., Holmström, M., Nurmi, M., Pakula, E., Suorsa, M., & Aro, E. M. (2011). A chloroplast-targeted DnaJ protein *AtJ8* is negatively regulated by light and has rapid turnover in darkness. *Journal of Plant Physiology*, *168*(15), 1780–1783. https://doi.org/10.1016/J.JPLPH.2011.04.001

Christ, B., Süssenbacher, I., Moser, S., Bichsel, N., Egert, A., Müller, T., Kräutler, B., & Hörtensteiner, S. (2013). Cytochrome P450 *CYP89A9* is involved in the formation of major chlorophyll catabolites during leaf senescence in Arabidopsis. *The Plant Cell*, *25*(5), 1868–1880. https://doi.org/10.1105/TPC.113.112151

DalCorso, G., Pesaresi, P., Masiero, S., Aseeva, E., Schünemann, D., Finazzi, G., Joliot, P., Barbato, R., & Leister, D. (2008). A complex containing *PGRL1* and *PGR5* is involved in the switch between linear and cyclic electron flow in Arabidopsis. *Cell*, *132*(2), 273–285. https://doi.org/10.1016/J.CELL.2007.12.028

D'Alessandro, S., Golin, S., Hardtke, C. S., lo Schiavo, F., & Zottini, M. (2015). The co-chaperone *p23* controls root development through the modulation of auxin distribution in the Arabidopsis root meristem. *Journal of Experimental Botany*, *66*(16), 5113–5122. https://doi.org/10.1093/JXB/ERV330

Dellero, Y., Mauve, C., Boex-Fontvieille, E., Flesch, V., Jossier, M., Tcherkez, G., & Hodges, M. (2015). Experimental evidence for a hydride transfer mechanism in plant glycolate oxidase catalysis. *Journal of Biological Chemistry*, *290*(3), 1689–1698. https://doi.org/10.1074/JBC.M114.618629

Dharmasiri, N., Dharmasiri, S., & Estelle, M. (2005). The F-box protein *TIR1* is an auxin receptor. *Nature*, *435*(7041), 441–445. https://doi.org/10.1038/NATURE03543

Dikilitas, M., Simsek, E., & Roychoudhury, A. (2020). Role of Proline and Glycine Betaine in Overcoming Abiotic Stresses. *Protective Chemical Agents in the Amelioration of Plant Abiotic Stress*, 1–23. https://doi.org/10.1002/9781119552154.CH1

Dorion, S., Ouellet, J. C., & Rivoal, J. (2021). Glutathione Metabolism in Plants under Stress: Beyond Reactive Oxygen Species Detoxification. *Metabolites*, *11*(9). https://doi.org/10.3390/METABO11090641

Dyson, B. C., Webster, R. E., & Johnson, G. N. (2014). GPT2: A glucose 6-phosphate/phosphate translocator with a novel role in the regulation of sugar signaling during seedling development. *Annals of Botany*, *113*(4), 643–652. https://doi.org/10.1093/AOB/MCT298

Edel, K. H., Marchadier, E., Brownlee, C., Kudla, J., & Hetherington, A. M. (2017). The Evolution of Calcium-Based Signaling in Plants. *Current Biology*, *27*(13), R667–R679. https://doi.org/10.1016/J.CUB.2017.05.020

Ejaz, S., Fahad, S., Anjum, M. A., Nawaz, A., Naz, S., Hussain, S., & Ahmad, S. (2020). *Role of Osmolytes in the Mechanisms of Antioxidant Defense of Plants* (pp. 95–117). Springer, Cham. https://doi.org/10.1007/978-3-030-38881-2_4

FAO. (2022). *Climate Change | Land & Water*. https://www.fao.org/land-water/overview/climate-change/en/

Farooq, M., Wahid, A., Kobayashi, N., Fujita, D., & Basra, S. M. A. (2009). Plant drought stress: effects, mechanisms and management. *Agronomy for Sustainable Development*, *29*(1), 185–212. https://doi.org/10.1051/agro:2008021

Fernández-Calvo, P., Chini, A., Fernández-Barbero, G., Chico, J. M., Gimenez-Ibanez, S., Geerinck, J., Eeckhout, D., Schweizer, F., Godoy, M., Franco-Zorrilla, J. M., Pauwels, L., Witters, E., Puga, M. I., Paz-Ares, J., Goossens, A., Reymond, P., de Jaeger, G., & Solano, R. (2011). The Arabidopsis bHLH transcription factors *MYC3* and *MYC4* are targets of JAZ repressors and act additively with *MYC2* in the activation of jasmonate responses. *The Plant Cell*, *23*(2), 701–715. https://doi.org/10.1105/TPC.110.080788

Feussner, I., & Polle, A. (2015). What the transcriptome does not tell - proteomics and metabolomics are closer to the plants' patho-phenotype. *Current Opinion in Plant Biology*, *26*, 26–31. https://doi.org/10.1016/j.pbi.2015.05.023

Fichtner, F., Olas, J. J., Feil, R., Watanabe, M., Krause, U., Hoefgen, R., Stitt, M., & Lunn, J. E. (2020). Functional features of *TREHALOSE-6-PHOSPHATE SYNTHASE1*, an essential enzyme in Arabidopsis. *Plant Cell*, *32*(6), 1949–1972. https://doi.org/10.1105/TPC.19.00837

Fracasso, A., Trindade, L. M., & Amaducci, S. (2016). Drought stress tolerance strategies revealed by RNA-Seq in two sorghum genotypes with contrasting WUE. *BMC Plant Biology*, *16*(1), 1–18. https://doi.org/10.1186/S12870-016-0800-X

Funck, D., Eckard, S., & Müller, G. (2010). Non-redundant functions of two proline dehydrogenase isoforms in Arabidopsis. *BMC Plant Biology*, *10*, 70–70. https://doi.org/10.1186/1471-2229-10-70

Gaxiola, R. A., Li, J., Undurraga, S., Dang, L. M., Allen, G. J., Alper, S. L., & Fink, G. R. (2001). Drought- and salt-tolerant plants result from overexpression of the *AVP1* H^+-pump. *Proceedings of the National Academy of Sciences of the United States of America*, *98*(20), 11444–11449. https://doi.org/10.1073/PNAS.191389398

Gill, S. S., & Tuteja, N. (2010). Reactive Oxygen Species and antioxidant machinery in abiotic stress tolerance in crop plants. *Plant Physiology and Biochemistry*, *48*(12), 909–930. https://doi.org/10.1016/j.plaphy.2010.08.016

Gisbert-Mullor, R., Pascual-Seva, N., Martínez-Gimeno, M. A., López-Serrano, L., Marín, E. B., Pérez-Pérez, J. G., Bonet, L., Padilla, Y. G., Calatayud, Á., Pascual, B., & López-Galarza, S. (2020). Grafting onto an appropriate rootstock reduces the impact on yield and quality of controlled deficit irrigated pepper crops. *Agronomy*, *10*(10). https://doi.org/10.3390/agronomy10101529

Gollhofer, J., Timofeev, R., Lan, P., Schmidt, W., & Buckhout, T. J. (2014). *Vacuolar-iron-transporter1-like* proteins mediate iron homeostasis in Arabidopsis. *PLoS ONE*, *9*(10). https://doi.org/10.1371/JOURNAL.PONE.0110468

Gonzalez-Guzman, M., Pizzio, G. A., Antoni, R., Vera-Sirera, F., Merilo, E., Bassel, G. W., Fernández, M. A., Holdsworth, M. J., Perez-Amador, M. A., Kollist, H., & Rodriguez, P. L. (2012). Arabidopsis PYR/PYL/RCAR receptors play a major role in quantitative regulation of stomatal aperture and transcriptional response to abscisic acid. *Plant Cell*, *24*(6), 2483–2496. https://doi.org/10.1105/TPC.112.098574/DC1

Ha, J. H., & Loh, S. N. (2012). Protein conformational switches: from nature to design. *Chemistry (Weinheim an Der Bergstrasse, Germany)*, *18*(26), 7984–7999. https://doi.org/10.1002/CHEM.201200348

Halfter, U., Ishitani, M., & Zhu, J. K. (2000). The Arabidopsis *SOS2* protein kinase physically interacts with and is activated by the calcium-binding protein *SOS3*. *Proceedings of the National Academy of Sciences of the United States of America*, *97*(7), 3735–3740. https://doi.org/10.1073/PNAS.97.7.3735

Hanzawa, Y., Imai, A., Michael, A. J., Komeda, Y., & Takahashi, T. (2002). Characterization of the spermidine synthase-related gene family in Arabidopsis thaliana. *FEBS Letters*, *527*(1–3), 176–180. https://doi.org/10.1016/S0014-5793(02)03217-9

Hao, Q., Yin, P., Li, W., Wang, L., Yan, C., Lin, Z., Wu, J. Z., Wang, J., Yan, S. F., & Yan, N. (2011). The molecular basis of ABA-independent inhibition of PP2Cs by a subclass of PYL proteins. *Molecular Cell*, *42*(5), 662–672. https://doi.org/10.1016/J.MOLCEL.2011.05.011

Hara, M., Kondo, M., & Kato, T. (2013). A KS-type dehydrin and its related domains reduce Cu-promoted radical generation and the histidine residues contribute to the radical-reducing activities. *Journal of Experimental Botany*, *64*(6), 1615–1624. https://doi.org/10.1093/JXB/ERT016

Hasanuzzaman, M., & Fujita, M. (2011). Selenium pretreatment upregulates the antioxidant defense and methylglyoxal detoxification system and confers enhanced tolerance to drought stress in rapeseed seedlings. *Biological Trace Element Research*, *143*(3), 1758–1776. https://doi.org/10.1007/S12011-011-8998-9

Hayashi, K.-I., Arai, K., Aoi, Y., Tanaka, Y., Hira, H., Guo, R., Hu, Y., Ge, C., Zhao, Y., Kasahara, H., & Fukui, K. (2021). The main oxidative inactivation pathway of the plant hormone auxin. *Nature Communications*, *12*(1), 6752. https://doi.org/10.1038/s41467-021-27020-1

Hayat, S., Hayat, Q., Alyemeni, M. N., Wani, A. S., Pichtel, J., & Ahmad, A. (2012). Role of proline under changing environments: A review. *Plant Signaling and Behavior*, *7*(11). https://doi.org/10.4161/psb.21949

Heyno, E., Innocenti, G., Lemaire, S. D., Issakidis-Bourguet, E., & Krieger-Liszkay, A. (2014). Putative role of the malate valve enzyme NADP-malate dehydrogenase in H_2O_2 signaling in Arabidopsis. *Philosophical Transactions of the Royal Society of London. Series B, Biological Sciences*, *369*(1640), 20130228–20130228. https://doi.org/10.1098/RSTB.2013.0228

Houben, M., & van de Poel, B. (2019). 1-aminocyclopropane-1-carboxylic acid oxidase (*ACO*): The enzyme that makes the plant hormone ethylene. *Frontiers in Plant Science*, *10*, 695. https://doi.org/10.3389/FPLS.2019.00695

Huang, L.-J., Li, N., Thurow, C., Wirtz, M., Hell, R., & Gatz, C. (2016). Ectopically expressed glutaredoxin *ROXY19* negatively regulates the detoxification pathway in Arabidopsis thaliana. *BMC Plant Biology 2016 16:1*, *16*(1), 1–12. https://doi.org/10.1186/S12870-016-0886-1

Hussain, S. S., Ali, M., Ahmad, M., & Siddique, K. H. M. (2011). Polyamines: Natural and engineered abiotic and biotic stress tolerance in plants. *Biotechnology Advances*, *29*(3), 300–311. https://doi.org/10.1016/J.BIOTECHADV.2011.01.003

Imai, A., Matsuyama, T., Hanzawa, Y., Akiyama, T., Tamaoki, M., Saji, H., Shirano, Y., Kato, T., Hayashi, H., Shibata, D., Tabata, S., Komeda, Y., & Takahashi, T. (2004). *Spermidine synthase* genes are essential for survival of arabidopsis. *Plant Physiology*, *135*(3), 1565–1573. https://doi.org/10.1104/PP.104.041699

Iovieno, P., Punzo, P., Guida, G., Mistretta, C., van Oosten, M. J., Nurcato, R., Bostan, H., Colantuono, C., Costa, A., Bagnaresi, P., Chiusano, M. L., Albrizio, R., Giorio, P., Batelli, G., & Grillo, S. (2016). Transcriptomic changes drive physiological responses to progressive drought stress and rehydration in tomato. *Frontiers in Plant Science*, *7*(MAR2016), 371. https://doi.org/10.3389/FPLS.2016.00371

Iqbal, N., & Nazar, R. (2016). Osmolytes and Plants Acclimation to Changing Environment: Emerging Omics Technologies. In N. Iqbal, R. Nazar, & N. A. Khan (Eds.), *Osmolytes and Plants Acclimation to Changing Environment: Emerging Omics Technologies*. Springer India. https://doi.org/10.1007/978-81-322-2616-1

Iturriaga, G., Suárez, R., & Nova-Franco, B. (2009). Trehalose Metabolism: From Osmoprotection to Signaling. *International Journal of Molecular Sciences 2009, Vol. 10, Pages 3793-3810*, *10*(9), 3793–3810. https://doi.org/10.3390/IJMS10093793

Jafari, Z., Haddad, R., Hosseini, R., & Garoosi, G. (2013). Cloning, identification and expression analysis of *ACC oxidase* gene involved in ethylene production pathway. *Molecular Biology Reports*, *40*(2), 1341–1350. https://doi.org/10.1007/S11033-012-2178-7

Jang, H. J., Pih, K. T., Kang, S. G., Lim, J. H., Jin, J. B., Piao, H. L., & Hwang, I. (1998). Molecular cloning of a novel Ca^{2+}-binding protein that is induced by NaCl stress. *Plant Molecular Biology*, *37*(5), 839–847. https://doi.org/10.1023/A:1006043006211

Jogawat, A. (2019). Osmolytes and their Role in Abiotic Stress Tolerance in Plants. In *Molecular Plant Abiotic Stress* (pp. 91–104). Wiley. https://doi.org/10.1002/9781119463665.ch5

Jurić, S., Hazler-Pilepić, K., Tomašić, A., Lepeduš, H., Jeličić, B., Puthiyaveetil, S., Bionda, T., Vojta, L., Allen, J. F., Schleiff, E., & Fulgosi, H. (2009). Tethering of *ferredoxin:NADP$^+$ oxidoreductase* to thylakoid membranes is mediated by novel chloroplast protein *TROL*. *The Plant Journal: For Cell and Molecular Biology*, *60*(5), 783–794. https://doi.org/10.1111/J.1365-313X.2009.03999.X

Kamada-Nobusada, T., Hayashi, M., Fukazawa, M., Sakakibara, H., & Nishimura, M. (2008). A putative peroxisomal polyamine oxidase, *AtPAO4*, is involved in polyamine catabolism in Arabidopsis thaliana. *Plant & Cell Physiology*, *49*(9), 1272–1282. https://doi.org/10.1093/PCP/PCN114

Kang, W. H., Sim, Y. M., Koo, N., Nam, J. Y., Lee, J., Kim, N., Jang, H., Kim, Y. M., & Yeom, S. I. (2020). Transcriptome profiling of abiotic responses to heat, cold, salt, and osmotic stress of *Capsicum annuum* L. *Scientific Data 2020 7:1*, *7*(1), 1–7. https://doi.org/10.1038/s41597-020-0352-7

Kaur, G., & Asthir, B. (2017). Molecular responses to drought stress in plants. *Biologia Plantarum*, *61*(2), 201–209. https://doi.org/10.1007/s10535-016-0700-9

Keller, Y., Bouvier, F., D'Harlingue, A., & Camara, B. (1998). Metabolic compartmentation of plastid prenyllipid biosynthesis - Evidence for the involvement of a multifunctional *geranylgeranyl reductase*. *European Journal of Biochemistry*, *251*(1–2), 413–417. https://doi.org/10.1046/J.1432-1327.1998.2510413.X

Khan, R., Zhou, P., Ma, X., Zhou, L., Wu, Y., Ullah, Z., & Wang, S. (2019). Transcriptome Profiling, Biochemical and Physiological Analyses Provide New Insights towards Drought Tolerance in *Nicotiana tabacum* L. *Genes 2019, Vol. 10, Page 1041*, *10*(12), 1041. https://doi.org/10.3390/GENES10121041

Kim, D., Paggi, J. M., Park, C., Bennett, C., & Salzberg, S. L. (2019). Graph-based genome alignment and genotyping with HISAT2 and HISAT-genotype. *Nature Biotechnology 2019 37:8*, *37*(8), 907–915. https://doi.org/10.1038/s41587-019-0201-4

Kim, S. A., Punshon, T., Lanzirotti, A., Li, A., Alonso, J. M., Ecker, J. R., Kaplan, J., & Guerinot, M. lou. (2006). Localization of iron in Arabidopsis seed requires the vacuolar membrane transporter *VIT1*. *Science*, *314*(5803), 1295–1298. https://doi.org/10.1126/SCIENCE.1132563

Kirch, H. H., Bartels, D., Wei, Y., Schnable, P. S., & Wood, A. J. (2004). The *ALDH* gene superfamily of Arabidopsis. *Trends in Plant Science*, *9*(8), 371–377. https://doi.org/10.1016/J.TPLANTS.2004.06.004

Kochhar, A., Khurana, J. P., & Tyagi, A. K. (1996). Nucleotide sequence of the *psbP* gene encoding precursor of 23-kDa polypeptide of oxygen-evolving complex in *Arabidopsis thaliana* and its expression in the wild-type and a constitutively photomorphogenic mutant. *DNA Research*, *3*(5), 277–285. https://doi.org/10.1093/DNARES/3.5.277

Kumari, S., Kumar, V., Beilsmith, K., Seaver, S. M. D., Canon, S., Dehal, P., Gu, T., Joachimiak, M., Lerma-Ortiz, C., Liu, F., Lu, Z., Pearson, E., Ranjan, P., Riel, W., Henry, C. S., Arkin, A. P., & Ware, D. (2021). A KBase case study on genome-wide transcriptomics and plant primary metabolism in response to drought stress in Sorghum. *Current Plant Biology*, *28*, 100229. https://doi.org/10.1016/J.CPB.2021.100229

Kurepa, J., & Smalle, J. A. (2022). Auxin/Cytokinin Antagonistic Control of the Shoot/Root Growth Ratio and Its Relevance for Adaptation to Drought and Nutrient Deficiency Stresses. *International Journal of Molecular Sciences 2022, Vol. 23, Page 1933*, *23*(4), 1933. https://doi.org/10.3390/IJMS23041933

Kuroha, T., Tokunaga, H., Kojima, M., Ueda, N., Ishida, T., Nagawa, S., Fukuda, H., Sugimoto, K., & Sakakibara, H. (2009). Functional analyses of *LONELY GUY* cytokinin-activating enzymes reveal the importance of the direct activation pathway in Arabidopsis. *Plant Cell*, *21*(10), 3152–3169. https://doi.org/10.1105/TPC.109.068676

Kushiro, T., Okamoto, M., Nakabayashi, K., Yamagishi, K., Kitamura, S., Asami, T., Hirai, N., Koshiba, T., Kamiya, Y., & Nambara, E. (2004). The Arabidopsis cytochrome P450 *CYP707A* encodes *ABA 8'-hydroxylases*: key enzymes in ABA catabolism. *The EMBO Journal*, *23*(7), 1647–1656. https://doi.org/10.1038/SJ.EMBOJ.7600121

Landi, S., de Lillo, A., Nurcato, R., Grillo, S., & Esposito, S. (2017). In-field study on traditional Italian tomato landraces: The constitutive activation of the ROS scavenging machinery reduces effects of drought stress. *Plant Physiology and Biochemistry*, *118*, 150–160. https://doi.org/10.1016/J.PLAPHY.2017.06.011

Lee, J., Shim, D., Moon, S., Kim, H., Bae, W., Kim, K., Kim, Y.-H., Rhee, S.-K., Hong, C. P., Hong, S.-Y., Lee, Y.-J., Sung, J., & Ryu, H. (2018). Genome-wide transcriptomic analysis of BR-deficient Micro-Tom reveals correlations between drought stress tolerance and brassinosteroid signaling in tomato. *Plant Physiology and Biochemistry*, *127*, 553–560. https://doi.org/10.1016/j.plaphy.2018.04.031

Lee, S. C., Lan, W., Buchanan, B. B., & Luan, S. (2009). A protein kinase-phosphatase pair interacts with an ion channel to regulate ABA signaling in plant guard cells. *Proceedings of the National Academy of Sciences of the United States of America*, *106*(50), 21419–21424. https://doi.org/10.1073/PNAS.0910601106

Li, H., Yue, H., Xie, J., Bu, J., Li, L., Xin, X., Zhao, Y., Zhang, H., Yang, L., Wang, J., & Jiang, X. (2021). Transcriptomic profiling of the high-vigour maize (*Zea mays* L.) hybrid variety response to cold and drought stresses during seed germination. *Scientific Reports 2021 11:1*, *11*(1), 1–16. https://doi.org/10.1038/s41598-021-98907-8

Li, J., Besseau, S., Törönen, P., Sipari, N., Kollist, H., Holm, L., & Palva, E. T. (2013). Defense-related transcription factors *WRKY70* and *WRKY54* modulate osmotic stress tolerance by regulating stomatal aperture in Arabidopsis. *The New Phytologist*, *200*(2), 457–472. https://doi.org/10.1111/NPH.12378

Li, Y., Li, Y., Liu, Y., Wu, Y., & Xie, Q. (2018). The *sHSP22* Heat Shock Protein Requires the *ABI1* Protein Phosphatase to Modulate Polar Auxin Transport and Downstream Responses. *Plant Physiology*, *176*(3), 2406–2425. https://doi.org/10.1104/pp.17.01206

Li, Y., Yang, X., & Li, X. (2019). Role of jasmonate signaling pathway in resistance to dehydration stress in Arabidopsis. *Acta Physiologiae Plantarum*, *41*(6), 1–12. https://doi.org/10.1007/S11738-019-2897-7

Locascio, A., Marqués, M. C., García-Martínez, G., Corratgé-Faillie, C., Andrés-Colás, N., Rubio, L., Fernández, J. A., Véry, A. A., Mulet, J. M., & Yenush, L. (2019). *BCl$_2$-associated Athanogene 4* regulates the *KAT1* potassium channel and controls stomatal movement. *Plant Physiology*, *181*(3), 1277–1294. https://doi.org/10.1104/PP.19.00224

López-Serrano, L., Calatayud, Á., López-Galarza, S., Serrano, R., & Bueso, E. (2021). Uncovering salt tolerance mechanisms in pepper plants: a physiological and transcriptomic approach. *BMC Plant Biology*, *21*(1), 169. https://doi.org/10.1186/s12870-021-02938-2

López-Serrano, L., Canet-Sanchis, G., Selak, G. V., Penella, C., San Bautista, A., López-Galarza, S., & Calatayud, Á. (2020). Physiological characterization of a pepper hybrid rootstock designed to cope with salinity stress. *Plant Physiology and Biochemistry: PPB*, *148*, 207–219. https://doi.org/10.1016/j.plaphy.2020.01.016

Love, M. I., Huber, W., & Anders, S. (2014). Moderated estimation of fold change and dispersion for RNA-seq data with DESeq2. *Genome Biology*, *15*(12), 1–21. https://doi.org/10.1186/S13059-014-0550-8

Martin, M. (2011). Cutadapt removes adapter sequences from high-throughput sequencing reads. *EMBnet.Journal*, *17*(1), 10–12. https://doi.org/10.14806/EJ.17.1.200

McCormack, E., & Braam, J. (2003). Calmodulins and related potential calcium sensors of Arabidopsis. *New Phytologist*, *159*(3), 585–598. https://doi.org/10.1046/J.1469-8137.2003.00845.X

Mi, H., Muruganujan, A., Huang, X., Ebert, D., Mills, C., Guo, X., & Thomas, P. D. (2019). Protocol Update for large-scale genome and gene function analysis with the PANTHER classification system (v.14.0). *Nature Protocols 2019 14:3*, *14*(3), 703–721. https://doi.org/10.1038/s41596-019-0128-8

Mia, Md. S., Liu, H., Wang, X., Zhang, C., & Yan, G. (2020). Root transcriptome profiling of contrasting wheat genotypes provides an insight to their adaptive strategies to water deficit. *Scientific Reports*, *10*(1), 4854. https://doi.org/10.1038/s41598-020-61680-1

Missihoun, T. D., Willèe, E., Guegan, J. P., Berardocco, S., Shafiq, M. R., Bouchereau, A., & Bartels, D. (2015). Overexpression of *ALDH10A8* and *ALDH10A9* Genes Provides Insight into Their Role in Glycine Betaine Synthesis and Affects Primary Metabolism in *Arabidopsis thaliana*. *Plant & Cell Physiology*, *56*(9), 1798–1807. https://doi.org/10.1093/PCP/PCV105

Mochizuki, N., Brusslan, J. A., Larkin, R., Nagatani, A., & Chory, J. (2001). Arabidopsis *genomes uncoupled 5* (*GUN5*) mutant reveals the involvement of MG-chelatase H subunit in plastid-to-nucleus signal transduction. *Proceedings of the National Academy of Sciences of the United States of America*, *98*(4), 2053–2058. https://doi.org/10.1073/PNAS.98.4.2053

Mori, I. C., & Schroeder, J. I. (2004). Reactive Oxygen Species Activation of Plant Ca^{2+} Channels. A Signaling Mechanism in Polar Growth, Hormone Transduction, Stress Signaling, and Hypothetically Mechanotransduction. *Plant Physiology*, *135*(2), 702. https://doi.org/10.1104/PP.104.042069

Moriwaki, T., Miyazawa, Y., Kobayashi, A., Uchida, M., Watanabe, C., Fujii, N., & Takahashi, H. (2011). Hormonal regulation of lateral root development in Arabidopsis modulated by *MIZ1* and requirement of *GNOM* activity for *MIZ1* function. *Plant Physiology*, *157*(3), 1209–1220. https://doi.org/10.1104/PP.111.186270

Mulangi, V., Chibucos, M. C., Phuntumart, V., & Morris, P. F. (2012). Kinetic and phylogenetic analysis of plant polyamine uptake transporters. *Planta*, *236*(4), 1261–1273. https://doi.org/10.1007/S00425-012-1668-0

Müller, M., & Hasanuzzaman, M. (2021). Foes or Friends: ABA and Ethylene Interaction under Abiotic Stress. *Plants 2021, Vol. 10, Page 448*, *10*(3), 448. https://doi.org/10.3390/PLANTS10030448

Munekage, Y., Takeda, S., Endo, T., Jahns, P., Hashimoto, T., & Shikanai, T. (2001). Cytochrome b(6)f mutation specifically affects thermal dissipation of absorbed light energy in Arabidopsis. *The Plant Journal: For Cell and Molecular Biology*, *28*(3), 351–359. https://doi.org/10.1046/J.1365-313X.2001.01178.X

Nawrocki, W. J., Bailleul, B., Picot, D., Cardol, P., Rappaport, F., Wollman, F. A., & Joliot, P. (2019). The mechanism of cyclic electron flow. *Biochimica et Biophysica Acta (BBA) - Bioenergetics*, *1860*(5), 433–438. https://doi.org/10.1016/J.BBABIO.2018.12.005

Negi, J., Matsuda, O., Nagasawa, T., Oba, Y., Takahashi, H., Kawai-Yamada, M., Uchimiya, H., Hashimoto, M., & Iba, K. (2008). CO_2 regulator *SLAC1* and its homologues are essential for anion homeostasis in plant cells. *Nature*, *452*(7186), 483–486. https://doi.org/10.1038/NATURE06720

Nishizawa, A., Yabuta, Y., & Shigeoka, S. (2008). Galactinol and Raffinose Constitute a Novel Function to Protect Plants from Oxidative Damage. *Plant Physiology*, *147*(3), 1251–1263. https://doi.org/10.1104/pp.108.122465

Olson, B. J. S. C., Skavdahl, M., Ramberg, H., Osterman, J. C., & Markwell, J. (2000). Formate dehydrogenase in Arabidopsis thaliana: characterization and possible targeting to the chloroplast. *Plant Science: An International Journal of Experimental Plant Biology*, *159*(2), 205–212. https://doi.org/10.1016/S0168-9452(00)00337-X

Ortbauer, M. (2013). Abiotic Stress Adaptation: Protein Folding Stability and Dynamics. In *Abiotic Stress - Plant Responses and Applications in Agriculture*. InTech. https://doi.org/10.5772/53129

Ozturk, M., Turkyilmaz Unal, B., García-Caparrós, P., Khursheed, A., Gul, A., & Hasanuzzaman, M. (2021). Osmoregulation and its actions during the drought stress in plants. *Physiologia Plantarum*, *172*(2), 1321–1335. https://doi.org/10.1111/PPL.13297

Padilla, Y. G., Gisbert-Mullor, R., López-Serrano, L., López-Galarza, S., & Calatayud, Á. (2021). Grafting Enhances Pepper Water Stress Tolerance by Improving Photosynthesis and Antioxidant Defense Systems. *Antioxidants 2021, Vol. 10, Page 576*, *10*(4), 576. https://doi.org/10.3390/ANTIOX10040576

Penella, C., Nebauer, S. G., López-Galarza, S., San Bautista, A., Rodríguez-Burruezo, A., & Calatayud, A. (2014). Evaluation of some pepper genotypes as rootstocks in water stress conditions. *Horticultural Science*, *41*(No. 4), 192–200. https://doi.org/10.17221/163/2013-HORTSCI

Pirayesh, N., Giridhar, M., ben Khedher, A., Vothknecht, U. C., & Chigri, F. (2021). Organellar calcium signaling in plants: An update. *Biochimica et Biophysica Acta - Molecular Cell Research*, *1868*(4). https://doi.org/10.1016/J.BBAMCR.2021.118948

Pulido, P., Toledo-Ortiz, G., Phillips, M. A., Wright, L. P., & Rodríguez-Concepción, M. (2013). Arabidopsis J-protein *J20* delivers the first enzyme of the plastidial isoprenoid pathway to protein quality control. *The Plant Cell*, *25*(10), 4183–4194. https://doi.org/10.1105/TPC.113.113001

Quigley, F., Rosenberg, J. M., Shachar-Hill, Y., & Bohnert, H. J. (2001). From genome to function: the Arabidopsis aquaporins. *Genome Biology*, *3*(1), RESEARCH0001–RESEARCH0001. https://doi.org/10.1186/GB-2001-3-1-RESEARCH0001

Rentsch, D., Hirner, B., Schmelzer, E., & Frommer, W. B. (1996). Salt stress-induced proline transporters and salt stress-repressed broad specificity amino acid permeases identified by suppression of a yeast amino acid permease-targeting mutant. *The Plant Cell*, *8*(8), 1437–1446. https://doi.org/10.1105/TPC.8.8.1437

Rivero, R. M., Gimeno, J., van Deynze, A., Walia, H., & Blumwald, E. (2010). Enhanced Cytokinin Synthesis in Tobacco Plants Expressing *PSARK::IPT* Prevents the Degradation of Photosynthetic Protein Complexes During Drought. *Plant and Cell Physiology*, *51*(11), 1929–1941. https://doi.org/10.1093/PCP/PCQ143

Rocchetti, G., Ghilardelli, F., Bonini, P., Lucini, L., Masoero, F., & Gallo, A. (2021). Changes of Milk Metabolomic Profiles Resulting from a Mycotoxins-Contaminated Corn Silage Intake by Dairy Cows. *Metabolites*, *11*(8), 475. https://doi.org/10.3390/metabo11080475

Rocchetti, G., Zhang, L., Bocchi, S., Giuberti, G., Ak, G., Elbasan, F., Yıldıztugay, E., Ceylan, R., Picot-Allain, M. C. N., Mahomoodally, M. F., Lucini, L., & Zengin, G. (2022). The functional potential of nine Allium species related to their untargeted phytochemical characterization, antioxidant capacity and enzyme inhibitory ability. *Food Chemistry*, *368*, 130782. https://doi.org/10.1016/j.foodchem.2021.130782

Ruiz-partida, R., Rosario, S. M., & Lozano-juste, J. (2021). An Update on Crop ABA Receptors. *Plants 2021, Vol. 10, Page 1087*, *10*(6), 1087. https://doi.org/10.3390/PLANTS10061087

Růžička, K., Strader, L. C., Bailly, A., Yang, H., Blakeslee, J., Łangowski, Ł., Nejedlá, E., Fujita, H., Itoh, H., Syono, K., Hejátko, J., Gray, W. M., Martinoia, E., Geisler, M., Bartel, B., Murphy, A. S., & Friml, J. (2010). Arabidopsis *PIS1* encodes the *ABCG37* transporter of auxinic compounds including the auxin precursor indole-3-butyric acid. *Proceedings of the National Academy of Sciences of the United States of America*, *107*(23), 10749–10753. https://doi.org/10.1073/PNAS.1005878107

Sade, N., Vinocur, B. J., Diber, A., Shatil, A., Ronen, G., Nissan, H., Wallach, R., Karchi, H., & Moshelion, M. (2009). Improving plant stress tolerance and yield production: is the tonoplast aquaporin *SlTIP2;2* a key to isohydric to anisohydric conversion? *New Phytologist*, *181*(3), 651–661. https://doi.org/10.1111/J.1469-8137.2008.02689.X

Sagi, M., & Fluhr, R. (2006). Production of Reactive Oxygen Species by Plant NADPH Oxidases. *Plant Physiology*, *141*(2), 336–340. https://doi.org/10.1104/PP.106.078089

Sakuma, Y., Liu, Q., Dubouzet, J. G., Abe, H., Yamaguchi-Shinozaki, K., & Shinozaki, K. (2002). DNA-binding specificity of the ERF/AP2 domain of Arabidopsis *DREB*s, transcription factors involved in dehydration- and cold-inducible gene expression. *Biochemical and Biophysical Research Communications*, *290*(3), 998–1009. https://doi.org/10.1006/BBRC.2001.6299

Salehi-Lisar, S. Y., & Bakhshayeshan-Agdam, H. (2016). Drought stress in plants: Causes, consequences, and tolerance. *Drought Stress Tolerance in Plants, Vol 1: Physiology and Biochemistry*, *1*, 1–16. https://doi.org/10.1007/978-3-319-28899-4_1

Schwartz, S. H., Qin, X., & Zeevaart, J. A. D. (2001). Characterization of a novel carotenoid cleavage dioxygenase from plants. *The Journal of Biological Chemistry*, *276*(27), 25208–25211. https://doi.org/10.1074/JBC.M102146200

Schweighofer, A., Hirt, H., & Meskiene, I. (2004). Plant *PP2C phosphatases*: Emerging functions in stress signaling. *Trends in Plant Science*, *9*(5), 236–243. https://doi.org/10.1016/j.tplants.2004.03.007

Seleiman, M. F., Al-Suhaibani, N., Ali, N., Akmal, M., Alotaibi, M., Refay, Y., Dindaroglu, T., Abdul-Wajid, H. H., & Battaglia, M. L. (2021). Drought Stress Impacts on Plants and Different Approaches to Alleviate Its Adverse Effects. *Plants 2021, Vol. 10, Page 259*, *10*(2), 259. https://doi.org/10.3390/PLANTS10020259

Seo, M., Jikumaru, Y., & Kamiya, Y. (2011). Profiling of hormones and related metabolites in seed dormancy and germination studies. *Methods in Molecular Biology*, *773*, 99–111. https://doi.org/10.1007/978-1-61779-231-1_7

Song, K., Kim, H. C., Shin, S., Kim, K. H., Moon, J. C., Kim, J. Y., & Lee, B. M. (2017). Transcriptome analysis of flowering time genes under drought stress in maize leaves. *Frontiers in Plant Science*, *8*, 267. https://doi.org/10.3389/FPLS.2017.00267

Staswick, P. E., Serban, B., Rowe, M., Tiryaki, I., Maldonado, M. T., Maldonado, M. C., & Suza, W. (2005). Characterization of an Arabidopsis enzyme family that conjugates amino acids to indole-3-acetic acid. *The Plant Cell*, *17*(2), 616–627. https://doi.org/10.1105/TPC.104.026690

Sun, W., van Montagu, M., & Verbruggen, N. (2002). Small heat shock proteins and stress tolerance in plants. *Biochimica et Biophysica Acta (BBA) - Gene Structure and Expression*, *1577*(1), 1–9. https://doi.org/10.1016/S0167-4781(02)00417-7

Taji, T., Ohsumi, C., Iuchi, S., Seki, M., Kasuga, M., Kobayashi, M., Yamaguchi-Shinozaki, K., & Shinozaki, K. (2002). Important roles of drought- and cold-inducible genes for *galactinol synthase* in stress tolerance in *Arabidopsis thaliana*. *The Plant Journal: For Cell and Molecular Biology*, *29*(4), 417–426. https://doi.org/10.1046/J.0960-7412.2001.01227.X

Takano, J., Yoshinari, A., Luu, D.-T., Takano, J., & Yoshinari, A. (2017). *Plant Aquaporin Trafficking*. 47–81. https://doi.org/10.1007/978-3-319-49395-4_3

Takei, K., Sakakibara, H., & Sugiyama, T. (2001). Identification of genes encoding *adenylate isopentenyltransferase*, a cytokinin biosynthesis enzyme, in *Arabidopsis thaliana*. *The Journal of Biological Chemistry*, *276*(28), 26405–26410. https://doi.org/10.1074/JBC.M102130200

Tamang, B. G., Li, S., Rajasundaram, D., Lamichhane, S., & Fukao, T. (2021). Overlapping and stress-specific transcriptomic and hormonal responses to flooding and drought in soybean. *The Plant Journal*, *107*(1), 100–117. https://doi.org/10.1111/TPJ.15276

Thomas, S. C., Alhasawi, A., Auger, C., Omri, A., & Appanna, V. D. (2016). The role of formate in combatting oxidative stress. *Antonie van Leeuwenhoek*, *109*(2), 263–271. https://doi.org/10.1007/s10482-015-0629-6

Tognetti, V. B., Mühlenbock, P., & van Breusegem, F. (2012). Stress homeostasis - the redox and auxin perspective. *Plant, Cell & Environment*, *35*(2), 321–333. https://doi.org/10.1111/j.1365-3040.2011.02324.x

Tognetti, V. B., van Aken, O., Morreel, K., Vandenbroucke, K., van de Cotte, B., de Clercq, I., Chiwocha, S., Fenske, R., Prinsen, E., Boerjan, W., Genty, B., Stubbs, K. A., Inzé, D., & van Breusegem, F. (2010). Perturbation of Indole-3-Butyric Acid Homeostasis by the UDP-Glucosyltransferase *UGT74E2* Modulates *Arabidopsis* Architecture and Water Stress Tolerance. *The Plant Cell*, *22*(8), 2660–2679. https://doi.org/10.1105/tpc.109.071316

Tsuzuki, T., Takahashi, K., Inoue, S. ichiro, Okigaki, Y., Tomiyama, M., Hossain, M. A., Shimazaki, K. ichiro, Murata, Y., & Kinoshita, T. (2011). Mg-chelatase H subunit affects ABA signaling in stomatal guard cells, but is not an ABA receptor in *Arabidopsis thaliana*. *Journal of Plant Research*, *124*(4), 527–538. https://doi.org/10.1007/S10265-011-0426-X

Tzvetkova-Chevolleau, T., Franck, F., Alawady, A. E., Dall'Osto, L., Carrière, F., Bassi, R., Grimm, B., Nussaume, L., & Havaux, M. (2007). The light stress-induced protein *ELIP2* is a regulator of chlorophyll synthesis in *Arabidopsis thaliana*. *The Plant Journal*, *50*(5), 795–809. https://doi.org/10.1111/j.1365-313X.2007.03090.x

van Houtte, H., Vandesteene, L., López-Galvis, L., Lemmens, L., Kissel, E., Carpentier, S., Feil, R., Avonce, N., Beeckman, T., Lunn, J. E., & van Dijck, P. (2013). Overexpression of the Trehalase Gene *AtTRE1* Leads to Increased Drought Stress Tolerance in Arabidopsis and Is Involved in Abscisic Acid-Induced Stomatal Closure. *Plant Physiology*, *161*(3), 1158–1171. https://doi.org/10.1104/PP.112.211391

Varoquaux, N., Cole, B., Gao, C., Pierroz, G., Baker, C. R., Patel, D., Madera, M., Jeffers, T., Hollingsworth, J., Sievert, J., Yoshinaga, Y., Owiti, J. A., Singan, V. R., DeGraaf, S., Xu, L., Blow, M. J., Harrison, M. J., Visel, A., Jansson, C., … Purdom, E. (2019). Transcriptomic analysis of field-droughted sorghum from seedling to maturity reveals biotic and metabolic responses. *Proceedings of the National Academy of Sciences of the United States of America*, *116*(52), 27124–27132. https://doi.org/10.1073/PNAS.1907500116

Varotto, C., Pesaresi, P., Jahns, P., Leßnick, A., Tizzano, M., Schiavon, F., Salamini, F., & Leister, D. (2002). Single and double knockouts of the genes for *photosystem I subunits G, K,* and *H* of Arabidopsis. Effects on photosystem I composition, photosynthetic electron flow, and state transitions. *Plant Physiology*, *129*(2), 616–624. https://doi.org/10.1104/PP.002089

Verma, V., Ravindran, P., & Kumar, P. P. (2016). Plant hormone-mediated regulation of stress responses. *BMC Plant Biology*, *16*(1), 1–10. https://doi.org/10.1186/S12870-016-0771-Y

Vernoux, T., Wilson, R. C., Seeley, K. A., Reichheld, J.-P., Muroy, S., Brown, S., Maughan, S. C., Cobbett, C. S., van Montagu, M., Inzé, D., May, M. J., & Sung, Z. R. (2000). The *ROOT MERISTEMLESS1/CADMIUM SENSITIVE2* gene defines a glutathione-dependent pathway involved in initiation and maintenance of cell division during postembryonic root development. *The Plant Cell*, *12*(1), 97–110. https://doi.org/10.1105/TPC.12.1.97

Vogel, G., Aeschbacher, R. A., Müller, J., Boller, T., & Wiemken, A. (1998). *Trehalose-6-phosphate phosphatases* from *Arabidopsis thaliana*: identification by functional complementation of the yeast *tps2* mutant. *The Plant Journal*, *13*(5), 673–683. https://doi.org/10.1046/J.1365-313X.1998.00064.X

Wang, Q., Yang, S., Wan, S., & Li, X. (2019). The Significance of Calcium in Photosynthesis. *International Journal of Molecular Sciences 2019, Vol. 20, Page 1353*, *20*(6), 1353. https://doi.org/10.3390/IJMS20061353

Wang, W., Vinocur, B., Shoseyov, O., & Altman, A. (2004). Role of plant heat-shock proteins and molecular chaperones in the abiotic stress response. *Trends in Plant Science*, *9*(5), 244–252. https://doi.org/10.1016/j.tplants.2004.03.006

Wang, X., Song, S., Wang, X., Liu, J., & Dong, S. (2022). Transcriptomic and Metabolomic Analysis of Seedling-Stage Soybean Responses to PEG-Simulated Drought Stress. *International Journal of Molecular Sciences 2022, Vol. 23, Page 6869*, *23*(12), 6869. https://doi.org/10.3390/IJMS23126869

Werner, T., Motyka, V., Laucou, V., Smets, R., van Onckelen, H., & Schmülling, T. (2003). Cytokinin-deficient transgenic Arabidopsis plants show multiple developmental alterations indicating opposite functions of cytokinins in the regulation of shoot and root meristem activity. *The Plant Cell*, *15*(11), 2532–2550. https://doi.org/10.1105/TPC.014928

Wu, A., Allu, A. D., Garapati, P., Siddiqui, H., Dortay, H., Zanor, M. I., Asensi-Fabado, M. A., Munná-Bosch, S., Antonio, C., Tohge, T., Fernie, A. R., Kaufmann, K., Xue, G. P., Mueller-Roeber, B., & Balazadeh, S. (2012). *JUNGBRUNNEN1*, a Reactive Oxygen Species-responsive NAC transcription factor, regulates longevity in Arabidopsis. *Plant Cell*, *24*(2), 482–506. https://doi.org/10.1105/TPC.111.090894

Xia, X. J., Zhou, Y. H., Shi, K., Zhou, J., Foyer, C. H., & Yu, J. Q. (2015). Interplay between reactive oxygen species and hormones in the control of plant development and stress tolerance. *Journal of Experimental Botany*, *66*(10), 2839–2856. https://doi.org/10.1093/JXB/ERV089

Xu, C., Fan, J., Riekhof, W., Froehlich, J. E., & Benning, C. (2003). A permease-like protein involved in ER to thylakoid lipid transfer in Arabidopsis. *The EMBO Journal*, *22*(10), 2370–2379. https://doi.org/10.1093/EMBOJ/CDG234

Xu, C., Xia, C., Xia, Z., Zhou, X., Huang, J., Huang, Z., Liu, Y., Jiang, Y., Casteel, S., & Zhang, C. (2018). Physiological and transcriptomic responses of reproductive stage soybean to drought stress. *Plant Cell Reports*, *37*(12), 1611–1624. https://doi.org/10.1007/S00299-018-2332-3

Yamamoto, H., Peng, L., Fukao, Y., & Shikanai, T. (2011). An Src homology 3 domain-like fold protein forms a ferredoxin binding site for the chloroplast NADH dehydrogenase-like complex in Arabidopsis. *Plant Cell*, *23*(4), 1480–1493. https://doi.org/10.1105/TPC.110.080291

Yan, J., He, C., & Zhang, H. (2003). The BAG-family proteins in *Arabidopsis thaliana*. *Plant Science*, *165*(1), 1–7. https://doi.org/10.1016/S0168-9452(03)00121-3

Yang, H., Zhao, L., Zhao, S., Wang, J., & Shi, H. (2017). Biochemical and transcriptomic analyses of drought stress responses of LY1306 tobacco strain. *Scientific Reports 2017 7:1*, *7*(1), 1–10. https://doi.org/10.1038/s41598-017-17045-2

Yang, X., Lu, M., Wang, Y., Wang, Y., Liu, Z., & Chen, S. (2021). Response Mechanism of Plants to Drought Stress. *Horticulturae*, *7*(3), 50. https://doi.org/10.3390/horticulturae7030050

Yates, A. D., Allen, J., Amode, R. M., Azov, A. G., Barba, M., Becerra, A., Bhai, J., Campbell, L. I., Carbajo Martinez, M., Chakiachvili, M., Chougule, K., Christensen, M., Contreras-Moreira, B., Cuzick, A., da Rin Fioretto, L., Davis, P., de Silva, N. H., Diamantakis, S., Dyer, S., … Flicek, P. (2022). Ensembl Genomes 2022: an expanding genome resource for non-vertebrates. *Nucleic Acids Research*, *50*(D1), D996–D1003. https://doi.org/10.1093/NAR/GKAB1007

You, J., Zhang, Y., Liu, A., Li, D., Wang, X., Dossa, K., Zhou, R., Yu, J., Zhang, Y., Wang, L., & Zhang, X. (2019). Transcriptomic and metabolomic profiling of drought-tolerant and susceptible sesame genotypes in response to drought stress. *BMC Plant Biology*, *19*(1), 267. https://doi.org/10.1186/s12870-019-1880-1

Zenda, T., Liu, S., Wang, X., Liu, G., Jin, H., Dong, A., Yang, Y., & Duan, H. (2019). Key Maize Drought-Responsive Genes and Pathways Revealed by Comparative Transcriptome and Physiological Analyses of Contrasting Inbred Lines. *International Journal of Molecular Sciences 2019, Vol. 20, Page 1268*, *20*(6), 1268. https://doi.org/10.3390/IJMS20061268

Zhang, D., Zeng, T., Liu, X., Gao, C., Li, Y., Li, C., Song, Y., Shi, Y., Wang, T., & Li, Y. (2019). Transcriptomic profiling of sorghum leaves and roots responsive to drought stress at the seedling stage. *Journal of Integrative Agriculture*, *18*(9), 1980–1995. https://doi.org/10.1016/S2095-3119(18)62119-7

Zhang, S., Ai, G., Li, M., Ye, Z., & Zhang, J. (2018). Tomato *LrgB* regulates heat tolerance and the assimilation and partitioning of carbon. *Plant Science*, *274*, 309–319. https://doi.org/10.1016/J.PLANTSCI.2018.06.001

Zhao, Z., Zhang, Y., Liu, X., Zhang, X., Liu, S., Yu, X., Ren, Y., Zheng, X., Zhou, K., Jiang, L., Guo, X., Gai, Y., Wu, C., Zhai, H., Wang, H., & Wan, J. (2013). A role for a dioxygenase in auxin metabolism and reproductive development in rice. *Developmental Cell*, *27*(1), 113–122. https://doi.org/10.1016/J.DEVCEL.2013.09.005

Zheng, H., Yang, Z., Wang, W., Guo, S., Li, Z., Liu, K., & Sui, N. (2020). Transcriptome analysis of maize inbred lines differing in drought tolerance provides novel insights into the molecular mechanisms of drought responses in roots. *Plant Physiology and Biochemistry*, *149*, 11–26. https://doi.org/10.1016/J.PLAPHY.2020.01.027

Zhu, S. Y., Yu, X. C., Wang, X. J., Zhao, R., Li, Y., Fan, R. C., Shang, Y., Du, S. Y., Wang, X. F., Wu, F. Q., Xu, Y. H., Zhang, X. Y., & Zhang, D. P. (2007). Two calcium-dependent protein kinases, *CPK4* and *CPK11*, regulate abscisic acid signal transduction in Arabidopsis. *The Plant Cell*, *19*(10), 3019–3036. https://doi.org/10.1105/TPC.107.050666

Zulfiqar, F., Akram, N. A., & Ashraf, M. (2019). Osmoprotection in plants under abiotic stresses: new insights into a classical phenomenon. *Planta 2019 251:1*, *251*(1), 1–17. https://doi.org/10.1007/S00425-019-03293-1

3.8. Supplementary Material

Supplementary Figure 1. GO test on Molecular Function statistically over- and under-represented categories with $p < 0.01$.

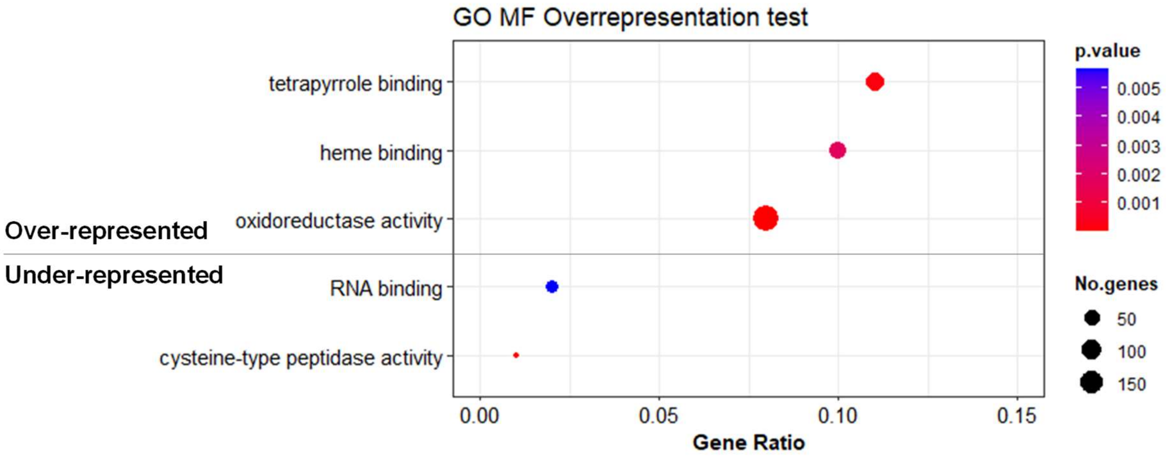

Supplementary Fig. 1. GO Overrepresentation test for the DEGs resulting from NIBER® in relation to A10 comparison under the control conditions showing the statistically over-and under-represented categories for Molecular Function. The Gene Ratio is the percentage of DEGs in relation to the total number of genes associated with the GO term in the *Capsicum annuum* genome.

Supplementary Figure 2. GO test on Cellular Component statistically over- and under-represented categories with $p < 0.05$.

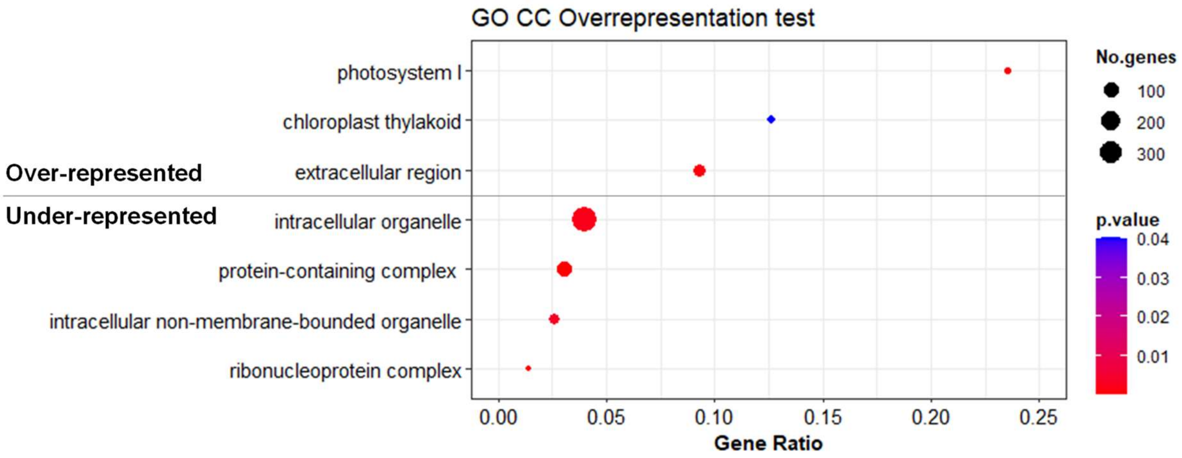

Supplementary Fig. 2. GO Overrepresentation test for the DEGs resulting from NIBER® in relation to A10 comparison under the control conditions showing the statistically over-and under-represented categories for Cellular Component. The Gene Ratio is the percentage of DEGs in relation to the total number of genes associated with the GO term in the *Capsicum annuum* genome.

Supplementary Table 1. **A**. Differentially expressed genes between both genotypes under the control conditions at T0 (NIBER®/A10).

Gene ID	log2FoldChange	lfcSE	stat	pvalue	padj
T459_02562	-9.2389	1.2196	-7.5757	0.0000	0.0000
T459_16565	-9.1845	1.2043	-7.6261	0.0000	0.0000
T459_02807	-9.1217	0.7308	-12.4817	0.0000	0.0000
T459_13944	-9.0628	1.2380	-7.3208	0.0000	0.0000
T459_28063	-8.9827	1.2167	-7.3830	0.0000	0.0000
T459_03230	-8.9534	1.2211	-7.3322	0.0000	0.0000
T459_00511	-8.6731	1.0348	-8.3818	0.0000	0.0000
T459_33789	-8.5670	1.0418	-8.2236	0.0000	0.0000
T459_02150	-8.5329	1.2214	-6.9861	0.0000	0.0000
T459_02802	-8.5198	0.8523	-9.9963	0.0000	0.0000
T459_28184	-8.4750	1.2017	-7.0526	0.0000	0.0000
T459_16780	-8.4093	0.8599	-9.7795	0.0000	0.0000
T459_13152	-8.3619	1.2863	-6.5009	0.0000	0.0000
T459_35644	-8.3522	1.2028	-6.9441	0.0000	0.0000
T459_24250	-7.5831	1.2319	-6.1558	0.0000	0.0000
T459_07196	-7.4627	1.2639	-5.9047	0.0000	0.0000
T459_28067	-7.4178	1.2587	-5.8934	0.0000	0.0000
T459_28065	-7.4035	1.2372	-5.9840	0.0000	0.0000
T459_16564	-7.1451	1.0531	-6.7850	0.0000	0.0000
T459_27777	-7.1181	0.3926	-18.1317	0.0000	0.0000
T459_29008	-7.0583	1.0582	-6.6699	0.0000	0.0000
T459_27571	-7.0259	1.2329	-5.6986	0.0000	0.0000
T459_28064	-7.0080	1.3359	-5.2458	0.0000	0.0000
T459_30788	-7.0011	0.5382	-13.0081	0.0000	0.0000
T459_02116	-6.9686	1.3106	-5.3172	0.0000	0.0000
T459_23514	-6.9225	1.2362	-5.5998	0.0000	0.0000
T459_04535	-6.5432	1.2702	-5.1511	0.0000	0.0000
T459_00869	-6.5375	1.0784	-6.0623	0.0000	0.0000
T459_16623	-6.5181	1.3436	-4.8512	0.0000	0.0000
T459_33575	-6.5143	1.2630	-5.1578	0.0000	0.0000
T459_14838	-6.3782	1.0940	-5.8301	0.0000	0.0000
T459_05002	-6.2478	0.5501	-11.3584	0.0000	0.0000
T459_03868	-6.1039	1.3822	-4.4159	0.0000	0.0002
T459_28863	-6.0834	0.6074	-10.0154	0.0000	0.0000
T459_33710	-6.0548	0.8979	-6.7432	0.0000	0.0000
T459_29009	-6.0262	1.4071	-4.2826	0.0000	0.0004
T459_15988	-5.9485	0.5712	-10.4145	0.0000	0.0000
T459_01116	-5.9443	0.6696	-8.8772	0.0000	0.0000
T459_07208	-5.8678	0.7993	-7.3415	0.0000	0.0000
T459_15624	-5.8330	1.2981	-4.4935	0.0000	0.0002
T459_26329	-5.8182	0.2556	-22.7601	0.0000	0.0000
T459_33470	-5.7155	1.3161	-4.3427	0.0000	0.0003
T459_08737	-5.6905	1.3253	-4.2939	0.0000	0.0004
T459_16303	-5.6368	1.3320	-4.2319	0.0000	0.0005

Gene ID	log2FoldChange	lfcSE	stat	pvalue	padj
T459_31883	-5.6190	0.6478	-8.6742	0.0000	0.0000
T459_32584	-5.6178	1.1495	-4.8871	0.0000	0.0000
T459_22353	-5.6017	0.5324	-10.5211	0.0000	0.0000
T459_26326	-5.5913	0.5267	-10.6149	0.0000	0.0000
T459_25500	-5.5896	0.7618	-7.3376	0.0000	0.0000
T459_15625	-5.5847	1.3148	-4.2474	0.0000	0.0004
T459_30283	-5.5562	1.3212	-4.2054	0.0000	0.0005
T459_12254	-5.5200	1.5013	-3.6769	0.0002	0.0037
T459_29702	-5.1750	0.6986	-7.4079	0.0000	0.0000
T459_33853	-5.1647	0.6795	-7.6003	0.0000	0.0000
T459_35491	-5.1396	1.5399	-3.3375	0.0008	0.0110
T459_11884	-5.1154	0.3864	-13.2398	0.0000	0.0000
T459_01928	-5.1140	0.4474	-11.4308	0.0000	0.0000
T459_01133	-5.1068	0.3317	-15.3958	0.0000	0.0000
T459_26921	-5.0704	0.5885	-8.6156	0.0000	0.0000
T459_35735	-4.9003	0.3294	-14.8784	0.0000	0.0000
T459_05160	-4.7175	0.7535	-6.2609	0.0000	0.0000
T459_22186	-4.7078	0.4373	-10.7660	0.0000	0.0000
T459_03043	-4.6189	0.8357	-5.5273	0.0000	0.0000
T459_15989	-4.6056	0.7933	-5.8058	0.0000	0.0000
T459_05205	-4.5341	0.4012	-11.3003	0.0000	0.0000
T459_26331	-4.2073	0.2610	-16.1171	0.0000	0.0000
T459_28234	-4.1701	0.3427	-12.1667	0.0000	0.0000
T459_05875	-4.1673	0.4349	-9.5828	0.0000	0.0000
T459_05161	-4.1075	0.5390	-7.6201	0.0000	0.0000
T459_32999	-4.0881	0.5636	-7.2541	0.0000	0.0000
T459_25292	-4.0563	0.3900	-10.3998	0.0000	0.0000
T459_04588	-4.0477	0.3939	-10.2766	0.0000	0.0000
T459_03997	-3.9891	0.4354	-9.1612	0.0000	0.0000
T459_31895	-3.9293	0.7355	-5.3427	0.0000	0.0000
T459_31982	-3.9184	0.7897	-4.9617	0.0000	0.0000
T459_35227	-3.8985	1.0441	-3.7339	0.0002	0.0031
T459_31977	-3.8882	0.7526	-5.1662	0.0000	0.0000
T459_03151	-3.8068	0.5380	-7.0754	0.0000	0.0000
T459_34633	-3.7691	0.6286	-5.9961	0.0000	0.0000
T459_14461	-3.6299	0.2640	-13.7498	0.0000	0.0000
T459_09705	-3.6077	0.5136	-7.0243	0.0000	0.0000
T459_15753	-3.4798	0.6499	-5.3547	0.0000	0.0000
T459_03219	-3.4430	0.7913	-4.3512	0.0000	0.0003
T459_20332	-3.4183	0.7031	-4.8617	0.0000	0.0000
T459_30903	-3.4173	0.8965	-3.8119	0.0001	0.0023
T459_21019	-3.3392	0.8655	-3.8582	0.0001	0.0020
T459_13878	-3.2906	0.1925	-17.0920	0.0000	0.0000
T459_00541	-3.2666	0.4724	-6.9151	0.0000	0.0000
T459_17608	-3.2325	1.1154	-2.8980	0.0038	0.0384
T459_03656	-3.1955	0.8599	-3.7160	0.0002	0.0033
T459_22573	-3.1944	0.4440	-7.1948	0.0000	0.0000

Gene ID	log2FoldChange	lfcSE	stat	pvalue	padj
T459_24273	-3.1181	0.7126	-4.3754	0.0000	0.0003
T459_22512	-3.0930	0.5511	-5.6122	0.0000	0.0000
T459_28257	-3.0523	0.5532	-5.5177	0.0000	0.0000
T459_02665	-3.0322	0.3967	-7.6439	0.0000	0.0000
T459_01745	-2.9828	0.5031	-5.9290	0.0000	0.0000
T459_34437	-2.9590	0.5987	-4.9428	0.0000	0.0000
T459_03550	-2.9099	0.5707	-5.0986	0.0000	0.0000
T459_34064	-2.8904	0.7058	-4.0951	0.0000	0.0008
T459_26953	-2.8659	0.6764	-4.2371	0.0000	0.0005
T459_18532	-2.8394	0.5072	-5.5978	0.0000	0.0000
T459_26091	-2.8353	0.5803	-4.8860	0.0000	0.0000
T459_19585	-2.8321	0.1453	-19.4883	0.0000	0.0000
T459_28618	-2.8191	0.4561	-6.1806	0.0000	0.0000
T459_26777	-2.8046	0.6876	-4.0787	0.0000	0.0009
T459_20228	-2.7683	0.4545	-6.0911	0.0000	0.0000
T459_34189	-2.7668	0.6387	-4.3317	0.0000	0.0003
T459_34632	-2.7564	0.3969	-6.9445	0.0000	0.0000
T459_01638	-2.7450	0.2396	-11.4551	0.0000	0.0000
T459_10257	-2.7447	0.2284	-12.0145	0.0000	0.0000
T459_03551	-2.7296	0.9171	-2.9763	0.0029	0.0311
T459_29116	-2.7287	0.5530	-4.9346	0.0000	0.0000
T459_02476	-2.7193	0.1227	-22.1603	0.0000	0.0000
T459_29829	-2.7176	0.5901	-4.6053	0.0000	0.0001
T459_23921	-2.6802	0.5307	-5.0501	0.0000	0.0000
T459_18943	-2.6701	0.3393	-7.8691	0.0000	0.0000
T459_29548	-2.6589	0.5350	-4.9703	0.0000	0.0000
T459_31089	-2.6464	0.3807	-6.9512	0.0000	0.0000
T459_15787	-2.6354	0.5086	-5.1818	0.0000	0.0000
T459_05004	-2.6198	0.5904	-4.4370	0.0000	0.0002
T459_05223	-2.5912	0.3513	-7.3762	0.0000	0.0000
T459_05876	-2.5714	0.3700	-6.9487	0.0000	0.0000
T459_10270	-2.5445	0.6968	-3.6514	0.0003	0.0041
T459_34272	-2.5165	0.7898	-3.1865	0.0014	0.0174
T459_17149	-2.5016	0.4759	-5.2568	0.0000	0.0000
T459_29316	-2.4907	0.5360	-4.6464	0.0000	0.0001
T459_09775	-2.4884	0.5984	-4.1582	0.0000	0.0006
T459_34443	-2.4587	0.5786	-4.2497	0.0000	0.0004
T459_34683	-2.4532	0.1839	-13.3427	0.0000	0.0000
T459_21241	-2.4426	0.2510	-9.7319	0.0000	0.0000
T459_12727	-2.4350	0.1803	-13.5056	0.0000	0.0000
T459_09737	-2.4251	0.8043	-3.0150	0.0026	0.0281
T459_05222	-2.4178	0.2884	-8.3835	0.0000	0.0000
T459_34760	-2.4055	0.5326	-4.5163	0.0000	0.0001
T459_27616	-2.4045	0.5176	-4.6454	0.0000	0.0001
T459_01614	-2.4029	0.7386	-3.2534	0.0011	0.0143
T459_33161	-2.3754	0.3870	-6.1373	0.0000	0.0000
T459_10040	-2.3753	0.5826	-4.0773	0.0000	0.0009

Gene ID	log2FoldChange	lfcSE	stat	pvalue	padj
T459_14112	-2.3660	0.4219	-5.6083	0.0000	0.0000
T459_18672	-2.3507	0.3682	-6.3838	0.0000	0.0000
T459_26328	-2.3444	0.4608	-5.0871	0.0000	0.0000
T459_16092	-2.3381	0.3853	-6.0678	0.0000	0.0000
T459_22747	-2.3149	0.3872	-5.9784	0.0000	0.0000
T459_33278	-2.2982	0.6116	-3.7578	0.0002	0.0028
T459_31118	-2.2432	0.4082	-5.4960	0.0000	0.0000
T459_14111	-2.2383	0.6234	-3.5906	0.0003	0.0049
T459_07877	-2.2327	0.6387	-3.4956	0.0005	0.0067
T459_06143	-2.2241	0.4519	-4.9220	0.0000	0.0000
T459_04466	-2.2019	0.2509	-8.7764	0.0000	0.0000
T459_24052	-2.1999	0.7841	-2.8057	0.0050	0.0481
T459_07603	-2.1810	0.5090	-4.2850	0.0000	0.0004
T459_19397	-2.1807	0.3767	-5.7893	0.0000	0.0000
T459_03540	-2.1797	0.6020	-3.6210	0.0003	0.0045
T459_21035	-2.1776	0.2687	-8.1033	0.0000	0.0000
T459_29809	-2.1768	0.3791	-5.7420	0.0000	0.0000
T459_07844	-2.1698	0.2976	-7.2912	0.0000	0.0000
T459_29293	-2.1642	0.4878	-4.4367	0.0000	0.0002
T459_25314	-2.1553	0.2865	-7.5230	0.0000	0.0000
T459_12710	-2.1459	0.4174	-5.1408	0.0000	0.0000
T459_34097	-2.1410	0.3023	-7.0817	0.0000	0.0000
T459_32578	-2.1363	0.2907	-7.3496	0.0000	0.0000
T459_31191	-2.1212	0.3877	-5.4713	0.0000	0.0000
T459_04004	-2.1044	0.4053	-5.1928	0.0000	0.0000
T459_25295	-2.0969	0.4218	-4.9712	0.0000	0.0000
T459_13126	-2.0966	0.4489	-4.6704	0.0000	0.0001
T459_22562	-2.0886	0.1805	-11.5718	0.0000	0.0000
T459_07163	-2.0877	0.3143	-6.6433	0.0000	0.0000
T459_33259	-2.0843	0.5110	-4.0788	0.0000	0.0009
T459_04854	-2.0802	0.3421	-6.0806	0.0000	0.0000
T459_28926	-2.0801	0.3094	-6.7229	0.0000	0.0000
T459_01683	-2.0796	0.3437	-6.0511	0.0000	0.0000
T459_26047	-2.0789	0.3617	-5.7481	0.0000	0.0000
T459_33400	-2.0592	0.5781	-3.5620	0.0004	0.0054
T459_03936	-2.0508	0.4937	-4.1536	0.0000	0.0007
T459_15343	-2.0507	0.2225	-9.2184	0.0000	0.0000
T459_05058	-2.0483	0.6896	-2.9703	0.0030	0.0316
T459_29549	-2.0307	0.4785	-4.2441	0.0000	0.0005
T459_07123	-2.0051	0.5413	-3.7040	0.0002	0.0034
T459_30756	-1.9982	0.5524	-3.6174	0.0003	0.0046
T459_12694	-1.9912	0.4151	-4.7971	0.0000	0.0000
T459_08797	-1.9817	0.6821	-2.9052	0.0037	0.0377
T459_26502	-1.9611	0.2868	-6.8374	0.0000	0.0000
T459_04714	-1.9579	0.5236	-3.7395	0.0002	0.0030
T459_18834	-1.9423	0.6501	-2.9877	0.0028	0.0303
T459_33260	-1.9408	0.2764	-7.0213	0.0000	0.0000

Gene ID	log2FoldChange	lfcSE	stat	pvalue	padj
T459_30718	-1.9371	0.1913	-10.1250	0.0000	0.0000
T459_24769	-1.9356	0.4923	-3.9318	0.0001	0.0015
T459_33852	-1.9308	0.6832	-2.8260	0.0047	0.0458
T459_32099	-1.9265	0.5203	-3.7024	0.0002	0.0034
T459_05021	-1.9075	0.3529	-5.4059	0.0000	0.0000
T459_01927	-1.9014	0.0926	-20.5397	0.0000	0.0000
T459_31710	-1.9000	0.3614	-5.2572	0.0000	0.0000
T459_21143	-1.8916	0.3798	-4.9801	0.0000	0.0000
T459_25458	-1.8752	0.1452	-12.9149	0.0000	0.0000
T459_20351	-1.8585	0.2506	-7.4154	0.0000	0.0000
T459_13884	-1.8554	0.5299	-3.5017	0.0005	0.0066
T459_27780	-1.8412	0.5426	-3.3933	0.0007	0.0093
T459_34694	-1.8362	0.4969	-3.6955	0.0002	0.0035
T459_08904	-1.8309	0.2974	-6.1559	0.0000	0.0000
T459_19291	-1.8291	0.1680	-10.8886	0.0000	0.0000
T459_24229	-1.8256	0.6440	-2.8347	0.0046	0.0448
T459_26048	-1.8188	0.2397	-7.5888	0.0000	0.0000
T459_25306	-1.8081	0.5393	-3.3529	0.0008	0.0105
T459_09665	-1.8009	0.1926	-9.3527	0.0000	0.0000
T459_05779	-1.7894	0.6238	-2.8684	0.0041	0.0412
T459_31475	-1.7868	0.5514	-3.2402	0.0012	0.0149
T459_25990	-1.7844	0.2868	-6.2223	0.0000	0.0000
T459_10518	-1.7739	0.3283	-5.4035	0.0000	0.0000
T459_26094	-1.7637	0.6207	-2.8415	0.0045	0.0441
T459_09663	-1.7538	0.5201	-3.3721	0.0007	0.0099
T459_13190	-1.7479	0.3558	-4.9122	0.0000	0.0000
T459_27227	-1.7405	0.3504	-4.9667	0.0000	0.0000
T459_31778	-1.7345	0.4331	-4.0052	0.0001	0.0012
T459_18555	-1.7156	0.2697	-6.3617	0.0000	0.0000
T459_06771	-1.6953	0.2268	-7.4758	0.0000	0.0000
T459_06587	-1.6786	0.5091	-3.2973	0.0010	0.0124
T459_01250	-1.6748	0.5693	-2.9418	0.0033	0.0343
T459_09619	-1.6682	0.3363	-4.9606	0.0000	0.0000
T459_04323	-1.6676	0.5248	-3.1774	0.0015	0.0179
T459_33851	-1.6671	0.4590	-3.6319	0.0003	0.0043
T459_33927	-1.6636	0.4390	-3.7894	0.0002	0.0025
T459_34271	-1.6506	0.3983	-4.1447	0.0000	0.0007
T459_26371	-1.6505	0.1756	-9.3976	0.0000	0.0000
T459_31247	-1.6373	0.2412	-6.7873	0.0000	0.0000
T459_32515	-1.6188	0.2867	-5.6471	0.0000	0.0000
T459_27819	-1.6186	0.2051	-7.8910	0.0000	0.0000
T459_32574	-1.6114	0.2978	-5.4109	0.0000	0.0000
T459_18546	-1.6100	0.3665	-4.3929	0.0000	0.0002
T459_29416	-1.5996	0.2772	-5.7701	0.0000	0.0000
T459_28224	-1.5851	0.5272	-3.0069	0.0026	0.0288
T459_03483	-1.5778	0.5539	-2.8485	0.0044	0.0433
T459_01295	-1.5727	0.3080	-5.1056	0.0000	0.0000

Gene ID	log2FoldChange	lfcSE	stat	pvalue	padj
T459_35632	-1.5726	0.3241	-4.8520	0.0000	0.0000
T459_21991	-1.5653	0.2630	-5.9524	0.0000	0.0000
T459_26375	-1.5562	0.0883	-17.6235	0.0000	0.0000
T459_07186	-1.5527	0.3989	-3.8925	0.0001	0.0017
T459_30884	-1.5525	0.2728	-5.6906	0.0000	0.0000
T459_23777	-1.5473	0.3692	-4.1912	0.0000	0.0006
T459_22421	-1.5450	0.3604	-4.2872	0.0000	0.0004
T459_15153	-1.5446	0.5458	-2.8299	0.0047	0.0454
T459_34688	-1.5428	0.3768	-4.0945	0.0000	0.0008
T459_25422	-1.5421	0.2316	-6.6575	0.0000	0.0000
T459_20103	-1.5293	0.3313	-4.6166	0.0000	0.0001
T459_19052	-1.5250	0.5027	-3.0337	0.0024	0.0268
T459_07898	-1.5250	0.2527	-6.0349	0.0000	0.0000
T459_26349	-1.5244	0.1852	-8.2317	0.0000	0.0000
T459_15847	-1.5139	0.2000	-7.5705	0.0000	0.0000
T459_06173	-1.4882	0.3663	-4.0630	0.0000	0.0009
T459_07637	-1.4852	0.4947	-3.0023	0.0027	0.0291
T459_31217	-1.4817	0.3279	-4.5193	0.0000	0.0001
T459_28372	-1.4787	0.3024	-4.8892	0.0000	0.0000
T459_22972	-1.4784	0.1395	-10.5996	0.0000	0.0000
T459_22569	-1.4769	0.1513	-9.7636	0.0000	0.0000
T459_19060	-1.4732	0.4833	-3.0480	0.0023	0.0257
T459_20387	-1.4727	0.2464	-5.9771	0.0000	0.0000
T459_18146	-1.4607	0.2853	-5.1198	0.0000	0.0000
T459_22748	-1.4603	0.3924	-3.7217	0.0002	0.0032
T459_32208	-1.4583	0.3307	-4.4094	0.0000	0.0002
T459_13587	-1.4510	0.3420	-4.2432	0.0000	0.0005
T459_15846	-1.4479	0.2511	-5.7661	0.0000	0.0000
T459_08259	-1.4437	0.4183	-3.4514	0.0006	0.0078
T459_32978	-1.4436	0.3830	-3.7693	0.0002	0.0027
T459_06787	-1.4381	0.3265	-4.4040	0.0000	0.0002
T459_07943	-1.4292	0.4255	-3.3587	0.0008	0.0103
T459_18219	-1.4265	0.3882	-3.6746	0.0002	0.0037
T459_21158	-1.4204	0.2977	-4.7708	0.0000	0.0000
T459_29580	-1.4132	0.4256	-3.3207	0.0009	0.0116
T459_05423	-1.4122	0.3709	-3.8080	0.0001	0.0024
T459_06015	-1.4098	0.2892	-4.8743	0.0000	0.0000
T459_03749	-1.4066	0.1106	-12.7151	0.0000	0.0000
T459_07006	-1.4049	0.4358	-3.2238	0.0013	0.0157
T459_14026	-1.4021	0.1720	-8.1530	0.0000	0.0000
T459_27259	-1.4007	0.3540	-3.9563	0.0001	0.0014
T459_09060	-1.3988	0.2101	-6.6589	0.0000	0.0000
T459_10426	-1.3955	0.2995	-4.6596	0.0000	0.0001
T459_34425	-1.3903	0.2802	-4.9625	0.0000	0.0000
T459_32064	-1.3902	0.3840	-3.6200	0.0003	0.0045
T459_28000	-1.3884	0.1630	-8.5185	0.0000	0.0000
T459_19854	-1.3826	0.1954	-7.0748	0.0000	0.0000

Gene ID	log2FoldChange	lfcSE	stat	pvalue	padj
T459_20322	-1.3820	0.4897	-2.8219	0.0048	0.0462
T459_30863	-1.3813	0.2288	-6.0376	0.0000	0.0000
T459_06698	-1.3812	0.3680	-3.7530	0.0002	0.0029
T459_29061	-1.3782	0.2208	-6.2430	0.0000	0.0000
T459_18851	-1.3768	0.2286	-6.0237	0.0000	0.0000
T459_09658	-1.3742	0.2748	-5.0009	0.0000	0.0000
T459_00118	-1.3689	0.1823	-7.5108	0.0000	0.0000
T459_24857	-1.3686	0.3484	-3.9282	0.0001	0.0015
T459_04064	-1.3679	0.3202	-4.2719	0.0000	0.0004
T459_14003	-1.3612	0.3014	-4.5167	0.0000	0.0001
T459_12995	-1.3376	0.3502	-3.8192	0.0001	0.0023
T459_21261	-1.3326	0.2024	-6.5850	0.0000	0.0000
T459_15306	-1.3321	0.2802	-4.7539	0.0000	0.0001
T459_05227	-1.3286	0.2354	-5.6448	0.0000	0.0000
T459_01153	-1.3228	0.2522	-5.2448	0.0000	0.0000
T459_27892	-1.3182	0.3980	-3.3125	0.0009	0.0118
T459_20643	-1.3152	0.3773	-3.4855	0.0005	0.0069
T459_31995	-1.3132	0.4473	-2.9361	0.0033	0.0348
T459_25169	-1.3108	0.3668	-3.5735	0.0004	0.0052
T459_27445	-1.3088	0.1949	-6.7134	0.0000	0.0000
T459_17315	-1.3020	0.4495	-2.8967	0.0038	0.0385
T459_07638	-1.2931	0.4331	-2.9859	0.0028	0.0303
T459_34292	-1.2862	0.3066	-4.1952	0.0000	0.0006
T459_35236	-1.2854	0.3016	-4.2614	0.0000	0.0004
T459_18858	-1.2789	0.4545	-2.8139	0.0049	0.0473
T459_14506	-1.2714	0.3598	-3.5332	0.0004	0.0059
T459_10862	-1.2707	0.3577	-3.5520	0.0004	0.0056
T459_03747	-1.2653	0.1851	-6.8339	0.0000	0.0000
T459_34540	-1.2648	0.1995	-6.3384	0.0000	0.0000
T459_30505	-1.2623	0.2372	-5.3208	0.0000	0.0000
T459_18439	-1.2583	0.4101	-3.0679	0.0022	0.0244
T459_18231	-1.2576	0.1621	-7.7578	0.0000	0.0000
T459_35222	-1.2573	0.2194	-5.7304	0.0000	0.0000
T459_07652	-1.2563	0.3874	-3.2429	0.0012	0.0148
T459_26842	-1.2558	0.2984	-4.2079	0.0000	0.0005
T459_18678	-1.2532	0.3073	-4.0782	0.0000	0.0009
T459_06286	-1.2378	0.3154	-3.9248	0.0001	0.0016
T459_29886	-1.2309	0.1474	-8.3479	0.0000	0.0000
T459_24903	-1.2304	0.3097	-3.9731	0.0001	0.0013
T459_31882	-1.2297	0.1941	-6.3351	0.0000	0.0000
T459_25801	-1.2272	0.2324	-5.2805	0.0000	0.0000
T459_12614	-1.2215	0.3204	-3.8126	0.0001	0.0023
T459_18560	-1.2204	0.2520	-4.8435	0.0000	0.0000
T459_09678	-1.2184	0.0938	-12.9959	0.0000	0.0000
T459_17188	-1.2163	0.3477	-3.4980	0.0005	0.0067
T459_09373	-1.2159	0.2615	-4.6490	0.0000	0.0001
T459_18047	-1.2112	0.3578	-3.3850	0.0007	0.0096

Gene ID	log2FoldChange	lfcSE	stat	pvalue	padj
T459_34441	-1.2097	0.1814	-6.6671	0.0000	0.0000
T459_31938	-1.2081	0.2248	-5.3751	0.0000	0.0000
T459_34478	-1.2049	0.2550	-4.7254	0.0000	0.0001
T459_10793	-1.1979	0.3565	-3.3603	0.0008	0.0103
T459_15576	-1.1966	0.2619	-4.5679	0.0000	0.0001
T459_34144	-1.1926	0.3049	-3.9114	0.0001	0.0016
T459_28271	-1.1920	0.1588	-7.5052	0.0000	0.0000
T459_15477	-1.1900	0.3637	-3.2717	0.0011	0.0135
T459_34477	-1.1850	0.1810	-6.5472	0.0000	0.0000
T459_24187	-1.1844	0.3933	-3.0118	0.0026	0.0284
T459_34590	-1.1833	0.3936	-3.0061	0.0026	0.0288
T459_19899	-1.1815	0.1486	-7.9522	0.0000	0.0000
T459_12901	-1.1695	0.2075	-5.6358	0.0000	0.0000
T459_21968	-1.1690	0.2673	-4.3729	0.0000	0.0003
T459_14277	-1.1676	0.3544	-3.2946	0.0010	0.0125
T459_04054	-1.1669	0.2449	-4.7638	0.0000	0.0000
T459_13455	-1.1662	0.2737	-4.2610	0.0000	0.0004
T459_06631	-1.1626	0.3277	-3.5472	0.0004	0.0057
T459_31012	-1.1607	0.1698	-6.8346	0.0000	0.0000
T459_05182	-1.1573	0.2956	-3.9148	0.0001	0.0016
T459_32062	-1.1479	0.2756	-4.1648	0.0000	0.0006
T459_11214	-1.1478	0.2680	-4.2828	0.0000	0.0004
T459_27999	-1.1451	0.1107	-10.3421	0.0000	0.0000
T459_24583	-1.1449	0.2921	-3.9191	0.0001	0.0016
T459_32186	-1.1431	0.2311	-4.9473	0.0000	0.0000
T459_31609	-1.1429	0.1304	-8.7680	0.0000	0.0000
T459_32341	-1.1409	0.2519	-4.5292	0.0000	0.0001
T459_21280	-1.1369	0.1976	-5.7545	0.0000	0.0000
T459_27700	-1.1353	0.1523	-7.4551	0.0000	0.0000
T459_24693	-1.1338	0.2889	-3.9239	0.0001	0.0016
T459_17950	-1.1336	0.2703	-4.1935	0.0000	0.0006
T459_01136	-1.1306	0.3137	-3.6041	0.0003	0.0047
T459_31358	-1.1287	0.3057	-3.6922	0.0002	0.0035
T459_09677	-1.1274	0.1870	-6.0287	0.0000	0.0000
T459_23088	-1.1265	0.3096	-3.6379	0.0003	0.0042
T459_15742	-1.1258	0.2850	-3.9499	0.0001	0.0014
T459_31857	-1.1256	0.2451	-4.5922	0.0000	0.0001
T459_25307	-1.1240	0.2354	-4.7746	0.0000	0.0000
T459_14124	-1.1240	0.3139	-3.5809	0.0003	0.0051
T459_18673	-1.1227	0.1229	-9.1322	0.0000	0.0000
T459_34720	-1.1226	0.1948	-5.7628	0.0000	0.0000
T459_25592	-1.1201	0.1482	-7.5571	0.0000	0.0000
T459_23079	-1.1174	0.3661	-3.0520	0.0023	0.0254
T459_29328	-1.1145	0.1503	-7.4165	0.0000	0.0000
T459_00051	-1.1119	0.3603	-3.0864	0.0020	0.0231
T459_06517	-1.1117	0.2933	-3.7905	0.0002	0.0025
T459_32063	-1.1109	0.3470	-3.2017	0.0014	0.0167

Gene ID	log2FoldChange	lfcSE	stat	pvalue	padj
T459_28911	-1.1088	0.3033	-3.6552	0.0003	0.0040
T459_26551	-1.1065	0.3742	-2.9569	0.0031	0.0328
T459_34226	-1.1028	0.3820	-2.8870	0.0039	0.0394
T459_09339	-1.0972	0.2940	-3.7315	0.0002	0.0031
T459_07799	-1.0969	0.1496	-7.3337	0.0000	0.0000
T459_31786	-1.0942	0.3810	-2.8715	0.0041	0.0409
T459_02332	-1.0898	0.3237	-3.3664	0.0008	0.0101
T459_25140	-1.0891	0.2570	-4.2375	0.0000	0.0005
T459_33262	-1.0879	0.2855	-3.8111	0.0001	0.0023
T459_09915	-1.0860	0.3862	-2.8119	0.0049	0.0474
T459_17136	-1.0844	0.3584	-3.0254	0.0025	0.0274
T459_35322	-1.0826	0.1943	-5.5724	0.0000	0.0000
T459_20699	-1.0817	0.2242	-4.8257	0.0000	0.0000
T459_18261	-1.0808	0.3862	-2.7989	0.0051	0.0488
T459_24413	-1.0805	0.2824	-3.8255	0.0001	0.0022
T459_20368	-1.0777	0.3062	-3.5191	0.0004	0.0062
T459_24139	-1.0763	0.3587	-3.0005	0.0027	0.0292
T459_31770	-1.0728	0.3331	-3.2206	0.0013	0.0158
T459_23969	-1.0679	0.3588	-2.9762	0.0029	0.0311
T459_00647	-1.0675	0.3495	-3.0548	0.0023	0.0252
T459_00276	-1.0669	0.1270	-8.4026	0.0000	0.0000
T459_22564	-1.0660	0.1208	-8.8230	0.0000	0.0000
T459_23239	-1.0634	0.3147	-3.3788	0.0007	0.0097
T459_31472	-1.0630	0.3440	-3.0903	0.0020	0.0229
T459_10146	-1.0600	0.1539	-6.8882	0.0000	0.0000
T459_23964	-1.0555	0.2332	-4.5267	0.0000	0.0001
T459_14828	-1.0545	0.2285	-4.6154	0.0000	0.0001
T459_11364	-1.0508	0.2834	-3.7078	0.0002	0.0033
T459_09712	-1.0504	0.1812	-5.7971	0.0000	0.0000
T459_07612	-1.0447	0.1913	-5.4603	0.0000	0.0000
T459_06703	-1.0413	0.1613	-6.4554	0.0000	0.0000
T459_35470	-1.0365	0.3517	-2.9475	0.0032	0.0337
T459_08278	-1.0326	0.2224	-4.6418	0.0000	0.0001
T459_17022	-1.0281	0.1738	-5.9160	0.0000	0.0000
T459_08260	-1.0272	0.2009	-5.1132	0.0000	0.0000
T459_34118	-1.0265	0.2393	-4.2892	0.0000	0.0004
T459_24568	-1.0222	0.3436	-2.9754	0.0029	0.0312
T459_07834	-1.0222	0.1624	-6.2930	0.0000	0.0000
T459_22567	-1.0178	0.1518	-6.7037	0.0000	0.0000
T459_24904	-1.0146	0.2873	-3.5312	0.0004	0.0060
T459_09676	-1.0130	0.2443	-4.1472	0.0000	0.0007
T459_33803	-1.0128	0.3379	-2.9977	0.0027	0.0295
T459_22563	-1.0102	0.2728	-3.7031	0.0002	0.0034
T459_15674	-1.0090	0.1990	-5.0706	0.0000	0.0000
T459_06469	-1.0063	0.1935	-5.2012	0.0000	0.0000
T459_27053	-1.0028	0.3565	-2.8131	0.0049	0.0473
T459_19483	1.0001	0.1200	8.3322	0.0000	0.0000

Gene ID	log2FoldChange	lfcSE	stat	pvalue	padj
T459_27859	1.0010	0.2208	4.5344	0.0000	0.0001
T459_01666	1.0024	0.3114	3.2189	0.0013	0.0159
T459_19482	1.0035	0.1295	7.7488	0.0000	0.0000
T459_03998	1.0067	0.1648	6.1092	0.0000	0.0000
T459_05635	1.0092	0.3576	2.8219	0.0048	0.0462
T459_03972	1.0113	0.3217	3.1433	0.0017	0.0197
T459_17009	1.0119	0.2152	4.7032	0.0000	0.0001
T459_00426	1.0134	0.2316	4.3761	0.0000	0.0003
T459_05721	1.0134	0.3044	3.3290	0.0009	0.0113
T459_25598	1.0150	0.0852	11.9080	0.0000	0.0000
T459_34989	1.0211	0.2721	3.7526	0.0002	0.0029
T459_33557	1.0242	0.1172	8.7377	0.0000	0.0000
T459_23188	1.0251	0.2499	4.1020	0.0000	0.0008
T459_06674	1.0321	0.1729	5.9690	0.0000	0.0000
T459_03735	1.0332	0.3148	3.2819	0.0010	0.0130
T459_18370	1.0333	0.0896	11.5375	0.0000	0.0000
T459_04410	1.0341	0.3167	3.2655	0.0011	0.0137
T459_01424	1.0356	0.3093	3.3485	0.0008	0.0106
T459_06009	1.0396	0.2875	3.6156	0.0003	0.0046
T459_32093	1.0397	0.1902	5.4664	0.0000	0.0000
T459_06340	1.0399	0.1543	6.7411	0.0000	0.0000
T459_27861	1.0403	0.2606	3.9922	0.0001	0.0012
T459_34399	1.0471	0.1976	5.2981	0.0000	0.0000
T459_00386	1.0554	0.1960	5.3832	0.0000	0.0000
T459_06317	1.0562	0.2567	4.1145	0.0000	0.0008
T459_07753	1.0588	0.2356	4.4943	0.0000	0.0002
T459_17419	1.0602	0.1935	5.4806	0.0000	0.0000
T459_15596	1.0617	0.2536	4.1867	0.0000	0.0006
T459_10460	1.0627	0.2498	4.2552	0.0000	0.0004
T459_31848	1.0637	0.1372	7.7538	0.0000	0.0000
T459_26945	1.0672	0.2470	4.3207	0.0000	0.0003
T459_01357	1.0676	0.2343	4.5571	0.0000	0.0001
T459_11052	1.0723	0.2375	4.5147	0.0000	0.0002
T459_19542	1.0731	0.1899	5.6519	0.0000	0.0000
T459_27951	1.0759	0.3445	3.1231	0.0018	0.0209
T459_05892	1.0764	0.3171	3.3951	0.0007	0.0093
T459_34298	1.0802	0.2108	5.1254	0.0000	0.0000
T459_16761	1.0804	0.1532	7.0524	0.0000	0.0000
T459_15451	1.0807	0.3872	2.7909	0.0053	0.0498
T459_03545	1.0829	0.3182	3.4034	0.0007	0.0091
T459_28687	1.0933	0.2424	4.5104	0.0000	0.0002
T459_08170	1.0974	0.2267	4.8416	0.0000	0.0000
T459_35167	1.0986	0.1632	6.7303	0.0000	0.0000
T459_11705	1.1013	0.2264	4.8636	0.0000	0.0000
T459_29175	1.1059	0.2598	4.2560	0.0000	0.0004
T459_20461	1.1101	0.3843	2.8888	0.0039	0.0392
T459_00329	1.1125	0.1705	6.5249	0.0000	0.0000

Gene ID	log2FoldChange	lfcSE	stat	pvalue	padj
T459_20093	1.1140	0.1862	5.9832	0.0000	0.0000
T459_00330	1.1161	0.1574	7.0914	0.0000	0.0000
T459_16126	1.1184	0.3413	3.2772	0.0010	0.0132
T459_17321	1.1195	0.2686	4.1686	0.0000	0.0006
T459_09948	1.1205	0.3325	3.3698	0.0008	0.0100
T459_00327	1.1216	0.2048	5.4754	0.0000	0.0000
T459_28617	1.1282	0.3276	3.4439	0.0006	0.0080
T459_34009	1.1298	0.1626	6.9472	0.0000	0.0000
T459_17102	1.1302	0.3372	3.3512	0.0008	0.0106
T459_12696	1.1306	0.2956	3.8246	0.0001	0.0022
T459_04840	1.1319	0.2781	4.0706	0.0000	0.0009
T459_24496	1.1333	0.3009	3.7663	0.0002	0.0027
T459_22503	1.1359	0.3932	2.8891	0.0039	0.0392
T459_31834	1.1403	0.3629	3.1425	0.0017	0.0197
T459_06287	1.1469	0.3604	3.1827	0.0015	0.0176
T459_06836	1.1475	0.2272	5.0508	0.0000	0.0000
T459_23978	1.1501	0.3131	3.6735	0.0002	0.0038
T459_21751	1.1525	0.2308	4.9934	0.0000	0.0000
T459_25112	1.1568	0.2361	4.9001	0.0000	0.0000
T459_05880	1.1670	0.2660	4.3871	0.0000	0.0003
T459_03272	1.1687	0.4156	2.8121	0.0049	0.0474
T459_30978	1.1691	0.2044	5.7205	0.0000	0.0000
T459_02596	1.1732	0.4180	2.8069	0.0050	0.0480
T459_31900	1.1732	0.2463	4.7636	0.0000	0.0000
T459_25966	1.1794	0.1546	7.6288	0.0000	0.0000
T459_05348	1.1868	0.3895	3.0468	0.0023	0.0258
T459_20028	1.1900	0.1485	8.0140	0.0000	0.0000
T459_25393	1.1914	0.3311	3.5988	0.0003	0.0048
T459_10402	1.1935	0.3223	3.7037	0.0002	0.0034
T459_06869	1.1944	0.1444	8.2720	0.0000	0.0000
T459_00979	1.1946	0.1979	6.0349	0.0000	0.0000
T459_07569	1.1955	0.3599	3.3222	0.0009	0.0115
T459_33787	1.1968	0.2265	5.2847	0.0000	0.0000
T459_31000	1.1970	0.2924	4.0937	0.0000	0.0008
T459_09108	1.2039	0.2426	4.9617	0.0000	0.0000
T459_04659	1.2058	0.3150	3.8277	0.0001	0.0022
T459_31637	1.2108	0.2579	4.6942	0.0000	0.0001
T459_26243	1.2228	0.3304	3.7010	0.0002	0.0034
T459_08160	1.2252	0.2588	4.7337	0.0000	0.0001
T459_00109	1.2265	0.4285	2.8625	0.0042	0.0418
T459_35563	1.2267	0.3400	3.6081	0.0003	0.0047
T459_18647	1.2272	0.4377	2.8036	0.0051	0.0483
T459_26014	1.2278	0.3182	3.8586	0.0001	0.0020
T459_23925	1.2296	0.2866	4.2897	0.0000	0.0004
T459_17714	1.2313	0.2162	5.6955	0.0000	0.0000
T459_10918	1.2318	0.4268	2.8860	0.0039	0.0395
T459_34685	1.2347	0.2224	5.5519	0.0000	0.0000

Gene ID	log2FoldChange	lfcSE	stat	pvalue	padj
T459_19889	1.2404	0.2145	5.7830	0.0000	0.0000
T459_15197	1.2414	0.1408	8.8197	0.0000	0.0000
T459_29288	1.2432	0.1739	7.1476	0.0000	0.0000
T459_10310	1.2437	0.2486	5.0037	0.0000	0.0000
T459_06370	1.2449	0.2524	4.9326	0.0000	0.0000
T459_18788	1.2469	0.3859	3.2310	0.0012	0.0153
T459_17544	1.2542	0.3750	3.3447	0.0008	0.0107
T459_03045	1.2553	0.2600	4.8286	0.0000	0.0000
T459_18795	1.2636	0.1137	11.1121	0.0000	0.0000
T459_34555	1.2688	0.3063	4.1428	0.0000	0.0007
T459_25700	1.2747	0.3338	3.8188	0.0001	0.0023
T459_05238	1.2765	0.1484	8.6039	0.0000	0.0000
T459_31988	1.2780	0.1058	12.0853	0.0000	0.0000
T459_17523	1.2785	0.2982	4.2874	0.0000	0.0004
T459_07062	1.2857	0.2938	4.3758	0.0000	0.0003
T459_26892	1.2902	0.4343	2.9705	0.0030	0.0316
T459_10753	1.2907	0.2516	5.1293	0.0000	0.0000
T459_07866	1.2925	0.3750	3.4465	0.0006	0.0079
T459_09686	1.2939	0.3042	4.2541	0.0000	0.0004
T459_23556	1.2960	0.2075	6.2461	0.0000	0.0000
T459_27860	1.2974	0.4411	2.9413	0.0033	0.0343
T459_10083	1.2979	0.3250	3.9940	0.0001	0.0012
T459_31638	1.2999	0.3232	4.0219	0.0001	0.0011
T459_05444	1.3055	0.1373	9.5094	0.0000	0.0000
T459_26620	1.3060	0.3551	3.6781	0.0002	0.0037
T459_29715	1.3069	0.3057	4.2747	0.0000	0.0004
T459_13916	1.3074	0.3540	3.6932	0.0002	0.0035
T459_07065	1.3083	0.2818	4.6424	0.0000	0.0001
T459_24671	1.3108	0.4158	3.1526	0.0016	0.0191
T459_21099	1.3118	0.1423	9.2180	0.0000	0.0000
T459_25745	1.3122	0.1662	7.8961	0.0000	0.0000
T459_11771	1.3126	0.2278	5.7611	0.0000	0.0000
T459_25791	1.3224	0.1568	8.4351	0.0000	0.0000
T459_31011	1.3243	0.2145	6.1746	0.0000	0.0000
T459_17980	1.3255	0.0788	16.8148	0.0000	0.0000
T459_15527	1.3285	0.4659	2.8516	0.0044	0.0429
T459_03860	1.3286	0.2621	5.0689	0.0000	0.0000
T459_31093	1.3326	0.3932	3.3895	0.0007	0.0095
T459_07594	1.3492	0.1723	7.8300	0.0000	0.0000
T459_19890	1.3509	0.2207	6.1224	0.0000	0.0000
T459_06175	1.3522	0.4816	2.8074	0.0050	0.0479
T459_25267	1.3546	0.2766	4.8970	0.0000	0.0000
T459_16124	1.3666	0.2283	5.9861	0.0000	0.0000
T459_05677	1.3667	0.4878	2.8016	0.0051	0.0485
T459_16102	1.3681	0.2704	5.0588	0.0000	0.0000
T459_23977	1.3697	0.2658	5.1535	0.0000	0.0000
T459_29936	1.3710	0.2697	5.0827	0.0000	0.0000

Gene ID	log2FoldChange	lfcSE	stat	pvalue	padj
T459_07759	1.3717	0.2629	5.2185	0.0000	0.0000
T459_06755	1.3750	0.2212	6.2149	0.0000	0.0000
T459_33669	1.3752	0.3162	4.3493	0.0000	0.0003
T459_31495	1.3780	0.2263	6.0899	0.0000	0.0000
T459_05669	1.3843	0.2814	4.9190	0.0000	0.0000
T459_13021	1.3848	0.3665	3.7786	0.0002	0.0026
T459_05089	1.3871	0.1830	7.5809	0.0000	0.0000
T459_22760	1.3903	0.1836	7.5705	0.0000	0.0000
T459_30533	1.3959	0.4564	3.0588	0.0022	0.0249
T459_10776	1.3961	0.4966	2.8114	0.0049	0.0475
T459_26283	1.4074	0.3565	3.9475	0.0001	0.0014
T459_34296	1.4135	0.2660	5.3143	0.0000	0.0000
T459_05088	1.4284	0.4126	3.4616	0.0005	0.0075
T459_09773	1.4321	0.2931	4.8861	0.0000	0.0000
T459_10082	1.4406	0.2555	5.6385	0.0000	0.0000
T459_24621	1.4488	0.2141	6.7658	0.0000	0.0000
T459_13251	1.4507	0.2750	5.2759	0.0000	0.0000
T459_04452	1.4582	0.2285	6.3807	0.0000	0.0000
T459_20160	1.4584	0.2549	5.7222	0.0000	0.0000
T459_25091	1.4645	0.4412	3.3196	0.0009	0.0116
T459_22468	1.4648	0.1551	9.4462	0.0000	0.0000
T459_00328	1.4680	0.2249	6.5277	0.0000	0.0000
T459_34127	1.4750	0.4822	3.0588	0.0022	0.0249
T459_27862	1.4754	0.3709	3.9776	0.0001	0.0013
T459_10081	1.4779	0.3932	3.7589	0.0002	0.0028
T459_33564	1.4834	0.3636	4.0792	0.0000	0.0009
T459_09093	1.4894	0.2370	6.2856	0.0000	0.0000
T459_25023	1.4983	0.3073	4.8751	0.0000	0.0000
T459_08611	1.5005	0.4064	3.6925	0.0002	0.0035
T459_03263	1.5040	0.2856	5.2661	0.0000	0.0000
T459_07881	1.5043	0.2851	5.2767	0.0000	0.0000
T459_16827	1.5110	0.2151	7.0233	0.0000	0.0000
T459_08353	1.5121	0.4308	3.5102	0.0004	0.0064
T459_25939	1.5125	0.3375	4.4819	0.0000	0.0002
T459_18565	1.5184	0.2842	5.3431	0.0000	0.0000
T459_00197	1.5189	0.3119	4.8699	0.0000	0.0000
T459_12083	1.5217	0.3485	4.3669	0.0000	0.0003
T459_15778	1.5388	0.3027	5.0829	0.0000	0.0000
T459_15104	1.5453	0.5285	2.9242	0.0035	0.0359
T459_02125	1.5469	0.4356	3.5513	0.0004	0.0056
T459_12695	1.5470	0.4389	3.5250	0.0004	0.0061
T459_34823	1.5499	0.2463	6.2924	0.0000	0.0000
T459_01358	1.5568	0.1658	9.3921	0.0000	0.0000
T459_09766	1.5617	0.2323	6.7232	0.0000	0.0000
T459_07195	1.5686	0.4388	3.5747	0.0004	0.0052
T459_33510	1.5688	0.1881	8.3424	0.0000	0.0000
T459_15945	1.5777	0.2429	6.4948	0.0000	0.0000

Gene ID	log2FoldChange	lfcSE	stat	pvalue	padj
T459_09837	1.5910	0.5146	3.0919	0.0020	0.0228
T459_22121	1.5949	0.3273	4.8725	0.0000	0.0000
T459_17322	1.6024	0.3972	4.0345	0.0001	0.0010
T459_33526	1.6048	0.2268	7.0770	0.0000	0.0000
T459_15040	1.6092	0.4325	3.7205	0.0002	0.0032
T459_07287	1.6102	0.3053	5.2737	0.0000	0.0000
T459_28315	1.6131	0.2300	7.0123	0.0000	0.0000
T459_21908	1.6190	0.3077	5.2611	0.0000	0.0000
T459_06573	1.6213	0.5463	2.9680	0.0030	0.0318
T459_30655	1.6216	0.3128	5.1841	0.0000	0.0000
T459_19053	1.6220	0.3933	4.1242	0.0000	0.0007
T459_33436	1.6251	0.4389	3.7029	0.0002	0.0034
T459_15780	1.6324	0.2195	7.4368	0.0000	0.0000
T459_03842	1.6343	0.2612	6.2557	0.0000	0.0000
T459_13871	1.6347	0.3601	4.5399	0.0000	0.0001
T459_22172	1.6379	0.1929	8.4922	0.0000	0.0000
T459_17503	1.6528	0.2044	8.0871	0.0000	0.0000
T459_08134	1.6592	0.1522	10.8999	0.0000	0.0000
T459_32272	1.6667	0.1816	9.1757	0.0000	0.0000
T459_28793	1.6686	0.5382	3.1003	0.0019	0.0222
T459_24048	1.6690	0.1134	14.7185	0.0000	0.0000
T459_15369	1.6697	0.4513	3.6997	0.0002	0.0034
T459_34126	1.6698	0.2873	5.8129	0.0000	0.0000
T459_03559	1.6781	0.2290	7.3274	0.0000	0.0000
T459_00326	1.6872	0.2753	6.1283	0.0000	0.0000
T459_00737	1.6930	0.4391	3.8555	0.0001	0.0020
T459_18426	1.6935	0.3092	5.4772	0.0000	0.0000
T459_15078	1.7012	0.5122	3.3211	0.0009	0.0116
T459_27008	1.7027	0.3799	4.4818	0.0000	0.0002
T459_13250	1.7100	0.3516	4.8637	0.0000	0.0000
T459_29938	1.7133	0.4147	4.1311	0.0000	0.0007
T459_00086	1.7174	0.5346	3.2125	0.0013	0.0162
T459_15901	1.7214	0.3157	5.4519	0.0000	0.0000
T459_05874	1.7441	0.1596	10.9283	0.0000	0.0000
T459_32753	1.7494	0.2753	6.3556	0.0000	0.0000
T459_27541	1.7565	0.3970	4.4240	0.0000	0.0002
T459_10147	1.7697	0.1558	11.3567	0.0000	0.0000
T459_09708	1.7987	0.2703	6.6555	0.0000	0.0000
T459_31879	1.7989	0.5754	3.1260	0.0018	0.0207
T459_15346	1.8200	0.2852	6.3822	0.0000	0.0000
T459_13835	1.8265	0.2383	7.6653	0.0000	0.0000
T459_29945	1.8405	0.2684	6.8585	0.0000	0.0000
T459_28583	1.8451	0.3031	6.0879	0.0000	0.0000
T459_05018	1.8598	0.2340	7.9469	0.0000	0.0000
T459_34082	1.8681	0.4134	4.5190	0.0000	0.0001
T459_03841	1.8711	0.2509	7.4585	0.0000	0.0000
T459_07424	1.8817	0.4186	4.4948	0.0000	0.0002

Gene ID	log2FoldChange	lfcSE	stat	pvalue	padj
T459_35139	1.8826	0.1944	9.6864	0.0000	0.0000
T459_12705	1.8892	0.4331	4.3622	0.0000	0.0003
T459_04510	1.8955	0.3977	4.7659	0.0000	0.0000
T459_03840	1.9162	0.3402	5.6322	0.0000	0.0000
T459_06712	1.9209	0.1647	11.6630	0.0000	0.0000
T459_28580	1.9473	0.3282	5.9334	0.0000	0.0000
T459_26666	1.9619	0.1877	10.4523	0.0000	0.0000
T459_28581	1.9621	0.2765	7.0967	0.0000	0.0000
T459_18809	1.9634	0.1917	10.2425	0.0000	0.0000
T459_25024	1.9762	0.2137	9.2487	0.0000	0.0000
T459_16024	1.9806	0.1359	14.5706	0.0000	0.0000
T459_18488	1.9938	0.3706	5.3802	0.0000	0.0000
T459_16218	1.9970	0.3414	5.8486	0.0000	0.0000
T459_33615	2.0249	0.2429	8.3365	0.0000	0.0000
T459_26265	2.0299	0.5072	4.0024	0.0001	0.0012
T459_27006	2.0415	0.4618	4.4205	0.0000	0.0002
T459_07192	2.0421	0.2444	8.3553	0.0000	0.0000
T459_22537	2.0635	0.2283	9.0376	0.0000	0.0000
T459_21462	2.0820	0.2205	9.4413	0.0000	0.0000
T459_19891	2.0883	0.2938	7.1088	0.0000	0.0000
T459_04212	2.1030	0.5436	3.8685	0.0001	0.0019
T459_32329	2.1054	0.2163	9.7343	0.0000	0.0000
T459_21981	2.1239	0.3608	5.8865	0.0000	0.0000
T459_10690	2.1275	0.5429	3.9190	0.0001	0.0016
T459_07860	2.1517	0.3395	6.3369	0.0000	0.0000
T459_25849	2.1904	0.1951	11.2252	0.0000	0.0000
T459_20407	2.1994	0.5814	3.7826	0.0002	0.0026
T459_28305	2.2002	0.2226	9.8844	0.0000	0.0000
T459_15080	2.2036	0.5703	3.8638	0.0001	0.0019
T459_18690	2.2105	0.4068	5.4345	0.0000	0.0000
T459_10246	2.2123	0.4334	5.1048	0.0000	0.0000
T459_30842	2.2261	0.4280	5.2009	0.0000	0.0000
T459_02590	2.2430	0.3755	5.9732	0.0000	0.0000
T459_16121	2.2527	0.1433	15.7154	0.0000	0.0000
T459_15081	2.2550	0.7681	2.9359	0.0033	0.0348
T459_30820	2.2610	0.6468	3.4957	0.0005	0.0067
T459_10788	2.2635	0.1728	13.0974	0.0000	0.0000
T459_00927	2.2725	0.5003	4.5424	0.0000	0.0001
T459_23252	2.2780	0.5017	4.5405	0.0000	0.0001
T459_24950	2.2821	0.5311	4.2966	0.0000	0.0004
T459_15288	2.2844	0.6595	3.4640	0.0005	0.0075
T459_16770	2.3010	0.3816	6.0300	0.0000	0.0000
T459_28052	2.3290	0.7982	2.9177	0.0035	0.0365
T459_29868	2.3331	0.3172	7.3562	0.0000	0.0000
T459_28582	2.3424	0.3323	7.0489	0.0000	0.0000
T459_15079	2.3622	0.6756	3.4965	0.0005	0.0067
T459_25894	2.3812	0.3437	6.9275	0.0000	0.0000

Gene ID	log2FoldChange	lfcSE	stat	pvalue	padj
T459_18689	2.4040	0.4431	5.4256	0.0000	0.0000
T459_28743	2.4090	0.4594	5.2436	0.0000	0.0000
T459_15129	2.4169	0.3084	7.8358	0.0000	0.0000
T459_19216	2.4284	0.2286	10.6213	0.0000	0.0000
T459_20537	2.4358	0.4410	5.5234	0.0000	0.0000
T459_18433	2.4621	0.2520	9.7684	0.0000	0.0000
T459_31014	2.4977	0.1842	13.5574	0.0000	0.0000
T459_04352	2.5064	0.4285	5.8489	0.0000	0.0000
T459_07296	2.5246	0.4433	5.6948	0.0000	0.0000
T459_16980	2.5370	0.6222	4.0773	0.0000	0.0009
T459_31811	2.5516	0.8920	2.8604	0.0042	0.0420
T459_15858	2.5576	0.5222	4.8981	0.0000	0.0000
T459_14538	2.5711	0.5591	4.5988	0.0000	0.0001
T459_35330	2.5975	0.4064	6.3917	0.0000	0.0000
T459_27195	2.6255	0.2575	10.1970	0.0000	0.0000
T459_24379	2.6266	0.5799	4.5298	0.0000	0.0001
T459_04287	2.6369	0.5503	4.7917	0.0000	0.0000
T459_17948	2.6655	0.3790	7.0324	0.0000	0.0000
T459_21979	2.6686	0.4933	5.4100	0.0000	0.0000
T459_29118	2.6778	0.5798	4.6187	0.0000	0.0001
T459_28937	2.6930	0.7909	3.4048	0.0007	0.0090
T459_35620	2.7115	0.6991	3.8786	0.0001	0.0018
T459_21301	2.7225	0.2648	10.2794	0.0000	0.0000
T459_05955	2.7313	0.2531	10.7913	0.0000	0.0000
T459_17077	2.7450	0.4698	5.8432	0.0000	0.0000
T459_32743	2.7790	0.2866	9.6980	0.0000	0.0000
T459_00505	2.7823	0.3224	8.6307	0.0000	0.0000
T459_08013	2.7827	0.2592	10.7346	0.0000	0.0000
T459_08990	2.8185	0.3435	8.2051	0.0000	0.0000
T459_16931	2.8212	0.7379	3.8234	0.0001	0.0022
T459_34410	2.8420	0.2360	12.0429	0.0000	0.0000
T459_28642	2.8604	0.4134	6.9192	0.0000	0.0000
T459_33984	2.8893	0.2855	10.1217	0.0000	0.0000
T459_32717	2.9929	0.2047	14.6224	0.0000	0.0000
T459_14681	3.0088	0.5846	5.1466	0.0000	0.0000
T459_01301	3.0265	0.6006	5.0391	0.0000	0.0000
T459_31505	3.0487	0.8002	3.8097	0.0001	0.0024
T459_09647	3.0514	0.3635	8.3948	0.0000	0.0000
T459_19222	3.0667	0.8650	3.5452	0.0004	0.0057
T459_04649	3.1292	0.6253	5.0042	0.0000	0.0000
T459_24370	3.1343	0.3526	8.8892	0.0000	0.0000
T459_07278	3.1579	0.6671	4.7337	0.0000	0.0001
T459_05780	3.1636	0.2531	12.4972	0.0000	0.0000
T459_05210	3.1892	0.6820	4.6766	0.0000	0.0001
T459_13441	3.2293	0.7843	4.1174	0.0000	0.0008
T459_33300	3.2501	0.4791	6.7833	0.0000	0.0000
T459_13071	3.2658	0.6484	5.0370	0.0000	0.0000

Gene ID	log2FoldChange	lfcSE	stat	pvalue	padj
T459_06148	3.2765	0.8482	3.8630	0.0001	0.0019
T459_09514	3.2899	0.3126	10.5254	0.0000	0.0000
T459_09622	3.3199	0.2188	15.1739	0.0000	0.0000
T459_06454	3.3343	0.3217	10.3634	0.0000	0.0000
T459_31986	3.4288	0.7610	4.5057	0.0000	0.0002
T459_31291	3.4694	0.7116	4.8752	0.0000	0.0000
T459_26516	3.4981	0.3998	8.7505	0.0000	0.0000
T459_20531	3.5137	0.5152	6.8204	0.0000	0.0000
T459_35711	3.5151	0.6640	5.2936	0.0000	0.0000
T459_19245	3.5165	0.2526	13.9235	0.0000	0.0000
T459_16439	3.6015	0.5884	6.1207	0.0000	0.0000
T459_34352	3.6320	0.5660	6.4174	0.0000	0.0000
T459_05668	3.6672	0.8854	4.1420	0.0000	0.0007
T459_11465	3.6962	0.2378	15.5436	0.0000	0.0000
T459_25765	3.7057	0.8022	4.6197	0.0000	0.0001
T459_24830	3.7199	1.0994	3.3835	0.0007	0.0096
T459_31463	3.7287	0.2667	13.9817	0.0000	0.0000
T459_00004	3.8593	0.4474	8.6251	0.0000	0.0000
T459_34288	3.9051	0.4059	9.6205	0.0000	0.0000
T459_00242	3.9387	0.6421	6.1336	0.0000	0.0000
T459_08129	3.9412	0.2563	15.3755	0.0000	0.0000
T459_29415	3.9704	0.6310	6.2925	0.0000	0.0000
T459_27154	3.9889	0.6013	6.6336	0.0000	0.0000
T459_25793	3.9928	0.9194	4.3428	0.0000	0.0003
T459_16041	3.9999	0.6723	5.9495	0.0000	0.0000
T459_35562	4.0924	0.5202	7.8666	0.0000	0.0000
T459_30754	4.1208	0.6501	6.3391	0.0000	0.0000
T459_00579	4.1686	0.4732	8.8100	0.0000	0.0000
T459_32663	4.2094	0.9177	4.5869	0.0000	0.0001
T459_07809	4.2818	0.3619	11.8331	0.0000	0.0000
T459_24945	4.3660	0.5101	8.5592	0.0000	0.0000
T459_15779	4.3776	0.3158	13.8622	0.0000	0.0000
T459_34931	4.3948	1.2127	3.6238	0.0003	0.0045
T459_27542	4.4537	1.0169	4.3797	0.0000	0.0003
T459_15922	4.4606	0.6458	6.9071	0.0000	0.0000
T459_27524	4.5326	0.3981	11.3867	0.0000	0.0000
T459_34553	4.5670	0.3147	14.5134	0.0000	0.0000
T459_12482	4.6839	1.1687	4.0078	0.0001	0.0011
T459_29261	4.7040	1.6773	2.8045	0.0050	0.0482
T459_23871	4.7043	0.5101	9.2216	0.0000	0.0000
T459_07774	4.8224	0.8496	5.6760	0.0000	0.0000
T459_12750	4.8488	0.4884	9.9283	0.0000	0.0000
T459_04168	4.8945	0.8466	5.7814	0.0000	0.0000
T459_02250	5.0036	0.8374	5.9750	0.0000	0.0000
T459_26503	5.0665	1.3747	3.6855	0.0002	0.0036
T459_29062	5.1020	0.4631	11.0177	0.0000	0.0000
T459_33125	5.1102	0.9484	5.3883	0.0000	0.0000

Gene ID	log2FoldChange	lfcSE	stat	pvalue	padj
T459_34940	5.1746	0.3919	13.2031	0.0000	0.0000
T459_21750	5.1997	0.6831	7.6114	0.0000	0.0000
T459_33968	5.2509	1.1374	4.6166	0.0000	0.0001
T459_29882	5.2911	1.3574	3.8981	0.0001	0.0017
T459_30897	5.3497	0.4351	12.2952	0.0000	0.0000
T459_18786	5.4083	0.2697	20.0503	0.0000	0.0000
T459_35190	5.4087	0.6485	8.3407	0.0000	0.0000
T459_27579	5.4244	1.3498	4.0186	0.0001	0.0011
T459_01111	5.4575	1.3648	3.9987	0.0001	0.0012
T459_10685	5.5083	0.2677	20.5743	0.0000	0.0000
T459_23503	5.5308	0.7115	7.7737	0.0000	0.0000
T459_29862	5.5426	1.4827	3.7382	0.0002	0.0030
T459_21239	5.6532	1.1223	5.0371	0.0000	0.0000
T459_14638	5.6686	0.7944	7.1359	0.0000	0.0000
T459_11617	5.6905	1.3167	4.3217	0.0000	0.0003
T459_08365	5.7236	0.3265	17.5325	0.0000	0.0000
T459_35707	5.7556	1.4289	4.0279	0.0001	0.0011
T459_32185	5.7771	0.6549	8.8217	0.0000	0.0000
T459_11980	5.8136	0.7928	7.3327	0.0000	0.0000
T459_15863	5.8522	1.4137	4.1396	0.0000	0.0007
T459_01110	5.8992	1.4159	4.1666	0.0000	0.0006
T459_23378	5.9199	0.9097	6.5079	0.0000	0.0000
T459_17323	5.9711	1.0915	5.4704	0.0000	0.0000
T459_35329	6.0143	1.1021	5.4570	0.0000	0.0000
T459_28374	6.0252	0.9587	6.2846	0.0000	0.0000
T459_34939	6.0272	0.2376	25.3674	0.0000	0.0000
T459_16926	6.0504	0.7097	8.5258	0.0000	0.0000
T459_02224	6.0656	1.2812	4.7342	0.0000	0.0001
T459_17454	6.0658	1.2949	4.6845	0.0000	0.0001
T459_20099	6.0946	0.6357	9.5865	0.0000	0.0000
T459_34383	6.1081	0.7982	7.6527	0.0000	0.0000
T459_16639	6.1417	1.4131	4.3463	0.0000	0.0003
T459_16769	6.1578	0.7726	7.9702	0.0000	0.0000
T459_25404	6.1613	1.2990	4.7430	0.0000	0.0001
T459_35732	6.1836	1.3919	4.4427	0.0000	0.0002
T459_01163	6.2494	1.0822	5.7748	0.0000	0.0000
T459_01086	6.2655	1.1040	5.6753	0.0000	0.0000
T459_25639	6.2860	1.3858	4.5360	0.0000	0.0001
T459_35188	6.2862	0.8903	7.0605	0.0000	0.0000
T459_34392	6.3246	1.0808	5.8516	0.0000	0.0000
T459_26858	6.3250	1.3628	4.6411	0.0000	0.0001
T459_34278	6.3660	0.8885	7.1647	0.0000	0.0000
T459_34684	6.4115	1.2629	5.0769	0.0000	0.0000
T459_28744	6.4118	1.2736	5.0342	0.0000	0.0000
T459_22541	6.4191	1.3775	4.6601	0.0000	0.0001
T459_15349	6.4199	0.6265	10.2477	0.0000	0.0000
T459_15872	6.4229	1.3535	4.7452	0.0000	0.0001

Gene ID	log2FoldChange	lfcSE	stat	pvalue	padj
T459_18566	6.4516	1.3360	4.8291	0.0000	0.0000
T459_23852	6.4759	1.2623	5.1301	0.0000	0.0000
T459_15862	6.4819	1.3334	4.8611	0.0000	0.0000
T459_32662	6.5405	1.3285	4.9231	0.0000	0.0000
T459_12136	6.5429	0.8822	7.4164	0.0000	0.0000
T459_34393	6.6349	1.2557	5.2838	0.0000	0.0000
T459_28212	6.6582	0.5750	11.5800	0.0000	0.0000
T459_15154	6.6756	1.0665	6.2593	0.0000	0.0000
T459_15783	6.6807	0.6763	9.8786	0.0000	0.0000
T459_05443	6.7003	0.6807	9.8430	0.0000	0.0000
T459_04877	6.7042	1.3142	5.1012	0.0000	0.0000
T459_24124	6.7335	0.4229	15.9225	0.0000	0.0000
T459_25046	6.7338	1.3438	5.0108	0.0000	0.0000
T459_20092	6.7821	1.3152	5.1567	0.0000	0.0000
T459_33000	6.7969	1.2634	5.3796	0.0000	0.0000
T459_03602	6.8239	1.4157	4.8201	0.0000	0.0000
T459_24123	6.8683	0.4418	15.5463	0.0000	0.0000
T459_10779	6.8740	1.2991	5.2913	0.0000	0.0000
T459_20380	6.8768	1.2638	5.4413	0.0000	0.0000
T459_34938	7.0210	0.8754	8.0208	0.0000	0.0000
T459_18730	7.0356	0.5469	12.8644	0.0000	0.0000
T459_17458	7.0635	1.2486	5.6573	0.0000	0.0000
T459_23428	7.0647	1.3066	5.4071	0.0000	0.0000
T459_34479	7.0929	0.5386	13.1704	0.0000	0.0000
T459_19586	7.0948	1.0556	6.7212	0.0000	0.0000
T459_23916	7.1239	1.2910	5.5180	0.0000	0.0000
T459_28101	7.1447	1.2793	5.5850	0.0000	0.0000
T459_25568	7.2140	0.7498	9.6214	0.0000	0.0000
T459_21229	7.2143	1.1038	6.5357	0.0000	0.0000
T459_15917	7.3022	0.6909	10.5684	0.0000	0.0000
T459_28041	7.3386	1.2737	5.7617	0.0000	0.0000
T459_33667	7.3856	1.2324	5.9929	0.0000	0.0000
T459_19238	7.4056	1.2633	5.8621	0.0000	0.0000
T459_32664	7.4517	1.2213	6.1017	0.0000	0.0000
T459_04961	7.4996	1.2726	5.8933	0.0000	0.0000
T459_21523	7.5421	0.7503	10.0526	0.0000	0.0000
T459_00651	7.5966	1.2549	6.0533	0.0000	0.0000
T459_32526	7.6317	1.0455	7.2997	0.0000	0.0000
T459_18564	7.6898	1.2570	6.1177	0.0000	0.0000
T459_29609	7.7004	1.0476	7.3508	0.0000	0.0000
T459_02191	7.7109	1.2170	6.3360	0.0000	0.0000
T459_15864	7.7678	1.2463	6.2326	0.0000	0.0000
T459_23974	7.8865	0.5322	14.8178	0.0000	0.0000
T459_05241	7.8969	1.2426	6.3553	0.0000	0.0000
T459_21788	7.9514	1.2406	6.4093	0.0000	0.0000
T459_14979	7.9956	1.2740	6.2761	0.0000	0.0000
T459_32527	8.0074	1.2091	6.6226	0.0000	0.0000

Gene ID	log2FoldChange	lfcSE	stat	pvalue	padj
T459_03520	8.0458	1.2438	6.4689	0.0000	0.0000
T459_15784	8.0780	1.2170	6.6374	0.0000	0.0000
T459_15740	8.1443	1.2395	6.5709	0.0000	0.0000
T459_06634	8.2447	1.2319	6.6925	0.0000	0.0000
T459_19663	8.3916	1.2068	6.9538	0.0000	0.0000
T459_01013	8.4827	1.2199	6.9535	0.0000	0.0000
T459_34391	8.6333	1.2205	7.0738	0.0000	0.0000
T459_09200	8.7041	1.2186	7.1428	0.0000	0.0000
T459_24224	8.7989	1.2134	7.2517	0.0000	0.0000
T459_34279	9.8042	1.1981	8.1828	0.0000	0.0000

Supplementary Table 1. **B**. Differentially expressed genes between both genotypes under the control conditions at T1 (NIBER®/A10).

Gene ID	log2FoldChange	lfcSE	stat	pvalue	padj
T459_27777	-10.7560	1.0281	-10.4621	0.0000	0.0000
T459_33710	-10.2565	1.1990	-8.5545	0.0000	0.0000
T459_00511	-10.1242	1.1947	-8.4741	0.0000	0.0000
T459_02807	-10.0193	1.0533	-9.5123	0.0000	0.0000
T459_03230	-9.9388	1.2022	-8.2670	0.0000	0.0000
T459_19432	-9.5750	1.2004	-7.9768	0.0000	0.0000
T459_33789	-9.5430	1.1911	-8.0118	0.0000	0.0000
T459_28063	-9.4916	1.2023	-7.8944	0.0000	0.0000
T459_28184	-9.1968	1.0333	-8.9002	0.0000	0.0000
T459_28065	-9.1049	1.2105	-7.5215	0.0000	0.0000
T459_01116	-8.8998	0.8547	-10.4133	0.0000	0.0000
T459_02802	-8.8629	1.0469	-8.4659	0.0000	0.0000
T459_02150	-8.8452	1.2251	-7.2201	0.0000	0.0000
T459_16780	-8.7244	1.2017	-7.2601	0.0000	0.0000
T459_13152	-8.4777	1.2799	-6.6238	0.0000	0.0000
T459_00869	-8.1418	1.2307	-6.6154	0.0000	0.0000
T459_16565	-8.1188	1.0426	-7.7873	0.0000	0.0000
T459_14838	-7.9941	1.2383	-6.4556	0.0000	0.0000
T459_02562	-7.9933	1.2141	-6.5834	0.0000	0.0000
T459_33470	-7.8211	1.2411	-6.3019	0.0000	0.0000
T459_29008	-7.7673	1.2545	-6.1917	0.0000	0.0000
T459_28064	-7.7211	1.2543	-6.1558	0.0000	0.0000
T459_28067	-7.6216	1.2529	-6.0832	0.0000	0.0000
T459_26326	-7.6171	0.8594	-8.8636	0.0000	0.0000
T459_11884	-7.5643	1.2275	-6.1624	0.0000	0.0000
T459_08764	-7.5233	1.2675	-5.9357	0.0000	0.0000
T459_05002	-7.5077	0.7507	-10.0012	0.0000	0.0000
T459_27571	-7.4925	1.2214	-6.1341	0.0000	0.0000
T459_13944	-7.4770	1.2218	-6.1195	0.0000	0.0000
T459_30788	-7.4736	0.8586	-8.7045	0.0000	0.0000
T459_10015	-7.4174	1.3285	-5.5831	0.0000	0.0000

Gene ID	log2FoldChange	lfcSE	stat	pvalue	padj
T459_19264	-7.4118	1.2892	-5.7492	0.0000	0.0000
T459_23514	-7.3298	1.2810	-5.7219	0.0000	0.0000
T459_33575	-7.3112	1.3323	-5.4878	0.0000	0.0000
T459_21019	-7.2841	1.2264	-5.9395	0.0000	0.0000
T459_01091	-6.9141	1.2996	-5.3201	0.0000	0.0000
T459_35644	-6.8752	0.8751	-7.8561	0.0000	0.0000
T459_31895	-6.8622	1.2429	-5.5210	0.0000	0.0000
T459_33853	-6.8195	1.0643	-6.4077	0.0000	0.0000
T459_02117	-6.7256	1.3440	-5.0041	0.0000	0.0000
T459_04535	-6.6525	1.3234	-5.0267	0.0000	0.0000
T459_35557	-6.5839	1.3294	-4.9526	0.0000	0.0000
T459_07196	-6.5800	1.0679	-6.1615	0.0000	0.0000
T459_06112	-6.5281	1.3466	-4.8478	0.0000	0.0000
T459_02116	-6.5212	1.3264	-4.9166	0.0000	0.0000
T459_16564	-6.4665	1.0736	-6.0230	0.0000	0.0000
T459_12254	-6.4082	1.3323	-4.8099	0.0000	0.0000
T459_10016	-6.4064	1.4365	-4.4597	0.0000	0.0001
T459_03868	-6.3822	1.3510	-4.7240	0.0000	0.0000
T459_29009	-6.3778	1.3356	-4.7752	0.0000	0.0000
T459_35491	-6.3412	1.3433	-4.7205	0.0000	0.0000
T459_35735	-6.2207	0.5828	-10.6745	0.0000	0.0000
T459_28863	-6.2114	0.5763	-10.7783	0.0000	0.0000
T459_26100	-6.0865	0.5692	-10.6936	0.0000	0.0000
T459_24250	-5.9422	1.0951	-5.4264	0.0000	0.0000
T459_22353	-5.9154	0.5918	-9.9956	0.0000	0.0000
T459_20017	-5.8439	1.4288	-4.0902	0.0000	0.0005
T459_08737	-5.6769	1.1072	-5.1274	0.0000	0.0000
T459_17608	-5.6114	1.3252	-4.2342	0.0000	0.0003
T459_14475	-5.5320	1.3446	-4.1143	0.0000	0.0005
T459_06323	-5.5006	1.4563	-3.7771	0.0002	0.0017
T459_26329	-5.4505	0.2569	-21.2201	0.0000	0.0000
T459_15645	-5.3784	1.5092	-3.5636	0.0004	0.0034
T459_05160	-5.3691	0.9175	-5.8520	0.0000	0.0000
T459_26953	-5.3674	0.6769	-7.9290	0.0000	0.0000
T459_15988	-5.3249	0.3982	-13.3731	0.0000	0.0000
T459_07841	-5.2981	0.6556	-8.0818	0.0000	0.0000
T459_05875	-5.1817	0.6750	-7.6772	0.0000	0.0000
T459_07208	-5.1788	0.6571	-7.8813	0.0000	0.0000
T459_15989	-5.0011	0.2922	-17.1143	0.0000	0.0000
T459_07299	-4.9145	0.8704	-5.6464	0.0000	0.0000
T459_34633	-4.7565	0.9713	-4.8969	0.0000	0.0000
T459_07298	-4.7220	0.4995	-9.4542	0.0000	0.0000
T459_16623	-4.7150	0.9961	-4.7334	0.0000	0.0000
T459_25292	-4.5434	0.3973	-11.4364	0.0000	0.0000
T459_02367	-4.5271	1.4537	-3.1143	0.0018	0.0138
T459_19585	-4.3946	0.1365	-32.2035	0.0000	0.0000
T459_26921	-4.3420	0.7716	-5.6271	0.0000	0.0000

Gene ID	log2FoldChange	lfcSE	stat	pvalue	padj
T459_30283	-4.3183	0.9908	-4.3586	0.0000	0.0002
T459_28234	-4.3151	0.2684	-16.0763	0.0000	0.0000
T459_10257	-4.2815	0.5083	-8.4227	0.0000	0.0000
T459_04047	-4.2521	1.2462	-3.4120	0.0006	0.0056
T459_05205	-4.2484	0.8324	-5.1040	0.0000	0.0000
T459_34760	-4.2214	0.2768	-15.2496	0.0000	0.0000
T459_05161	-4.1633	0.6292	-6.6170	0.0000	0.0000
T459_15416	-4.1319	0.4974	-8.3062	0.0000	0.0000
T459_01745	-4.0880	0.4820	-8.4815	0.0000	0.0000
T459_19480	-4.0229	0.6290	-6.3953	0.0000	0.0000
T459_31930	-4.0183	0.8872	-4.5294	0.0000	0.0001
T459_29702	-3.9770	0.3951	-10.0659	0.0000	0.0000
T459_01928	-3.9705	0.3910	-10.1547	0.0000	0.0000
T459_29116	-3.9248	0.4103	-9.5652	0.0000	0.0000
T459_16803	-3.8553	0.8315	-4.6369	0.0000	0.0001
T459_33852	-3.8284	1.0436	-3.6685	0.0002	0.0024
T459_23249	-3.8120	0.7635	-4.9930	0.0000	0.0000
T459_08570	-3.7845	0.4338	-8.7250	0.0000	0.0000
T459_28257	-3.7670	0.5531	-6.8110	0.0000	0.0000
T459_25500	-3.7657	0.3338	-11.2813	0.0000	0.0000
T459_07300	-3.6803	0.4694	-7.8401	0.0000	0.0000
T459_18879	-3.6489	0.4259	-8.5682	0.0000	0.0000
T459_26777	-3.6340	0.6335	-5.7360	0.0000	0.0000
T459_26331	-3.6199	0.2545	-14.2218	0.0000	0.0000
T459_34636	-3.5859	0.7871	-4.5561	0.0000	0.0001
T459_01133	-3.5451	0.6421	-5.5208	0.0000	0.0000
T459_34064	-3.5378	0.6039	-5.8583	0.0000	0.0000
T459_35227	-3.5190	0.7863	-4.4754	0.0000	0.0001
T459_07652	-3.4598	0.3903	-8.8650	0.0000	0.0000
T459_28405	-3.4465	0.4648	-7.4158	0.0000	0.0000
T459_17149	-3.3932	0.3061	-11.0863	0.0000	0.0000
T459_00963	-3.3708	0.9176	-3.6733	0.0002	0.0024
T459_22888	-3.3334	0.5097	-6.5400	0.0000	0.0000
T459_26091	-3.2884	0.5821	-5.6490	0.0000	0.0000
T459_25797	-3.2849	0.5436	-6.0431	0.0000	0.0000
T459_22186	-3.2567	0.3834	-8.4948	0.0000	0.0000
T459_15753	-3.2055	0.6015	-5.3294	0.0000	0.0000
T459_07877	-3.1915	0.6693	-4.7682	0.0000	0.0000
T459_04588	-3.1715	0.3957	-8.0157	0.0000	0.0000
T459_13532	-3.1704	0.5216	-6.0778	0.0000	0.0000
T459_23034	-3.1583	0.2686	-11.7605	0.0000	0.0000
T459_10270	-3.1540	0.5522	-5.7116	0.0000	0.0000
T459_00106	-3.1498	0.3112	-10.1229	0.0000	0.0000
T459_24857	-3.1475	0.5399	-5.8299	0.0000	0.0000
T459_30903	-3.1447	0.5134	-6.1256	0.0000	0.0000
T459_06039	-3.1422	0.5389	-5.8303	0.0000	0.0000
T459_06587	-3.1339	0.5391	-5.8127	0.0000	0.0000

Gene ID	log2FoldChange	lfcSE	stat	pvalue	padj
T459_22562	-3.1195	0.2271	-13.7342	0.0000	0.0000
T459_10224	-3.0934	0.5621	-5.5038	0.0000	0.0000
T459_26588	-3.0647	0.9467	-3.2373	0.0012	0.0096
T459_05876	-3.0429	0.5519	-5.5136	0.0000	0.0000
T459_26502	-3.0419	0.2671	-11.3877	0.0000	0.0000
T459_09758	-3.0268	0.5073	-5.9668	0.0000	0.0000
T459_05588	-2.9942	0.5294	-5.6562	0.0000	0.0000
T459_26328	-2.9933	0.3896	-7.6828	0.0000	0.0000
T459_14112	-2.9798	0.3516	-8.4742	0.0000	0.0000
T459_14461	-2.9606	0.2325	-12.7353	0.0000	0.0000
T459_13878	-2.9415	0.1890	-15.5623	0.0000	0.0000
T459_00466	-2.9163	0.7345	-3.9704	0.0001	0.0008
T459_16225	-2.9113	0.6555	-4.4411	0.0000	0.0001
T459_21143	-2.8255	0.4593	-6.1517	0.0000	0.0000
T459_15625	-2.8234	0.7295	-3.8702	0.0001	0.0012
T459_14111	-2.8116	0.3783	-7.4322	0.0000	0.0000
T459_05587	-2.7853	0.5444	-5.1160	0.0000	0.0000
T459_29287	-2.7848	0.3358	-8.2944	0.0000	0.0000
T459_03997	-2.7802	0.2698	-10.3054	0.0000	0.0000
T459_19854	-2.7571	0.2389	-11.5385	0.0000	0.0000
T459_26524	-2.7463	0.3487	-7.8750	0.0000	0.0000
T459_10747	-2.7439	0.7549	-3.6349	0.0003	0.0027
T459_07843	-2.7382	0.6312	-4.3381	0.0000	0.0002
T459_02665	-2.7080	0.5345	-5.0666	0.0000	0.0000
T459_32999	-2.7068	0.5039	-5.3722	0.0000	0.0000
T459_24273	-2.6862	0.5359	-5.0126	0.0000	0.0000
T459_07779	-2.6749	0.6352	-4.2111	0.0000	0.0003
T459_07645	-2.6336	0.5380	-4.8948	0.0000	0.0000
T459_07842	-2.6307	0.8181	-3.2155	0.0013	0.0103
T459_33570	-2.6306	0.5160	-5.0985	0.0000	0.0000
T459_07425	-2.6165	0.3941	-6.6396	0.0000	0.0000
T459_00541	-2.6102	0.5152	-5.0665	0.0000	0.0000
T459_19287	-2.5908	0.4765	-5.4368	0.0000	0.0000
T459_18129	-2.5804	0.8583	-3.0062	0.0026	0.0186
T459_02476	-2.5557	0.1228	-20.8135	0.0000	0.0000
T459_14211	-2.5507	0.6923	-3.6842	0.0002	0.0023
T459_29235	-2.5421	0.8539	-2.9771	0.0029	0.0202
T459_05136	-2.5351	0.5539	-4.5773	0.0000	0.0001
T459_21241	-2.5334	0.1999	-12.6734	0.0000	0.0000
T459_18804	-2.5278	0.6825	-3.7036	0.0002	0.0021
T459_15787	-2.5074	0.5160	-4.8593	0.0000	0.0000
T459_20608	-2.4913	0.3147	-7.9168	0.0000	0.0000
T459_13580	-2.4861	0.4445	-5.5930	0.0000	0.0000
T459_33012	-2.4787	0.5724	-4.3302	0.0000	0.0002
T459_21261	-2.4667	0.1904	-12.9532	0.0000	0.0000
T459_13607	-2.4606	0.3143	-7.8285	0.0000	0.0000
T459_01250	-2.4602	0.2714	-9.0640	0.0000	0.0000

Gene ID	log2FoldChange	lfcSE	stat	pvalue	padj
T459_05004	-2.4370	0.2345	-10.3932	0.0000	0.0000
T459_15153	-2.4259	0.4487	-5.4069	0.0000	0.0000
T459_03960	-2.4209	0.5031	-4.8114	0.0000	0.0000
T459_27616	-2.4143	0.4914	-4.9132	0.0000	0.0000
T459_04234	-2.4102	0.6515	-3.6997	0.0002	0.0022
T459_13884	-2.4041	0.6386	-3.7644	0.0002	0.0017
T459_22419	-2.3995	0.3433	-6.9903	0.0000	0.0000
T459_17755	-2.3955	0.3463	-6.9170	0.0000	0.0000
T459_06243	-2.3913	0.5925	-4.0362	0.0001	0.0006
T459_03219	-2.3896	0.4348	-5.4962	0.0000	0.0000
T459_23921	-2.3885	0.5209	-4.5853	0.0000	0.0001
T459_22512	-2.3758	0.4281	-5.5499	0.0000	0.0000
T459_09339	-2.3533	0.5940	-3.9620	0.0001	0.0008
T459_30980	-2.3460	0.4702	-4.9896	0.0000	0.0000
T459_05222	-2.3381	0.2834	-8.2504	0.0000	0.0000
T459_32412	-2.3371	0.5130	-4.5554	0.0000	0.0001
T459_15847	-2.3296	0.2234	-10.4274	0.0000	0.0000
T459_27227	-2.3209	0.3195	-7.2633	0.0000	0.0000
T459_09552	-2.3198	0.4044	-5.7365	0.0000	0.0000
T459_12939	-2.3123	0.5784	-3.9976	0.0001	0.0007
T459_16744	-2.3048	0.6729	-3.4251	0.0006	0.0054
T459_25295	-2.2798	0.6328	-3.6030	0.0003	0.0030
T459_07123	-2.2777	0.7889	-2.8870	0.0039	0.0256
T459_05726	-2.2519	0.5463	-4.1222	0.0000	0.0005
T459_31121	-2.2460	0.7789	-2.8837	0.0039	0.0258
T459_16092	-2.2386	0.3007	-7.4437	0.0000	0.0000
T459_13626	-2.2351	0.8293	-2.6953	0.0070	0.0412
T459_14788	-2.2286	0.3795	-5.8723	0.0000	0.0000
T459_01927	-2.2258	0.1127	-19.7449	0.0000	0.0000
T459_34097	-2.2246	0.2019	-11.0170	0.0000	0.0000
T459_18532	-2.2180	0.3868	-5.7340	0.0000	0.0000
T459_02675	-2.2053	0.6701	-3.2910	0.0010	0.0082
T459_13955	-2.2031	0.8180	-2.6934	0.0071	0.0414
T459_25644	-2.2023	0.4047	-5.4423	0.0000	0.0000
T459_31089	-2.1927	0.3748	-5.8510	0.0000	0.0000
T459_24674	-2.1870	0.3528	-6.1987	0.0000	0.0000
T459_07933	-2.1674	0.4326	-5.0104	0.0000	0.0000
T459_27446	-2.1662	0.6338	-3.4177	0.0006	0.0055
T459_18198	-2.1661	0.4765	-4.5462	0.0000	0.0001
T459_33368	-2.1619	0.3517	-6.1479	0.0000	0.0000
T459_29549	-2.1586	0.3635	-5.9381	0.0000	0.0000
T459_15987	-2.1585	0.7927	-2.7230	0.0065	0.0386
T459_24718	-2.1546	0.3970	-5.4265	0.0000	0.0000
T459_32338	-2.1419	0.7276	-2.9436	0.0032	0.0221
T459_22009	-2.1335	0.5481	-3.8922	0.0001	0.0011
T459_15837	-2.1288	0.5238	-4.0639	0.0000	0.0006
T459_18672	-2.1273	0.2629	-8.0920	0.0000	0.0000

Gene ID	log2FoldChange	lfcSE	stat	pvalue	padj
T459_20284	-2.1134	0.4836	-4.3701	0.0000	0.0002
T459_13190	-2.1095	0.2201	-9.5820	0.0000	0.0000
T459_34632	-2.1070	0.3616	-5.8268	0.0000	0.0000
T459_24708	-2.0975	0.4469	-4.6935	0.0000	0.0000
T459_07943	-2.0847	0.3235	-6.4442	0.0000	0.0000
T459_33803	-2.0799	0.4100	-5.0727	0.0000	0.0000
T459_33519	-2.0786	0.2824	-7.3611	0.0000	0.0000
T459_14612	-2.0764	0.2063	-10.0661	0.0000	0.0000
T459_05021	-2.0668	0.2761	-7.4845	0.0000	0.0000
T459_19291	-2.0661	0.2202	-9.3825	0.0000	0.0000
T459_06698	-2.0652	0.6475	-3.1894	0.0014	0.0111
T459_21739	-2.0629	0.3409	-6.0514	0.0000	0.0000
T459_19397	-2.0621	0.2622	-7.8657	0.0000	0.0000
T459_14159	-2.0608	0.6942	-2.9684	0.0030	0.0206
T459_22281	-2.0493	0.4918	-4.1672	0.0000	0.0004
T459_25910	-2.0432	0.3691	-5.5349	0.0000	0.0000
T459_25458	-2.0412	0.2025	-10.0796	0.0000	0.0000
T459_34683	-2.0387	0.1594	-12.7876	0.0000	0.0000
T459_13465	-2.0311	0.5549	-3.6603	0.0003	0.0025
T459_33520	-2.0292	0.2072	-9.7924	0.0000	0.0000
T459_20322	-2.0286	0.7694	-2.6368	0.0084	0.0474
T459_24433	-2.0256	0.7043	-2.8760	0.0040	0.0263
T459_20889	-2.0213	0.6374	-3.1712	0.0015	0.0117
T459_30756	-2.0140	0.3928	-5.1268	0.0000	0.0000
T459_05320	-2.0129	0.5782	-3.4811	0.0005	0.0045
T459_15092	-2.0119	0.2828	-7.1131	0.0000	0.0000
T459_07331	-1.9866	0.4748	-4.1842	0.0000	0.0004
T459_33784	-1.9838	0.3955	-5.0165	0.0000	0.0000
T459_23777	-1.9830	0.3126	-6.3437	0.0000	0.0000
T459_20699	-1.9813	0.2222	-8.9154	0.0000	0.0000
T459_18858	-1.9756	0.4079	-4.8434	0.0000	0.0000
T459_14397	-1.9692	0.3576	-5.5060	0.0000	0.0000
T459_03540	-1.9688	0.2280	-8.6363	0.0000	0.0000
T459_28088	-1.9684	0.3743	-5.2591	0.0000	0.0000
T459_34443	-1.9631	0.3802	-5.1638	0.0000	0.0000
T459_33851	-1.9562	0.4494	-4.3530	0.0000	0.0002
T459_13275	-1.9528	0.5348	-3.6515	0.0003	0.0026
T459_04269	-1.9476	0.6135	-3.1749	0.0015	0.0116
T459_28332	-1.9445	0.3715	-5.2347	0.0000	0.0000
T459_25619	-1.9419	0.6534	-2.9720	0.0030	0.0204
T459_04732	-1.9405	0.2702	-7.1822	0.0000	0.0000
T459_26127	-1.9282	0.5057	-3.8129	0.0001	0.0015
T459_30657	-1.9276	0.4754	-4.0544	0.0001	0.0006
T459_21991	-1.9063	0.2773	-6.8734	0.0000	0.0000
T459_20328	-1.9022	0.4541	-4.1891	0.0000	0.0004
T459_29293	-1.9003	0.2986	-6.3647	0.0000	0.0000
T459_28559	-1.8990	0.5111	-3.7159	0.0002	0.0020

Gene ID	log2FoldChange	lfcSE	stat	pvalue	padj
T459_34425	-1.8978	0.2579	-7.3590	0.0000	0.0000
T459_04043	-1.8960	0.3528	-5.3739	0.0000	0.0000
T459_32672	-1.8927	0.5337	-3.5462	0.0004	0.0036
T459_07898	-1.8919	0.1627	-11.6285	0.0000	0.0000
T459_32978	-1.8901	0.3749	-5.0412	0.0000	0.0000
T459_22747	-1.8861	0.4374	-4.3121	0.0000	0.0002
T459_11118	-1.8683	0.3270	-5.7128	0.0000	0.0000
T459_12727	-1.8682	0.2270	-8.2288	0.0000	0.0000
T459_25618	-1.8585	0.3794	-4.8991	0.0000	0.0000
T459_19808	-1.8499	0.5114	-3.6176	0.0003	0.0029
T459_05135	-1.8469	0.3787	-4.8768	0.0000	0.0000
T459_31866	-1.8464	0.3151	-5.8593	0.0000	0.0000
T459_07834	-1.8426	0.1621	-11.3702	0.0000	0.0000
T459_15606	-1.8385	0.5682	-3.2357	0.0012	0.0097
T459_32337	-1.8376	0.3981	-4.6154	0.0000	0.0001
T459_34551	-1.8373	0.2274	-8.0804	0.0000	0.0000
T459_01638	-1.8328	0.2156	-8.5029	0.0000	0.0000
T459_30863	-1.8322	0.3390	-5.4052	0.0000	0.0000
T459_25422	-1.8321	0.1718	-10.6669	0.0000	0.0000
T459_28926	-1.8320	0.3813	-4.8046	0.0000	0.0000
T459_09775	-1.8312	0.2695	-6.7952	0.0000	0.0000
T459_00647	-1.8310	0.4839	-3.7836	0.0002	0.0016
T459_21035	-1.8162	0.3077	-5.9025	0.0000	0.0000
T459_15624	-1.8154	0.6216	-2.9205	0.0035	0.0236
T459_04004	-1.8149	0.2659	-6.8267	0.0000	0.0000
T459_17919	-1.8132	0.5973	-3.0354	0.0024	0.0172
T459_34437	-1.8118	0.3900	-4.6459	0.0000	0.0001
T459_05252	-1.8109	0.4984	-3.6335	0.0003	0.0027
T459_10792	-1.8059	0.4365	-4.1370	0.0000	0.0004
T459_16891	-1.8053	0.6459	-2.7951	0.0052	0.0322
T459_32578	-1.7976	0.2181	-8.2417	0.0000	0.0000
T459_30884	-1.7961	0.3404	-5.2772	0.0000	0.0000
T459_24585	-1.7851	0.4773	-3.7402	0.0002	0.0019
T459_24769	-1.7830	0.5087	-3.5050	0.0005	0.0041
T459_00935	-1.7757	0.2857	-6.2148	0.0000	0.0000
T459_07612	-1.7729	0.1574	-11.2628	0.0000	0.0000
T459_13633	-1.7720	0.2950	-6.0066	0.0000	0.0000
T459_08904	-1.7700	0.1583	-11.1823	0.0000	0.0000
T459_04466	-1.7678	0.2736	-6.4622	0.0000	0.0000
T459_07967	-1.7623	0.4529	-3.8913	0.0001	0.0011
T459_32515	-1.7620	0.3722	-4.7336	0.0000	0.0000
T459_09619	-1.7557	0.2618	-6.7066	0.0000	0.0000
T459_29061	-1.7492	0.2208	-7.9233	0.0000	0.0000
T459_30505	-1.7491	0.2676	-6.5366	0.0000	0.0000
T459_09302	-1.7413	0.5679	-3.0661	0.0022	0.0158
T459_15961	-1.7382	0.4742	-3.6651	0.0002	0.0024
T459_27819	-1.7379	0.1358	-12.7989	0.0000	0.0000

Gene ID	log2FoldChange	lfcSE	stat	pvalue	padj
T459_10793	-1.7359	0.2744	-6.3273	0.0000	0.0000
T459_29548	-1.7287	0.3992	-4.3309	0.0000	0.0002
T459_20547	-1.7260	0.2043	-8.4465	0.0000	0.0000
T459_06244	-1.7246	0.1790	-9.6368	0.0000	0.0000
T459_09478	-1.7193	0.1566	-10.9781	0.0000	0.0000
T459_15846	-1.7160	0.2191	-7.8308	0.0000	0.0000
T459_15576	-1.6949	0.2628	-6.4501	0.0000	0.0000
T459_17106	-1.6913	0.2171	-7.7923	0.0000	0.0000
T459_33221	-1.6912	0.4118	-4.1071	0.0000	0.0005
T459_23742	-1.6909	0.6337	-2.6685	0.0076	0.0440
T459_08649	-1.6904	0.1702	-9.9339	0.0000	0.0000
T459_12694	-1.6884	0.3323	-5.0818	0.0000	0.0000
T459_20228	-1.6878	0.3391	-4.9772	0.0000	0.0000
T459_22671	-1.6868	0.4943	-3.4126	0.0006	0.0056
T459_10040	-1.6811	0.6178	-2.7213	0.0065	0.0388
T459_34780	-1.6776	0.2073	-8.0908	0.0000	0.0000
T459_03550	-1.6757	0.5478	-3.0592	0.0022	0.0161
T459_15071	-1.6752	0.2731	-6.1335	0.0000	0.0000
T459_24190	-1.6748	0.2455	-6.8218	0.0000	0.0000
T459_31710	-1.6738	0.4172	-4.0123	0.0001	0.0007
T459_31249	-1.6697	0.4908	-3.4019	0.0007	0.0058
T459_03747	-1.6691	0.2908	-5.7399	0.0000	0.0000
T459_17928	-1.6685	0.2840	-5.8750	0.0000	0.0000
T459_27892	-1.6646	0.3844	-4.3300	0.0000	0.0002
T459_23761	-1.6636	0.4616	-3.6037	0.0003	0.0030
T459_28658	-1.6635	0.2362	-7.0440	0.0000	0.0000
T459_28556	-1.6623	0.3086	-5.3873	0.0000	0.0000
T459_33809	-1.6564	0.4845	-3.4187	0.0006	0.0055
T459_00160	-1.6549	0.4102	-4.0342	0.0001	0.0006
T459_20387	-1.6477	0.2516	-6.5500	0.0000	0.0000
T459_04694	-1.6386	0.3020	-5.4250	0.0000	0.0000
T459_18287	-1.6369	0.5215	-3.1388	0.0017	0.0129
T459_09665	-1.6368	0.2097	-7.8070	0.0000	0.0000
T459_27046	-1.6338	0.3543	-4.6108	0.0000	0.0001
T459_34688	-1.6284	0.3564	-4.5683	0.0000	0.0001
T459_31475	-1.6249	0.2084	-7.7963	0.0000	0.0000
T459_16895	-1.6005	0.5942	-2.6933	0.0071	0.0414
T459_25513	-1.5997	0.2405	-6.6500	0.0000	0.0000
T459_18956	-1.5996	0.5931	-2.6971	0.0070	0.0411
T459_22326	-1.5975	0.5158	-3.0970	0.0020	0.0145
T459_32208	-1.5884	0.4252	-3.7352	0.0002	0.0019
T459_15343	-1.5868	0.2460	-6.4495	0.0000	0.0000
T459_26412	-1.5836	0.2172	-7.2909	0.0000	0.0000
T459_26554	-1.5815	0.2116	-7.4749	0.0000	0.0000
T459_15460	-1.5748	0.3220	-4.8901	0.0000	0.0000
T459_28616	-1.5721	0.2339	-6.7223	0.0000	0.0000
T459_14746	-1.5699	0.5946	-2.6405	0.0083	0.0471

Gene ID	log2FoldChange	lfcSE	stat	pvalue	padj
T459_35632	-1.5606	0.5485	-2.8449	0.0044	0.0285
T459_28000	-1.5580	0.1758	-8.8603	0.0000	0.0000
T459_26375	-1.5565	0.1075	-14.4822	0.0000	0.0000
T459_24413	-1.5520	0.4852	-3.1988	0.0014	0.0108
T459_23717	-1.5520	0.5360	-2.8957	0.0038	0.0251
T459_24139	-1.5507	0.4395	-3.5288	0.0004	0.0038
T459_03652	-1.5504	0.4811	-3.2226	0.0013	0.0100
T459_00118	-1.5464	0.1926	-8.0314	0.0000	0.0000
T459_05319	-1.5448	0.3465	-4.4586	0.0000	0.0001
T459_18050	-1.5371	0.3209	-4.7900	0.0000	0.0000
T459_31786	-1.5342	0.2737	-5.6047	0.0000	0.0000
T459_04599	-1.5325	0.5469	-2.8022	0.0051	0.0316
T459_04396	-1.5323	0.3252	-4.7122	0.0000	0.0000
T459_00896	-1.5297	0.2010	-7.6110	0.0000	0.0000
T459_04042	-1.5290	0.3154	-4.8474	0.0000	0.0000
T459_17976	-1.5280	0.2808	-5.4425	0.0000	0.0000
T459_29259	-1.5260	0.4301	-3.5482	0.0004	0.0036
T459_00120	-1.5248	0.3929	-3.8810	0.0001	0.0011
T459_00830	-1.5244	0.5025	-3.0336	0.0024	0.0173
T459_34694	-1.5237	0.2510	-6.0696	0.0000	0.0000
T459_20126	-1.5217	0.3498	-4.3503	0.0000	0.0002
T459_28618	-1.5124	0.4416	-3.4249	0.0006	0.0054
T459_18555	-1.5110	0.2829	-5.3418	0.0000	0.0000
T459_02212	-1.5102	0.4650	-3.2474	0.0012	0.0094
T459_04064	-1.4930	0.3177	-4.6996	0.0000	0.0000
T459_26830	-1.4927	0.3489	-4.2787	0.0000	0.0002
T459_16885	-1.4924	0.1639	-9.1065	0.0000	0.0000
T459_05634	-1.4912	0.3119	-4.7804	0.0000	0.0000
T459_03656	-1.4889	0.5293	-2.8130	0.0049	0.0309
T459_05793	-1.4874	0.2824	-5.2676	0.0000	0.0000
T459_08278	-1.4866	0.2458	-6.0487	0.0000	0.0000
T459_30790	-1.4848	0.2373	-6.2577	0.0000	0.0000
T459_09272	-1.4833	0.5319	-2.7886	0.0053	0.0328
T459_18546	-1.4830	0.3425	-4.3300	0.0000	0.0002
T459_26349	-1.4804	0.1777	-8.3325	0.0000	0.0000
T459_26876	-1.4729	0.5069	-2.9056	0.0037	0.0245
T459_08785	-1.4613	0.1872	-7.8058	0.0000	0.0000
T459_29285	-1.4575	0.3584	-4.0666	0.0000	0.0006
T459_05316	-1.4530	0.2710	-5.3608	0.0000	0.0000
T459_10649	-1.4530	0.1395	-10.4180	0.0000	0.0000
T459_34912	-1.4463	0.3917	-3.6925	0.0002	0.0022
T459_28081	-1.4401	0.1773	-8.1228	0.0000	0.0000
T459_18783	-1.4400	0.4687	-3.0724	0.0021	0.0155
T459_06692	-1.4398	0.1697	-8.4825	0.0000	0.0000
T459_23150	-1.4390	0.3626	-3.9685	0.0001	0.0008
T459_29809	-1.4376	0.3143	-4.5746	0.0000	0.0001
T459_09878	-1.4333	0.4195	-3.4170	0.0006	0.0055

Gene ID	log2FoldChange	lfcSE	stat	pvalue	padj
T459_32792	-1.4308	0.4354	-3.2864	0.0010	0.0083
T459_22341	-1.4293	0.3200	-4.4666	0.0000	0.0001
T459_27445	-1.4279	0.1650	-8.6551	0.0000	0.0000
T459_02811	-1.4264	0.2224	-6.4138	0.0000	0.0000
T459_24915	-1.4259	0.3419	-4.1701	0.0000	0.0004
T459_00829	-1.4238	0.3059	-4.6538	0.0000	0.0001
T459_29886	-1.4233	0.1909	-7.4575	0.0000	0.0000
T459_28372	-1.4196	0.2464	-5.7609	0.0000	0.0000
T459_30265	-1.4173	0.4854	-2.9200	0.0035	0.0236
T459_27776	-1.4167	0.2270	-6.2404	0.0000	0.0000
T459_00587	-1.4162	0.2968	-4.7712	0.0000	0.0000
T459_07844	-1.4153	0.2192	-6.4570	0.0000	0.0000
T459_00870	-1.4151	0.2719	-5.2051	0.0000	0.0000
T459_15306	-1.4130	0.2279	-6.2011	0.0000	0.0000
T459_10518	-1.4125	0.2296	-6.1532	0.0000	0.0000
T459_29489	-1.4105	0.1891	-7.4596	0.0000	0.0000
T459_06533	-1.4080	0.3362	-4.1883	0.0000	0.0004
T459_13796	-1.4074	0.2708	-5.1979	0.0000	0.0000
T459_17927	-1.4013	0.1165	-12.0273	0.0000	0.0000
T459_10824	-1.3984	0.2554	-5.4743	0.0000	0.0000
T459_15163	-1.3960	0.2567	-5.4380	0.0000	0.0000
T459_24367	-1.3954	0.3709	-3.7621	0.0002	0.0017
T459_31012	-1.3951	0.1466	-9.5190	0.0000	0.0000
T459_05227	-1.3943	0.1601	-8.7105	0.0000	0.0000
T459_12955	-1.3938	0.4749	-2.9352	0.0033	0.0226
T459_06053	-1.3936	0.1797	-7.7564	0.0000	0.0000
T459_13455	-1.3933	0.2566	-5.4305	0.0000	0.0000
T459_23048	-1.3889	0.1769	-7.8529	0.0000	0.0000
T459_10096	-1.3887	0.1155	-12.0284	0.0000	0.0000
T459_07979	-1.3877	0.2378	-5.8353	0.0000	0.0000
T459_20103	-1.3867	0.2746	-5.0495	0.0000	0.0000
T459_29396	-1.3843	0.4992	-2.7731	0.0056	0.0341
T459_35322	-1.3806	0.1679	-8.2211	0.0000	0.0000
T459_10335	-1.3773	0.2950	-4.6693	0.0000	0.0000
T459_22211	-1.3768	0.3992	-3.4485	0.0006	0.0050
T459_09792	-1.3717	0.3488	-3.9329	0.0001	0.0009
T459_07638	-1.3707	0.3066	-4.4707	0.0000	0.0001
T459_07439	-1.3705	0.4574	-2.9965	0.0027	0.0191
T459_04054	-1.3684	0.1652	-8.2809	0.0000	0.0000
T459_13998	-1.3679	0.1564	-8.7434	0.0000	0.0000
T459_07453	-1.3654	0.2900	-4.7082	0.0000	0.0000
T459_33446	-1.3646	0.1683	-8.1094	0.0000	0.0000
T459_09658	-1.3586	0.3617	-3.7560	0.0002	0.0018
T459_10606	-1.3549	0.1633	-8.2978	0.0000	0.0000
T459_11205	-1.3541	0.4840	-2.7976	0.0051	0.0320
T459_02332	-1.3510	0.3921	-3.4454	0.0006	0.0050
T459_27700	-1.3506	0.2577	-5.2415	0.0000	0.0000

Gene ID	log2FoldChange	lfcSE	stat	pvalue	padj
T459_14010	-1.3471	0.3107	-4.3361	0.0000	0.0002
T459_34438	-1.3465	0.4194	-3.2107	0.0013	0.0104
T459_23964	-1.3448	0.3720	-3.6154	0.0003	0.0029
T459_10860	-1.3448	0.2225	-6.0431	0.0000	0.0000
T459_12710	-1.3425	0.2607	-5.1505	0.0000	0.0000
T459_18222	-1.3394	0.4117	-3.2534	0.0011	0.0092
T459_20956	-1.3379	0.1939	-6.9017	0.0000	0.0000
T459_35286	-1.3367	0.4061	-3.2913	0.0010	0.0082
T459_10457	-1.3328	0.3032	-4.3954	0.0000	0.0002
T459_10452	-1.3313	0.2370	-5.6181	0.0000	0.0000
T459_05423	-1.3294	0.3052	-4.3555	0.0000	0.0002
T459_28271	-1.3288	0.1716	-7.7426	0.0000	0.0000
T459_05960	-1.3268	0.1572	-8.4420	0.0000	0.0000
T459_13524	-1.3250	0.3518	-3.7665	0.0002	0.0017
T459_20700	-1.3250	0.3142	-4.2172	0.0000	0.0003
T459_20400	-1.3121	0.4526	-2.8994	0.0037	0.0248
T459_01225	-1.2964	0.4255	-3.0470	0.0023	0.0167
T459_01295	-1.2931	0.3902	-3.3142	0.0009	0.0077
T459_13211	-1.2923	0.4366	-2.9599	0.0031	0.0211
T459_31770	-1.2906	0.4025	-3.2063	0.0013	0.0105
T459_35236	-1.2865	0.2293	-5.6098	0.0000	0.0000
T459_04157	-1.2863	0.4719	-2.7257	0.0064	0.0384
T459_15327	-1.2841	0.2793	-4.5982	0.0000	0.0001
T459_24693	-1.2812	0.2391	-5.3589	0.0000	0.0000
T459_12256	-1.2784	0.3517	-3.6353	0.0003	0.0027
T459_16555	-1.2781	0.1886	-6.7753	0.0000	0.0000
T459_31358	-1.2778	0.2048	-6.2389	0.0000	0.0000
T459_14436	-1.2766	0.4314	-2.9589	0.0031	0.0212
T459_06156	-1.2727	0.2401	-5.3013	0.0000	0.0000
T459_33467	-1.2681	0.3906	-3.2463	0.0012	0.0094
T459_28640	-1.2677	0.3187	-3.9771	0.0001	0.0008
T459_18678	-1.2616	0.2073	-6.0850	0.0000	0.0000
T459_32099	-1.2561	0.4788	-2.6232	0.0087	0.0490
T459_23333	-1.2556	0.3806	-3.2994	0.0010	0.0080
T459_18673	-1.2545	0.1602	-7.8325	0.0000	0.0000
T459_34687	-1.2539	0.1984	-6.3214	0.0000	0.0000
T459_05047	-1.2536	0.1773	-7.0711	0.0000	0.0000
T459_32574	-1.2532	0.3300	-3.7971	0.0001	0.0015
T459_05274	-1.2505	0.3276	-3.8176	0.0001	0.0014
T459_18703	-1.2496	0.3858	-3.2387	0.0012	0.0096
T459_09676	-1.2493	0.2234	-5.5913	0.0000	0.0000
T459_03900	-1.2427	0.2085	-5.9606	0.0000	0.0000
T459_16120	-1.2387	0.1961	-6.3152	0.0000	0.0000
T459_17005	-1.2321	0.2737	-4.5012	0.0000	0.0001
T459_15575	-1.2305	0.4223	-2.9135	0.0036	0.0240
T459_12614	-1.2299	0.3820	-3.2197	0.0013	0.0101
T459_06799	-1.2277	0.1496	-8.2094	0.0000	0.0000

Gene ID	log2FoldChange	lfcSE	stat	pvalue	padj
T459_14639	-1.2277	0.1978	-6.2077	0.0000	0.0000
T459_04844	-1.2271	0.2438	-5.0340	0.0000	0.0000
T459_25584	-1.2251	0.2193	-5.5851	0.0000	0.0000
T459_22051	-1.2236	0.1858	-6.5841	0.0000	0.0000
T459_20601	-1.2197	0.3181	-3.8341	0.0001	0.0014
T459_05643	-1.2197	0.2482	-4.9144	0.0000	0.0000
T459_24151	-1.2174	0.4109	-2.9626	0.0031	0.0210
T459_19506	-1.2172	0.2285	-5.3258	0.0000	0.0000
T459_20630	-1.2168	0.2194	-5.5466	0.0000	0.0000
T459_15672	-1.2131	0.2249	-5.3943	0.0000	0.0000
T459_18047	-1.2122	0.4104	-2.9532	0.0031	0.0215
T459_18447	-1.2097	0.4449	-2.7192	0.0065	0.0390
T459_19288	-1.2088	0.2759	-4.3813	0.0000	0.0002
T459_33424	-1.2054	0.3253	-3.7053	0.0002	0.0021
T459_18146	-1.2054	0.2284	-5.2777	0.0000	0.0000
T459_33291	-1.2036	0.1802	-6.6786	0.0000	0.0000
T459_10888	-1.2013	0.1871	-6.4219	0.0000	0.0000
T459_25075	-1.2009	0.2163	-5.5514	0.0000	0.0000
T459_26008	-1.1975	0.4331	-2.7651	0.0057	0.0348
T459_09678	-1.1972	0.1021	-11.7290	0.0000	0.0000
T459_13444	-1.1964	0.1846	-6.4807	0.0000	0.0000
T459_22748	-1.1958	0.3102	-3.8549	0.0001	0.0013
T459_09682	-1.1953	0.3843	-3.1103	0.0019	0.0140
T459_21770	-1.1952	0.1689	-7.0744	0.0000	0.0000
T459_17973	-1.1946	0.3787	-3.1550	0.0016	0.0123
T459_03749	-1.1946	0.1621	-7.3703	0.0000	0.0000
T459_30713	-1.1928	0.1788	-6.6711	0.0000	0.0000
T459_20351	-1.1927	0.2275	-5.2425	0.0000	0.0000
T459_32413	-1.1925	0.2274	-5.2443	0.0000	0.0000
T459_11005	-1.1917	0.2137	-5.5775	0.0000	0.0000
T459_15101	-1.1903	0.2652	-4.4877	0.0000	0.0001
T459_05380	-1.1884	0.4041	-2.9407	0.0033	0.0223
T459_32155	-1.1882	0.3173	-3.7448	0.0002	0.0018
T459_07637	-1.1881	0.3431	-3.4630	0.0005	0.0047
T459_33560	-1.1817	0.2295	-5.1498	0.0000	0.0000
T459_11119	-1.1799	0.2939	-4.0148	0.0001	0.0007
T459_22854	-1.1799	0.2006	-5.8813	0.0000	0.0000
T459_16524	-1.1791	0.1659	-7.1053	0.0000	0.0000
T459_09677	-1.1780	0.1868	-6.3060	0.0000	0.0000
T459_05485	-1.1735	0.2957	-3.9683	0.0001	0.0008
T459_03994	-1.1697	0.1480	-7.9040	0.0000	0.0000
T459_15095	-1.1687	0.1764	-6.6252	0.0000	0.0000
T459_34477	-1.1681	0.1803	-6.4801	0.0000	0.0000
T459_07607	-1.1676	0.1185	-9.8541	0.0000	0.0000
T459_22212	-1.1668	0.4050	-2.8810	0.0040	0.0260
T459_13126	-1.1646	0.2019	-5.7679	0.0000	0.0000
T459_19444	-1.1633	0.1974	-5.8917	0.0000	0.0000

Gene ID	log2FoldChange	lfcSE	stat	pvalue	padj
T459_31701	-1.1598	0.2981	-3.8906	0.0001	0.0011
T459_28400	-1.1590	0.2567	-4.5144	0.0000	0.0001
T459_18943	-1.1587	0.2551	-4.5413	0.0000	0.0001
T459_31320	-1.1576	0.2752	-4.2070	0.0000	0.0003
T459_02059	-1.1553	0.2125	-5.4362	0.0000	0.0000
T459_18378	-1.1552	0.2695	-4.2864	0.0000	0.0002
T459_33005	-1.1545	0.2454	-4.7039	0.0000	0.0000
T459_25932	-1.1528	0.2831	-4.0723	0.0000	0.0006
T459_24494	-1.1515	0.3949	-2.9161	0.0035	0.0238
T459_03063	-1.1513	0.2187	-5.2632	0.0000	0.0000
T459_33815	-1.1509	0.2294	-5.0172	0.0000	0.0000
T459_24566	-1.1496	0.2380	-4.8300	0.0000	0.0000
T459_06703	-1.1473	0.4351	-2.6367	0.0084	0.0474
T459_18379	-1.1471	0.2859	-4.0118	0.0001	0.0007
T459_05995	-1.1465	0.1682	-6.8169	0.0000	0.0000
T459_15674	-1.1452	0.2998	-3.8205	0.0001	0.0014
T459_10524	-1.1448	0.2486	-4.6059	0.0000	0.0001
T459_04323	-1.1446	0.4157	-2.7531	0.0059	0.0358
T459_21280	-1.1444	0.1983	-5.7710	0.0000	0.0000
T459_17139	-1.1437	0.1628	-7.0243	0.0000	0.0000
T459_28576	-1.1428	0.2561	-4.4623	0.0000	0.0001
T459_22563	-1.1415	0.2869	-3.9782	0.0001	0.0008
T459_07935	-1.1357	0.3011	-3.7713	0.0002	0.0017
T459_22720	-1.1319	0.3603	-3.1412	0.0017	0.0128
T459_32285	-1.1308	0.2536	-4.4585	0.0000	0.0001
T459_22564	-1.1273	0.1461	-7.7149	0.0000	0.0000
T459_18327	-1.1264	0.2411	-4.6724	0.0000	0.0000
T459_34540	-1.1257	0.3172	-3.5484	0.0004	0.0036
T459_22213	-1.1241	0.2973	-3.7809	0.0002	0.0016
T459_13141	-1.1209	0.3771	-2.9724	0.0030	0.0204
T459_22972	-1.1200	0.1691	-6.6240	0.0000	0.0000
T459_06075	-1.1199	0.2094	-5.3488	0.0000	0.0000
T459_21980	-1.1124	0.2901	-3.8350	0.0001	0.0014
T459_25140	-1.1109	0.2558	-4.3435	0.0000	0.0002
T459_17003	-1.1104	0.1440	-7.7107	0.0000	0.0000
T459_28087	-1.1068	0.2759	-4.0119	0.0001	0.0007
T459_13934	-1.1068	0.3672	-3.0144	0.0026	0.0182
T459_17246	-1.1066	0.2223	-4.9777	0.0000	0.0000
T459_28920	-1.1053	0.2578	-4.2881	0.0000	0.0002
T459_30912	-1.1041	0.3813	-2.8958	0.0038	0.0251
T459_28395	-1.1020	0.3989	-2.7622	0.0057	0.0350
T459_10283	-1.1013	0.1813	-6.0760	0.0000	0.0000
T459_17022	-1.1008	0.1548	-7.1087	0.0000	0.0000
T459_05009	-1.0985	0.4031	-2.7250	0.0064	0.0384
T459_05720	-1.0972	0.2204	-4.9791	0.0000	0.0000
T459_32622	-1.0972	0.2005	-5.4714	0.0000	0.0000
T459_13825	-1.0970	0.3895	-2.8165	0.0049	0.0307

Gene ID	log2FoldChange	lfcSE	stat	pvalue	padj
T459_09914	-1.0962	0.3016	-3.6348	0.0003	0.0027
T459_17528	-1.0956	0.1895	-5.7821	0.0000	0.0000
T459_18560	-1.0916	0.3031	-3.6013	0.0003	0.0030
T459_08259	-1.0901	0.3921	-2.7799	0.0054	0.0335
T459_12653	-1.0880	0.1540	-7.0660	0.0000	0.0000
T459_34285	-1.0856	0.2343	-4.6337	0.0000	0.0001
T459_05454	-1.0835	0.2256	-4.8028	0.0000	0.0000
T459_14160	-1.0812	0.2871	-3.7667	0.0002	0.0017
T459_31205	-1.0808	0.4059	-2.6630	0.0077	0.0446
T459_30901	-1.0806	0.2272	-4.7556	0.0000	0.0000
T459_01519	-1.0806	0.2385	-4.5311	0.0000	0.0001
T459_19400	-1.0805	0.2253	-4.7970	0.0000	0.0000
T459_25801	-1.0805	0.1505	-7.1792	0.0000	0.0000
T459_10124	-1.0803	0.1587	-6.8072	0.0000	0.0000
T459_31422	-1.0800	0.2953	-3.6574	0.0003	0.0025
T459_20127	-1.0799	0.2746	-3.9331	0.0001	0.0009
T459_30370	-1.0793	0.2722	-3.9658	0.0001	0.0008
T459_22565	-1.0774	0.3878	-2.7785	0.0055	0.0336
T459_28925	-1.0769	0.2846	-3.7845	0.0002	0.0016
T459_22210	-1.0767	0.2369	-4.5440	0.0000	0.0001
T459_20685	-1.0728	0.1623	-6.6089	0.0000	0.0000
T459_24838	-1.0727	0.3935	-2.7261	0.0064	0.0384
T459_26032	-1.0708	0.2362	-4.5332	0.0000	0.0001
T459_23332	-1.0695	0.1679	-6.3707	0.0000	0.0000
T459_30718	-1.0674	0.2127	-5.0180	0.0000	0.0000
T459_04254	-1.0672	0.1307	-8.1662	0.0000	0.0000
T459_33656	-1.0649	0.2536	-4.1984	0.0000	0.0003
T459_09663	-1.0644	0.3925	-2.7118	0.0067	0.0396
T459_17230	-1.0640	0.1933	-5.5035	0.0000	0.0000
T459_22484	-1.0636	0.3286	-3.2365	0.0012	0.0096
T459_34478	-1.0625	0.2077	-5.1149	0.0000	0.0000
T459_26257	-1.0617	0.3516	-3.0199	0.0025	0.0180
T459_24029	-1.0606	0.1715	-6.1849	0.0000	0.0000
T459_34682	-1.0603	0.3553	-2.9838	0.0028	0.0198
T459_03587	-1.0600	0.1885	-5.6221	0.0000	0.0000
T459_09060	-1.0596	0.1681	-6.3029	0.0000	0.0000
T459_06607	-1.0594	0.2894	-3.6610	0.0003	0.0025
T459_05113	-1.0586	0.1795	-5.8986	0.0000	0.0000
T459_35119	-1.0579	0.2202	-4.8043	0.0000	0.0000
T459_21969	-1.0572	0.1357	-7.7884	0.0000	0.0000
T459_01685	-1.0558	0.2993	-3.5272	0.0004	0.0038
T459_25139	-1.0547	0.3235	-3.2597	0.0011	0.0090
T459_32045	-1.0544	0.2585	-4.0788	0.0000	0.0005
T459_06157	-1.0537	0.2507	-4.2022	0.0000	0.0003
T459_29968	-1.0535	0.3737	-2.8195	0.0048	0.0304
T459_10253	-1.0534	0.2486	-4.2373	0.0000	0.0003
T459_01423	-1.0519	0.3075	-3.4204	0.0006	0.0054

Gene ID	log2FoldChange	lfcSE	stat	pvalue	padj
T459_02583	-1.0518	0.3547	-2.9649	0.0030	0.0208
T459_24583	-1.0477	0.2232	-4.6945	0.0000	0.0000
T459_29328	-1.0473	0.1717	-6.1000	0.0000	0.0000
T459_24904	-1.0454	0.3788	-2.7601	0.0058	0.0352
T459_09213	-1.0414	0.3216	-3.2388	0.0012	0.0096
T459_18084	-1.0405	0.1581	-6.5823	0.0000	0.0000
T459_26124	-1.0360	0.3553	-2.9162	0.0035	0.0238
T459_27568	-1.0347	0.1516	-6.8243	0.0000	0.0000
T459_18231	-1.0329	0.1892	-5.4588	0.0000	0.0000
T459_23598	-1.0328	0.2107	-4.9019	0.0000	0.0000
T459_26371	-1.0323	0.2759	-3.7420	0.0002	0.0019
T459_24342	-1.0321	0.3674	-2.8097	0.0050	0.0311
T459_21735	-1.0314	0.1237	-8.3387	0.0000	0.0000
T459_33904	-1.0283	0.3449	-2.9817	0.0029	0.0199
T459_26551	-1.0282	0.2729	-3.7676	0.0002	0.0017
T459_27999	-1.0276	0.1319	-7.7927	0.0000	0.0000
T459_20119	-1.0225	0.1686	-6.0651	0.0000	0.0000
T459_24338	-1.0225	0.2854	-3.5823	0.0003	0.0032
T459_31733	-1.0209	0.3404	-2.9990	0.0027	0.0190
T459_18223	-1.0201	0.1702	-5.9916	0.0000	0.0000
T459_06592	-1.0200	0.2361	-4.3205	0.0000	0.0002
T459_10512	-1.0173	0.3259	-3.1215	0.0018	0.0136
T459_03518	-1.0155	0.2436	-4.1684	0.0000	0.0004
T459_15429	-1.0153	0.2105	-4.8228	0.0000	0.0000
T459_23784	-1.0136	0.1930	-5.2529	0.0000	0.0000
T459_14420	-1.0131	0.1581	-6.4096	0.0000	0.0000
T459_32186	-1.0122	0.2136	-4.7390	0.0000	0.0000
T459_28862	-1.0099	0.2700	-3.7405	0.0002	0.0019
T459_15458	-1.0096	0.2754	-3.6654	0.0002	0.0024
T459_00130	-1.0089	0.1758	-5.7380	0.0000	0.0000
T459_11214	-1.0083	0.2747	-3.6698	0.0002	0.0024
T459_34418	-1.0080	0.1510	-6.6768	0.0000	0.0000
T459_16317	-1.0074	0.1669	-6.0361	0.0000	0.0000
T459_11983	-1.0073	0.3578	-2.8150	0.0049	0.0308
T459_08260	-1.0060	0.1625	-6.1922	0.0000	0.0000
T459_27964	-1.0057	0.2220	-4.5313	0.0000	0.0001
T459_17950	-1.0055	0.3044	-3.3034	0.0010	0.0079
T459_21302	1.0005	0.1314	7.6143	0.0000	0.0000
T459_09093	1.0015	0.2219	4.5130	0.0000	0.0001
T459_08896	1.0087	0.2166	4.6558	0.0000	0.0001
T459_26283	1.0096	0.1983	5.0924	0.0000	0.0000
T459_05677	1.0097	0.1979	5.1021	0.0000	0.0000
T459_17125	1.0106	0.3759	2.6884	0.0072	0.0419
T459_27389	1.0116	0.3630	2.7866	0.0053	0.0329
T459_33223	1.0126	0.2008	5.0425	0.0000	0.0000
T459_02937	1.0129	0.2581	3.9247	0.0001	0.0010
T459_22368	1.0134	0.2020	5.0176	0.0000	0.0000

Gene ID	log2FoldChange	lfcSE	stat	pvalue	padj
T459_33564	1.0138	0.3219	3.1491	0.0016	0.0125
T459_04659	1.0171	0.2889	3.5202	0.0004	0.0039
T459_24882	1.0176	0.2854	3.5655	0.0004	0.0034
T459_32123	1.0177	0.1920	5.2998	0.0000	0.0000
T459_33547	1.0219	0.2900	3.5235	0.0004	0.0039
T459_13782	1.0225	0.3579	2.8567	0.0043	0.0276
T459_31490	1.0226	0.2344	4.3629	0.0000	0.0002
T459_25596	1.0239	0.1109	9.2320	0.0000	0.0000
T459_27448	1.0276	0.1244	8.2593	0.0000	0.0000
T459_22667	1.0283	0.3279	3.1363	0.0017	0.0130
T459_11705	1.0286	0.1807	5.6923	0.0000	0.0000
T459_30471	1.0291	0.1864	5.5201	0.0000	0.0000
T459_15997	1.0324	0.3347	3.0846	0.0020	0.0150
T459_21829	1.0330	0.2569	4.0208	0.0001	0.0007
T459_28305	1.0332	0.1910	5.4106	0.0000	0.0000
T459_32255	1.0373	0.1985	5.2254	0.0000	0.0000
T459_19483	1.0379	0.1147	9.0514	0.0000	0.0000
T459_32005	1.0386	0.1822	5.6996	0.0000	0.0000
T459_22325	1.0395	0.2194	4.7378	0.0000	0.0000
T459_26523	1.0407	0.1328	7.8377	0.0000	0.0000
T459_13294	1.0407	0.2079	5.0053	0.0000	0.0000
T459_06370	1.0439	0.1850	5.6430	0.0000	0.0000
T459_25716	1.0453	0.2846	3.6734	0.0002	0.0024
T459_07675	1.0462	0.1972	5.3062	0.0000	0.0000
T459_19762	1.0504	0.2138	4.9132	0.0000	0.0000
T459_20389	1.0533	0.2439	4.3180	0.0000	0.0002
T459_15945	1.0535	0.1543	6.8271	0.0000	0.0000
T459_18325	1.0540	0.3102	3.3978	0.0007	0.0058
T459_12288	1.0546	0.2368	4.4529	0.0000	0.0001
T459_07033	1.0551	0.2984	3.5363	0.0004	0.0037
T459_34296	1.0560	0.2013	5.2464	0.0000	0.0000
T459_30489	1.0570	0.1202	8.7944	0.0000	0.0000
T459_05880	1.0572	0.2781	3.8009	0.0001	0.0015
T459_35376	1.0599	0.2209	4.7985	0.0000	0.0000
T459_07963	1.0631	0.1768	6.0123	0.0000	0.0000
T459_21342	1.0637	0.3684	2.8877	0.0039	0.0256
T459_07424	1.0651	0.2346	4.5397	0.0000	0.0001
T459_16126	1.0669	0.4041	2.6402	0.0083	0.0471
T459_27502	1.0695	0.3694	2.8949	0.0038	0.0251
T459_13916	1.0707	0.3027	3.5378	0.0004	0.0037
T459_14050	1.0712	0.3046	3.5167	0.0004	0.0040
T459_25953	1.0724	0.1762	6.0874	0.0000	0.0000
T459_28012	1.0729	0.2431	4.4128	0.0000	0.0001
T459_24352	1.0764	0.1597	6.7396	0.0000	0.0000
T459_10523	1.0787	0.2558	4.2169	0.0000	0.0003
T459_13621	1.0805	0.1974	5.4729	0.0000	0.0000
T459_02822	1.0820	0.3550	3.0478	0.0023	0.0167

Gene ID	log2FoldChange	lfcSE	stat	pvalue	padj
T459_27911	1.0846	0.2271	4.7760	0.0000	0.0000
T459_08122	1.0849	0.3294	3.2934	0.0010	0.0081
T459_06119	1.0853	0.3995	2.7166	0.0066	0.0392
T459_25393	1.0855	0.3364	3.2267	0.0013	0.0099
T459_27394	1.0858	0.2966	3.6606	0.0003	0.0025
T459_06623	1.0886	0.2429	4.4812	0.0000	0.0001
T459_23444	1.0889	0.1884	5.7797	0.0000	0.0000
T459_01044	1.0920	0.1381	7.9048	0.0000	0.0000
T459_21293	1.0936	0.2202	4.9676	0.0000	0.0000
T459_15873	1.0965	0.2386	4.5958	0.0000	0.0001
T459_11882	1.0966	0.1375	7.9773	0.0000	0.0000
T459_15814	1.0971	0.2286	4.7986	0.0000	0.0000
T459_25939	1.0979	0.3923	2.7989	0.0051	0.0319
T459_27388	1.1003	0.2570	4.2819	0.0000	0.0002
T459_22348	1.1003	0.3373	3.2618	0.0011	0.0089
T459_07336	1.1017	0.4168	2.6434	0.0082	0.0467
T459_27048	1.1021	0.1923	5.7313	0.0000	0.0000
T459_34102	1.1021	0.2582	4.2692	0.0000	0.0003
T459_13179	1.1032	0.2573	4.2881	0.0000	0.0002
T459_01440	1.1089	0.2296	4.8291	0.0000	0.0000
T459_21098	1.1118	0.1407	7.9004	0.0000	0.0000
T459_22431	1.1127	0.2464	4.5167	0.0000	0.0001
T459_17254	1.1161	0.2516	4.4361	0.0000	0.0001
T459_18795	1.1162	0.1330	8.3926	0.0000	0.0000
T459_15141	1.1169	0.3059	3.6510	0.0003	0.0026
T459_03316	1.1179	0.2830	3.9502	0.0001	0.0009
T459_22555	1.1199	0.2679	4.1798	0.0000	0.0004
T459_30978	1.1221	0.2487	4.5118	0.0000	0.0001
T459_26475	1.1227	0.2760	4.0670	0.0000	0.0006
T459_31503	1.1230	0.3660	3.0682	0.0022	0.0157
T459_13788	1.1239	0.1570	7.1573	0.0000	0.0000
T459_32329	1.1259	0.2086	5.3977	0.0000	0.0000
T459_20713	1.1292	0.3854	2.9301	0.0034	0.0229
T459_10139	1.1302	0.1585	7.1311	0.0000	0.0000
T459_19552	1.1320	0.0997	11.3492	0.0000	0.0000
T459_09843	1.1336	0.2739	4.1382	0.0000	0.0004
T459_26318	1.1407	0.1828	6.2390	0.0000	0.0000
T459_30018	1.1410	0.3381	3.3748	0.0007	0.0063
T459_06582	1.1415	0.2588	4.4111	0.0000	0.0001
T459_01450	1.1441	0.3347	3.4179	0.0006	0.0055
T459_29286	1.1448	0.1679	6.8189	0.0000	0.0000
T459_09108	1.1454	0.1691	6.7749	0.0000	0.0000
T459_02320	1.1501	0.2854	4.0291	0.0001	0.0007
T459_06837	1.1526	0.1792	6.4319	0.0000	0.0000
T459_16156	1.1542	0.3611	3.1959	0.0014	0.0109
T459_11261	1.1564	0.3728	3.1014	0.0019	0.0143
T459_07697	1.1616	0.2407	4.8258	0.0000	0.0000

Gene ID	log2FoldChange	lfcSE	stat	pvalue	padj
T459_02853	1.1634	0.1837	6.3319	0.0000	0.0000
T459_05238	1.1636	0.1249	9.3161	0.0000	0.0000
T459_34178	1.1646	0.3779	3.0818	0.0021	0.0151
T459_20708	1.1671	0.1473	7.9213	0.0000	0.0000
T459_26243	1.1678	0.2637	4.4277	0.0000	0.0001
T459_24963	1.1740	0.1273	9.2195	0.0000	0.0000
T459_09433	1.1744	0.1934	6.0732	0.0000	0.0000
T459_05003	1.1798	0.2510	4.6995	0.0000	0.0000
T459_26733	1.1803	0.3293	3.5842	0.0003	0.0032
T459_33965	1.1806	0.1707	6.9149	0.0000	0.0000
T459_23977	1.1821	0.2256	5.2398	0.0000	0.0000
T459_01356	1.1821	0.4435	2.6653	0.0077	0.0444
T459_08134	1.1839	0.1168	10.1378	0.0000	0.0000
T459_31096	1.1840	0.1789	6.6177	0.0000	0.0000
T459_15105	1.1844	0.3177	3.7284	0.0002	0.0020
T459_10144	1.1851	0.2187	5.4177	0.0000	0.0000
T459_06693	1.1882	0.4237	2.8045	0.0050	0.0315
T459_15732	1.1886	0.3443	3.4522	0.0006	0.0049
T459_33697	1.1889	0.1515	7.8470	0.0000	0.0000
T459_00169	1.1905	0.1770	6.7260	0.0000	0.0000
T459_32109	1.1912	0.3972	2.9993	0.0027	0.0190
T459_07062	1.1962	0.2402	4.9805	0.0000	0.0000
T459_18292	1.2019	0.3946	3.0459	0.0023	0.0167
T459_08806	1.2033	0.1993	6.0366	0.0000	0.0000
T459_17054	1.2045	0.2291	5.2580	0.0000	0.0000
T459_29936	1.2062	0.2418	4.9874	0.0000	0.0000
T459_15815	1.2070	0.1608	7.5060	0.0000	0.0000
T459_22739	1.2081	0.3160	3.8230	0.0001	0.0014
T459_14547	1.2094	0.3956	3.0571	0.0022	0.0162
T459_27865	1.2103	0.1411	8.5796	0.0000	0.0000
T459_20093	1.2145	0.1325	9.1688	0.0000	0.0000
T459_06630	1.2153	0.4051	3.0001	0.0027	0.0189
T459_07594	1.2207	0.2078	5.8752	0.0000	0.0000
T459_03011	1.2221	0.1644	7.4346	0.0000	0.0000
T459_18996	1.2240	0.1416	8.6429	0.0000	0.0000
T459_26888	1.2281	0.3709	3.3112	0.0009	0.0077
T459_26001	1.2295	0.3747	3.2809	0.0010	0.0084
T459_22097	1.2341	0.2605	4.7373	0.0000	0.0000
T459_33447	1.2344	0.1276	9.6729	0.0000	0.0000
T459_28439	1.2396	0.4527	2.7379	0.0062	0.0372
T459_18482	1.2396	0.3239	3.8270	0.0001	0.0014
T459_05874	1.2399	0.2326	5.3299	0.0000	0.0000
T459_12705	1.2415	0.2564	4.8426	0.0000	0.0000
T459_04175	1.2418	0.1658	7.4902	0.0000	0.0000
T459_29120	1.2443	0.1646	7.5612	0.0000	0.0000
T459_03860	1.2444	0.2033	6.1199	0.0000	0.0000
T459_23555	1.2462	0.1711	7.2856	0.0000	0.0000

Gene ID	log2FoldChange	lfcSE	stat	pvalue	padj
T459_00979	1.2463	0.3390	3.6763	0.0002	0.0024
T459_02769	1.2463	0.2326	5.3585	0.0000	0.0000
T459_25745	1.2476	0.1484	8.4050	0.0000	0.0000
T459_13048	1.2477	0.2901	4.3011	0.0000	0.0002
T459_08353	1.2494	0.3688	3.3877	0.0007	0.0060
T459_04015	1.2521	0.4573	2.7380	0.0062	0.0372
T459_18365	1.2535	0.4174	3.0028	0.0027	0.0188
T459_23978	1.2537	0.2471	5.0733	0.0000	0.0000
T459_13538	1.2540	0.2849	4.4020	0.0000	0.0002
T459_15135	1.2592	0.3010	4.1838	0.0000	0.0004
T459_09243	1.2621	0.3648	3.4598	0.0005	0.0048
T459_21099	1.2630	0.1137	11.1064	0.0000	0.0000
T459_30732	1.2664	0.4544	2.7871	0.0053	0.0329
T459_20407	1.2681	0.4254	2.9810	0.0029	0.0199
T459_30838	1.2693	0.2690	4.7182	0.0000	0.0000
T459_11136	1.2714	0.4059	3.1322	0.0017	0.0131
T459_10753	1.2730	0.1503	8.4719	0.0000	0.0000
T459_17523	1.2775	0.4423	2.8882	0.0039	0.0255
T459_03588	1.2787	0.3875	3.2999	0.0010	0.0080
T459_27347	1.2802	0.4095	3.1264	0.0018	0.0134
T459_21752	1.2840	0.4016	3.1976	0.0014	0.0108
T459_07833	1.2841	0.3551	3.6166	0.0003	0.0029
T459_23785	1.2871	0.2770	4.6458	0.0000	0.0001
T459_18658	1.2911	0.3117	4.1423	0.0000	0.0004
T459_23437	1.2916	0.3345	3.8609	0.0001	0.0012
T459_00030	1.2923	0.4131	3.1280	0.0018	0.0133
T459_21260	1.2927	0.3024	4.2748	0.0000	0.0003
T459_31879	1.2929	0.1895	6.8229	0.0000	0.0000
T459_25767	1.2973	0.2019	6.4263	0.0000	0.0000
T459_13149	1.2978	0.3417	3.7976	0.0001	0.0015
T459_05000	1.2979	0.2471	5.2521	0.0000	0.0000
T459_27274	1.3006	0.4227	3.0766	0.0021	0.0154
T459_23190	1.3027	0.2097	6.2110	0.0000	0.0000
T459_21840	1.3028	0.3103	4.1982	0.0000	0.0003
T459_09951	1.3090	0.3692	3.5457	0.0004	0.0036
T459_17784	1.3106	0.2284	5.7372	0.0000	0.0000
T459_08557	1.3146	0.3166	4.1521	0.0000	0.0004
T459_03972	1.3178	0.2582	5.1043	0.0000	0.0000
T459_07751	1.3181	0.1770	7.4453	0.0000	0.0000
T459_29367	1.3206	0.2334	5.6578	0.0000	0.0000
T459_31947	1.3242	0.2981	4.4423	0.0000	0.0001
T459_29707	1.3243	0.3272	4.0470	0.0001	0.0006
T459_15527	1.3254	0.4160	3.1861	0.0014	0.0112
T459_17431	1.3323	0.5015	2.6565	0.0079	0.0453
T459_16473	1.3338	0.2787	4.7865	0.0000	0.0000
T459_08105	1.3341	0.4405	3.0287	0.0025	0.0175
T459_18370	1.3346	0.1345	9.9234	0.0000	0.0000

Gene ID	log2FoldChange	lfcSE	stat	pvalue	padj
T459_04840	1.3350	0.1650	8.0928	0.0000	0.0000
T459_24964	1.3352	0.1082	12.3356	0.0000	0.0000
T459_34004	1.3376	0.3089	4.3298	0.0000	0.0002
T459_25776	1.3461	0.2704	4.9780	0.0000	0.0000
T459_02544	1.3481	0.3315	4.0673	0.0000	0.0006
T459_27006	1.3485	0.4469	3.0172	0.0026	0.0181
T459_03841	1.3486	0.1506	8.9566	0.0000	0.0000
T459_35563	1.3513	0.4424	3.0542	0.0023	0.0164
T459_25267	1.3524	0.2991	4.5212	0.0000	0.0001
T459_18108	1.3544	0.3362	4.0290	0.0001	0.0007
T459_22503	1.3584	0.2210	6.1458	0.0000	0.0000
T459_22443	1.3617	0.1821	7.4761	0.0000	0.0000
T459_27008	1.3740	0.3136	4.3812	0.0000	0.0002
T459_17321	1.3780	0.3289	4.1903	0.0000	0.0004
T459_13760	1.3794	0.4274	3.2272	0.0012	0.0099
T459_03842	1.3794	0.1548	8.9086	0.0000	0.0000
T459_17980	1.3801	0.0994	13.8846	0.0000	0.0000
T459_34009	1.3852	0.1739	7.9644	0.0000	0.0000
T459_21300	1.3859	0.3024	4.5825	0.0000	0.0001
T459_03559	1.3862	0.1668	8.3102	0.0000	0.0000
T459_07472	1.3894	0.4052	3.4286	0.0006	0.0053
T459_27951	1.3900	0.4981	2.7903	0.0053	0.0326
T459_09708	1.3901	0.1925	7.2227	0.0000	0.0000
T459_32620	1.3953	0.5088	2.7425	0.0061	0.0368
T459_34354	1.4077	0.4025	3.4975	0.0005	0.0042
T459_16942	1.4092	0.4656	3.0263	0.0025	0.0176
T459_34549	1.4144	0.3807	3.7155	0.0002	0.0020
T459_14095	1.4158	0.2926	4.8386	0.0000	0.0000
T459_33620	1.4159	0.2680	5.2826	0.0000	0.0000
T459_34082	1.4183	0.3380	4.1961	0.0000	0.0003
T459_07860	1.4207	0.2782	5.1073	0.0000	0.0000
T459_27243	1.4220	0.4730	3.0062	0.0026	0.0186
T459_26415	1.4228	0.2121	6.7071	0.0000	0.0000
T459_06535	1.4321	0.2096	6.8321	0.0000	0.0000
T459_07759	1.4443	0.1407	10.2663	0.0000	0.0000
T459_31848	1.4527	0.1892	7.6765	0.0000	0.0000
T459_14090	1.4539	0.4505	3.2271	0.0013	0.0099
T459_15320	1.4589	0.2497	5.8418	0.0000	0.0000
T459_35139	1.4653	0.2690	5.4481	0.0000	0.0000
T459_05390	1.4684	0.4443	3.3046	0.0010	0.0079
T459_26620	1.4690	0.3352	4.3829	0.0000	0.0002
T459_22121	1.4699	0.4869	3.0188	0.0025	0.0180
T459_04510	1.4718	0.3161	4.6568	0.0000	0.0001
T459_29715	1.4725	0.1883	7.8199	0.0000	0.0000
T459_22502	1.4728	0.4983	2.9557	0.0031	0.0213
T459_17555	1.4732	0.3924	3.7542	0.0002	0.0018
T459_03840	1.4850	0.1774	8.3709	0.0000	0.0000

Gene ID	log2FoldChange	lfcSE	stat	pvalue	padj
T459_33510	1.4851	0.1139	13.0424	0.0000	0.0000
T459_34347	1.4873	0.1466	10.1490	0.0000	0.0000
T459_02123	1.4877	0.1397	10.6476	0.0000	0.0000
T459_16182	1.4900	0.2674	5.5732	0.0000	0.0000
T459_34126	1.4958	0.3831	3.9046	0.0001	0.0010
T459_13821	1.4985	0.1013	14.7884	0.0000	0.0000
T459_24377	1.5013	0.3082	4.8709	0.0000	0.0000
T459_00327	1.5026	0.1040	14.4426	0.0000	0.0000
T459_27040	1.5054	0.5050	2.9810	0.0029	0.0199
T459_28527	1.5073	0.5267	2.8620	0.0042	0.0273
T459_28936	1.5084	0.3787	3.9835	0.0001	0.0008
T459_26844	1.5094	0.3955	3.8164	0.0001	0.0014
T459_04016	1.5125	0.5461	2.7697	0.0056	0.0343
T459_24012	1.5182	0.2981	5.0937	0.0000	0.0000
T459_23556	1.5212	0.2263	6.7210	0.0000	0.0000
T459_33615	1.5235	0.2943	5.1772	0.0000	0.0000
T459_25824	1.5260	0.4369	3.4931	0.0005	0.0043
T459_35555	1.5280	0.4717	3.2392	0.0012	0.0096
T459_02596	1.5295	0.5487	2.7875	0.0053	0.0329
T459_05797	1.5309	0.2687	5.6984	0.0000	0.0000
T459_00109	1.5357	0.2687	5.7157	0.0000	0.0000
T459_10427	1.5362	0.1575	9.7547	0.0000	0.0000
T459_11848	1.5364	0.4313	3.5622	0.0004	0.0034
T459_03045	1.5408	0.1768	8.7138	0.0000	0.0000
T459_28315	1.5411	0.1931	7.9813	0.0000	0.0000
T459_04872	1.5440	0.2449	6.3042	0.0000	0.0000
T459_31988	1.5483	0.1207	12.8295	0.0000	0.0000
T459_26095	1.5488	0.3606	4.2956	0.0000	0.0002
T459_13546	1.5498	0.4848	3.1968	0.0014	0.0108
T459_34555	1.5502	0.3607	4.2976	0.0000	0.0002
T459_08067	1.5524	0.4256	3.6478	0.0003	0.0026
T459_33436	1.5573	0.5058	3.0787	0.0021	0.0153
T459_15238	1.5573	0.3585	4.3439	0.0000	0.0002
T459_00834	1.5642	0.5182	3.0184	0.0025	0.0180
T459_01627	1.5699	0.3482	4.5082	0.0000	0.0001
T459_32804	1.5790	0.1835	8.6048	0.0000	0.0000
T459_09169	1.5809	0.2790	5.6666	0.0000	0.0000
T459_25024	1.5907	0.1662	9.5706	0.0000	0.0000
T459_19053	1.5938	0.2094	7.6103	0.0000	0.0000
T459_26014	1.5961	0.2677	5.9619	0.0000	0.0000
T459_10310	1.5970	0.4968	3.2145	0.0013	0.0103
T459_31886	1.5979	0.4871	3.2806	0.0010	0.0085
T459_17130	1.6042	0.2329	6.8869	0.0000	0.0000
T459_25849	1.6153	0.1194	13.5248	0.0000	0.0000
T459_08993	1.6158	0.3323	4.8625	0.0000	0.0000
T459_06213	1.6218	0.2995	5.4147	0.0000	0.0000
T459_31173	1.6311	0.4641	3.5146	0.0004	0.0040

Gene ID	log2FoldChange	lfcSE	stat	pvalue	padj
T459_34305	1.6393	0.5127	3.1972	0.0014	0.0108
T459_07866	1.6442	0.4406	3.7320	0.0002	0.0019
T459_06320	1.6456	0.2223	7.4010	0.0000	0.0000
T459_16761	1.6550	0.1409	11.7445	0.0000	0.0000
T459_18490	1.6551	0.1757	9.4216	0.0000	0.0000
T459_10083	1.6557	0.2332	7.1006	0.0000	0.0000
T459_00330	1.6560	0.0998	16.5878	0.0000	0.0000
T459_21689	1.6584	0.6126	2.7070	0.0068	0.0401
T459_17419	1.6612	0.2307	7.2018	0.0000	0.0000
T459_15040	1.6665	0.4097	4.0677	0.0000	0.0006
T459_00766	1.6716	0.4848	3.4478	0.0006	0.0050
T459_15203	1.6755	0.4193	3.9965	0.0001	0.0007
T459_31000	1.6815	0.3282	5.1233	0.0000	0.0000
T459_18788	1.6880	0.4421	3.8183	0.0001	0.0014
T459_02663	1.6885	0.1195	14.1248	0.0000	0.0000
T459_29938	1.6891	0.4034	4.1869	0.0000	0.0004
T459_23853	1.6903	0.4177	4.0463	0.0001	0.0006
T459_04410	1.6903	0.2808	6.0206	0.0000	0.0000
T459_31688	1.6908	0.2531	6.6797	0.0000	0.0000
T459_05928	1.6911	0.4846	3.4896	0.0005	0.0043
T459_18809	1.6968	0.2262	7.5002	0.0000	0.0000
T459_22366	1.7058	0.6105	2.7943	0.0052	0.0323
T459_31869	1.7063	0.4726	3.6103	0.0003	0.0029
T459_00242	1.7065	0.3620	4.7135	0.0000	0.0000
T459_34989	1.7169	0.3260	5.2665	0.0000	0.0000
T459_22830	1.7264	0.3940	4.3819	0.0000	0.0002
T459_14471	1.7314	0.2937	5.8957	0.0000	0.0000
T459_07881	1.7337	0.4424	3.9186	0.0001	0.0010
T459_21981	1.7379	0.4094	4.2450	0.0000	0.0003
T459_31011	1.7461	0.1746	10.0016	0.0000	0.0000
T459_15451	1.7475	0.3635	4.8081	0.0000	0.0000
T459_01090	1.7509	0.2225	7.8680	0.0000	0.0000
T459_17102	1.7529	0.5083	3.4482	0.0006	0.0050
T459_30533	1.7761	0.3328	5.3363	0.0000	0.0000
T459_13901	1.7767	0.2027	8.7673	0.0000	0.0000
T459_31295	1.7794	0.1247	14.2727	0.0000	0.0000
T459_27541	1.7869	0.5043	3.5432	0.0004	0.0036
T459_10460	1.7894	0.1753	10.2071	0.0000	0.0000
T459_15369	1.7919	0.6105	2.9350	0.0033	0.0226
T459_27353	1.8024	0.2130	8.4626	0.0000	0.0000
T459_17874	1.8072	0.4799	3.7660	0.0002	0.0017
T459_27998	1.8498	0.3364	5.4992	0.0000	0.0000
T459_04060	1.8499	0.2482	7.4535	0.0000	0.0000
T459_21301	1.8504	0.1394	13.2743	0.0000	0.0000
T459_06869	1.8591	0.1331	13.9684	0.0000	0.0000
T459_14205	1.8612	0.3063	6.0765	0.0000	0.0000
T459_16124	1.8637	0.2569	7.2533	0.0000	0.0000

Gene ID	log2FoldChange	lfcSE	stat	pvalue	padj
T459_02309	1.8683	0.3797	4.9205	0.0000	0.0000
T459_27195	1.8822	0.2165	8.6940	0.0000	0.0000
T459_25018	1.8851	0.6406	2.9429	0.0033	0.0221
T459_26265	1.8915	0.2699	7.0081	0.0000	0.0000
T459_06712	1.8990	0.1778	10.6780	0.0000	0.0000
T459_28580	1.8991	0.2598	7.3097	0.0000	0.0000
T459_19451	1.9001	0.6299	3.0162	0.0026	0.0181
T459_00231	1.9112	0.3104	6.1571	0.0000	0.0000
T459_24621	1.9120	0.2926	6.5343	0.0000	0.0000
T459_23692	1.9163	0.4615	4.1521	0.0000	0.0004
T459_15080	1.9202	0.3501	5.4854	0.0000	0.0000
T459_20160	1.9247	0.4311	4.4641	0.0000	0.0001
T459_04649	1.9266	0.3750	5.1372	0.0000	0.0000
T459_08131	1.9273	0.5085	3.7902	0.0002	0.0016
T459_00426	1.9308	0.3410	5.6631	0.0000	0.0000
T459_33526	1.9361	0.3339	5.7982	0.0000	0.0000
T459_10581	1.9368	0.4747	4.0804	0.0000	0.0005
T459_00329	1.9404	0.1164	16.6697	0.0000	0.0000
T459_34823	1.9520	0.2035	9.5922	0.0000	0.0000
T459_25112	1.9578	0.2049	9.5554	0.0000	0.0000
T459_08275	1.9649	0.2592	7.5810	0.0000	0.0000
T459_10402	1.9654	0.2685	7.3191	0.0000	0.0000
T459_28617	1.9704	0.6789	2.9024	0.0037	0.0247
T459_18426	1.9854	0.3723	5.3322	0.0000	0.0000
T459_26516	1.9901	0.3678	5.4110	0.0000	0.0000
T459_20222	1.9949	0.2933	6.8017	0.0000	0.0000
T459_19891	1.9958	0.3239	6.1617	0.0000	0.0000
T459_31731	1.9963	0.3872	5.1560	0.0000	0.0000
T459_20192	2.0019	0.4601	4.3506	0.0000	0.0002
T459_07287	2.0042	0.2221	9.0255	0.0000	0.0000
T459_08013	2.0048	0.2856	7.0200	0.0000	0.0000
T459_22468	2.0097	0.1371	14.6587	0.0000	0.0000
T459_04884	2.0185	0.4824	4.1845	0.0000	0.0004
T459_35787	2.0243	0.6136	3.2989	0.0010	0.0080
T459_15860	2.0356	0.6131	3.3202	0.0009	0.0075
T459_21462	2.0403	0.2367	8.6189	0.0000	0.0000
T459_05892	2.0411	0.3848	5.3037	0.0000	0.0000
T459_27886	2.0456	0.5248	3.8974	0.0001	0.0011
T459_05088	2.0479	0.4145	4.9410	0.0000	0.0000
T459_08990	2.0581	0.2378	8.6554	0.0000	0.0000
T459_03998	2.0608	0.2037	10.1143	0.0000	0.0000
T459_06561	2.0763	0.5802	3.5786	0.0003	0.0032
T459_29941	2.0776	0.4188	4.9610	0.0000	0.0000
T459_07883	2.0798	0.4855	4.2841	0.0000	0.0002
T459_23468	2.0818	0.3993	5.2140	0.0000	0.0000
T459_28581	2.0824	0.2330	8.9354	0.0000	0.0000
T459_00326	2.0909	0.1635	12.7848	0.0000	0.0000

Gene ID	log2FoldChange	lfcSE	stat	pvalue	padj
T459_05604	2.0916	0.3104	6.7395	0.0000	0.0000
T459_15078	2.0996	0.3502	5.9948	0.0000	0.0000
T459_23181	2.1060	0.5388	3.9085	0.0001	0.0010
T459_18667	2.1184	0.5014	4.2246	0.0000	0.0003
T459_22172	2.1592	0.1509	14.3109	0.0000	0.0000
T459_10788	2.1622	0.1621	13.3388	0.0000	0.0000
T459_00328	2.1740	0.1551	14.0123	0.0000	0.0000
T459_26665	2.1763	0.8039	2.7072	0.0068	0.0401
T459_13441	2.1803	0.6971	3.1278	0.0018	0.0133
T459_24950	2.1890	0.6080	3.6004	0.0003	0.0030
T459_09948	2.1950	0.7123	3.0816	0.0021	0.0151
T459_25537	2.2019	0.3443	6.3958	0.0000	0.0000
T459_32220	2.2044	0.4056	5.4352	0.0000	0.0000
T459_12583	2.2058	0.6195	3.5608	0.0004	0.0034
T459_08267	2.2107	0.3201	6.9064	0.0000	0.0000
T459_34298	2.2148	0.2588	8.5575	0.0000	0.0000
T459_30842	2.2169	0.5595	3.9624	0.0001	0.0008
T459_29945	2.2247	0.1787	12.4470	0.0000	0.0000
T459_06920	2.2380	0.6866	3.2594	0.0011	0.0090
T459_28582	2.2439	0.2936	7.6437	0.0000	0.0000
T459_35711	2.2501	0.5737	3.9223	0.0001	0.0010
T459_09393	2.2584	0.6095	3.7050	0.0002	0.0021
T459_07278	2.3252	0.8269	2.8119	0.0049	0.0310
T459_00927	2.3263	0.6400	3.6345	0.0003	0.0027
T459_09647	2.3263	0.4290	5.4233	0.0000	0.0000
T459_10610	2.3319	0.5875	3.9694	0.0001	0.0008
T459_18700	2.3446	0.5624	4.1689	0.0000	0.0004
T459_35633	2.3459	0.5397	4.3471	0.0000	0.0002
T459_04516	2.3486	0.4951	4.7439	0.0000	0.0000
T459_16121	2.3599	0.2109	11.1918	0.0000	0.0000
T459_22460	2.3759	0.3092	7.6832	0.0000	0.0000
T459_33787	2.3770	0.3198	7.4328	0.0000	0.0000
T459_04352	2.4111	0.2750	8.7673	0.0000	0.0000
T459_18433	2.4197	0.2869	8.4340	0.0000	0.0000
T459_18565	2.4466	0.3590	6.8141	0.0000	0.0000
T459_10073	2.4580	0.4521	5.4367	0.0000	0.0000
T459_33984	2.4678	0.2344	10.5303	0.0000	0.0000
T459_07192	2.4708	0.3002	8.2312	0.0000	0.0000
T459_05018	2.4772	0.2802	8.8420	0.0000	0.0000
T459_10147	2.4781	0.1642	15.0881	0.0000	0.0000
T459_29636	2.4877	0.7953	3.1279	0.0018	0.0133
T459_31624	2.4916	0.6082	4.0970	0.0000	0.0005
T459_28583	2.4948	0.3081	8.0975	0.0000	0.0000
T459_32753	2.4958	0.3310	7.5401	0.0000	0.0000
T459_16218	2.4987	0.3202	7.8026	0.0000	0.0000
T459_18690	2.5084	0.2792	8.9854	0.0000	0.0000
T459_31495	2.5104	0.1544	16.2573	0.0000	0.0000

Gene ID	log2FoldChange	lfcSE	stat	pvalue	padj
T459_09956	2.5235	0.3317	7.6081	0.0000	0.0000
T459_15858	2.5235	0.5420	4.6557	0.0000	0.0001
T459_05516	2.5389	0.1617	15.7052	0.0000	0.0000
T459_21289	2.5467	0.5368	4.7440	0.0000	0.0000
T459_30490	2.5914	0.5218	4.9663	0.0000	0.0000
T459_20537	2.5926	0.4839	5.3575	0.0000	0.0000
T459_14052	2.6090	0.3276	7.9634	0.0000	0.0000
T459_34239	2.6240	0.2999	8.7508	0.0000	0.0000
T459_35330	2.6241	0.4701	5.5822	0.0000	0.0000
T459_15901	2.6333	0.2858	9.2130	0.0000	0.0000
T459_03735	2.6424	0.3833	6.8933	0.0000	0.0000
T459_09168	2.6485	0.2451	10.8058	0.0000	0.0000
T459_00505	2.6636	0.3093	8.6113	0.0000	0.0000
T459_17873	2.6682	0.4113	6.4867	0.0000	0.0000
T459_32199	2.6771	0.6880	3.8913	0.0001	0.0011
T459_14053	2.7127	0.4623	5.8676	0.0000	0.0000
T459_00737	2.7153	0.2521	10.7694	0.0000	0.0000
T459_31014	2.7245	0.2070	13.1651	0.0000	0.0000
T459_16024	2.7289	0.1489	18.3314	0.0000	0.0000
T459_17036	2.7321	0.8556	3.1932	0.0014	0.0110
T459_34410	2.7329	0.2284	11.9644	0.0000	0.0000
T459_32272	2.7391	0.4556	6.0123	0.0000	0.0000
T459_07809	2.7509	0.2306	11.9278	0.0000	0.0000
T459_26666	2.7647	0.2126	13.0069	0.0000	0.0000
T459_12483	2.8039	0.4844	5.7879	0.0000	0.0000
T459_04330	2.8579	0.9553	2.9915	0.0028	0.0193
T459_34553	2.8645	0.2016	14.2087	0.0000	0.0000
T459_07065	2.8781	0.2316	12.4249	0.0000	0.0000
T459_29868	2.8878	0.2824	10.2251	0.0000	0.0000
T459_07099	2.8885	0.8486	3.4039	0.0007	0.0057
T459_17322	2.8962	0.9587	3.0210	0.0025	0.0179
T459_14538	2.8997	0.2367	12.2503	0.0000	0.0000
T459_17077	2.9283	0.2961	9.8887	0.0000	0.0000
T459_05780	2.9310	0.1553	18.8742	0.0000	0.0000
T459_23871	2.9390	0.3070	9.5726	0.0000	0.0000
T459_24370	2.9448	0.3810	7.7283	0.0000	0.0000
T459_14836	2.9546	0.1488	19.8528	0.0000	0.0000
T459_06576	2.9553	0.7577	3.9004	0.0001	0.0011
T459_18689	2.9650	0.3070	9.6579	0.0000	0.0000
T459_14681	2.9837	0.5081	5.8718	0.0000	0.0000
T459_04287	2.9890	0.3800	7.8666	0.0000	0.0000
T459_20592	2.9916	0.6728	4.4464	0.0000	0.0001
T459_17503	3.0119	0.2271	13.2647	0.0000	0.0000
T459_32743	3.0138	0.2703	11.1482	0.0000	0.0000
T459_07774	3.0165	0.7663	3.9366	0.0001	0.0009
T459_05955	3.0174	0.1686	17.8976	0.0000	0.0000
T459_17948	3.0438	0.2647	11.4989	0.0000	0.0000

Gene ID	log2FoldChange	lfcSE	stat	pvalue	padj
T459_21750	3.0469	0.3402	8.9573	0.0000	0.0000
T459_07861	3.0997	0.8925	3.4731	0.0005	0.0046
T459_17223	3.1156	1.1845	2.6302	0.0085	0.0482
T459_05665	3.1437	0.5221	6.0217	0.0000	0.0000
T459_25894	3.1564	0.3680	8.5775	0.0000	0.0000
T459_08800	3.2097	0.9739	3.2958	0.0010	0.0081
T459_03008	3.2173	0.4027	7.9890	0.0000	0.0000
T459_29118	3.2383	0.6569	4.9300	0.0000	0.0000
T459_19216	3.2757	0.2387	13.7207	0.0000	0.0000
T459_27154	3.3078	0.5452	6.0677	0.0000	0.0000
T459_00004	3.3080	0.3222	10.2659	0.0000	0.0000
T459_24005	3.3348	1.1241	2.9667	0.0030	0.0207
T459_24945	3.3554	0.6005	5.5872	0.0000	0.0000
T459_05442	3.3637	0.7881	4.2679	0.0000	0.0003
T459_22173	3.3871	0.3824	8.8583	0.0000	0.0000
T459_29539	3.3905	0.5176	6.5506	0.0000	0.0000
T459_35562	3.4080	0.3392	10.0463	0.0000	0.0000
T459_21979	3.4326	0.5612	6.1162	0.0000	0.0000
T459_16041	3.4983	0.6707	5.2157	0.0000	0.0000
T459_07296	3.5023	0.4768	7.3460	0.0000	0.0000
T459_16604	3.5056	0.5410	6.4793	0.0000	0.0000
T459_28374	3.5178	0.3297	10.6700	0.0000	0.0000
T459_31463	3.5226	0.4694	7.5045	0.0000	0.0000
T459_23252	3.5325	0.3621	9.7569	0.0000	0.0000
T459_11465	3.5526	0.2841	12.5028	0.0000	0.0000
T459_16690	3.5554	1.1203	3.1736	0.0015	0.0116
T459_28743	3.5614	0.3959	8.9953	0.0000	0.0000
T459_25023	3.6115	0.5954	6.0662	0.0000	0.0000
T459_13226	3.6344	0.6961	5.2212	0.0000	0.0000
T459_06454	3.6753	0.4423	8.3089	0.0000	0.0000
T459_32717	3.6852	0.2408	15.3025	0.0000	0.0000
T459_18820	3.6939	0.4642	7.9566	0.0000	0.0000
T459_34288	3.7083	0.3954	9.3790	0.0000	0.0000
T459_09773	3.7475	0.2748	13.6364	0.0000	0.0000
T459_33300	3.7529	0.7973	4.7068	0.0000	0.0000
T459_22447	3.7568	0.4515	8.3209	0.0000	0.0000
T459_24378	3.7718	0.7532	5.0078	0.0000	0.0000
T459_24379	3.7840	0.6213	6.0909	0.0000	0.0000
T459_07195	3.7927	0.3643	10.4100	0.0000	0.0000
T459_08129	3.7927	0.2170	17.4778	0.0000	0.0000
T459_15780	3.7953	0.1774	21.3892	0.0000	0.0000
T459_35594	3.8664	0.9088	4.2542	0.0000	0.0003
T459_15778	3.8764	0.2351	16.4872	0.0000	0.0000
T459_04168	3.8967	0.8073	4.8269	0.0000	0.0000
T459_24612	3.9667	0.9081	4.3680	0.0000	0.0002
T459_15129	4.0624	0.9775	4.1561	0.0000	0.0004
T459_29869	4.0982	0.4864	8.4251	0.0000	0.0000

Gene ID	log2FoldChange	lfcSE	stat	pvalue	padj
T459_31811	4.1127	0.7358	5.5894	0.0000	0.0000
T459_19245	4.1324	0.2736	15.1064	0.0000	0.0000
T459_29882	4.1456	1.5041	2.7561	0.0058	0.0355
T459_02590	4.1685	0.3484	11.9652	0.0000	0.0000
T459_21298	4.2009	0.5800	7.2429	0.0000	0.0000
T459_09622	4.2182	0.2871	14.6925	0.0000	0.0000
T459_22537	4.2768	0.1199	35.6570	0.0000	0.0000
T459_31608	4.3362	0.8058	5.3816	0.0000	0.0000
T459_27082	4.3630	0.2635	16.5558	0.0000	0.0000
T459_30754	4.3634	0.3322	13.1354	0.0000	0.0000
T459_16025	4.3792	0.9849	4.4463	0.0000	0.0001
T459_19222	4.4161	0.4617	9.5649	0.0000	0.0000
T459_31291	4.5222	0.8729	5.1810	0.0000	0.0000
T459_06459	4.5437	1.4615	3.1090	0.0019	0.0140
T459_29415	4.5577	0.6264	7.2755	0.0000	0.0000
T459_00538	4.6051	0.8733	5.2733	0.0000	0.0000
T459_09514	4.6233	0.5837	7.9211	0.0000	0.0000
T459_32663	4.6473	0.8435	5.5097	0.0000	0.0000
T459_35671	4.6606	1.4361	3.2453	0.0012	0.0094
T459_00579	4.6759	0.4884	9.5745	0.0000	0.0000
T459_07666	4.6802	0.4398	10.6420	0.0000	0.0000
T459_34352	4.7001	0.6041	7.7801	0.0000	0.0000
T459_35190	4.7112	0.4951	9.5153	0.0000	0.0000
T459_03009	4.7135	1.1827	3.9854	0.0001	0.0008
T459_10685	4.9380	0.2512	19.6578	0.0000	0.0000
T459_12482	4.9737	0.8290	5.9996	0.0000	0.0000
T459_02250	4.9976	0.8243	6.0630	0.0000	0.0000
T459_16439	5.0504	0.8306	6.0807	0.0000	0.0000
T459_18670	5.1619	0.9311	5.5438	0.0000	0.0000
T459_12750	5.1685	0.5802	8.9075	0.0000	0.0000
T459_27524	5.2116	0.4409	11.8210	0.0000	0.0000
T459_20092	5.2573	1.5105	3.4804	0.0005	0.0045
T459_15354	5.2586	1.3452	3.9093	0.0001	0.0010
T459_14638	5.2721	0.8041	6.5563	0.0000	0.0000
T459_05542	5.3177	1.4945	3.5582	0.0004	0.0035
T459_18786	5.3787	0.3477	15.4709	0.0000	0.0000
T459_22538	5.4443	1.4792	3.6805	0.0002	0.0023
T459_34931	5.4788	1.1242	4.8737	0.0000	0.0000
T459_13071	5.4960	0.6687	8.2191	0.0000	0.0000
T459_08365	5.5209	0.4090	13.4970	0.0000	0.0000
T459_35182	5.5602	1.4472	3.8420	0.0001	0.0013
T459_23428	5.5690	0.9144	6.0906	0.0000	0.0000
T459_17323	5.5922	0.7989	7.0000	0.0000	0.0000
T459_29062	5.5940	0.4279	13.0722	0.0000	0.0000
T459_15863	5.6286	1.3106	4.2946	0.0000	0.0002
T459_13895	5.6684	1.4279	3.9697	0.0001	0.0008
T459_11617	5.6768	1.1031	5.1464	0.0000	0.0000

Gene ID	log2FoldChange	lfcSE	stat	pvalue	padj
T459_05210	5.7802	1.2990	4.4498	0.0000	0.0001
T459_16298	5.8347	1.3055	4.4692	0.0000	0.0001
T459_20099	5.8851	0.6428	9.1548	0.0000	0.0000
T459_06174	5.9097	0.9562	6.1803	0.0000	0.0000
T459_15349	5.9340	0.5946	9.9804	0.0000	0.0000
T459_34940	5.9357	0.4574	12.9764	0.0000	0.0000
T459_26290	6.0382	1.4115	4.2780	0.0000	0.0002
T459_29261	6.0718	1.3823	4.3926	0.0000	0.0002
T459_16769	6.1156	0.7734	7.9077	0.0000	0.0000
T459_33667	6.1869	1.0910	5.6711	0.0000	0.0000
T459_27579	6.2183	1.3754	4.5212	0.0000	0.0001
T459_15872	6.2251	1.3752	4.5266	0.0000	0.0001
T459_32664	6.2723	0.7698	8.1483	0.0000	0.0000
T459_22811	6.2853	1.3480	4.6627	0.0000	0.0000
T459_26825	6.3304	0.8853	7.1503	0.0000	0.0000
T459_33125	6.3589	1.2794	4.9703	0.0000	0.0000
T459_29862	6.4176	1.3357	4.8047	0.0000	0.0000
T459_34939	6.4190	0.2527	25.4017	0.0000	0.0000
T459_34383	6.4479	0.8768	7.3538	0.0000	0.0000
T459_18566	6.4762	1.3269	4.8808	0.0000	0.0000
T459_28373	6.4801	1.2720	5.0945	0.0000	0.0000
T459_14784	6.5610	1.3190	4.9744	0.0000	0.0000
T459_35732	6.5846	1.3276	4.9598	0.0000	0.0000
T459_24123	6.5895	0.9113	7.2308	0.0000	0.0000
T459_05912	6.6400	1.3143	5.0520	0.0000	0.0000
T459_26859	6.7703	1.2429	5.4473	0.0000	0.0000
T459_05326	6.8818	1.2930	5.3222	0.0000	0.0000
T459_32185	6.8893	0.6744	10.2158	0.0000	0.0000
T459_23852	6.9889	1.2903	5.4166	0.0000	0.0000
T459_15917	7.0110	1.0575	6.6300	0.0000	0.0000
T459_26858	7.0902	1.2936	5.4807	0.0000	0.0000
T459_04877	7.1171	1.0590	6.7207	0.0000	0.0000
T459_34938	7.1290	1.2362	5.7667	0.0000	0.0000
T459_20380	7.1479	1.2760	5.6017	0.0000	0.0000
T459_19663	7.1619	1.2785	5.6017	0.0000	0.0000
T459_03101	7.2386	1.2731	5.6858	0.0000	0.0000
T459_34393	7.3364	1.2631	5.8082	0.0000	0.0000
T459_19238	7.3531	1.2628	5.8228	0.0000	0.0000
T459_18730	7.3613	0.3780	19.4758	0.0000	0.0000
T459_28041	7.3717	1.2671	5.8178	0.0000	0.0000
T459_24872	7.4036	1.2670	5.8436	0.0000	0.0000
T459_15779	7.4821	0.5817	12.8623	0.0000	0.0000
T459_28744	7.5237	1.2315	6.1093	0.0000	0.0000
T459_05241	7.5323	1.2260	6.1435	0.0000	0.0000
T459_22541	7.6917	1.2500	6.1534	0.0000	0.0000
T459_21788	7.7204	1.2472	6.1903	0.0000	0.0000
T459_16639	7.7484	1.2570	6.1641	0.0000	0.0000

Gene ID	log2FoldChange	lfcSE	stat	pvalue	padj
T459_15783	7.8044	0.7448	10.4785	0.0000	0.0000
T459_02224	7.8048	1.2438	6.2751	0.0000	0.0000
T459_35188	7.8265	1.2156	6.4385	0.0000	0.0000
T459_35329	7.8365	1.2412	6.3135	0.0000	0.0000
T459_28101	7.8378	1.2393	6.3242	0.0000	0.0000
T459_29609	7.8787	1.0437	7.5485	0.0000	0.0000
T459_25404	7.8840	1.2405	6.3554	0.0000	0.0000
T459_01163	7.8963	1.2404	6.3657	0.0000	0.0000
T459_15154	7.9336	1.2479	6.3577	0.0000	0.0000
T459_17458	7.9795	1.2346	6.4634	0.0000	0.0000
T459_15864	8.0222	1.2312	6.5157	0.0000	0.0000
T459_01111	8.0318	1.2371	6.4926	0.0000	0.0000
T459_04961	8.0525	1.2333	6.5294	0.0000	0.0000
T459_19586	8.0625	1.2371	6.5172	0.0000	0.0000
T459_22932	8.0854	1.2417	6.5114	0.0000	0.0000
T459_21239	8.0974	1.2332	6.5661	0.0000	0.0000
T459_34684	8.1287	1.2324	6.5959	0.0000	0.0000
T459_23916	8.2035	1.2312	6.6630	0.0000	0.0000
T459_34392	8.2265	1.2300	6.6884	0.0000	0.0000
T459_35385	8.2449	1.2254	6.7282	0.0000	0.0000
T459_32526	8.2499	1.2116	6.8092	0.0000	0.0000
T459_25639	8.2772	1.2513	6.6151	0.0000	0.0000
T459_17454	8.3443	1.2342	6.7611	0.0000	0.0000
T459_01086	8.4083	1.2039	6.9841	0.0000	0.0000
T459_18564	8.4308	1.2258	6.8779	0.0000	0.0000
T459_25568	8.4679	1.2022	7.0440	0.0000	0.0000
T459_00651	8.5186	1.2874	6.6171	0.0000	0.0000
T459_23378	8.5971	1.2184	7.0560	0.0000	0.0000
T459_34391	8.6698	1.2291	7.0540	0.0000	0.0000
T459_03520	8.6719	1.2193	7.1125	0.0000	0.0000
T459_15740	8.7557	1.2172	7.1934	0.0000	0.0000
T459_24224	8.8376	1.2118	7.2928	0.0000	0.0000
T459_32527	8.8702	1.2186	7.2793	0.0000	0.0000
T459_21523	9.0152	0.4418	20.4062	0.0000	0.0000
T459_23503	9.0445	1.2160	7.4381	0.0000	0.0000
T459_02191	9.0497	1.2118	7.4679	0.0000	0.0000
T459_11980	9.0861	1.2075	7.5245	0.0000	0.0000
T459_04876	9.0896	1.2064	7.5343	0.0000	0.0000
T459_01013	9.1654	1.2088	7.5824	0.0000	0.0000
T459_30897	9.2316	1.2039	7.6679	0.0000	0.0000
T459_09200	9.2481	1.2077	7.6577	0.0000	0.0000
T459_28212	9.4627	1.1930	7.9316	0.0000	0.0000
T459_05443	9.5334	1.2065	7.9016	0.0000	0.0000
T459_16926	9.6851	1.1985	8.0809	0.0000	0.0000
T459_34278	9.7091	1.1998	8.0921	0.0000	0.0000
T459_34479	9.7170	0.5596	17.3651	0.0000	0.0000
T459_15784	9.7807	1.2038	8.1251	0.0000	0.0000

Gene ID	log2FoldChange	lfcSE	stat	pvalue	padj
T459_12136	9.9883	1.1953	8.3563	0.0000	0.0000
T459_33000	10.0092	0.4932	20.2952	0.0000	0.0000
T459_03602	10.3291	1.3879	7.4420	0.0000	0.0000
T459_24124	10.4426	1.2188	8.5677	0.0000	0.0000
T459_34279	11.1895	1.1904	9.4000	0.0000	0.0000
T459_23974	11.8514	1.4189	8.3525	0.0000	0.0000

Supplementary Table 1. **C**. Differentially expressed genes between both genotypes under the control conditions at T2 (NIBER®/A10).

Gene ID	log2FoldChange	lfcSE	stat	pvalue	padj
T459_16565	-9.4053	1.2022	-7.8235	0.0000	0.0000
T459_03230	-8.8866	1.2171	-7.3014	0.0000	0.0000
T459_33710	-8.8723	1.2182	-7.2834	0.0000	0.0000
T459_02802	-8.7867	1.0554	-8.3252	0.0000	0.0000
T459_19432	-8.7336	1.2281	-7.1117	0.0000	0.0000
T459_27777	-8.6872	0.6194	-14.0245	0.0000	0.0000
T459_16780	-8.6715	1.0435	-8.3104	0.0000	0.0000
T459_28065	-8.6273	1.2220	-7.0598	0.0000	0.0000
T459_31883	-8.5700	1.1504	-7.4499	0.0000	0.0000
T459_28063	-8.5561	1.2226	-6.9980	0.0000	0.0000
T459_02150	-8.5370	1.2210	-6.9917	0.0000	0.0000
T459_02807	-8.5050	1.2661	-6.7173	0.0000	0.0000
T459_28184	-8.4616	1.2020	-7.0397	0.0000	0.0000
T459_33789	-8.3867	1.0383	-8.0770	0.0000	0.0000
T459_16564	-8.0646	1.2101	-6.6642	0.0000	0.0000
T459_32542	-7.9774	1.2459	-6.4030	0.0000	0.0000
T459_30788	-7.9746	0.7484	-10.6559	0.0000	0.0000
T459_35644	-7.8841	1.2141	-6.4938	0.0000	0.0000
T459_23514	-7.6012	1.2607	-6.0292	0.0000	0.0000
T459_04535	-7.5371	1.2721	-5.9250	0.0000	0.0000
T459_13944	-7.5054	1.2626	-5.9444	0.0000	0.0000
T459_07208	-7.4431	1.2265	-6.0684	0.0000	0.0000
T459_33575	-7.3239	1.2805	-5.7197	0.0000	0.0000
T459_28064	-7.1781	1.2881	-5.5725	0.0000	0.0000
T459_01116	-7.0598	0.8963	-7.8768	0.0000	0.0000
T459_28863	-7.0238	0.8645	-8.1244	0.0000	0.0000
T459_28067	-6.9985	1.3057	-5.3599	0.0000	0.0000
T459_14838	-6.9158	1.2458	-5.5511	0.0000	0.0000
T459_02562	-6.8912	0.8941	-7.7071	0.0000	0.0000
T459_33470	-6.8357	1.3116	-5.2117	0.0000	0.0000
T459_00869	-6.7841	1.2779	-5.3088	0.0000	0.0000
T459_00511	-6.7391	0.6209	-10.8542	0.0000	0.0000
T459_05002	-6.5870	0.6211	-10.6047	0.0000	0.0000
T459_24250	-6.4755	1.0795	-5.9988	0.0000	0.0000
T459_05161	-6.3258	1.0818	-5.8475	0.0000	0.0000
T459_27571	-6.2560	1.0862	-5.7595	0.0000	0.0000

Gene ID	log2FoldChange	lfcSE	stat	pvalue	padj
T459_17043	-6.2504	1.2724	-4.9121	0.0000	0.0000
T459_31895	-6.2345	1.2912	-4.8284	0.0000	0.0000
T459_26326	-6.1833	0.6429	-9.6174	0.0000	0.0000
T459_22353	-6.0683	0.6737	-9.0076	0.0000	0.0000
T459_12254	-6.0539	1.3853	-4.3699	0.0000	0.0003
T459_29008	-6.0505	0.9267	-6.5289	0.0000	0.0000
T459_26329	-5.8886	0.2937	-20.0526	0.0000	0.0000
T459_11884	-5.8873	0.5175	-11.3771	0.0000	0.0000
T459_29009	-5.8133	1.4466	-4.0186	0.0001	0.0012
T459_02116	-5.8074	1.3133	-4.4220	0.0000	0.0002
T459_35557	-5.6754	1.4448	-3.9282	0.0001	0.0016
T459_35227	-5.6399	1.3416	-4.2040	0.0000	0.0006
T459_07196	-5.4252	1.1754	-4.6156	0.0000	0.0001
T459_01928	-5.3774	0.5641	-9.5323	0.0000	0.0000
T459_10270	-5.1470	1.1805	-4.3601	0.0000	0.0003
T459_08737	-5.0995	1.1379	-4.4813	0.0000	0.0002
T459_05875	-5.0572	0.5750	-8.7948	0.0000	0.0000
T459_32584	-5.0169	1.1549	-4.3440	0.0000	0.0003
T459_32999	-4.8740	0.5993	-8.1329	0.0000	0.0000
T459_16392	-4.8669	1.2416	-3.9198	0.0001	0.0017
T459_05205	-4.8664	0.6261	-7.7726	0.0000	0.0000
T459_35735	-4.8589	0.3757	-12.9336	0.0000	0.0000
T459_05160	-4.8267	0.8396	-5.7490	0.0000	0.0000
T459_26921	-4.6107	0.9367	-4.9221	0.0000	0.0000
T459_22512	-4.5796	0.6871	-6.6646	0.0000	0.0000
T459_01133	-4.5038	0.7461	-6.0368	0.0000	0.0000
T459_28234	-4.4681	0.4275	-10.4516	0.0000	0.0000
T459_33853	-4.2126	0.5389	-7.8165	0.0000	0.0000
T459_15989	-4.2039	0.4307	-9.7609	0.0000	0.0000
T459_22186	-4.1785	0.4127	-10.1251	0.0000	0.0000
T459_26331	-4.1782	0.2790	-14.9779	0.0000	0.0000
T459_28257	-3.9949	0.6296	-6.3449	0.0000	0.0000
T459_17149	-3.9917	0.5704	-6.9982	0.0000	0.0000
T459_15988	-3.9766	0.6187	-6.4276	0.0000	0.0000
T459_04588	-3.8428	0.3984	-9.6449	0.0000	0.0000
T459_13878	-3.8344	0.3432	-11.1715	0.0000	0.0000
T459_18943	-3.7532	0.4573	-8.2073	0.0000	0.0000
T459_29829	-3.7493	0.8199	-4.5729	0.0000	0.0001
T459_29702	-3.7134	0.4783	-7.7644	0.0000	0.0000
T459_06039	-3.5359	0.9025	-3.9180	0.0001	0.0017
T459_05223	-3.5313	0.4706	-7.5034	0.0000	0.0000
T459_25500	-3.5023	0.4421	-7.9219	0.0000	0.0000
T459_15624	-3.4458	0.7908	-4.3573	0.0000	0.0003
T459_03997	-3.4448	0.4083	-8.4367	0.0000	0.0000
T459_20332	-3.4058	0.7652	-4.4508	0.0000	0.0002
T459_25292	-3.3723	0.3510	-9.6075	0.0000	0.0000
T459_26091	-3.3382	0.6888	-4.8461	0.0000	0.0000

Gene ID	log2FoldChange	lfcSE	stat	pvalue	padj
T459_21019	-3.3340	0.8903	-3.7446	0.0002	0.0031
T459_10257	-3.3338	0.2669	-12.4910	0.0000	0.0000
T459_22573	-3.3297	0.6738	-4.9416	0.0000	0.0000
T459_03936	-3.3199	0.5200	-6.3842	0.0000	0.0000
T459_30903	-3.3199	0.7397	-4.4881	0.0000	0.0002
T459_34633	-3.3007	0.7336	-4.4991	0.0000	0.0002
T459_05004	-3.2981	0.5704	-5.7821	0.0000	0.0000
T459_13884	-3.2915	0.7688	-4.2812	0.0000	0.0004
T459_26328	-3.2685	0.4421	-7.3934	0.0000	0.0000
T459_17389	-3.2229	0.8867	-3.6347	0.0003	0.0044
T459_34437	-3.1652	0.7188	-4.4034	0.0000	0.0003
T459_14461	-3.1563	0.2384	-13.2385	0.0000	0.0000
T459_33278	-3.1015	0.5803	-5.3450	0.0000	0.0000
T459_15987	-2.9859	0.8252	-3.6184	0.0003	0.0046
T459_03151	-2.9695	0.4656	-6.3781	0.0000	0.0000
T459_05876	-2.9341	0.3634	-8.0732	0.0000	0.0000
T459_29549	-2.9246	0.4991	-5.8601	0.0000	0.0000
T459_02476	-2.8847	0.1563	-18.4546	0.0000	0.0000
T459_16092	-2.8629	0.4594	-6.2314	0.0000	0.0000
T459_19585	-2.8529	0.1248	-22.8567	0.0000	0.0000
T459_15787	-2.8327	0.4858	-5.8308	0.0000	0.0000
T459_00541	-2.8021	0.7490	-3.7411	0.0002	0.0031
T459_34683	-2.7700	0.3198	-8.6612	0.0000	0.0000
T459_03550	-2.6954	0.7199	-3.7443	0.0002	0.0031
T459_18532	-2.6346	0.5602	-4.7031	0.0000	0.0001
T459_31118	-2.6217	0.5003	-5.2406	0.0000	0.0000
T459_12614	-2.6099	0.4497	-5.8032	0.0000	0.0000
T459_34438	-2.5929	0.6508	-3.9842	0.0001	0.0013
T459_07943	-2.5729	0.4145	-6.2070	0.0000	0.0000
T459_14111	-2.5508	0.5193	-4.9120	0.0000	0.0000
T459_34064	-2.5353	0.5643	-4.4931	0.0000	0.0002
T459_34760	-2.5325	0.2873	-8.8141	0.0000	0.0000
T459_31995	-2.4956	0.6262	-3.9856	0.0001	0.0013
T459_24903	-2.3981	0.3801	-6.3096	0.0000	0.0000
T459_27616	-2.3949	0.5670	-4.2236	0.0000	0.0005
T459_16225	-2.3807	0.5167	-4.6072	0.0000	0.0001
T459_31089	-2.3746	0.4239	-5.6023	0.0000	0.0000
T459_09619	-2.3661	0.3954	-5.9838	0.0000	0.0000
T459_12727	-2.3470	0.2760	-8.5024	0.0000	0.0000
T459_10040	-2.3451	0.6139	-3.8201	0.0001	0.0024
T459_24904	-2.2825	0.3956	-5.7704	0.0000	0.0000
T459_34443	-2.2517	0.4884	-4.6107	0.0000	0.0001
T459_20351	-2.2486	0.3592	-6.2598	0.0000	0.0000
T459_19397	-2.2453	0.4263	-5.2674	0.0000	0.0000
T459_19287	-2.2381	0.5313	-4.2127	0.0000	0.0006
T459_14112	-2.2372	0.4768	-4.6918	0.0000	0.0001
T459_04466	-2.2332	0.2412	-9.2571	0.0000	0.0000

Gene ID	log2FoldChange	lfcSE	stat	pvalue	padj
T459_21035	-2.2309	0.2859	-7.8043	0.0000	0.0000
T459_05222	-2.2271	0.3106	-7.1707	0.0000	0.0000
T459_25295	-2.2246	0.5453	-4.0796	0.0000	0.0009
T459_33259	-2.2165	0.4763	-4.6534	0.0000	0.0001
T459_21241	-2.2164	0.2270	-9.7630	0.0000	0.0000
T459_26502	-2.2126	0.3742	-5.9129	0.0000	0.0000
T459_13190	-2.2096	0.5120	-4.3160	0.0000	0.0004
T459_15847	-2.1931	0.2128	-10.3037	0.0000	0.0000
T459_27892	-2.1711	0.4647	-4.6719	0.0000	0.0001
T459_25458	-2.1495	0.1636	-13.1408	0.0000	0.0000
T459_08570	-2.1437	0.4632	-4.6280	0.0000	0.0001
T459_08904	-2.1416	0.2169	-9.8745	0.0000	0.0000
T459_19291	-2.1221	0.1705	-12.4473	0.0000	0.0000
T459_15846	-2.1221	0.2642	-8.0314	0.0000	0.0000
T459_18672	-2.1178	0.3466	-6.1095	0.0000	0.0000
T459_06771	-2.0647	0.2134	-9.6770	0.0000	0.0000
T459_00466	-2.0567	0.5267	-3.9046	0.0001	0.0018
T459_22211	-2.0401	0.3098	-6.5851	0.0000	0.0000
T459_33270	-2.0332	0.4747	-4.2830	0.0000	0.0004
T459_23969	-2.0201	0.4212	-4.7960	0.0000	0.0000
T459_01683	-2.0084	0.3283	-6.1171	0.0000	0.0000
T459_32515	-1.9957	0.3938	-5.0681	0.0000	0.0000
T459_07645	-1.9910	0.3752	-5.3065	0.0000	0.0000
T459_13607	-1.9838	0.4406	-4.5026	0.0000	0.0002
T459_01927	-1.9359	0.1576	-12.2840	0.0000	0.0000
T459_30808	-1.9114	0.2951	-6.4764	0.0000	0.0000
T459_29155	-1.9045	0.3320	-5.7369	0.0000	0.0000
T459_08659	-1.8712	0.4977	-3.7601	0.0002	0.0029
T459_07898	-1.8604	0.1964	-9.4732	0.0000	0.0000
T459_02665	-1.8580	0.3559	-5.2201	0.0000	0.0000
T459_09665	-1.8493	0.2292	-8.0683	0.0000	0.0000
T459_22212	-1.8370	0.3125	-5.8791	0.0000	0.0000
T459_27227	-1.8218	0.2676	-6.8075	0.0000	0.0000
T459_33519	-1.8072	0.3093	-5.8436	0.0000	0.0000
T459_12710	-1.8030	0.3496	-5.1569	0.0000	0.0000
T459_09677	-1.7898	0.2143	-8.3517	0.0000	0.0000
T459_29416	-1.7842	0.3243	-5.5016	0.0000	0.0000
T459_27700	-1.7831	0.2146	-8.3095	0.0000	0.0000
T459_13825	-1.7804	0.4569	-3.8967	0.0001	0.0018
T459_15343	-1.7752	0.2331	-7.6144	0.0000	0.0000
T459_34688	-1.7748	0.3696	-4.8021	0.0000	0.0000
T459_13126	-1.7469	0.2704	-6.4612	0.0000	0.0000
T459_05021	-1.7389	0.1917	-9.0708	0.0000	0.0000
T459_05227	-1.7365	0.2446	-7.1002	0.0000	0.0000
T459_06692	-1.7357	0.3862	-4.4945	0.0000	0.0002
T459_33520	-1.7177	0.2915	-5.8936	0.0000	0.0000
T459_35236	-1.7167	0.3148	-5.4533	0.0000	0.0000

Gene ID	log2FoldChange	lfcSE	stat	pvalue	padj
T459_30863	-1.7096	0.2425	-7.0500	0.0000	0.0000
T459_31191	-1.6998	0.3986	-4.2648	0.0000	0.0005
T459_34694	-1.6859	0.3637	-4.6360	0.0000	0.0001
T459_25618	-1.6857	0.3561	-4.7345	0.0000	0.0001
T459_28000	-1.6664	0.1858	-8.9680	0.0000	0.0000
T459_03129	-1.6650	0.4518	-3.6851	0.0002	0.0037
T459_21150	-1.6525	0.3647	-4.5307	0.0000	0.0002
T459_18555	-1.6424	0.3581	-4.5866	0.0000	0.0001
T459_01685	-1.6353	0.3004	-5.4441	0.0000	0.0000
T459_20228	-1.6202	0.3250	-4.9850	0.0000	0.0000
T459_31358	-1.6184	0.4027	-4.0192	0.0001	0.0012
T459_10793	-1.6069	0.3499	-4.5920	0.0000	0.0001
T459_10860	-1.6018	0.3040	-5.2683	0.0000	0.0000
T459_15460	-1.5955	0.3631	-4.3935	0.0000	0.0003
T459_26375	-1.5923	0.1065	-14.9467	0.0000	0.0000
T459_30790	-1.5913	0.4260	-3.7351	0.0002	0.0032
T459_10518	-1.5794	0.2886	-5.4717	0.0000	0.0000
T459_22972	-1.5790	0.1634	-9.6641	0.0000	0.0000
T459_32208	-1.5725	0.4007	-3.9241	0.0001	0.0016
T459_32782	-1.5692	0.2717	-5.7754	0.0000	0.0000
T459_11341	-1.5608	0.3291	-4.7427	0.0000	0.0001
T459_34540	-1.5551	0.2825	-5.5047	0.0000	0.0000
T459_05997	-1.5524	0.2591	-5.9903	0.0000	0.0000
T459_17654	-1.5514	0.3117	-4.9775	0.0000	0.0000
T459_25990	-1.5499	0.2918	-5.3123	0.0000	0.0000
T459_34720	-1.5492	0.2448	-6.3293	0.0000	0.0000
T459_20328	-1.5429	0.4165	-3.7044	0.0002	0.0035
T459_08260	-1.5320	0.3330	-4.6011	0.0000	0.0001
T459_15101	-1.5274	0.3643	-4.1924	0.0000	0.0006
T459_26349	-1.5185	0.1738	-8.7358	0.0000	0.0000
T459_13587	-1.5181	0.3733	-4.0666	0.0000	0.0010
T459_30884	-1.5154	0.2512	-6.0326	0.0000	0.0000
T459_05911	-1.5153	0.3542	-4.2777	0.0000	0.0004
T459_27445	-1.5100	0.2831	-5.3344	0.0000	0.0000
T459_06053	-1.5098	0.2602	-5.8026	0.0000	0.0000
T459_22213	-1.5046	0.2300	-6.5408	0.0000	0.0000
T459_20387	-1.4912	0.2916	-5.1144	0.0000	0.0000
T459_33260	-1.4884	0.2941	-5.0606	0.0000	0.0000
T459_26531	-1.4813	0.3730	-3.9717	0.0001	0.0014
T459_05306	-1.4709	0.3927	-3.7459	0.0002	0.0031
T459_22569	-1.4667	0.1367	-10.7291	0.0000	0.0000
T459_31882	-1.4620	0.2197	-6.6560	0.0000	0.0000
T459_22747	-1.4592	0.3972	-3.6736	0.0002	0.0039
T459_17412	-1.4385	0.3125	-4.6026	0.0000	0.0001
T459_29886	-1.4360	0.1785	-8.0469	0.0000	0.0000
T459_09373	-1.4318	0.2586	-5.5372	0.0000	0.0000
T459_24117	-1.4201	0.3620	-3.9232	0.0001	0.0016

Gene ID	log2FoldChange	lfcSE	stat	pvalue	padj
T459_10606	-1.4081	0.2155	-6.5330	0.0000	0.0000
T459_34441	-1.4044	0.1640	-8.5622	0.0000	0.0000
T459_27819	-1.4012	0.1717	-8.1621	0.0000	0.0000
T459_07993	-1.3993	0.3373	-4.1482	0.0000	0.0007
T459_28926	-1.3987	0.2679	-5.2217	0.0000	0.0000
T459_22888	-1.3925	0.2823	-4.9320	0.0000	0.0000
T459_05016	-1.3918	0.2348	-5.9281	0.0000	0.0000
T459_20601	-1.3857	0.3364	-4.1196	0.0000	0.0008
T459_32578	-1.3703	0.2570	-5.3313	0.0000	0.0000
T459_03768	-1.3624	0.3628	-3.7553	0.0002	0.0030
T459_18678	-1.3604	0.2403	-5.6621	0.0000	0.0000
T459_10426	-1.3593	0.3119	-4.3585	0.0000	0.0003
T459_17106	-1.3562	0.3130	-4.3335	0.0000	0.0003
T459_20699	-1.3557	0.2457	-5.5167	0.0000	0.0000
T459_10987	-1.3556	0.3242	-4.1810	0.0000	0.0006
T459_34425	-1.3517	0.2690	-5.0256	0.0000	0.0000
T459_00118	-1.3432	0.1681	-7.9888	0.0000	0.0000
T459_35470	-1.3396	0.3406	-3.9331	0.0001	0.0016
T459_00896	-1.3396	0.3559	-3.7636	0.0002	0.0029
T459_18231	-1.3389	0.2217	-6.0384	0.0000	0.0000
T459_32574	-1.3379	0.3130	-4.2743	0.0000	0.0004
T459_06419	-1.3355	0.2682	-4.9801	0.0000	0.0000
T459_31475	-1.3333	0.2383	-5.5948	0.0000	0.0000
T459_31012	-1.3238	0.1973	-6.7081	0.0000	0.0000
T459_21812	-1.3111	0.1706	-7.6841	0.0000	0.0000
T459_34478	-1.3104	0.3157	-4.1508	0.0000	0.0007
T459_03749	-1.3098	0.1287	-10.1738	0.0000	0.0000
T459_07260	-1.3005	0.2923	-4.4497	0.0000	0.0002
T459_10146	-1.2964	0.1593	-8.1361	0.0000	0.0000
T459_30852	-1.2947	0.2563	-5.0516	0.0000	0.0000
T459_34477	-1.2907	0.2156	-5.9858	0.0000	0.0000
T459_21143	-1.2875	0.3468	-3.7125	0.0002	0.0034
T459_11364	-1.2845	0.3501	-3.6687	0.0002	0.0039
T459_31878	-1.2839	0.3124	-4.1094	0.0000	0.0008
T459_35322	-1.2669	0.1288	-9.8373	0.0000	0.0000
T459_15087	-1.2658	0.3485	-3.6326	0.0003	0.0044
T459_26830	-1.2563	0.3034	-4.1414	0.0000	0.0007
T459_18084	-1.2471	0.1975	-6.3154	0.0000	0.0000
T459_17139	-1.2346	0.1684	-7.3321	0.0000	0.0000
T459_18673	-1.2289	0.1177	-10.4413	0.0000	0.0000
T459_19854	-1.2250	0.1602	-7.6451	0.0000	0.0000
T459_08649	-1.2193	0.2616	-4.6607	0.0000	0.0001
T459_13624	-1.2192	0.1747	-6.9772	0.0000	0.0000
T459_34682	-1.2133	0.3264	-3.7173	0.0002	0.0034
T459_06015	-1.2059	0.2958	-4.0775	0.0000	0.0009
T459_10096	-1.2032	0.1696	-7.0934	0.0000	0.0000
T459_04295	-1.1957	0.3132	-3.8179	0.0001	0.0024

Gene ID	log2FoldChange	lfcSE	stat	pvalue	padj
T459_09920	-1.1936	0.3071	-3.8861	0.0001	0.0019
T459_07668	-1.1823	0.2217	-5.3334	0.0000	0.0000
T459_00276	-1.1821	0.1279	-9.2398	0.0000	0.0000
T459_33005	-1.1817	0.1887	-6.2627	0.0000	0.0000
T459_08278	-1.1807	0.2424	-4.8702	0.0000	0.0000
T459_21280	-1.1751	0.2740	-4.2882	0.0000	0.0004
T459_15100	-1.1706	0.3009	-3.8899	0.0001	0.0019
T459_18546	-1.1687	0.2691	-4.3424	0.0000	0.0003
T459_12901	-1.1674	0.2314	-5.0454	0.0000	0.0000
T459_13163	-1.1608	0.2951	-3.9336	0.0001	0.0016
T459_28920	-1.1589	0.2665	-4.3479	0.0000	0.0003
T459_27999	-1.1570	0.1733	-6.6759	0.0000	0.0000
T459_26371	-1.1538	0.2966	-3.8898	0.0001	0.0019
T459_05599	-1.1439	0.1255	-9.1174	0.0000	0.0000
T459_19981	-1.1408	0.2962	-3.8514	0.0001	0.0021
T459_32341	-1.1390	0.2569	-4.4342	0.0000	0.0002
T459_23598	-1.1388	0.2074	-5.4905	0.0000	0.0000
T459_12979	-1.1324	0.2775	-4.0813	0.0000	0.0009
T459_17589	-1.1254	0.1533	-7.3392	0.0000	0.0000
T459_15674	-1.1223	0.2188	-5.1304	0.0000	0.0000
T459_23964	-1.1187	0.2539	-4.4056	0.0000	0.0003
T459_17370	-1.1182	0.2043	-5.4733	0.0000	0.0000
T459_24763	-1.1168	0.1936	-5.7690	0.0000	0.0000
T459_18146	-1.1158	0.2925	-3.8149	0.0001	0.0024
T459_20718	-1.1151	0.2837	-3.9307	0.0001	0.0016
T459_00829	-1.1150	0.2661	-4.1906	0.0000	0.0006
T459_25801	-1.1147	0.2172	-5.1329	0.0000	0.0000
T459_25422	-1.1138	0.1509	-7.3801	0.0000	0.0000
T459_24583	-1.1138	0.2381	-4.6784	0.0000	0.0001
T459_12307	-1.1058	0.2317	-4.7721	0.0000	0.0001
T459_13105	-1.1045	0.2368	-4.6646	0.0000	0.0001
T459_09678	-1.0983	0.1121	-9.7942	0.0000	0.0000
T459_10893	-1.0950	0.2077	-5.2710	0.0000	0.0000
T459_00664	-1.0889	0.2590	-4.2035	0.0000	0.0006
T459_30505	-1.0881	0.2826	-3.8499	0.0001	0.0021
T459_00100	-1.0874	0.2969	-3.6626	0.0002	0.0040
T459_18075	-1.0795	0.2350	-4.5937	0.0000	0.0001
T459_22567	-1.0744	0.1432	-7.5035	0.0000	0.0000
T459_10649	-1.0725	0.1699	-6.3108	0.0000	0.0000
T459_29328	-1.0678	0.1749	-6.1069	0.0000	0.0000
T459_31247	-1.0630	0.1882	-5.6472	0.0000	0.0000
T459_18785	-1.0592	0.2843	-3.7254	0.0002	0.0033
T459_26451	-1.0577	0.2381	-4.4413	0.0000	0.0002
T459_31182	-1.0533	0.2781	-3.7872	0.0002	0.0027
T459_31609	-1.0505	0.1352	-7.7684	0.0000	0.0000
T459_06156	-1.0502	0.2713	-3.8709	0.0001	0.0020
T459_22210	-1.0500	0.2200	-4.7730	0.0000	0.0001

Gene ID	log2FoldChange	lfcSE	stat	pvalue	padj
T459_29768	-1.0490	0.1823	-5.7550	0.0000	0.0000
T459_18773	-1.0463	0.1983	-5.2761	0.0000	0.0000
T459_24029	-1.0441	0.1820	-5.7381	0.0000	0.0000
T459_21261	-1.0424	0.2388	-4.3658	0.0000	0.0003
T459_33446	-1.0384	0.2077	-4.9988	0.0000	0.0000
T459_00607	-1.0381	0.2605	-3.9856	0.0001	0.0013
T459_18941	-1.0361	0.2140	-4.8421	0.0000	0.0000
T459_27044	-1.0345	0.2317	-4.4645	0.0000	0.0002
T459_28271	-1.0318	0.2128	-4.8496	0.0000	0.0000
T459_14828	-1.0302	0.2553	-4.0353	0.0001	0.0011
T459_03994	-1.0204	0.2817	-3.6222	0.0003	0.0046
T459_25513	-1.0171	0.2751	-3.6974	0.0002	0.0036
T459_16120	-1.0055	0.2153	-4.6700	0.0000	0.0001
T459_03347	-1.0029	0.2250	-4.4566	0.0000	0.0002
T459_07595	1.0112	0.2314	4.3704	0.0000	0.0003
T459_00327	1.0130	0.1286	7.8794	0.0000	0.0000
T459_00328	1.0196	0.2259	4.5135	0.0000	0.0002
T459_33557	1.0203	0.1236	8.2555	0.0000	0.0000
T459_34399	1.0239	0.1871	5.4719	0.0000	0.0000
T459_06370	1.0252	0.2263	4.5308	0.0000	0.0002
T459_25791	1.0262	0.2132	4.8133	0.0000	0.0000
T459_25537	1.0277	0.2316	4.4379	0.0000	0.0002
T459_17419	1.0281	0.2495	4.1207	0.0000	0.0008
T459_04647	1.0428	0.2259	4.6158	0.0000	0.0001
T459_33787	1.0461	0.2408	4.3433	0.0000	0.0003
T459_20093	1.0464	0.2381	4.3941	0.0000	0.0003
T459_33991	1.0499	0.1686	6.2254	0.0000	0.0000
T459_31637	1.0517	0.2848	3.6932	0.0002	0.0036
T459_06755	1.0524	0.2797	3.7622	0.0002	0.0029
T459_06406	1.0588	0.1763	6.0049	0.0000	0.0000
T459_19483	1.0599	0.1046	10.1367	0.0000	0.0000
T459_03221	1.0632	0.2873	3.7005	0.0002	0.0036
T459_03045	1.0712	0.2271	4.7167	0.0000	0.0001
T459_23978	1.0793	0.2903	3.7183	0.0002	0.0034
T459_26818	1.0794	0.2928	3.6860	0.0002	0.0037
T459_21761	1.0844	0.2434	4.4551	0.0000	0.0002
T459_06674	1.0867	0.2570	4.2280	0.0000	0.0005
T459_34174	1.0901	0.2722	4.0052	0.0001	0.0012
T459_13294	1.1024	0.2257	4.8838	0.0000	0.0000
T459_17009	1.1048	0.2065	5.3498	0.0000	0.0000
T459_13538	1.1181	0.2895	3.8623	0.0001	0.0020
T459_25598	1.1264	0.1024	11.0046	0.0000	0.0000
T459_34009	1.1267	0.1570	7.1778	0.0000	0.0000
T459_21260	1.1281	0.3111	3.6267	0.0003	0.0045
T459_22736	1.1283	0.2540	4.4419	0.0000	0.0002
T459_19693	1.1348	0.2558	4.4367	0.0000	0.0002
T459_08959	1.1372	0.2399	4.7405	0.0000	0.0001

Gene ID	log2FoldChange	lfcSE	stat	pvalue	padj
T459_30824	1.1382	0.2944	3.8661	0.0001	0.0020
T459_16827	1.1398	0.2617	4.3561	0.0000	0.0003
T459_08170	1.1450	0.2042	5.6068	0.0000	0.0000
T459_34555	1.1496	0.3131	3.6713	0.0002	0.0039
T459_30838	1.1522	0.3101	3.7155	0.0002	0.0034
T459_08085	1.1526	0.2770	4.1606	0.0000	0.0007
T459_17102	1.1543	0.3059	3.7741	0.0002	0.0028
T459_31988	1.1575	0.0943	12.2748	0.0000	0.0000
T459_21751	1.1583	0.2696	4.2965	0.0000	0.0004
T459_35139	1.1598	0.3020	3.8404	0.0001	0.0022
T459_05880	1.1652	0.3141	3.7099	0.0002	0.0034
T459_17544	1.1733	0.3003	3.9070	0.0001	0.0017
T459_00566	1.1735	0.2731	4.2969	0.0000	0.0004
T459_05892	1.1748	0.2404	4.8868	0.0000	0.0000
T459_17321	1.1794	0.2596	4.5433	0.0000	0.0002
T459_01853	1.1835	0.2729	4.3363	0.0000	0.0003
T459_32093	1.1835	0.3074	3.8495	0.0001	0.0021
T459_32944	1.1860	0.2699	4.3938	0.0000	0.0003
T459_07675	1.1866	0.2951	4.0209	0.0001	0.0011
T459_20474	1.1964	0.2733	4.3773	0.0000	0.0003
T459_17496	1.1991	0.1845	6.4988	0.0000	0.0000
T459_31848	1.2000	0.1598	7.5110	0.0000	0.0000
T459_00386	1.2027	0.2271	5.2965	0.0000	0.0000
T459_23437	1.2051	0.3016	3.9954	0.0001	0.0013
T459_09727	1.2097	0.3200	3.7798	0.0002	0.0027
T459_34685	1.2097	0.2278	5.3096	0.0000	0.0000
T459_34901	1.2111	0.2942	4.1171	0.0000	0.0008
T459_25091	1.2222	0.2246	5.4410	0.0000	0.0000
T459_27048	1.2261	0.1947	6.2988	0.0000	0.0000
T459_20160	1.2301	0.3332	3.6913	0.0002	0.0037
T459_23651	1.2371	0.3328	3.7173	0.0002	0.0034
T459_28012	1.2373	0.2856	4.3330	0.0000	0.0003
T459_34823	1.2498	0.3144	3.9747	0.0001	0.0014
T459_13901	1.2632	0.2747	4.5978	0.0000	0.0001
T459_19542	1.2639	0.1689	7.4818	0.0000	0.0000
T459_23556	1.2689	0.2855	4.4440	0.0000	0.0002
T459_04872	1.2824	0.2294	5.5906	0.0000	0.0000
T459_15596	1.2850	0.3354	3.8311	0.0001	0.0023
T459_10460	1.2857	0.1903	6.7554	0.0000	0.0000
T459_32005	1.2891	0.2713	4.7522	0.0000	0.0001
T459_06340	1.2895	0.1698	7.5951	0.0000	0.0000
T459_14092	1.2911	0.3579	3.6078	0.0003	0.0048
T459_28305	1.2918	0.3084	4.1881	0.0000	0.0006
T459_10360	1.3020	0.3470	3.7519	0.0002	0.0030
T459_34298	1.3148	0.2267	5.7989	0.0000	0.0000
T459_08105	1.3219	0.3174	4.1647	0.0000	0.0007
T459_09766	1.3245	0.2769	4.7837	0.0000	0.0001

Gene ID	log2FoldChange	lfcSE	stat	pvalue	padj
T459_14246	1.3248	0.3050	4.3432	0.0000	0.0003
T459_09785	1.3273	0.2878	4.6125	0.0000	0.0001
T459_21099	1.3426	0.1169	11.4818	0.0000	0.0000
T459_32804	1.3443	0.2394	5.6166	0.0000	0.0000
T459_03263	1.3449	0.3410	3.9440	0.0001	0.0015
T459_04659	1.3455	0.3670	3.6659	0.0002	0.0040
T459_10139	1.3467	0.2646	5.0898	0.0000	0.0000
T459_33510	1.3548	0.1774	7.6361	0.0000	0.0000
T459_11771	1.3549	0.2997	4.5207	0.0000	0.0002
T459_10082	1.3606	0.2242	6.0693	0.0000	0.0000
T459_09093	1.3611	0.2354	5.7818	0.0000	0.0000
T459_07424	1.3646	0.3590	3.8006	0.0001	0.0025
T459_31011	1.3652	0.2700	5.0566	0.0000	0.0000
T459_23925	1.3698	0.3670	3.7324	0.0002	0.0032
T459_18996	1.3719	0.3370	4.0713	0.0000	0.0010
T459_05655	1.3726	0.3137	4.3753	0.0000	0.0003
T459_17980	1.3731	0.0903	15.2137	0.0000	0.0000
T459_18795	1.3758	0.1182	11.6442	0.0000	0.0000
T459_22172	1.3819	0.1653	8.3617	0.0000	0.0000
T459_26265	1.3840	0.3250	4.2584	0.0000	0.0005
T459_29945	1.3851	0.2539	5.4545	0.0000	0.0000
T459_16761	1.3885	0.1008	13.7735	0.0000	0.0000
T459_09108	1.3901	0.2544	5.4632	0.0000	0.0000
T459_09786	1.3906	0.3419	4.0675	0.0000	0.0010
T459_03735	1.3910	0.2762	5.0365	0.0000	0.0000
T459_13021	1.3928	0.2829	4.9234	0.0000	0.0000
T459_25267	1.3936	0.3580	3.8926	0.0001	0.0018
T459_34296	1.3966	0.2546	5.4851	0.0000	0.0000
T459_33908	1.4024	0.3458	4.0550	0.0001	0.0010
T459_05238	1.4115	0.1259	11.2103	0.0000	0.0000
T459_15372	1.4157	0.3485	4.0622	0.0000	0.0010
T459_01357	1.4172	0.2588	5.4760	0.0000	0.0000
T459_06719	1.4314	0.3445	4.1555	0.0000	0.0007
T459_16124	1.4343	0.1745	8.2194	0.0000	0.0000
T459_13916	1.4345	0.2649	5.4156	0.0000	0.0000
T459_25745	1.4399	0.2646	5.4415	0.0000	0.0000
T459_04840	1.4459	0.2596	5.5701	0.0000	0.0000
T459_05410	1.4531	0.2553	5.6926	0.0000	0.0000
T459_16689	1.4547	0.1832	7.9390	0.0000	0.0000
T459_00426	1.4594	0.2258	6.4631	0.0000	0.0000
T459_00326	1.4647	0.2289	6.3979	0.0000	0.0000
T459_34126	1.4667	0.3358	4.3684	0.0000	0.0003
T459_26014	1.4696	0.3685	3.9879	0.0001	0.0013
T459_08463	1.4799	0.3725	3.9732	0.0001	0.0014
T459_23977	1.4857	0.3234	4.5944	0.0000	0.0001
T459_32743	1.4922	0.3031	4.9233	0.0000	0.0000
T459_12367	1.4958	0.3553	4.2105	0.0000	0.0006

Gene ID	log2FoldChange	lfcSE	stat	pvalue	padj
T459_09386	1.4964	0.3409	4.3894	0.0000	0.0003
T459_29288	1.5012	0.1917	7.8320	0.0000	0.0000
T459_18108	1.5042	0.3248	4.6318	0.0000	0.0001
T459_01358	1.5062	0.1933	7.7916	0.0000	0.0000
T459_07751	1.5283	0.3278	4.6629	0.0000	0.0001
T459_05669	1.5306	0.4126	3.7100	0.0002	0.0034
T459_25824	1.5419	0.3354	4.5978	0.0000	0.0001
T459_07062	1.5466	0.3044	5.0803	0.0000	0.0000
T459_15732	1.5473	0.3487	4.4375	0.0000	0.0002
T459_31879	1.5501	0.3420	4.5332	0.0000	0.0002
T459_22503	1.5555	0.4230	3.6776	0.0002	0.0038
T459_15320	1.5560	0.3311	4.7000	0.0000	0.0001
T459_05089	1.5576	0.3707	4.2017	0.0000	0.0006
T459_15597	1.5633	0.3562	4.3889	0.0000	0.0003
T459_18565	1.5703	0.3471	4.5245	0.0000	0.0002
T459_31163	1.5729	0.2329	6.7544	0.0000	0.0000
T459_35540	1.5739	0.3361	4.6826	0.0000	0.0001
T459_33564	1.5784	0.3950	3.9956	0.0001	0.0013
T459_08134	1.5836	0.1599	9.9048	0.0000	0.0000
T459_27911	1.5970	0.3966	4.0267	0.0001	0.0011
T459_03842	1.6036	0.2226	7.2037	0.0000	0.0000
T459_20531	1.6103	0.3817	4.2183	0.0000	0.0005
T459_29936	1.6162	0.3004	5.3797	0.0000	0.0000
T459_13943	1.6188	0.4146	3.9043	0.0001	0.0018
T459_09620	1.6313	0.3631	4.4928	0.0000	0.0002
T459_24048	1.6379	0.1365	11.9983	0.0000	0.0000
T459_28315	1.6388	0.2041	8.0296	0.0000	0.0000
T459_13200	1.6496	0.4510	3.6575	0.0003	0.0041
T459_06869	1.6571	0.2070	8.0039	0.0000	0.0000
T459_06213	1.6690	0.4612	3.6192	0.0003	0.0046
T459_18690	1.6950	0.4108	4.1257	0.0000	0.0008
T459_07986	1.7013	0.3300	5.1556	0.0000	0.0000
T459_12695	1.7046	0.3698	4.6101	0.0000	0.0001
T459_00508	1.7083	0.3005	5.6846	0.0000	0.0000
T459_05874	1.7246	0.1830	9.4258	0.0000	0.0000
T459_07881	1.7288	0.2975	5.8108	0.0000	0.0000
T459_07287	1.7352	0.2360	7.3514	0.0000	0.0000
T459_15780	1.7414	0.1646	10.5799	0.0000	0.0000
T459_12705	1.7685	0.4692	3.7692	0.0002	0.0028
T459_16024	1.7689	0.1289	13.7222	0.0000	0.0000
T459_34025	1.7704	0.3540	5.0015	0.0000	0.0000
T459_17503	1.7794	0.2527	7.0428	0.0000	0.0000
T459_17555	1.7878	0.4758	3.7572	0.0002	0.0030
T459_17523	1.7949	0.3222	5.5706	0.0000	0.0000
T459_15778	1.7969	0.3234	5.5565	0.0000	0.0000
T459_18426	1.8018	0.1847	9.7555	0.0000	0.0000
T459_32753	1.8023	0.4294	4.1974	0.0000	0.0006

Gene ID	log2FoldChange	lfcSE	stat	pvalue	padj
T459_17431	1.8065	0.4156	4.3472	0.0000	0.0003
T459_27998	1.8205	0.3783	4.8124	0.0000	0.0000
T459_20028	1.8388	0.1530	12.0221	0.0000	0.0000
T459_03841	1.8422	0.1988	9.2681	0.0000	0.0000
T459_16218	1.8442	0.3630	5.0807	0.0000	0.0000
T459_07860	1.8505	0.4314	4.2897	0.0000	0.0004
T459_29715	1.8527	0.2904	6.3793	0.0000	0.0000
T459_07440	1.8677	0.4171	4.4784	0.0000	0.0002
T459_17948	1.8725	0.3940	4.7527	0.0000	0.0001
T459_05348	1.8899	0.4204	4.4954	0.0000	0.0002
T459_27006	1.9315	0.4370	4.4197	0.0000	0.0002
T459_27082	1.9369	0.2836	6.8288	0.0000	0.0000
T459_04410	1.9485	0.2140	9.1061	0.0000	0.0000
T459_10083	1.9576	0.2285	8.5661	0.0000	0.0000
T459_09647	1.9593	0.4519	4.3360	0.0000	0.0003
T459_21752	1.9662	0.5235	3.7556	0.0002	0.0030
T459_05018	1.9686	0.3453	5.7018	0.0000	0.0000
T459_25112	1.9726	0.2585	7.6311	0.0000	0.0000
T459_04884	1.9736	0.5069	3.8936	0.0001	0.0018
T459_24377	1.9847	0.2942	6.7468	0.0000	0.0000
T459_03840	2.0076	0.2913	6.8920	0.0000	0.0000
T459_06712	2.0217	0.1703	11.8685	0.0000	0.0000
T459_28581	2.0303	0.2557	7.9403	0.0000	0.0000
T459_31495	2.0390	0.1927	10.5797	0.0000	0.0000
T459_10147	2.0407	0.1596	12.7859	0.0000	0.0000
T459_16866	2.0452	0.4811	4.2508	0.0000	0.0005
T459_22760	2.0614	0.1791	11.5093	0.0000	0.0000
T459_15901	2.0654	0.2919	7.0762	0.0000	0.0000
T459_07195	2.0767	0.3519	5.9011	0.0000	0.0000
T459_16121	2.0771	0.1939	10.7143	0.0000	0.0000
T459_25849	2.0844	0.1849	11.2724	0.0000	0.0000
T459_26666	2.0992	0.2862	7.3341	0.0000	0.0000
T459_28583	2.1001	0.2898	7.2470	0.0000	0.0000
T459_01301	2.1214	0.5054	4.1977	0.0000	0.0006
T459_27008	2.1581	0.3387	6.3713	0.0000	0.0000
T459_32329	2.1639	0.2329	9.2918	0.0000	0.0000
T459_29869	2.1664	0.5702	3.7993	0.0001	0.0026
T459_17322	2.1679	0.3664	5.9173	0.0000	0.0000
T459_12483	2.1704	0.5161	4.2052	0.0000	0.0006
T459_30490	2.1965	0.5198	4.2254	0.0000	0.0005
T459_33098	2.2046	0.5763	3.8254	0.0001	0.0023
T459_04374	2.2141	0.3722	5.9485	0.0000	0.0000
T459_21981	2.2279	0.2918	7.6355	0.0000	0.0000
T459_16770	2.2284	0.5202	4.2837	0.0000	0.0004
T459_10788	2.2359	0.1761	12.6988	0.0000	0.0000
T459_18809	2.2505	0.1939	11.6043	0.0000	0.0000
T459_25036	2.2512	0.5259	4.2804	0.0000	0.0004

Gene ID	log2FoldChange	lfcSE	stat	pvalue	padj
T459_16102	2.2574	0.1922	11.7448	0.0000	0.0000
T459_28580	2.2804	0.3193	7.1426	0.0000	0.0000
T459_26283	2.2807	0.3286	6.9412	0.0000	0.0000
T459_22173	2.2962	0.4150	5.5326	0.0000	0.0000
T459_33809	2.3012	0.4143	5.5547	0.0000	0.0000
T459_08013	2.3177	0.2587	8.9578	0.0000	0.0000
T459_28937	2.3230	0.3655	6.3552	0.0000	0.0000
T459_33615	2.3743	0.2865	8.2875	0.0000	0.0000
T459_02590	2.3816	0.3186	7.4749	0.0000	0.0000
T459_21301	2.3908	0.2476	9.6563	0.0000	0.0000
T459_31014	2.4031	0.2197	10.9380	0.0000	0.0000
T459_22537	2.4070	0.2740	8.7841	0.0000	0.0000
T459_28582	2.4076	0.3059	7.8715	0.0000	0.0000
T459_00737	2.4145	0.3886	6.2133	0.0000	0.0000
T459_05955	2.4211	0.2133	11.3492	0.0000	0.0000
T459_30533	2.4223	0.5646	4.2900	0.0000	0.0004
T459_29868	2.4408	0.3018	8.0861	0.0000	0.0000
T459_22468	2.4441	0.1704	14.3468	0.0000	0.0000
T459_35330	2.4526	0.5768	4.2523	0.0000	0.0005
T459_18689	2.4799	0.5233	4.7386	0.0000	0.0001
T459_21462	2.4881	0.1662	14.9688	0.0000	0.0000
T459_00065	2.4949	0.6699	3.7243	0.0002	0.0033
T459_07060	2.5216	0.5452	4.6253	0.0000	0.0001
T459_19216	2.5237	0.4907	5.1433	0.0000	0.0000
T459_04352	2.5413	0.4314	5.8914	0.0000	0.0000
T459_15080	2.5456	0.5465	4.6582	0.0000	0.0001
T459_04516	2.5462	0.5916	4.3042	0.0000	0.0004
T459_19891	2.5594	0.3470	7.3746	0.0000	0.0000
T459_09914	2.5853	0.5828	4.4361	0.0000	0.0002
T459_07192	2.5865	0.2539	10.1886	0.0000	0.0000
T459_15129	2.5914	0.4991	5.1919	0.0000	0.0000
T459_34082	2.6530	0.4978	5.3294	0.0000	0.0000
T459_17077	2.6697	0.4574	5.8370	0.0000	0.0000
T459_09708	2.6740	0.2771	9.6507	0.0000	0.0000
T459_00505	2.6748	0.3559	7.5148	0.0000	0.0000
T459_14681	2.7410	0.6391	4.2886	0.0000	0.0004
T459_04510	2.7629	0.5901	4.6820	0.0000	0.0001
T459_18488	2.7761	0.3475	7.9887	0.0000	0.0000
T459_00242	2.7825	0.5448	5.1071	0.0000	0.0000
T459_26516	2.7825	0.4758	5.8484	0.0000	0.0000
T459_25894	2.7865	0.3451	8.0735	0.0000	0.0000
T459_16931	2.7898	0.6652	4.1936	0.0000	0.0006
T459_05780	2.8468	0.3186	8.9343	0.0000	0.0000
T459_35594	2.8944	0.7596	3.8106	0.0001	0.0025
T459_00477	2.9066	0.5113	5.6844	0.0000	0.0000
T459_12583	2.9179	0.6569	4.4415	0.0000	0.0002
T459_35620	2.9200	0.6907	4.2277	0.0000	0.0005

Gene ID	log2FoldChange	lfcSE	stat	pvalue	padj
T459_14052	2.9327	0.5585	5.2506	0.0000	0.0000
T459_24950	2.9708	0.6723	4.4186	0.0000	0.0002
T459_33984	2.9883	0.2633	11.3480	0.0000	0.0000
T459_08990	3.0152	0.2679	11.2530	0.0000	0.0000
T459_35248	3.0196	0.3578	8.4396	0.0000	0.0000
T459_32717	3.0322	0.2844	10.6606	0.0000	0.0000
T459_31986	3.0690	0.8388	3.6587	0.0003	0.0041
T459_07296	3.1333	0.3721	8.4196	0.0000	0.0000
T459_09773	3.1715	0.3256	9.7390	0.0000	0.0000
T459_16041	3.1979	0.5068	6.3098	0.0000	0.0000
T459_00066	3.2078	0.7564	4.2406	0.0000	0.0005
T459_24370	3.2204	0.3224	9.9894	0.0000	0.0000
T459_29314	3.2261	0.7956	4.0550	0.0001	0.0010
T459_15858	3.2620	0.5882	5.5454	0.0000	0.0000
T459_24379	3.2703	0.7286	4.4883	0.0000	0.0002
T459_18433	3.2803	0.4115	7.9710	0.0000	0.0000
T459_09622	3.2966	0.2387	13.8092	0.0000	0.0000
T459_06454	3.3403	0.3568	9.3608	0.0000	0.0000
T459_20538	3.3835	0.5352	6.3222	0.0000	0.0000
T459_14538	3.3957	0.7721	4.3980	0.0000	0.0003
T459_34410	3.4185	0.3183	10.7406	0.0000	0.0000
T459_04649	3.4396	0.2648	12.9872	0.0000	0.0000
T459_20537	3.4420	0.5221	6.5923	0.0000	0.0000
T459_20539	3.4564	0.5821	5.9378	0.0000	0.0000
T459_35711	3.4610	0.7223	4.7917	0.0000	0.0001
T459_30754	3.4659	0.5381	6.4415	0.0000	0.0000
T459_23252	3.4734	0.6913	5.0244	0.0000	0.0000
T459_24945	3.4974	0.7195	4.8609	0.0000	0.0000
T459_32663	3.5171	0.9319	3.7739	0.0002	0.0028
T459_35562	3.5224	0.4636	7.5978	0.0000	0.0000
T459_28052	3.5930	0.8604	4.1759	0.0000	0.0006
T459_31608	3.6859	0.8053	4.5770	0.0000	0.0001
T459_08129	3.6898	0.3657	10.0895	0.0000	0.0000
T459_29415	3.6961	0.5690	6.4958	0.0000	0.0000
T459_19245	3.7123	0.3041	12.2082	0.0000	0.0000
T459_34288	3.8051	0.4175	9.1139	0.0000	0.0000
T459_03008	3.8788	0.6632	5.8482	0.0000	0.0000
T459_04067	3.9747	1.0520	3.7783	0.0002	0.0028
T459_06459	4.0142	0.9809	4.0922	0.0000	0.0009
T459_31463	4.0370	0.3671	10.9963	0.0000	0.0000
T459_09514	4.0616	0.2278	17.8305	0.0000	0.0000
T459_12482	4.1138	0.9165	4.4884	0.0000	0.0002
T459_27154	4.1321	0.6786	6.0891	0.0000	0.0000
T459_11465	4.1764	0.2926	14.2749	0.0000	0.0000
T459_34553	4.2379	0.2955	14.3428	0.0000	0.0000
T459_05209	4.2448	0.6554	6.4768	0.0000	0.0000
T459_00004	4.2498	0.4997	8.5038	0.0000	0.0000

Gene ID	log2FoldChange	lfcSE	stat	pvalue	padj
T459_07809	4.2506	0.3845	11.0546	0.0000	0.0000
T459_28743	4.2826	0.5000	8.5652	0.0000	0.0000
T459_34352	4.4461	0.2931	15.1672	0.0000	0.0000
T459_27524	4.4770	0.4074	10.9900	0.0000	0.0000
T459_19222	4.5145	1.0003	4.5133	0.0000	0.0002
T459_04287	4.5203	0.8954	5.0486	0.0000	0.0000
T459_35190	4.5839	0.7234	6.3370	0.0000	0.0000
T459_15922	4.6453	0.7634	6.0852	0.0000	0.0000
T459_23871	4.6932	0.5772	8.1309	0.0000	0.0000
T459_13071	4.7121	0.5967	7.8969	0.0000	0.0000
T459_15325	4.7143	0.9299	5.0694	0.0000	0.0000
T459_05210	4.7456	0.9813	4.8358	0.0000	0.0000
T459_15779	4.7605	0.3504	13.5847	0.0000	0.0000
T459_31337	4.9049	0.8403	5.8367	0.0000	0.0000
T459_34931	5.1254	0.9146	5.6041	0.0000	0.0000
T459_28041	5.1460	1.1874	4.3340	0.0000	0.0003
T459_28373	5.1464	0.8942	5.7556	0.0000	0.0000
T459_00579	5.2312	0.7545	6.9332	0.0000	0.0000
T459_16298	5.2477	1.3793	3.8045	0.0001	0.0025
T459_25793	5.2505	1.4100	3.7238	0.0002	0.0033
T459_10685	5.3878	0.3407	15.8147	0.0000	0.0000
T459_33125	5.3917	1.0169	5.3022	0.0000	0.0000
T459_20040	5.4578	1.4345	3.8047	0.0001	0.0025
T459_16439	5.4816	0.9477	5.7842	0.0000	0.0000
T459_28374	5.4911	0.5788	9.4869	0.0000	0.0000
T459_08365	5.5622	1.0719	5.1893	0.0000	0.0000
T459_35707	5.5854	1.4847	3.7620	0.0002	0.0029
T459_29862	5.6422	1.4805	3.8109	0.0001	0.0025
T459_11645	5.6837	1.3167	4.3166	0.0000	0.0004
T459_15349	5.6963	0.4860	11.7219	0.0000	0.0000
T459_14638	5.7077	0.9349	6.1048	0.0000	0.0000
T459_15917	5.7110	0.6039	9.4561	0.0000	0.0000
T459_03101	5.7318	1.5097	3.7967	0.0001	0.0026
T459_17323	5.7858	1.1155	5.1866	0.0000	0.0000
T459_06634	5.8137	0.8406	6.9165	0.0000	0.0000
T459_29062	5.8356	0.4394	13.2796	0.0000	0.0000
T459_18730	5.8433	0.3597	16.2436	0.0000	0.0000
T459_35465	5.8576	1.4445	4.0552	0.0001	0.0010
T459_21239	5.8620	1.1094	5.2839	0.0000	0.0000
T459_01110	5.8960	1.4240	4.1405	0.0000	0.0007
T459_17454	5.9357	1.3319	4.4567	0.0000	0.0002
T459_24452	5.9651	1.3309	4.4821	0.0000	0.0002
T459_35732	5.9703	1.4610	4.0864	0.0000	0.0009
T459_18786	6.0277	0.3301	18.2625	0.0000	0.0000
T459_15872	6.1918	1.3860	4.4675	0.0000	0.0002
T459_21750	6.2229	0.6772	9.1896	0.0000	0.0000
T459_32185	6.2590	0.8521	7.3458	0.0000	0.0000

Gene ID	log2FoldChange	lfcSE	stat	pvalue	padj
T459_06174	6.3141	0.9098	6.9397	0.0000	0.0000
T459_26858	6.3527	1.3909	4.5672	0.0000	0.0001
T459_04276	6.3672	1.5081	4.2219	0.0000	0.0005
T459_11617	6.4053	1.2807	5.0015	0.0000	0.0000
T459_20380	6.4233	1.2810	5.0144	0.0000	0.0000
T459_20092	6.4328	1.4966	4.2984	0.0000	0.0004
T459_32664	6.4712	1.0835	5.9724	0.0000	0.0000
T459_18566	6.5305	1.3578	4.8094	0.0000	0.0000
T459_16639	6.5397	1.3479	4.8519	0.0000	0.0000
T459_25639	6.6436	1.3305	4.9934	0.0000	0.0000
T459_34940	6.6602	0.4602	14.4708	0.0000	0.0000
T459_12750	6.6792	0.6359	10.5033	0.0000	0.0000
T459_34938	6.7146	0.8739	7.6835	0.0000	0.0000
T459_27579	6.7216	1.3608	4.9393	0.0000	0.0000
T459_05241	6.7239	1.2499	5.3796	0.0000	0.0000
T459_04961	6.8758	1.3063	5.2635	0.0000	0.0000
T459_28744	6.9319	1.2502	5.5448	0.0000	0.0000
T459_22541	6.9484	1.3033	5.3312	0.0000	0.0000
T459_25404	6.9702	1.3024	5.3518	0.0000	0.0000
T459_23916	7.0384	1.3040	5.3975	0.0000	0.0000
T459_26859	7.0460	1.3014	5.4142	0.0000	0.0000
T459_23852	7.0846	1.3017	5.4427	0.0000	0.0000
T459_28101	7.1359	1.3024	5.4790	0.0000	0.0000
T459_16769	7.1740	1.0590	6.7742	0.0000	0.0000
T459_15740	7.2037	1.2527	5.7508	0.0000	0.0000
T459_34392	7.2170	1.2345	5.8462	0.0000	0.0000
T459_30897	7.2576	0.7576	9.5802	0.0000	0.0000
T459_04876	7.2890	1.3431	5.4272	0.0000	0.0000
T459_19238	7.3080	1.2793	5.7124	0.0000	0.0000
T459_18564	7.3133	1.2947	5.6488	0.0000	0.0000
T459_04877	7.3651	1.2824	5.7431	0.0000	0.0000
T459_34939	7.3710	0.2573	28.6480	0.0000	0.0000
T459_34393	7.3767	1.2867	5.7332	0.0000	0.0000
T459_35289	7.3791	1.3943	5.2922	0.0000	0.0000
T459_23428	7.4137	1.2768	5.8067	0.0000	0.0000
T459_35329	7.4186	1.3294	5.5804	0.0000	0.0000
T459_20099	7.4657	1.0572	7.0615	0.0000	0.0000
T459_02224	7.5484	1.2725	5.9319	0.0000	0.0000
T459_32527	7.6118	1.2284	6.1967	0.0000	0.0000
T459_17381	7.6220	1.3844	5.5056	0.0000	0.0000
T459_25568	7.6227	0.8621	8.8421	0.0000	0.0000
T459_01163	7.6481	1.2565	6.0867	0.0000	0.0000
T459_34684	7.6511	1.2589	6.0776	0.0000	0.0000
T459_33667	7.6829	1.2639	6.0785	0.0000	0.0000
T459_33149	7.7236	1.2205	6.3282	0.0000	0.0000
T459_01086	7.7456	1.2547	6.1731	0.0000	0.0000
T459_12136	7.8372	1.2156	6.4473	0.0000	0.0000

Gene ID	log2FoldChange	lfcSE	stat	pvalue	padj
T459_17458	7.8485	1.2543	6.2571	0.0000	0.0000
T459_19187	7.8631	1.3260	5.9298	0.0000	0.0000
T459_19586	7.9121	1.2180	6.4958	0.0000	0.0000
T459_15783	8.0185	0.8599	9.3253	0.0000	0.0000
T459_14979	8.1444	1.2402	6.5670	0.0000	0.0000
T459_34278	8.1594	1.2624	6.4634	0.0000	0.0000
T459_21788	8.2337	1.2397	6.6415	0.0000	0.0000
T459_23378	8.3049	1.2419	6.6872	0.0000	0.0000
T459_02191	8.3377	1.2376	6.7372	0.0000	0.0000
T459_35188	8.3610	1.2313	6.7905	0.0000	0.0000
T459_09200	8.4488	1.2279	6.8807	0.0000	0.0000
T459_00651	8.4590	1.2367	6.8399	0.0000	0.0000
T459_01013	8.4751	1.2457	6.8034	0.0000	0.0000
T459_23503	8.5455	1.2224	6.9910	0.0000	0.0000
T459_33000	8.5703	1.0787	7.9453	0.0000	0.0000
T459_34391	8.5750	1.2210	7.0231	0.0000	0.0000
T459_05443	8.6319	1.2178	7.0881	0.0000	0.0000
T459_11980	8.6654	1.2234	7.0833	0.0000	0.0000
T459_34383	9.1200	1.2088	7.5448	0.0000	0.0000
T459_24123	9.1290	0.9445	9.6654	0.0000	0.0000
T459_32526	9.2309	1.2114	7.6199	0.0000	0.0000
T459_34479	9.2408	0.4576	20.1948	0.0000	0.0000
T459_16926	9.2840	1.2067	7.6937	0.0000	0.0000
T459_15154	9.3622	1.2171	7.6919	0.0000	0.0000
T459_03602	9.4123	0.6276	14.9963	0.0000	0.0000
T459_34279	9.4831	1.2330	7.6909	0.0000	0.0000
T459_21523	9.5147	0.6529	14.5728	0.0000	0.0000
T459_29609	9.5238	1.2260	7.7681	0.0000	0.0000
T459_15784	9.5460	1.2091	7.8949	0.0000	0.0000
T459_19663	9.5878	1.2347	7.7652	0.0000	0.0000
T459_24124	9.7365	0.6196	15.7149	0.0000	0.0000
T459_28212	9.9981	1.2008	8.3260	0.0000	0.0000
T459_23974	12.9429	1.2715	10.1792	0.0000	0.0000

Supplementary Table 1. **D**. Differentially expressed genes between A10 under water stress and A10 under the control conditions at T1 (A10 PEG/A10 Control).

Gene ID	log2FoldChange	lfcSE	stat	pvalue	padj
T459_04005	-5.0330	0.9639	-5.2214	0.0000	0.0000
T459_25316	-4.9054	1.5691	-3.1262	0.0018	0.0326
T459_05997	-4.3187	1.1888	-3.6328	0.0003	0.0086
T459_12349	-4.2223	0.9543	-4.4247	0.0000	0.0006
T459_12276	-4.2215	0.8785	-4.8053	0.0000	0.0001
T459_32064	-4.1800	1.1847	-3.5284	0.0004	0.0117
T459_21833	-4.1713	1.2781	-3.2636	0.0011	0.0233
T459_32063	-4.0822	0.5488	-7.4389	0.0000	0.0000
T459_12275	-4.0788	0.6111	-6.6741	0.0000	0.0000

Gene ID	log2FoldChange	lfcSE	stat	pvalue	padj
T459_18120	-3.8339	0.6251	-6.1329	0.0000	0.0000
T459_05911	-3.8337	0.7278	-5.2674	0.0000	0.0000
T459_15100	-3.8335	1.0018	-3.8267	0.0001	0.0049
T459_21981	-3.8222	1.0457	-3.6551	0.0003	0.0081
T459_32062	-3.7652	0.3976	-9.4690	0.0000	0.0000
T459_22213	-3.7361	0.2953	-12.6503	0.0000	0.0000
T459_03880	-3.7105	0.4605	-8.0569	0.0000	0.0000
T459_24052	-3.6937	0.9160	-4.0324	0.0001	0.0025
T459_08151	-3.6809	0.7170	-5.1335	0.0000	0.0000
T459_15101	-3.6584	0.5842	-6.2621	0.0000	0.0000
T459_15477	-3.5982	0.5468	-6.5806	0.0000	0.0000
T459_33467	-3.5692	0.8629	-4.1364	0.0000	0.0017
T459_22502	-3.5610	1.0455	-3.4059	0.0007	0.0161
T459_12852	-3.5360	0.9579	-3.6912	0.0002	0.0073
T459_09472	-3.4323	0.4762	-7.2075	0.0000	0.0000
T459_33921	-3.3946	0.4473	-7.5893	0.0000	0.0000
T459_05978	-3.3259	0.5506	-6.0400	0.0000	0.0000
T459_01685	-3.2173	0.2846	-11.3029	0.0000	0.0000
T459_14651	-3.2134	0.7370	-4.3604	0.0000	0.0008
T459_09492	-3.2109	0.4435	-7.2397	0.0000	0.0000
T459_15111	-3.1659	0.8294	-3.8173	0.0001	0.0050
T459_04295	-3.1450	0.5541	-5.6763	0.0000	0.0000
T459_19480	-3.1270	0.6858	-4.5596	0.0000	0.0004
T459_15113	-3.1166	0.5889	-5.2919	0.0000	0.0000
T459_33622	-3.1068	0.8415	-3.6919	0.0002	0.0073
T459_14969	-3.1006	0.6919	-4.4810	0.0000	0.0005
T459_00197	-3.0825	0.7513	-4.1030	0.0000	0.0020
T459_18119	-3.0785	0.6046	-5.0917	0.0000	0.0000
T459_07163	-3.0326	0.3109	-9.7539	0.0000	0.0000
T459_17404	-2.9592	0.6257	-4.7294	0.0000	0.0002
T459_08856	-2.9417	0.5020	-5.8601	0.0000	0.0000
T459_01973	-2.9193	0.5432	-5.3739	0.0000	0.0000
T459_23239	-2.8193	0.4033	-6.9911	0.0000	0.0000
T459_22211	-2.7918	0.3635	-7.6800	0.0000	0.0000
T459_05984	-2.7866	0.6250	-4.4583	0.0000	0.0005
T459_01091	-2.7628	0.7389	-3.7389	0.0002	0.0064
T459_01683	-2.7365	0.4544	-6.0223	0.0000	0.0000
T459_27700	-2.7318	0.4904	-5.5704	0.0000	0.0000
T459_22212	-2.7236	0.3377	-8.0654	0.0000	0.0000
T459_09625	-2.6357	0.5950	-4.4296	0.0000	0.0006
T459_22210	-2.6074	0.2962	-8.8042	0.0000	0.0000
T459_13152	-2.5974	0.6154	-4.2207	0.0000	0.0013
T459_09473	-2.5701	0.4621	-5.5616	0.0000	0.0000
T459_16939	-2.5453	0.4545	-5.6006	0.0000	0.0000
T459_18426	-2.5389	0.6764	-3.7537	0.0002	0.0061
T459_06119	-2.5272	0.5453	-4.6347	0.0000	0.0003
T459_14054	-2.5148	0.7617	-3.3016	0.0010	0.0212

Gene ID	log2FoldChange	lfcSE	stat	pvalue	padj
T459_29549	-2.4954	0.4946	-5.0459	0.0000	0.0000
T459_31204	-2.4893	0.4515	-5.5139	0.0000	0.0000
T459_15087	-2.4616	0.3871	-6.3590	0.0000	0.0000
T459_04157	-2.4597	0.6594	-3.7301	0.0002	0.0065
T459_27641	-2.4570	0.5098	-4.8196	0.0000	0.0001
T459_13687	-2.4452	0.7087	-3.4501	0.0006	0.0143
T459_17401	-2.4430	0.3928	-6.2190	0.0000	0.0000
T459_33012	-2.4319	0.7391	-3.2901	0.0010	0.0218
T459_26764	-2.4206	0.7226	-3.3498	0.0008	0.0188
T459_24674	-2.4132	0.5133	-4.7010	0.0000	0.0002
T459_33922	-2.4055	0.4107	-5.8569	0.0000	0.0000
T459_00607	-2.3943	0.3092	-7.7442	0.0000	0.0000
T459_31320	-2.3938	0.7346	-3.2585	0.0011	0.0235
T459_32921	-2.3204	0.5951	-3.8992	0.0001	0.0039
T459_02267	-2.2893	0.4637	-4.9373	0.0000	0.0001
T459_23950	-2.2731	0.4706	-4.8299	0.0000	0.0001
T459_32228	-2.2640	0.2741	-8.2582	0.0000	0.0000
T459_31475	-2.2606	0.4667	-4.8436	0.0000	0.0001
T459_25725	-2.2302	0.3554	-6.2747	0.0000	0.0000
T459_16407	-2.1942	0.3698	-5.9341	0.0000	0.0000
T459_12502	-2.1545	0.6657	-3.2365	0.0012	0.0248
T459_11375	-2.1402	0.6510	-3.2874	0.0010	0.0220
T459_00051	-2.1226	0.6388	-3.3228	0.0009	0.0202
T459_29581	-2.1129	0.5370	-3.9349	0.0001	0.0035
T459_17412	-2.0949	0.5958	-3.5160	0.0004	0.0121
T459_33987	-2.0905	0.5000	-4.1806	0.0000	0.0015
T459_05089	-2.0703	0.2311	-8.9571	0.0000	0.0000
T459_30270	-2.0661	0.6023	-3.4306	0.0006	0.0149
T459_13275	-2.0463	0.5853	-3.4964	0.0005	0.0127
T459_12756	-2.0190	0.4324	-4.6690	0.0000	0.0002
T459_03898	-2.0176	0.4125	-4.8913	0.0000	0.0001
T459_12761	-1.9919	0.6142	-3.2430	0.0012	0.0245
T459_00820	-1.9423	0.5210	-3.7283	0.0002	0.0065
T459_05788	-1.9325	0.4216	-4.5836	0.0000	0.0003
T459_06597	-1.9243	0.4287	-4.4892	0.0000	0.0005
T459_13879	-1.9196	0.5598	-3.4292	0.0006	0.0150
T459_26812	-1.9179	0.6302	-3.0434	0.0023	0.0399
T459_13461	-1.9109	0.4025	-4.7479	0.0000	0.0002
T459_15707	-1.8999	0.5447	-3.4879	0.0005	0.0130
T459_07924	-1.8941	0.3914	-4.8392	0.0000	0.0001
T459_26349	-1.8904	0.2324	-8.1352	0.0000	0.0000
T459_11050	-1.8871	0.5551	-3.3997	0.0007	0.0163
T459_17633	-1.8837	0.5027	-3.7473	0.0002	0.0062
T459_26760	-1.8813	0.6268	-3.0015	0.0027	0.0436
T459_13825	-1.8691	0.4656	-4.0144	0.0001	0.0027
T459_31209	-1.8653	0.2656	-7.0218	0.0000	0.0000
T459_17755	-1.8403	0.4268	-4.3121	0.0000	0.0010

Gene ID	log2FoldChange	lfcSE	stat	pvalue	padj
T459_16904	-1.8383	0.3717	-4.9461	0.0000	0.0001
T459_33699	-1.8276	0.4756	-3.8429	0.0001	0.0047
T459_22503	-1.8264	0.2838	-6.4361	0.0000	0.0000
T459_12531	-1.8206	0.4931	-3.6922	0.0002	0.0073
T459_32088	-1.8124	0.2962	-6.1186	0.0000	0.0000
T459_19850	-1.8034	0.5215	-3.4581	0.0005	0.0140
T459_03835	-1.7937	0.3791	-4.7310	0.0000	0.0002
T459_34912	-1.7870	0.4435	-4.0289	0.0001	0.0026
T459_22194	-1.7869	0.4629	-3.8606	0.0001	0.0044
T459_06592	-1.7840	0.1932	-9.2319	0.0000	0.0000
T459_25932	-1.7728	0.3847	-4.6078	0.0000	0.0003
T459_32951	-1.7563	0.3400	-5.1651	0.0000	0.0000
T459_32940	-1.7443	0.3686	-4.7324	0.0000	0.0002
T459_07017	-1.7441	0.4885	-3.5705	0.0004	0.0103
T459_34615	-1.7390	0.3969	-4.3815	0.0000	0.0007
T459_31453	-1.7338	0.4872	-3.5584	0.0004	0.0106
T459_02989	-1.7318	0.2575	-6.7266	0.0000	0.0000
T459_25901	-1.7284	0.4342	-3.9802	0.0001	0.0030
T459_17893	-1.7245	0.5141	-3.3545	0.0008	0.0186
T459_17576	-1.7221	0.4319	-3.9867	0.0001	0.0029
T459_32149	-1.7091	0.5114	-3.3418	0.0008	0.0191
T459_10968	-1.7046	0.2557	-6.6675	0.0000	0.0000
T459_20013	-1.7027	0.2516	-6.7674	0.0000	0.0000
T459_12179	-1.6933	0.4947	-3.4231	0.0006	0.0152
T459_00160	-1.6881	0.5549	-3.0421	0.0023	0.0400
T459_01474	-1.6797	0.2391	-7.0240	0.0000	0.0000
T459_26831	-1.6779	0.4431	-3.7870	0.0002	0.0056
T459_21376	-1.6727	0.3827	-4.3706	0.0000	0.0008
T459_01425	-1.6562	0.3484	-4.7539	0.0000	0.0002
T459_31431	-1.6527	0.4514	-3.6615	0.0003	0.0080
T459_33545	-1.6521	0.3648	-4.5287	0.0000	0.0004
T459_04218	-1.6519	0.3650	-4.5263	0.0000	0.0004
T459_08417	-1.6510	0.3661	-4.5095	0.0000	0.0004
T459_31866	-1.6448	0.3261	-5.0444	0.0000	0.0000
T459_18222	-1.6441	0.4457	-3.6888	0.0002	0.0074
T459_05974	-1.6432	0.3777	-4.3505	0.0000	0.0008
T459_18434	-1.6336	0.4750	-3.4391	0.0006	0.0147
T459_20146	-1.6310	0.3486	-4.6793	0.0000	0.0002
T459_31006	-1.6290	0.3987	-4.0855	0.0000	0.0021
T459_26047	-1.6208	0.3211	-5.0467	0.0000	0.0000
T459_32792	-1.6161	0.5013	-3.2239	0.0013	0.0255
T459_00233	-1.6150	0.3678	-4.3909	0.0000	0.0007
T459_18479	-1.6093	0.4232	-3.8022	0.0001	0.0053
T459_25035	-1.6037	0.4490	-3.5720	0.0004	0.0103
T459_01911	-1.5969	0.3030	-5.2697	0.0000	0.0000
T459_07935	-1.5866	0.2867	-5.5334	0.0000	0.0000
T459_29707	-1.5746	0.4314	-3.6498	0.0003	0.0082

Gene ID	log2FoldChange	lfcSE	stat	pvalue	padj
T459_08291	-1.5689	0.3273	-4.7938	0.0000	0.0001
T459_06178	-1.5683	0.2741	-5.7226	0.0000	0.0000
T459_28294	-1.5405	0.4259	-3.6173	0.0003	0.0090
T459_00556	-1.5400	0.3403	-4.5253	0.0000	0.0004
T459_19556	-1.5358	0.3206	-4.7902	0.0000	0.0002
T459_12430	-1.5294	0.2049	-7.4629	0.0000	0.0000
T459_13134	-1.5097	0.3171	-4.7615	0.0000	0.0002
T459_07440	-1.5070	0.5038	-2.9915	0.0028	0.0447
T459_18879	-1.5059	0.2834	-5.3144	0.0000	0.0000
T459_03555	-1.4913	0.4292	-3.4745	0.0005	0.0134
T459_21054	-1.4879	0.4759	-3.1262	0.0018	0.0326
T459_22888	-1.4862	0.4216	-3.5254	0.0004	0.0118
T459_04043	-1.4853	0.3658	-4.0602	0.0000	0.0023
T459_29777	-1.4823	0.2882	-5.1440	0.0000	0.0000
T459_29580	-1.4780	0.2747	-5.3807	0.0000	0.0000
T459_09708	-1.4762	0.1774	-8.3213	0.0000	0.0000
T459_31452	-1.4724	0.4432	-3.3219	0.0009	0.0202
T459_10224	-1.4698	0.4438	-3.3119	0.0009	0.0206
T459_03029	-1.4671	0.3703	-3.9616	0.0001	0.0032
T459_31451	-1.4637	0.3794	-3.8584	0.0001	0.0045
T459_11049	-1.4546	0.3053	-4.7647	0.0000	0.0002
T459_20808	-1.4546	0.4066	-3.5771	0.0003	0.0102
T459_27054	-1.4545	0.3736	-3.8933	0.0001	0.0039
T459_08979	-1.4531	0.3209	-4.5287	0.0000	0.0004
T459_22009	-1.4521	0.4863	-2.9863	0.0028	0.0452
T459_08410	-1.4459	0.3550	-4.0733	0.0000	0.0022
T459_26655	-1.4418	0.3649	-3.9514	0.0001	0.0033
T459_32705	-1.4407	0.4796	-3.0038	0.0027	0.0434
T459_04683	-1.4407	0.4165	-3.4594	0.0005	0.0139
T459_14199	-1.4324	0.3987	-3.5927	0.0003	0.0097
T459_24190	-1.4218	0.2775	-5.1236	0.0000	0.0000
T459_28305	-1.4172	0.3881	-3.6519	0.0003	0.0082
T459_10759	-1.4168	0.3749	-3.7791	0.0002	0.0057
T459_09428	-1.4123	0.3527	-4.0043	0.0001	0.0028
T459_21738	-1.4085	0.2341	-6.0165	0.0000	0.0000
T459_23598	-1.4076	0.2628	-5.3564	0.0000	0.0000
T459_16064	-1.4048	0.1947	-7.2146	0.0000	0.0000
T459_05992	-1.3950	0.2954	-4.7226	0.0000	0.0002
T459_09604	-1.3914	0.2674	-5.2030	0.0000	0.0000
T459_02807	-1.3896	0.4628	-3.0030	0.0027	0.0434
T459_18595	-1.3847	0.3933	-3.5208	0.0004	0.0119
T459_15116	-1.3809	0.4095	-3.3719	0.0007	0.0176
T459_02958	-1.3799	0.4313	-3.1995	0.0014	0.0270
T459_10658	-1.3790	0.2854	-4.8322	0.0000	0.0001
T459_20093	-1.3789	0.1787	-7.7173	0.0000	0.0000
T459_25045	-1.3733	0.1772	-7.7477	0.0000	0.0000
T459_31734	-1.3693	0.4072	-3.3623	0.0008	0.0182

Gene ID	log2FoldChange	lfcSE	stat	pvalue	padj
T459_27086	-1.3666	0.3369	-4.0567	0.0000	0.0023
T459_09203	-1.3652	0.3844	-3.5515	0.0004	0.0108
T459_16377	-1.3617	0.3825	-3.5602	0.0004	0.0106
T459_30187	-1.3608	0.4112	-3.3091	0.0009	0.0207
T459_05789	-1.3583	0.3548	-3.8284	0.0001	0.0049
T459_23736	-1.3548	0.3845	-3.5233	0.0004	0.0118
T459_13010	-1.3543	0.2131	-6.3562	0.0000	0.0000
T459_32515	-1.3533	0.3644	-3.7138	0.0002	0.0068
T459_33443	-1.3524	0.4049	-3.3401	0.0008	0.0192
T459_14845	-1.3423	0.4245	-3.1619	0.0016	0.0298
T459_17614	-1.3417	0.3429	-3.9130	0.0001	0.0037
T459_12384	-1.3387	0.3906	-3.4275	0.0006	0.0150
T459_14080	-1.3271	0.1885	-7.0394	0.0000	0.0000
T459_22459	-1.3267	0.2869	-4.6247	0.0000	0.0003
T459_14767	-1.3249	0.4126	-3.2109	0.0013	0.0265
T459_15544	-1.3215	0.3470	-3.8080	0.0001	0.0052
T459_04036	-1.3133	0.3752	-3.5002	0.0005	0.0126
T459_19812	-1.3111	0.3339	-3.9268	0.0001	0.0036
T459_25618	-1.3103	0.3511	-3.7319	0.0002	0.0065
T459_24499	-1.3024	0.3103	-4.1978	0.0000	0.0014
T459_26502	-1.2991	0.2643	-4.9155	0.0000	0.0001
T459_34754	-1.2989	0.4306	-3.0164	0.0026	0.0420
T459_21205	-1.2959	0.3367	-3.8489	0.0001	0.0046
T459_14318	-1.2951	0.4068	-3.1839	0.0015	0.0282
T459_12710	-1.2946	0.3250	-3.9829	0.0001	0.0030
T459_00726	-1.2932	0.3862	-3.3483	0.0008	0.0189
T459_29637	-1.2931	0.3378	-3.8283	0.0001	0.0049
T459_08990	-1.2928	0.3446	-3.7512	0.0002	0.0062
T459_23703	-1.2890	0.2776	-4.6440	0.0000	0.0003
T459_00418	-1.2887	0.3945	-3.2665	0.0011	0.0231
T459_06593	-1.2869	0.3085	-4.1712	0.0000	0.0016
T459_33221	-1.2868	0.4266	-3.0166	0.0026	0.0420
T459_24671	-1.2846	0.3439	-3.7359	0.0002	0.0064
T459_13944	-1.2840	0.3171	-4.0496	0.0001	0.0024
T459_17496	-1.2828	0.3929	-3.2652	0.0011	0.0232
T459_07986	-1.2753	0.2774	-4.5978	0.0000	0.0003
T459_16166	-1.2734	0.3116	-4.0871	0.0000	0.0021
T459_26097	-1.2706	0.3353	-3.7895	0.0002	0.0055
T459_14897	-1.2689	0.2845	-4.4604	0.0000	0.0005
T459_04323	-1.2669	0.4182	-3.0296	0.0024	0.0409
T459_07841	-1.2655	0.3090	-4.0950	0.0000	0.0020
T459_24585	-1.2637	0.4184	-3.0207	0.0025	0.0417
T459_08514	-1.2565	0.3228	-3.8930	0.0001	0.0039
T459_10299	-1.2546	0.3122	-4.0183	0.0001	0.0027
T459_33998	-1.2485	0.3325	-3.7551	0.0002	0.0061
T459_25025	-1.2458	0.3175	-3.9232	0.0001	0.0036
T459_18082	-1.2306	0.3734	-3.2959	0.0010	0.0215

Gene ID	log2FoldChange	lfcSE	stat	pvalue	padj
T459_09971	-1.2283	0.4154	-2.9569	0.0031	0.0481
T459_27798	-1.2278	0.2545	-4.8248	0.0000	0.0001
T459_16214	-1.2262	0.3508	-3.4951	0.0005	0.0128
T459_20168	-1.2227	0.3511	-3.4820	0.0005	0.0131
T459_16131	-1.2163	0.2124	-5.7273	0.0000	0.0000
T459_04439	-1.2110	0.2603	-4.6519	0.0000	0.0003
T459_19802	-1.2108	0.2735	-4.4275	0.0000	0.0006
T459_29293	-1.2072	0.2862	-4.2178	0.0000	0.0013
T459_30957	-1.2071	0.3008	-4.0131	0.0001	0.0027
T459_06181	-1.2038	0.2626	-4.5843	0.0000	0.0003
T459_03838	-1.2003	0.2264	-5.3009	0.0000	0.0000
T459_30803	-1.1966	0.3462	-3.4565	0.0005	0.0140
T459_06354	-1.1955	0.2814	-4.2481	0.0000	0.0012
T459_21908	-1.1922	0.3471	-3.4348	0.0006	0.0148
T459_00922	-1.1920	0.3105	-3.8386	0.0001	0.0048
T459_23977	-1.1919	0.3213	-3.7103	0.0002	0.0069
T459_33247	-1.1899	0.1920	-6.1964	0.0000	0.0000
T459_28400	-1.1891	0.3988	-2.9815	0.0029	0.0457
T459_05246	-1.1844	0.2009	-5.8962	0.0000	0.0000
T459_27534	-1.1844	0.2551	-4.6437	0.0000	0.0003
T459_00201	-1.1829	0.3854	-3.0695	0.0021	0.0376
T459_05835	-1.1770	0.2823	-4.1698	0.0000	0.0016
T459_11868	-1.1723	0.2962	-3.9583	0.0001	0.0032
T459_09908	-1.1715	0.3452	-3.3937	0.0007	0.0166
T459_27087	-1.1674	0.3106	-3.7581	0.0002	0.0061
T459_13019	-1.1672	0.3808	-3.0653	0.0022	0.0380
T459_26656	-1.1668	0.3762	-3.1018	0.0019	0.0345
T459_05321	-1.1508	0.3609	-3.1890	0.0014	0.0278
T459_33111	-1.1507	0.2672	-4.3072	0.0000	0.0010
T459_22368	-1.1488	0.3797	-3.0255	0.0025	0.0412
T459_33596	-1.1482	0.3147	-3.6489	0.0003	0.0082
T459_17280	-1.1478	0.3503	-3.2767	0.0011	0.0225
T459_18223	-1.1448	0.1909	-5.9967	0.0000	0.0000
T459_32056	-1.1433	0.3181	-3.5939	0.0003	0.0096
T459_16714	-1.1337	0.2205	-5.1415	0.0000	0.0000
T459_17741	-1.1332	0.2758	-4.1090	0.0000	0.0019
T459_25305	-1.1326	0.3238	-3.4978	0.0005	0.0127
T459_08119	-1.1232	0.3425	-3.2791	0.0010	0.0224
T459_05431	-1.1182	0.3163	-3.5357	0.0004	0.0114
T459_10112	-1.1177	0.3672	-3.0440	0.0023	0.0399
T459_33430	-1.1109	0.2633	-4.2201	0.0000	0.0013
T459_27736	-1.1055	0.2518	-4.3908	0.0000	0.0007
T459_00751	-1.1018	0.3093	-3.5621	0.0004	0.0105
T459_08690	-1.1005	0.2559	-4.3005	0.0000	0.0010
T459_04042	-1.0960	0.3024	-3.6238	0.0003	0.0089
T459_20141	-1.0929	0.3715	-2.9418	0.0033	0.0498
T459_34205	-1.0918	0.1148	-9.5127	0.0000	0.0000

Gene ID	log2FoldChange	lfcSE	stat	pvalue	padj
T459_04280	-1.0892	0.1730	-6.2948	0.0000	0.0000
T459_00379	-1.0877	0.1818	-5.9833	0.0000	0.0000
T459_27353	-1.0876	0.3356	-3.2407	0.0012	0.0246
T459_20367	-1.0864	0.3580	-3.0351	0.0024	0.0404
T459_22748	-1.0845	0.3138	-3.4564	0.0005	0.0140
T459_20708	-1.0809	0.3281	-3.2940	0.0010	0.0216
T459_20462	-1.0795	0.2708	-3.9867	0.0001	0.0029
T459_14467	-1.0779	0.1813	-5.9450	0.0000	0.0000
T459_20474	-1.0772	0.3421	-3.1485	0.0016	0.0309
T459_27416	-1.0737	0.2939	-3.6529	0.0003	0.0082
T459_20051	-1.0721	0.2156	-4.9729	0.0000	0.0001
T459_09620	-1.0645	0.3099	-3.4347	0.0006	0.0148
T459_08182	-1.0633	0.2604	-4.0830	0.0000	0.0021
T459_17635	-1.0599	0.2611	-4.0599	0.0000	0.0023
T459_29377	-1.0593	0.3487	-3.0378	0.0024	0.0401
T459_21092	-1.0565	0.2682	-3.9390	0.0001	0.0034
T459_32257	-1.0559	0.2235	-4.7246	0.0000	0.0002
T459_23039	-1.0548	0.1909	-5.5255	0.0000	0.0000
T459_03030	-1.0542	0.2141	-4.9231	0.0000	0.0001
T459_14039	-1.0538	0.3389	-3.1097	0.0019	0.0338
T459_26228	-1.0533	0.2488	-4.2342	0.0000	0.0013
T459_21271	-1.0508	0.1969	-5.3378	0.0000	0.0000
T459_00785	-1.0502	0.2768	-3.7938	0.0001	0.0054
T459_05874	-1.0464	0.3213	-3.2570	0.0011	0.0235
T459_08381	-1.0425	0.2392	-4.3586	0.0000	0.0008
T459_02841	-1.0399	0.2441	-4.2603	0.0000	0.0012
T459_05021	-1.0336	0.3305	-3.1274	0.0018	0.0326
T459_09786	-1.0329	0.3305	-3.1255	0.0018	0.0326
T459_04105	-1.0328	0.2767	-3.7329	0.0002	0.0065
T459_22402	-1.0323	0.2353	-4.3866	0.0000	0.0007
T459_00730	-1.0260	0.3125	-3.2833	0.0010	0.0222
T459_06943	-1.0258	0.3232	-3.1741	0.0015	0.0288
T459_31701	-1.0248	0.2909	-3.5229	0.0004	0.0119
T459_15721	-1.0189	0.2549	-3.9975	0.0001	0.0028
T459_22045	-1.0183	0.2958	-3.4421	0.0006	0.0146
T459_01371	-1.0168	0.2359	-4.3098	0.0000	0.0010
T459_33308	-1.0074	0.2644	-3.8097	0.0001	0.0052
T459_01759	-1.0071	0.2539	-3.9666	0.0001	0.0031
T459_05227	-1.0069	0.2719	-3.7031	0.0002	0.0071
T459_12992	-1.0023	0.2754	-3.6392	0.0003	0.0085
T459_17556	1.0002	0.1475	6.7796	0.0000	0.0000
T459_20976	1.0047	0.3038	3.3077	0.0009	0.0208
T459_00195	1.0068	0.3113	3.2339	0.0012	0.0250
T459_13161	1.0070	0.2363	4.2619	0.0000	0.0011
T459_22263	1.0076	0.3396	2.9665	0.0030	0.0471
T459_27667	1.0174	0.3344	3.0427	0.0023	0.0399
T459_10470	1.0201	0.2762	3.6934	0.0002	0.0073

Gene ID	log2FoldChange	lfcSE	stat	pvalue	padj
T459_24347	1.0204	0.2793	3.6534	0.0003	0.0082
T459_06473	1.0241	0.1948	5.2584	0.0000	0.0000
T459_03057	1.0278	0.3347	3.0706	0.0021	0.0376
T459_08061	1.0394	0.2260	4.5990	0.0000	0.0003
T459_30106	1.0415	0.3519	2.9592	0.0031	0.0479
T459_12859	1.0433	0.3067	3.4021	0.0007	0.0162
T459_15245	1.0439	0.3090	3.3788	0.0007	0.0174
T459_31185	1.0440	0.2913	3.5842	0.0003	0.0099
T459_05808	1.0441	0.3269	3.1943	0.0014	0.0274
T459_04757	1.0489	0.3302	3.1767	0.0015	0.0287
T459_08907	1.0513	0.2951	3.5628	0.0004	0.0105
T459_33719	1.0553	0.2090	5.0484	0.0000	0.0000
T459_24743	1.0589	0.3405	3.1103	0.0019	0.0338
T459_06047	1.0591	0.2797	3.7865	0.0002	0.0056
T459_12990	1.0593	0.3196	3.3144	0.0009	0.0205
T459_32030	1.0632	0.3461	3.0722	0.0021	0.0375
T459_05687	1.0661	0.2784	3.8290	0.0001	0.0049
T459_35222	1.0718	0.2997	3.5765	0.0003	0.0102
T459_06005	1.0780	0.3092	3.4869	0.0005	0.0130
T459_28151	1.0806	0.2897	3.7305	0.0002	0.0065
T459_10609	1.0864	0.3359	3.2346	0.0012	0.0249
T459_05976	1.0923	0.3421	3.1933	0.0014	0.0275
T459_20080	1.0932	0.3003	3.6408	0.0003	0.0085
T459_17066	1.0941	0.2793	3.9182	0.0001	0.0037
T459_15472	1.0967	0.2900	3.7815	0.0002	0.0057
T459_28369	1.0979	0.2436	4.5066	0.0000	0.0005
T459_05301	1.1020	0.2975	3.7046	0.0002	0.0071
T459_06058	1.1046	0.3718	2.9709	0.0030	0.0468
T459_13107	1.1095	0.3118	3.5584	0.0004	0.0106
T459_16444	1.1125	0.2368	4.6982	0.0000	0.0002
T459_20975	1.1173	0.2729	4.0939	0.0000	0.0020
T459_26878	1.1197	0.2812	3.9823	0.0001	0.0030
T459_31997	1.1293	0.3548	3.1833	0.0015	0.0282
T459_33045	1.1321	0.2544	4.4491	0.0000	0.0006
T459_13430	1.1337	0.3524	3.2170	0.0013	0.0261
T459_15047	1.1491	0.3475	3.3065	0.0009	0.0209
T459_19604	1.1527	0.2932	3.9313	0.0001	0.0035
T459_21823	1.1587	0.2773	4.1785	0.0000	0.0015
T459_10783	1.1598	0.3364	3.4482	0.0006	0.0143
T459_18405	1.1659	0.2685	4.3425	0.0000	0.0009
T459_17174	1.1681	0.2449	4.7699	0.0000	0.0002
T459_13330	1.1706	0.2446	4.7863	0.0000	0.0002
T459_26096	1.1725	0.3752	3.1251	0.0018	0.0326
T459_19682	1.1738	0.2996	3.9178	0.0001	0.0037
T459_04872	1.1816	0.3040	3.8873	0.0001	0.0040
T459_17304	1.1870	0.3601	3.2959	0.0010	0.0215
T459_31929	1.1883	0.3369	3.5271	0.0004	0.0117

Gene ID	log2FoldChange	lfcSE	stat	pvalue	padj
T459_20564	1.1893	0.2759	4.3113	0.0000	0.0010
T459_13497	1.1920	0.3563	3.3457	0.0008	0.0190
T459_05466	1.1943	0.4004	2.9826	0.0029	0.0455
T459_06780	1.2050	0.2760	4.3657	0.0000	0.0008
T459_05520	1.2061	0.2456	4.9112	0.0000	0.0001
T459_22589	1.2083	0.3683	3.2807	0.0010	0.0223
T459_06801	1.2095	0.2669	4.5320	0.0000	0.0004
T459_27048	1.2199	0.3713	3.2859	0.0010	0.0220
T459_21812	1.2264	0.2327	5.2704	0.0000	0.0000
T459_32099	1.2313	0.3354	3.6706	0.0002	0.0077
T459_06923	1.2347	0.3593	3.4361	0.0006	0.0147
T459_29341	1.2354	0.3942	3.1342	0.0017	0.0321
T459_15582	1.2374	0.3962	3.1231	0.0018	0.0328
T459_10117	1.2406	0.3859	3.2147	0.0013	0.0262
T459_26099	1.2499	0.2619	4.7724	0.0000	0.0002
T459_08371	1.2517	0.4136	3.0266	0.0025	0.0411
T459_23347	1.2534	0.3197	3.9210	0.0001	0.0036
T459_07508	1.2540	0.3593	3.4903	0.0005	0.0129
T459_10899	1.2566	0.3084	4.0749	0.0000	0.0022
T459_13246	1.2633	0.2947	4.2864	0.0000	0.0010
T459_17545	1.2660	0.2227	5.6859	0.0000	0.0000
T459_00316	1.2662	0.3669	3.4508	0.0006	0.0142
T459_08313	1.2714	0.3972	3.2007	0.0014	0.0270
T459_27224	1.2750	0.3070	4.1530	0.0000	0.0016
T459_03056	1.2792	0.4109	3.1133	0.0018	0.0336
T459_25550	1.2814	0.4001	3.2024	0.0014	0.0270
T459_05406	1.2844	0.3673	3.4965	0.0005	0.0127
T459_10514	1.2937	0.2746	4.7112	0.0000	0.0002
T459_27834	1.2959	0.3949	3.2818	0.0010	0.0223
T459_03043	1.3018	0.3848	3.3829	0.0007	0.0172
T459_01139	1.3037	0.1936	6.7341	0.0000	0.0000
T459_18335	1.3039	0.2783	4.6846	0.0000	0.0002
T459_34573	1.3061	0.3097	4.2174	0.0000	0.0013
T459_06626	1.3092	0.3980	3.2892	0.0010	0.0219
T459_23071	1.3135	0.3682	3.5671	0.0004	0.0104
T459_05513	1.3218	0.4357	3.0339	0.0024	0.0405
T459_13568	1.3266	0.3861	3.4361	0.0006	0.0147
T459_27879	1.3269	0.4081	3.2517	0.0011	0.0239
T459_23984	1.3355	0.3164	4.2214	0.0000	0.0013
T459_16565	1.3376	0.3509	3.8120	0.0001	0.0051
T459_17126	1.3638	0.4596	2.9672	0.0030	0.0471
T459_08268	1.3701	0.4078	3.3596	0.0008	0.0183
T459_29934	1.3738	0.3634	3.7802	0.0002	0.0057
T459_20343	1.3977	0.3582	3.9018	0.0001	0.0039
T459_16799	1.4008	0.4018	3.4859	0.0005	0.0130
T459_15141	1.4015	0.4565	3.0702	0.0021	0.0376
T459_07113	1.4049	0.4207	3.3398	0.0008	0.0192

Gene ID	log2FoldChange	lfcSE	stat	pvalue	padj
T459_26266	1.4086	0.4599	3.0630	0.0022	0.0382
T459_04236	1.4102	0.4516	3.1224	0.0018	0.0328
T459_08282	1.4112	0.4179	3.3769	0.0007	0.0174
T459_19681	1.4278	0.4583	3.1152	0.0018	0.0335
T459_10437	1.4283	0.3895	3.6673	0.0002	0.0078
T459_12318	1.4475	0.3835	3.7740	0.0002	0.0057
T459_27911	1.4526	0.4500	3.2277	0.0012	0.0253
T459_31642	1.4549	0.4783	3.0421	0.0023	0.0400
T459_23464	1.4575	0.3592	4.0575	0.0000	0.0023
T459_32400	1.4592	0.4378	3.3331	0.0009	0.0195
T459_16504	1.4601	0.3467	4.2121	0.0000	0.0013
T459_10508	1.4655	0.4235	3.4607	0.0005	0.0139
T459_06869	1.4723	0.4004	3.6770	0.0002	0.0076
T459_25345	1.4763	0.3749	3.9381	0.0001	0.0034
T459_20281	1.4771	0.2823	5.2324	0.0000	0.0000
T459_33863	1.4897	0.4570	3.2595	0.0011	0.0235
T459_24968	1.4899	0.5042	2.9550	0.0031	0.0483
T459_09655	1.4930	0.4789	3.1175	0.0018	0.0332
T459_15238	1.5128	0.4243	3.5654	0.0004	0.0104
T459_01755	1.5342	0.5041	3.0436	0.0023	0.0399
T459_08838	1.5421	0.5134	3.0038	0.0027	0.0434
T459_03982	1.5444	0.4674	3.3045	0.0010	0.0210
T459_23083	1.5460	0.5017	3.0812	0.0021	0.0366
T459_00795	1.5512	0.3986	3.8912	0.0001	0.0040
T459_31982	1.5529	0.5021	3.0926	0.0020	0.0354
T459_32071	1.5532	0.2713	5.7259	0.0000	0.0000
T459_21708	1.5603	0.5100	3.0596	0.0022	0.0385
T459_02489	1.5777	0.3746	4.2118	0.0000	0.0013
T459_32648	1.5970	0.4742	3.3676	0.0008	0.0178
T459_06630	1.6013	0.3390	4.7243	0.0000	0.0002
T459_25967	1.6090	0.3809	4.2243	0.0000	0.0013
T459_26060	1.6127	0.3683	4.3792	0.0000	0.0007
T459_19890	1.6138	0.4910	3.2867	0.0010	0.0220
T459_00717	1.6333	0.5002	3.2652	0.0011	0.0232
T459_18362	1.6393	0.4561	3.5944	0.0003	0.0096
T459_06704	1.6512	0.4216	3.9163	0.0001	0.0037
T459_11506	1.6584	0.3489	4.7537	0.0000	0.0002
T459_15634	1.6647	0.3020	5.5119	0.0000	0.0000
T459_14090	1.6650	0.5656	2.9436	0.0032	0.0496
T459_23388	1.6656	0.4507	3.6954	0.0002	0.0073
T459_04804	1.6662	0.3952	4.2164	0.0000	0.0013
T459_02320	1.6670	0.3695	4.5122	0.0000	0.0004
T459_19889	1.6762	0.4614	3.6330	0.0003	0.0086
T459_27971	1.6779	0.4818	3.4826	0.0005	0.0131
T459_33642	1.6781	0.5069	3.3105	0.0009	0.0207
T459_10427	1.6808	0.2928	5.7401	0.0000	0.0000
T459_13377	1.6819	0.4889	3.4398	0.0006	0.0147

Gene ID	log2FoldChange	lfcSE	stat	pvalue	padj
T459_18702	1.6872	0.5465	3.0870	0.0020	0.0360
T459_13190	1.6885	0.4450	3.7946	0.0001	0.0054
T459_28895	1.6911	0.4400	3.8437	0.0001	0.0047
T459_18313	1.6956	0.4076	4.1596	0.0000	0.0016
T459_07874	1.6996	0.5520	3.0788	0.0021	0.0368
T459_15105	1.7107	0.5118	3.3427	0.0008	0.0191
T459_23231	1.7214	0.4112	4.1858	0.0000	0.0015
T459_05690	1.7250	0.5621	3.0691	0.0021	0.0376
T459_13164	1.7425	0.5009	3.4790	0.0005	0.0132
T459_06169	1.7446	0.4795	3.6381	0.0003	0.0085
T459_04998	1.7509	0.4825	3.6291	0.0003	0.0087
T459_13417	1.7521	0.5191	3.3750	0.0007	0.0175
T459_35454	1.7553	0.4801	3.6563	0.0003	0.0081
T459_24753	1.7671	0.5611	3.1491	0.0016	0.0308
T459_05908	1.7906	0.4469	4.0067	0.0001	0.0028
T459_15261	1.7973	0.4810	3.7368	0.0002	0.0064
T459_29265	1.8035	0.4716	3.8242	0.0001	0.0049
T459_34044	1.8064	0.3876	4.6601	0.0000	0.0002
T459_22449	1.8074	0.4377	4.1292	0.0000	0.0018
T459_23082	1.8219	0.5814	3.1338	0.0017	0.0321
T459_23487	1.8266	0.4018	4.5462	0.0000	0.0004
T459_13674	1.8391	0.4377	4.2016	0.0000	0.0014
T459_30286	1.8589	0.3452	5.3853	0.0000	0.0000
T459_05020	1.8601	0.3064	6.0714	0.0000	0.0000
T459_05380	1.8779	0.5622	3.3401	0.0008	0.0192
T459_02495	1.8981	0.5254	3.6128	0.0003	0.0091
T459_18261	1.8990	0.5167	3.6749	0.0002	0.0076
T459_22117	1.9089	0.3634	5.2526	0.0000	0.0000
T459_20592	1.9133	0.6026	3.1748	0.0015	0.0288
T459_31981	1.9208	0.5785	3.3201	0.0009	0.0202
T459_16533	1.9273	0.3909	4.9307	0.0000	0.0001
T459_08132	1.9336	0.5053	3.8268	0.0001	0.0049
T459_04895	1.9399	0.4288	4.5244	0.0000	0.0004
T459_22005	1.9402	0.6110	3.1757	0.0015	0.0288
T459_07904	1.9460	0.4433	4.3901	0.0000	0.0007
T459_06895	1.9507	0.5312	3.6721	0.0002	0.0077
T459_26777	1.9514	0.3910	4.9908	0.0000	0.0001
T459_13083	1.9527	0.5246	3.7220	0.0002	0.0067
T459_06105	1.9545	0.5096	3.8351	0.0001	0.0048
T459_21949	1.9628	0.5115	3.8373	0.0001	0.0048
T459_17598	1.9642	0.5231	3.7550	0.0002	0.0061
T459_20479	1.9683	0.3794	5.1885	0.0000	0.0000
T459_00299	1.9880	0.4449	4.4683	0.0000	0.0005
T459_14095	1.9881	0.5848	3.3996	0.0007	0.0163
T459_06393	2.0002	0.4500	4.4446	0.0000	0.0006
T459_02622	2.0167	0.5629	3.5825	0.0003	0.0100
T459_18130	2.0244	0.4270	4.7413	0.0000	0.0002

Gene ID	log2FoldChange	lfcSE	stat	pvalue	padj
T459_24642	2.0374	0.5670	3.5933	0.0003	0.0096
T459_14992	2.0401	0.6078	3.3567	0.0008	0.0185
T459_32634	2.0550	0.4849	4.2376	0.0000	0.0013
T459_31878	2.0868	0.2613	7.9860	0.0000	0.0000
T459_29475	2.0869	0.6130	3.4042	0.0007	0.0161
T459_07595	2.0898	0.4397	4.7531	0.0000	0.0002
T459_20703	2.1046	0.4474	4.7035	0.0000	0.0002
T459_06931	2.1092	0.5794	3.6403	0.0003	0.0085
T459_07109	2.1382	0.5347	3.9985	0.0001	0.0028
T459_13757	2.1424	0.6184	3.4647	0.0005	0.0137
T459_09323	2.1436	0.5598	3.8292	0.0001	0.0049
T459_07005	2.1552	0.5365	4.0172	0.0001	0.0027
T459_05623	2.1928	0.4461	4.9157	0.0000	0.0001
T459_32584	2.1949	0.5450	4.0274	0.0001	0.0026
T459_22258	2.2223	0.3036	7.3195	0.0000	0.0000
T459_32610	2.2336	0.3892	5.7390	0.0000	0.0000
T459_29474	2.2370	0.6201	3.6077	0.0003	0.0092
T459_09685	2.2544	0.6012	3.7496	0.0002	0.0062
T459_28527	2.2638	0.5655	4.0034	0.0001	0.0028
T459_15631	2.2720	0.4384	5.1825	0.0000	0.0000
T459_29611	2.2821	0.3486	6.5466	0.0000	0.0000
T459_09338	2.2842	0.6186	3.6924	0.0002	0.0073
T459_32234	2.3488	0.5226	4.4941	0.0000	0.0005
T459_27250	2.3507	0.4611	5.0978	0.0000	0.0000
T459_09858	2.3589	0.4223	5.5854	0.0000	0.0000
T459_22281	2.3594	0.7210	3.2725	0.0011	0.0228
T459_07809	2.3624	0.5658	4.1756	0.0000	0.0015
T459_00728	2.3776	0.4512	5.2694	0.0000	0.0000
T459_10441	2.3890	0.5257	4.5441	0.0000	0.0004
T459_12450	2.3971	0.4583	5.2305	0.0000	0.0000
T459_24935	2.4038	0.5901	4.0738	0.0000	0.0022
T459_20275	2.4065	0.4507	5.3390	0.0000	0.0000
T459_28941	2.4093	0.4745	5.0779	0.0000	0.0000
T459_31554	2.4276	0.4446	5.4596	0.0000	0.0000
T459_07329	2.4357	0.4311	5.6494	0.0000	0.0000
T459_20471	2.4439	0.3155	7.7464	0.0000	0.0000
T459_09958	2.4659	0.3584	6.8805	0.0000	0.0000
T459_00315	2.4670	0.3489	7.0712	0.0000	0.0000
T459_12310	2.4958	0.5233	4.7689	0.0000	0.0002
T459_33529	2.4980	0.6783	3.6827	0.0002	0.0075
T459_03312	2.5009	0.5090	4.9136	0.0000	0.0001
T459_06917	2.5027	0.5042	4.9636	0.0000	0.0001
T459_05688	2.5050	0.4447	5.6330	0.0000	0.0000
T459_17950	2.5051	0.5201	4.8163	0.0000	0.0001
T459_23080	2.5608	0.4885	5.2422	0.0000	0.0000
T459_26035	2.5777	0.4579	5.6295	0.0000	0.0000
T459_14092	2.6354	0.5823	4.5257	0.0000	0.0004

Gene ID	log2FoldChange	lfcSE	stat	pvalue	padj
T459_12184	2.6484	0.3742	7.0782	0.0000	0.0000
T459_09533	2.7207	0.5186	5.2458	0.0000	0.0000
T459_00869	2.7238	0.5116	5.3239	0.0000	0.0000
T459_18515	2.7308	0.6144	4.4450	0.0000	0.0006
T459_07900	2.7655	0.5156	5.3632	0.0000	0.0000
T459_03058	2.8005	0.4110	6.8142	0.0000	0.0000
T459_32612	2.8213	0.7723	3.6532	0.0003	0.0082
T459_33927	2.8243	0.6214	4.5451	0.0000	0.0004
T459_35114	2.8545	0.4963	5.7516	0.0000	0.0000
T459_27223	2.8616	0.5086	5.6269	0.0000	0.0000
T459_06392	2.8654	0.8267	3.4661	0.0005	0.0136
T459_27222	2.8958	0.4954	5.8457	0.0000	0.0000
T459_31977	2.9007	0.5775	5.0226	0.0000	0.0001
T459_25506	2.9024	0.6960	4.1703	0.0000	0.0016
T459_01486	2.9182	0.5452	5.3526	0.0000	0.0000
T459_21752	2.9575	0.8287	3.5689	0.0004	0.0104
T459_32014	2.9716	0.3925	7.5716	0.0000	0.0000
T459_02795	2.9777	0.3704	8.0399	0.0000	0.0000
T459_08285	2.9795	0.6094	4.8892	0.0000	0.0001
T459_18683	3.0002	0.5762	5.2069	0.0000	0.0000
T459_18526	3.0312	0.5770	5.2532	0.0000	0.0000
T459_24730	3.0343	1.0270	2.9545	0.0031	0.0483
T459_13096	3.0455	0.7119	4.2782	0.0000	0.0011
T459_25929	3.0538	0.5246	5.8209	0.0000	0.0000
T459_13934	3.1062	0.9813	3.1653	0.0015	0.0295
T459_17054	3.1173	0.4920	6.3359	0.0000	0.0000
T459_32043	3.1194	0.5055	6.1704	0.0000	0.0000
T459_14053	3.1554	0.6752	4.6730	0.0000	0.0002
T459_01666	3.1581	0.5026	6.2831	0.0000	0.0000
T459_12817	3.1673	0.7196	4.4016	0.0000	0.0007
T459_20565	3.1984	0.5720	5.5920	0.0000	0.0000
T459_20467	3.2121	0.9842	3.2636	0.0011	0.0233
T459_31894	3.2718	0.8565	3.8201	0.0001	0.0050
T459_10808	3.2968	1.1106	2.9686	0.0030	0.0470
T459_01049	3.2983	0.9572	3.4460	0.0006	0.0144
T459_06461	3.3045	1.0074	3.2803	0.0010	0.0223
T459_20468	3.3104	0.8081	4.0963	0.0000	0.0020
T459_19699	3.3395	0.7249	4.6065	0.0000	0.0003
T459_31978	3.3597	0.9234	3.6384	0.0003	0.0085
T459_33323	3.3696	0.8880	3.7944	0.0001	0.0054
T459_11069	3.3867	1.0455	3.2393	0.0012	0.0247
T459_15482	3.4469	1.1351	3.0367	0.0024	0.0402
T459_09948	3.4554	0.6076	5.6872	0.0000	0.0000
T459_31980	3.4585	0.9231	3.7464	0.0002	0.0062
T459_17731	3.4970	0.5193	6.7345	0.0000	0.0000
T459_05078	3.5003	0.7394	4.7338	0.0000	0.0002
T459_34874	3.5125	0.5623	6.2461	0.0000	0.0000

Gene ID	log2FoldChange	lfcSE	stat	pvalue	padj
T459_20883	3.5424	0.9634	3.6771	0.0002	0.0076
T459_27508	3.5501	0.6270	5.6621	0.0000	0.0000
T459_24029	3.5985	0.8675	4.1482	0.0000	0.0017
T459_30004	3.6305	0.6440	5.6375	0.0000	0.0000
T459_07331	3.6441	0.4486	8.1235	0.0000	0.0000
T459_20283	3.6556	0.4962	7.3678	0.0000	0.0000
T459_19900	3.6809	1.1037	3.3351	0.0009	0.0194
T459_15127	3.7736	0.9480	3.9804	0.0001	0.0030
T459_22923	3.8078	0.8395	4.5359	0.0000	0.0004
T459_00314	3.8755	0.6132	6.3202	0.0000	0.0000
T459_20431	3.9286	0.8559	4.5901	0.0000	0.0003
T459_29286	3.9491	0.9383	4.2087	0.0000	0.0014
T459_32522	3.9900	0.8469	4.7111	0.0000	0.0002
T459_18527	4.0339	1.0487	3.8464	0.0001	0.0047
T459_12583	4.0547	1.2566	3.2267	0.0013	0.0253
T459_13524	4.0843	1.1632	3.5114	0.0004	0.0122
T459_32501	4.1068	1.0494	3.9133	0.0001	0.0037
T459_05079	4.1746	1.0191	4.0963	0.0000	0.0020
T459_11057	4.1802	1.1005	3.7985	0.0001	0.0054
T459_05010	4.2025	0.6008	6.9949	0.0000	0.0000
T459_08010	4.2064	1.1459	3.6708	0.0002	0.0077
T459_09899	4.2583	1.0815	3.9374	0.0001	0.0035
T459_30935	4.4046	1.0713	4.1114	0.0000	0.0019
T459_27229	4.4563	1.0030	4.4430	0.0000	0.0006
T459_33926	4.5105	1.1322	3.9840	0.0001	0.0030
T459_14050	4.7044	0.8844	5.3194	0.0000	0.0000
T459_24005	4.7170	1.1651	4.0486	0.0001	0.0024
T459_22737	4.9673	1.1467	4.3320	0.0000	0.0009
T459_19946	5.0606	1.0603	4.7726	0.0000	0.0002
T459_13044	5.0816	0.7014	7.2446	0.0000	0.0000
T459_22830	5.2478	1.2138	4.3236	0.0000	0.0009
T459_17035	5.4060	1.0737	5.0350	0.0000	0.0001
T459_22736	5.4145	1.0504	5.1548	0.0000	0.0000
T459_17036	5.5722	0.7695	7.2411	0.0000	0.0000
T459_13034	5.6542	1.1968	4.7244	0.0000	0.0002
T459_05058	5.8089	0.8932	6.5036	0.0000	0.0000
T459_01048	5.8515	1.3047	4.4849	0.0000	0.0005
T459_29288	5.8588	1.1360	5.1574	0.0000	0.0000
T459_20117	6.8815	1.2122	5.6767	0.0000	0.0000

Supplementary Table 1. **E**. Differentially expressed genes between A10 under water stress and A10 under the control conditions at T2 (A10 PEG/A10 Control).

Gene ID	log2FoldChange	lfcSE	stat	pvalue	padj
T459_20070	-2.7781	0.6539	-4.2483	0.0000	0.0053
T459_27465	-1.8668	0.4646	-4.0177	0.0001	0.0108
T459_09550	-1.7972	0.5112	-3.5158	0.0004	0.0467

Gene ID	log2FoldChange	lfcSE	stat	pvalue	padj
T459_12289	-1.6977	0.4585	-3.7027	0.0002	0.0285
T459_06497	-1.6703	0.3297	-5.0667	0.0000	0.0002
T459_10290	-1.5372	0.3738	-4.1129	0.0000	0.0082
T459_20966	-1.4267	0.3722	-3.8331	0.0001	0.0196
T459_17432	-1.2037	0.3034	-3.9677	0.0001	0.0125
T459_24398	-1.1275	0.3188	-3.5366	0.0004	0.0445
T459_30808	-1.1015	0.2414	-4.5637	0.0000	0.0017
T459_29611	1.0030	0.2506	4.0028	0.0001	0.0111
T459_12693	1.0265	0.2709	3.7899	0.0002	0.0217
T459_09958	1.0270	0.2860	3.5910	0.0003	0.0374
T459_19171	1.0399	0.2341	4.4419	0.0000	0.0027
T459_28553	1.0548	0.2574	4.0975	0.0000	0.0084
T459_32944	1.0712	0.2529	4.2355	0.0000	0.0055
T459_29253	1.0734	0.2351	4.5659	0.0000	0.0017
T459_18743	1.0854	0.2255	4.8126	0.0000	0.0007
T459_20900	1.0974	0.2852	3.8479	0.0001	0.0186
T459_07005	1.1122	0.2524	4.4059	0.0000	0.0030
T459_22468	1.1138	0.2551	4.3670	0.0000	0.0035
T459_06393	1.1487	0.1752	6.5576	0.0000	0.0000
T459_30568	1.1492	0.3137	3.6629	0.0002	0.0315
T459_19900	1.1508	0.2711	4.2450	0.0000	0.0053
T459_12479	1.1593	0.2725	4.2541	0.0000	0.0053
T459_32234	1.1669	0.2817	4.1427	0.0000	0.0076
T459_29247	1.2012	0.3000	4.0034	0.0001	0.0111
T459_18958	1.2188	0.2682	4.5439	0.0000	0.0018
T459_34060	1.2230	0.3390	3.6075	0.0003	0.0361
T459_09686	1.2379	0.3364	3.6800	0.0002	0.0303
T459_15105	1.2485	0.3295	3.7887	0.0002	0.0217
T459_12994	1.3167	0.2949	4.4642	0.0000	0.0025
T459_18996	1.3197	0.3104	4.2519	0.0000	0.0053
T459_08701	1.3301	0.2608	5.0995	0.0000	0.0002
T459_20283	1.3414	0.3578	3.7492	0.0002	0.0251
T459_26266	1.3440	0.2886	4.6563	0.0000	0.0012
T459_28936	1.3552	0.3673	3.6901	0.0002	0.0293
T459_03904	1.3613	0.3161	4.3060	0.0000	0.0045
T459_29286	1.3663	0.3516	3.8859	0.0001	0.0163
T459_34352	1.3821	0.1816	7.6130	0.0000	0.0000
T459_13934	1.3841	0.3037	4.5573	0.0000	0.0017
T459_06392	1.3997	0.2060	6.7951	0.0000	0.0000
T459_23393	1.4071	0.3677	3.8271	0.0001	0.0196
T459_11633	1.4340	0.3635	3.9450	0.0001	0.0133
T459_32043	1.4463	0.3865	3.7423	0.0002	0.0255
T459_24566	1.4534	0.3006	4.8346	0.0000	0.0006
T459_31660	1.4633	0.4019	3.6406	0.0003	0.0332
T459_34025	1.4829	0.4034	3.6762	0.0002	0.0304
T459_08085	1.4959	0.3190	4.6890	0.0000	0.0011
T459_01321	1.4977	0.3695	4.0530	0.0001	0.0099

Gene ID	log2FoldChange	lfcSE	stat	pvalue	padj
T459_02320	1.5270	0.1697	8.9965	0.0000	0.0000
T459_30803	1.5363	0.1634	9.4012	0.0000	0.0000
T459_22736	1.5388	0.2738	5.6193	0.0000	0.0000
T459_31879	1.5618	0.2833	5.5128	0.0000	0.0000
T459_20703	1.5786	0.4394	3.5925	0.0003	0.0374
T459_00035	1.6062	0.4546	3.5336	0.0004	0.0448
T459_22332	1.6154	0.4256	3.7953	0.0001	0.0217
T459_33926	1.6205	0.4538	3.5712	0.0004	0.0395
T459_05020	1.6334	0.3469	4.7093	0.0000	0.0010
T459_13674	1.6353	0.3434	4.7624	0.0000	0.0008
T459_14986	1.6523	0.2544	6.4956	0.0000	0.0000
T459_31642	1.6610	0.3179	5.2249	0.0000	0.0001
T459_22503	1.6935	0.3354	5.0498	0.0000	0.0002
T459_29982	1.7157	0.2333	7.3548	0.0000	0.0000
T459_29255	1.7279	0.4812	3.5907	0.0003	0.0374
T459_06173	1.7307	0.4738	3.6528	0.0003	0.0323
T459_05761	1.8056	0.4051	4.4575	0.0000	0.0025
T459_32189	1.8255	0.2942	6.2044	0.0000	0.0000
T459_07849	1.9207	0.3785	5.0748	0.0000	0.0002
T459_17416	2.0329	0.4225	4.8116	0.0000	0.0007
T459_26588	2.0453	0.4319	4.7351	0.0000	0.0009
T459_07754	2.1785	0.4503	4.8384	0.0000	0.0006
T459_05058	2.1824	0.3931	5.5513	0.0000	0.0000
T459_00888	2.2087	0.3411	6.4746	0.0000	0.0000
T459_16555	2.4510	0.4279	5.7285	0.0000	0.0000
T459_06174	2.5219	0.7060	3.5720	0.0004	0.0395
T459_06704	2.5226	0.3087	8.1721	0.0000	0.0000
T459_22504	2.5522	0.4151	6.1488	0.0000	0.0000
T459_05010	2.6170	0.6114	4.2805	0.0000	0.0048
T459_04332	2.6264	0.6259	4.1962	0.0000	0.0061
T459_20061	2.6459	0.6592	4.0135	0.0001	0.0109
T459_06129	2.6830	0.4655	5.7636	0.0000	0.0000
T459_33809	2.8293	0.3845	7.3575	0.0000	0.0000
T459_13096	2.8426	0.6868	4.1390	0.0000	0.0076
T459_22093	3.5473	0.6202	5.7191	0.0000	0.0000
T459_09956	3.7750	0.8287	4.5552	0.0000	0.0017
T459_32612	3.8343	0.8100	4.7339	0.0000	0.0009
T459_20117	3.8550	0.6461	5.9664	0.0000	0.0000
T459_31337	5.0245	0.8578	5.8572	0.0000	0.0000

Supplementary Table 1. **F.** Differentially expressed genes between NIBER® under water stress and NIBER® under the control conditions at T1 (NIBER® PEG/ NIBER® Control).

Gene ID	log2FoldChange	lfcSE	stat	pvalue	padj
T459_05911	-4.9977	0.6143	-8.1362	0.0000	0.0000
T459_25316	-4.9137	0.7071	-6.9491	0.0000	0.0000
T459_32064	-4.7150	0.4505	-10.4660	0.0000	0.0000

Gene ID	log2FoldChange	lfcSE	stat	pvalue	padj
T459_00406	-4.4996	0.6534	-6.8860	0.0000	0.0000
T459_15100	-4.4072	0.4115	-10.7096	0.0000	0.0000
T459_14969	-4.3481	0.7488	-5.8067	0.0000	0.0000
T459_12276	-4.3007	0.5577	-7.7108	0.0000	0.0000
T459_08230	-4.2414	1.2037	-3.5237	0.0004	0.0160
T459_22213	-3.9477	0.4927	-8.0118	0.0000	0.0000
T459_08151	-3.8883	0.5845	-6.6529	0.0000	0.0000
T459_15101	-3.8412	0.3850	-9.9767	0.0000	0.0000
T459_05984	-3.6681	0.4510	-8.1325	0.0000	0.0000
T459_12275	-3.6098	0.4349	-8.2998	0.0000	0.0000
T459_24052	-3.5606	0.9831	-3.6219	0.0003	0.0119
T459_32062	-3.4944	0.4824	-7.2430	0.0000	0.0000
T459_12349	-3.3442	0.4935	-6.7764	0.0000	0.0000
T459_17412	-3.3018	0.3369	-9.8017	0.0000	0.0000
T459_05997	-3.2545	0.6250	-5.2071	0.0000	0.0000
T459_27700	-3.2353	0.4609	-7.0201	0.0000	0.0000
T459_15477	-3.2294	0.5157	-6.2619	0.0000	0.0000
T459_32063	-3.2177	0.4181	-7.6958	0.0000	0.0000
T459_31320	-3.1977	0.5583	-5.7278	0.0000	0.0000
T459_05978	-3.1066	0.5099	-6.0925	0.0000	0.0000
T459_31641	-3.0829	0.8225	-3.7481	0.0002	0.0079
T459_15087	-3.0731	0.4071	-7.5479	0.0000	0.0000
T459_22212	-3.0718	0.3477	-8.8338	0.0000	0.0000
T459_15113	-3.0138	0.4030	-7.4785	0.0000	0.0000
T459_19222	-2.9427	0.3922	-7.5027	0.0000	0.0000
T459_22211	-2.8997	0.3143	-9.2254	0.0000	0.0000
T459_16407	-2.8636	0.6277	-4.5622	0.0000	0.0004
T459_04295	-2.8263	0.3861	-7.3208	0.0000	0.0000
T459_05496	-2.6384	0.4133	-6.3832	0.0000	0.0000
T459_07336	-2.5973	0.6061	-4.2854	0.0000	0.0013
T459_26450	-2.4009	0.4959	-4.8416	0.0000	0.0001
T459_18120	-2.3659	0.4593	-5.1512	0.0000	0.0000
T459_17404	-2.3578	0.5390	-4.3740	0.0000	0.0009
T459_20341	-2.3416	0.6670	-3.5108	0.0004	0.0167
T459_32730	-2.3370	0.3430	-6.8139	0.0000	0.0000
T459_22210	-2.2924	0.3553	-6.4512	0.0000	0.0000
T459_01685	-2.2588	0.4525	-4.9918	0.0000	0.0001
T459_12756	-2.2015	0.4291	-5.1311	0.0000	0.0000
T459_03110	-2.1757	0.5474	-3.9749	0.0001	0.0038
T459_00197	-2.1678	0.3208	-6.7579	0.0000	0.0000
T459_23950	-2.1523	0.3200	-6.7267	0.0000	0.0000
T459_18119	-2.1226	0.6429	-3.3018	0.0010	0.0298
T459_26812	-2.0858	0.5100	-4.0902	0.0000	0.0026
T459_32228	-2.0847	0.2886	-7.2238	0.0000	0.0000
T459_11198	-2.0802	0.5537	-3.7567	0.0002	0.0078
T459_33921	-2.0700	0.2909	-7.1148	0.0000	0.0000
T459_31204	-2.0659	0.5152	-4.0099	0.0001	0.0034

Gene ID	log2FoldChange	lfcSE	stat	pvalue	padj
T459_26480	-2.0528	0.5265	-3.8989	0.0001	0.0048
T459_06409	-2.0054	0.6171	-3.2497	0.0012	0.0344
T459_29159	-1.9690	0.5008	-3.9317	0.0001	0.0044
T459_22503	-1.9010	0.2957	-6.4289	0.0000	0.0000
T459_05604	-1.8961	0.5457	-3.4746	0.0005	0.0184
T459_08856	-1.8931	0.4813	-3.9330	0.0001	0.0043
T459_28461	-1.8849	0.2946	-6.3971	0.0000	0.0000
T459_33922	-1.8328	0.4019	-4.5603	0.0000	0.0004
T459_19850	-1.8229	0.2298	-7.9338	0.0000	0.0000
T459_24545	-1.8166	0.2957	-6.1443	0.0000	0.0000
T459_07883	-1.8046	0.4988	-3.6177	0.0003	0.0121
T459_26863	-1.7956	0.3734	-4.8091	0.0000	0.0002
T459_12384	-1.7678	0.3069	-5.7604	0.0000	0.0000
T459_26831	-1.7219	0.4275	-4.0277	0.0001	0.0032
T459_01911	-1.7181	0.2344	-7.3297	0.0000	0.0000
T459_32921	-1.7174	0.4697	-3.6562	0.0003	0.0107
T459_17486	-1.7076	0.3252	-5.2510	0.0000	0.0000
T459_01472	-1.6937	0.5112	-3.3132	0.0009	0.0291
T459_17784	-1.6830	0.4778	-3.5227	0.0004	0.0161
T459_29941	-1.6819	0.5273	-3.1896	0.0014	0.0403
T459_20398	-1.6680	0.3990	-4.1808	0.0000	0.0019
T459_04385	-1.6657	0.5036	-3.3078	0.0009	0.0294
T459_25725	-1.6493	0.4277	-3.8558	0.0001	0.0055
T459_15707	-1.6418	0.3860	-4.2529	0.0000	0.0014
T459_05062	-1.6397	0.4220	-3.8859	0.0001	0.0050
T459_14845	-1.6353	0.4253	-3.8446	0.0001	0.0057
T459_11103	-1.5775	0.4521	-3.4890	0.0005	0.0177
T459_12761	-1.5758	0.3896	-4.0445	0.0001	0.0030
T459_00607	-1.5611	0.3387	-4.6095	0.0000	0.0004
T459_05021	-1.5558	0.3569	-4.3587	0.0000	0.0010
T459_12288	-1.5204	0.2802	-5.4256	0.0000	0.0000
T459_32693	-1.5062	0.3604	-4.1797	0.0000	0.0019
T459_13449	-1.4756	0.3727	-3.9597	0.0001	0.0040
T459_17487	-1.4723	0.3287	-4.4792	0.0000	0.0006
T459_23239	-1.4641	0.4548	-3.2192	0.0013	0.0374
T459_15379	-1.4632	0.4227	-3.4616	0.0005	0.0191
T459_00233	-1.4590	0.3099	-4.7078	0.0000	0.0002
T459_34590	-1.4564	0.3172	-4.5919	0.0000	0.0004
T459_09971	-1.4537	0.2542	-5.7180	0.0000	0.0000
T459_01474	-1.4386	0.3430	-4.1942	0.0000	0.0018
T459_16904	-1.4293	0.2797	-5.1097	0.0000	0.0000
T459_31287	-1.4220	0.3429	-4.1469	0.0000	0.0021
T459_12750	-1.4172	0.2825	-5.0171	0.0000	0.0001
T459_21376	-1.4165	0.3706	-3.8220	0.0001	0.0062
T459_20146	-1.4125	0.3229	-4.3740	0.0000	0.0009
T459_32869	-1.3907	0.4312	-3.2249	0.0013	0.0367
T459_12992	-1.3835	0.3020	-4.5812	0.0000	0.0004

Gene ID	log2FoldChange	lfcSE	stat	pvalue	padj
T459_05657	-1.3830	0.2723	-5.0793	0.0000	0.0000
T459_10815	-1.3783	0.4268	-3.2291	0.0012	0.0363
T459_33430	-1.3639	0.3260	-4.1844	0.0000	0.0018
T459_20683	-1.3625	0.2943	-4.6300	0.0000	0.0003
T459_15041	-1.3567	0.3517	-3.8578	0.0001	0.0055
T459_07279	-1.3459	0.2790	-4.8249	0.0000	0.0001
T459_25023	-1.3440	0.4258	-3.1564	0.0016	0.0441
T459_06178	-1.3427	0.1909	-7.0322	0.0000	0.0000
T459_09601	-1.3421	0.2798	-4.7973	0.0000	0.0002
T459_34549	-1.3338	0.3801	-3.5091	0.0004	0.0168
T459_26516	-1.3324	0.3451	-3.8603	0.0001	0.0055
T459_18426	-1.3311	0.4283	-3.1082	0.0019	0.0498
T459_08690	-1.3243	0.2799	-4.7309	0.0000	0.0002
T459_18338	-1.3105	0.3594	-3.6465	0.0003	0.0110
T459_03836	-1.3023	0.1786	-7.2934	0.0000	0.0000
T459_28400	-1.2997	0.2772	-4.6896	0.0000	0.0003
T459_09168	-1.2907	0.2846	-4.5343	0.0000	0.0005
T459_03932	-1.2610	0.3480	-3.6238	0.0003	0.0118
T459_17301	-1.2574	0.3663	-3.4324	0.0006	0.0207
T459_20367	-1.2565	0.2572	-4.8846	0.0000	0.0001
T459_06926	-1.2356	0.3733	-3.3101	0.0009	0.0293
T459_01425	-1.2344	0.3150	-3.9194	0.0001	0.0045
T459_04647	-1.2268	0.3622	-3.3869	0.0007	0.0237
T459_12179	-1.2240	0.2867	-4.2689	0.0000	0.0014
T459_31286	-1.2175	0.2212	-5.5051	0.0000	0.0000
T459_07594	-1.2125	0.2795	-4.3375	0.0000	0.0010
T459_31096	-1.1970	0.3718	-3.2193	0.0013	0.0374
T459_03141	-1.1970	0.2962	-4.0412	0.0001	0.0030
T459_21211	-1.1901	0.2419	-4.9207	0.0000	0.0001
T459_20711	-1.1883	0.3374	-3.5223	0.0004	0.0161
T459_05658	-1.1749	0.2948	-3.9848	0.0001	0.0037
T459_14318	-1.1610	0.3346	-3.4694	0.0005	0.0186
T459_02793	-1.1590	0.3226	-3.5929	0.0003	0.0130
T459_32705	-1.1377	0.2107	-5.4001	0.0000	0.0000
T459_20013	-1.1342	0.2964	-3.8269	0.0001	0.0061
T459_30814	-1.1339	0.2247	-5.0458	0.0000	0.0001
T459_20168	-1.1300	0.2327	-4.8551	0.0000	0.0001
T459_00664	-1.1297	0.3083	-3.6647	0.0002	0.0104
T459_20836	-1.1289	0.3466	-3.2570	0.0011	0.0339
T459_02853	-1.1188	0.3144	-3.5586	0.0004	0.0144
T459_14199	-1.1130	0.2242	-4.9645	0.0000	0.0001
T459_03004	-1.1062	0.3085	-3.5858	0.0003	0.0132
T459_11511	-1.0919	0.2688	-4.0623	0.0000	0.0028
T459_06772	-1.0866	0.2386	-4.5547	0.0000	0.0004
T459_09433	-1.0864	0.2109	-5.1509	0.0000	0.0000
T459_04280	-1.0818	0.3138	-3.4478	0.0006	0.0198
T459_29300	-1.0807	0.3229	-3.3467	0.0008	0.0263

Gene ID	log2FoldChange	lfcSE	stat	pvalue	padj
T459_20708	-1.0666	0.1484	-7.1852	0.0000	0.0000
T459_35378	-1.0597	0.2775	-3.8188	0.0001	0.0062
T459_24757	-1.0553	0.2010	-5.2509	0.0000	0.0000
T459_33064	-1.0539	0.3158	-3.3373	0.0008	0.0272
T459_28765	-1.0462	0.2398	-4.3630	0.0000	0.0009
T459_23957	-1.0458	0.2758	-3.7914	0.0001	0.0068
T459_13010	-1.0363	0.1580	-6.5590	0.0000	0.0000
T459_06858	-1.0360	0.2236	-4.6329	0.0000	0.0003
T459_31451	-1.0254	0.2818	-3.6385	0.0003	0.0113
T459_17966	-1.0253	0.2583	-3.9688	0.0001	0.0039
T459_05115	-1.0252	0.2698	-3.7999	0.0001	0.0066
T459_13163	-1.0242	0.2610	-3.9245	0.0001	0.0045
T459_32743	-1.0082	0.2336	-4.3161	0.0000	0.0011
T459_10759	-1.0026	0.2919	-3.4346	0.0006	0.0205
T459_10253	1.0013	0.2466	4.0595	0.0000	0.0028
T459_10702	1.0023	0.2277	4.4021	0.0000	0.0008
T459_22589	1.0045	0.1580	6.3572	0.0000	0.0000
T459_06933	1.0178	0.2797	3.6381	0.0003	0.0113
T459_10514	1.0183	0.2486	4.0953	0.0000	0.0025
T459_13126	1.0199	0.3133	3.2548	0.0011	0.0341
T459_24398	1.0219	0.3221	3.1730	0.0015	0.0421
T459_18335	1.0233	0.2310	4.4298	0.0000	0.0007
T459_33289	1.0281	0.2126	4.8357	0.0000	0.0001
T459_08907	1.0298	0.2533	4.0648	0.0000	0.0028
T459_31929	1.0298	0.2589	3.9782	0.0001	0.0037
T459_20470	1.0303	0.2343	4.3981	0.0000	0.0008
T459_00195	1.0322	0.1821	5.6700	0.0000	0.0000
T459_25345	1.0362	0.2291	4.5234	0.0000	0.0005
T459_22396	1.0367	0.1327	7.8093	0.0000	0.0000
T459_06813	1.0453	0.3157	3.3114	0.0009	0.0292
T459_20984	1.0463	0.1868	5.6010	0.0000	0.0000
T459_18261	1.0560	0.3183	3.3174	0.0009	0.0288
T459_00057	1.0674	0.3077	3.4686	0.0005	0.0187
T459_32620	1.0710	0.3191	3.3558	0.0008	0.0258
T459_06780	1.0713	0.1833	5.8437	0.0000	0.0000
T459_23984	1.0771	0.1821	5.9133	0.0000	0.0000
T459_06445	1.0838	0.3350	3.2355	0.0012	0.0356
T459_23071	1.0969	0.2845	3.8558	0.0001	0.0055
T459_23464	1.1009	0.3256	3.3812	0.0007	0.0241
T459_30564	1.1010	0.3195	3.4462	0.0006	0.0199
T459_15138	1.1064	0.2520	4.3907	0.0000	0.0009
T459_31503	1.1075	0.3406	3.2513	0.0011	0.0343
T459_05020	1.1188	0.2317	4.8298	0.0000	0.0001
T459_13107	1.1307	0.2481	4.5569	0.0000	0.0004
T459_15105	1.1330	0.3610	3.1386	0.0017	0.0459
T459_10139	1.1353	0.2089	5.4356	0.0000	0.0000
T459_04757	1.1556	0.1803	6.4083	0.0000	0.0000

Gene ID	log2FoldChange	lfcSE	stat	pvalue	padj
T459_32673	1.1696	0.2983	3.9213	0.0001	0.0045
T459_18252	1.1751	0.2389	4.9181	0.0000	0.0001
T459_05681	1.1752	0.2164	5.4307	0.0000	0.0000
T459_33234	1.1773	0.3203	3.6751	0.0002	0.0101
T459_22854	1.1825	0.3790	3.1204	0.0018	0.0481
T459_29163	1.1890	0.3243	3.6662	0.0002	0.0104
T459_29783	1.1896	0.1629	7.3026	0.0000	0.0000
T459_26096	1.1898	0.3555	3.3470	0.0008	0.0263
T459_34200	1.1929	0.2661	4.4827	0.0000	0.0006
T459_13633	1.1959	0.3464	3.4526	0.0006	0.0196
T459_10824	1.2148	0.2416	5.0271	0.0000	0.0001
T459_30732	1.2178	0.2725	4.4692	0.0000	0.0006
T459_19845	1.2192	0.1324	9.2116	0.0000	0.0000
T459_22117	1.2265	0.3687	3.3262	0.0009	0.0281
T459_33719	1.2274	0.3005	4.0847	0.0000	0.0026
T459_07967	1.2287	0.3511	3.4992	0.0005	0.0172
T459_18708	1.2303	0.2117	5.8124	0.0000	0.0000
T459_35222	1.2326	0.3090	3.9888	0.0001	0.0036
T459_05406	1.2410	0.2241	5.5376	0.0000	0.0000
T459_10457	1.2450	0.2883	4.3187	0.0000	0.0011
T459_33965	1.2587	0.3365	3.7401	0.0002	0.0080
T459_16533	1.2596	0.3924	3.2101	0.0013	0.0383
T459_21110	1.2628	0.3120	4.0472	0.0001	0.0030
T459_32008	1.2681	0.3046	4.1632	0.0000	0.0020
T459_06923	1.2744	0.3648	3.4932	0.0005	0.0175
T459_21812	1.2770	0.2836	4.5027	0.0000	0.0005
T459_26060	1.2779	0.3433	3.7224	0.0002	0.0086
T459_05475	1.2796	0.1482	8.6335	0.0000	0.0000
T459_21823	1.2798	0.3885	3.2940	0.0010	0.0304
T459_05400	1.2838	0.4108	3.1250	0.0018	0.0476
T459_05623	1.2887	0.2316	5.5633	0.0000	0.0000
T459_23487	1.2908	0.3738	3.4529	0.0006	0.0196
T459_07904	1.3110	0.3424	3.8286	0.0001	0.0061
T459_33717	1.3234	0.3992	3.3146	0.0009	0.0290
T459_28486	1.3318	0.3859	3.4515	0.0006	0.0196
T459_09862	1.3353	0.4250	3.1421	0.0017	0.0456
T459_07109	1.3355	0.3973	3.3611	0.0008	0.0255
T459_31878	1.3357	0.2147	6.2208	0.0000	0.0000
T459_15492	1.3462	0.3472	3.8770	0.0001	0.0052
T459_10528	1.3463	0.4208	3.1993	0.0014	0.0392
T459_00728	1.3466	0.3031	4.4424	0.0000	0.0007
T459_13246	1.3477	0.3264	4.1289	0.0000	0.0022
T459_06056	1.3546	0.2702	5.0124	0.0000	0.0001
T459_19604	1.3572	0.3021	4.4929	0.0000	0.0006
T459_07595	1.3620	0.3924	3.4706	0.0005	0.0186
T459_11261	1.3643	0.2959	4.6110	0.0000	0.0004
T459_08313	1.3731	0.2061	6.6618	0.0000	0.0000

Gene ID	log2FoldChange	lfcSE	stat	pvalue	padj
T459_05301	1.3798	0.2799	4.9295	0.0000	0.0001
T459_34004	1.3871	0.3984	3.4815	0.0005	0.0181
T459_10437	1.4036	0.2949	4.7592	0.0000	0.0002
T459_23388	1.4413	0.3475	4.1473	0.0000	0.0021
T459_06895	1.4537	0.2491	5.8350	0.0000	0.0000
T459_20275	1.4604	0.3650	4.0015	0.0001	0.0035
T459_20565	1.4784	0.3975	3.7190	0.0002	0.0087
T459_31554	1.4886	0.1902	7.8259	0.0000	0.0000
T459_14003	1.4895	0.3489	4.2695	0.0000	0.0014
T459_22419	1.4956	0.4668	3.2040	0.0014	0.0388
T459_26839	1.5075	0.3408	4.4237	0.0000	0.0007
T459_00299	1.5195	0.3068	4.9520	0.0000	0.0001
T459_04931	1.5230	0.4213	3.6148	0.0003	0.0121
T459_24718	1.5329	0.4549	3.3696	0.0008	0.0249
T459_12450	1.5507	0.3315	4.6778	0.0000	0.0003
T459_32234	1.5702	0.3031	5.1810	0.0000	0.0000
T459_22258	1.5712	0.2486	6.3202	0.0000	0.0000
T459_12482	1.5873	0.3012	5.2698	0.0000	0.0000
T459_00717	1.5954	0.4105	3.8862	0.0001	0.0050
T459_09552	1.5958	0.4797	3.3268	0.0009	0.0280
T459_13377	1.6026	0.5095	3.1457	0.0017	0.0453
T459_08159	1.6142	0.2192	7.3638	0.0000	0.0000
T459_32610	1.6214	0.2927	5.5387	0.0000	0.0000
T459_05908	1.6233	0.4636	3.5018	0.0005	0.0171
T459_33863	1.6235	0.4131	3.9298	0.0001	0.0044
T459_12184	1.6262	0.2897	5.6131	0.0000	0.0000
T459_15631	1.6331	0.2682	6.0885	0.0000	0.0000
T459_11506	1.6384	0.4646	3.5268	0.0004	0.0159
T459_12583	1.6579	0.4424	3.7472	0.0002	0.0079
T459_29265	1.6748	0.2990	5.6017	0.0000	0.0000
T459_09766	1.6767	0.3068	5.4647	0.0000	0.0000
T459_14992	1.6842	0.4295	3.9214	0.0001	0.0045
T459_04404	1.6846	0.3822	4.4081	0.0000	0.0008
T459_01666	1.6867	0.2525	6.6796	0.0000	0.0000
T459_17897	1.6929	0.4026	4.2045	0.0000	0.0017
T459_07005	1.6944	0.4792	3.5355	0.0004	0.0155
T459_20471	1.6955	0.2509	6.7564	0.0000	0.0000
T459_17054	1.7072	0.4475	3.8151	0.0001	0.0063
T459_06461	1.7082	0.4838	3.5306	0.0004	0.0158
T459_32292	1.7111	0.4917	3.4798	0.0005	0.0181
T459_26035	1.7131	0.2732	6.2715	0.0000	0.0000
T459_20479	1.7230	0.1400	12.3061	0.0000	0.0000
T459_07645	1.7295	0.3226	5.3611	0.0000	0.0000
T459_10508	1.7344	0.3256	5.3266	0.0000	0.0000
T459_05688	1.7378	0.4400	3.9500	0.0001	0.0041
T459_14092	1.7467	0.4483	3.8962	0.0001	0.0049
T459_06393	1.7546	0.3813	4.6017	0.0000	0.0004

Gene ID	log2FoldChange	lfcSE	stat	pvalue	padj
T459_22197	1.7602	0.4826	3.6470	0.0003	0.0110
T459_02795	1.7651	0.4090	4.3155	0.0000	0.0011
T459_14345	1.7677	0.3492	5.0618	0.0000	0.0001
T459_13439	1.7997	0.5739	3.1362	0.0017	0.0461
T459_20235	1.8025	0.3204	5.6249	0.0000	0.0000
T459_09958	1.8276	0.2974	6.1445	0.0000	0.0000
T459_34044	1.8339	0.4735	3.8728	0.0001	0.0053
T459_27223	1.8481	0.5758	3.2097	0.0013	0.0383
T459_01486	1.8779	0.4204	4.4673	0.0000	0.0006
T459_00315	1.8878	0.2007	9.4071	0.0000	0.0000
T459_13934	1.9044	0.5210	3.6551	0.0003	0.0107
T459_33642	1.9160	0.3791	5.0543	0.0000	0.0001
T459_27222	1.9197	0.5680	3.3798	0.0007	0.0242
T459_05078	1.9210	0.5396	3.5601	0.0004	0.0144
T459_07933	1.9456	0.1977	9.8404	0.0000	0.0000
T459_12483	1.9477	0.3385	5.7545	0.0000	0.0000
T459_20487	1.9639	0.6041	3.2511	0.0011	0.0343
T459_09858	1.9686	0.2582	7.6244	0.0000	0.0000
T459_32043	1.9765	0.5014	3.9416	0.0001	0.0042
T459_28743	1.9888	0.4288	4.6384	0.0000	0.0003
T459_32471	1.9906	0.6408	3.1066	0.0019	0.0500
T459_23080	1.9974	0.4338	4.6043	0.0000	0.0004
T459_32860	2.0201	0.4827	4.1853	0.0000	0.0018
T459_08132	2.0223	0.5496	3.6797	0.0002	0.0099
T459_04998	2.0239	0.4510	4.4871	0.0000	0.0006
T459_05942	2.0274	0.3664	5.5339	0.0000	0.0000
T459_28941	2.0351	0.3700	5.5005	0.0000	0.0000
T459_06917	2.0414	0.2382	8.5683	0.0000	0.0000
T459_22738	2.0415	0.6044	3.3778	0.0007	0.0243
T459_13535	2.0457	0.4098	4.9918	0.0000	0.0001
T459_10116	2.0710	0.3084	6.7150	0.0000	0.0000
T459_07329	2.1195	0.4337	4.8870	0.0000	0.0001
T459_25910	2.1308	0.3060	6.9636	0.0000	0.0000
T459_20889	2.1369	0.6135	3.4833	0.0005	0.0180
T459_09533	2.1499	0.4237	5.0737	0.0000	0.0000
T459_23095	2.1542	0.3435	6.2706	0.0000	0.0000
T459_24029	2.1751	0.4658	4.6697	0.0000	0.0003
T459_13190	2.2255	0.4069	5.4695	0.0000	0.0000
T459_32014	2.2328	0.2727	8.1889	0.0000	0.0000
T459_20468	2.2373	0.3983	5.6177	0.0000	0.0000
T459_25929	2.2626	0.3092	7.3187	0.0000	0.0000
T459_10441	2.2730	0.6625	3.4310	0.0006	0.0207
T459_13674	2.3375	0.5412	4.3192	0.0000	0.0011
T459_35454	2.3378	0.7196	3.2485	0.0012	0.0344
T459_05079	2.3633	0.4080	5.7916	0.0000	0.0000
T459_34874	2.3651	0.3580	6.6072	0.0000	0.0000
T459_05380	2.3658	0.4266	5.5459	0.0000	0.0000

Gene ID	log2FoldChange	lfcSE	stat	pvalue	padj
T459_07900	2.3664	0.4377	5.4070	0.0000	0.0000
T459_03058	2.3672	0.3220	7.3509	0.0000	0.0000
T459_17598	2.3921	0.5070	4.7185	0.0000	0.0002
T459_01049	2.3951	0.5369	4.4612	0.0000	0.0006
T459_20467	2.4312	0.2309	10.5278	0.0000	0.0000
T459_22843	2.4379	0.5378	4.5329	0.0000	0.0005
T459_00314	2.4405	0.5034	4.8485	0.0000	0.0001
T459_20283	2.4533	0.4000	6.1341	0.0000	0.0000
T459_17950	2.4544	0.4577	5.3627	0.0000	0.0000
T459_31548	2.4758	0.6350	3.8991	0.0001	0.0048
T459_06392	2.4893	0.5221	4.7679	0.0000	0.0002
T459_24935	2.5295	0.4169	6.0667	0.0000	0.0000
T459_31616	2.5443	0.4792	5.3095	0.0000	0.0000
T459_16352	2.5553	0.6514	3.9225	0.0001	0.0045
T459_27250	2.5694	0.7191	3.5729	0.0004	0.0138
T459_35114	2.5918	0.8125	3.1898	0.0014	0.0403
T459_29611	2.5999	0.3412	7.6200	0.0000	0.0000
T459_33713	2.6077	0.6856	3.8033	0.0001	0.0065
T459_20703	2.6453	0.5152	5.1344	0.0000	0.0000
T459_07809	2.6619	0.3777	7.0482	0.0000	0.0000
T459_18312	2.6675	0.6420	4.1549	0.0000	0.0020
T459_20883	2.6830	0.6010	4.4643	0.0000	0.0006
T459_17731	2.7411	0.4113	6.6640	0.0000	0.0000
T459_21300	2.7608	0.8763	3.1507	0.0016	0.0447
T459_14050	2.8884	0.4989	5.7899	0.0000	0.0000
T459_03312	3.0264	0.6015	5.0317	0.0000	0.0001
T459_27508	3.0526	0.3274	9.3240	0.0000	0.0000
T459_29286	3.0651	0.5388	5.6884	0.0000	0.0000
T459_18683	3.0696	0.4489	6.8374	0.0000	0.0000
T459_19900	3.1098	0.9079	3.4251	0.0006	0.0211
T459_13044	3.1371	0.6956	4.5102	0.0000	0.0005
T459_27229	3.2183	0.5093	6.3188	0.0000	0.0000
T459_22923	3.3262	0.8137	4.0879	0.0000	0.0026
T459_15711	3.3706	0.9621	3.5032	0.0005	0.0171
T459_17036	3.4142	0.5284	6.4609	0.0000	0.0000
T459_24730	3.6055	1.1053	3.2619	0.0011	0.0335
T459_20431	3.6401	0.7954	4.5766	0.0000	0.0004
T459_00763	3.6699	1.0652	3.4453	0.0006	0.0199
T459_33926	3.6947	1.0657	3.4668	0.0005	0.0188
T459_07331	3.7523	0.8892	4.2199	0.0000	0.0016
T459_09899	3.7567	0.9828	3.8226	0.0001	0.0062
T459_25223	3.9469	1.2699	3.1080	0.0019	0.0498
T459_13524	3.9508	0.6691	5.9044	0.0000	0.0000
T459_22736	3.9839	0.5467	7.2877	0.0000	0.0000
T459_22830	3.9892	0.8554	4.6638	0.0000	0.0003
T459_29287	4.0080	1.1464	3.4961	0.0005	0.0174
T459_29288	4.1762	0.8600	4.8558	0.0000	0.0001

Gene ID	log2FoldChange	lfcSE	stat	pvalue	padj
T459_31894	4.2023	1.0224	4.1104	0.0000	0.0024
T459_10808	4.3332	1.2689	3.4150	0.0006	0.0218
T459_33530	4.3450	1.0768	4.0350	0.0001	0.0031
T459_17035	4.3857	0.8080	5.4280	0.0000	0.0000
T459_05058	4.5224	0.4529	9.9851	0.0000	0.0000
T459_22737	4.5567	1.0932	4.1684	0.0000	0.0019
T459_19946	4.8297	1.0147	4.7596	0.0000	0.0002
T459_02490	4.8489	0.8030	6.0383	0.0000	0.0000
T459_13034	4.8564	0.8817	5.5080	0.0000	0.0000
T459_20117	5.9998	1.0167	5.9015	0.0000	0.0000

Supplementary Table 1. **G.** Differentially expressed genes between NIBER® under water stress and NIBER® under the control conditions at T2 (NIBER® PEG/ NIBER® Control).

Gene ID	log2FoldChange	lfcSE	stat	pvalue	padj
T459_33149	-8.6662	1.2187	-7.1110	0.0000	0.0000
T459_20070	-4.8132	1.3708	-3.5111	0.0004	0.0283
T459_04970	-2.7442	0.7531	-3.6439	0.0003	0.0201
T459_31821	-2.2782	0.5564	-4.0943	0.0000	0.0049
T459_06497	-2.1362	0.3133	-6.8184	0.0000	0.0000
T459_07135	-2.0699	0.4524	-4.5758	0.0000	0.0009
T459_20966	-2.0149	0.3680	-5.4750	0.0000	0.0000
T459_33809	-1.9584	0.4898	-3.9984	0.0001	0.0065
T459_10290	-1.7263	0.3674	-4.6988	0.0000	0.0006
T459_32688	-1.6915	0.4690	-3.6064	0.0003	0.0223
T459_22455	-1.6850	0.3141	-5.3649	0.0000	0.0000
T459_20068	-1.5523	0.3094	-5.0166	0.0000	0.0001
T459_09210	-1.5109	0.3034	-4.9802	0.0000	0.0002
T459_27612	-1.4731	0.4136	-3.5619	0.0004	0.0251
T459_20687	-1.4526	0.3481	-4.1725	0.0000	0.0038
T459_20453	-1.4038	0.3905	-3.5946	0.0003	0.0232
T459_20065	-1.3621	0.3078	-4.4252	0.0000	0.0016
T459_20965	-1.3355	0.3943	-3.3868	0.0007	0.0388
T459_09727	-1.2726	0.3247	-3.9200	0.0001	0.0084
T459_17509	-1.2404	0.3453	-3.5924	0.0003	0.0233
T459_20064	-1.2142	0.2926	-4.1501	0.0000	0.0041
T459_18733	-1.2026	0.3025	-3.9754	0.0001	0.0070
T459_26842	-1.2019	0.2860	-4.2026	0.0000	0.0035
T459_22516	-1.2016	0.3452	-3.4807	0.0005	0.0306
T459_26764	-1.2012	0.3156	-3.8058	0.0001	0.0121
T459_27933	-1.1791	0.1104	-10.6782	0.0000	0.0000
T459_24073	-1.1695	0.2069	-5.6523	0.0000	0.0000
T459_34804	-1.1589	0.2020	-5.7367	0.0000	0.0000
T459_16555	-1.1536	0.3327	-3.4673	0.0005	0.0317
T459_31033	-1.1137	0.2856	-3.8998	0.0001	0.0090
T459_17432	-1.0294	0.3051	-3.3735	0.0007	0.0405
T459_07170	1.0041	0.2711	3.7044	0.0002	0.0168

Gene ID	log2FoldChange	lfcSE	stat	pvalue	padj
T459_34967	1.0167	0.2973	3.4201	0.0006	0.0356
T459_17550	1.0178	0.1469	6.9284	0.0000	0.0000
T459_21895	1.0291	0.2537	4.0563	0.0000	0.0054
T459_21211	1.0319	0.1128	9.1439	0.0000	0.0000
T459_28553	1.0499	0.1583	6.6307	0.0000	0.0000
T459_14080	1.0592	0.3148	3.3646	0.0008	0.0415
T459_14897	1.0616	0.1844	5.7575	0.0000	0.0000
T459_17769	1.0785	0.2787	3.8694	0.0001	0.0100
T459_12696	1.0848	0.2828	3.8361	0.0001	0.0111
T459_02931	1.0947	0.1174	9.3228	0.0000	0.0000
T459_20471	1.0962	0.2426	4.5192	0.0000	0.0011
T459_00100	1.1046	0.3327	3.3199	0.0009	0.0458
T459_17731	1.1049	0.3113	3.5492	0.0004	0.0258
T459_03483	1.1069	0.3198	3.4615	0.0005	0.0322
T459_32254	1.1112	0.3170	3.5055	0.0005	0.0288
T459_17633	1.1124	0.2347	4.7403	0.0000	0.0005
T459_08128	1.1209	0.2234	5.0166	0.0000	0.0001
T459_12439	1.1453	0.2342	4.8913	0.0000	0.0003
T459_04029	1.1528	0.2222	5.1885	0.0000	0.0001
T459_22736	1.1855	0.2879	4.1177	0.0000	0.0045
T459_06160	1.1927	0.3229	3.6935	0.0002	0.0172
T459_18901	1.2012	0.2355	5.1008	0.0000	0.0001
T459_16404	1.2019	0.2567	4.6820	0.0000	0.0006
T459_16939	1.2033	0.3590	3.3520	0.0008	0.0425
T459_33266	1.2214	0.2581	4.7323	0.0000	0.0005
T459_20400	1.2315	0.3279	3.7562	0.0002	0.0141
T459_20020	1.2336	0.2092	5.8959	0.0000	0.0000
T459_34102	1.2466	0.3681	3.3869	0.0007	0.0388
T459_13892	1.2645	0.3521	3.5916	0.0003	0.0233
T459_24067	1.2785	0.3391	3.7700	0.0002	0.0135
T459_20900	1.2787	0.2212	5.7804	0.0000	0.0000
T459_24566	1.2836	0.3912	3.2807	0.0010	0.0497
T459_18215	1.2910	0.2286	5.6469	0.0000	0.0000
T459_16386	1.3126	0.2433	5.3941	0.0000	0.0000
T459_06933	1.3235	0.3083	4.2930	0.0000	0.0025
T459_13377	1.3292	0.3818	3.4810	0.0005	0.0306
T459_27229	1.3434	0.3799	3.5359	0.0004	0.0266
T459_34043	1.3536	0.3098	4.3687	0.0000	0.0020
T459_25891	1.3576	0.2511	5.4076	0.0000	0.0000
T459_26828	1.3722	0.2458	5.5835	0.0000	0.0000
T459_05383	1.3808	0.3119	4.4267	0.0000	0.0016
T459_05604	1.3832	0.3611	3.8309	0.0001	0.0113
T459_14985	1.3911	0.2338	5.9498	0.0000	0.0000
T459_03020	1.3935	0.3403	4.0954	0.0000	0.0049
T459_06136	1.3961	0.2944	4.7420	0.0000	0.0005
T459_09169	1.3991	0.3420	4.0912	0.0000	0.0049
T459_32234	1.4029	0.3406	4.1185	0.0000	0.0045

Gene ID	log2FoldChange	lfcSE	stat	pvalue	padj
T459_12692	1.4106	0.3008	4.6896	0.0000	0.0006
T459_12695	1.4120	0.3424	4.1244	0.0000	0.0045
T459_33234	1.4185	0.3256	4.3560	0.0000	0.0020
T459_06042	1.4378	0.2622	5.4840	0.0000	0.0000
T459_15090	1.4406	0.3565	4.0409	0.0001	0.0056
T459_29287	1.4469	0.3679	3.9327	0.0001	0.0081
T459_33161	1.4546	0.4107	3.5416	0.0004	0.0261
T459_22504	1.4580	0.4079	3.5744	0.0004	0.0243
T459_19698	1.4789	0.3532	4.1870	0.0000	0.0037
T459_05384	1.4838	0.3059	4.8503	0.0000	0.0003
T459_12693	1.4846	0.3421	4.3400	0.0000	0.0021
T459_28219	1.4974	0.4516	3.3158	0.0009	0.0461
T459_26373	1.5010	0.3774	3.9770	0.0001	0.0070
T459_12610	1.5763	0.4055	3.8874	0.0001	0.0093
T459_26551	1.5788	0.3902	4.0459	0.0001	0.0056
T459_29968	1.6260	0.2463	6.6028	0.0000	0.0000
T459_06371	1.6361	0.3784	4.3236	0.0000	0.0022
T459_12994	1.6493	0.3184	5.1803	0.0000	0.0001
T459_20275	1.6982	0.4620	3.6759	0.0002	0.0182
T459_09686	1.7401	0.3250	5.3540	0.0000	0.0000
T459_14986	1.7543	0.3995	4.3918	0.0000	0.0018
T459_18958	1.8160	0.3460	5.2486	0.0000	0.0001
T459_05496	1.8317	0.3640	5.0323	0.0000	0.0001
T459_10800	1.8663	0.4982	3.7458	0.0002	0.0146
T459_30803	1.8936	0.3397	5.5748	0.0000	0.0000
T459_08701	1.9693	0.3450	5.7086	0.0000	0.0000
T459_10640	1.9901	0.5327	3.7361	0.0002	0.0151
T459_22843	2.0670	0.4870	4.2444	0.0000	0.0030
T459_20407	2.1141	0.4848	4.3611	0.0000	0.0020
T459_03366	2.1299	0.4599	4.6315	0.0000	0.0007
T459_32501	2.1369	0.5905	3.6190	0.0003	0.0215
T459_29810	2.1505	0.5094	4.2220	0.0000	0.0033
T459_33713	2.2249	0.6440	3.4551	0.0006	0.0326
T459_00888	2.2270	0.5065	4.3967	0.0000	0.0017
T459_06909	2.4281	0.4109	5.9089	0.0000	0.0000
T459_01328	2.4515	0.7146	3.4305	0.0006	0.0347
T459_05058	2.4868	0.5105	4.8715	0.0000	0.0003
T459_11057	2.5956	0.7263	3.5737	0.0004	0.0243
T459_31982	2.8629	0.6986	4.0978	0.0000	0.0049
T459_03090	3.0972	0.8038	3.8531	0.0001	0.0105
T459_03125	3.1146	0.6839	4.5543	0.0000	0.0010
T459_31977	3.1850	0.6195	5.1416	0.0000	0.0001
T459_09274	3.3196	0.8143	4.0766	0.0000	0.0051
T459_31978	3.4641	0.6489	5.3386	0.0000	0.0000
T459_13757	3.5122	1.0692	3.2848	0.0010	0.0493
T459_31980	3.5361	0.7255	4.8738	0.0000	0.0003
T459_09275	3.5812	0.5899	6.0708	0.0000	0.0000

Gene ID	log2FoldChange	lfcSE	stat	pvalue	padj
T459_15940	3.6174	1.0802	3.3489	0.0008	0.0425
T459_03089	3.8704	0.7490	5.1671	0.0000	0.0001
T459_14326	4.0965	0.9827	4.1685	0.0000	0.0039
T459_35359	6.1204	0.8009	7.6415	0.0000	0.0000

CHAPTER III

Short-term water stress responses of grafted pepper plants are associated with changes in the hormonal balance

Yaiza Gara Padilla[1], Ramón Gisbert-Mullor[2], Alfonso Albacete[3,4], Purificación A. Martínez-Melgarejo[3], Salvador López-Galarza[2] and Ángeles Calatayud[1]

1 Departamento de Horticultura, Centro de Citricultura y Producción Vegetal, Instituto Valenciano de Investigaciones Agrarias (IVIA), CV-315, Km 10,7, Moncada, 46113 Valencia, Spain.

2 Departamento de Producción Vegetal, Centro Valenciano de Estudios sobre el Riego, Universitat Politècnica de València (UPV), Camí de Vera s/n, 46022 Valencia, Spain.

3 Department of Plant Nutrition, Centro de Edafología y Biología Aplicada del Segura (CEBAS-CSIC), Murcia, Spain.

4 Institute for Agro-Environmental Research and Development of Murcia (IMIDA), Department of Plant Production and Agrotechnology, Murcia, Spain.

Frontiers in Plant Science **2023**, 14, 1170021.
doi.org/10.3389/fpls.2023.1170021

4.1. Abstract

Phytohormones play an important role in regulating the plant behavior to drought. In previous studies, NIBER® pepper rootstock showed tolerance to drought in terms of production and fruit quality compared to ungrafted plants. In this study, our hypothesis was that short-term exposure to water stress in young, grafted pepper plants would shed light on tolerance to drought in terms of modulation of the hormonal balance. To validate this hypothesis, fresh weight, water use efficiency (WUE) and the main hormone classes were analyzed in self-grafted pepper plants (variety onto variety, V/V) and variety grafted onto NIBER® (V/N) at 4, 24, and 48h after severe water stress was induced by PEG addition. After 48h, WUE in V/N was higher than in V/V, due to major stomata closure to maintain water retention in the leaves. This can be explained by the higher abscisic acid (ABA) levels observed in the leaves of V/N plants. Despite the interaction between ABA and the ethylene precursor, 1-aminocyclopropane-1- carboxylic acid (ACC), in relation to stomata closure is controversial, we observed an important increase of ACC at the end of the experiment in V/N plants coinciding with an important rise of the WUE and ABA. The maximum concentration of jasmonic acid and salicylic acid after 48h was found in the leaves of V/N, associated with their role in abiotic stress signaling and tolerance. Respect to auxins and cytokinins, the highest concentrations were linked to water stress and NIBER®, but this effect did not occur for gibberellins. These results show that hormone balance was affected by water stress and rootstock genotype, where NIBER® rootstock displayed a better ability to overcome short-term water stress.

4.2. Introduction

Drought stress is one of the most important environmental factors negatively affecting agriculture production and it has been aggravated in the last decade by climatic change worldwide (Gray and Brady, 2016). Most crops are highly vulnerable to drought stress, resulting in growth and production impairment with relevant economic consequences (Vicente-Serrano, 2007).

Plants have developed several adaptive strategies to mitigate the negative effects of water scarcity, evolving morpho-physiological, phenological, biochemical, and genetic mechanisms (Basu et al., 2016; Ullah et al., 2018). Plant roots are the first organs sensing soil water deficit and this perception induces a complex signaling network from root to shoot (and shoot to root), in which hormones, reactive oxygen species (ROS), sugars, other metabolites, and small nucleotides are mainly involved (Albacete et al., 2014). Among them, phytohormones are the key mediators of plant responses to drought stress, they are involved in the tolerance strategies (Pérez-Alfocea et al., 2011; Ullah et al., 2018) by producing chemical messengers which activate various physiological processes to overcome drought stress (Fahad et al., 2015).

Drought provokes osmotic stress that induces abscisic acid (ABA) synthesis, which is implicated in the synthesis of compatible osmolytes, the regulation of drought-responsive genes expression, and the regulation of stomatal closure. Generally, ABA synthesis occurs in the roots from where it is translocated to the leaves via the xylem sap, inducing stomatal closure to decrease water loss. However, several experiments have demonstrated that ABA biosynthesis also takes place in leaves (Holbrook et al., 2002; Manzi et al., 2017; López-Serrano et al., 2020), but also stomatal closure can occur without the assistance of ABA root synthesis (Holbrook et al., 2002).

Ethylene or its direct precursor 1-aminocyclopropane-1-carboxyl acid (ACC) is highly mobile within the cell and can be translocated basipetally via the phloem or acropetally through the xylem (Druege, 2006). Both have been considered important regulators of water stress responses by inducing leaf senescence, epinasty, organs abscission, and leaf growth inhibition (Acosta-Motos et al., 2020; Fatma et al., 2022).

Other hormones, such as auxins (IAA), cytokinins (CKs), and gibberellins (GAs) are directly involved in the control of plant growth and their concentrations can be environmentally modulated (Werner et al., 2001; Sachs, 2005), playing critical roles during water stress. However, they can have an opposite effect since high auxin levels have been associated with drought tolerance, while GA accumulation decreased tolerance (Ullah et al., 2018). CKs have shown a dual role under water stress since positive but also negative effects on drought tolerance have been reported (Zwack and Rashotte, 2015; Li et al., 2016). A decrease in CK transport from the root to the shoot could inhibit leaf growth while a low CK content would promote root growth and modify the root/shoot ratio (Rahayu, 2005).

Furthermore, jasmonic acid (JA) and salicylic acid (SA) are hormones classically involved in biotic stress tolerance signaling (Li et al., 2003), and it is only recently that their importance in abiotic stress responses has been revealed (Muñoz-Espinoza et al., 2015). Water deficit increased JA levels in several species (Brossa et al., 2011; Chen et al., 2016; de Ollas et al., 2018). Moreover, JA and SA regulate stomatal conductance, increase root hydraulic conductivity, enhance the scavenging of ROS by antioxidant activity stimulation, and promote root development, thus contributing to drought tolerance (Munné-Bosch and

Peñuelas, 2003; Saruhan et al., 2012; Aslam et al., 2021). Their function is directly related to their relative and absolute concentrations, when SA and JA were equally applied externally at low concentrations they acted synergistically, whereas applying high concentrations of one hormone antagonized the other one (Mur et al., 2006).

It is important to note that the role of each phytohormone has been frequently described considering individual signaling pathways and not the hormonal interaction network, the spatial organ distribution, the long-distance hormonal signaling, and the type of crosstalk between hormones (positive or negative), which can be dependent of the magnitude (time and intensity) of the water stress. Indeed, different studies have demonstrated the hormonal interactions taking place under drought stress, highlighting the complexity of hormonal signaling cascades (Davies et al., 2005; Muñoz-Espinoza et al., 2015; de Ollas et al., 2018; Ullah et al., 2018; Devireddy et al., 2021; Huntenburg et al., 2022).

An important approach for discovering how long-distance hormonal communication and how roots can alter the shoot perception (or vice versa) under stress is the use of grafted plants. Vegetable grafting has become an effective strategy to increase tolerance under water stress (Rouphael et al., 2008; Penella et al., 2014; Sánchez-Rodríguez et al., 2016; López-Serrano et al., 2019; Gisbert-Mullor et al., 2020; Padilla et al., 2021) by the use of tolerant rootstocks that improve the physiological performance of plants under drought conditions. Some studies have demonstrated that the efficiency of tolerant rootstocks in overcoming water stress is related to their higher capacity to absorb water and nutrients, maintain root growth, achieve an active osmotic adjustment, and activate the antioxidant defense systems (Rouphael et al., 2008; Yao et al., 2016; Zhang et al., 2019a). This higher root efficiency under water stress contributes to maintain the metabolic processes taking place in the scion, sustaining plant growth and productivity. In addition, hormonal communication plays an important role in achieving water stress adaptation of grafted plants. Different combinations of rootstocks and scions have different modes of phytohormone synthesis transport (Lacombe and Achard, 2016; Lu et al., 2020) and affect plant adaptability to stress. ABA is the main hormone studied in grafted plants under water stress, because of its function in controlling stomata closure. Most studies have been done in tomato (Holbrook et al., 2002; Dodd et al., 2009; Ghanem et al., 2011; Cantero-Navarro et al., 2016; Gaion et al., 2018; Zhang et al., 2019b) and cucumber (Liu et al., 2016). However, there are no reports on hormonal balance regulation in grafted pepper plants exposed to water stress, being sweet pepper an important vegetable crop, thoroughly cultivated in the Mediterranean area, where water shortage is a major problem limiting productivity (Penella et al., 2014). Even more, the availability of rootstocks tolerant to water stress is lacking in pepper plants (Lee et al., 2010; Penella et al., 2014; Kyriacou et al., 2017). Nevertheless, to fill this gap we have obtained by a classic breeding program a water stress tolerant rootstock, NIBER®, an F1 hybrid that has been tested under field conditions achieving greater yields than the ungrafted variety (Gisbert-Mullor et al., 2020). Mechanisms by which NIBER® rootstock modulates plant performance under water stress, particularly hormonal balance, neither have not been fully unraveled.

Therefore, the present work aimed to determine whether the water stress tolerance observed in pepper plants grafted onto NIBER® in terms of productivity is associated with changes in the hormonal balance in early stage of grafted plant development and identify the hormones role responsible for the drought tolerance in rootstock and scion. Understanding the interactive hormonal mechanism can be effective for the development to tolerant rootstocks.

To fulfill this, we compared the hormonal profiles (ACC, CKs, GAs, ABA, IAA, JA, and SA) in roots and leaves of two pepper graft combinations (variety grafted onto NIBER® and self-grafted variety) under optimal and short-term water stress conditions.

4.3. Materials and Methods

4.3.1. Plant Material

Based on our previous studies (Gisbert-Mullor et al., 2020), a hybrid pepper rootstock tolerant to water stress i.e., NIBER® (Capsicum annuum x C. annuum, abbreviated as N) was employed in this study. Two plant combinations were herein used: the commercial pepper variety “Maestral F1” (sweet pepper, California-type, Semillas Fitó, Spain, abbreviated as V) was grafted onto NIBER® (abbreviated as V/N) and the self-grafted plants (abbreviated as V/V), thus considering the grafting effect. Early in March, the seeds of V and N were sown in 104 seedling trays filled with a peat-based substrate for germination. The grafts were performed after 2 months using the tube-grafting method (Penella et al., 2015). The grafted plants were maintained in a chamber with relative humidity above 95% and air temperature around 28-29°C for a 4-6 day period to successfully join rootstock and scion (Penella et al., 2014).

4.3.2. Hydroponic greenhouse conditions

Three weeks after grafting (by the beginning of June), seedlings were removed from the substrate and their roots were cleaned before being placed in 2L polyethylene pots in a Venlo-type greenhouse situated in Valencia (Spain, 39° 29’ 1.135” N 0° 20’ 27.315” W) under natural light conditions (610-870 μmol m^{-2} s^{-1}) and temperature and relative humidity ranges of 21-25°C and 52-72%, respectively. Pots were filled with a nutrient solution containing (in mmol L-1): 13.0 NO_3^-, 1.0 $H2PO^{4-}$, 2.45 $SO4^{2-}$, 1.6 Cl^-, 1.0 NH_4^+, 6.0 K^+, 4.0 Ca^{2+}, 2.5 Mg^{2+}, 0.5Na^+ and micronutrients (15.8 μM Fe^{2+}, 10.3 μM Mn^{2+}, 4.2 μM Zn^{2+}, 43.5 μM B^+, 2.14 μM Cu^{2+}), that were artificially aerated with an air pump. The electrical conductivity and pH of the nutrient solution were 2.1 dSm^{-1} and 6.7, respectively. After 7 days of seedling acclimation to the pots, the water stress treatment was initiated by adding 5% PEG 8000 (Sigma Co.) to the nutrient solution. The osmotic potential of the nutrient solutions, measured by a vapor osmometer (Digital osmometer, Wescor, Logan, USA), were -0.55 MPa for 5% PEG and -0.05 MPa for the control solution (0% PEG). The layout was a completely randomized design with 20 plants per combination (V/V and V/N) and treatment (5% PEG and control).

4.3.3. Fresh weight determination

Fresh weight determinations were performed at the end of the experiment (48h) using the plants that were not used for the hormonal analysis. Four plants per graft combination and treatment were analyzed by measuring the fresh weight of leaves and roots. The data are shown as a percentage of water stress over control conditions for self-grated (V/V) and variety grafted onto NIBER® (V/N).

4.3.4. Photosynthesis analysis

Gas exchange measurements were performed at the beginning (T0) and the end of the experiment (T48). The gas exchange measurements were taken in the morning (9.30 am to 10.30 am GMT) with four plants per graft combination and treatment. The net CO_2 assimilation rate (A_N, mmol CO_2 m^{-2} s^{-1}), stomatal conductance (g_s, mol H_2O m^{-2} s^{-1}), and transpiration rate (E, mmol H_2O m^{-2} s^{-1}) were determined on fully expanded leaves (3rd - 4th leaf from the apex) in the steady-state under saturating light conditions (1000 mmol m^{-2} s^{-1}) and with 400 ppm CO_2 by a LI-6400 infrared gas analyzer (LI-COR, Nebraska, USA) at 24 ± 2°C and 65 ± 10% relative humidity. Parameters A_N/g_s and A_N/E_{leaf} were calculated as intrinsic water use efficiency and instantaneous water use efficiency, respectively.

4.3.5. Sampling for hormonal analysis

The samples (leaves and roots) for hormonal analysis were taken before PEG addition (T0), and 4h (T4), 24h (T24), and 48h (T48) after water stress treatment began. Measurements were taken in fully expanded mature leaves (3rd – 4th leaf from the shoot apex) and 2 cm from distal roots. The layout was randomized with 4 samples of independent plants. The samples were frozen in liquid nitrogen immediately after harvest, conserved at −80°C, and afterwards freeze-dried.

4.3.6 Hormone extraction and analysis

Cytokinins (trans-zeatin, tZ, zeatin riboside, ZR, and isopentenyl adenine, iP), gibberellins (GA1, GA3, and GA4), indole-3-acetic acid (IAA), abscisic acid (ABA), salicylic acid (SA), jasmonic acid (JA) and the ethylene precursor 1-aminocyclopropane-1-carboxylic acid (ACC) were analyzed according to Albacete et al. (2008) and Großkinsky et al. (2014) with some modifications. Briefly, 40 mg of freeze-dried plant material were homogenized and dropped in 1 ml of cold (-20°C) extraction mixture of methanol/water (80/20, v/v). Solids were separated by centrifugation (20000 *g*, 15 min) and re-extracted for 30 min at 4°C in additional 1mL of the same extraction solution. Pooled supernatants were passed through Sep-Pak Plus †C18 cartridge (SepPak Plus, Waters, USA) to remove interfering lipids and part of plant pigments and evaporated at 40°C under vacuum either to near dryness or until the organic solvent was removed. The residue was dissolved in 0.5 mL methanol/water (20/80, v/v) solution using an ultrasonic bath. The dissolved samples were filtered through 13 mm diameter Millex filters with 0.22 µm pore size nylon membrane (Millipore, Bedford, MA, USA).

Ten µL of filtrated extract were injected in a U-HPLC-MS system consisting of an Accela Series U-HPLC (ThermoFisher Scientific, Waltham, MA, USA) coupled to an Exactive mass spectrometer (ThermoFisher Scientific, Waltham, MA, USA) using a heated electrospray ionization (HESI) interface. Mass spectra were obtained using the Xcalibur software version 2.2 (ThermoFisher Scientific, Waltham, MA, USA). For quantification of the plant hormones, calibration curves were constructed for each analyzed component (1, 10, 50, and 100 µg L^{-1}) and corrected for 10 µg L^{-1} deuterated internal standards. Recovery percentages ranged between 92 and 95%.

4.3.7 Statistical analysis

Data for each measure time (T0, T4, T24 and T48) and parameter were subject to an analysis of variance using Statgraphics Centurion 18 (Statgraphics Technologies, Inc., The Plains, Virgina, USA). The mean comparisons were performed using Fisher's least significance difference (LSD) test at $P \leq 0.05$.

4.4. Results

4.4.1 Fresh weight

The fresh weight of leaves (Figure 1A) was affected by water stress at the end of the experiment with significant differences for both plant combinations, with a 28% and 83% reduction in V/N and V/V respectively, compared with control conditions. The fresh root weight (Figure 1B) was less affected by water stress without significant differences, the reduction was 12% and 8% for V/V and V/N, respectively and respect to their controls.

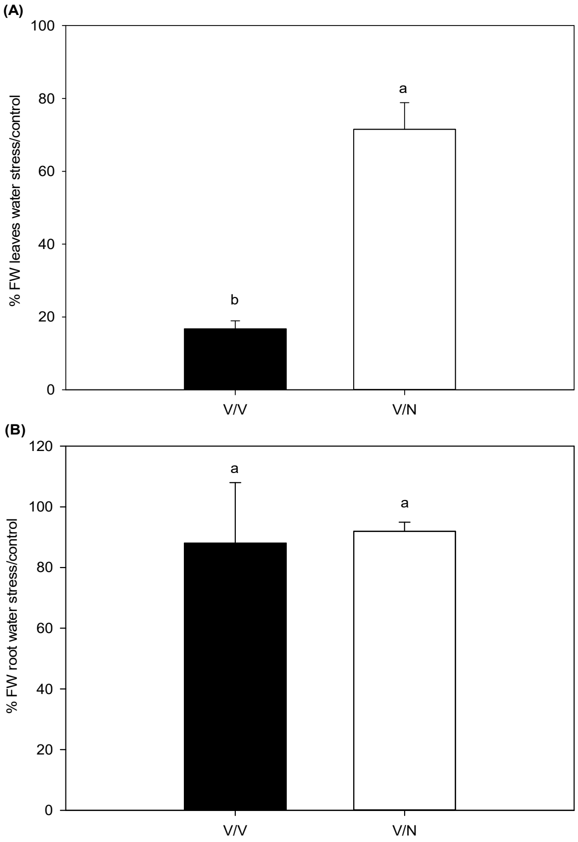

Figure 1. Percentage fresh weight in leaves **(A)** and roots **(B)** under water stress conditions compared to control conditions in the selfgrafted plants (V/V) and V grafted onto NIBER® (V/N). Values are mean for n = 4. Different letters are statistically different according with LSD test ($P \leq 0.05$).

4.4.2 Photosynthetic parameters

Instantaneous water use efficiency (A_N/E) (Figure 2A) did not show significant differences at T0 for V/V and V/N with values between 1.8-2.2. After 48h, all plants with PEG treatment increased significantly the A_N/E values. The increase with respect to its control plants was 47% for V/V and 44% for V/N, being the highest values for V/N-WS. Regarding intrinsic water use efficiency (A_N/g_s) (Figure 2B), differences between genotypes were already observed at T0, V/V showed lower values compared with V/ N. At the end of the experiment, plants under PEG treatment exhibited higher values with significant differences respect to control plants, plus the highest rise was observed in V/N plants.

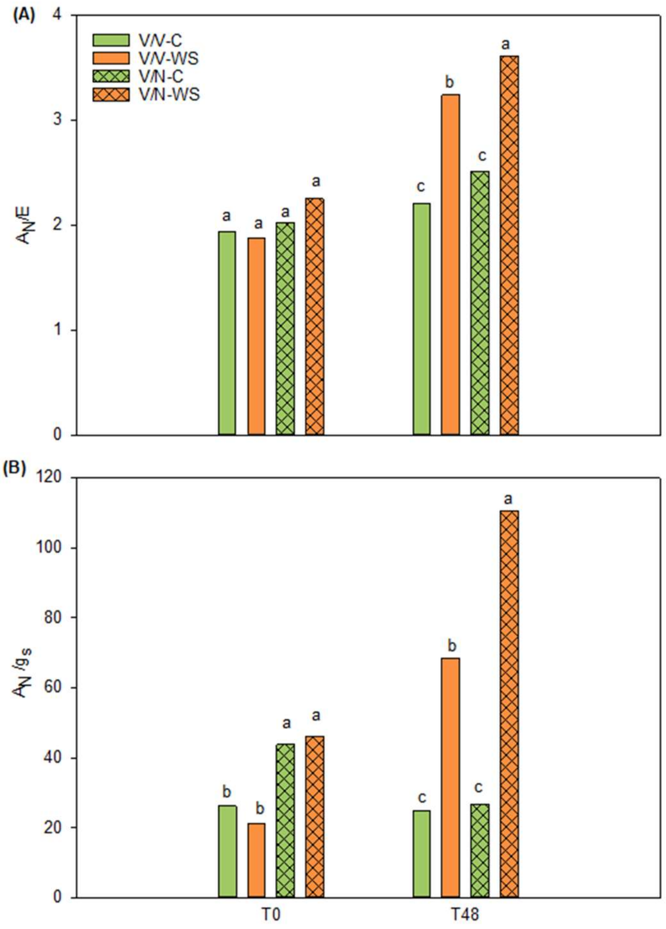

Figure 2. Instantaneous water use efficiency (A_N/E) **(A)** and intrinsic water use efficiency (A_N/g_s) **(B)** in the self-grafted pepper plants (V/V) and the plants grafted onto NIBER® (V/N) at 0% PEG (control, C) or 5% PEG (water stress, WS). Measurements were taken on T0 and T48 (hours after treatment with PEG began). Data are the mean values for n = 4. For each studied time, different letters indicate significant differences at P ≤ 0.05 (LSD test).

4.4.3 Hormonal profiling

4.4.3.1 ACC

In general terms, ACC levels were higher in roots than in leaves, reaching up to 4.5-fold as a mean value for all times and all plant combinations. At T0, in the control treatment, V/V and V/N did not show significant differences either in roots or in leaves (Figures 3A, B). From T4 to T48, ACC concentration remained constant for each plant combination and treatment except at T24 for V/V in roots and at T48 for V/N in leaves, when the highest ACC levels were observed in response to water stress.

4.4.3.2 ABA

In contrast to ACC, the ABA concentrations were higher in leaves than in roots. Similar to ACC at T0, ABA levels in roots and leaves (Figures 3C, D) did not display significant differences between V/V and V/N. In roots, at T4 and T24 the highest values were found in V/N-WS, while at the end of the experiment (T48) the ABA levels for this plant combination decreased by 54%. In leaves, V/N-WS ABA concentrations reached the highest values at T48 with significant differences. At T48 in roots and leaves, the lowest ABA values were found in V/V control plants, with significant differences to the rest of the plant combinations and treatments.

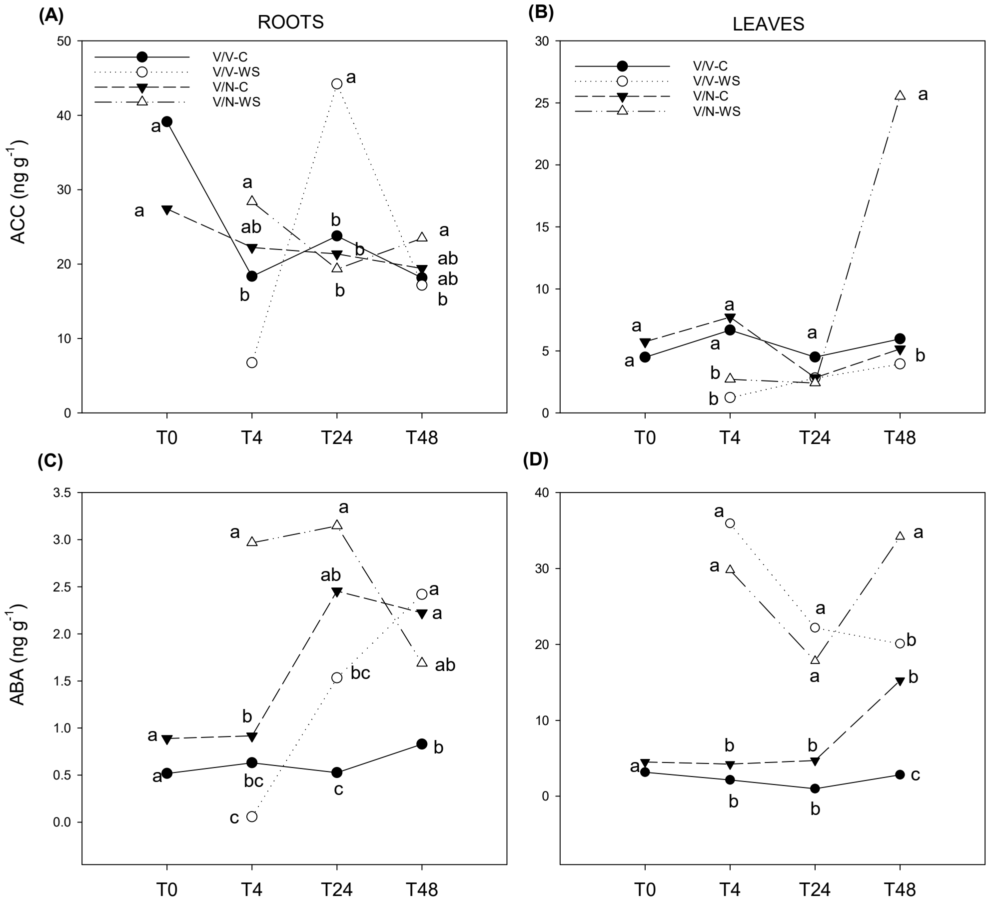

Figure 3. ACC **(A, B)** and ABA **(C, D)** levels in roots and leaves of self-grafted pepper plants (V/V) and the plants grafted onto NIBER® (V/N) at 0% PEG (control, C) or 5% PEG (water stress, WS). Measurements were taken on T0, T4, T24 and T48 (hours after treatment with PEG began). Data are the mean values for n = 4. For each studied time, different letters indicate significant differences at $P \leq 0.05$ (LSD test).

4.4.3.3 IAA

In roots, IAA concentration (Figure 4A) remained constant in V/N control and in V/V-WS decreased along the experiment. Nevertheless, for the rest of the plant combinations and treatments there was an erratic behavior, highlighting the IAA decrease from T24 to T48 for V/V control and the increase for V/N-WS. In leaves, IAA levels (Figure 4B) increased along the experiment (except for V/V control), reaching the maximum values at the end of the experiment in V/V-WS and V/N control, without significant differences with V/N-WS.

4.4.3.4 CKs

CKs levels were 9-fold lower in leaves than roots, showing different dynamics in both organs. In roots, CKs levels (Figure 4C) remained constant after a decrease from T0 to T4, except for a sustained increase in V/N-WS at T24, following a decrease to the lowest CKs concentrations at the end of the experiment. In leaves

(Figure 4D), CKs behavior resembled IAA role, with an increase from T4 to T48 for all plant combinations and treatments without significant differences between them at the end of experiment.

4.4.3.5 GAs

The concentrations of GAs were similar in leaves and roots (Figures 4E, F). In roots, an increase was observed in V/N control and V/V-WS from T4 to T48. In leaves, in response to water stress, a peak of GAs was detected at T24 in V/N-WS, decreasing later to reach similar values to the control plants. The lowest GA values were found in V/V plants under control and water stress conditions.

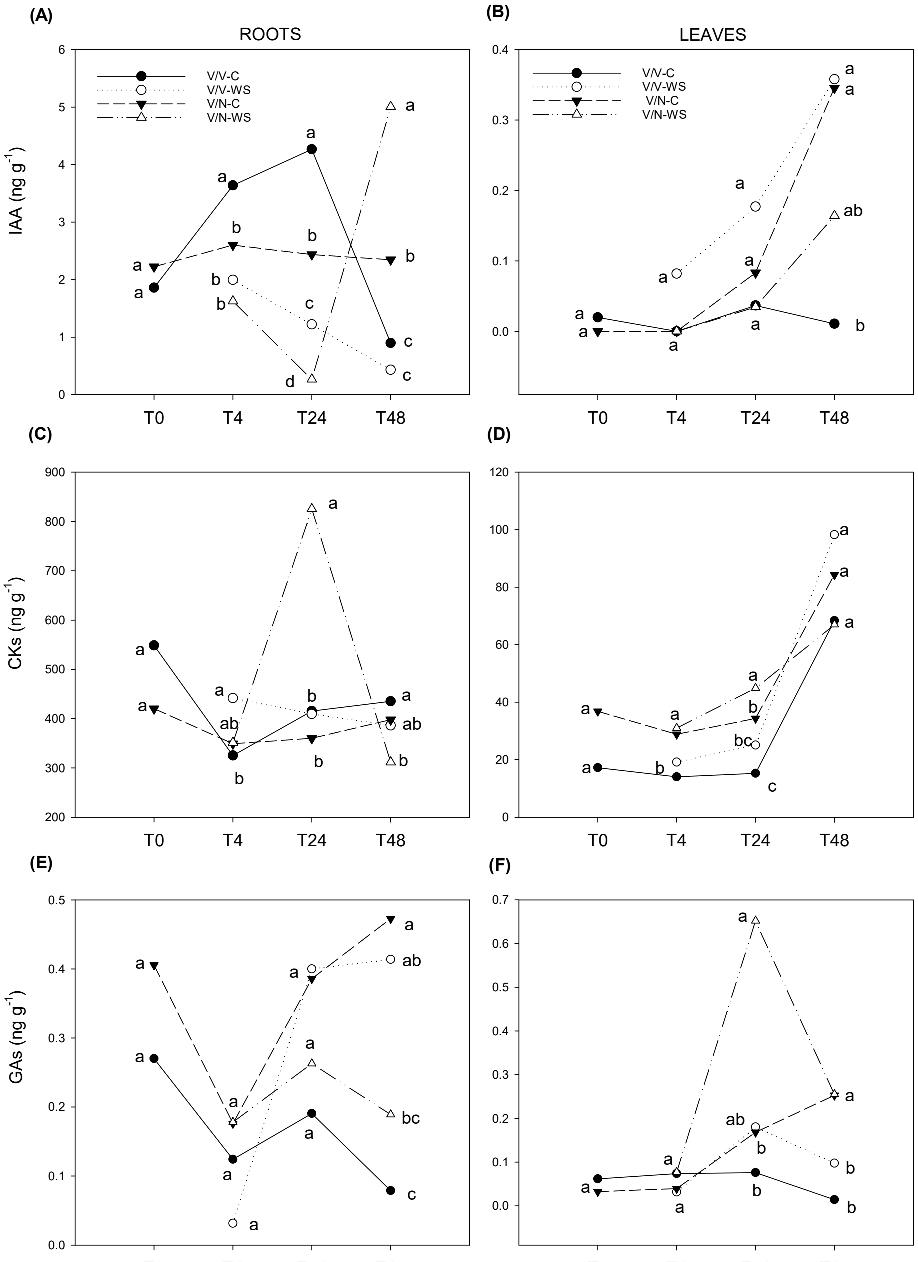

Figure 4. IAA **(A, B)**, CKs **(C, D)** and GAs **(E, F)** levels in roots and leaves of self-grafted pepper plants (V/V) and the plants grafted onto NIBER® (V/N) at 0% PEG (control, C) or 5% PEG (water stress, WS). Measurements were taken on T0, T4, T24 and T48 (hours after treatment with PEG began). Data are the mean values for n = 4. For each studied time, different letters indicate significant differences at P ≤ 0.05 (LSD test).

4.4.3.6 JA

In roots, the levels of JA (Figure 5A) were 9-fold (as average) higher than in leaves. In roots, both treatments showed a differential trend. The highest values were observed in control conditions with a peak in both plant combinations at T24. Under water stress, V/V and V/N displayed the lowest values, without significant differences between them. However, in leaves (Figure 5B), a peak at T24 in the JA levels was observed for all plant combinations and treatments, following a decrease until T48, being the highest values for V/N-WS and the lowest values for V/V-WS, with significant differences.

4.4.3.7 SA

In roots, increased SA concentrations in response to water stress were detected at T24 for V/V and V/N (Figure 5C). From T24 to T48 SA levels decreased to similar values for all plant combinations and treatments, without significant differences between them. A different evolution was observed in leaves (Figure 5D) with respect to roots, with a constant drop along the experiment in all plants and treatments, standing up V/N-WS with the highest concentration at T4. At the end of the experiment, two groups were separated, with highest SA levels belonging to water-stressed plants and lowest values to control plants.

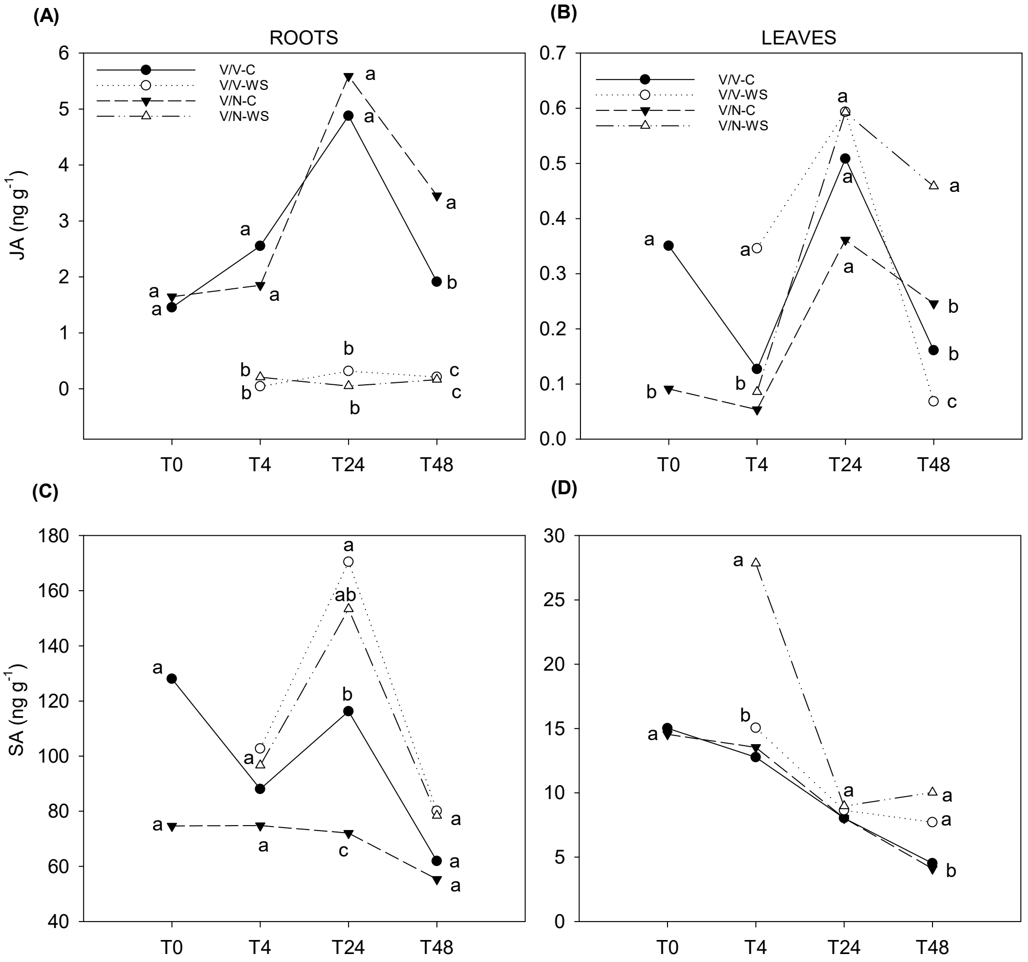

Figure 5. JA **(A, B)** and SA **(C, D)** levels in roots and leaves of self-grafted pepper plants (V/V) and the plants grafted onto NIBER® (V/N) at 0% PEG (control, C) or 5% PEG (water stress, WS). Measurements were taken on T0, T4, T24 and T48 (hours after treatment with PEG began). Data are the mean values for n = 4. For each studied time, different letters indicate significant differences at P ≤ 0.05 (LSD test).

4.5 Discussion

The study of hormone signaling fine-tuning during the early state of water stress exposure could help to distinguish and understand the tolerance responses in grafted plants mediated by efficient rootstocks. Indeed, plant hormones play a key role in controlling the adaptive processes to water stress, involving long-distance communication between different organs of plants together with in situ phytohormone synthesis (Albacete et al., 2008; Acosta- Motos et al., 2020; Lu et al., 2020).

Under water stress, roots are the first organs to perceive the osmotic stress, causing a rapid loss of shoot turgor and stomata closure, within minutes and hours (Munns, 2002). In this study, we observed at 48h that osmotic stress provoked a higher increase in A_N/g_s in V/N than in V/V. This indicates that the regulation of stomatal closure is more efficient in the V/N combination, thus allowing major water accumulation in the leaves. In this sense, the fresh weight loss on leaves caused by osmotic stress was reduced in V/N plants compared to V/V, since N was considered as a tolerant rootstock. However, no effect was detected in the fresh weight of the roots in both graft combinations, indicating that the leaves were more sensitive to osmotic stress than the roots. Several authors (Hsiao and Xu, 2000; Sharp, 2002; López-Serrano et al., 2019) have also observed this differential response between roots and leaves. This is interesting because V/N water requirements and use should be lower, implicating positive economic and environmental effects. Indeed, graft technology has been used as an effective tool to increase WUE under water stress in vegetable crops like tomato (Cantero-Navarro et al., 2016; Gaion et al., 2018; Fullana-Pericàs et al., 2020), pepper (Gisbert-Mullor et al., 2020; Padilla et al., 2021) or cucumber (Liu et al., 2016).

Water relations traits are controlled by hormonal signals from root to shoot and shoot to root. Currently, ABA is the primary hormone that modulates stomatal performance contributing to the regulation of water-mediated stomatal closure and plays a key role in drought resistance (Holbrook et al., 2002; Gaion et al., 2018; Yang et al., 2022). Under short-term water stress, it has been described that ABA is synthesized mainly in the roots and afterward transported into guard cells to trigger stomata closure in leaves (Wilkinson and Davies, 2002; Allario et al., 2013; Sarwat and Tuteja, 2017). We found a fast induction (T4) of ABA concentration under water stress in V/N for roots and leaves, but only for the leaves in V/ V. This suggests that the roots of a tolerant water stress rootstock such as NIBER® were more sensitive to changes in the osmotic potential of the nutrient solution. As a consequence, V/N speeded up ABA synthesis in roots and transport to the leaves (Liu et al., 2016), as it can be observed in ABA rise at T48 in leaves coinciding with ABA decrease in roots. Hence, a differential rootstock behavior was observed under water stress, with an ABA hypersensitivity or biosynthesis to ABA in V/N plants that can increase WUE in the scion thus enhancing stress tolerance. Similar responses were observed in different vegetable-grafted plants using tolerant rootstocks under water stress, such as cucumber grafted onto luffa (Liu et al., 2016) and tomato grafted onto different recombinant inbred lines from *Solanum pimpinellifolium* (Cantero-Navarro et al., 2016). Considering that the ABA levels in leaves were higher than in the roots in all plant combinations and treatments, the synthesis of ABA in the scion cannot be ruled out (Manzi et al., 2017; López-Serrano et al., 2020).

ABA and ethylene (or its precursor ACC) regulate stress responses in coordinated ways, in senescence, flooding, drought, and wounding stresses, and have been considered important WUE regulators under stress conditions (Wilkinson, 2004; Cantero-Navarro et al., 2016). However, the interaction between ethylene and ABA in relation to stomata closure is controversial and still not fully understood (Wilkinson et al., 2012; Chen et al., 2013). Generally, ABA and JA are positive regulators of stomata closure, while IAA and CKs have been described as negative regulators. However, the regulatory role of ethylene on stomata behavior is ambiguous, acting as a positive or negative regulator depending on the tissue and environmental conditions (Nemhauser et al., 2006; Huang et al., 2008; Daszkowska-Golec and Szarejko, 2013). In this sense, under water stress, elevated ABA levels usually limited ethylene production in maize plants (Sharp et al., 1994). In *Arabidopsis thaliana*, ethylene physiologically inhibited ABA-dependent stomata closure through the ethylene signaling pathway (Tanaka et al., 2005). Despite the apparent antagonist relation between ABA and ethylene under water stress (Spollen et al., 2000), in *A. thaliana* ethylene signaling was promoted during short-term ABA treatment (*ERF1*, *EDF1* and *EDF4* up-regulated) (Yang et al., 2014). In citrus (Tudela and Primo-Millo, 1992) and pea (Belimov et al., 2009), water stress induced an increase in ACC concentrations. Additionally, in grafted tomato plants, ACC in the roots could increase agronomic WUE (Cantero-Navarro et al., 2016). These results show that ethylene also plays an important role in stomatal control (Desikan et al., 2006; Vysotskaya et al., 2011). We did not find dramatic changes in ACC levels in leaves, except for an important increase at the end of the experiment (after 48h of water stress) in plants grafted onto NIBER®, coinciding with a significant rise of intrinsic WUE and ABA. These results could indicate that ACC is promoted at the initial stage of ABA-dependent control of water stress, using ACC as a rapid response to accelerate tolerance in V/N (Yang et al., 2014). Importantly, this effect was not observed in V/V plants, and only a maximum ACC concentration was measured at T24 in roots following an important decrease at T48h. This drop was not associated with an increase in leaves, which could indicate ACC degradation in the roots.

In addition to ABA and ethylene, JA and SA are also involved in the stomata response under water stress (Nazareno and Hernandez, 2017; Munemasa et al., 2019; Müller and Munné-Bosch, 2021). JA and 12-OPDA (JA precursor) are positive regulators of stomata closure, leading to increased drought stress tolerance (Savchenko and Dehesh, 2014). However, we did not find any change in JA concentrations in the root system under water stress, indicating that JA is not a primary hormonal factor controlling drought stress and/ or there was an early transient increase. Similarly, other studies did not find changes in JA under water stress, possibly due to JA accumulation being characterized as early transient (within 3h), therefore being dependent on the measure time (Luo et al., 2019; Wang et al., 2020; Huntenburg et al., 2022). In the leaves, the highest JA levels at the end of the experiment were found in V/N under water stress, which coincides with increased levels of ABA and ACC and stomata closure. Regarding SA, its role has been associated with biotic stress defense responses (Vlot et al., 2009). Recently, different research works have suggested that SA can have an important contribution to abiotic stress-induced signaling and tolerance (Miura and Tada, 2014; Zandalinas et al., 2016). However, the effect of SA on water stress tolerance is still unclear (Borsani et al., 2001). In our experimental conditions, SA increased at T24h in the roots mainly under water stress in both plant combinations, thus indicating that SA may be involved in drought responses. SA content augmented approximately 2-fold with water stress in barley roots associated to ABA increase (Bandurska and Stroinski, 2005), corresponding to our observations at T24h. In leaves, SA has been described to be implicated in stomata closure (Mori et al., 2001; Liu et al., 2013; Prodhan et al., 2018), and in the enhancement of antioxidants and antioxidant enzymes mainly to protect the photosynthetic apparatus (Miura and Tada, 2014; Khan et al., 2015; Zandalinas et al., 2016). The endogenous SA accumulation in leaves has been detected in several crops like citrus (Zandalinas et al., 2016), mustard (Alam et al., 2013), and *Phyllyrea angustifolia*, where SA levels were correlated with the water stress degree, increasing up to 5-fold under severe stress, thus suggesting a role for SA in drought tolerance (Munné-Bosch and Peñuelas, 2003). In pepper leaves, a drastic SA increase occurred immediately after water stress was applied only in V/N plants. Afterwards, SA concentrations decreased to reach values similar to V/V values, but higher than V/N control plants. This could indicate that SA accumulation is related to water stress, but it is also dependent on the rootstock genotype.

IAA, CKs, and GAs are hormones related to plant growth and development, and they are also involved in regulating drought responses (Devireddy et al., 2021; Raza et al., 2022). However, the variations of these hormones content under water stress are contradictory in our experiment. In roots under water stress, IAA content showed a gradual decline in V/V from T4 until the end of the experiment, but in V/N plants the IAA decrease occurred at T24 and, thereafter, IAA concentration increased up to a maximum. Regarding the concentrations of CKs under water stress, a transient increase at T24 in V/N was observed in roots and then CK levels declined to reach values similar to the optimal watering conditions and to the rest of the plant combinations and treatments. In both hormones, the highest concentrations were linked to water stress and to water stress tolerant rootstock (NIBER®), but this effect was not observed for GAs. IAA and CKs promote root branching and root growth, having a potential role in drought-tolerance mechanisms (Verma et al., 2016; Ullah et al., 2018). By using NIBER® as rootstock under salinity conditions for 10 days, a significant increase in root length was stated (López-Serrano et al., 2020), which could explain the increase in IAA and CKs when NIBER® is used under the osmotic treatment. In addition, increasing endogenous IAA levels in roots under osmotic stress have been associated with enhanced tolerance in *Arabidopsis* (Kim et al., 2013) and *Prosopis strombulifera* (halophyte) (Llanes et al., 2014) due to an increase in lateral root formation and enlarged root system (Llanes et al., 2016).

However, the GA trend in roots did not seem to be dependent on either water stress or rootstock genotype, considering that there were no significant differences between V/V and V/N at the end of the experiment.

In the leaves, IAA and CK levels increased along the experiment, but no significant differences were observed between both rootstock and treatments, which could indicate a poor relation with water stress. Increasing IAA in maize leaves was observed on the first day under water stress (provoked by PEG addition, -0.4MPa) (Wang et al., 2008) with an osmotic potential similar to the one used in this experiment. The increase of CKs has been related to an amelioration of the effect of water stress by stimulating osmotic adjustment and allowing water absorption. However, the increase in IAA and CKs in the majority of studies is associated with stimulated stomata opening and they are considered as ABA antagonists (Pospíšilová, 2003; Gaion et al., 2018). The stomata closure observed in our study could be the consequence of crosstalk between concentration and action place (Ullah et al., 2018; Iqbal et al., 2022).

Regarding GAs in leaves, they can modulate drought responses through stomata development and responses (Nir et al., 2014; Gaion et al., 2018). In our results, an important transient increase in leaves at T24 was recorded in V/N under water stress. Subsequently, GA levels declined to reach control values, and no differences in GA content associated with water stress were observed at the end of the experiment, although there were significant differences between rootstocks. Several studies have demonstrated that the reduction of GA levels contributes to plant growth restriction under drought (Llanes et al., 2016). Besides, in halophyte and some no-halophyte tolerant plants, GA concentrations in leaves increased in response to an osmotic potential decrease to maintain the growth (Li et al., 2012; Colebrook et al., 2014; Llanes et al., 2016). The transient increase observed in V/N under water stress could be associated with GA modulation and signaling for growth preservation.

The knowledge about endogenous phytohormone modulation in response to water stress remains scarce given that most plants' hormonal studies are based on exogenous applications. Overall, this work reflects the fast modulation of the balance of major phytohormones during short-term water stress in young pepper plants, self-grafted or grafted onto a water stress tolerant rootstock such as NIBER®. Phytohormone levels during early water stress exposure (up to 48h) revealed natural variability present in V/V and V/N and how V/N integrates various hormonal signals to tolerate drought imposition. It is essential to determine the water stress tolerance mechanisms and to find the key factors responsible for short-term tolerance, such as hormones. Therefore, this study will allow to understand the early differential responses to water stress in grafted pepper plants and the contribution of NIBER® rootstock hormonal balance to scion water stress improvement. This study will be crucial to extend knowledge and open the door to future biotechnological strategies to improve drought tolerance. However, due to the high level of complexity of the phytohormones network, further studies are required.

4.6 References

Acosta-Motos, J. R., Rothwell, S. A., Massam, M. J., Albacete, A., Zhang, H., and Dodd, I. C. (2020). Alternate wetting and drying irrigation increases water and phosphorus use efficiency independent of substrate phosphorus status of vegetative rice plants. *Plant Physiol. Biochem*. 155, 914–926. doi: 10.1016/j.plaphy.2020.06.017

Alam, M. M., Hasanuzzaman, M., Nahar, K., and Fujita, M. (2013). Exogenous salicylic acid ameliorates short-term drought stress in mustard (*Brassica juncea* L.) seedlings by up-regulating the antioxidant defense and glyoxalase system. *Aust J Crop Sci* 7, 1053–1063.

Albacete, A. A., Martínez-Andújar, C., and Pérez-Alfocea, F. (2014). Hormonal and metabolic regulation of source–sink relations under salinity and drought: From plant survival to crop yield stability. *Biotechnol Adv* 32, 12–30. doi: 10.1016/j.biotechadv.2013.10.005.

Albacete, A., Ghanem, M. E., Martinez-Andujar, C., Acosta, M., Sanchez-Bravo, J., Martinez, V., et al. (2008). Hormonal changes in relation to biomass partitioning and shoot growth impairment in salinized tomato (*Solanum lycopersicum* L.) plants. *J Exp Bot* 59, 4119–4131. doi: 10.1093/jxb/ern251.

Allario, T., Brumos, J., Colmenero-Flores, J. M., Iglesias, D. J., Pina, J. A., Navarro, L., et al. (2013). Tetraploid Rangpur lime rootstock increases drought tolerance via enhanced constitutive root abscisic acid production. *Plant Cell Environ* 36, 856–868. doi: 10.1111/pce.12021.

Aslam, S., Gul, N., Mir, M. A., Asgher, Mohd., Al-Sulami, N., Abulfaraj, A. A., et al. (2021). Role of Jasmonates, Calcium, and Glutathione in Plants to Combat Abiotic Stresses Through Precise Signaling Cascade. *Front Plant Sci* 12. doi: 10.3389/fpls.2021.668029.

Bandurska, H., and Stroinski, A. (2005). The effect of salicylic acid on barley response to water deficit. *Acta Physiol Plant* 27, 379–386. doi: 10.1007/s11738-005-0015-5.

Basu, S., Ramegowda, V., Kumar, A., and Pereira, A. (2016). Plant adaptation to drought stress. *F1000Res* 5, 1554. doi: 10.12688/f1000research.7678.1.

Belimov, A. A., Dodd, I. C., Hontzeas, N., Theobald, J. C., Safronova, V. I., and Davies, W. J. (2009). Rhizosphere bacteria containing 1-aminocyclopropane-1-carboxylate deaminase increase yield of plants grown in drying soil via both local and systemic hormone signalling. *New Phytologist* 181, 413–423. doi: 10.1111/j.1469-8137.2008.02657.x.

Borsani, O., Valpuesta, V., and Botella, M. A. (2001). Evidence for a Role of Salicylic Acid in the Oxidative Damage Generated by NaCl and Osmotic Stress in Arabidopsis Seedlings. *Plant Physiol* 126, 1024–1030. doi: 10.1104/pp.126.3.1024.

Brossa, R., López-Carbonell, M., Jubany-Marí, T., and Alegre, L. (2011). Interplay Between Abscisic Acid and Jasmonic Acid and its Role in Water-oxidative Stress in Wild-type, ABA-deficient, JA-deficient, and Ascorbate-deficient Arabidopsis Plants. *J Plant Growth Regul* 30, 322–333. doi: 10.1007/s00344-011-9194-z.

Cantero-Navarro, E., Romero-Aranda, R., Fernández-Muñoz, R., Martínez-Andújar, C., Pérez-Alfocea, F., and Albacete, A. (2016). Improving agronomic water use efficiency in tomato by rootstock-mediated hormonal regulation of leaf biomass. *Plant Science* 251, 90–100. doi: 10.1016/j.plantsci.2016.03.001.

Chen, H., Hsieh, E., Cheng, M., Chen, C., Hwang, S., and Lin, T. (2016). ORA47 (octadecanoid-responsive AP2/ERF-domain transcription factor 47) regulates jasmonic acid and abscisic acid biosynthesis and signaling through binding to a novel *cis* -element. *New Phytologist* 211, 599–613. doi: 10.1111/nph.13914.

Chen, L., Dodd, I. C., Davies, W. J., and Wilkinson, S. (2013). Ethylene limits abscisic acid- or soil drying-induced stomatal closure in aged wheat leaves. *Plant Cell Environ* 36, 1850–1859. doi: 10.1111/pce.12094.

Colebrook, E. H., Thomas, S. G., Phillips, A. L., and Hedden, P. (2014). The role of gibberellin signalling in plant responses to abiotic stress. *Journal of Experimental Biology* 217, 67–75. doi: 10.1242/jeb.089938.

Daszkowska-Golec, A., and Szarejko, I. (2013). Open or Close the Gate – Stomata Action Under the Control of Phytohormones in Drought Stress Conditions. *Front Plant Sci* 4. doi: 10.3389/fpls.2013.00138.

Davies, W. J., Kudoyarova, G., and Hartung, W. (2005). Long-distance ABA Signaling and Its Relation to Other Signaling Pathways in the Detection of Soil Drying and the Mediation of the Plant's Response to Drought. *J Plant Growth Regul* 24, 285. doi: 10.1007/s00344-005-0103-1.

de Ollas, C., Arbona, V., Gómez-Cadenas, A., and Dodd, I. C. (2018). Attenuated accumulation of jasmonates modifies stomatal responses to water deficit. *J Exp Bot* 69, 2103–2116. doi: 10.1093/jxb/ery045.

Desikan, R., Last, K., Harrett-Williams, R., Tagliavia, C., Harter, K., Hooley, R., et al. (2006). Ethylene-induced stomatal closure in Arabidopsis occurs via AtrbohF-mediated hydrogen peroxide synthesis. *The Plant Journal* 47, 907–916. doi: 10.1111/j.1365-313X.2006.02842.x.

Devireddy, A. R., Zandalinas, S. I., Fichman, Y., and Mittler, R. (2021). Integration of reactive oxygen species and hormone signaling during abiotic stress. *The Plant Journal* 105, 459–476. doi: 10.1111/tpj.15010.

Dodd, I. C., Theobald, J. C., Richer, S. K., & Davies, W. J. (2009). Partial phenotypic reversion of ABA-deficient flacca tomato (*Solanum lycopersicum*) scions by a wild-type rootstock: normalizing shoot ethylene relations promotes leaf area but does not diminish whole plant transpiration rate. *Journal of Experimental Botany*, 60(14), 4029–4039. https://doi.org/10.1093/JXB/ERP236

Ghanem, M. E., Albacete, A., Smigocki, A. C., Frébort, I., Pospíílová, H., Martínez-Andújar, C., Acosta, M., Sánchez-Bravo, J., Lutts, S., Dodd, I. C., & Pérez-Alfocea, F. (2011). Root-synthesized cytokinins improve shoot growth and fruit yield in salinized tomato (*Solanum lycopersicum* L.) plants. *Journal of Experimental Botany*, 62(1), 125–140. https://doi.org/10.1093/JXB/ERQ266

Druege, U. (2006). “Ethylene and Plant Responses to Abiotic Stress,” in *Ethylene Action in Plants* (Berlin, Heidelberg: Springer Berlin Heidelberg), 81–118. doi: 10.1007/978-3-540-32846-9_5.

Fahad, S., Nie, L., Chen, Y., Wu, C., Xiong, D., Saud, S., et al. (2015). “Crop Plant Hormones and Environmental Stress,” in, 371–400. doi: 10.1007/978-3-319-09132-7_10.

Fatma, M., Asgher, M., Iqbal, N., Rasheed, F., Sehar, Z., Sofo, A., et al. (2022). Ethylene Signaling under Stressful Environments: Analyzing Collaborative Knowledge. *Plants* 11, 2211. doi: 10.3390/plants11172211.

Fullana-Pericàs, M., Conesa, M. À., Ribas-Carbó, M., and Galmés, J. (2020). The Use of a Tomato Landrace as Rootstock Improves the Response of Commercial Tomato under Water Deficit Conditions. *Agronomy* 10, 748. doi: 10.3390/agronomy10050748.

Gaion, L. A., Braz, L. T., and Carvalho, R. F. (2018). Grafting in Vegetable Crops: A Great Technique for Agriculture. *International Journal of Vegetable Science* 24, 85–102. doi: 10.1080/19315260.2017.1357062.

Gisbert-Mullor, R., Pascual-Seva, N., Martínez-Gimeno, M. A., López-Serrano, L., Badal Marín, E., Pérez-Pérez, J. G., et al. (2020). Grafting onto an Appropriate Rootstock Reduces the Impact on Yield and Quality of Controlled Deficit Irrigated Pepper Crops. *Agronomy* 10, 1529. doi: 10.3390/agronomy10101529.

Gray, S. B., and Brady, S. M. (2016). Plant developmental responses to climate change. *Dev Biol* 419, 64–77. doi: 10.1016/j.ydbio.2016.07.023.

Großkinsky, D. K., Albacete, A., Jammer, A., Krbez, P., van der Graaff, E., Pfeifhofer, H., et al. (2014). A Rapid Phytohormone and Phytoalexin Screening Method for Physiological Phenotyping. *Mol Plant* 7, 1053–1056. doi: 10.1093/mp/ssu015.

Holbrook, N. M., Shashidhar, V. R., James, R. A., and Munns, R. (2002). Stomatal control in tomato with ABA-deficient roots: response of grafted plants to soil drying. *J Exp Bot* 53, 1503–1514. doi: 10.1093/JEXBOT/53.373.1503.

Hsiao, T. C., and Xu, L. (2000). Sensitivity of growth of roots versus leaves to water stress: biophysical analysis and relation to water transport. *J Exp Bot* 51, 1595–1616. doi: 10.1093/jexbot/51.350.1595.

Huang, D., Wu, W., Abrams, S. R., and Cutler, A. J. (2008). The relationship of drought-related gene expression in Arabidopsis thaliana to hormonal and environmental factors. *J Exp Bot* 59, 2991–3007. doi: 10.1093/jxb/ern155.

Huntenburg, K., Puértolas, J., de Ollas, C., and Dodd, I. C. (2022). Bi-directional, long-distance hormonal signalling between roots and shoots of soil water availability. *Physiol Plant* 174. doi: 10.1111/ppl.13697.

Iqbal, N., Fatma, M., Gautam, H., Sehar, Z., Rasheed, F., Khan, M. I. R., et al. (2022). Salicylic Acid Increases Photosynthesis of Drought Grown Mustard Plants Effectively with Sufficient-N via Regulation of Ethylene, Abscisic Acid, and Nitrogen-Use Efficiency. *J Plant Growth Regul* 41, 1966–1977. doi: 10.1007/s00344-021-10565-2.

Khan, M. I. R., Fatma, M., Per, T. S., Anjum, N. A., and Khan, N. A. (2015). Salicylic acid-induced abiotic stress tolerance and underlying mechanisms in plants. *Front Plant Sci* 6. doi: 10.3389/fpls.2015.00462.

Kim, J. I., Baek, D., Park, H. C., Chun, H. J., Oh, D.-H., Lee, M. K., et al. (2013). Overexpression of Arabidopsis *YUCCA6* in Potato Results in High-Auxin Developmental Phenotypes and Enhanced Resistance to Water Deficit. *Mol Plant* 6, 337–349. doi: 10.1093/mp/sss100.

Kyriacou, M. C., Rouphael, Y., Colla, G., Zrenner, R., and Schwarz, D. (2017). Vegetable Grafting: The Implications of a Growing Agronomic Imperative for Vegetable Fruit Quality and Nutritive Value. *Front Plant Sci* 8. doi: 10.3389/fpls.2017.00741.

Lacombe, B., and Achard, P. (2016). Long-distance transport of phytohormones through the plant vascular system. *Curr Opin Plant Biol* 34, 1–8. doi: 10.1016/j.pbi.2016.06.007.

Lee, J.-M., Kubota, C., Tsao, S. J., Bie, Z., Echevarria, P. H., Morra, L., et al. (2010). Current status of vegetable grafting: Diffusion, grafting techniques, automation. *Sci Hortic* 127, 93–105. doi: 10.1016/j.scienta.2010.08.003.

Li, C., Liu, G., Xu, C., Lee, G. I., Bauer, P., Ling, H.-Q., et al. (2003). The Tomato *Suppressor of prosystemin-mediated responses2* Gene Encodes a Fatty Acid Desaturase Required for the Biosynthesis of Jasmonic Acid and the Production of a Systemic Wound Signal for Defense Gene Expression. *Plant Cell* 15, 1646–1661. doi: 10.1105/tpc.012237.

Li, J., Sima, W., Ouyang, B., Wang, T., Ziaf, K., Luo, Z., et al. (2012). Tomato *SlDREB* gene restricts leaf expansion and internode elongation by downregulating key genes for gibberellin biosynthesis. *J Exp Bot* 63, 6407–6420. doi: 10.1093/jxb/ers295.

Li, W., Herrera-Estrella, L., and Tran, L.-S. P. (2016). The Yin–Yang of Cytokinin Homeostasis and Drought Acclimation/Adaptation. *Trends Plant Sci* 21, 548–550. doi: 10.1016/j.tplants.2016.05.006.

Liu, P., Xu, Z.-S., Pan-Pan, L., Hu, D., Chen, M., Li, L.-C., et al. (2013). A wheat *PI4K* gene whose product possesses threonine autophophorylation activity confers tolerance to drought and salt in Arabidopsis. *J Exp Bot* 64, 2915–2927. doi: 10.1093/jxb/ert133.

Liu, S., Li, H., Lv, X., Ahammed, G. J., Xia, X., Zhou, J., et al. (2016). Grafting cucumber onto luffa improves drought tolerance by increasing ABA biosynthesis and sensitivity. *Sci Rep* 6, 20212. doi: 10.1038/srep20212.

Llanes, A., Arbona, V., Gómez-Cadenas, A., and Luna, V. (2016). Metabolomic profiling of the halophyte *Prosopis strombulifera* shows sodium salt- specific response. *Plant Physiology and Biochemistry* 108, 145–157. doi: 10.1016/j.plaphy.2016.07.010.

Llanes, A., Masciarelli, O., and Luna, V. (2014). Growth responses to sulfate and chloride are related to different phytohormone profiles in the halophyte *Prosopis strombulifera*. *Emir J Food Agric* 26, 1097. doi: 10.9755/ejfa.v26i12.19121.

López-Serrano, L., Canet-Sanchis, G., Selak, G. V., Penella, C., San Bautista, A., López-Galarza, S., et al. (2020). Physiological characterization of a pepper hybrid rootstock designed to cope with salinity stress. *Plant Physiology and Biochemistry* 148, 207–219. doi: 10.1016/j.plaphy.2020.01.016.

López-Serrano, L., Canet-Sanchis, G., Vuletin Selak, G., Penella, C., San Bautista, A., López-Galarza, S., et al. (2019). Pepper Rootstock and Scion Physiological Responses Under Drought Stress. *Front Plant Sci* 10. doi: 10.3389/fpls.2019.00038.

Lu, X., Liu, W., Wang, T., Zhang, J., Li, X., and Zhang, W. (2020). Systemic Long-Distance Signaling and Communication Between Rootstock and Scion in Grafted Vegetables. *Front Plant Sci* 11. doi: 10.3389/fpls.2020.00460.

Luo, Z., Kong, X., Zhang, Y., Li, W., Zhang, D., Dai, J., et al. (2019). Leaf-Derived Jasmonate Mediates Water Uptake from Hydrated Cotton Roots under Partial Root-Zone Irrigation. *Plant Physiol* 180, 1660–1676. doi: 10.1104/pp.19.00315.

Manzi, M., Pitarch-Bielsa, M., Arbona, V., and Gómez-Cadenas, A. (2017). Leaf dehydration is needed to induce abscisic acid accumulation in roots of citrus plants. *Environ Exp Bot* 139, 116–126. doi: 10.1016/j.envexpbot.2017.05.004.

Miura, K., and Tada, Y. (2014). Regulation of water, salinity, and cold stress responses by salicylic acid. *Front Plant Sci* 5. doi: 10.3389/fpls.2014.00004.

Mori, I. C., Pinontoan, R., Kawano, T., and Muto, S. (2001). Involvement of Superoxide Generation in Salicylic Acid-Induced Stomatal Closure in *Vicia faba*. *Plant Cell Physiol* 42, 1383–1388. doi: 10.1093/pcp/pce176.

Müller, M., and Munné-Bosch, S. (2021). Hormonal impact on photosynthesis and photoprotection in plants. *Plant Physiol* 185, 1500–1522. doi: 10.1093/plphys/kiaa119.

Munemasa, S., Hirao, Y., Tanami, K., Mimata, Y., Nakamura, Y., and Murata, Y. (2019). Ethylene Inhibits Methyl Jasmonate-Induced Stomatal Closure by Modulating Guard Cell Slow-Type Anion Channel Activity via the *OPEN STOMATA 1/SnRK2.6* Kinase-Independent Pathway in Arabidopsis. *Plant Cell Physiol* 60, 2263–2271. doi: 10.1093/pcp/pcz121.

Munné-Bosch, S., and Peñuelas, J. (2003). Photo- and antioxidative protection, and a role for salicylic acid during drought and recovery in field-grown *Phillyrea angustifolia* plants. *Planta* 217, 758–766. doi: 10.1007/s00425-003-1037-0.

Munns, R. (2002). Comparative physiology of salt and water stress. *Plant Cell Environ* 25, 239–250. doi: 10.1046/j.0016-8025.2001.00808.x.

Muñoz-Espinoza, V. A., López-Climent, M. F., Casaretto, J. A., and Gómez-Cadenas, A. (2015). Water Stress Responses of Tomato Mutants Impaired in Hormone Biosynthesis Reveal Abscisic Acid, Jasmonic Acid and Salicylic Acid Interactions. *Front Plant Sci* 6. doi: 10.3389/fpls.2015.00997.

Mur, L. A. J., Kenton, P., Atzorn, R., Miersch, O., and Wasternack, C. (2006). The Outcomes of Concentration-Specific Interactions between Salicylate and Jasmonate Signaling Include Synergy, Antagonism, and Oxidative Stress Leading to Cell Death. *Plant Physiol* 140, 249–262. doi: 10.1104/pp.105.072348.

Nazareno, A. L., and Hernandez, B. S. (2017). A mathematical model of the interaction of abscisic acid, ethylene and methyl jasmonate on stomatal closure in plants. *PLoS One* 12, e0171065. doi: 10.1371/journal.pone.0171065.

Nemhauser, J. L., Hong, F., and Chory, J. (2006). Different Plant Hormones Regulate Similar Processes through Largely Nonoverlapping Transcriptional Responses. *Cell* 126, 467–475. doi: 10.1016/j.cell.2006.05.050.

Nir, I., Moshelion, M., and Weiss, D. (2014). The *Arabidopsis GIBBERELLIN METHYL TRANSFERASE 1* suppresses gibberellin activity, reduces whole-plant transpiration and promotes drought tolerance in transgenic tomato. *Plant Cell Environ* 37, 113–123. doi: 10.1111/pce.12135.

Padilla, Y. G., Gisbert-Mullor, R., López-Serrano, L., López-Galarza, S., and Calatayud, Á. (2021). Grafting Enhances Pepper Water Stress Tolerance by Improving Photosynthesis and Antioxidant Defense Systems. *Antioxidants* 10, 576. doi: 10.3390/antiox10040576.

Penella, C., Nebauer, S. G., Bautista, A. S., López-Galarza, S., and Calatayud, Á. (2014). Rootstock alleviates PEG-induced water stress in grafted pepper seedlings: Physiological responses. *J Plant Physiol* 171, 842–851. doi: 10.1016/j.jplph.2014.01.013.

Penella, C., Nebauer, S. G., Quiñones, A., San Bautista, A., López-Galarza, S., and Calatayud, A. (2015). Some rootstocks improve pepper tolerance to mild salinity through ionic regulation. *Plant Science* 230, 12–22. doi: 10.1016/j.plantsci.2014.10.007.

Pérez-Alfocea, F., Ghanem, M. E., Gómez-Cadenas, A., and Dodd, I. C. (2011). *Omics* of Root-to-Shoot Signaling Under Salt Stress and Water Deficit. *OMICS* 15, 893–901. doi: 10.1089/omi.2011.0092.

Pospíšilová, J. (2003). Participation of Phytohormones in the Stomatal Regulation of Gas Exchange During Water Stress. *Biol Plant* 46, 491–506. doi: 10.1023/A:1024894923865.

Prodhan, M. Y., Munemasa, S., Nahar, M. N. E. N., Nakamura, Y., and Murata, Y. (2018). Guard Cell Salicylic Acid Signaling Is Integrated into Abscisic Acid Signaling via the Ca2+/CPK-Dependent Pathway. *Plant Physiol* 178, 441–450. doi: 10.1104/PP.18.00321.

Rahayu, Y. S. (2005). Root-derived cytokinins as long-distance signals for NO_3-induced stimulation of leaf growth. *J Exp Bot* 56, 1143–1152. doi: 10.1093/jxb/eri107.

Raza, A., Salehi, H., Rahman, M. A., Zahid, Z., Madadkar Haghjou, M., Najafi-Kakavand, S., et al. (2022). Plant hormones and neurotransmitter interactions mediate antioxidant defenses under induced oxidative stress in plants. *Front Plant Sci* 13. doi: 10.3389/fpls.2022.961872.

Rouphael, Y., Cardarelli, M., Colla, G., and Rea, E. (2008). Yield, Mineral Composition, Water Relations, and Water Use Efficiency of Grafted Mini-watermelon Plants Under Deficit Irrigation. *HortScience* 43, 730–736. doi: 10.21273/HORTSCI.43.3.730.

Sachs, T. (2005). Auxin's role as an example of the mechanisms of shoot/root relations. *Plant Soil* 268, 13–19. doi: 10.1007/s11104-004-0173-z.

Sánchez-Rodríguez, E., Romero, L., and Ruiz, J. M. (2016). Accumulation of free polyamines enhances the antioxidant response in fruits of grafted tomato plants under water stress. *J Plant Physiol* 190, 72–78. doi: 10.1016/j.jplph.2015.10.010.

Saruhan, N., Saglam, A., and Kadioglu, A. (2012). Salicylic acid pretreatment induces drought tolerance and delays leaf rolling by inducing antioxidant systems in maize genotypes. *Acta Physiol Plant* 34, 97–106. doi: 10.1007/s11738-011-0808-7.

Sarwat, M., and Tuteja, N. (2017). Hormonal signaling to control stomatal movement during drought stress. *Plant Gene* 11, 143–153. doi: 10.1016/j.plgene.2017.07.007.

Savchenko, T., and Dehesh, K. (2014). Drought stress modulates oxylipin signature by eliciting *12-OPDA* as a potent regulator of stomatal aperture. *Plant Signal Behav* 9, e28304. doi: 10.4161/psb.28304.

Sharp, R. E. (2002). Interaction with ethylene: changing views on the role of abscisic acid in root and shoot growth responses to water stress. *Plant Cell Environ* 25, 211–222. doi: 10.1046/j.1365-3040.2002.00798.x.

Sharp, R. E., Wu, Y., Voetberg, G. S., Saab, I. N., and LeNoble, M. E. (1994). Confirmation that abscisic acid accumulation is required for maize primary root elongation at low water potentials. *J Exp Bot* 45, 1743–1751. doi: 10.1093/jxb/45.Special_Issue.1743.

Spollen, W. G., LeNoble, M. E., Samuels, T. D., Bernstein, N., and Sharp, R. E. (2000). Abscisic Acid Accumulation Maintains Maize Primary Root Elongation at Low Water Potentials by Restricting Ethylene Production. *Plant Physiol* 122, 967–976. doi: 10.1104/pp.122.3.967.

Tanaka, Y., Sano, T., Tamaoki, M., Nakajima, N., Kondo, N., and Hasezawa, S. (2005). Ethylene Inhibits Abscisic Acid-Induced Stomatal Closure in Arabidopsis. *Plant Physiol* 138, 2337–2343. doi: 10.1104/pp.105.063503.

Tudela, D., and Primo-Millo, E. (1992). 1-Aminocyclopropane-1-Carboxylic Acid Transported from Roots to Shoots Promotes Leaf Abscission in Cleopatra Mandarin (*Citrus reshni* Hort. ex Tan.) Seedlings Rehydrated after Water Stress. *Plant Physiol* 100, 131–137. doi: 10.1104/pp.100.1.131.

Ullah, A., Manghwar, H., Shaban, M., Khan, A. H., Akbar, A., Ali, U., et al. (2018). Phytohormones enhanced drought tolerance in plants: a coping strategy. *Environmental Science and Pollution Research* 25, 33103–33118. doi: 10.1007/s11356-018-3364-5.

Verma, V., Ravindran, P., and Kumar, P. P. (2016). Plant hormone-mediated regulation of stress responses. *BMC Plant Biol* 16, 86. doi: 10.1186/s12870-016-0771-y.

Vicente-Serrano, S. M. (2007). Evaluating the Impact of Drought Using Remote Sensing in a Mediterranean, Semi-arid Region. *Natural Hazards* 40, 173–208. doi: 10.1007/s11069-006-0009-7.

Vlot, A. C., Dempsey, D. A., and Klessig, D. F. (2009). Salicylic Acid, a Multifaceted Hormone to Combat Disease. *Annu Rev Phytopathol* 47, 177–206. doi: 10.1146/annurev.phyto.050908.135202.

Vysotskaya, L., Wilkinson, S., Davies, W. J., Arkhipova, T., and Kudoyarova, G. (2011). The effect of competition from neighbours on stomatal conductance in lettuce and tomato plants. *Plant Cell Environ* 34, 729–737. doi: 10.1111/j.1365-3040.2011.02277.x.

Wang, C., Yang, A., Yin, H., and Zhang, J. (2008). Influence of Water Stress on Endogenous Hormone Contents and Cell Damage of Maize Seedlings. *J Integr Plant Biol* 50, 427–434. doi: 10.1111/j.1774-7909.2008.00638.x.

Wang, J., Song, L., Gong, X., Xu, J., and Li, M. (2020). Functions of Jasmonic Acid in Plant Regulation and Response to Abiotic Stress. *Int J Mol Sci* 21, 1446. doi: 10.3390/ijms21041446.

Werner, T., Motyka, V., Strnad, M., and Schmülling, T. (2001). Regulation of plant growth by cytokinin. *Proceedings of the National Academy of Sciences* 98, 10487–10492. doi: 10.1073/pnas.171304098.

Wilkinson, S. (2004). “Water use efficiency and chemical signalling,” in *Water use efficiency in Plant Biology*, ed. M. A. Bacon (Blackwell Publishing), 75–112.

Wilkinson, S., and Davies, W. J. (2002). ABA-based chemical signalling: the co-ordination of responses to stress in plants. *Plant Cell Environ* 25, 195–210. doi: 10.1046/j.0016-8025.2001.00824.x.

Wilkinson, S., Kudoyarova, G. R., Veselov, D. S., Arkhipova, T. N., and Davies, W. J. (2012). Plant hormone interactions: innovative targets for crop breeding and management. *J Exp Bot* 63, 3499–3509. doi: 10.1093/jxb/ers148.

Yang, C., Liu, J., Dong, X., Cai, Z., Tian, W., and Wang, X. (2014). Short-Term and Continuing Stresses Differentially Interplay with Multiple Hormones to Regulate Plant Survival and Growth. *Mol Plant* 7, 841–855. doi: 10.1093/mp/ssu013.

Yang, L., Xia, L., Zeng, Y., Han, Q., and Zhang, S. (2022). Grafting enhances plants drought resistance: Current understanding, mechanisms, and future perspectives. *Front Plant Sci* 13. doi: 10.3389/fpls.2022.1015317.

Yao, X., Yang, R., Zhao, F., Wang, S., Li, C., and Zhao, W. (2016). An analysis of physiological index of differences in drought tolerance of tomato rootstock seedlings. *Journal of Plant Biology* 59, 311–321. doi: 10.1007/s12374-016-0071-y.

Zandalinas, S. I., Rivero, R. M., Martínez, V., Gómez-Cadenas, A., and Arbona, V. (2016). Tolerance of citrus plants to the combination of high temperatures and drought is associated to the increase in transpiration modulated by a reduction in abscisic acid levels. *BMC Plant Biol* 16, 105. doi: 10.1186/s12870-016-0791-7.

Zhang, Z., Cao, B., Gao, S., and Xu, K. (2019a). Grafting improves tomato drought tolerance through enhancing photosynthetic capacity and reducing ROS accumulation. *Protoplasma* 256, 1013–1024. doi: 10.1007/s00709-019-01357-3.

Zhang, Z., Cao, B., Li, N., Chen, Z., and Xu, K. (2019b). Comparative transcriptome analysis of the regulation of ABA signaling genes in different rootstock grafted tomato seedlings under drought stress. *Environ Exp Bot* 166, 103814. doi: 10.1016/j.envexpbot.2019.103814.

Zwack, P. J., and Rashotte, A. M. (2015). Interactions between cytokinin signalling and abiotic stress responses. *J Exp Bot* 66, 4863–4871. doi: 10.1093/jxb/erv172

CHAPTER IV

Leaves and roots metabolomic signatures underlying rootstock-mediated water stress tolerance in grafted pepper plants

Yaiza Gara Padilla[1], Begoña Miras-Moreno[2], Ramón Gisbert-Mullor[3], Luigi Lucini[2], Salvador López-Galarza[3], Ángeles Calatayud[1]

1 Departamento de Horticultura, Centro de Citricultura y Producción Vegetal, Instituto Valenciano de Investigaciones Agrarias (IVIA), CV-315, Km 10,7, Moncada, 46113 Valencia, Spain.

2 Department for Sustainable Food Process, Research Centre for Nutrigenomics and Proteomics, Università Cattolica del Sacro Cuore, 29122 Piacenza, Italy.

3 Departamento de Producción Vegetal, Centro Valenciano de Estudios sobre el Riego, Universitat Politècnica de València (UPV), Camí de Vera s/n, 46022 Valencia, Spain.

Under review

5.1. Abstract

Pepper rootstock NIBER® mitigates water stress effects on the grafted variety and increases biomass and yields. We comparatively explored the metabolomic responses to water stress in the pepper variety grafted onto NIBER® (V/N) and self-grafted variety (V/V). Untargeted analysis in leaves and roots allowed to find differences at the metabolome level. In V/V, the leaf biomass decreased under water stress, while the root biomass did not change. Contrarily, the leaf biomass in V/N was not affected by water stress, and the root biomass increased. Our results indicate that NIBER® modulates the grafted variety response to water stress, consistently with the differential metabolomic profiles in leaves and roots. The V/N-enriched metabolic pathways showed that the NIBER® response to water stress involves cutin and suberin biosynthesis, which act as protection layers, and jasmonic acid and jasmonates biosynthesis to favor signaling pathways. NIBER® avoided inducing flavonols and Chl b synthesis, probably to promote anthocyanins biosynthesis and an undisturbed Chla:Chlb ratio. Moreover, NIBER® increased vitamin B6, anthocyanins and stearic acid concentration in the variety leaves, whereas siroheme content rose in roots to improve nitrogen assimilation. The contribution of secondary metabolites (chlorogenic acid, shisonin, pinosylvin, glycoalkaloids, glucosinolates) to NIBER® water stress tolerance should be further studied.

5.2. Introduction

Drought is one of the most threatening natural phenomena to affect agriculture and, due to the climate change scenario, droughts have become more frequent, severer and longer. According to the FAO, 40 percent of the world population depends on agriculture to survive, and the impact of drought on developing countries is even worse for having an effect on not only the economy, but also on society [1].

The final consequence of drought stress for plants is significant productivity and yield losses, but in the meantime, processes such as nutrients uptake, CO_2 net assimilation and radiation use efficiency are negatively affected by water deficit [2]. The effects of drought on nutrients uptake extend to nutrients transport from roots to shoots. There is communication between both organs to sense the presence of water stress in soil and to transmit information through the vascular system [3].

This signal induced in the root that leads to adjustments in the shoot due to water stress conditions in soil can be assessed using suitable rootstocks. It has been proved that grafting onto tolerant rootstocks is a convenient strategy to overcome water stress in plants [4]. Focusing on vegetable grafting, several studies [5,6] report promising results when employing tolerant rootstocks under water stress conditions through different approaches like vigorous root-rootstock [7], active osmotic adjustment [8], ability to enhance the antioxidant defense system [9], photosynthesis maintenance [10], hormonal synthesis regulation [11], among other physiological mechanisms.

It is necessary to further understand the mechanism involved in water shortage tolerance. In this sense, “omics” sciences have been recently considered a powerful tool to uncover changes in the rootstock functional properties that affect the scion under environmental stresses and to understand the mechanisms that underlie tolerance (or sensitivity) in grafted plants to a greater extent [12]. In particular, untargeted metabolomics spots the differential accumulation of metabolites in both the rootstock and scion, including the biochemical changes that occur under water stress [13,14] and understanding adaptation to stresses in grafted plants from a holistic perspective. The metabolomic profile in plants includes a wide diversity of low-molecular-weight compounds, including sugar alcohols, polyamines, phenols, lipids, carbohydrates, amino acids, among others. Many of them are important and essential compounds for plant acclimation under stress conditions [15,16]. Variations in primary metabolism are easily recognized as a response to abiotic stresses (i.e., sugars, polyols, amino acids), yet secondary metabolism alterations are more specific of stress conditions and species and should not be left behind [17].

Accordingly, grafting has been reported as a factor for regulating the metabolome of a plant [18]. Some studies evaluate the metabolomics of low-temperature-exposed pepper rootstock roots [19] or the volatiles profile of pepper-grafted fruits [20]. Other studies show the effects of drought on the metabolic profile of pepper fruit [21], or pepper roots and shoots [22]. However, information about the metabolic changes that lead to grafted pepper plants’ increased tolerance to overcome water stress is lacking, with only a little evidence in tomato and citrus [4,23]. In our previous works, by a breeding program we obtained a hybrid pepper (NIBER®, F1) with greater vigor and more growth to be used as a rootstock. Then we tested the hybrid under water stress conditions in the field **[24]** to demonstrate that grafting a pepper cultivar onto an appropriate rootstock (NIBER®) overcomes the negative effects of sustained water stress conditions. All this was attributed to a less marked reduction in shoot dry weight (DW), which allowed greater whole photosynthesis by maintaining sink activity and higher plant biomass production and fruit yields compared to ungrafted plants.

By bearing this background in mind, we hypothesize in this study that the stress mitigation in the grafted plants using tolerant rootstock (NIBER®) compared to self-grafted plants under water shortage conditions could be ascribed to a distinct modulation of metabolic profiles after grafting under water stress. Accordingly, the aim of the present work was to evaluate and identify traits of tolerant rootstock NIBER® and the scion associated with early metabolic responses, and to elucidate biochemical bases under water stress conditions by the untargeted metabolomics approach.

5.3. Results

5.3.1. Dry biomass changes

Water stress has a significant impact on leaves DW at the end of the experiment (T48h), with significant differences obtained for V/V and V/N, and a 40% reduction in V/V and no reduction in V/N compared to the control conditions (Fig. 1A). The root DW displayed significant differences between V/V and V/N, and this DW did not lower in the V/V plants and increased for the V/N plants (up to 140%) versus the control conditions (Fig. 1B).

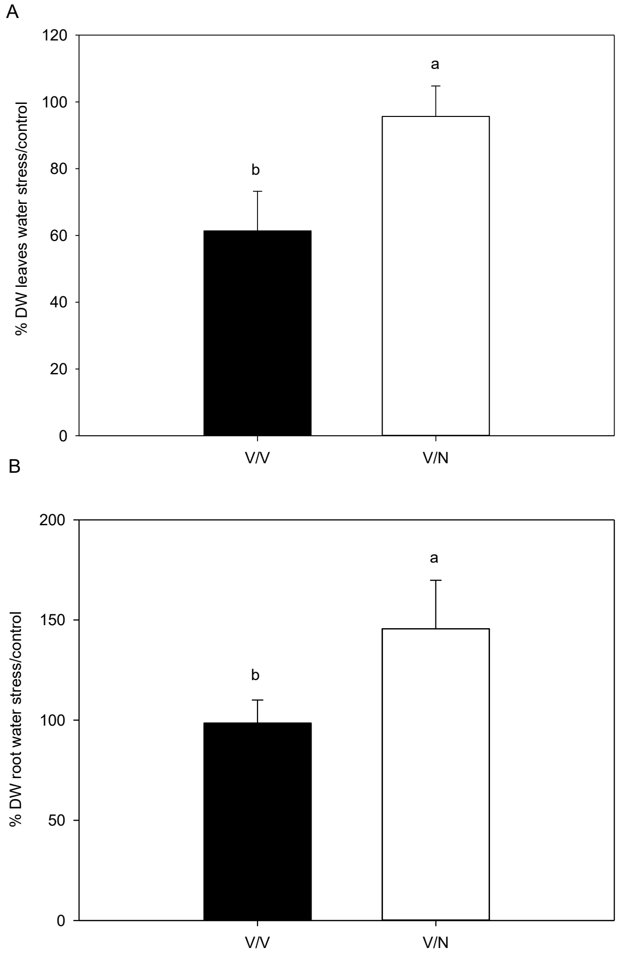

Fig. 1. Dry weight percentage of water stress in relation to the control conditions in the leaves **(A)** and roots **(B)** for V/V and V/N. Different letters indicate statistical differences for the LSD test with a p-value of <0.05 for n=5.

5.3.2. Untargeted metabolomics analysis of leaves and roots

An untargeted metabolomics approach was carried out to evaluate the effect of water stress on the V/V and V/N plants, from which 3995 and 4097 compounds were putatively annotated for leaves and roots, respectively (Supplementary Table 1).

The unsupervised fold-change-based hierarchical clustering (HCA) output on the metabolomic profile of leaves and roots (Fig. 2) was used to identify similarities and dissimilarities among treatments and plant combinations. This analysis pointed out that water stress was the main factor in clustering for both leaves (Fig. 2A) and roots (Fig. 2B). In fact two main clusters were observed to separate the control plants from the PEG-treated plants, and regardless of plant combinations. Nevertheless, V/V and V/N were clearly separated in two subclusters in water stress, and a similar trend for both leaves and roots was observed. This separation was further confirmed by the supervised OPLS model (Supplementary Figure 1), where first latent vector clearly separated the control plants from those treated with PEG, while the second vector separated samples according to rootstock (V and N).

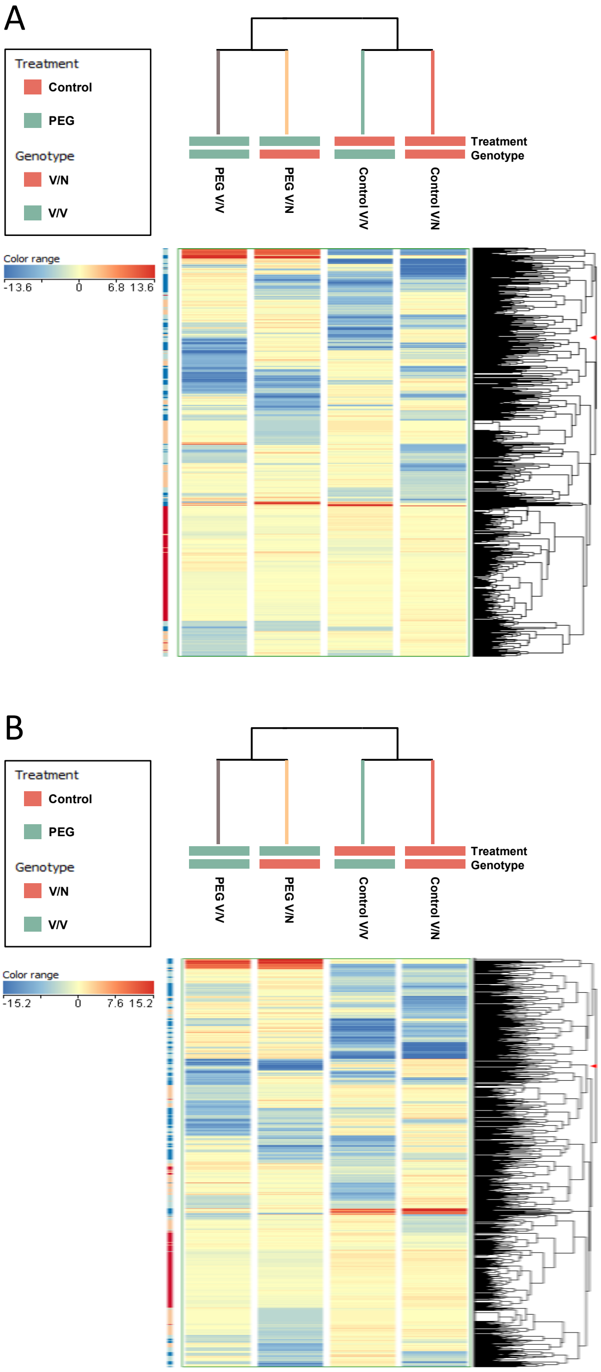

Fig. 2. Unsupervised hierarchical cluster analysis (HCA) (Euclidean similarity; Ward linkage rule) from the leaves **(A)** and roots **(B)** metabolomic profile of V/V and V/N under water stress (PEG) and the control conditions, obtained by UHPLC/QTOF-MS untargeted metabolomics. Clustering was performed on heat maps, which were based on fold change from compound intensity.

5.3.3. Water stress impact on plant metabolism

A Volcano analysis was carried out to identify differentially accumulated metabolites as a result of water stress exposure for each plant combination (V/V and V/N) and organ (leaves and roots) compared to the control plants (Supplementary Table 2). The Venn diagram performed using these significant compounds showed in leaves that 76 differentially up-accumulated metabolites overlapped between V/N and V/V (44% of all the metabolites) (Fig. 3A), and the number of specific up-accumulated metabolites was similar for both plant combinations (48 and 49, respectively). Nevertheless, only seven down-accumulated metabolites were in common for both plant combinations (15% of all the metabolites) (Fig. 3B). Additionally, 16 and 25 down-accumulated metabolites were specific for V/N and V/V, respectively. In all, the number of down-accumulated metabolites was bigger for V/V (32) than for V/N (23).

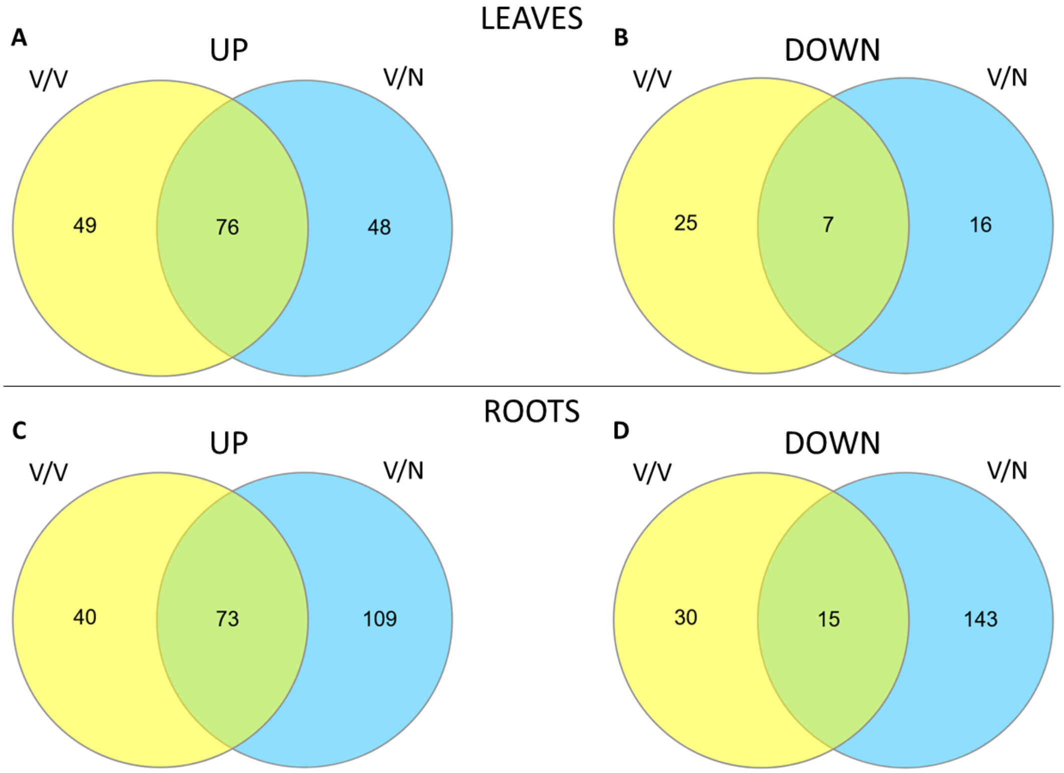

Fig. 3. Venn diagrams for the differential accumulated metabolites (DAM) under water stress in relation to the control conditions. **(A)** and **(B)** show the up-accumulated and down-accumulated DAMs in leaves, respectively. **(C)** and **(D)** denote the up-accumulated and down-accumulated DAMs in roots, respectively. Orange depicts the DAMs exclusive for V/N, blue is the DAMs specific for V/V and green represents the DAMs shared by both plant combinations.

In roots, the number of both up- (Fig. 3C) and down-accumulated (Fig. 3D) metabolites was larger in V/N than in V/V (182 vs. 113 and 158 vs. 45, respectively). Similarly to what happened with leaves, in roots water stress induced more common up-modulated metabolites (73) than common down-modulated metabolites (15), which represented 67% and 8% of all the metabolites, respectively. In addition, the number of specific up- and down-accumulated metabolites for V/N (109 and 143, respectively) was bigger than for V/V (40 and 30, respectively).

5.3.4. Metabolic pathways associated with water stress

In order to examine in-depth the observed variations on the metabolic profile of leaves and roots in V/N and V/V when exposed to water stress, we performed the PMN Pathway Enrichment analysis for the differentially accumulated metabolites using the Fisher Exact test and $p<0.05$ in the *Capsicum annuum* database. Several biosynthesis pathways were enriched for the aforementioned compounds according to the Pathway Tools pathway ontology (Supplementary Table 3).

Amino acid biosynthesis pathways (Figure 4A) were enriched in leaves and included "L-serine biosynthesis I" (V/V and V/N), "superpathway of L-lysine, L-threonine and L-methionine biosynthesis II" (V/V) and, forming part of the latter, "L-methionine biosynthesis II (plants)" (V/V). Amine- and polyamine biosynthesis-enriched pathways (Figure 4B) were "phosphatidylethanolamine biosynthesis II" and "superpathway of choline biosynthesis", both in V/V leaves. Regarding carbohydrate biosynthesis pathways (Figure 4C), the involved compounds came from the V/V leaves for "UDP-sugar biosynthesis" and the V/N leaves for "GDP-L-fucose biosynthesis I (from GDP-D-mannose)". Cell structure biosynthesis pathways (Figure 4D) "cutin biosynthesis" and "suberin monomers biosynthesis" were enriched in compounds in the V/N roots. The pathways related to cofactor, carrier and vitamin biosynthesis (Figure 4E) were only enriched in leaves, with "NAD metabolism" and "NAD biosynthesis" for both plant combinations and "vitamin B6 biosynthesis" for V/N, specifically "pyridoxal 5'-phosphate biosynthesis II" in leaves. Both the leaves and roots of V/V and V/N were enriched in fatty acid and lipid biosynthesis pathways (Figure 4F); i.e., "superpathway of phospholipid biosynthesis II (plants)" was enriched in the V/V leaves, whereas "fatty acid biosynthesis" was enriched in the leaves of V/V and V/N and roots of V/V. As part of the latter, "very long fatty acid biosynthesis II" was enriched in all the plant combinations and organs, while "stearate biosynthesis II (bacteria and plants)" and "polyunsaturated fatty acid biosynthesis pathways" were enriched only in the V/N leaves. Regarding nucleotide and nucleoside biosynthesis pathways (Figure 4G), "superpathway of pyrimidine ribonucleosides salvage" was enriched in the leaves of both plant combinations, "superpathway of pyrimidine deoxyribonucleoside salvage" in the V/V roots, "superpathway of purine nucleotides de novo biosynthesis I" in the V/V leaves and V/N roots and, pertaining to the last one, "adenosine ribonucleotides de novo biosynthesis I" and "inosine-5'-phosphate biosynthesis II" in the V/V leaves and V/N roots. The pathways belonging to other biosynthesis (Figure 4H) were enriched in leaves, i.e., the "curcumin glucoside biosynthesis" pathway was enriched in both plant combinations. As for polyprenyl biosynthesis (Figure 4I), enrichment was present only in the V/V leaves for "superpathway of geranylgeranyl diphosphate biosynthesis II (via MEP)". Last, tetrapyrrole biosynthesis pathways (Figure 4J) were exclusively enriched in roots; that is, "porphyrin compound biosynthesis" in V/V and "siroheme biosynthesis" in both plant combinations.

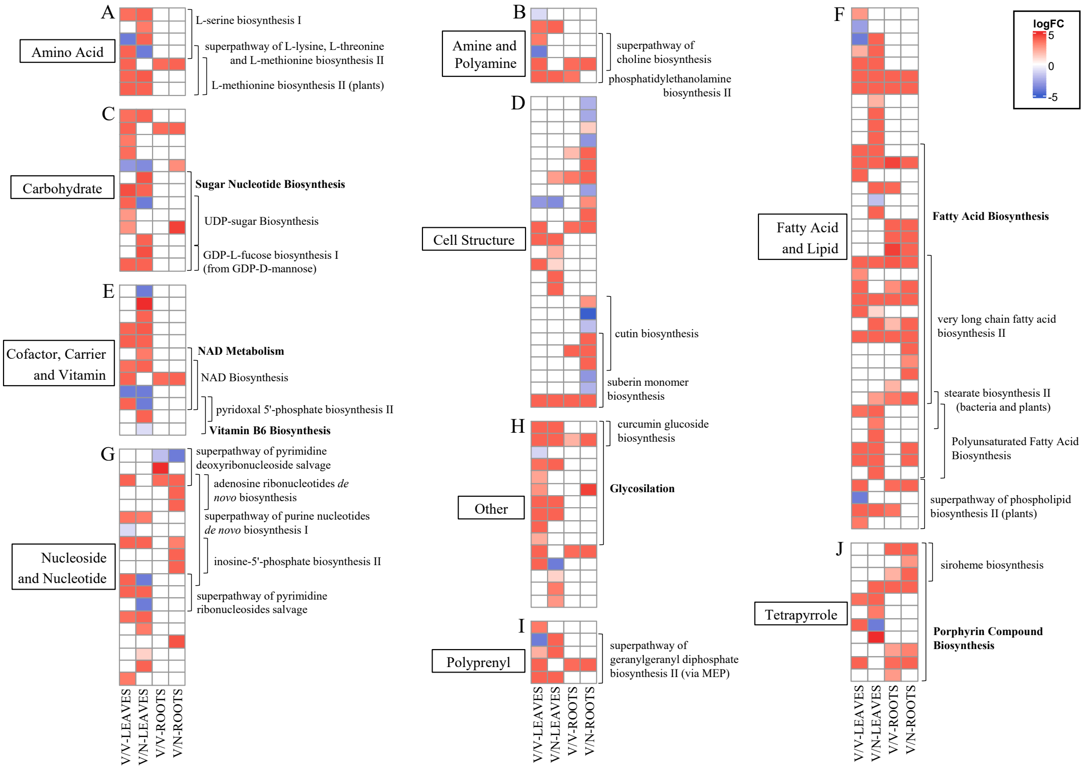

Fig. 4. Enriched biosynthesis metabolic pathways under water stress in relation to the control conditions in V/V and V/N leaves and roots. Heat maps were based on metabolites log (fold change, FC) in water stress versus the control conditions. Red depicts up-accumulation under water stress (positive logFC), blue denotes down-accumulation (negative logFC) and white indicates no differences between treatments.

Given the amount of differentially accumulated metabolites associated with the secondary metabolism, enriched secondary metabolites biosynthesis pathways are represented independently in Figure 5. Nitrogen-containing glucoside biosynthesis pathways (Figure 5A) were associated mainly with glucosinolates biosynthesis and enriched in the leaves of both plant combinations and V/N roots. Other nitrogen-containing secondary compound biosynthesis (Figure 5B) only included “alpha-solanine/alpha-chaconine biosynthesis” as an enriched pathway in the roots of both plant combinations and V/V leaves, despite many compounds being differentially accumulated in the V/N roots. Regarding hormone biosynthesis pathways (Figure 5C), “trans-zeatin biosynthesis” was enriched in the V/V leaves, “jasmonate biosynthesis” in the leaves of both plant combinations and V/N roots and, as part of the latter, “jasmonic acid biosynthesis” in the leaves of both plant combinations. Terpenoid biosynthesis (Figure 5D) showed only enriched pathways in V/V, with “methylerythritol phosphate pathway I” and “methylerythritol phosphate pathway II” in leaves, and “olivetol biosynthesis” in roots. Regarding phenylpropanoid derivative biosynthesis pathways, the enriched flavonoid biosynthesis pathways (Figure 5E) were “flavonol biosynthesis” in the V/V leaves, which comprised “quercetin gentiotetraside biosynthesis” in the leaves of both plant combinations. Also belonging to flavonoid biosynthesis (Figure 5E), the “anthocyanin biosynthesis pathway” was enriched in the leaves of V/N and included “cyanidin 3,7-diglucoside polyacylation biosynthesis” and “shisonin biosynthesis” enriched in the V/V roots, and “viodelphin biosynthesis” enriched in the leaves of both plant combinations and V/V roots. Other phenylpropanoid derivative biosynthesis enriched pathways (Figure 5F) were “stilbene phytoalexin biosynthesis” in the V/V roots, “cinnamate biosynthesis” and, forming part of the latter, “chlorogenic acid biosynthesis II” in the V/N roots, “hydrolyzable tannin biosynthesis” in the leaves of both plant combinations and, pertaining to the latter, “ellagitannin biosynthesis” in both V/V leaves and V/N roots.

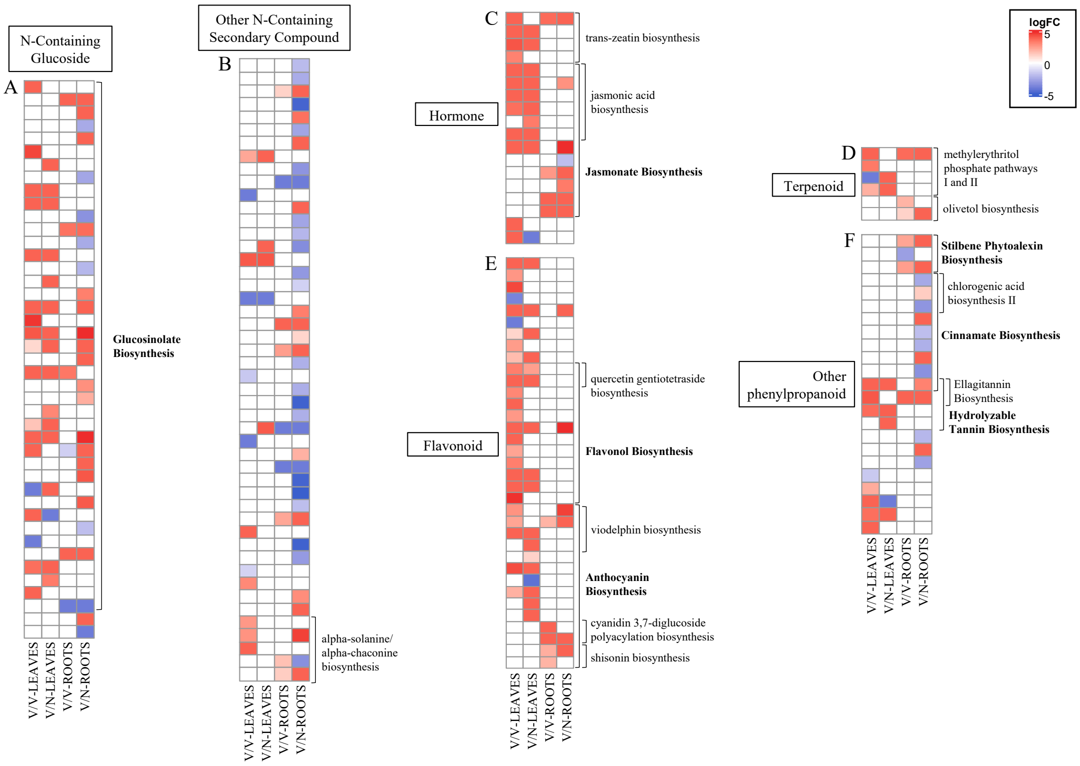

Figure 5. Enriched secondary metabolites biosynthesis metabolic pathways under water stress in relation to the control conditions in V/V and V/N leaves and roots. Heat maps were based on metabolites log (fold change, FC) in water stress versus the control conditions. Red depicts up-accumulation under water stress (positive logFC), blue refers to down-accumulation (negative logFC) and white denotes no differences between treatments.

5.4. Discussion

5.4.1. Pepper metabolic response to water stress

Water stress is an important constraint and, as such, understanding tolerance mechanisms for the development of tolerant crops is urgent. In this study, we performed a water stress experiment on self-grafted pepper plants (V/V) and plants grafted onto tolerant pepper rootstock NIBER® (V/N) **[24,25]**.

Plant metabolism is entirely affected by water stress, and both primary and secondary metabolisms are disturbed together with metabolic networks, which reprogram to counteract the detrimental effects of stress **[26,27]**. In our experiment, a strong impact was noted in the early water stress exposure stage on the metabolism because the biggest differences in metabolic profiles were found between treatments (water stress and control conditions) in both plant combinations (V/V and V/N) and organs (leaves and roots) (Figure 2). These results evidence the importance of studying the metabolic profile to understand the metabolic responses to short-term water stress and the associated metabolites.

Several authors report many "drought-responsive" metabolites. You et al. (2019) **[27]** identified more than half the metabolites as being drought-responsive metabolites (113 of 221 metabolites) in common for drought-tolerant and -sensitive sesame genotypes. Ma et al. (2021) **[28]** obtained similar results in the metabolic profile of drought-tolerant and -sensitive alfalfa cultivars under drought stress, with 131/427 metabolites shared by both cultivars. In the present study, of the 138 differentially accumulated metabolites (up- and down-) in leaves, 83 metabolites accumulated in both V/V and V/N as a response to the water stress conditions (Figure 3A,B). In roots, the number of common accumulated metabolites between both plant combinations under water stress (88) in relation to the total number of accumulated metabolites (322) was lower than in leaves. In fact the total number of accumulated metabolites (up- and down-) in relation to the control conditions was significantly bigger in roots than in leaves (322 vs. 138) (Figure 3). This result evidences that the rootstock influences the metabolic response to water stress because most metabolites differentially accumulate in roots and these metabolites are not common between V/V and V/N.

Our results indicate that rootstock affects the metabolome of the variety (leaves). This differential metabolic profile was manifested in the variety grafted onto rootstock NIBER® under water stress, and no significant reduction occurred in the leaf biomass in the water-stressed V/N plants compared to the control V/N plants and the root biomass considerably increased (Figure 1). The differential biomass response in V/V and V/N under water stress could be associated with the metabolomic profiles in the V/N and V/V plants, which could provide useful information in water stress tolerance mechanisms.

5.4.2. Enriched metabolic pathways under water stress

The water stress-responsive metabolites in this study were associated with biosynthesis (Figure 4) and secondary metabolism biosynthetic pathways (Figure 5).

The *L-serine biosynthesis I pathway*, also called the *phosphorylated pathway of L-serine biosynthesis* (PPSB), was enriched in the leaves of V/V and V/N. The PPSB is crucial for plant development and metabolism, and is responsible for providing serine under abiotic stress conditions **[29]**. Serine is used for the biosynthesis of phospholipids and amines, but also in signaling and the creation of reducing power **[30]**. Phospholipids are mainly found in non plastid membranes in plants as phosphatidylethanolamine and phosphatidylcholine. Both the *phosphatidylethanolamine biosynthesis II pathway* and the *superpathway of choline biosynthesis* were enriched in the V/V leaves. However, there is a competition between CDP-choline and CDP-ethanolamine to produce either phosphatidylcholine or phosphatidylethanolamine **[31]**. In our experiment, the V/V leaves seemed to prefer phosphatidylethanolamine biosynthesis over phosphatidylcholine, despite choline having been identified as a precursor for glycine betaine and its synthesis pathway being enhanced in salt stress for osmoprotection **[32,33]**. In fact intermediate CDP-ethanolamine was up-accumulated in the V/V and V/N leaves, even though this pathway was not enriched in V/N. Moreover, the first enzyme in the *phosphatidylethanolamine biosynthesis II pathway*, named serine decarboxylase, is strongly activity-dependent on pyridoxal 5'-phosphate (PLP) **[34]**. PLP was up-accumulated in the V/N leaves, in which the *pyridoxal 5'-phosphate biosynthesis II pathway* and *vitamin B6 biosynthesis* were enriched. PLP is the biochemically active form of vitamin B6, whose antioxidant role is emerging, and is also used as cofactor to catalyze numerous reactions **[35]**. The vitamin B6 antioxidant ability of reactive oxygen species (ROS) scavenging has been linked with abiotic stress tolerance **[36]**.

NAD^+ is another cofactor that is widely used in many metabolic reactions, and the *NAD de novo biosynthesis I (from aspartate) pathway* was enriched in the V/V and V/N leaves. Abiotic stress unbalances the redox system in cells that depends on the reducing power of NAD^+ and $NADP^+$ to reduce glutathione and ascorbate, among other antioxidant compounds **[37]**. NAD^+ was up-accumulated under water stress for both plant combinations, but NADH only increased in the V/N leaves. This NADH in leaves could be an advantage for V/N to regenerate the NAD^+ pool and to increase reducing power under water stress.

NAD^+ also participates in the biosynthesis of fatty acids, whose associated *very long chain fatty acid biosynthesis II pathway* was enriched in V/V and V/N leaves and roots. The first compound in this pathway is stearoyl-CoA, which is converted into 3-oxoicosanoyl-CoA and was up-accumulated in the V/V roots and V/N roots and leaves. Gundaraniya et al. (2020) **[38]** observed an up-accumulation of stearic acid in the leaves of a drought-tolerant genotype and in the roots of a drought-sensitive genotype in peanut under water stress. This compound is synthesized by means of the *stearate biosynthesis II (bacteria and plants) pathway*, which was enriched in the V/N leaves. This finding suggests that rootstock NIBER® had an effect on promoting stearate biosynthesis in the leaves of the grafted variety. The above-mentioned pathway derives from the *palmitate biosynthesis II (bacteria and plants) pathway*, which is also further extended to *suberin monomers biosynthesis* and *cutin biosynthesis*. These two pathways were enriched in the V/N roots, and they play an important role in maintaining the stock of extracellular barrier constituents, i.e., cutin and suberin **[39]**. Zhang et al. (2021) **[40]** studied the lipidomic response to drought in sorghum genotypes and reported an increase in cutin and its monomers only in the drought-tolerant genotype. In V/N, several compounds involved in these pathways were up-accumulated in leaves (docosanoyl-CoA, 22-carboxy-docosanoyl-CoA, 10,16-dihydroxypalmitoyl-CoA) and roots (22-oxo-docosanoyl-CoA, palmitoyl-CoA, 16-hydroxypalmitoyl-CoA, 10,16-dihydroxypalmitoyl-CoA), probably to favor cutin and suberin biosynthesis, which act as barriers that control non stomatal fluxes of water, solutes and gases to protect plants from water stress **[41]**.

According to He et al. (2020) **[39]**, apart from being extracellular barrier constituents and membrane components, unsaturated fatty acids are involved in stress defense as the precursors of bioactive and signaling molecules (i.e., jasmonic acid (JA), nitroalkenes). In this experiment, the *jasmonic acid biosynthesis pathway* was enriched in the leaves of both plant combinations and *jasmonate biosynthesis*, which refers to JA precursors and derivatives, was enriched in the V/V leaves and V/N leaves and roots. An increase in JA was quantified in the NIBER® roots under water stress in relation to the control conditions **[42]**, and coincided with the up-regulation of transcription factor *MYC2*, which promotes the gene expression of dehydration resistance-associated genes **[43]**. Taken together, these results support the involvement of JA in NIBER® tolerance under water stress. However, the *trans-zeatin biosynthesis pathway*, the other hormone biosynthesis pathway enriched in this analysis, displayed contrasting behavior in both V/V and V/N. Cytokinins regulate the shoot/root ratio to promote shoot growth over root growth, and changes in this ratio are common under water stress **[44]**. The pathway was exclusively enriched in the V/V leaves in which intermediate metabolites were up-accumulated, and the opposite was observed in the V/N roots, where trans-zeatin and other intermediates were down-accumulated. These results suggest a more limited involvement of cytokinins in the NIBER® response to water stress, and was manifested in the markedly increased root DW in the V/N plants. Nevertheless, CKs concentration at 24 h under water stress was significantly higher in the NIBER® roots **[11]**, following a decrease until the end of the experiment (48 h), which suggests that CKs synthesis is not prevented in the very early response to water stress (24 h) and regulation mechanisms could be later promoted (48 h).

The *trans-zeatin biosynthesis pathway* needs a source for the prenyl group, which can be the *mevalonate pathway* (MVA) in the cytosol or the *methylerythritol phosphate pathway* (MEP) in plastids **[45]**. In our study, the *MEP pathways I and II* were enriched in the V/V leaves and, in addition to the prenyl group, they provide isopentenyl diphosphate for the *geranylgeranyl diphosphate biosynthesis pathway*, which was also enriched in the V/V leaves. Geranylgeranyl diphosphate (GGPP) that comes from the *MEP pathway* in plastids is an intermediate to synthesize gibberellins, carotenoids, tocopherols, chlorophylls, among others **[46]**. Nevertheless, in V/V we did not observe enrichment on any biosynthesis pathways associated with these essential metabolites. Hence they must have a different purpose or may be modulated by feedback regulation. The overexpression of the *MEP pathway* enzymes only achieved bigger plastidial isoprenoids production because post-transcriptional regulation prevented marked increases in the enzyme's activity **[47]**.

Chlorophyll a (Chl a) was up-accumulated in the V/N (leaves and roots) and V/V leaves, whereas 71-dihydroxychlorophyllide a was up-accumulated in the V/V roots. 71-

dihydroxychlorophyllide a is an intermediate in chlorophyll b (Chl b) biosynthesis, which is performed by chlorophyllide a oxygenase (CAO) in the chlorophyll cycle **[48]**. In previous experiments **[42]**, the *CAO* gene was down-regulated in NIBER® vs. A10 (a water stress-sensitive accession) under the control conditions. It may seem that NIBER® does not promote Chl b biosynthesis, perhaps to avoid changes in the Chl a:Chl b ratio that usually lowers under water stress, and this reduction is faster in drought-sensitive genotypes **[49]**. Chl a is a tetrapyrrole, specifically a porphyrin compound, and the *porphyrin compound biosynthesis pathway* was enriched in both the V/V roots and V/N leaves. The *siroheme biosynthesis pathway* was enriched in the roots of both plant combinations. This compound is a modified tetrapyrrole that is similar in structure to chlorophyll. Some intermediates of this pathway were up-accumulated in roots (preuroporphyrinogen, percorrin-1, percorrin-2), as well as siroheme. Siroheme is an iron-containing prosthetic group in sulfite and nitrite reductases and, thus, plays a main role in nitrogen assimilation **[50]**. In preceding experiments, when NIBER® was used as a rootstock under salt stress, its roots showed a slighter decrease in nitrate reductase activity than the self-grafted and ungrafted variety compared to the control conditions **[51]**. Moreover in Padilla et al. (2023) **[42]**, up to five genes coding for vacuolar iron transporters were down-regulated in the NIBER® roots under water stress. Taking together previous and present results, it may seem that NIBER® attempts to perform better nitrogen assimilation by modulating nitrate and nitrite reductases activity, the latter by increasing siroheme synthesis, which is favored by less iron compartmentation in the vacuole.

S-adenosyl-L-methionine (SAM) is a methyl donor in siroheme biosynthesis that derives from L-methionine and the L-*methionine biosynthesis II (plants) pathway* was enriched in the V/V leaves. Methionine is a protein constituent and the precursor of SAM, which participates in the synthesis of ethylene and polyamines (spermine and spermidine), among others **[52]**. However, no SAM- or ethylene- and polyamines-related pathways or metabolites accumulated in V/V. Another function of methionine through SAM is the regulation of cellular processes by transferring methyl groups to SAM-dependent methyltransferases, whose substrates are primary and secondary metabolites (i.e., flavonoids, other phenylpropanoids, alkaloids, glucosinolates) **[53]**. When plants are affected by stress, their metabolism can switch between primary and secondary metabolisms to cope with unfavorable conditions **[54]**. Secondary metabolites like phenolic compounds are promoted during abiotic stress to help plants to adapt to stress conditions, probably due to their antioxidant properties that derive from hydroxyl groups **[38]**.

The phenylpropanoid derivative-enriched biosynthesis pathways in this study include cinnamates, flavonoids, hydrolyzable tannins and stilbenes biosynthesis pathways. The *cinnamate biosynthesis pathway* was enriched in the V/N roots, together with the *chlorogenic acid biosynthesis II pathway*. Despite chlorogenic acid (CGA) having the potentiality to play a detoxifying role in drought stress to diminish oxidative damage in plants, two intermediate metabolites were down-accumulated in the V/N roots. Indeed Nouraei et al. (2018) **[55]** observed increases in CGA in drought-stressed artichokes leaves and heads, which coincided with reduced chlorophyll, relative water content, growth and yield produced by oxidative stress (higher lipid peroxidation and H_2O_2). The down-accumulation in the NIBER® roots may play a role in preventing decreases in growth, chlorophyll and yields because the V/N root DW under water stress was significantly higher in relation to the control conditions and V/V in both treatments. Therefore, the role of CGA in the water stress response should be further investigated.

Regarding flavonoids, the *flavonol biosynthesis pathway* was enriched in the V/V leaves. Among flavonols, the *quercetin gentiotetraside biosynthesis pathway* was enriched in the leaves of both plant combinations, and several quercetin and kaempferol metabolites were up-accumulated mainly in the V/V leaves. Flavonols like quercetin and kaempferol, and their related metabolites, have been linked with photoprotection under light stress in *Arabidopsis* and *Vitis vinifera* (L.), and increases in these metabolites have been associated with elevated ROS production and reduced photosynthesis under high irradiation and drought stress **[56,57]**. In conclusion, flavonols are important ROS scavengers that could be helpful to reduce ROS in V/V, but these ROS may be a product of enhanced oxidative stress and these metabolites could be indicators of plants suffering from water stress **[58]**. It would seem that the NIBER® response to water stress does not involve flavonols biosynthesis under the water stress conditions of this experiment.

Anthoncyanin is another class of flavonoids that is a known powerful antioxidant and the *anthocyanin biosynthesis pathway* was enriched in the V/N leaves. Anthocyanins content increases in pea leaves by UV-B radiation and drought **[59]**, and their function in ROS scavenging has been proposed because they are usually located in vacuoles, near ROS production sites like chloroplasts and peroxisomes **[60]**. Viodelphin is an anthocyanin that up-accumulated in the leaves of both plant combinations and the V/V roots, and the *viodelphin biosynthesis pathway* was enriched. The acyl-glucose donor on this pathway (i.e., 1-O-4-hydroxybenzoyl-β-D-glucose) was up-accumulated in the V/V roots. It was also the donor on the *cyanidin 3,7-diglucoside polyacylation biosynthesis pathway*, which was enriched in the V/V roots. Last, the *shisonin biosynthesis pathway* was enriched in the V/V roots and its final product, i.e., malonylshisonin, was up-accumulated in the roots of V/V and V/N. Interestingly, this pathway and the implicated metabolites have been mostly described in *Perilla frutescens* (L.), in which malonylshisonin increased after high light treatment **[61]**. Thus its implications in the water stress response should be further studied.

Malonyl-CoA is a substrate in malonylshisonin biosynthesis, but is also involved in other phenylpropanoid derivative biosynthesis pathways like the stilbene *phytoalexin biosynthesis pathway*, which was enriched in the V/V roots. Several compounds of pinosylvin metabolism were up-accumulated in the roots of both plant combinations, and pinosylvin increases have been observed after ozone or UV light treatment **[62]**. However, information about additional stilbenes apart from resveratrol, which has been widely studied and described for its health-promoting properties, is lacking **[63]**.

Nitrogen-containing secondary compounds derive from amino acids and principally perform a defensive function. In this experiment, nitrogen-containing secondary compounds were differentially accumulated in both plant combinations and organs, and mainly belong to alkaloids and nitrogen-containing glucosides. The *alpha-solanine/alpha-chaconine biosynthesis pathway* was enriched in the roots of both plant combinations and V/V leaves. Alpha-solanine and alpha-chaconine are glycoalkaloids (GAs) that are toxic metabolites found in the Solanaceae family **[64]**. Bejarano et al. (2000) **[65]** observed an increase in GAs in drought-sensitive potatoes, but a slighter increase or no increase in drought-tolerant potatoes under drought conditions. Alpha-chaconine was up-accumulated in the V/V roots and down-accumulated in the V/N roots. α-chaconine is more toxic than is α-solanine given its greater ability to disrupt cholesterol-containing cell membranes **[66]**. Apart from the aforementioned role in drought-stressed potatoes, α-solanine and α-chaconine have not been associated with abiotic stress responses. Other nitrogen-containing class of compounds are glucosinolates, whose biosynthesis pathway was enriched in the leaves of both plant combinations and V/N roots. Glucosinolates contain a considerable amount of plant sulfur and drought stress modulates sulfur metabolism, mainly for ROS detoxification mediated by glutathione **[67]**. The V/V and V/N leaves seemed to promote glucosinolates biosynthesis because many involved metabolites were up-accumulated, whereas the V/N roots did not follow a marked trend, but showed up- and down-accumulated metabolites. Indeed glucosinolates have been linked with drought tolerance by means of crosstalk with phytohormones, i.e., auxins and stomatal regulation **[68]**.

5.5. Conclusion

To conclude, focusing on NIBER® and its tolerance mechanisms, distinct metabolomic signatures could be observed in both roots and leaves. In particular, a broad reprogramming was triggered at metabolome level by the NIBER® rootstock, indicating specific stress mitigation processes. This rootstock increased the vitamin B6, stearic acid and anthocyanins contents in the leaves of the grafted variety. Moreover, the NIBER® roots increased siroheme content for better nitrogen assimilation and decreased trans-zeatin content to give a higher root/shoot ratio. Besides, V/N enhanced cutin and suberin biosynthesis, which act as protection barriers, and jasmonic acid and jasmonates biosynthesis to promote tolerance signaling. Finally, NIBER® did not stimulate flavonols and Chl b biosynthesis to favor anthocyanins biosynthesis and to maintain the Chl a:Chl b ratio. The contribution to the water stress response of several secondary metabolites like CGA, shisonin, pinosylvin, glycoalkaloids and glucosinolates should be studied in-depth because most of them have not been previously described in pepper and information about their role in water stress tolerance is lacking.

5.6 Material and methods

5.6.1. Plant material

Pepper variety “Maestral F1” (abbreviated as V) (sweet pepper, California-type, Semillas Fitó, Spain) was self-grafted and grafted onto the pepper hybrid rootstock named NIBER® (abbreviated as N) (*Capsicum annuum* x *C. annuum*), which is tolerant to water stress **[24,25]**. Two plant combinations were herein used: self-grafted V plants (V/V, by showing the graft effect) and V grafted onto N (V/N). Early in March, the seeds of V and N were sown in 104 seedling trays filled with a peat-based substrate for germination. After 2 months, the grafted plant combinations were performed by the tube-grafting method **[69]**. Plants were maintained in a chamber with relative humidity above 95% and air temperature around 28-29° C for a 4-6-day period **[8]**.

5.6.2. Hydroponic greenhouse conditions

Three weeks after grafting (by the beginning of June), seedlings were removed from substrate and their roots were cleaned before being placed in 2 L polyethylene pots covered with aluminum sheets. Pots were filled with a nutrient solution containing (expressed as mmol L^{-1}): 13.0 NO_3^-, 1.0 $H_2PO_4^-$, 2.45 SO_4^{2-}, 1.6 Cl^-, 1.0 NH_4^+, 6.0 K^+, 4.0 Ca^{2+}, 2.5 Mg^{2+}, 0.5 Na^+ and micronutrients (15.8 μM Fe^{2+}, 10.3 μM Mn^{2+}, 4.2 μM Zn^{2+}, 43.5 μM B^+, 2.14 μM Cu^{2+}), and were artificially aerated with an air pump. Electrical conductivity and pH were 2.1 dS m^{-1} and 6.7, respectively. After seedling plants’ acclimatation to pots for 7 days, the water stress treatment was initiated by adding 5% PEG 8000 (Sigma Co.) to the nutrient solution. The osmotic potential of the solutions measured by a vapor osmometer (Digital osmometer, Wescor, Logan, USA) was -0.55 MPa for 5% PEG and -0.05 MPa for the control solution (0% PEG). Plants remained in a Venlo-type greenhouse under natural light conditions (610-870 μmol m^{-2} s^{-1}) for 48 h. Temperature and relative humidity ranges were 21-25°C and 52-72%, respectively. The layout was completely randomized, with ten plants per combination (V/V and V/N).

5.6.3. Dry weight determination

Weight determination was performed at the end of the experiment (48 h) using the plants that were not involved in the metabolomic analyses. Five plants per plant combination and treatment were used. Leaves were separated from roots and weighed to obtain the leaves and roots fresh weight, respectively. Immediately afterward, they were dried by placing them in an oven at 65°C for 72 h. Then everything was weighed again to determine leaves and roots dry weight (DW). Data are shown as the DW percentage of water stress in relation to the control conditions for V/V and V/N. Samples were tested by a one-way ANalysis Of VAriance (ANOVA) with Statgraphics Centurion XVIII (Statgraphics Technologies, Inc., The Plains, Virginia, USA). Fisher’s Least Significant Difference test (LSD) was performed at $p<0.05$.

5.6.4. Untargeted metabolomics analysis

The samples for the metabolomics analysis (leaves and roots) were taken 48 h after water stress treatment began (T48). Measurements were taken with fully expanded mature leaves (3rd-4th leaf from the shoot apex) and 2 cm from the distal roots. Samples were frozen in liquid nitrogen immediately after harvest, conserved at - 80°C and later freeze-dried. The layout was randomized with five samples of independent plants.

Sample preparation was carried out as previously reported **[70]**. Briefly, the freeze-dried samples were extracted with an Ultra-Turrax (Ika T-25, Staufen, Germany) using a proportion of 1 g of sample: 20 mL of buffer containing methanol/water solution (80:20, v/v) and 0.1% HCOOH. Extracts were centrifuged (12000 x *g*) and filtered through a 0.22 µm cellulose membrane directly into amber vials for the untargeted metabolomics analysis. The metabolomics platform included a UHPLC 1290 chromatographic system coupled to a hybrid quadrupole-time-of-flight (Q-TOF) G6550 mass spectrometer (UHPLC/Q-TOF-MS) and a JetStream Dual Electrospray ionization source (Agilent Technologies, Santa Clara, CA, USA). The analysis was carried out as previously described by Formisano et al. (2021) **[70]**. Reverse-phase chromatographic separation was performed using an Agilent pentafluorophenylpropyl (PFP) column (2.0 × 100 mm, 3 µm) (Santa Clara, CA, USA) with a water-acetonitrile gradient elution from 6% to 94% in 33 min. The mass spectrometer worked in the SCAN mode from 100 to 1200 m/z, and extended the dynamic range mode with positive polarity.

Feature metabolites and post-acquisition processing were performed by the Agilent Profinder B.07 software tool as reported by Formisano et. al (2021) **[70]**. The combination of monoisotopic accurate mass and isotopes patterns allowed compounds annotation against the PlantCyc 12.6 database (Plant Metabolic Network; Release: October 2021; www.plantcyc.org) according to the COSMOS Metabolomics Standards Initiative for Level 2 of confidence (putatively annotated compounds) **[71]**.

5.6.5. Statistics and Chemometric Interpretation of Metabolites

Mass profiler Professional B.12.06 (Agilent Technologies, Santa Clara, CA, USA) was used for chemometric interpretation purposes. Compound abundance was log2-transformed, normalized at the 75th percentile and baselined against the median. The unsupervised hierarchical cluster analysis (HCA) was carried out based on fold-change values with the Wards agglomerative algorithm of Euclidean distances. A supervised orthogonal partial least squares discriminant analysis (OPLS-DA) was performed with the SIMCA 16 software (Umetrics, Sweden). Fitness parameters were also calculated and Hotelling's T2 was applied to exclude outliers. CV-ANOVA ($p < 0.01$) and permutation testing ($n = 100$) were used for model validation. Significant compounds compared to the control conditions were identified by a Volcano plot analysis (p-value < 0.05; FC > 2). A Plant Metabolic Network Pathway Enrichment analysis **[72]** was performed on PlantCyc for the differentially accumulated metabolites in stress compared to the control conditions using the Fisher Exact test ($p<0.05$) and the Capsicum annuum database. The significant pathways for V/V and V/N were classified according to the Pathway Tools pathway ontology **[73]**.

5.7. References

1. FAO. Drought and Agriculture. 2023. https://www.fao.org/land-water/water/drought/droughtandag/en/ (13 December 2021, last accesed).
2. Ullah H, Santiago-Arenas R, Ferdous Z *et al.* Improving water use efficiency, nitrogen use efficiency, and radiation use efficiency in field crops under drought stress: A review. *Advances in Agronomy*. Vol 156. Academic Press Inc., 2019, 109–57, DOI: 10.1016/bs.agron.2019.02.002.
3. Takahashi F, Kuromori T, Urano K *et al.* Drought Stress Responses and Resistance in Plants: From Cellular Responses to Long-Distance Intercellular Communication. *Front Plant Sci* 2020;**11**, DOI: 10.3389/fpls.2020.556972.
4. Sousa AR de O, Silva EM de A, Filho MAC *et al.* Metabolic responses to drought stress and rehydration in leaves and roots of three Citrus scion/rootstock combinations. *Sci Hortic* 2022;**292**:110490, DOI: 10.1016/J.SCIENTA.2021.110490.
5. Schwarz D, Rouphael Y, Colla G *et al.* Grafting as a tool to improve tolerance of vegetables to abiotic stresses: Thermal stress, water stress and organic pollutants. *Sci Hortic* 2010;**127**:162–71, DOI: 10.1016/j.scienta.2010.09.016
6. Kumar P, Rouphael Y, Cardarelli M *et al.* Vegetable Grafting as a Tool to Improve Drought Resistance and Water Use Efficiency. *Front Plant Sci* 2017;**8**:1130, DOI: 10.3389/fpls.2017.01130.
7. Yao X, Yang R, Zhao F *et al.* An analysis of physiological index of differences in drought tolerance of tomato rootstock seedlings. *Journal of Plant Biology* 2016;**59**:311–21, DOI: 10.1007/s12374-016-0071-y.
8. Penella C, Nebauer SG, Bautista AS *et al.* Rootstock alleviates PEG-induced water stress in grafted pepper seedlings: Physiological responses. *J Plant Physiol* 2014;**171**:842–51, DOI: 10.1016/j.jplph.2014.01.013.
9. Liu J, Li J, Su X *et al.* Grafting improves drought tolerance by regulating antioxidant enzyme activities and stress-responsive gene expression in tobacco. *Environ Exp Bot* 2014;**107**:173–9, DOI: 10.1016/j.envexpbot.2014.06.012.
10. López-Serrano L, Canet-Sanchis G, Vuletin Selak G *et al.* Pepper Rootstock and Scion Physiological Responses Under Drought Stress. *Front Plant Sci* 2019;**10**, DOI: 10.3389/fpls.2019.00038.
11. Padilla YG, Gisbert-Mullor R, López-Galarza S *et al.* Short-term water stress responses of grafted pepper plants are associated with changes in the hormonal balance. *Front Plant Sci* 2023;**14**:1412, DOI: 10.3389/FPLS.2023.1170021.
12. Lu X, Liu W, Wang T *et al.* Systemic Long-Distance Signaling and Communication Between Rootstock and Scion in Grafted Vegetables. *Front Plant Sci* 2020;**11**, DOI: 10.3389/fpls.2020.00460.
13. Lucini L, Miras-Moreno B, Busconi M *et al.* Molecular basis of rootstock-related tolerance to water deficit in Vitis vinifera L. cv. Sangiovese: A physiological and metabolomic combined approach. *Plant Science* 2020;**299**:110600, DOI: 10.1016/J.PLANTSCI.2020.110600.
14. Kumar P, Lucini L, Rouphael Y *et al.* Insight into the role of grafting and arbuscular mycorrhiza on cadmium stress tolerance in tomato. *Front Plant Sci* 2015;**6**:477, DOI: 10.3389/FPLS.2015.00477.
15. Fraser CM, Chapple C. The Phenylpropanoid Pathway in Arabidopsis. *The Arabidopsis Book / American Society of Plant Biologists* 2011;**9**:e0152, DOI: 10.1199/TAB.0152.
16. Zandalinas SI, Sales C, Beltrán J *et al.* Activation of secondary metabolism in citrus plants is associated to sensitivity to combined drought and high temperatures. *Front Plant Sci* 2017;**7**:1954, DOI: 10.3389/FPLS.2016.01954.
17. Arbona V, Manzi M, de Ollas C *et al.* Metabolomics as a Tool to Investigate Abiotic Stress Tolerance in Plants. *International Journal of Molecular Sciences 2013, Vol 14, Pages 4885-4911* 2013;**14**:4885–911, DOI: 10.3390/IJMS14034885.
18. Aslam A, Zhao S, Lu X *et al.* High-Throughput LC-ESI-MS/MS Metabolomics Approach Reveals Regulation of Metabolites Related to Diverse Functions in Mature Fruit of Grafted Watermelon. *Biomolecules 2021, Vol 11, Page 628* 2021;**11**:628, DOI: 10.3390/BIOM11050628.
19. Aidoo MK, Sherman T, Lazarovitch N *et al.* Physiology and metabolism of grafted bell pepper in response to low root-zone temperature. *Functional Plant Biology* 2019;**46**:339, DOI: 10.1071/FP18206.
20. Gisbert-Mullor R, Ceccanti C, Padilla YG *et al.* Effect of grafting on the production, physico-chemical characteristics and nutritional quality of fruit from pepper landraces. *Antioxidants* 2020;**9**, DOI: 10.3390/antiox9060501.
21. Borràs D, Plazas M, Moglia A *et al.* The influence of acute water stresses on the biochemical composition of bell pepper (*Capsicum annuum* L.) berries. *J Sci Food Agric* 2021;**101**:4724–34, DOI: 10.1002/JSFA.11118.
22. Vílchez JI, Niehaus K, Dowling DN *et al.* Protection of Pepper Plants from Drought by Microbacterium sp. 3J1 by Modulation of the Plant's Glutamine and α-ketoglutarate Content: A Comparative Metabolomics Approach. *Front Microbiol* 2018;**9**, DOI: 10.3389/fmicb.2018.00284.
23. Kalozoumis P, Savvas D, Aliferis K *et al.* Impact of Plant Growth-Promoting Rhizobacteria Inoculation and Grafting on Tolerance of Tomato to Combined Water and Nutrient Stress Assessed via Metabolomics Analysis. *Front Plant Sci* 2021;**12**:814, DOI: 10.3389/FPLS.2021.670236.
24. Gisbert-Mullor R, Pascual-Seva N, Martínez-Gimeno MA *et al.* Grafting onto an Appropriate Rootstock Reduces the Impact on Yield and Quality of Controlled Deficit Irrigated Pepper Crops. *Agronomy* 2020;**10**:1529, DOI: 10.3390/agronomy10101529.

25. Gisbert-Mullor R, Martín-García R, Bažon Zidarić I *et al.* A Water Stress–Tolerant Pepper Rootstock Improves the Behavior of Pepper Plants under Deficit Irrigation through Root Biomass Distribution and Physiological Adaptation. *Horticulturae* 2023;**9**:362, DOI: 10.3390/HORTICULTURAE9030362.

26. Obata T, Fernie AR. The use of metabolomics to dissect plant responses to abiotic stresses. *Cellular and Molecular Life Sciences 2012 69:19* 2012;**69**:3225–43, DOI: 10.1007/S00018-012-1091-5.

27. You J, Zhang Y, Liu A *et al.* Transcriptomic and metabolomic profiling of drought-tolerant and susceptible sesame genotypes in response to drought stress. *BMC Plant Biol* 2019;**19**:1–16, DOI: 10.1186/s12870-019-1880-1.

28. Ma Q, Xu X, Xie Y *et al.* Comparative metabolomic analysis of the metabolism pathways under drought stress in alfalfa leaves. *Environ Exp Bot* 2021;**183**:104329, DOI: 10.1016/J.ENVEXPBOT.2020.104329.

29. Ho CL, Saito K. Molecular biology of the plastidic phosphorylated serine biosynthetic pathway in Arabidopsis thaliana. *Amino Acids* 2001;**20**:243–59, DOI: 10.1007/S007260170042.

30. Kishor PBK, Suravajhala R, Rajasheker G *et al.* Lysine, Lysine-Rich, Serine, and Serine-Rich Proteins: Link Between Metabolism, Development, and Abiotic Stress Tolerance and the Role of ncRNAs in Their Regulation. *Front Plant Sci* 2020;**11**:1840, DOI: 10.3389/FPLS.2020.546213.

31. Dewey RE, Wilson RF, Novitzky WP *et al.* The *AAPT1* gene of soybean complements a cholinephosphotransferase-deficient mutant of yeast. *Plant Cell* 1994;**6**:1495–507, DOI: 10.1105/TPC.6.10.1495.

32. Summers PS, Weretilnyk EA. Choline Synthesis in Spinach in Relation to Salt Stress. *Plant Physiol* 1993;**103**:1269–76, DOI: 10.1104/PP.103.4.1269.

33. Nuccio ML, Ziemak MJ, Henry SA *et al.* cDNA cloning of phosphoethanolamine N-methyltransferase from spinach by complementation in *Schizosaccharomyces pombe* and characterization of the recombinant enzyme. *J Biol Chem* 2000;**275**:14095–101, DOI: 10.1074/JBC.275.19.14095.

34. Rontein D, Nishida I, Tashiro G *et al.* Plants synthesize ethanolamine by direct decarboxylation of serine using a pyridoxal phosphate enzyme. *J Biol Chem* 2001;**276**:35523–9, DOI: 10.1074/JBC.M106038200.

35. Tambasco-Studart M, Titiz O, Raschle T *et al.* Vitamin B6 biosynthesis in higher plants. *Proc Natl Acad Sci U S A* 2005;**102**:13687–92, DOI: 10.1073/PNAS.0506228102.

36. Mooney S, Hellmann H. Vitamin B6: Killing two birds with one stone? *Phytochemistry* 2010;**71**:495–501, DOI: 10.1016/J.PHYTOCHEM.2009.12.015.

37. Gakière B, Hao J, de Bont L *et al.* NAD + Biosynthesis and Signaling in Plants. *CRC Crit Rev Plant Sci* 2018;**37**:259–307, DOI: 10.1080/07352689.2018.1505591.

38. Gundaraniya SA, Ambalam PS, Tomar RS. Metabolomic Profiling of Drought-Tolerant and Susceptible Peanut (*Arachis hypogaea* L.) Genotypes in Response to Drought Stress. *ACS Omega* 2020;**5**:31209–19, DOI: 10.1021/ACSOMEGA.0C04601.

39. He M, Ding NZ. Plant Unsaturated Fatty Acids: Multiple Roles in Stress Response. *Front Plant Sci* 2020;**11**:1378, DOI: 10.3389/FPLS.2020.562785

40. Zhang X, Ni Y, Xu D *et al.* Integrative analysis of the cuticular lipidome and transcriptome of *Sorghum bicolor* reveals cultivar differences in drought tolerance. *Plant Physiology and Biochemistry* 2021;**163**:285–95, DOI: 10.1016/J.PLAPHY.2021.04.007.

41. Pollard M, Beisson F, Li Y *et al.* Building lipid barriers: biosynthesis of cutin and suberin. *Trends Plant Sci* 2008;**13**:236–46, DOI: 10.1016/J.TPLANTS.2008.03.003.

42. Padilla YG, Gisbert-Mullor R, Bueso E *et al.* New insights into short-term water stress tolerance through transcriptomic and metabolomic analyses on pepper roots. *Plant Science* 2023;**333**:111731, DOI: 10.1016/J.PLANTSCI.2023.111731.

43. Li Y, Yang X, Li X. Role of jasmonate signaling pathway in resistance to dehydration stress in Arabidopsis. *Acta Physiol Plant* 2019;**41**:1–12, DOI: 10.1007/S11738-019-2897-7.

44. Kurepa J, Smalle JA. Auxin/Cytokinin Antagonistic Control of the Shoot/Root Growth Ratio and Its Relevance for Adaptation to Drought and Nutrient Deficiency Stresses. *International Journal of Molecular Sciences 2022, Vol 23, Page 1933* 2022;**23**:1933, DOI: 10.3390/IJMS23041933.

45. Kasahara H, Takei K, Ueda N *et al.* Distinct isoprenoid origins of cis- and trans-zeatin biosyntheses in Arabidopsis. *J Biol Chem* 2004;**279**:14049–54, DOI: 10.1074/JBC.M314195200.

46. Rodríguez-Concepción M, Boronat A. Elucidation of the methylerythritol phosphate pathway for isoprenoid biosynthesis in bacteria and plastids. A metabolic milestone achieved through genomics. *Plant Physiol* 2002;**130**:1079–89, DOI: 10.1104/PP.007138.

47. Pulido P, Toledo-Ortiz G, Phillips MA *et al.* Arabidopsis J-Protein J20 Delivers the First Enzyme of the Plastidial Isoprenoid Pathway to Protein Quality Control. *Plant Cell* 2013;**25**:4183–94, DOI: 10.1105/TPC.113.113001.

48. Oster U, Tanaka R, Tanaka A *et al.* Cloning and functional expression of the gene encoding the key enzyme for chlorophyll b biosynthesis (CAO) from *Arabidopsis thaliana*. *The Plant Journal* 2000;**21**:305–10, DOI: 10.1046/J.1365-313X.2000.00672.X.

49. Majidi MM, Rashidi F, Sharafi Y. Physiological traits related to drought tolerance in Brassica. *Int J Plant Prod* 2015;**9**:541–59, ISSN: 1735-6814.

50. Murphy MJ, Siegel LM. Siroheme and Sirohydrochlorin. *Journal of Biological Chemistry* 1973;**248**:6911–9, DOI: 10.1016/s0021-9258(19)43436-4.

51. López-Serrano L, Canet-Sanchis G, Selak GV *et al.* Physiological characterization of a pepper hybrid rootstock designed to cope with salinity stress. *Plant Physiology and Biochemistry* 2020;**148**:207–19, DOI: 10.1016/j.plaphy.2020.01.016.

52. Amir R. Current understanding of the factors regulating methionine content in vegetative tissues of higher plants. *Amino Acids* 2010;**39**:917–31, DOI: 10.1007/S00726-010-0482-X.

53. Roje S. S-Adenosyl-l-methionine: Beyond the universal methyl group donor. *Phytochemistry* 2006;**67**:1686–98, DOI: 10.1016/J.PHYTOCHEM.2006.04.019.

54. Jia H, Wang L, Li J *et al.* Comparative metabolomics analysis reveals different metabolic responses to drought in tolerant and susceptible poplar species. *Physiol Plant* 2020;**168**:531–46, DOI: 10.1111/PPL.13036.

55. Nouraei S, Rahimmalek M, Saeidi G. Variation in polyphenolic composition, antioxidants and physiological characteristics of globe artichoke (*Cynara cardunculus* var. *scolymus* Hayek L.) as affected by drought stress. *Sci Hortic* 2018;**233**:378–85, DOI: 10.1016/J.SCIENTA.2017.12.060.

56. Havaux M, Kloppstech K. The protective functions of carotenoid and flavonoid pigments against excess visible radiation at chilling temperature investigated in Arabidopsis *npq* and *tt* mutants. *Planta* 2001;**213**:953–66, DOI: 10.1007/S004250100572.

57. Griesser M, Weingart G, Schoedl-Hummel K *et al.* Severe drought stress is affecting selected primary metabolites, polyphenols, and volatile metabolites in grapevine leaves (*Vitis vinifera* cv. *Pinot noir*). *Plant Physiology and Biochemistry* 2015;**88**:17–26, DOI: 10.1016/J.PLAPHY.2015.01.004.

58. Sharma D, Shree B, Kumar S *et al.* Stress induced production of plant secondary metabolites in vegetables: Functional approach for designing next generation super foods. *Plant Physiology and Biochemistry* 2022;**192**:252–72, DOI: 10.1016/J.PLAPHY.2022.09.034.

59. Nogués S, Allen DJ, Morison JIL *et al.* Ultraviolet-B Radiation Effects on Water Relations, Leaf Development, and Photosynthesis in Droughted Pea Plants. *Plant Physiol* 1998;**117**:173–81, DOI: 10.1104/PP.117.1.173.

60. Naing AH, Kim CK. Abiotic stress-induced anthocyanins in plants: Their role in tolerance to abiotic stresses. *Physiol Plant* 2021;**172**:1711–23, DOI: 10.1111/PPL.13373.

61. Xie G, Zou X, Liang Z *et al.* Integrated metabolomic and transcriptomic analyses reveal molecular response of anthocyanins biosynthesis in perilla to light intensity. *Front Plant Sci* 2022;**13**, DOI: 10.3389/FPLS.2022.976449.

62. Chong J, Poutaraud A, Hugueney P. Metabolism and roles of stilbenes in plants. *Plant Science* 2009;**177**:143–55, DOI: 10.1016/J.PLANTSCI.2009.05.012.

63. Valletta A, Iozia LM, Leonelli F. Impact of Environmental Factors on Stilbene Biosynthesis. *Plants 2021, Vol 10, Page 90* 2021;**10**:90, DOI: 10.3390/PLANTS10010090.

64. Papathanasiou F, Mitchell SH, Watson S *et al.* Effect of environmental stress during tuber development on accumulation of glycoalkaloids in potato (Solanum tuberosum L). *J Sci Food Agric* 1999;**79**:1183–9, DOI: 10.1002/(SICI)1097-0010(19990701)79:9<1183::AID-JSFA341>3.0.CO;2-4, ISSN: 0022-5142.

65. Bejarano L, Mignolet E, Devaux A *et al.* Glycoalkaloids in potato tubers: the effect of variety and drought stress on the a-solanine and a-chaconine contents of potatoes. *J Sci Food Agric* 2000;**80**:2096–100, DOI: 10.1002/1097-0010(200011)80:14.

66. Friedman M. Potato glycoalkaloids and metabolites: Roles in the plant and in the diet. *J Agric Food Chem* 2006;**54**:8655–81, DOI: 10.1021/JF061471T.

67. Chan KX, Wirtz M, Phua SY *et al.* Balancing metabolites in drought: the sulfur assimilation conundrum. *Trends Plant Sci* 2013;**18**:18–29, DOI: 10.1016/J.TPLANTS.2012.07.005.

68. Salehin M, Li B, Tang M *et al.* Auxin-sensitive Aux/IAA proteins mediate drought tolerance in Arabidopsis by regulating glucosinolate levels. *Nature Communications 2019 10:1* 2019;**10**:1–9, DOI: 10.1038/s41467-019-12002-1.

69. Penella C, Nebauer SG, Quiñones A *et al.* Some rootstocks improve pepper tolerance to mild salinity through ionic regulation. *Plant Science* 2015;**230**:12–22, DOI: 10.1016/j.plantsci.2014.10.007.

70. Formisano L, Miras-Moreno B, Ciriello M *et al.* Trichoderma and Phosphite Elicited Distinctive Secondary Metabolite Signatures in Zucchini Squash Plants. *Agronomy* 2021;**11**:1205, DOI: 10.3390/agronomy11061205.

71. Salek RM, Neumann S, Schober D *et al.* COordination of Standards in MetabOlomicS (COSMOS): facilitating integrated metabolomics data access. *Metabolomics* 2015;**11**:1587–97, DOI: 10.1007/s11306-015-0810-y.

72. Hawkins C, Ginzburg D, Zhao K *et al.* Plant Metabolic Network 15: A resource of genome-wide metabolism databases for 126 plants and algae. *J Integr Plant Biol* 2021;**63**:1888–905, DOI: 10.1111/jipb.13163.

73. Karp PD, Paley SM, Krummenacker M *et al.* Pathway Tools version 13.0: integrated software for pathway/genome informatics and systems biology. *Brief Bioinform* 2010;**11**:40–79, DOI: 10.1093/bib/bbp043.

5.8. Supplementary Material

Supplementary Figure 1A. OPLS model on leaves for each plant combination (V/V and V/N) under water tress (PEG) and the control conditions.

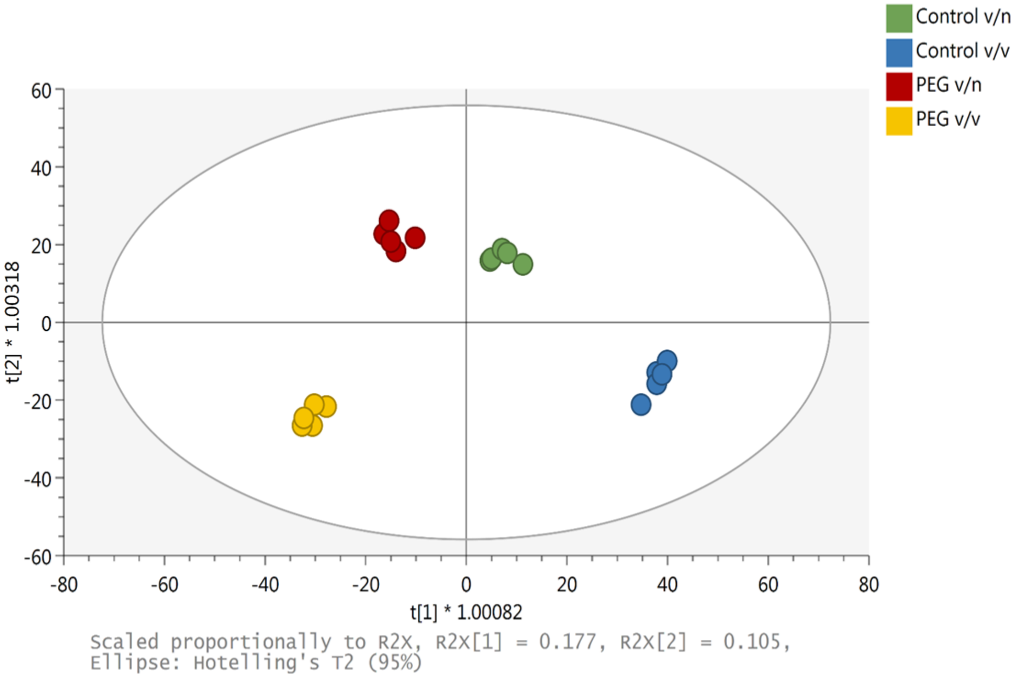

Supplementary Figure 1B. OPLS model on roots for each plant combination (V/V and V/N) under water tress (PEG) and the control conditions.

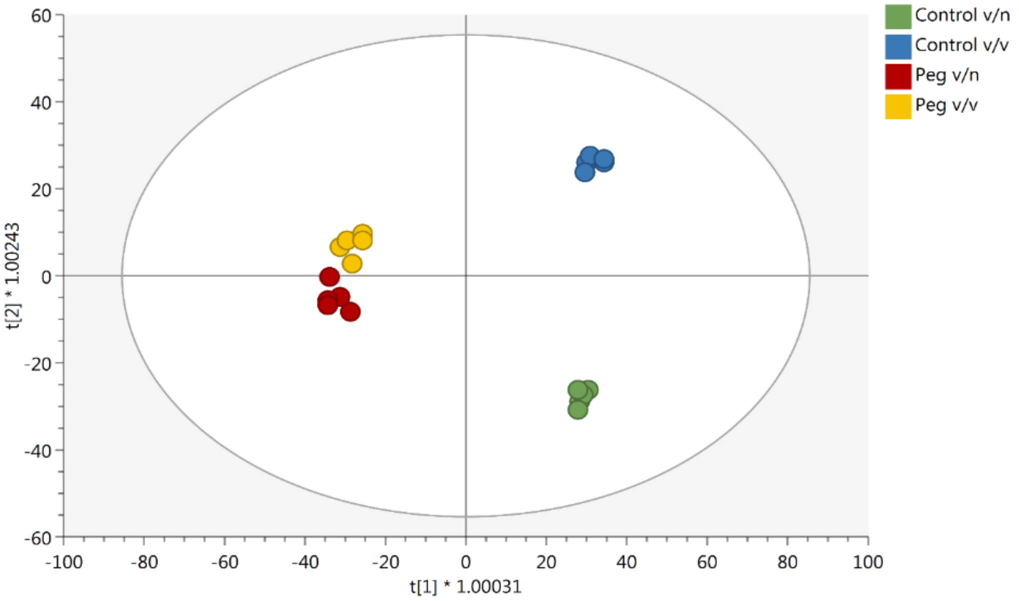

Supplementary Table 1A. Differentially accumulated metabolites from Volcano analysis for V/V leaves under water stress compared to the control plants.

Compound	p (Corr) (Peg Vs Control)	Log FC (Peg Vs Control)	Mass	Formula	Compound Name
tetra-acyl estolide	0	4.00	1208.978	C75 H132 O11	CPD-12262
violdelphin	0	2.40	1174.2971	C53 H58 O30	CPD-16561
cerotoyl-CoA	0	3.02	1141.4633	C47 H82 N7 O17 P3 S	CPD1G-277
(3R)-3-hydroxylignoceroyl-CoA	0	4.00	1129.4316	C45 H78 N7 O18 P3 S	CPD-14277
lignoceroyl-CoA	0	4.00	1113.4418	C45 H78 N7 O17 P3 S	CPD-10280
trans-lignocer-2-enoyl-CoA	0	4.00	1111.4312	C45 H76 N7 O17 P3 S	CPD-14282
dolichol-group	0	4.00	1093.019	C80 H132	DOLICHOL-GROUP
docosanoyl-CoA	0	4.00	1085.4152	C43 H74 N7 O17 P3 S	CPD-10279
3-oxo-auricoloyl-CoA	0	4.00	1083.3134	C41 H64 N7 O19 P3 S	CPD-17401
(7Z,10Z,13Z,16Z,19Z)-docosapentaenoyl-CoA	0	4.00	1075.3348	C43 H64 N7 O17 P3 S	CPD-14426
icosanoyl-CoA	0	4.00	1057.3923	C41 H70 N7 O17 P3 S	CPD-9965
3-oxo-2-(cis-2'-pentenyl)-cyclopentane-1-(3-oxooctanoyl)-CoA	0	4.00	1053.255	C39 H58 N7 O19 P3 S	CPD-11520
(2E,8Z,11Z,14Z,17Z)-icosapentaenoyl-CoA	0	4.00	1047.3059	C41 H60 N7 O17 P3 S	CPD-17264
10,16-dihydroxypalmitoyl-CoA	0	4.00	1033.31	C37 H62 N7 O19 P3 S	CPD-17627
3-oxo-2-(cis-2'-pentenyl)-cyclopentane-1-(3R-hydroxyhexanoyl)-CoA	0	4.00	1027.2509	C37 H56 N7 O19 P3 S	CPD-11523
gamma-linolenoyl-CoA	0	4.00	1023.3006	C39 H60 N7 O17 P3 S	GAMMA-LINOLENOYL-COA
curcumin 4',4"-O-beta-D-digentiobioside	0	4.00	1016.3342	C45 H60 O26	CPD-6626
3-oxo-2-(cis-2'-pentenyl)-cyclopentane-1-hexanoyl-CoA	0	4.00	1011.275	C37 H56 N7 O18 P3 S	CPD-11521
(S)-3-hydroxy-(5Z)-tetradecenoyl-CoA	0	4.00	987.2648	C35 H56 N7 O18 P3 S	CPD0-1163
3-oxo-2-(cis-2'-pentenyl)-cyclopentane-1-butanoyl-CoA	0	4.00	983.2353	C35 H52 N7 O18 P3 S	CPD-11525
sinapoyl-CoA	0	4.00	969.1364	C32 H42 N7 O20 P3 S	SINAPOYL-COA
3-hydroxy-indole-3-butyryl-CoA	0	4.00	968.1995	C33 H47 N8 O18 P3 S	CPD-10517
6'-hydroxyferuloyl-CoA	0	4.00	959.1577	C31 H44 N7 O20 P3 S	CPD4FS-4
quercetin-3-gentiotetraside	0	4.00	950.2559	C39 H50 O27	CPD-14822
lauroyl-CoA	0	4.00	945.2553	C33 H54 N7 O17 P3 S	LAUROYLCOA-CPD
1,2,3,4,6-pentagalloylglucose	4.86E-04	4.25	940.1223	C41 H32 O26	12346-PENTAKIS-O-GALLOYL-BETA-D-GLUC
tellimagrandin II	0	4.00	938.0994	C41 H30 O26	CPD-8949
pimeloyl-CoA	0	4.00	904.142	C28 H41 N7 O19 P3 S	CPD-558
4-chlorobenzoyl-coA	0	4.89	901.0678	C28 H35 Cl N7 O17 P3 S	CPD-1776

Compound	p (Corr) (Peg Vs Control)	Log FC (Peg Vs Control)	Mass	Formula	Compound Name
delphinidin 3-O-rutinoside-7-O-(6-O-(p-hydroxybenzoyl)-glucoside)	0	4.00	892.2178	C40 H44 O23	CPD-16559
1-methylpyrrolidine-2-acetyl-CoA	0	2.34	889.1775	C28 H44 N8 O17 P3 S	CPD-9771
cyanidin O-O-[6-O-(6-O-4-hydroxycinnamoyl-beta-D-glucosyl)-2-O-beta-D-xylosyl-beta-D-galactoside]	0	2.77	887.2238	C41 H43 O22	CPD-15000
(2E)-oct-2-enoyl-CoA	0	4.00	887.1698	C29 H44 N7 O17 P3 S	CPD0-2108
protochlorophyll a	1.95E-04	4.96	867.5427	C55 H71 N4 O5	CPD-8177
decaprenyl diphosphate	0	4.00	858.5667	C50 H84 O7 P2	CPDQT-22
(+)-sesaminol 2-O-beta-D-gentiotrioside	2.37E-03	2.22	856.263	C38 H48 O22	CPD-14841
curcumin 4'-O-beta-D-gentiobiosyl 4''-O-beta-D-glucoside	0	4.00	854.2765	C39 H50 O21	CPD-6625
cytochrome c	0	1.05	829.3583	C42 H53 N8 O6 S2	CPD-16495
quercetin-3-gentiotrioside	0	3.37	788.1967	C33 H40 O22	CPD-14821
quercetin 3-O-gentiobioside-7-O-rhamnoside	0	4.00	772.2139	C33 H40 O21	CPD-15024
isovitexin 2''-O-beta-D-glucosyl 7-O-galactoside	0	-4.00	756.2183	C33 H40 O20	CPD-18169
1-alpha-linolenoyl-2-palmitoyl-phosphatidylglycerol	0	-2.86	743.4893	C40 H72 O10 P	CPD-8087
1D-myo-inositol 3-diphosphate 1,2,4,5,6-pentakisphosphate	0	4.00	727.7311	C6 H7 O27 P7	CPD-11937
amaranthin	2.62E-03	4.22	724.165	C30 H32 N2 O19	CPD-8658
5-methyltetrahydropteroyl tri-L-glutamate	1.51E-04	3.96	713.2384	C30 H35 N9 O12	CPD-1302
delphinidin-3-O-(6''-O-malonyl)-beta-glucoside-3'-O-beta-glucoside	0	2.09	711.137	C30 H31 O20	CPD-7870
beta-chaconine	0	4.00	706.4486	C39 H64 N O10	CPD-9215
tetrahydropteroyl tri-L-glutamate	1.51E-04	4.08	699.2236	C29 H33 N9 O12	CPD-1301
pteroyl-gamma-glutamyl-gamma-glutamylglutamate	0	3.68	695.1862	C29 H29 N9 O12	CPD0-1473
a xylogalacturonan	0	-3.12	678.1475	C23 H34 O23	CPD-10235
NAD+	5.29E-03	3.74	662.1047	C21 H26 N7 O14 P2	NAD
bisorganyltrisulfane	0	5.04	644.128	C20 H32 N6 O12 S3	CPD-11763
rubusoside	0	-1.23	642.3274	C32 H50 O13	CPD-14505

Compound	p (Corr) (Peg Vs Control)	Log FC (Peg Vs Control)	Mass	Formula	Compound Name
dalpatein 7-O-beta-D-apiofuranosyl-(1->6)-beta-D-glucopyranoside	1.91E-03	4.57	636.1675	C29 H32 O16	CPD-9693
luteolin 7-O-beta-D-diglucuronide	0	1.80	636.0956	C27 H24 O18	LUTEOLIN-7-O-BETA-D-DIGLUCURONIDE
cyanidin 3-O-(3",6"-O-dimalonyl-beta-glucopyranoside)	0	4.46	617.0767	C27 H21 O17	CPD-7700
verdoheme	5.76E-04	3.44	615.165	C33 H29 Fe N4 O5	CPD-19719
kaempferol 3,7-bis-O-beta-D-glucoside	1.51E-04	4.94	610.1519	C27 H30 O16	CPD-8034
2-phospho-4-(cytidine 5'-diphospho)-2-C-methyl-D-erythritol	0	2.11	597.0206	C14 H22 N3 O17 P3	2-PHOSPHO-4-CYTIDINE-5-DIPHOSPHO-2-C-MET
2-sinapoyloxy-3-butenylglucosinolate	0	4.00	594.0919	C22 H28 N O14 S2	CPD-12423
trans-zeatin riboside triphosphate	3.11E-03	3.28	588.0323	C15 H21 N5 O14 P3	CPD-4202
baccatin III	0	4.00	586.2407	C31 H38 O11	BACCATIN-III
5-methyl-tetrahydropteroyl-alpha-glutamylglutamate	0	1.96	585.2054	C25 H29 N8 O9	CPD0-1474
GDP-4-dehydro-alpha-D-rhamnose	0	4.00	585.0539	C16 H21 N5 O15 P2	GDP-4-DEHYDRO-6-DEOXY-D-MANNOSE
Mg-protoporphyrin	0	1.19	582.2144	C34 H30 Mg N4 O4	MG-PROTOPORPHYRIN
3-sinapoyloxypropylglucosinolate	0	4.00	582.094	C21 H28 N O14 S2	CPD-12417
C-132-carboxypyropheophorbide a	0	4.00	577.2453	C34 H33 N4 O5	CPD-14963
3-all trans-hexaprenyl-4-hydroxy-5-methoxybenzoate	0	4.00	575.4081	C38 H55 O4	3-HEXAPRENYL-4-HYDROXY-5-METHOXYBENZOATE
UDP-alpha-D-galactose	0	2.73	564.04	C15 H22 N2 O17 P2	CPD-14553
ADP-D-ribose	0	4.00	557.0598	C15 H21 N5 O14 P2	ADENOSINE_DIPHOSPHATE_RIBOSE
(2E,10E,14E,18E)-lycopatetraene	0	3.78	554.5757	C40 H74	CPD-20659
UDP-beta-L-rhamnose	0	2.86	548.0434	C15 H22 N2 O16 P2	UDP-L-RHAMNOSE
dTDP-beta-L-rhamnose	0	4.44	546.0677	C16 H24 N2 O15 P2	DTDP-RHAMNOSE
afrormosin-7-O-glucoside-6''-O-malonate	3.11E-03	2.64	545.1402	C26 H25 O13	CPD-10081
10-deacetylbaccatin III	0	4.00	544.228	C29 H36 O10	10-DEACETYLBACCATIN-III
NAD stem group	0	4.00	541.0619	C15 H21 N5 O13 P2	NAD-STEM-GROUP
cyclic ADP-ribose	3.39E-04	3.75	540.0538	C15 H20 N5 O13 P2	CPD-14880

Compound	p (Corr) (Peg Vs Control)	Log FC (Peg Vs Control)	Mass	Formula	Compound Name
3-alpha(S)-strictosidine	0	-4.00	531.2244	C27 H35 N2 O9	STRICTOSIDINE
ketoconazole	0	3.74	530.1453	C26 H28 Cl2 N4 O4	CPD-4503
succinate-semialdehyde-thiamine PPi	0	4.33	527.0771	C16 H25 N4 O10 P2 S	SUCCINATE-SEMIALDEHYDE-THIAMINE-PPI
3,7,4'-trimethylquercetin 2'-O-beta-D-glucoside	3.49E-03	3.35	522.1341	C24 H26 O13	CPD-14858
apigenin 7-O-(6-malonyl-beta-D-glucoside)	0	-3.73	517.0979	C24 H21 O13	CPD-10318
2,2'-azino-bis-(3-ethylbenzothiazoline-6-sulfonate)	0	-4.00	511.996	C18 H16 N4 O6 S4	CPD-12796
trans-zeatin riboside diphosphate	0	4.31	508.0647	C15 H20 N5 O11 P2	CPD-4204
8-hydroxy-dATP	1.51E-04	4.91	504.9798	C10 H14 N5 O13 P3	CPD0-1093
malonyldaidzin	0	1.13	501.1084	C24 H21 O12	CPD-3425
BPH-652	8.66E-03	2.26	499.9232	C16 H16 K3 O7 P S	CPD-9926
patulitrin	0	4.00	493.0997	C22 H21 O13	CPD-14909
8-(methylsulfinyl)octyl-glucosinolate	0	1.57	492.1036	C16 H30 N O10 S3	CPDQT-299
N6-(Delta2-isopentenyl)-adenosine 5'-diphosphate	0	4.00	492.0755	C15 H20 N5 O10 P2	CPD-4203
2-benzoyloxy-3-butenylglucosinolate	0	4.00	492.0717	C18 H22 N O11 S2	CPD-12421
7,8-dihydroneopterin 3'-triphosphate	1.95E-03	2.89	490.9674	C9 H12 N5 O13 P3	DIHYDRONEOPTERIN-P3
dATP	6.42E-04	3.62	486.9718	C10 H12 N5 O12 P3	DATP
1-O,6-O-digalloyl-beta-D-glucose	7.46E-04	3.82	484.0868	C20 H20 O14	1-O6-O-DIGALLOYL-BETA-D-GLUCOSE
dodecyl icosanoate	0	4.00	480.4921	C32 H64 O2	CPD-14270
myricetin 3-O-beta-D-glucoside	0	4.00	480.0962	C21 H20 O13	CPD-14843
quercetagetin 7-O-glucoside	0	4.00	479.0898	C21 H19 O13	CPD-14908
CTP	1.10E-03	3.49	478.9546	C9 H12 N3 O14 P3	CTP
4-methoxyglucobrassicin	1.51E-04	4.87	477.0645	C17 H21 N2 O10 S2	4-METHOXY-3-INDOLYLMETHYL-GLUCOSINOLATE
2,4-dinitrophenyl-S-glutathione	0	4.00	472.0728	C16 H18 N5 O10 S	S-24-DINITROPHENYL GLUTATHIONE
quercetin 7-O-glucoside	3.11E-03	2.43	463.0935	C21 H19 O12	CPD-8006
4-hydroxyglucobrassicin	0	4.00	463.0604	C16 H19 N2 O10 S2	4-HYDROXY-3-INDOLYLMETHYL-GLUCOSINOLATE
mersalyl acid	1.67E-04	5.10	461.0598	C13 H15 Hg N O5	CPD0-1313
wogonin 7-O-beta-D-glucuronate	0	4.00	459.0897	C22 H19 O11	CPD-12728
(-)-epigallocatechin-3-O-gallate	1.91E-03	3.15	458.0938	C22 H18 O11	CPD-15291

Compound	p (Corr) (Peg Vs Control)	Log FC (Peg Vs Control)	Mass	Formula	Compound Name
5-(methylsulfinyl)pentyl-glucosinolate	0	1.05	450.0594	C13 H24 N O10 S3	CPDQT-284
5'-phosphoribosyl-4-(N-succinocarboxamide)-5-aminoimidazole	0	4.00	450.0332	C13 H15 N4 O12 P	P-RIBOSYL-4-SUCCCARB-AMINOIMIDAZOLE
6-(methylsulfanyl)hexyl-glucosinolate	0	4.00	448.0845	C14 H26 N O9 S3	CPDQT-420
kaempferol 3-O-beta-D-glucoside	0	4.00	447.0875	C21 H19 O11	CPD1F-453
glucobrassicin	0	4.00	447.0522	C16 H19 N2 O9 S2	CPD-1863
CDP-ethanolamine	0	4.00	445.0517	C11 H19 N4 O11 P2	CDP-ETHANOLAMINE
(E)-1-(glutathion-S-yl)-N-hydroxy-omega-(methylsulfanyl)butan-1-imine	0	4.00	437.1247	C15 H25 N4 O7 S2	CPD-12390
5-(methylsulfanyl)pentyl-glucosinolate	0	4.27	434.0515	C13 H24 N O9 S3	CPDQT-286
2'-azido-2'-deoxyuridine-5'-diphosphate	0	1.49	425.9799	C9 H10 N5 O11 P2	CPD0-1393
tetrahydrothiamine diphosphate	0	-1.76	425.0475	C12 H19 N4 O7 P2 S	CPD0-1354
IDP	0	4.00	424.985	C10 H11 N4 O11 P2	IDP
ADP	0	4.00	424.0128	C10 H12 N5 O10 P2	ADP
adenosine 3',5'-bisphosphate	0	4.00	422.9911	C10 H11 N5 O10 P2	3-5-ADP
2'-chloro-2'-deoxyuridine-5'-diphosphate	0	4.00	418.9536	C9 H10 Cl N2 O11 P2	CPD0-1394
D-myo-inositol (1,4,5)-trisphosphate	0	4.00	416.9397	C6 H12 O15 P3	inositol_145-trisphosphate
glucotropaeolin	0	-4.00	408.0434	C14 H18 N O9 S2	GLUCOTROPEOLIN
CDP	0	4.00	399.9822	C9 H12 N3 O11 P2	CDP
strictosidine aglycone	0	-1.27	369.1796	C21 H25 N2 O4	STRICTOSIDINE-AGLYCONE
N-acetyl-farnesylcysteine	0	4.00	366.213	C20 H32 N O3 S	CPD-12592
(+)-pinoresinol	0	-1.57	358.144	C20 H22 O6	CPD-8905
Fe(II)-nicotianamine	1.51E-04	-4.81	357.0811	C12 H21 Fe N3 O6	CPD-10157
IMP	0	-1.09	346.0296	C10 H11 N4 O8 P	IMP
methyl-2-alpha-L-fucopyranosyl-beta-D-galactoside	0	4.00	340.1398	C13 H24 O10	CPD-8198
dihydrosanguinarine	0	-1.60	333.1058	C20 H15 N O4	DIHYDROSANGUINARINE
beta-nicotinate D-ribonucleotide	0	-4.00	333.0316	C11 H12 N O9 P	NICOTINATE_NUCLEOTIDE
cyclic-AMP	0	-2.29	328.0531	C10 H11 N5 O6 P	CAMP
ribavirin-5'-monophosphate	0	-4.00	322.0235	C8 H11 N4 O8 P	CPD0-1492
ubiquinone-2	0	1.29	318.1836	C19 H26 O4	UBIQUINONE-2
2-S-cysteinyldopaquinone	0	-4.00	314.0521	C12 H14 N2 O6 S	CPD-20261
thebaine	0	3.11	312.1579	C19 H22 N O3	CPD-7710
porphyrin-ring	0	-4.00	308.1067	C20 H12 N4	PORPHYRIN-RING
tributyrin	0	-2.49	302.1731	C15 H26 O6	CPD-13014

Compound	p (Corr) (Peg Vs Control)	Log FC (Peg Vs Control)	Mass	Formula	Compound Name
5alpha-androstane-3,17-dione	0	4.00	288.2096	C19 H28 O2	CPD-342
(R)-coclaurine	0	-4.00	286.1442	C17 H20 N O3	R-COCLAURINE
2-(cystein-S-yl)-2-(1H-indol-3-yl)-acetonitrile	7.29E-04	2.87	275.0813	C13 H13 N3 O2 S	CPD-12636
alpha-D-glucosamine 1-phosphate	0	-4.00	258.0391	C6 H13 N O8 P	GLUCOSAMINE-1P
ancymidol	0	-1.18	256.1221	C15 H16 N2 O2	CPD-4022
zealexin A1	0	1.33	233.1554	C15 H21 O2	CPD-13573
geranyl monophosphate	0	1.81	232.0863	C10 H17 O4 P	CPD-13243
2-C-methyl-D-erythritol 4-phosphate	0	-4.00	214.0277	C5 H11 O7 P	2-C-METHYL-D-ERYTHRITOL-4-PHOSPHATE
4-methylene diaminopimelate	3.49E-03	-3.34	202.0983	C8 H14 N2 O4	CPD0-1500
N,N-dihydroxyhomomethionine	0	-4.00	194.0446	C6 H12 N O4 S	CPD-14046
leucodopachrome	0	-4.00	194.0443	C9 H8 N O4	CPD-8652
1-(1H-indol-3-yl)-2-aci-nitroethane	1.51E-04	4.59	190.0781	C10 H10 N2 O2	CPD-12386
3-phosphooxypyruvate	0	-4.00	180.9555	C3 H2 O7 P	3-P-HYDROXYPYRUVATE
O-ureido-L-homoserine	0	4.00	177.0761	C5 H11 N3 O4	O-UREIDOHOMOSERINE
S-(2-aminoethyl)-L-cysteine	0	1.75	165.0692	C5 H13 N2 O2 S	S-2-AMINOETHYL-L-CYSTEINE
2-oxoadipate	0	-4.00	158.0219	C6 H6 O5	2K-ADIPATE
L-glutamate	0	4.00	146.0463	C5 H8 N O4	GLT
O-phosphoethanolamine	0	-4.00	140.0113	C2 H7 N O4 P	PHOSPHORYL-ETHANOLAMINE
thiosulfate	0	-1.64	112.9377	H O3 S2	S2O3
catechol	9.24E-03	-1.65	110.0367	C6 H6 O2	CATECHOL

Supplementary Table 1B. Differentially accumulated metabolites from Volcano analysis for V/N leaves under water stress compared to the control plants.

Compound	p (Corr) (Peg Vs Control)	Log FC (Peg Vs Control)	Mass	Formula	Compound Name
7,8-diaminopelargonate	0	-4.00	189.1607	C9 H21 N2 O2	DIAMINONONANOATE
gamma-L-glutamyl-(S)-methyl-L-cysteine	0	2.92	263.0752	C9 H15 N2 O5 S	CPD-17447
CDP	0	4.00	399.9822	C9 H12 N3 O11 P2	CDP
2'-chloro-2'-deoxyuridine-5'-diphosphate	0	4.00	418.9536	C9 H10 Cl N2 O11 P2	CPD0-1394
dolichol-group	0	4.00	1093.019	C80 H132	DOLICHOL-GROUP
pyridoxal 5'-phosphate	0	4.00	245.005	C8 H8 N O6 P	PYRIDOXAL_PHOSPHATE
4-methylene diaminopimelate	6.96E-03	-1.84	202.0983	C8 H14 N2 O4	CPD0-1500

Compound	p (Corr) (Peg Vs Control)	Log FC (Peg Vs Control)	Mass	Formula	Compound Name
pyridoxamine	0	-1.02	169.098	C8 H13 N2 O2	PYRIDOXAMINE
ribavirin-5'-monophosphate	0	-4.00	322.0235	C8 H11 N4 O8 P	CPD0-1492
tetra-acyl estolide	0	4.00	1208.978	C75 H132 O11	CPD-12262
1D-myo-inositol 3-diphosphate 1,2,4,5,6-pentakisphosphate	0	4.00	727.7311	C6 H7 O27 P7	CPD-11937
1D-myoinositol 5-diphosphate 1,2,3,4,6-pentakisphosphate	0	1.83	726.7312	C6 H6 O27 P7	5-DIPHOSPHO-1D-MYO-INOSITOL-12346P
D-myo-inositol (1,4,5)-trisphosphate	0	4.00	416.9397	C6 H12 O15 P3	inositol_145-trisphosphate
tri-acyl estolide	0	2.04	930.745	C57 H102 O9	CPD-17374
di-trans,octa-cis-undecaprenyl group	0	4.00	750.7071	C55 H90	TRANS-CIS-UNDECAPRENYL-GROUP
chlorophyll a	0	4.00	891.5285	C55 H71 Mg N4 O5	CHLOROPHYLL-A
decaprenyl diphosphate	0	4.00	858.5667	C50 H84 O7 P2	CPDQT-22
L-glutamate	0	-4.00	146.0463	C5 H8 N O4	GLT
norfuraneol	0	-1.25	114.0319	C5 H6 O3	CPD-10204
(S)-dihydroorotate	0	4.00	157.0238	C5 H5 N2 O4	DI-H-OROTATE
2-C-methyl-D-erythritol 4-phosphate	0	4.00	214.0277	C5 H11 O7 P	2-C-METHYL-D-ERYTHRITOL-4-PHOSPHATE
2-O-digalloyl-1,3,4,6-tetra-O-beta-D-galloylglucose	0	4.00	1092.1367	C48 H36 O30	CPD-8953
(3R)-3-hydroxylignoceroyl-CoA	0	4.00	1129.4316	C45 H78 N7 O18 P3 S	CPD-14277
trans-lignocer-2-enoyl-CoA	0	4.00	1111.4312	C45 H76 N7 O17 P3 S	CPD-14282
curcumin 4',4"-O-beta-D-digentiobioside	0	4.00	1016.3342	C45 H60 O26	CPD-6626
UDP-2-N,3-O-bis[(3R)-3-hydroxytetradecanoyl]-alpha-D-glucosamine	0	4.00	1015.4511	C43 H75 N3 O20 P2	OH-MYRISTOYL
docosanoyl-CoA	0	1.11	1085.4152	C43 H74 N7 O17 P3 S	CPD-10279
22-carboxy-docosanoyl-CoA	0	2.08	1114.3752	C43 H71 N7 O19 P3 S	CPD-14775
(7Z,10Z,13Z,16Z,19Z)-docosapentaenoyl-CoA	0	4.00	1075.3348	C43 H64 N7 O17 P3 S	CPD-14426
(5Z,8Z,11Z,14Z,17Z)-3-oxodocosapentaenoyl-CoA	0	4.00	1089.3115	C43 H62 N7 O18 P3 S	CPD-14423
peonidin-3-(p-coumaroyl)-rutinoside-5-glucoside	0	4.00	917.2713	C43 H49 O22	CPD-10504
cyanidin O-O-[6-O-(6-O-feruloyl-beta-D-glucosyl)-2-O-beta-D-xylosyl-beta-D-galactoside]	0	4.00	917.2362	C42 H45 O23	CPD-16529
(3R)-3-hydroxy-arachidoyl-CoA	0	4.00	1073.3789	C41 H70 N7 O18 P3 S	CPD-14275
icosanoyl-CoA	0	4.00	1057.3923	C41 H70 N7 O17 P3 S	CPD-9965
(11Z)-icosenoyl-CoA	0	4.00	1055.3455	C41 H68 N7 O17 P3 S	CPD-15363
3-oxo-auricoloyl-CoA	0	4.00	1083.3134	C41 H64 N7 O19 P3 S	CPD-17401
(2E,11Z,14Z)-icosatrienoyl-CoA	0	4.00	1051.3177	C41 H64 N7 O17 P3 S	CPD-17348
(2E,8Z,11Z,14Z,17Z)-icosapentaenoyl-CoA	0	4.00	1047.3059	C41 H60 N7 O17 P3 S	CPD-17264

Compound	p (Corr) (Peg Vs Control)	Log FC (Peg Vs Control)	Mass	Formula	Compound Name
tellimagrandin II	0	4.00	938.0994	C41 H30 O26	CPD-8949
1-linoleoyl-2-(3E)-hexadecenoyl-phosphatidylglycerol	0	4.00	743.4893	C40 H72 O10 P	CPD-2185
delphinidin 3-O-rutinoside-7-O-(6-O-(p-hydroxybenzoyl)-glucoside)	0	4.00	892.2178	C40 H44 O23	CPD-16559
3-cyano-L-alanine	0	-4.00	113.0353	C4 H5 N2 O2	CPD-603
uracil	0	-4.00	112.0274	C4 H4 N2 O2	URACIL
stearoyl-CoA	0	2.59	1029.3523	C39 H66 N7 O17 P3 S	STEAROYL-COA
3-oxo-2-(cis-2'-pentenyl)-cyclopentane-1-(3-oxooctanoyl)-CoA	0	4.00	1053.255	C39 H58 N7 O19 P3 S	CPD-11520
quercetin-3-gentiotetraside	0	4.00	950.2559	C39 H50 O27	CPD-14822
curcumin 4'-O-beta-D-gentiobiosyl 4''-O-beta-D-glucoside	0	4.00	854.2765	C39 H50 O21	CPD-6625
3-all trans-hexaprenyl-4-hydroxy-5-methoxybenzoate	0	4.00	575.4081	C38 H55 O4	3-HEXAPRENYL-4-HYDROXY-5-METHOXYBENZOATE
10,16-dihydroxypalmitoyl-CoA	0	4.00	1033.31	C37 H62 N7 O19 P3 S	CPD-17627
3-oxo-2-(cis-2'-pentenyl)-cyclopentane-1-(3R-hydroxyhexanoyl)-CoA	0	4.00	1027.2509	C37 H56 N7 O19 P3 S	CPD-11523
3-oxo-2-(cis-2'-pentenyl)-cyclopentane-1-hexanoyl-CoA	0	4.00	1011.275	C37 H56 N7 O18 P3 S	CPD-11521
coproporphyrin III	0	4.03	650.2406	C36 H34 N4 O8	COPROPORPHYRIN_III
(S)-3-hydroxy-(5Z)-tetradecenoyl-CoA	0	4.00	987.2648	C35 H56 N7 O18 P3 S	CPD0-1163
3-oxo-2-(cis-2'-pentenyl)-cyclopentane-1-butanoyl-CoA	0	4.00	983.2353	C35 H52 N7 O18 P3 S	CPD-11525
kaempferide triglycoside	0	4.00	770.2207	C34 H42 O20	CPD-14960
C-132-carboxypyropheophorbide a	0	4.36	577.2453	C34 H33 N4 O5	CPD-14963
lauroyl-CoA	0	4.00	945.2553	C33 H54 N7 O17 P3 S	LAUROYLCOA-CPD
quercetin-3-gentiotrioside	0	2.55	788.1967	C33 H40 O22	CPD-14821
delphinidin 3-O-rutinoside-7-O-glucoside	0	4.00	772.2139	C33 H40 O21	CPD-16558
lampranthin I	0	4.20	695.1682	C33 H31 N2 O15	CPD-15300
dodecyl icosanoate	0	4.00	480.4921	C32 H64 O2	CPD-14270
6'-hydroxyferuloyl-CoA	0	4.00	959.1577	C31 H44 N7 O20 P3 S	CPD4FS-4
baccatin III	0	4.00	586.2407	C31 H38 O11	BACCATIN-III
5-methyltetrahydropteroyl tri-L-glutamate	0	4.21	713.2384	C30 H35 N9 O12	CPD-1302
amaranthin	6.75E-03	4.27	724.165	C30 H32 N2 O19	CPD-8658
delphinidin-3-O-(6''-O-malonyl)-beta-glucoside-3'-O-beta-glucoside	0	4.00	711.137	C30 H31 O20	CPD-7870

Compound	p (Corr) (Peg Vs Control)	Log FC (Peg Vs Control)	Mass	Formula	Compound Name
3-phosphooxypyruvate	0	4.00	180.9555	C3 H2 O7 P	3-P-HYDROXYPYRUVATE
(2E)-oct-2-enoyl-CoA	0	4.00	887.1698	C29 H44 N7 O17 P3 S	CPD0-2108
10-deacetylbaccatin III	0	4.00	544.228	C29 H36 O10	10-DEACETYLBACCATIN-III
tetrahydropteroyl tri-L-glutamate	7.38E-05	4.03	699.2236	C29 H33 N9 O12	CPD-1301
pteroyl-gamma-glutamyl-gamma-glutamylglutamate	0	4.00	695.1862	C29 H29 N9 O12	CPD0-1473
1-methylpyrrolidine-2-acetyl-CoA	0	4.00	889.1775	C28 H44 N8 O17 P3 S	CPD-9771
pimeloyl-CoA	0	4.00	904.142	C28 H41 N7 O19 P3 S	CPD-558
luteolin 7-O-beta-D-diglucuronide	0	4.00	636.0956	C27 H24 O18	LUTEOLIN-7-O-BETA-D-DIGLUCURONIDE
cyanidin 3-O-(3",6"-O-dimalonyl-beta-glucopyranoside)	0	4.00	617.0767	C27 H21 O17	CPD-7700
6-O-methyl-N-deacetylisoipecoside	0	4.00	538.2224	C26 H36 N O11	CPD-14812
cyanidin 3-O-beta-D-sambubioside	7.53E-03	-4.35	579.1353	C26 H27 O15	CPD-16535
malonyldaidzin	0	4.00	501.1084	C24 H21 O12	CPD-3425
a xylogalacturonan	0	-3.53	678.1475	C23 H34 O23	CPD-10235
eupatolitin 3-glucoside	3.59E-03	2.77	508.1249	C23 H24 O13	CPD-14911
2-sinapoyloxy-3-butenylglucosinolate	0	4.00	594.0919	C22 H28 N O14 S2	CPD-12423
patulitrin	0	4.00	493.0997	C22 H21 O13	CPD-14909
wogonin 7-O-beta-D-glucuronate	0	4.00	459.0897	C22 H19 O11	CPD-12728
3-sinapoyloxypropylglucosinolate	0	4.00	582.094	C21 H28 N O14 S2	CPD-12417
NADH	0	3.45	663.1057	C21 H27 N7 O14 P2	NADH
NAD+	0	4.00	662.1047	C21 H26 N7 O14 P2	NAD
(+)-7-epi-12-hydroxyjasmonoyl-L-phenylalanine	0	1.21	372.1777	C21 H26 N O5	CPD-19818
myricetin 3-O-beta-D-glucoside	0	4.00	480.0962	C21 H20 O13	CPD-14843
quercetagetin 7-O-glucoside	0	4.00	479.0898	C21 H19 O13	CPD-14908
kaempferol 7-O-glucoside	0	4.00	447.0875	C21 H19 O11	CPD-8007
pelargonidin-3-O-beta-D-glucoside	0	1.20	431.1007	C21 H19 O10	PELARGONIDIN-3-GLUCOSIDE-CMPD
bisorganyltrisulfane	0	4.00	644.128	C20 H32 N6 O12 S3	CPD-11763
abieta-7,13-diene-18-oate	0	-1.97	301.2183	C20 H29 O2	CPD-8694
1-O,6-O-digalloyl-beta-D-glucose	0	4.08	484.0868	C20 H20 O14	1-O6-O-DIGALLOYL-BETA-D-GLUCOSE
(9Z)-12,13,17-trihydroxyoctadeca-9-enoate	0	4.00	329.2302	C18 H33 O5	CPD-13087
(9Z,12Z)-15,16-dihydroxyoctadeca-9,12-dienoate	0	-1.86	311.2236	C18 H31 O4	CPD-13093

Compound	p (Corr) (Peg Vs Control)	Log FC (Peg Vs Control)	Mass	Formula	Compound Name
4-benzoyloxybutylglucosinolate	0	4.00	494.0762	C18 H24 N O11 S2	CPD-12420
2-benzoyloxy-3-butenylglucosinolate	0	4.00	492.0717	C18 H22 N O11 S2	CPD-12421
UDP-N-acetyl-alpha-D-glucosamine	0	4.00	605.0673	C17 H25 N3 O17 P2	UDP-N-ACETYL-D-GLUCOSAMINE
CMP-3-deoxy-beta-D-manno-octulosonate	0	4.35	541.0875	C17 H24 N3 O15 P	CMP-KDO
FMNH2	0	4.00	456.1001	C17 H21 N4 O9 P	FMNH2
(R)-coclaurine	0	-1.36	286.1442	C17 H20 N O3	R-COCLAURINE
FMN	0	4.00	453.0822	C17 H18 N4 O9 P	FMN
(S)-tetrahydroprotoberberine	3.24E-04	-2.67	236.1442	C17 H18 N	S-781314-TETRAHYDROPROTOBERBERINE
3,3'-dimethylquercetin	0	-4.00	330.0655	C17 H14 O7	CPD-14946
8-(methylsulfinyl)octyl-glucosinolate	0	4.00	492.1036	C16 H30 N O10 S3	CPDQT-299
succinate-semialdehyde-thiamine PPi	0	4.00	527.0771	C16 H25 N4 O10 P2 S	SUCCINATE-SEMIALDEHYDE-THIAMINE-PPI
dTDP-beta-L-rhamnose	0	4.00	546.0677	C16 H24 N2 O15 P2	DTDP-RHAMNOSE
GDP-beta-L-fucose	3.91E-05	4.41	587.0687	C16 H23 N5 O15 P2	CPD-13118
GDP-4-dehydro-alpha-D-rhamnose	0	4.00	585.0539	C16 H21 N5 O15 P2	GDP-4-DEHYDRO-6-DEOXY-D-MANNOSE
elwesine	0	-1.64	275.1501	C16 H21 N O3	CPD-19423
4-hydroxyglucobrassicin	0	4.00	463.0604	C16 H19 N2 O10 S2	4-HYDROXY-3-INDOLYLMETHYL-GLUCOSINOLATE
2,4-dinitrophenyl-S-glutathione	0	4.00	472.0728	C16 H18 N5 O10 S	S-24-DINITROPHENYLGLUTATHIONE
7-(methylsulfanyl)heptyl-glucosinolate	0	3.16	462.098	C15 H28 N O9 S3	CPDQT-296
FAD stem group	5.56E-03	2.47	559.0898	C15 H25 N6 O13 P2	FAD-STEM-GROUP
UDP-6-deoxy-alpha-D-galactose	0	4.00	548.0434	C15 H22 N2 O16 P2	CPD0-1898
zealexin A1	0	1.71	233.1554	C15 H21 O2	CPD-13573
ADP-D-ribose	0	4.00	557.0598	C15 H21 N5 O14 P2	ADENOSINE_DIPHOSPHATE_RIBOSE
NAD stem group	0	4.00	541.0619	C15 H21 N5 O13 P2	NAD-STEM-GROUP
epoxypseudoisoeugenol-2-methylbutanoate	5.56E-03	-2.46	264.1376	C15 H20 O4	CPD-9948
trans-zeatin riboside diphosphate	0	4.00	508.0647	C15 H20 N5 O11 P2	CPD-4204
N6-(Delta2-isopentenyl)-adenosine 5'-diphosphate	0	4.00	492.0755	C15 H20 N5 O10 P2	CPD-4203
6-(methylsulfanyl)hexyl-glucosinolate	0	4.00	448.0845	C14 H26 N O9 S3	CPDQT-420
2-phospho-4-(cytidine 5'-diphospho)-2-C-methyl-D-erythritol	0	4.00	597.0206	C14 H22 N3 O17 P3	2-PHOSPHO-4-CYTIDINE-5-DIPHOSPHO-2-C-MET
salidroside	0	1.98	300.1248	C14 H20 O7	CPD-13354

Compound	p (Corr) (Peg Vs Control)	Log FC (Peg Vs Control)	Mass	Formula	Compound Name
glucotropaeolin	0	4.00	408.0434	C14 H18 N O9 S2	GLUCOTROPEOLIN
tetrahydropteroate	0	-2.41	315.1181	C14 H15 N6 O3	CPD-9020
petivericin	0	4.00	262.048	C14 H14 O S2	CPD-12487
methyl-2-alpha-L-fucopyranosyl-beta-D-galactoside	0	4.00	340.1398	C13 H24 O10	CPD-8198
5-(methylsulfanyl)pentyl-glucosinolate	0	4.00	434.0515	C13 H24 N O9 S3	CPDQT-286
5-(methylsulfinyl)pentyl-glucosinolate	0	4.00	450.0594	C13 H24 N O10 S3	CPDQT-284
5'-phosphoribosyl-4-(N-succinocarboxamide)-5-aminoimidazole	0	4.00	450.0332	C13 H15 N4 O12 P	P-RIBOSYL-4-SUCCCARB-AMINOIMIDAZOLE
N-(2-methoxy-4-pyridyl)-N'-phenylurea	0	-1.00	243.1001	C13 H13 N3 O2	CPD-5482
2-[(2'-methylsulfanyl)heptyl]maleate	0	4.00	258.0918	C12 H18 O4 S	CPD-19481
2-S-cysteinyldopaquinone	0	-4.00	314.0521	C12 H14 N2 O6 S	CPD-20261
CDP-ethanolamine	0	4.00	445.0517	C11 H19 N4 O11 P2	CDP-ETHANOLAMINE
triacsin C	0	1.44	207.1397	C11 H17 N3 O	CPD-14770
beta-nicotinate D-ribonucleotide	0	-4.00	333.0316	C11 H12 N O9 P	NICOTINATE_NUCLEOTIDE
8-hydroxy-dATP	3.19E-05	4.87	504.9798	C10 H14 N5 O13 P3	CPD0-1093
thymidine	0	1.22	242.0912	C10 H14 N2 O5	THYMIDINE
adenylyl-imidodiphosphate	1.43E-04	3.64	501.9766	C10 H13 N6 O12 P3	CPD0-1054
porphobilinogen	0	5.41	225.0852	C10 H13 N2 O4	PORPHOBILINOGEN
8-oxo-GTP	1.28E-03	-2.59	534.9495	C10 H12 N5 O15 P3	CPD-12366
dATP	1.43E-04	3.43	486.9718	C10 H12 N5 O12 P3	DATP
cyclic-AMP	0	-1.98	328.0531	C10 H11 N5 O6 P	CAMP
adenosine 3',5'-bisphosphate	0	4.00	422.9911	C10 H11 N5 O10 P2	3-5-ADP
IDP	0	4.00	424.985	C10 H11 N4 O11 P2	IDP

Supplementary Table 1C. Differentially accumulated metabolites from Volcano analysis for V/V roots under water stress compared to the control plants.

Compound	p (Corr) (Peg Vs Control)	Log FC (Peg Vs Control)	Mass	Formula	Compound Name
(+)-7-epi-12-hydroxyjasmonoyl-L-phenylalanine	0	-3.12	37218	C21 H26 N O5	CPD-19818
8-oxo-GTP	0	-3.06	5349495	C10 H12 N5 O15 P3	CPD-12366
p-coumaroyltriacetate	0	-2.87	2890685	C15 H13 O6	CPD-6954
5-O-methylthujaplicatin	0	-2.58	3881606	C21 H24 O7	CPD-17593
9-oxononanoate	0	-2.54	1711013	C9 H15 O3	CPD-8686
(S)-tetrahydroprotoberberine	0	-2.36	2361429	C17 H18 N	S-781314-TETRAHYDROPROTOBERBERINE
2,3-dioctanoylglyceramide	0	-2.09	3572553	C19 H35 N O5	CPD0-1807

Compound	p (Corr) (Peg Vs Control)	Log FC (Peg Vs Control)	Mass	Formula	Compound Name
p-coumaroylserotonin	0	-1.88	3221345	$C_{19}H_{18}N_{2}O_{3}$	CPD-8936
dethiobiotin	0	-1.88	2131252	$C_{10}H_{17}N_{2}O_{3}$	DETHIOBIOTIN
(indol-3-yl)acetate	0	-1.84	1740564	$C_{10}H_{8}NO_{2}$	INDOLE_ACETATE_AUXIN
3-glc-glc-rha, 28-glc medicagenic acid	0	-1.84	1134543	$C_{54}H_{86}O_{25}$	CPD2GG-5257
chrysin	0	-1.82	2530542	$C_{15}H_{9}O_{4}$	CPD-8184
indolepropanol phosphate	0	-1.82	2530542	$C_{11}H_{12}NO_{4}P$	CPD-12164
4-O-methyl-DIBOA-glucoside	0	-1.68	3571077	$C_{15}H_{19}NO_{9}$	CPD-6627
epi-cholestanol	0	-1.59	3883755	$C_{27}H_{48}O$	CPD-7193
2,3-diphospho-D-glycerate	0	-1.27	2609214	$C_{3}H_{3}O_{10}P_{2}$	23-DIPHOSPHOGLYCERATE
feruloylacetyl-CoA	0	-1.23	9811445	$C_{33}H_{42}N_{7}O_{20}P_{3}S$	CPD-12180
chromate	0	-1.21	1149331	$CrHO_{4}$	CPD-4422
D-gluconate 6-phosphate	0	-1.11	2729955	$C_{6}H_{10}O_{10}P$	CPD-2961
butanoate	0	-1.00	870471	$C_{4}H_{7}O_{2}$	BUTYRIC_ACID
3-methoxy-4-hydroxy-5-all-trans-nonaprenylbenzoate	0	-9.56	779592	$C_{53}H_{79}O_{4}$	CPD-9898
p-nitrophenyl-beta-D-cellobioside	4.29E+06	-6.08	4631311	$C_{18}H_{25}NO_{13}$	CPD-13199
(E)-1-(L-cysteinylglycin-S-yl)-N-hydroxy-2-(1H-indol-3-yl)ethan-1-imine	0	-5.11	35011	$C_{15}H_{18}N_{4}O_{4}S$	CPD-12388
7-hydroxy-4'5'-dimethoxyisoflavone	0	-2.18	2980809	$C_{17}H_{14}O_{5}$	CPD-9530
2'-deoxycytidine	0	-1.91	2270947	$C_{9}H_{13}N_{3}O_{4}$	DEOXYCYTIDINE
kaempferide triglycoside	0	-1.86	7702295	$C_{34}H_{42}O_{20}$	CPD-14960
beta-nicotinamide D-ribonucleotide	0	-1.75	3330493	$C_{11}H_{14}N_{2}O_{8}P$	NICOTINAMIDE_NUCLEOTIDE
7,8-dihydroneopterin 3'-phosphate	0	-1.75	3330494	$C_{9}H_{12}N_{5}O_{7}P$	DIHYDRONEOPTERIN-P
glucobrassicin	0	-1.39	4470568	$C_{16}H_{19}N_{2}O_{9}S_{2}$	CPD-1863
4-fluorobenzoate	0	-1.08	1390178	$C_{7}H_{4}FO_{2}$	4-FLUOROBENZOATE
(-)-isopiperitenone	0	-4.00	1501047	$C_{10}H_{14}O$	CPD-1090
1-pyrroline-2-carboxylate	0	-4.00	1120403	$C_{5}H_{6}NO_{2}$	DELTA1-PYRROLINE_2-CARBOXYLATE
3,4-dihydroxypyridin	0	-4.00	1110325	$C_{5}H_{5}NO_{2}$	DIHYDROXYPIRIDIN-CPD
3',5'-di-C-glucosylphloretin	0	-4.00	5981937	$C_{27}H_{34}O_{15}$	CPD-20011
3-sulfanylpropanoate	0	-4.00	1050037	$C_{3}H_{5}O_{2}S$	CPD-7673
4-vinylpyridine	0	-4.00	1050584	$C_{7}H_{7}N$	CPD-5542
9'-hydroxyabscisate	0	-4.00	2791232	$C_{15}H_{19}O_{5}$	CPD-7728
D-alanine	0	-4.00	890505	$C_{3}H_{7}NO_{2}$	D-ALANINE
D-glucarate	0	-4.00	2080208	$C_{6}H_{8}O_{8}$	D-GLUCARATE
DL -alpha-difluoromethyllysine	0	-4.00	197107	$C_{7}H_{15}F_{2}N_{2}O_{2}$	CPD-7990

Compound	p (Corr) (Peg Vs Control)	Log FC (Peg Vs Control)	Mass	Formula	Compound Name
hamamelose-21,5-bisphosphate	0	-4.00	3399949	C6 H14 O12 P2	CPDQT-7
lampranthin I	0	-4.00	6951719	C33 H31 N2 O15	CPD-15300
methylconiine	0	-4.00	1421602	C9 H20 N	CPD-9426
pheophorbide b	0	-4.00	6052382	C35 H33 N4 O6	CPD-7062
sinigrin	0	-4.00	3580288	C10 H16 N O9 S2	2-PROPENYL-GLUCOSINOLATE
alpha-terpinyl cation	0	4.00	1391538	C10 H19	CPD-12228
beta-myrcene	0	4.00	1361293	C10 H16	CPD-4888
(-)-curcuquinone	0	4.00	2321458	C15 H20 O2	CPD-9877
(E)-1-(L-cystein-S-yl)-N-hydroxy-omega-(methylsulfanyl)pentan-1-imine	0	4.00	2660702	C9 H18 N2 O3 S2	CPDQT-406
(3R)-3-hydroxylignoceroyl-CoA	0	4.00	11294409	C45 H78 N7 O18 P3 S	CPD-14277
(6R)-4a-hydroxy-tetrahydrobiopterin	0	4.00	2571133	C9 H15 N5 O4	CPD-5881
(8Z,11Z,14Z,17Z)-3-oxoicosatetraenoyl-CoA	0	4.00	10633085	C41 H60 N7 O18 P3 S	CPD-17262
(9Z,12Z,15Z)-hexadeca-9,12,15-trienoyl-CoA	0	4.00	9952752	C37 H56 N7 O17 P3 S	CPD-10255
(S)-3-hydroxy-(5Z)-tetradecenoyl-CoA	0	4.00	9872648	C35 H56 N7 O18 P3 S	CPD0-1163
N2,N2-dihydroxy-L-tryptophan	0	4.00	2350723	C11 H11 N2 O4	CPD-13027
p-nitrophenyl-beta-D-xylopyranoside	0	4.00	2710715	C11 H13 N O7	CPD-13210
trans-1,4-diaminocyclohexane	0	4.00	1161319	C6 H16 N2	CPD-19537
trans-lignocer-2-enoyl-CoA	0	4.00	11114312	C45 H76 N7 O17 P3 S	CPD-14282
1,2,3,4,6-pentagalloylglucose	0	4.00	940113	C41 H32 O26	12346-PENTAKIS-O-GALLOYL-BETA-D-GLUC
1-O-4-hydroxybenzoyl-beta-D-glucose	0	4.00	3000869	C13 H16 O8	CPD-15283
10,16-dihydroxypalmitoyl-CoA	0	4.00	10333066	C37 H62 N7 O19 P3 S	CPD-17627
18-hydroxylinoleoyl-CoA	0	4.00	10413188	C39 H62 N7 O18 P3 S	CPD-17371
1D-myo-inositol 3-diphosphate 1,2,4,5,6-pentakisphosphate	0	4.00	7277311	C6 H7 O27 P7	CPD-11937
3,5,7-trioxododecanoyl-CoA	0	4.00	9871782	C33 H48 N7 O20 P3 S	CPD-14615
3,5-dioxodecanoyl-CoA	0	4.00	9451863	C31 H46 N7 O19 P3 S	CPD-14687
3-oxo-2-(cis-2'-pentenyl)-cyclopentane-1-(3-oxohexanoyl)-CoA	0	4.00	10252354	C37 H54 N7 O19 P3 S	CPD-11524
3-oxo-2-(cis-2'-pentenyl)-cyclopentane-1-(E-buta-2-enoyl)-CoA	0	4.00	9812059	C35 H50 N7 O18 P3 S	CPD-11526
3-oxo-2-(cis-2'-pentenyl)-cyclopentane-1-(E-octa-2-enoyl)-CoA	0	4.00	10372815	C39 H58 N7 O18 P3 S	CPD-11518

Compound	p (Corr) (Peg Vs Control)	Log FC (Peg Vs Control)	Mass	Formula	Compound Name
4-deoxypyridoxine 5'-phosphate	0	4.00	231028	$C_{8}H_{10}NO_{5}P$	CPD0-1221
4-hydroxybutanoate	0	4.00	1030399	$C_{4}H_{7}O_{3}$	4-HYDROXY-BUTYRATE
6'-hydroxyferuloyl-CoA	0	4.00	9591577	$C_{31}H_{44}N_{7}O_{20}P_{3}S$	CPD4FS-4
7,8-dihydroneopterin 3'-triphosphate	0	4.00	4909648	$C_{9}H_{12}N_{5}O_{13}P_{3}$	DIHYDRONEOPTERIN-P3
acryloyl-CoA	0	4.00	8170953	$C_{24}H_{34}N_{7}O_{17}P_{3}S$	ACRYLYL-COA
bisdemethoxycurcumin	0	4.00	3081059	$C_{19}H_{16}O_{4}$	CPD-12188
bromohydrin of isopentenyl pyrophosphate	0	4.00	3389069	$C_{5}H_{10}BrO_{8}P_{2}$	CPD0-1025
C33 botryococcene	0	4.00	4524488	$C_{33}H_{56}$	CPD-14289
CDP group	0	4.00	4009941	$C_{9}H_{13}N_{3}O_{11}P_{2}$	CDP-GROUP
celosianin II	0	4.00	9002102	$C_{40}H_{40}N_{2}O_{22}$	CPD-8676
chelidamate	0	4.00	1810046	$C_{7}H_{3}NO_{5}$	CPD0-1271
chlorophyll a	0	4.00	8915356	$C_{55}H_{71}MgN_{4}O_{5}$	CHLOROPHYLL-A
clorgyline	0	4.00	2710474	$C_{13}H_{15}Cl_{2}NO$	CPD-7656
cyanidin 3-O-[6-O-(4-O-beta-D-glucosyl-p-coumaroyl)-2-O-(beta-D-xylosyl)-beta-D-glucosyl]-5-O-(6-O-malonyl-beta-D-glucoside)	0	4.00	11352714	$C_{50}H_{55}O_{30}$	CPD-15234
cyanidin 3-O-glucoside-7-O-(6-O-(4-O-(6-O-(p-hydroxybenzoyl)-glucosyl)-oxybenzoyl)-glucoside)	0	4.00	10122421	$C_{47}H_{48}O_{25}$	CPD-16604
delphinidin 3-O-glucosyl-5-O-(caffeoylglucoside-3'-O-glucoside)	0	4.00	9502331	$C_{42}H_{46}O_{25}$	CPD-7963
D-sorbitol 6-phosphate	0	4.00	2600303	$C_{6}H_{13}O_{9}P$	D-SORBITOL-6-P
elwesine	0	4.00	2751501	$C_{16}H_{21}NO_{3}$	CPD-19423
FADH2	0	4.00	7851599	$C_{27}H_{33}N_{9}O_{15}P_{2}$	FADH2
gypsogenin-28-beta-D-glucoside	0	4.00	6323895	$C_{36}H_{56}O_{9}$	CPD-9472
hydroxymethyl-dCDP	0	4.00	4140069	$C_{10}H_{14}N_{3}O_{11}P_{2}$	CPD0-1345
loganin	0	4.00	3901507	$C_{17}H_{26}O_{10}$	LOGANIN
mizoribine 5'-monophosphate	0	4.00	3370248	$C_{9}H_{12}N_{3}O_{9}P$	CPD-12503
oleoyl-CoA	0	4.00	10273246	$C_{39}H_{64}N_{7}O_{17}P_{3}S$	OLEOYL-COA
precorrin-1	0	4.00	842226	$C_{41}H_{38}N_{4}O_{16}$	CPD-9038
quercetin 3-sulfate	0	4.00	3799874	$C_{15}H_{8}O_{10}S$	CPD-1822
ribavirin-5'-monophosphate	0	4.00	3220375	$C_{8}H_{11}N_{4}O_{8}P$	CPD0-1492
sucrose 6G-phosphate	0	4.00	4200625	$C_{12}H_{21}O_{14}P$	CPD-15716
tetra-acyl estolide	0	4.00	1208978	$C_{75}H_{132}O_{11}$	CPD-12262
thidiazuron	0	4.00	2200374	$C_{9}H_{8}N_{4}OS$	THIDIAZURON
(3R)-3-amino-3-phenylpropanoyl-CoA	0	1.64	9111596	$C_{30}H_{42}N_{8}O_{17}P_{3}S$	CPD-9207
3-phenylpropanoyl-CoA	0	2.40	8951321	$C_{30}H_{40}N_{7}O_{17}P_{3}S$	CPD-503

Compound	p (Corr) (Peg Vs Control)	Log FC (Peg Vs Control)	Mass	Formula	Compound Name
cinnamoyl-CoA	0	2.57	8931235	C30 H38 N7 O17 P3 S	CINNAMOYL-COA
(E)-glutaconyl-CoA	0	2.74	8740918	C26 H35 N7 O19 P3 S	GLUTACONYL-COA
P1,P5-bis(5'-adenosyl) pentaphosphate	0	2.89	9109598	C20 H24 N10 O22 P5	CPD0-1137
lignoceroyl-CoA	0	3.00	11134323	C45 H78 N7 O17 P3 S	CPD-10280
3-[(3'-methylsulfanyl)propyl]malate	0	3.66	220037	C8 H12 O5 S	CPDQT-36
gamma-Glu-Cys-gamma-Glu-Cys-beta-Ala	0	4.51	5511417	C19 H29 N5 O10 S2	CPD-13498
3-oxo-auricoloyl-CoA	0	4.65	10833267	C41 H64 N7 O19 P3 S	CPD-17401
plastoquinol-9	0	1.10	75265	C53 H84 O2	CPDQT-459
4-(2-amino-3-hydroxyphenyl)-2,4-dioxobutanoate	0	1.19	2220387	C10 H8 N O5	CPD-11552
hexanoyl-CoA	0	1.20	8611546	C27 H42 N7 O17 P3 S	HEXANOYL-COA
(E,E)-piperoyl-CoA	0	1.21	9631311	C33 H40 N7 O19 P3 S	EE-PIPEROYL-COA
beta-solanine	0	1.35	7214392	C39 H63 N O11	CPD-9212
glutathione disulfide	0	1.35	610136	C20 H30 N6 O12 S2	OXIDIZED-GLUTATHIONE
homoglutathione	0	1.54	3200901	C11 H18 N3 O6 S	CPD-211
alizarin	0	1.58	2400411	C14 H8 O4	ALIZARIN
eupatolin	0	1.62	4921212	C23 H24 O12	CPD-14912
alpha-chaconine	0	1.66	8525128	C45 H74 N O14	CPD-9214
7-hydroxylauroyl-CoA	0	1.81	9612503	C33 H54 N7 O18 P3 S	CPD-17638
(3R)-3-hydroxy-arachidoyl-CoA	0	1.83	10733639	C41 H70 N7 O18 P3 S	CPD-14275
3-oxohexanoyl-CoA	0	2.00	875137	C27 H40 N7 O18 P3 S	K-HEXANOYL-COA
(2S,3S)-3-hydroxy-2-methylbutanoyl-CoA	0	2.00	8631434	C26 H40 N7 O18 P3 S	2-METHYL-3-HYDROXY-BUTYRYL-COA
malonyl-CoA	0	2.01	8480787	C24 H33 N7 O19 P3 S	MALONYL-COA
violdelphin	0	2.01	11742963	C53 H58 O30	CPD-16561
siroheme	0	2.05	9061571	C42 H36 Fe N4 O16	SIROHEME
curcumin 4',4''-O-beta-D-digentiobioside	0	2.05	10163318	C45 H60 O26	CPD-6626
1-(18-hydroxyoleoyl)-sn-glycrol 3-phosphate	0	2.11	4502359	C21 H39 O8 P	CPD-17372
3-oxooctanoyl-CoA	0	2.15	9031555	C29 H44 N7 O18 P3 S	CPD0-2106
malonylshisonin	0	2.16	8411872	C39 H37 O21	CPD-7708
thiamine diphosphate	0	2.22	4220276	C12 H16 N4 O7 P2 S	THIAMINE-PYROPHOSPHATE
N-methylanthraniloyl-CoA	0	2.35	8961273	C29 H39 N8 O17 P3 S	N-METHYLANTHRANILOYL-COA
salidroside	0	2.46	3001205	C14 H20 O7	CPD-13354
preuroporphyrinogen	0	2.54	8462116	C40 H38 N4 O17	HYDROXYMETHYLBILANE
uroporphyrinogen-I	0	2.54	8282102	C40 H36 N4 O16	CPD-11444
N-dimethylethanolamine	0	2.57	9009	C4 H12 N O	CPD-5602

Compound	p (Corr) (Peg Vs Control)	Log FC (Peg Vs Control)	Mass	Formula	Compound Name
anthraniloyl-CoA	0	2.57	8821133	C28 H37 N8 O17 P3 S	2-AMINOBENZOYL-COA
syringin	0	2.63	3721427	C17 H24 O9	CPD-63
2,4-dinitrophenyl-S-glutathione	0	2.64	4720728	C16 H18 N5 O10 S	S-24-DINITROPHENYL GLUTATHIONE
2-[(7'-methylsulfanyl)heptyl]malate	0	2.64	276102	C12 H20 O5 S	CPDQT-35
8-(methylsulfanyl)octyl-glucosinolate	0	2.66	4761065	C16 H30 N O9 S3	CPDQT-300
71-hydroxychlorophyllide a	0	2.68	6282149	C35 H32 Mg N4 O6	CPD-7015
cis-12-sulfojasmonate	0	2.72	3040577	C12 H16 O7 S	CPD-19816
benzoyl-beta-D-glucopyranose	0	3.00	284092	C13 H16 O7	CPD-12630
CDP-alpha-D-glucose	0	3.50	563063	C15 H23 N3 O16 P2	CDP-D-GLUCOSE
stearoyl-CoA	0	3.52	10293424	C39 H66 N7 O17 P3 S	STEAROYL-COA
6-(methylsulfanyl)hexyl-glucosinolate	0	3.55	4480788	C14 H26 N O9 S3	CPDQT-420
CDP-ethanolamine	0	3.61	4450517	C11 H19 N4 O11 P2	CDP-ETHANOLAMINE
kaempferol 7-O-glucoside	0	3.71	4470875	C21 H19 O11	CPD-8007
ADP	0	3.82	4240128	C10 H12 N5 O10 P2	ADP
P1-uridyl-P2-phenyl diphosphate	0	3.90	478019	C15 H16 N2 O12 P2	CPD0-1324
(11Z)-icosenoyl-CoA	0	3.91	10553685	C41 H68 N7 O17 P3 S	CPD-15363
D-myo-inositol (1,4,5)-trisphosphate	0	4.07	4169399	C6 H12 O15 P3	inositol_145-trisphosphate
aureobasidin A	0	4.19	11006729	C60 H92 N8 O11	CPD-14755
icosanoyl-CoA	0	4.22	10573794	C41 H70 N7 O17 P3 S	CPD-9965
linoleoyl-CoA	0	4.72	1025295	C39 H62 N7 O17 P3 S	CPD-18
(2E,5Z)-tetradecenoyl-CoA	0	4.82	969256	C35 H54 N7 O17 P3 S	CPD0-1162
(20S)-ginsenoside Rh2	0	5.58	6224436	C36 H62 O8	CPD-12104
dCTP	4.29E+06	5.85	462956	C9 H12 N3 O13 P3	DCTP
NAD stem group	0	6.10	5410619	C15 H21 N5 O13 P2	NAD-STEM-GROUP

Supplementary Table 1D. Differentially accumulated metabolites from Volcano analysis for V/N roots under water stress compared to the control plants.

Compound	p (Corr) (Peg Vs Control)	Log FC (Peg Vs Control)	Mass	Formula	Compound Name
thymine	0	-9.94	1260423	C5 H6 N2 O2	THYMINE
difluoromethylornithine	4.17E-02	-5.42	1830933	C6 H13 F2 N2 O2	DIFLUOROMETHYLORNITHINE
p-coumaroyltyramine	2.50E-02	-4.91	2831227	C17 H17 N O3	CPD-8943
hemanthamine	2.50E-02	-4.91	3011332	C17 H19 N O4	CPD-19429
3-methyl-1,2-didehydro-2,3-dihydrosqualene	0	-4.48	4244153	C31 H52	CPD-14263
N-(beta-D-glucosyl)-(indol-3-yl)acetyl-L-glutamate	0	-4.31	4641388	C21 H24 N2 O10	CPD-9573

Compound	p (Corr) (Peg Vs Control)	Log FC (Peg Vs Control)	Mass	Formula	Compound Name
dihydrosterculate	2.08E-02	-4.07	2952655	C19 H35 O2	DIHYDROSTERCULIC-ACID
1-(p-butylphenyl)-2,2-dimethyl-4,6-diamino-1,2-dihydro-s-triazine	2.50E-02	-4.00	2731964	C15 H23 N5	CPD0-1590
(3Z)-hex-3-en-1-yl acetate	8.74E+06	-3.97	1421003	C8 H14 O2	CPD-12846
alpha-tocotrienol	5.57E-02	-3.96	4243352	C29 H44 O2	CPD-15836
1-18:2-2-18:2-digalactosyldiacylglycerol	5.96E-02	-3.88	9406127	C51 H88 O15	CPD-8082
thiosulfinate	0	-3.72	1620117	C6 H10 O S2	CPD-9306
indolin-2-one	4.23E+06	-3.67	1330528	C8 H7 N O	CPD-6361
3-(1H-indol-3-yl)propanoate	6.20E-02	-3.42	1880725	C11 H10 N O2	INDOLE-PROPIONATE
alpha-chaconine	0	-3.36	8525128	C45 H74 N O14	CPD-9214
(-)-jasmonoyl-1-aminocyclopropane-1 carboxylate	5.96E-02	-3.32	2921546	C16 H22 N O4	CPD-19728
O-sinapoylcholine	6.20E-02	-3.31	3101653	C16 H24 N O5	O-SINAPOYLCHOLINE
1,4-dihydroxy-6,7,8-trimethoxy-2-methylanthraquinone	4.23E+06	-3.31	3440832	C18 H16 O7	CPD-9632
dihydropinosylvin	4.94E+06	-3.30	214097	C14 H14 O2	CPD-6963
3-(methylsulfanyl)propyl-desulfoglucosinolate	4.30E+06	-3.29	3270803	C11 H21 N O6 S2	3-METHYLTHIOPROPYL-DESULFO-GLUCOSINOLATE
D-erythro-imidazole-glycerol-phosphate	0	-3.28	2360213	C6 H9 N2 O6 P	D-ERYTHRO-IMIDAZOLE-GLYCEROL-P
beta-methylenecyclopropyl pyruvate	2.43E+06	-3.25	1390403	C7 H7 O3	CPD-9739
stigmasterol 3-O-beta-D-glucoside	0	-3.25	5744264	C35 H58 O6	CPD-11606
cis-indole-2,3-dihydrodiol	5.96E+06	-3.23	1510638	C8 H9 N O2	CPD-10523
3,4-dihydroxybenzaldehyde	2.43E+06	-3.21	1380324	C7 H6 O3	CPD-7616
10,16-dihydroxypalmitate	8.87E-02	-3.19	2872211	C16 H31 O4	9--OR-1016-DIHYDROXYPALMITATE
trans-5-O-(4-coumaroyl)shikimate	3.56E-02	-3.18	31908	C16 H15 O7	CPD-412
1-18:2-2-18:2-monogalactosyldiacylglycerol	7.63E-02	-3.18	7785664	C45 H78 O10	CPD-8165
16-oxo-palmitate	8.87E-02	-3.17	2692109	C16 H29 O3	CPD-10512
3-(O-beta-glucosyl)-(2-oxindol-3-yl)acetyl-L-aspartate	7.67E+05	-3.14	4821169	C20 H22 N2 O12	3-O-BETA-GLUCOSYL-2-OXINDOLE-3-ACETYL-
scopolamine	1.87E+06	-3.03	3031494	C17 H21 N O4	SCOPOLAMINE
coumestrol	4.23E+06	-3.02	2680365	C15 H8 O5	CPD-11779
acifluorfen	4.73E-02	-3.01	3599808	C14 H6 Cl F3 N O5	ACIFLUORFEN
3-(phosphonoacetylamido)-L-alanine	2.88E+06	-3.01	2250266	C5 H10 N2 O6 P	CPD0-1454
indole	1.44E+06	-2.99	1170584	C8 H7 N	INDOLE
apigeninidin 5-O-glucoside	2.27E+06	-2.94	4161116	C21 H20 O9	CPD-15272
4-O-oxalyl-L-threonate	3.37E+06	-2.92	2060081	C6 H6 O8	CPD-13911

Compound	p (Corr) (Peg Vs Control)	Log FC (Peg Vs Control)	Mass	Formula	Compound Name
4-guanidinobutyraldehyde	6.95E+05	-2.89	1300965	C5 H12 N3 O	CPD-825
raffinose	5.22E+06	-2.88	5041691	C18 H32 O16	CPD-1099
soyasaponin I	0	-2.86	9415207	C48 H77 O18	CPD-13255
16-feruloyloxypalmitate	0	-2.86	4472752	C26 H39 O6	CPD-11591
1,3,5,6-tetrahydroxyxanthone	6.49E+06	-2.84	25903	C13 H7 O6	CPD-6886
O-phospho-L-tyrosine	6.49E+06	-2.84	2590299	C9 H10 N O6 P	CPD-3728
methylcinnamate	6.20E-02	-2.80	162069	C10 H10 O2	CPD-6421
1-palmitoyl-2-alpha-linolenoyl-phosphatidylcholine	2.79E+05	-2.77	7555453	C42 H78 N O8 P	CPD-8159
L-cycloserine	5.92E+06	-2.76	1030505	C3 H7 N2 O2	CPD-2483
butyl propanoate	4.61E+06	-2.75	1300965	C7 H14 O2	CPD-19956
11-hydroxyvittatine	4.90E+06	-2.70	2871154	C16 H17 N O4	CPD-19447
1,4-dihydroxy-2-naphthoate	7.39E-02	-2.65	2030343	C11 H7 O4	DIHYDROXYNAPHTHOATE
(S)-5-hydroxyisourate	4.23E+06	-2.61	1840264	C5 H4 N4 O4	5-HYDROXYISOURATE
pelargonidin	5.46E+06	-2.57	2690444	C15 H9 O5	PELARGONIDIN-CMPD
trans-5-O-(4-coumaroyl)-D-quinate	2.58E+06	-2.57	3370905	C16 H17 O8	4-COUMAROYLQUINATE
(E)-7-(methyltsulfanyl)heptanal oxime	0	-2.52	1751009	C8 H17 N O S	CPDQT-405
3-[(4'-methylsulfanyl)butyl]malate	0	-2.51	2340515	C9 H14 O5 S	CPDQT-37
1,2-dioctanoyl-1,2,3-butanetriol	1.99E+06	-2.50	3582719	C20 H38 O5	CPD0-1762
S-sulfanylglutathione	0	-2.48	3380517	C10 H16 N3 O6 S2	CPD-11281
(6E)-8-hydroxygeranial	6.49E+06	-2.46	1681145	C10 H16 O2	CPD-9977
N-beta-D-glucosyl-(indol-3-yl)acetyl-L-aspartate	7.48E+06	-2.46	4501235	C20 H22 N2 O10	CPD-9568
uridine	9.76E+06	-2.43	2440649	C9 H12 N2 O6	URIDINE
gramine	5.86E+06	-2.40	1751212	C11 H15 N2	CPD-8915
5'-(aminoiminomethyl)amino-5'-deoxyadenosine	0	-2.39	3091449	C11 H17 N8 O3	CPD0-1401
2-pentadecanone	5.99E+06	-2.38	2262298	C15 H30 O	CPD-7898
hordatine A	4.90E+06	-2.38	5523211	C28 H40 N8 O4	CPD-12232
2-carboxy-L-threo-pentonate	0	-2.36	2080208	C6 H8 O8	CPD-13912
4alpha-formyl,4beta,14alpha-dimethyl-9beta,19-cyclo-5alpha-cholest-24-en-3beta-ol	6.49E+06	-2.36	4403683	C30 H48 O2	CPD-12918
coniferyl alcohol	1.94E+05	-2.36	1800795	C10 H12 O3	CONIFERYL-ALCOHOL
betaine aldehyde hydrate	9.34E+06	-2.35	1201026	C5 H14 N O2	BETAINE-ALDEHYDE-HYDRATE
N6-(Delta2-isopentenyl)-adenosine 5'-monophosphate	2.96E+06	-2.35	4131176	C15 H20 N5 O7 P	CPD-4205
ribitol	9.65E+06	-2.33	1520691	C5 H12 O5	RIBITOL

Compound	p (Corr) (Peg Vs Control)	Log FC (Peg Vs Control)	Mass	Formula	Compound Name
brassinolide 22-O-sulfate	5.29E+06	-2.30	5592941	C28 H47 O9 S	CPD-19794
(6S)-5-formyl-tetrahydrofolate mono-L-glutamate	2.60E+06	-2.22	4711513	C20 H21 N7 O7	5-FORMYL-THF
a triketide alpha-pyrone	2.27E+06	-2.22	1810874	C10 H13 O3	CPD-11507
(-)-yatein	0	-2.20	4001497	C22 H24 O7	CPD-17595
cerulenin	4.99E+06	-2.19	2231222	C12 H17 N O3	CPD-6901
3-hydroxy-3-phenylpropanoate	5.22E+06	-2.17	1650564	C9 H9 O3	CPD-12218
1-O-caffeoyl-beta-D-glucose	2.51E+06	-2.15	3421033	C15 H18 O9	CPD-16550
4-(methylsulfanyl)butyl-desulfoglucosinolate	2.51E+06	-2.14	3410959	C12 H23 N O6 S2	CPDQT-416
digitoxigenin	3.92E+05	-2.14	3742455	C23 H34 O4	CPD-10537
methotrexate	2.80E+05	-2.13	4521597	C20 H20 N8 O5	CPD-6041
coumaryl acetate	2.27E+06	-2.12	1920799	C11 H12 O3	CPD-12215
gossypol-6,6'-dimethyl ether	0	-2.11	5462283	C32 H34 O8	CPD-9527
L-indospicine	3.26E+06	-2.10	174124	C7 H16 N3 O2	CPD0-1690
gibberellin A19	2.76E+06	-2.04	3601597	C20 H24 O6	CPD1F-96
adhyperforin	0	-2.04	5504014	C36 H54 O4	CPD-14533
(1H-indol-3-yl)-N-methylmethanamine	6.49E+06	-2.01	1611088	C10 H13 N2	CPD-8914
2-(2-methylpyridin-3-yl)ethanol	4.61E+06	-1.98	1370846	C8 H11 N O	CPD-15779
3,5-dimethoxytoluene	2.88E+06	-1.95	1520873	C9 H12 O2	CPD-9502
N-formyldemecolcine	4.98E+06	-1.93	3991682	C22 H25 N O6	CPD-14544
L-phenylalanine	4.90E+06	-1.91	16508	C9 H11 N O2	PHE
4alpha-carboxy-4beta,14alpha-dimethyl-9beta,19-cyclo-5alpha-ergost-24(241)-en-3beta-ol	4.23E+06	-1.88	4693689	C31 H49 O3	CPD-12867
16-alpha-hydroxygypsogenate	0	-1.81	5003133	C30 H44 O6	CPD-9476
5,10-methenyl-THF	9.45E+06	-1.80	4561643	C20 H22 N7 O6	510-methenyl-thf
L-cystine	9.12E+05	-1.72	2400282	C6 H12 N2 O4 S2	CYSTINE
acenaphthenequinone	9.65E+06	-1.72	1820396	C12 H6 O2	ACENAPHTHENE QUINONE
trans-zeatin	4.90E+06	-1.71	2191123	C10 H13 N5 O	CPD-4210
abietatriene	0	-1.35	2702345	C20 H30	CPD-8721
betalamate	0	-1.34	2090322	C9 H7 N O5	CPD-8651
N-(5-phosphoribosyl)-anthranilate	0	-1.17	3460339	C12 H13 N O9 P	N-5-PHOSPHORIBOSYL-ANTHRANILATE
2-hydroxy-3-nitropropionate	0	-1.17	1340134	C3 H4 N O5	CPD0-2489
campestanol	0	-1.16	4023843	C28 H50 O	CPD-710
L-azaserine	0	-1.14	1740563	C5 H8 N3 O4	L-AZASERINE
4-deoxypyridoxine 5'-phosphate	0	-1.03	231028	C8 H10 N O5 P	CPD0-1221
AMP group	0	-1.02	3450438	C10 H12 N5 O7 P	AMP-GROUP
beta-peltatin-A methyl ether	2.06E+06	-5.45	4281419	C23 H24 O8	CPD-8961
N-feruloyltyramine	2.08E-02	-5.07	3131332	C18 H19 N O4	CPD-440

Compound	p (Corr) (Peg Vs Control)	Log FC (Peg Vs Control)	Mass	Formula	Compound Name
morphinone	2.83E-02	-4.83	2841305	C17 H18 N O3	MORPHINONE
(S)-6-O-methylnorlaudanosoline	2.83E-02	-4.82	3021411	C17 H20 N O4	6-O-METHYLNORLAUDANOSOLINE
S-methyl-5'-thioadenosine	0	-4.79	2970914	C11 H15 N5 O3 S	5-METHYLTHIOADENOSINE
2-amino-4-methyl-5-hydroxyethylthiazole	0	-4.23	1590593	C6 H11 N2 O S	CPD-15755
15-hydroxypentadecanoate	1.85E-02	-4.21	2572118	C15 H29 O3	CPD-11594
L-arginine	3.63E+06	-3.19	1751207	C6 H15 N4 O2	ARG
benzoate	2.64E+06	-3.10	1210297	C7 H5 O2	BENZOATE
5-fluoropyrimidin-2-one-ribonucleoside	2.58E+06	-2.94	2460628	C9 H11 F N2 O5	CPD0-1311
1,2-dibutyrin	8.25E+06	-2.89	2321327	C11 H20 O5	CPD-13040
(indol-3-yl)acetyl-myo-inositol L-arabinoside	3.26E+06	-2.78	4691558	C21 H27 N O11	INDOL-YLACETYL-MYO-INOSITOL-ARABINOSIDE
2-[(2'-methylsulfanyl)hexyl]maleate	6.86E+06	-2.65	2440744	C11 H16 O4 S	CPD-19480
gibberellin A43	1.26E+06	-2.57	3911357	C20 H23 O8	CPD-6222
N-beta-D-glucosyl-(indol-3-yl)acetate	0	-2.41	3361087	C16 H18 N O7	CPD-9567
Nomega-phosphocreatine	0	-2.33	2090145	C4 H8 N3 O5 P	CREATINE-P
(9R,10S)-dihydroxystearate	2.43E+06	-2.25	3152539	C18 H35 O4	CPD-10515
6-hydroxyprotopine	5.96E+06	-2.16	3691214	C20 H19 N O6	6-HYDROXYPROTOPINE
lycopaoctaene	6.31E+06	-2.11	5465163	C40 H66	CPD-20653
1,8-dihydroxy-3-methylnaphthalene	2.43E+06	-2.07	1740691	C11 H10 O2	CPD-11688
L-arginino-succinate	4.94E+06	-2.05	2891148	C10 H17 N4 O6	L-ARGININO-SUCCINATE
7,8,4'-trihydroxyflavone	0	-2.01	27006	C15 H10 O5	CPD-15480
malonyl-furaneol glucopyranoside	5.96E+06	-1.69	3750903	C15 H19 O11	CPD-17454
4-hydroxylamino-2,6-dinitrotoluene-O-glucoside	5.96E+06	-1.69	3750901	C13 H17 N3 O10	CPD-10460
2-phenylethyl beta-D-glucopyranoside	4.23E+06	-5.92	2841309	C14 H20 O6	CPD-14528
6-O-methyl-N-deacetylisoipecoside	2.51E+06	-3.46	5382283	C26 H36 N O11	CPD-14812
4,5-seco-dopa	3.49E+06	-2.69	2280518	C9 H10 N O6	CPD-253
N-hydroxy DAP	8.89E+06	-2.47	2050874	C7 H13 N2 O5	CPD0-1499
alpha-(2,6-anhydro-3-deoxy-D-arabino-heptulopyranosid)onate 7-phosphonate	0	-4.00	2570384	C7 H14 O8 P	CPD0-1372
alpha-glucose 1,6-bisphosphate	0	-4.00	3359666	C6 H10 O12 P2	ALPHA-GLUCOSE-16-BISPHOSPHATE
(2S)-pinocembrin	0	-4.00	255062	C15 H11 O4	CPD-6991
trans-1,4-diaminocyclohexane	0	-4.00	1161319	C6 H16 N2	CPD-19537
1,2-dipalmitoyl-sn-glycerol	0	-4.00	5685095	C35 H68 O5	CPD66-34

Compound	p (Corr) (Peg Vs Control)	Log FC (Peg Vs Control)	Mass	Formula	Compound Name
1-pyrroline-2-carboxylate	0	-4.00	1120403	C5 H6 N O2	DELTA1-PYRROLINE_2-CARBOXYLATE
2,3-dioctanoylglyceramide	0	-4.00	3572553	C19 H35 N O5	CPD0-1807
2,6,7,4'-tetrahydroxyisoflavanone	0	-4.00	2880633	C15 H12 O6	CPD-6997
2-S-cysteinyldopaquinone	0	-4.00	3140659	C12 H14 N2 O6 S	CPD-20261
2'-deoxycytidine	0	-4.00	2270947	C9 H13 N3 O4	DEOXYCYTIDINE
3,4-dihydroxypyridin	0	-4.00	1110325	C5 H5 N O2	DIHYDROXYPIRIDIN-CPD
3',5'-di-C-glucosylphloretin	0	-4.00	5981937	C27 H34 O15	CPD-20011
3-sulfanylpropanoate	0	-4.00	1050037	C3 H5 O2 S	CPD-7673
4-isopropylbenzyl alcohol	0	-4.00	1501047	C10 H14 O	CPD-1002
4'-phosphopantetheine	0	-4.00	3560763	C11 H21 N2 O7 P S	PANTETHEINE-P
4-vinylpyridine	0	-4.00	1050584	C7 H7 N	CPD-5542
9'-hydroxyabscisate	0	-4.00	2791232	C15 H19 O5	CPD-7728
butanoate	0	-4.00	870471	C4 H7 O2	BUTYRIC_ACID
chrysin	0	-4.00	2530542	C15 H9 O4	CPD-8184
D-alanine	0	-4.00	890505	C3 H7 N O2	D-ALANINE
furcatin	0	-4.00	4281702	C20 H28 O10	CPD-14703
indolepropanol phosphate	0	-4.00	2530542	C11 H12 N O4 P	CPD-12164
lampranthin I	0	-4.00	6951719	C33 H31 N2 O15	CPD-15300
methylconiine	0	-4.00	1421602	C9 H20 N	CPD-9426
nicotinate	0	-4.00	1220243	C6 H4 N O2	NIACINE
phenylmercuric chloride	0	-4.00	3079796	C6 H5 Cl Hg	CPD-14709
sinigrin	0	-4.00	3580288	C10 H16 N O9 S2	2-PROPENYL-GLUCOSINOLATE
alpha-terpinyl cation	0	4.00	1391538	C10 H19	CPD-12228
beta-myrcene	0	4.00	1361293	C10 H16	CPD-4888
beta-solanine	0	4.00	7214392	C39 H63 N O11	CPD-9212
(E)-omega-(methylsulfanyl)hexyl-thiohydroximate	0	4.00	1930585	C7 H15 N O S2	CPDQT-412
(E)-1-(L-cystein-S-yl)-N-hydroxy-omega-(methylsulfanyl)pentan-1-imine	0	4.00	2660702	C9 H18 N2 O3 S2	CPDQT-406
(E)-1-(L-cysteinylglycin-S-yl)-N-hydroxy-omega-(methylsulfanyl)heptan-1-imine	0	4.00	3511291	C13 H25 N3 O4 S2	CPD-12400
(S)-3-hydroxy-isobutanoate	0	4.00	1030399	C4 H7 O3	CPD-12175
(14E,18E)-lycopadiene	0	4.00	5586106	C40 H78	CPD-13313
(2E,8Z,11Z,14Z,17Z)-icosapentaenoyl-CoA	0	4.00	10473059	C41 H60 N7 O17 P3 S	CPD-17264
(2S,3S)-3-hydroxy-2-methylbutanoyl-CoA	0	4.00	8631434	C26 H40 N7 O18 P3 S	2-METHYL-3-HYDROXY-BUTYRYL-COA
(2S,5R)-2-(2-hydroxypropan-2-yl)-5,9-dimethyl-1-oxaspiro[5.5]undec-8-ene-7,10-dione	0	4.00	2661537	C15 H22 O4	CPD-9884

Compound	p (Corr) (Peg Vs Control)	Log FC (Peg Vs Control)	Mass	Formula	Compound Name
(3R)-3-hydroxy-arachidoyl-CoA	0	4.00	10733639	C41 H70 N7 O18 P3 S	CPD-14275
(3R)-3-hydroxybehenoyl-CoA	0	4.00	11014067	C43 H74 N7 O18 P3 S	CPD-14276
(3R)-3-hydroxylignoceroyl-CoA	0	4.00	11294409	C45 H78 N7 O18 P3 S	CPD-14277
(4S)-2,3-dehydro-leucocyanidin	0	4.00	3040574	C15 H12 O7	CPD-19726
(7Z,10Z,13Z,16Z,19Z)-docosapentaenoyl-CoA	0	4.00	10753348	C43 H64 N7 O17 P3 S	CPD-14426
(8Z,11Z,14Z,17Z)-3-oxoicosatetraenoyl-CoA	0	4.00	10633085	C41 H60 N7 O18 P3 S	CPD-17262
(9Z,12Z,15Z)-hexadeca-9,12,15-trienoyl-CoA	0	4.00	9952752	C37 H56 N7 O17 P3 S	CPD-10255
(E,E)-piperoyl-CoA	0	4.00	9631311	C33 H40 N7 O19 P3 S	EE-PIPEROYL-COA
(S)-3-hydroxy-(5Z)-tetradecenoyl-CoA	0	4.00	9872648	C35 H56 N7 O18 P3 S	CPD0-1163
cis-12-sulfojasmonate	0	4.00	3040577	C12 H16 O7 S	CPD-19816
N-dimethylethanolamine	0	4.00	9009	C4 H12 N O	CPD-5602
N-methylanthraniloyl-CoA	0	4.00	8961273	C29 H39 N8 O17 P3 S	N-METHYLANTHRANILOYL-COA
N2,N2-dihydroxy-L-tryptophan	0	4.00	2350723	C11 H11 N2 O4	CPD-13027
P1,P5-bis(5'-adenosyl) pentaphosphate	0	4.00	9109598	C20 H24 N10 O22 P5	CPD0-1137
trans-cerot-2-enoyl-CoA	0	4.00	113945	C47 H80 N7 O17 P3 S	CPD-14283
trans-lignocer-2-enoyl-CoA	0	4.00	11114312	C45 H76 N7 O17 P3 S	CPD-14282
1,2,3,4,6-pentagalloylglucose	0	4.00	940113	C41 H32 O26	12346-PENTAKIS-O-GALLOYL-BETA-D-GLUC
1,2-di-O-sinapoyl-beta-D-glucose	0	4.00	5921796	C28 H32 O14	12-BIS-O-SINAPOYL-BETA-D-GLUCOSIDE
10,16-dihydroxypalmitoyl-CoA	0	4.00	10333066	C37 H62 N7 O19 P3 S	CPD-17627
16-hydroxypalmitoyl-CoA	0	4.00	10173159	C37 H62 N7 O18 P3 S	CPD-17621
16-hydroxytabersonine	0	4.00	3531856	C21 H25 N2 O3	16-HYDROXYTABERSONINE
18-hydroxylinoleoyl-CoA	0	4.00	10413188	C39 H62 N7 O18 P3 S	CPD-17371
18-hydroxystearoyl-CoA	0	4.00	10453326	C39 H66 N7 O18 P3 S	CPD-17641
2,4,6-trihydroxycinnamoyl-CoA	0	4.00	9411118	C30 H38 N7 O20 P3 S	CPD-18078
2-O-acetyl-3-O-trans-coutarate	0	4.00	3360528	C15 H12 O9	CPD-16579
2-amino-4,6-dinitrotoluene	0	4.00	1980544	C7 H8 N3 O4	CPD-10450
2'-deoxyuridine 3'-monophosphate	0	4.00	3060325	C9 H11 N2 O8 P	CPD-15393
2-succinylbenzoate	0	4.00	2200363	C11 H8 O5	O-SUCCINYLBENZOATE
2-trans-indole-3-butyryl-CoA	0	4.00	9501839	C33 H45 N8 O17 P3 S	CPD-10516
3,4-dihydroxymandelonitrile beta-D-glucoside	0	4.00	3270954	C14 H17 N O8	CPD-14593
3,5,7-trioxododecanoyl-CoA	0	4.00	9871782	C33 H48 N7 O20 P3 S	CPD-14615

Compound	p (Corr) (Peg Vs Control)	Log FC (Peg Vs Control)	Mass	Formula	Compound Name
3,5-dioxodecanoyl-CoA	0	4.00	9451863	C31 H46 N7 O19 P3 S	CPD-14687
3-methylbutanol	0	4.00	880864	C5 H12 O	CPD-7032
3-oxo-2-(cis-2'-pentenyl)-cyclopentane-1-(3-oxohexanoyl)-CoA	0	4.00	10252354	C37 H54 N7 O19 P3 S	CPD-11524
3-oxo-2-(cis-2'-pentenyl)-cyclopentane-1-(E-buta-2-enoyl)-CoA	0	4.00	9812059	C35 H50 N7 O18 P3 S	CPD-11526
3-oxo-2-(cis-2'-pentenyl)-cyclopentane-1-(E-octa-2-enoyl)-CoA	0	4.00	10372815	C39 H58 N7 O18 P3 S	CPD-11518
3-oxo-auricoloyl-CoA	0	4.00	10833267	C41 H64 N7 O19 P3 S	CPD-17401
3-oxohexanoyl-CoA	0	4.00	875137	C27 H40 N7 O18 P3 S	K-HEXANOYL-COA
3-oxooctanoyl-CoA	0	4.00	9031555	C29 H44 N7 O18 P3 S	CPD0-2106
3-phenylpropanoyl-CoA	0	4.00	8951321	C30 H40 N7 O17 P3 S	CPD-503
4-(2-amino-3-hydroxyphenyl)-2,4-dioxobutanoate	0	4.00	2220387	C10 H8 N O5	CPD-11552
4-fluorobenzoate	0	4.00	1390178	C7 H4 F O2	4-FLUOROBENZOATE
4-hydroxyglucobrassicin	0	4.00	4630565	C16 H19 N2 O10 S2	4-HYDROXY-3-INDOLYLMETHYL-GLUCOSINOLATE
5-(methylsulfinyl)pentyl-glucosinolate	0	4.00	4500548	C13 H24 N O10 S3	CPDQT-284
5-amino-1-(5-phospho-D-ribosyl)imidazole-4-carboxamide	0	4.00	3360525	C9 H13 N4 O8 P	AICAR
5-formamido-1-(5-phospho-D-ribosyl)-imidazole-4-carboxamide	0	4.00	3640481	C10 H13 N4 O9 P	PHOSPHORIBOSYL-FORMAMIDO-CARBOXAMIDE
6-(methylsulfanyl)-2-oxohexanoate	0	4.00	1750468	C7 H11 O3 S	CPDQT-27
6'-hydroxyferuloyl-CoA	0	4.00	9591577	C31 H44 N7 O20 P3 S	CPD4FS-4
7,8-dihydroneopterin 3'-triphosphate	0	4.00	4909648	C9 H12 N5 O13 P3	DIHYDRONEOPTERIN-P3
7-hydroxylauroyl-CoA	0	4.00	9612503	C33 H54 N7 O18 P3 S	CPD-17638
adenylo-succinate	0	4.00	4590433	C14 H14 N5 O11 P	ADENYLOSUCC
ADP	0	4.00	4240128	C10 H12 N5 O10 P2	ADP
allantoate	0	4.00	1750459	C4 H7 N4 O4	ALLANTOATE
bromohydrin of isopentenyl pyrophosphate	0	4.00	3389069	C5 H10 Br O8 P2	CPD0-1025
C33 botryococcene	0	4.00	4524488	C33 H56	CPD-14289
CDP group	0	4.00	4009941	C9 H13 N3 O11 P2	CDP-GROUP
celosianin II	0	4.00	9002102	C40 H40 N2 O22	CPD-8676
chlorophyll a	0	4.00	8915356	C55 H71 Mg N4 O5	CHLOROPHYLL-A
cinnamoyl-CoA	0	4.00	8931235	C30 H38 N7 O17 P3 S	CINNAMOYL-COA
clorgyline	0	4.00	2710474	C13 H15 Cl2 N O	CPD-7656
curcumin 4',4''-O-beta-D-digentiobioside	0	4.00	10163318	C45 H60 O26	CPD-6626

Compound	p (Corr) (Peg Vs Control)	Log FC (Peg Vs Control)	Mass	Formula	Compound Name
cyanidin 3-O-[6-O-(4-O-beta-D-glucosyl-p-coumaroyl)-2-O-(beta-D-xylosyl)-beta-D-glucosyl]-5-O-(6-O-malonyl-beta-D-glucoside)	0	4.00	11352714	C50 H55 O30	CPD-15234
cyanidin 3-O-glucoside-7-O-(6-O-(4-O-(6-O-(p-hydroxybenzoyl)-glucosyl)-oxybenzoyl)-glucoside)	0	4.00	10122421	C47 H48 O25	CPD-16604
D-myo-inositol (1,4,5)-trisphosphate	0	4.00	4169399	C6 H12 O15 P3	inositol_145-trisphosphate
delphinidin 3-O-glucosyl-5-O-(caffeoylglucoside-3'-O-glucoside)	0	4.00	9502331	C42 H46 O25	CPD-7963
FADH2	0	4.00	7851599	C27 H33 N9 O15 P2	FADH2
feruloylacetyl-CoA	0	4.00	9811445	C33 H42 N7 O20 P3 S	CPD-12180
GDP	0	4.00	4400045	C10 H12 N5 O11 P2	GDP
glucobrassicin	0	4.00	4470568	C16 H19 N2 O9 S2	CPD-1863
glucoiberverin	0	4.00	4060306	C11 H20 N O9 S3	3-METHYLTHIOPROPYL-GLUCOSINOLATE
gypsogenin-28-beta-D-glucoside	0	4.00	6323895	C36 H56 O9	CPD-9472
hexanoyl-CoA	0	4.00	8611546	C27 H42 N7 O17 P3 S	HEXANOYL-COA
hydroxymethyl-dCDP	0	4.00	4140069	C10 H14 N3 O11 P2	CPD0-1345
icosanoyl-CoA	0	4.00	10573794	C41 H70 N7 O17 P3 S	CPD-9965
indole-3-carboxylate	0	4.00	1600394	C9 H6 N O2	CPD-13135
L-cystathionine	0	4.00	2220685	C7 H14 N2 O4 S	L-CYSTATHIONINE
lignoceroyl-CoA	0	4.00	11134323	C45 H78 N7 O17 P3 S	CPD-10280
linoleoyl-CoA	0	4.00	1025295	C39 H62 N7 O17 P3 S	CPD-18
lipid X	0	4.00	7094165	C34 H64 N O12 P	BISOHMYR-GLUCOSAMINYL-1P
malonylshisonin	0	4.00	8411872	C39 H37 O21	CPD-7708
maltoheptaose	0	4.00	11523817	C42 H72 O36	CPD0-1133
mizoribine 5'-monophosphate	0	4.00	3370248	C9 H12 N3 O9 P	CPD-12503
octanoyl-CoA	0	4.00	8891891	C29 H46 N7 O17 P3 S	CPD-196
octoketide	0	4.00	3170668	C16 H13 O7	CPD-11555
oleoyl-CoA	0	4.00	10273246	C39 H64 N7 O17 P3 S	OLEOYL-COA
O-sinapoylglucarate	0	4.00	4140791	C17 H18 O12	O-SINAPOYLGLUCARATE
P1-uridyl-P2-phenyl diphosphate	0	4.00	478019	C15 H16 N2 O12 P2	CPD0-1324
palmitoyl-CoA	0	4.00	10013112	C37 H62 N7 O17 P3 S	PALMITYL-COA
pelargonidin 5-O-beta-D-glucoside 3-O-beta-D-sambubioside	0	4.00	7262012	C32 H38 O19	CPD-18093
phaselate	0	4.00	2940368	C13 H10 O8	CPD-11724
p-hydroxymercuribenzoate	0	4.00	3329966	C7 H5 Hg O3	PHMB
phytyl monophosphate	0	4.00	3742613	C20 H39 O4 P	CPD-7025

Compound	p (Corr) (Peg Vs Control)	Log FC (Peg Vs Control)	Mass	Formula	Compound Name
precorrin-1	0	4.00	842226	C41 H38 N4 O16	CPD-9038
quercetin 3-sulfate	0	4.00	3799874	C15 H8 O10 S	CPD-1822
ribavirin-5'-monophosphate	0	4.00	3220375	C8 H11 N4 O8 P	CPD0-1492
salvianin	0	4.00	9261688	C42 H38 O24	CPD-7142
siroheme	0	4.00	9061571	C42 H36 Fe N4 O16	SIROHEME
stearoyl-CoA	0	4.00	10293424	C39 H66 N7 O17 P3 S	STEAROYL-COA
sucrose 6G-phosphate	0	4.00	4200625	C12 H21 O14 P	CPD-15716
syringin	0	4.00	3721427	C17 H24 O9	CPD-63
taxusin	0	4.00	5042701	C28 H40 O8	CPD-13925
ternatin C3	0	4.00	1018222	C45 H46 O27	CPD-15371
tetra-acyl estolide	0	4.00	1208978	C75 H132 O11	CPD-12262
thiamine diphosphate	0	4.00	4220276	C12 H16 N4 O7 P2 S	THIAMINE-PYROPHOSPHATE
UDP-3-O-(3-hydroxymyristoyl)-alpha-D-glucosamine	0	4.00	7902561	C29 H50 N3 O18 P2	UDP-OHMYR-GLUCOSAMINE
vindorosine	0	4.00	4272262	C24 H31 N2 O5	CPD-19895
violdelphin	0	4.00	11742963	C53 H58 O30	CPD-16561
wogonin 7-O-beta-D-glucuronate	0	4.00	4590897	C22 H19 O11	CPD-12728
a xyloglucan	0	4.00	10623319	C39 H66 O33	CPD-10123
(S)-magnoflorine	0	3.69	3421717	C20 H24 N O4	CPD-9936
2'-deoxyadenosine	2.50E-02	4.33	2511041	C10 H13 N5 O3	DEOXYADENOSINE
5-(methylsulfanyl)pentyl-glucosinolate	1.85E+06	5.49	4340515	C13 H24 N O9 S3	CPDQT-286
castasterone-23-O-glucoside	1.85E-02	6.33	626402	C34 H58 O10	CPDQT-522
ADP-D-ribose	0	1.85	5570598	C15 H21 N5 O14 P2	ADENOSINE_DIPHOSPHATE_RIBOSE
2,5,7-trihydroxyflavanone	0	2.14	2710648	C15 H11 O5	CPD-15080
7-(methylsulfanyl)-2-oxoheptanoate	4.94E+06	2.16	1890554	C8 H13 O3 S	CPDQT-28
(11Z,14Z)-3-oxoicosadienoyl-CoA	5.92E+06	2.50	10673195	C41 H64 N7 O18 P3 S	CPD-17346
p-chloromercuriphenylsulfonate	1.99E+06	2.54	3869209	C6 H4 Cl Hg O3 S	CPD-5401
plumbagin	2.17E+06	2.85	1880466	C11 H8 O3	CPD-4461
22-oxo-docosanoyl-CoA	0	2.85	10993868	C43 H72 N7 O18 P3 S	CPD-17633
3-oxo-2-(cis-2'-pentenyl)-cyclopentane-1-butanoyl-CoA	0	2.88	9832353	C35 H52 N7 O18 P3 S	CPD-11525
a xylogalacturonan	5.22E+06	3.01	6781492	C23 H34 O23	CPD-10235
luteolinidin 5-O-glucoside	2.50E-02	3.61	4321081	C21 H20 O10	CPD-15269
NAD stem group	0	3.87	5410619	C15 H21 N5 O13 P2	NAD-STEM-GROUP
(2E,5Z)-tetradecenoyl-CoA	1.85E-02	4.19	969256	C35 H54 N7 O17 P3 S	CPD0-1162
(2R,3S,4S)-leucocyanidin	5.57E-02	4.22	3060742	C15 H14 O7	CPD-590
glucoraphanin	1.85E-02	4.27	4360412	C12 H22 N O10 S3	CPDQT-280
N-acetyl-S-geranylgeranyl-L-cysteine	6.46E-02	4.38	4342705	C25 H40 N O3 S	CPD-12753

Compound	p (Corr) (Peg Vs Control)	Log FC (Peg Vs Control)	Mass	Formula	Compound Name
UDP-beta-L-rhamnose	0	4.69	5480434	C15 H22 N2 O16 P2	UDP-L-RHAMNOSE
1D-myo-inositol 3-diphosphate 1,2,4,5,6-pentakisphosphate	0	1.12	7277311	C6 H7 O27 P7	CPD-11937
cephaeline	0	1.12	468302	C28 H40 N2 O4	CPD-14816
L-quinate	0	1.34	1910576	C7 H11 O6	QUINATE
methoxydihydrosorgoleone	0	1.48	3582497	C23 H34 O3	CPD-12348
suberate	0	1.64	172074	C8 H12 O4	CPD0-1264
L-glucose	4.61E+06	1.91	1800646	C6 H12 O6	CPD-3607
macarpine	5.86E+06	2.07	3921139	C22 H18 N O6	CPD-7848
deoxycholate	5.58E+06	2.17	3912845	C24 H39 O4	DEOXYCHOLATE
docosanedioate	3.33E+06	2.25	3682936	C22 H40 O4	CPD-13101
luteolin 7-O-beta-D-glucuronide	6.49E+06	2.45	4610809	C21 H17 O12	LUTEOLIN-7-O-BETA-D-GLUCURONIDE
1,2-dioctanoyl-1,2,6-hexanetriol	3.30E+06	2.46	3863031	C22 H42 O5	CPD0-1761
isorhamnetin 3, 4'-bisulfate	0	2.57	4729489	C16 H9 O13 S2	CPD-11018
beta-D-glucopyranosyl abscisate	4.23E+06	2.65	4261896	C21 H30 O9	CPD-7727
2-methylacetoacetyl-CoA	6.74E+05	2.75	8611209	C26 H38 N7 O18 P3 S	2-METHYL-ACETO-ACETYL-COA
hypoglycin B	2.78E+06	2.75	2691146	C12 H17 N2 O5	CPD-9700
2,4-diamino-6-ethyl-5,3'-(2-trifluoromethylphenoxy)prop-1'-yloxypyrimidine	1.67E+06	2.76	3561497	C16 H19 F3 N4 O2	CPD0-1585
2'-methoxythiamine pyrophosphate	0	2.77	4380148	C12 H16 N4 O8 P2 S	CPD0-2022
precorrin-2	0	2.78	8572465	C42 H41 N4 O16	DIHYDROSIROHYDROCHLORIN
6-methylsulfinylhexyl-glucosinolate	0	2.93	4640687	C14 H26 N O10 S3	CPDQT-288
phenyllactatyl-CoA	1.45E+06	2.98	9171767	C30 H46 N7 O18 P3 S	CPD-9918
scoparone	2.58E+06	3.01	2060574	C11 H10 O4	CPD-9836
vincristine	6.20E-02	3.02	8244055	C46 H56 N4 O10	CPD-19894
3-epihydroxymugineate	1.18E+06	3.05	3341042	C12 H18 N2 O9	CPD-7289
3-oxoicosanoyl-CoA	0	3.07	10713464	C41 H68 N7 O18 P3 S	CPD-14271
L-alpha-amino-epsilon-keto-pimelate	3.37E+06	3.11	188057	C7 H10 N O5	L-ALPHA-AMINO-EPSILON-KETO-PIMELATE
3R-hydroxy-lesqueroloyl-CoA	4.61E+06	3.19	10873625	C41 H68 N7 O19 P3 S	CPD-15369
preuroporphyrinogen	0	3.28	8462116	C40 H38 N4 O17	HYDROXYMETHYLBILANE
tellimagrandin II	5.29E+06	3.28	9381046	C41 H30 O26	CPD-8949
5'-phosphoribosyl-4-(N-succinocarboxamide)-5-aminoimidazole	0	3.34	4500468	C13 H15 N4 O12 P	P-RIBOSYL-4-SUCCCARB-AMINOIMIDAZOLE
4-hydroxybutylglucosinolate	0	3.34	3900578	C11 H20 N O10 S2	CPDQT-274
cathinone	2.30E+06	3.37	1500906	C9 H12 N O	CPD-9950
(+)-7-epi-jasmonoyl-CoA	0	3.45	9551858	C33 H48 N7 O18 P3 S	CPD-11529
uroporphyrinogen-I	0	3.51	8282102	C40 H36 N4 O16	CPD-11444
emodin dianthrone	5.96E-02	3.57	5081188	C30 H20 O8	CPD-9558

Compound	p (Corr) (Peg Vs Control)	Log FC (Peg Vs Control)	Mass	Formula	Compound Name
3-[(3'-methylsulfanyl)propyl]malate	1.85E-02	3.81	220037	$C_8H_{12}O_5S$	CPDQT-36
3-methoxytyramine	5.73E-02	3.98	1681014	$C_9H_{14}NO_2$	CPD-7650
(+)-sesaminol 2-O-beta-D-glucoside	0	4.10	5321559	$C_{26}H_{28}O_{12}$	CPD-14838
glutathione	5.57E-02	4.21	3060746	$C_{10}H_{16}N_3O_6S$	GLUTATHIONE
D-mannitol	1.85E-02	4.57	1820819	$C_6H_{14}O_6$	MANNITOL
isovitexin 2"-O-arabinoside	0	4.57	5631451	$C_{26}H_{27}O_{14}$	CPD-18156
BPH-700	1.85E-02	5.08	4839255	$C_{16}H_{16}K_3O_6PS$	CPD-9928
adenosine 3',5'-bisphosphate	0	6.35	4229911	$C_{10}H_{11}N_5O_{10}P_2$	3-5-ADP

Supplementary Table 2A. Pathway Enrichment Analysis for V/V leaves under water stress compared to the control plants.

Pathways	p-value	Matches
Purine Riboucleotide De Novo Biosynthesis	1.18E-03	ADP // L-glutamate // IMP // NAD+ // 5'-phosphoribosyl-4-(N-succinocarboxamide)-5-aminoimidazole
Sugar Nucleotide Biosynthesis	2.08E-03	CTP // ADP // NAD+ // UDP-beta-L-rhamnose // L-glutamate // dTDP-beta-L-rhamnose // GDP-4-dehydro-alpha-D-rhamnose // UDP-alpha-D-galactose
superpathway of pyrimidine ribonucleosides salvage	2.44E-03	CDP // CTP // ADP // L-glutamate
jasmonic acid biosynthesis	2.54E-03	3-oxo-2-(cis-2'-pentenyl)-cyclopentane-1-hexanoyl-CoA // 3-oxo-2-(cis-2'-pentenyl)-cyclopentane-1-butanoyl-CoA // 3-oxo-2-(cis-2'-pentenyl)-cyclopentane-1-(3-oxooctanoyl)-CoA // NAD+ // 3-oxo-2-(cis-2'-pentenyl)-cyclopentane-1-(3R-hydroxyhexanoyl)-CoA
Flavonoid Biosynthesis	3.03E-03	myricetin 3-O-beta-D-glucoside // cyanidin O-O-[6-O-(6-O-4-hydroxycinnamoyl-beta-D-glucosyl)-2-O-beta-D-xylosyl-beta-D-galactoside] // UDP-alpha-D-galactose // UDP-beta-L-rhamnose // dalpatein 7-O-beta-D-apiofuranosyl-(1->6)-beta-D-glucopyranoside // apigenin 7-O-(6-malonyl-beta-D-glucoside) // delphinidin-3-O-(6''-O-malonyl)-beta-glucoside-3'-O-beta-glucoside // 3,7,4'-trimethylquercetin 2'-O-beta-D-glucoside // quercetin-3-gentiotrioside // quercetin-3-gentiotetraside // cyanidin 3-O-(3'',6''-O-dimalonyl-beta-glucopyranoside) // wogonin 7-O-beta-D-glucuronate // quercetin 7-O-glucoside // patulitrin // quercetagetin 7-O-glucoside // kaempferol 3-O-beta-D-glucoside // kaempferol 3,7-bis-O-beta-D-glucoside // isovitexin 2''-O-beta-D-glucosyl 7-O-galactoside // quercetin 3-O-gentiobioside-7-O-rhamnoside // malonyldaidzin // afrormosin-7-O-glucoside-6''-O-malonate // adenosine 3',5'-bisphosphate // (-)-epigallocatechin-3-O-gallate // violdelphin // delphinidin 3-O-rutinoside-7-O-(6-O-(p-hydroxybenzoyl)-glucoside) // luteolin 7-O-beta-D-diglucuronide
superpathway of purine nucleotides de novo biosynthesis I	3.32E-03	ADP // IMP // dATP // 5'-phosphoribosyl-4-(N-succinocarboxamide)-5-aminoimidazole // L-glutamate
Other Biosynthesis	3.46E-03	L-glutamate // ADP // curcumin 4'-O-beta-D-gentiobiosyl 4''-O-beta-D-glucoside // curcumin 4',4''-O-beta-D-digentiobioside // rubusoside // NAD+ // quercetin 7-O-glucoside // UDP-beta-L-rhamnose // patulitrin // quercetagetin 7-O-glucoside // kaempferol 3-O-beta-D-glucoside // (+)-sesaminol 2-O-beta-D-gentiotrioside
L-serine biosynthesis I	3.50E-03	NAD+ // 3-phosphooxypyruvate // L-glutamate
trans-zeatin biosynthesis	3.52E-03	ADP // N6-(Delta2-isopentenyl)-adenosine 5'-diphosphate // trans-zeatin riboside diphosphate // trans-zeatin riboside triphosphate
methylerythritol phosphate pathway II	3.52E-03	CTP // 2-C-methyl-D-erythritol 4-phosphate // 2-phospho-4-(cytidine 5'-diphospho)-2-C-methyl-D-erythritol // ADP
Jasmonate Biosynthesis	3.58E-03	adenosine 3',5'-bisphosphate // 3-oxo-2-(cis-2'-pentenyl)-cyclopentane-1-hexanoyl-CoA // 3-oxo-2-(cis-2'-pentenyl)-cyclopentane-1-butanoyl-CoA // 3-oxo-2-(cis-2'-pentenyl)-cyclopentane-1-(3-oxooctanoyl)-CoA // NAD+ // 3-oxo-2-(cis-2'-pentenyl)-cyclopentane-1-(3R-hydroxyhexanoyl)-CoA
Nitrogen-Containing Secondary Compound Biosynthesis	3.67E-03	L-glutamate // adenosine 3',5'-bisphosphate // glucotropaeolin // beta-nicotinate D-ribonucleotide // NAD+ // sinapoyl-CoA // 6-(methylsulfanyl)hexyl-glucosinolate // 2-sinapoyloxy-3-butenylglucosinolate // 2-benzoyloxy-3-butenylglucosinolate // UDP-alpha-D-galactose // 3-alpha(S)-strictosidine // amaranthin // leucodopachrome // O-ureido-L-homoserine // 1-methylpyrrolidine-2-acetyl-CoA // glucobrassicin // 1-(1H-indol-3-yl)-2-aci-nitroethane // 4-hydroxyglucobrassicin // 4-methoxyglucobrassicin // thebaine // 3-sinapoyloxypropylglucosinolate // (E)-1-(glutathion-S-yl)-N-hydroxy-omega-(methylsulfanyl)butan-1-imine // N,N-dihydroxyhomomethionine // UDP-beta-L-rhamnose // beta-chaconine // dihydrosanguinarine // strictosidine aglycone // 5-(methylsulfinyl)pentyl-glucosinolate // 5-(methylsulfanyl)pentyl-glucosinolate // 8-(methylsulfinyl)octyl-glucosinolate

Pathways	p-value	Matches
Purine Nucleotide Biosynthesis	3.95E-03	ADP // L-glutamate // IMP // NAD+ // dATP // 5'-phosphoribosyl-4-(N-succinocarboxamide)-5-aminoimidazole
phosphatidylethanolamine biosynthesis II	4.23E-03	CDP-ethanolamine // CTP // O-phosphoethanolamine // ADP
alpha-solanine/alpha-chaconine biosynthesis	4.57E-03	UDP-alpha-D-galactose // UDP-beta-L-rhamnose // beta-chaconine
violdelphin biosynthesis	4.57E-03	violdelphin // delphinidin 3-O-rutinoside-7-O-(6-O-(p-hydroxybenzoyl)-glucoside) // UDP-beta-L-rhamnose
methylerythritol phosphate pathway I	4.89E-03	CTP // 2-C-methyl-D-erythritol 4-phosphate // 2-phospho-4-(cytidine 5'-diphospho)-2-C-methyl-D-erythritol // ADP
Methylerythritol Phosphate Pathways	4.89E-03	CTP // 2-C-methyl-D-erythritol 4-phosphate // 2-phospho-4-(cytidine 5'-diphospho)-2-C-methyl-D-erythritol // ADP
Nucleoside and Nucleotide Biosynthesis	5.05E-03	ADP // L-glutamate // IMP // NAD+ // CDP // CTP // dATP // 5'-phosphoribosyl-4-(N-succinocarboxamide)-5-aminoimidazole
Phenylpropanoid Derivative Biosynthesis	5.27E-03	cyanidin O-O-[6-O-(6-O-4-hydroxycinnamoyl-beta-D-glucosyl)-2-O-beta-D-xylosyl-beta-D-galactoside] // UDP-alpha-D-galactose // wogonin 7-O-beta-D-glucuronate // quercetin 7-O-glucoside // L-glutamate // (+)-pinoresinol // NAD+ // 3,7,4'-trimethylquercetin 2'-O-beta-D-glucoside // delphinidin-3-O-(6''-O-malonyl)-beta-glucoside-3'-O-beta-glucoside // sinapoyl-CoA // UDP-beta-L-rhamnose // apigenin 7-O-(6-malonyl-beta-D-glucoside) // myricetin 3-O-beta-D-glucoside // curcumin 4'-O-beta-D-gentiobiosyl 4''-O-beta-D-glucoside // curcumin 4',4''-O-beta-D-digentiobioside // (-)-epigallocatechin-3-O-gallate // cyanidin 3-O-(3'',6''-O-dimalonyl-beta-glucopyranoside) // malonyldaidzin // isovitexin 2''-O-beta-D-glucosyl 7-O-galactoside // violdelphin // delphinidin 3-O-rutinoside-7-O-(6-O-(p-hydroxybenzoyl)-glucoside) // 1,2,3,4,6-pentagalloylglucose // tellimagrandin II // 1-O,6-O-digalloyl-beta-D-glucose // kaempferol 3-O-beta-D-glucoside // adenosine 3',5'-bisphosphate // patulitrin // quercetagetin 7-O-glucoside // afrormosin-7-O-glucoside-6''-O-malonate // quercetin 3-O-gentiobioside-7-O-rhamnoside // quercetin-3-gentiotrioside // quercetin-3-gentiotetraside // (+)-sesaminol 2-O-beta-D-gentiotrioside // dalpatein 7-O-beta-D-apiofuranosyl-(1->6)-beta-D-glucopyranoside // luteolin 7-O-beta-D-diglucuronide // kaempferol 3,7-bis-O-beta-D-glucoside
lysine degradation III	5.69E-03	ADP // NAD+ // 2-oxoadipate // L-glutamate
Flavonol Biosynthesis	6.15E-03	(-)-epigallocatechin-3-O-gallate // kaempferol 3-O-beta-D-glucoside // UDP-alpha-D-galactose // adenosine 3',5'-bisphosphate // UDP-beta-L-rhamnose // quercetin 3-O-gentiobioside-7-O-rhamnoside // quercetin 7-O-glucoside // quercetin-3-gentiotrioside // quercetin-3-gentiotetraside // 3,7,4'-trimethylquercetin 2'-O-beta-D-glucoside // patulitrin // quercetagetin 7-O-glucoside // myricetin 3-O-beta-D-glucoside // kaempferol 3,7-bis-O-beta-D-glucoside
superpathway of geranylgeranyl diphosphate biosynthesis II (via MEP)	7.54E-03	CTP // 2-C-methyl-D-erythritol 4-phosphate // 2-phospho-4-(cytidine 5'-diphospho)-2-C-methyl-D-erythritol // ADP
Nucleoside and Nucleotide Degradation	8.02E-03	NAD+ // CTP // ADP // L-glutamate // CDP // IMP
Ellagitannin Biosynthesis	8.19E-03	tellimagrandin II // 1,2,3,4,6-pentagalloylglucose
Sugar Biosynthesis	9.40E-03	NAD+ // ADP // CTP // UDP-beta-L-rhamnose // L-glutamate // dTDP-beta-L-rhamnose // GDP-4-dehydro-alpha-D-rhamnose // UDP-alpha-D-galactose
Inosine-5'-phosphate Biosynthesis	1.07E-02	IMP // 5'-phosphoribosyl-4-(N-succinocarboxamide)-5-aminoimidazole // ADP

Pathways	p-value	Matches
inosine-5'-phosphate biosynthesis II	1.07E-02	IMP // 5'-phosphoribosyl-4-(N-succinocarboxamide)-5-aminoimidazole // ADP
Polyprenyl Biosynthesis	1.08E-02	CTP // CDP // ADP // 2-C-methyl-D-erythritol 4-phosphate // 2-phospho-4-(cytidine 5'-diphospho)-2-C-methyl-D-erythritol
Biosynthesis	1.25E-02	gamma-linolenoyl-CoA // NAD+ // 5-methyltetrahydropteroyl tri-L-glutamate // tetrahydropteroyl tri-L-glutamate // ADP // L-glutamate // dATP // malonyldaidzin // UDP-beta-L-rhamnose // glucobrassicin // 1-(1H-indol-3-yl)-2-aci-nitroethane // 4-hydroxyglucobrassicin // 4-methoxyglucobrassicin // adenosine 3',5'-bisphosphate // CTP // 2-C-methyl-D-erythritol 4-phosphate // 2-phospho-4-(cytidine 5'-diphospho)-2-C-methyl-D-erythritol // beta-nicotinate D-ribonucleotide // O-phosphoethanolamine // 3-oxo-2-(cis-2'-pentenyl)-cyclopentane-1-hexanoyl-CoA // 3-oxo-2-(cis-2'-pentenyl)-cyclopentane-1-butanoyl-CoA // 3-oxo-2-(cis-2'-pentenyl)-cyclopentane-1-(3-oxooctanoyl)-CoA // 3-oxo-2-(cis-2'-pentenyl)-cyclopentane-1-(3R-hydroxyhexanoyl)-CoA // wogonin 7-O-beta-D-glucuronate // luteolin 7-O-beta-D-diglucuronide // amaranthin // leucodopachrome // delphinidin-3-O-(6''-O-malonyl)-beta-glucoside-3'-O-beta-glucoside // UDP-alpha-D-galactose // IMP // docosanoyl-CoA // sinapoyl-CoA // tellimagrandin II // 1,2,3,4,6-pentagalloylglucose // kaempferol 3-O-beta-D-glucoside // kaempferol 3,7-bis-O-beta-D-glucoside // quercetin 7-O-glucoside // patulitrin // quercetagetin 7-O-glucoside // curcumin 4'-O-beta-D-gentiobiosyl 4''-O-beta-D-glucoside // curcumin 4',4''-O-beta-D-digentiobioside // 1-O,6-O-digalloyl-beta-D-glucose // strictosidine aglycone // 3-alpha(S)-strictosidine // 3-oxo-auricoloyl-CoA // tetra-acyl estolide // a xylogalacturonan // zealexin A1 // catechol // (2E,10E,14E,18E)-lycopatetraene // GDP-4-dehydro-alpha-D-rhamnose // 3-sinapoyloxypropylglucosinolate // (E)-1-(glutathion-S-yl)-N-hydroxy-omega-(methylsulfanyl)butan-1-imine // N,N-dihydroxyhomomethionine // cyanidin O-O-[6-O-(6-O-4-hydroxycinnamoyl-beta-D-glucosyl)-2-O-beta-D-xylosyl-beta-D-galactoside] // rubusoside // lauroyl-CoA // (+)-pinoresinol // icosanoyl-CoA // dTDP-beta-L-rhamnose // CDP // (-)-epigallocatechin-3-O-gallate // 5'-phosphoribosyl-4-(N-succinocarboxamide)-5-aminoimidazole // quercetin-3-gentiotrioside // quercetin-3-gentiotetraside // glucotropaeolin // (2E)-oct-2-enoyl-CoA // 7,8-dihydroneopterin 3'-triphosphate // cerotoyl-CoA // lignoceroyl-CoA // trans-lignocer-2-enoyl-CoA // (3R)-3-hydroxylignoceroyl-CoA // 2-sinapoyloxy-3-butenylglucosinolate // 2-benzoyloxy-3-butenylglucosinolate // 3,7,4'-trimethylquercetin 2'-O-beta-D-glucoside // CDP-ethanolamine // quercetin 3-O-gentiobioside-7-O-rhamnoside // 8-(methylsulfinyl)octyl-glucosinolate // cyanidin 3-O-(3'',6''-O-dimalonyl-beta-glucopyranoside) // 2-(cystein-S-yl)-2-(1H-indol-3-yl)-acetonitrile // O-ureido-L-homoserine // violdelphin // delphinidin 3-O-rutinoside-7-O-(6-O-(p-hydroxybenzoyl)-glucoside) // 3-hydroxy-indole-3-butyryl-CoA // apigenin 7-O-(6-malonyl-beta-D-glucoside) // isovitexin 2''-O-beta-D-glucosyl 7-O-galactoside // (+)-sesaminol 2-O-beta-D-gentiotrioside // 1-alpha-linolenoyl-2-palmitoyl-phosphatidylglycerol // 1-methylpyrrolidine-2-acetyl-CoA // baccatin III // 10-deacetylbaccatin III // N6-(Delta2-isopentenyl)-adenosine 5'-diphosphate // trans-zeatin riboside diphosphate // trans-zeatin riboside triphosphate // thebaine // beta-chaconine // myricetin 3-O-beta-D-glucoside // (2E,8Z,11Z,14Z,17Z)-icosapentaenoyl-CoA // dihydrosanguinarine // Mg-protoporphyrin // 5-(methylsulfinyl)pentyl-glucosinolate // 5-(methylsulfanyl)pentyl-glucosinolate // dalpatein 7-O-beta-D-apiofuranosyl-(1->6)-beta-D-glucopyranoside // (7Z,10Z,13Z,16Z,19Z)-docosapentaenoyl-CoA // afrormosin-7-O-glucoside-6''-O-malonate // 6-(methylsulfanyl)hexyl-glucosinolate // 3-phosphooxypyruvate // 10,16-dihydroxypalmitoyl-CoA
L-methionine De Novo Biosynthesis	1.27E-02	5-methyltetrahydropteroyl tri-L-glutamate // tetrahydropteroyl tri-L-glutamate // ADP
L-methionine biosynthesis II (plants)	1.27E-02	5-methyltetrahydropteroyl tri-L-glutamate // tetrahydropteroyl tri-L-glutamate // ADP
2'-Deoxyribonucleotide Biosynthesis	1.29E-02	CTP // ADP // CDP // dATP // L-glutamate
UDP-sugar Biosynthesis	1.29E-02	NAD+ // UDP-beta-L-rhamnose // ADP // L-glutamate // UDP-alpha-D-galactose
Glycosylation	1.30E-02	curcumin 4'-O-beta-D-gentiobiosyl 4''-O-beta-D-glucoside // curcumin 4',4''-O-beta-D-digentiobioside // rubusoside // NAD+ // quercetin 7-O-glucoside // UDP-beta-L-rhamnose // patulitrin // quercetagetin 7-O-glucoside // kaempferol 3-O-beta-D-glucoside // (+)-sesaminol 2-O-beta-D-gentiotrioside
Purine Nucleotide De Novo Biosynthesis	1.31E-02	ADP // L-glutamate // IMP // NAD+ // dATP // 5'-phosphoribosyl-4-(N-succinocarboxamide)-5-aminoimidazole

Pathways	p-value	Matches
L-serine Biosynthesis	1.54E-02	NAD+ // L-glutamate // ADP // 3-phosphooxypyruvate
superpathway of L-lysine, L-threonine and L-methionine biosynthesis II	1.54E-02	L-glutamate // ADP // 5-methyltetrahydropteroyl tri-L-glutamate // tetrahydropteroyl tri-L-glutamate
Isopentenyl Diphosphate Biosynthesis	1.70E-02	CTP // 2-C-methyl-D-erythritol 4-phosphate // 2-phospho-4-(cytidine 5'-diphospho)-2-C-methyl-D-erythritol // ADP
Hydrolyzable Tannin Biosynthesis	1.99E-02	1,2,3,4,6-pentagalloylglucose // tellimagrandin II // 1-O,6-O-digalloyl-beta-D-glucose
NAD de novo biosynthesis I (from aspartate)	1.99E-02	beta-nicotinate D-ribonucleotide // NAD+ // L-glutamate
Phosphatidylcholine Biosynthesis	1.99E-02	CTP // O-phosphoethanolamine // ADP
Hemiterpene Biosynthesis	2.07E-02	ADP // CTP // 2-C-methyl-D-erythritol 4-phosphate // 2-phospho-4-(cytidine 5'-diphospho)-2-C-methyl-D-erythritol
Fatty Acid Derivative Biosynthesis	2.07E-02	3-oxo-2-(cis-2'-pentenyl)-cyclopentane-1-hexanoyl-CoA // 3-oxo-2-(cis-2'-pentenyl)-cyclopentane-1-butanoyl-CoA // 3-oxo-2-(cis-2'-pentenyl)-cyclopentane-1-(3-oxooctanoyl)-CoA // NAD+ // 3-oxo-2-(cis-2'-pentenyl)-cyclopentane-1-(3R-hydroxyhexanoyl)-CoA
quercetin gentiotetraside biosynthesis	2.16E-02	quercetin-3-gentiotrioside // quercetin-3-gentiotetraside
Inorganic Nutrient Metabolism	2.25E-02	NAD+ // L-glutamate // ADP // Fe(II)-nicotianamine // 5-methyltetrahydropteroyl tri-L-glutamate // tetrahydropteroyl tri-L-glutamate // thiosulfate
Geranylgeranyl Diphosphate Biosynthesis	2.27E-02	ADP // CTP // 2-C-methyl-D-erythritol 4-phosphate // 2-phospho-4-(cytidine 5'-diphospho)-2-C-methyl-D-erythritol
Secondary Metabolite Biosynthesis	2.41E-02	UDP-alpha-D-galactose // UDP-beta-L-rhamnose // beta-chaconine // ADP // quercetin 7-O-glucoside // dalpatein 7-O-beta-D-apiofuranosyl-(1->6)-beta-D-glucopyranoside // CTP // 2-C-methyl-D-erythritol 4-phosphate // 2-phospho-4-(cytidine 5'-diphospho)-2-C-methyl-D-erythritol // L-glutamate // 5-(methylsulfinyl)pentyl-glucosinolate // 5-(methylsulfanyl)pentyl-glucosinolate // adenosine 3',5'-bisphosphate // NAD+ // malonyldaidzin // lauroyl-CoA // glucobrassicin // 1-(1H-indol-3-yl)-2-aci-nitroethane // 4-hydroxyglucobrassicin // 4-methoxyglucobrassicin // beta-nicotinate D-ribonucleotide // sinapoyl-CoA // 2-sinapoyloxy-3-butenylglucosinolate // 2-benzoyloxy-3-butenylglucosinolate // 3,7,4'-trimethylquercetin 2'-O-beta-D-glucoside // delphinidin-3-O-(6"-O-malonyl)-beta-glucoside-3'-O-beta-glucoside // wogonin 7-O-beta-D-glucuronate // 8-(methylsulfinyl)octyl-glucosinolate // quercetin 3-O-gentiobioside-7-O-rhamnoside // 3-oxo-2-(cis-2'-pentenyl)-cyclopentane-1-hexanoyl-CoA // 3-oxo-2-(cis-2'-pentenyl)-cyclopentane-1-butanoyl-CoA // 3-oxo-2-(cis-2'-pentenyl)-cyclopentane-1-(3-oxooctanoyl)-CoA // 3-oxo-2-(cis-2'-pentenyl)-cyclopentane-1-(3R-hydroxyhexanoyl)-CoA // amaranthin // leucodopachrome // 3-alpha(S)-strictosidine // O-ureido-L-homoserine // luteolin 7-O-beta-D-diglucuronide // kaempferol 3-O-beta-D-glucoside // 2-(cystein-S-yl)-2-(1H-indol-3-yl)-acetonitrile // (+)-pinoresinol // violdelphin // delphinidin 3-O-rutinoside-7-O-(6-O-(p-hydroxybenzoyl)-glucoside) // cyanidin 3-O-(3",6"-O-dimalonyl-beta-glucopyranoside) // 3-hydroxy-indole-3-butyryl-CoA // kaempferol 3,7-bis-O-beta-D-glucoside // curcumin 4'-O-beta-D-gentiobiosyl 4"-O-beta-D-glucoside // curcumin 4',4"-O-beta-D-digentiobioside // apigenin 7-O-(6-malonyl-beta-D-glucoside) // 1-O,6-O-digalloyl-beta-D-glucose // 1,2,3,4,6-pentagalloylglucose // (+)-sesaminol 2-O-beta-D-gentiotrioside // CDP // tellimagrandin II // isovitexin 2"-O-beta-D-glucosyl 7-O-galactoside // patulitrin // quercetagetin 7-O-glucoside // (2E,10E,14E,18E)-lycopatetraene // strictosidine aglycone // zealexin A1 // N6-(Delta2-isopentenyl)-adenosine 5'-diphosphate // trans-zeatin riboside diphosphate // trans-zeatin riboside triphosphate // 1-methylpyrrolidine-2-acetyl-CoA // cyanidin O-O-[6-O-(6-O-4-hydroxycinnamoyl-beta-D-glucosyl)-2-O-beta-D-xylosyl-beta-D-galactoside] // (-)-epigallocatechin-3-O-gallate // baccatin III // 10-deacetylbaccatin III // 3-sinapoyloxypropylglucosinolate // (E)-1-(glutathion-S-yl)-N-hydroxy-omega-(methylsulfanyl)butan-1-imine // N,N-dihydroxyhomomethionine // rubusoside // dihydrosanguinarine // quercetin-3-gentiotrioside // quercetin-3-gentiotetraside // myricetin 3-O-beta-D-glucoside // afrormosin-7-O-glucoside-6"-O-malonate // dTDP-beta-L-rhamnose // glucotropaeolin // 6-(methylsulfanyl)hexyl-glucosinolate // thebaine // (2E)-oct-2-enoyl-CoA

Pathways	p-value	Matches
Fatty Acid Biosynthesis	2.46E-02	NAD+ // cerotoyl-CoA // lignoceroyl-CoA // trans-lignocer-2-enoyl-CoA // docosanoyl-CoA // icosanoyl-CoA // (3R)-3-hydroxylignoceroyl-CoA // lauroyl-CoA // 3-oxo-auricoloyl-CoA // gamma-linolenoyl-CoA // (2E,8Z,11Z,14Z,17Z)-icosapentaenoyl-CoA // (7Z,10Z,13Z,16Z,19Z)-docosapentaenoyl-CoA
Glucosinolate Activation	2.56E-02	glucobrassicin // L-glutamate // 4-hydroxyglucobrassicin // 4-methoxyglucobrassicin // glucotropaeolin
NAD Biosynthesis	2.70E-02	beta-nicotinate D-ribonucleotide // L-glutamate // NAD+ // ADP
Activation	2.84E-02	glucobrassicin // L-glutamate // 4-hydroxyglucobrassicin // 4-methoxyglucobrassicin // ADP // glucotropaeolin
Plant Hormone Biosynthesis	2.88E-02	3-hydroxy-indole-3-butyryl-CoA // L-glutamate // NAD+ // adenosine 3',5'-bisphosphate // 3-oxo-2-(cis-2'-pentenyl)-cyclopentane-1-hexanoyl-CoA // 3-oxo-2-(cis-2'-pentenyl)-cyclopentane-1-butanoyl-CoA // 3-oxo-2-(cis-2'-pentenyl)-cyclopentane-1-(3-oxooctanoyl)-CoA // 3-oxo-2-(cis-2'-pentenyl)-cyclopentane-1-(3R-hydroxyhexanoyl)-CoA // ADP // N6-(Delta2-isopentenyl)-adenosine 5'-diphosphate // trans-zeatin riboside diphosphate // trans-zeatin riboside triphosphate
Transport	3.18E-02	L-glutamate // ADP // NAD+ // Fe(II)-nicotianamine
Choline Biosynthesis	3.25E-02	CTP // O-phosphoethanolamine // ADP
superpathway of choline biosynthesis	3.25E-02	CTP // O-phosphoethanolamine // ADP
Ceramide and Sphingolipid Recycling and Degradation	3.35E-02	O-phosphoethanolamine // ADP
ceramide degradation	3.35E-02	O-phosphoethanolamine // ADP
Sugars Degradation	3.35E-02	UDP-alpha-D-galactose // ADP
UDP-galactose biosynthesis (salvage pathway from galactose using UDP-glucose)	3.35E-02	UDP-alpha-D-galactose // ADP
Carbohydrate Biosynthesis	3.64E-02	NAD+ // ADP // CTP // (2E,10E,14E,18E)-lycopatetraene // UDP-beta-L-rhamnose // L-glutamate // dTDP-beta-L-rhamnose // GDP-4-dehydro-alpha-D-rhamnose // UDP-alpha-D-galactose // a xylogalacturonan
NAD Metabolism	3.70E-02	beta-nicotinate D-ribonucleotide // L-glutamate // NAD+ // ADP
superpathway of phospholipid biosynthesis II (plants)	3.70E-02	CDP-ethanolamine // CTP // O-phosphoethanolamine // ADP
Amine and Polyamine Biosynthesis	3.97E-02	CTP // NAD+ // O-phosphoethanolamine // ADP // IMP
L-lysine Degradation	3.98E-02	ADP // NAD+ // 2-oxoadipate // L-glutamate
curcumin glucoside biosynthesis	4.01E-02	curcumin 4'-O-beta-D-gentiobiosyl 4''-O-beta-D-glucoside // curcumin 4',4''-O-beta-D-digentiobioside

Pathways	p-value	Matches
adenosine ribonucleotides de novo biosynthesis	4.01E-02	ADP // IMP
Hormone Biosynthesis	4.21E-02	3-hydroxy-indole-3-butyryl-CoA // L-glutamate // NAD+ // adenosine 3',5'-bisphosphate // 3-oxo-2-(cis-2'-pentenyl)-cyclopentane-1-hexanoyl-CoA // 3-oxo-2-(cis-2'-pentenyl)-cyclopentane-1-butanoyl-CoA // 3-oxo-2-(cis-2'-pentenyl)-cyclopentane-1-(3-oxooctanoyl)-CoA // 3-oxo-2-(cis-2'-pentenyl)-cyclopentane-1-(3R-hydroxyhexanoyl)-CoA // ADP // N6-(Delta2-isopentenyl)-adenosine 5'-diphosphate // trans-zeatin riboside diphosphate // trans-zeatin riboside triphosphate
Fatty Acid and Lipid Biosynthesis	4.99E-02	UDP-alpha-D-galactose // CDP-ethanolamine // CTP // O-phosphoethanolamine // ADP // NAD+ // 1-alpha-linolenoyl-2-palmitoyl-phosphatidylglycerol // CDP // 2-C-methyl-D-erythritol 4-phosphate // 2-phospho-4-(cytidine 5'-diphospho)-2-C-methyl-D-erythritol // gamma-linolenoyl-CoA // cerotoyl-CoA // lignoceroyl-CoA // trans-lignocer-2-enoyl-CoA // docosanoyl-CoA // icosanoyl-CoA // (3R)-3-hydroxylignoceroyl-CoA // 3-oxo-auricoloyl-CoA // (2E,8Z,11Z,14Z,17Z)-icosapentaenoyl-CoA // 10,16-dihydroxypalmitoyl-CoA // lauroyl-CoA // (7Z,10Z,13Z,16Z,19Z)-docosapentaenoyl-CoA // tetra-acyl estolide
very long chain fatty acid biosynthesis II	5.13E-02	cerotoyl-CoA // lignoceroyl-CoA // trans-lignocer-2-enoyl-CoA // docosanoyl-CoA // icosanoyl-CoA // (3R)-3-hydroxylignoceroyl-CoA
Phosphatidylethanolamine Biosynthesis	7.72E-02	CDP-ethanolamine // CTP // O-phosphoethanolamine // ADP
Glucosinolate Biosynthesis	1.25E-01	L-glutamate // 5-(methylsulfinyl)pentyl-glucosinolate // 5-(methylsulfanyl)pentyl-glucosinolate // adenosine 3',5'-bisphosphate // 8-(methylsulfinyl)octyl-glucosinolate // glucotropaeolin // sinapoyl-CoA // 3-sinapoyloxypropylglucosinolate // (E)-1-(glutathion-S-yl)-N-hydroxy-omega-(methylsulfanyl)butan-1-imine // N,N-dihydroxyhomomethionine // 2-sinapoyloxy-3-butenylglucosinolate // 2-benzoyloxy-3-butenylglucosinolate // NAD+ // glucobrassicin // 1-(1H-indol-3-yl)-2-aci-nitroethane // 4-hydroxyglucobrassicin // 4-methoxyglucobrassicin // 6-(methylsulfanyl)hexyl-glucosinolate
Nitrogen-Containing Glucoside Biosynthesis	1.92E-01	L-glutamate // 5-(methylsulfinyl)pentyl-glucosinolate // 5-(methylsulfanyl)pentyl-glucosinolate // adenosine 3',5'-bisphosphate // 8-(methylsulfinyl)octyl-glucosinolate // glucotropaeolin // sinapoyl-CoA // 3-sinapoyloxypropylglucosinolate // (E)-1-(glutathion-S-yl)-N-hydroxy-omega-(methylsulfanyl)butan-1-imine // N,N-dihydroxyhomomethionine // 2-sinapoyloxy-3-butenylglucosinolate // 2-benzoyloxy-3-butenylglucosinolate // NAD+ // glucobrassicin // 1-(1H-indol-3-yl)-2-aci-nitroethane // 4-hydroxyglucobrassicin // 4-methoxyglucobrassicin // 6-(methylsulfanyl)hexyl-glucosinolate

Supplementary Table 2B. Pathway Enrichment Analysis for V/N leaves under water stress compared to the control plants.

Pathways	p-value	Matches
Nucleoside and Nucleotide Biosynthesis	1.07E-03	L-glutamate // NAD+ // NADH // CDP // thymidine // dATP // (S)-dihydroorotate // 5'-phosphoribosyl-4-(N-succinocarboxamide)-5-aminoimidazole // uracil
Biosynthesis	1.48E-03	petivericin // NADH // NAD+ // 5-methyltetrahydropteroyl tri-L-glutamate // tetrahydropteroyl tri-L-glutamate // L-glutamate // dATP // malonyldaidzin // gamma-L-glutamyl-(S)-methyl-L-cysteine // cyanidin 3-O-beta-D-sambubioside // pelargonidin-3-O-beta-D-glucoside // 4-hydroxyglucobrassicin // adenosine 3',5'-bisphosphate // 2-C-methyl-D-erythritol 4-phosphate // 2-phospho-4-(cytidine 5'-diphospho)-2-C-methyl-D-erythritol // beta-nicotinate D-ribonucleotide // FMN // (2E,11Z,14Z)-icosatrienoyl-CoA // 7-(methylsulfanyl)heptyl-glucosinolate // 3-oxo-2-(cis-2'-pentenyl)-cyclopentane-1-hexanoyl-CoA // 3-oxo-2-(cis-2'-pentenyl)-cyclopentane-1-butanoyl-CoA // 3-oxo-2-(cis-2'-pentenyl)-cyclopentane-1-(3-oxooctanoyl)-CoA // 3-oxo-2-(cis-2'-pentenyl)-cyclopentane-1-(3R-hydroxyhexanoyl)-CoA // wogonin 7-O-beta-D-glucuronate // thymidine // luteolin 7-O-beta-D-diglucuronide // amaranthin // delphinidin-3-O-(6''-O-malonyl)-beta-glucoside-3'-O-beta-glucoside // uracil // (S)-dihydroorotate // 22-carboxy-docosanoyl-CoA // docosanoyl-CoA // tellimagrandin II // kaempferol 7-O-glucoside // chlorophyll a // eupatolitin 3-glucoside // patulitrin // quercetagetin 7-O-glucoside // curcumin 4'-O-beta-D-gentiobiosyl 4''-O-beta-D-glucoside // curcumin 4',4''-O-beta-D-digentiobioside // 1-O,6-O-digalloyl-beta-D-glucose // elwesine // (11Z)-icosenoyl-CoA // 3-oxo-auricoloyl-CoA // tri-acyl estolide // tetra-acyl estolide // a xylogalacturonan // zealexin A1 // GDP-beta-L-fucose // GDP-4-dehydro-alpha-D-rhamnose // 3-sinapoyloxypropylglucosinolate // cyanidin O-O-[6-O-(6-O-feruloyl-beta-D-glucosyl)-2-O-beta-D-xylosyl-beta-D-galactoside] // epoxypseudoisoeugenol-2-methylbutanoate // pyridoxal 5'-phosphate // pyridoxamine // lauroyl-CoA // 3,3'-dimethylquercetin // 2-O-digalloyl-1,3,4,6-tetra-O-beta-D-galloylglucose // icosanoyl-CoA // dTDP-beta-L-rhamnose // CDP // abieta-7,13-diene-18-oate // 5'-phosphoribosyl-4-(N-succinocarboxamide)-5-aminoimidazole // quercetin-3-gentiotrioside // quercetin-3-gentiotetraside // porphobilinogen // glucotropaeolin // (2E)-oct-2-enoyl-CoA // lampranthin I // CMP-3-deoxy-beta-D-manno-octulosonate // trans-lignocer-2-enoyl-CoA // (3R)-3-hydroxylignoceroyl-CoA // (3R)-3-hydroxy-arachidoyl-CoA // stearoyl-CoA // 2-sinapoyloxy-3-butenylglucosinolate // 4-benzoyloxybutylglucosinolate // 2-benzoyloxy-3-butenylglucosinolate // UDP-N-acetyl-alpha-D-glucosamine // CDP-ethanolamine // 8-(methylsulfinyl)octyl-glucosinolate // cyanidin 3-O-(3'',6''-O-dimalonyl-beta-glucopyranoside) // peonidin-3-(p-coumaroyl)-rutinoside-5-glucoside // UDP-2-N,3-O-bis[(3R)-3-hydroxytetradecanoyl]-alpha-D-glucosamine // 2-[(2'-methylsulfanyl)heptyl]maleate // delphinidin 3-O-rutinoside-7-O-(6-O-(p-hydroxybenzoyl)-glucoside) // delphinidin 3-O-rutinoside-7-O-glucoside // kaempferide triglycoside // (9Z,12Z)-15,16-dihydroxyoctadeca-9,12-dienoate // (9Z)-12,13,17-trihydroxyoctadeca-9-enoate // 1-linoleoyl-2-(3E)-hexadecenoyl-phosphatidylglycerol // 1-methylpyrrolidine-2-acetyl-CoA // baccatin III // 10-deacetylbaccatin III // 6-O-methyl-N-deacetylisoipecoside // N6-(Delta2-isopentenyl)-adenosine 5'-diphosphate // trans-zeatin riboside diphosphate // myricetin 3-O-beta-D-glucoside // salidroside // (2E,8Z,11Z,14Z,17Z)-icosapentaenoyl-CoA // 5-(methylsulfinyl)pentyl-glucosinolate // 5-(methylsulfanyl)pentyl-glucosinolate // 7,8-diaminopelargonate // (7Z,10Z,13Z,16Z,19Z)-docosapentaenoyl-CoA // (5Z,8Z,11Z,14Z,17Z)-3-oxodocosapentaenoyl-CoA // 6-(methylsulfanyl)hexyl-glucosinolate // 3-phosphooxypyruvate // 10,16-dihydroxypalmitoyl-CoA
Nitrogen-Containing Glucoside Biosynthesis	1.74E-03	L-glutamate // 5-(methylsulfinyl)pentyl-glucosinolate // 5-(methylsulfanyl)pentyl-glucosinolate // adenosine 3',5'-bisphosphate // 8-(methylsulfinyl)octyl-glucosinolate // glucotropaeolin // 3-sinapoyloxypropylglucosinolate // 2-sinapoyloxy-3-butenylglucosinolate // 4-benzoyloxybutylglucosinolate // 2-benzoyloxy-3-butenylglucosinolate // NAD+ // NADH // 2-[(2'-methylsulfanyl)heptyl]maleate // 4-hydroxyglucobrassicin // 6-(methylsulfanyl)hexyl-glucosinolate // 7-(methylsulfanyl)heptyl-glucosinolate
Sugar Nucleotide Biosynthesis	1.75E-03	CMP-3-deoxy-beta-D-manno-octulosonate // GDP-beta-L-fucose // NAD+ // NADH // UDP-N-acetyl-alpha-D-glucosamine // L-glutamate // dTDP-beta-L-rhamnose // GDP-4-dehydro-alpha-D-rhamnose
L-serine biosynthesis I	1.84E-03	NAD+ // 3-phosphooxypyruvate // NADH // L-glutamate

Pathways	p-value	Matches
Fatty Acid and Lipid Biosynthesis	2.92E-03	CDP-ethanolamine // (2E,11Z,14Z)-icosatrienoyl-CoA // NAD+ // NADH // stearoyl-CoA // 1-linoleoyl-2-(3E)-hexadecenoyl-phosphatidylglycerol // CDP // 2-C-methyl-D-erythritol 4-phosphate // 2-phospho-4-(cytidine 5'-diphospho)-2-C-methyl-D-erythritol // (9Z,12Z)-15,16-dihydroxyoctadeca-9,12-dienoate // (9Z)-12,13,17-trihydroxyoctadeca-9-enoate // trans-lignocer-2-enoyl-CoA // docosanoyl-CoA // icosanoyl-CoA // (3R)-3-hydroxylignoceroyl-CoA // (3R)-3-hydroxy-arachidoyl-CoA // (11Z)-icosenoyl-CoA // 3-oxo-auricoloyl-CoA // (2E,8Z,11Z,14Z,17Z)-icosapentaenoyl-CoA // 10,16-dihydroxypalmitoyl-CoA // lauroyl-CoA // UDP-N-acetyl-alpha-D-glucosamine // UDP-2-N,3-O-bis[(3R)-3-hydroxytetradecanoyl]-alpha-D-glucosamine // (7Z,10Z,13Z,16Z,19Z)-docosapentaenoyl-CoA // (5Z,8Z,11Z,14Z,17Z)-3-oxodocosapentaenoyl-CoA // tri-acyl estolide // tetra-acyl estolide
jasmonic acid biosynthesis	2.93E-03	3-oxo-2-(cis-2'-pentenyl)-cyclopentane-1-hexanoyl-CoA // 3-oxo-2-(cis-2'-pentenyl)-cyclopentane-1-butanoyl-CoA // 3-oxo-2-(cis-2'-pentenyl)-cyclopentane-1-(3-oxooctanoyl)-CoA // NAD+ // NADH // 3-oxo-2-(cis-2'-pentenyl)-cyclopentane-1-(3R-hydroxyhexanoyl)-CoA
Fatty Acid Derivative Biosynthesis	4.18E-03	3-oxo-2-(cis-2'-pentenyl)-cyclopentane-1-hexanoyl-CoA // 3-oxo-2-(cis-2'-pentenyl)-cyclopentane-1-butanoyl-CoA // 3-oxo-2-(cis-2'-pentenyl)-cyclopentane-1-(3-oxooctanoyl)-CoA // NAD+ // NADH // 3-oxo-2-(cis-2'-pentenyl)-cyclopentane-1-(3R-hydroxyhexanoyl)-CoA
Purine Nucleotide De Novo Biosynthesis	5.34E-03	L-glutamate // NAD+ // NADH // dATP // 5'-phosphoribosyl-4-(N-succinocarboxamide)-5-aminoimidazole
Enzyme Cofactor Biosynthesis	6.08E-03	7,8-diaminopelargonate // NAD+ // NADH // beta-nicotinate D-ribonucleotide // L-glutamate // porphobilinogen // FMN // 5-methyltetrahydropteroyl tri-L-glutamate // tetrahydropteroyl tri-L-glutamate // pyridoxal 5'-phosphate // pyridoxamine
Purine Riboucleotide De Novo Biosynthesis	7.83E-03	L-glutamate // NAD+ // NADH // 5'-phosphoribosyl-4-(N-succinocarboxamide)-5-aminoimidazole
Sugar Biosynthesis	8.03E-03	NAD+ // NADH // CMP-3-deoxy-beta-D-manno-octulosonate // GDP-beta-L-fucose // UDP-N-acetyl-alpha-D-glucosamine // L-glutamate // dTDP-beta-L-rhamnose // GDP-4-dehydro-alpha-D-rhamnose
Fatty Acid Biosynthesis	1.15E-02	NAD+ // NADH // trans-lignocer-2-enoyl-CoA // docosanoyl-CoA // icosanoyl-CoA // (3R)-3-hydroxylignoceroyl-CoA // (3R)-3-hydroxy-arachidoyl-CoA // stearoyl-CoA // lauroyl-CoA // (11Z)-icosenoyl-CoA // 3-oxo-auricoloyl-CoA // (9Z,12Z)-15,16-dihydroxyoctadeca-9,12-dienoate // (9Z)-12,13,17-trihydroxyoctadeca-9-enoate // (2E,8Z,11Z,14Z,17Z)-icosapentaenoyl-CoA // (7Z,10Z,13Z,16Z,19Z)-docosapentaenoyl-CoA // (5Z,8Z,11Z,14Z,17Z)-3-oxodocosapentaenoyl-CoA // (2E,11Z,14Z)-icosatrienoyl-CoA
L-serine Biosynthesis	1.40E-02	NAD+ // NADH // L-glutamate // 3-phosphooxypyruvate
Pyrimidine Nucleotide Salvage	1.55E-02	CDP // thymidine // uracil // L-glutamate
Purine Nucleotide Biosynthesis	1.60E-02	L-glutamate // NAD+ // NADH // dATP // 5'-phosphoribosyl-4-(N-succinocarboxamide)-5-aminoimidazole
Polyunsaturated Fatty Acid Biosynthesis	1.67E-02	NADH // NAD+ // (2E,8Z,11Z,14Z,17Z)-icosapentaenoyl-CoA // (7Z,10Z,13Z,16Z,19Z)-docosapentaenoyl-CoA // (5Z,8Z,11Z,14Z,17Z)-3-oxodocosapentaenoyl-CoA // (2E,11Z,14Z)-icosatrienoyl-CoA
Cell Structure Biosynthesis	1.69E-02	stearoyl-CoA // lauroyl-CoA // 10,16-dihydroxypalmitoyl-CoA // 22-carboxy-docosanoyl-CoA // docosanoyl-CoA // a xylogalacturonan // UDP-N-acetyl-alpha-D-glucosamine // UDP-2-N,3-O-bis[(3R)-3-hydroxytetradecanoyl]-alpha-D-glucosamine

Pathways	p-value	Matches
Glucosinolate Biosynthesis	1.69E-02	L-glutamate // 5-(methylsulfinyl)pentyl-glucosinolate // 5-(methylsulfanyl)pentyl-glucosinolate // adenosine 3',5'-bisphosphate // 8-(methylsulfinyl)octyl-glucosinolate // glucotropaeolin // 3-sinapoyloxypropylglucosinolate // 2-sinapoyloxy-3-butenylglucosinolate // 4-benzoyloxybutylglucosinolate // 2-benzoyloxy-3-butenylglucosinolate // NAD+ // NADH // 2-[(2'-methylsulfanyl)heptyl]maleate // 4-hydroxyglucobrassicin // 6-(methylsulfanyl)hexyl-glucosinolate // 7-(methylsulfanyl)heptyl-glucosinolate
Anthocyanin Biosynthesis	1.77E-02	pelargonidin-3-O-beta-D-glucoside // cyanidin 3-O-(3'',6''-O-dimalonyl-beta-glucopyranoside) // cyanidin 3-O-beta-D-sambubioside // delphinidin 3-O-rutinoside-7-O-(6-O-(p-hydroxybenzoyl)-glucoside) // delphinidin 3-O-rutinoside-7-O-glucoside // delphinidin-3-O-(6''-O-malonyl)-beta-glucoside-3'-O-beta-glucoside // peonidin-3-(p-coumaroyl)-rutinoside-5-glucoside // cyanidin O-O-[6-O-(6-O-feruloyl-beta-D-glucosyl)-2-O-beta-D-xylosyl-beta-D-galactoside]
Hydrolyzable Tannin Biosynthesis	1.86E-02	2-O-digalloyl-1,3,4,6-tetra-O-beta-D-galloylglucose // tellimagrandin II // 1-O,6-O-digalloyl-beta-D-glucose
NAD de novo biosynthesis I (from aspartate)	1.86E-02	beta-nicotinate D-ribonucleotide // NAD+ // L-glutamate
Stearate Biosynthesis	1.86E-02	stearoyl-CoA // NAD+ // NADH
stearate biosynthesis II (bacteria and plants)	1.86E-02	stearoyl-CoA // NAD+ // NADH
superpathway of pyrimidine ribonucleosides salvage	1.86E-02	CDP // L-glutamate // uracil
GDP-L-fucose biosynthesis I (from GDP-D-mannose)	2.06E-02	GDP-beta-L-fucose // GDP-4-dehydro-alpha-D-rhamnose
quercetin gentiotetraside biosynthesis	2.06E-02	quercetin-3-gentiotrioside // quercetin-3-gentiotetraside
Vitamin B6 Biosynthesis	2.12E-02	pyridoxal 5'-phosphate // L-glutamate // pyridoxamine
Pyrimidine Nucleotide Biosynthesis	2.15E-02	CDP // thymidine // L-glutamate // (S)-dihydroorotate // uracil
Nucleoside and Nucleotide Degradation	2.82E-02	NAD+ // NADH // L-glutamate // CDP // uracil
pyridoxal 5'-phosphate biosynthesis II	3.18E-02	pyridoxal 5'-phosphate // L-glutamate
Porphyrin Compound Biosynthesis	3.19E-02	chlorophyll a // NAD+ // NADH // L-glutamate // porphobilinogen
Tetrapyrrole Biosynthesis	3.19E-02	chlorophyll a // NAD+ // NADH // L-glutamate // porphobilinogen

Pathways	p-value	Matches
Degradation/Utilization/Assimilation - Other	3.40E-02	3-cyano-L-alanine // L-glutamate // NAD+ // NADH
NAD Metabolism	3.40E-02	beta-nicotinate D-ribonucleotide // L-glutamate // NAD+ // NADH
curcumin glucoside biosynthesis	3.82E-02	curcumin 4'-O-beta-D-gentiobiosyl 4''-O-beta-D-glucoside // curcumin 4',4''-O-beta-D-digentiobioside
very long chain fatty acid biosynthesis II	4.40E-02	trans-lignocer-2-enoyl-CoA // docosanoyl-CoA // icosanoyl-CoA // (3R)-3-hydroxylignoceroyl-CoA // (3R)-3-hydroxy-arachidoyl-CoA // stearoyl-CoA
Unsaturated Fatty Acid Biosynthesis	4.47E-02	NAD+ // NADH // (2E,8Z,11Z,14Z,17Z)-icosapentaenoyl-CoA // icosanoyl-CoA // (7Z,10Z,13Z,16Z,19Z)-docosapentaenoyl-CoA // (5Z,8Z,11Z,14Z,17Z)-3-oxodocosapentaenoyl-CoA // (2E,11Z,14Z)-icosatrienoyl-CoA
violdelphin biosynthesis	4.50E-02	delphinidin 3-O-rutinoside-7-O-(6-O-(p-hydroxybenzoyl)-glucoside) // delphinidin 3-O-rutinoside-7-O-glucoside
Pyrimidine Nucleotide Degradation	4.52E-02	L-glutamate // CDP // uracil
2'-Deoxyribonucleotide Biosynthesis	4.81E-02	CDP // dATP // L-glutamate // (S)-dihydroorotate
UDP-sugar Biosynthesis	4.81E-02	NAD+ // NADH // UDP-N-acetyl-alpha-D-glucosamine // L-glutamate
Other Biosynthesis	4.98E-02	L-glutamate // pelargonidin-3-O-beta-D-glucoside // curcumin 4'-O-beta-D-gentiobiosyl 4''-O-beta-D-glucoside // curcumin 4',4''-O-beta-D-digentiobioside // NADH // NAD+ // eupatolitin 3-glucoside // patulitrin // quercetagetin 7-O-glucoside
Jasmonate Biosynthesis	5.53E-02	adenosine 3',5'-bisphosphate // 3-oxo-2-(cis-2'-pentenyl)-cyclopentane-1-hexanoyl-CoA // 3-oxo-2-(cis-2'-pentenyl)-cyclopentane-1-butanoyl-CoA // 3-oxo-2-(cis-2'-pentenyl)-cyclopentane-1-(3-oxooctanoyl)-CoA // NAD+ // NADH // 3-oxo-2-(cis-2'-pentenyl)-cyclopentane-1-(3R-hydroxyhexanoyl)-CoA

Supplementary Table 2C. Pathway Enrichment Analysis for V/V roots under water stress compared to the control plants.

Pathways	p-value	Matches
Stilbene Phytoalexin Biosynthesis	1.29E-03	malonyl-CoA // 3-phenylpropanoyl-CoA // cinnamoyl-CoA // p-coumaroyltriacetate
Stilbene Biosynthesis	2.00E-03	malonyl-CoA // 3-phenylpropanoyl-CoA // cinnamoyl-CoA // p-coumaroyltriacetate
Porphyrin Compound Biosynthesis	9.39E-03	chlorophyll a // precorrin-1 // siroheme // preuroporphyrinogen // ADP // 71-hydroxychlorophyllide a
Tetrapyrrole Biosynthesis	9.39E-03	chlorophyll a // precorrin-1 // siroheme // preuroporphyrinogen // ADP // 71-hydroxychlorophyllide a
superpathway of pyrimidine deoxyribonucleoside salvage	1.73E-02	2'-deoxycytidine // ADP // dCTP
cyanidin 3,7-diglucoside polyacylation biosynthesis	2.16E-02	1-O-4-hydroxybenzoyl-beta-D-glucose // cyanidin 3-O-glucoside-7-O-(6-O-(4-O-(6-O-(p-hydroxybenzoyl)-glucosyl)-oxybenzoyl)-glucoside)
Fatty Acid Biosynthesis	2.46E-02	lignoceroyl-CoA // trans-lignocer-2-enoyl-CoA // icosanoyl-CoA // (3R)-3-hydroxylignoceroyl-CoA // (3R)-3-hydroxy-arachidoyl-CoA // malonyl-CoA // stearoyl-CoA // (11Z)-icosenoyl-CoA // 3-oxo-auricoloyl-CoA // oleoyl-CoA // linoleoyl-CoA // (8Z,11Z,14Z,17Z)-3-oxoicosatetraenoyl-CoA
olivetol biosynthesis	3.35E-02	malonyl-CoA // hexanoyl-CoA
resveratrol biosynthesis	3.35E-02	p-coumaroyltriacetate // malonyl-CoA
shisonin biosynthesis	3.35E-02	malonyl-CoA // malonylshisonin
siroheme biosynthesis	4.01E-02	precorrin-1 // siroheme
alpha-solanine/alpha-chaconine biosynthesis	4.72E-02	beta-solanine // alpha-chaconine
violdelphin biosynthesis	4.72E-02	1-O-4-hydroxybenzoyl-beta-D-glucose // violdelphin
very long chain fatty acid biosynthesis II	3.77E-01	lignoceroyl-CoA // trans-lignocer-2-enoyl-CoA // icosanoyl-CoA // (3R)-3-hydroxylignoceroyl-CoA // (3R)-3-hydroxy-arachidoyl-CoA // malonyl-CoA // stearoyl-CoA

Supplementary Table 2D. Pathway Enrichment Analysis for V/N roots under water stress compared to the control plants.

Pathways	p-value	Matches
Nitrogen-Containing Secondary Compound Biosynthesis	1.33E-03	L-phenylalanine // glutathione // adenosine 3',5'-bisphosphate // betalamate // N-methylanthraniloyl-CoA // nicotinate // benzoate // cathinone // p-coumaroyltyramine // cinnamoyl-CoA // N-feruloyltyramine // (E)-1-(L-cysteinylglycin-S-yl)-N-hydroxy-omega-(methylsulfanyl)heptan-1-imine // (E)-7-(methyltsulfanyl)heptanal oxime // 6-methylsulfinylhexyl-glucosinolate // hordatine A // (E)-1-(L-cystein-S-yl)-N-hydroxy-omega-(methylsulfanyl)pentan-1-imine // 4-hydroxybutylglucosinolate // glucoraphanin // 4-(methylsulfanyl)butyl-desulfoglucosinolate // celosianin II // 6-O-methyl-N-deacetylisoipecoside // cephaeline // 3,4-dihydroxypyridin // N2,N2-dihydroxy-L-tryptophan // scopolamine // glucobrassicin // 4-hydroxyglucobrassicin // 4,5-seco-dopa // morphinone // sinigrin // glucoiberverin // 3-(methylsulfanyl)propyl-desulfoglucosinolate // lampranthin I // (S)-magnoflorine // (6E)-8-hydroxygeranial // UDP-beta-L-rhamnose // beta-solanine // alpha-chaconine // 7-(methylsulfanyl)-2-oxoheptanoate // 6-(methylsulfanyl)-2-oxohexanoate // 3-[(4'-methylsulfanyl)butyl]malate // 3-[(3'-methylsulfanyl)propyl]malate // 2-[(2'-methylsulfanyl)hexyl]maleate // 3-methoxytyramine // macarpine // 6-hydroxyprotopine // methylconiine // (E)-omega-(methylsulfanyl)hexyl-thiohydroximate // 5-(methylsulfinyl)pentyl-glucosinolate // 5-(methylsulfanyl)pentyl-glucosinolate // (1H-indol-3-yl)-N-methylmethanamine // gramine // (E,E)-piperoyl-CoA // coniferyl alcohol // 3,4-dihydroxymandelonitrile beta-D-glucoside // 11-hydroxyvittatine // hemanthamine // 3,4-dihydroxybenzaldehyde // (S)-6-O-methylnorlaudanosoline // vincristine // vindorosine // 16-hydroxytabersonine // N-formyldemecolcine
Glucosinolate Biosynthesis	1.60E-03	(E)-omega-(methylsulfanyl)hexyl-thiohydroximate // glutathione // 5-(methylsulfinyl)pentyl-glucosinolate // 5-(methylsulfanyl)pentyl-glucosinolate // adenosine 3',5'-bisphosphate // L-phenylalanine // sinigrin // glucoiberverin // 3-(methylsulfanyl)propyl-desulfoglucosinolate // (E)-1-(L-cystein-S-yl)-N-hydroxy-omega-(methylsulfanyl)pentan-1-imine // 4-hydroxybutylglucosinolate // glucoraphanin // 4-(methylsulfanyl)butyl-desulfoglucosinolate // 7-(methylsulfanyl)-2-oxoheptanoate // 6-(methylsulfanyl)-2-oxohexanoate // 3-[(4'-methylsulfanyl)butyl]malate // 3-[(3'-methylsulfanyl)propyl]malate // 2-[(2'-methylsulfanyl)hexyl]maleate // glucobrassicin // N2,N2-dihydroxy-L-tryptophan // 4-hydroxyglucobrassicin // (E)-1-(L-cysteinylglycin-S-yl)-N-hydroxy-omega-(methylsulfanyl)heptan-1-imine // (E)-7-(methyltsulfanyl)heptanal oxime // 6-methylsulfinylhexyl-glucosinolate
Cinnamate Biosynthesis	6.87E-03	O-sinapoylglucarate // L-phenylalanine // coniferyl alcohol // trans-5-O-(4-coumaroyl)-D-quinate // L-quinate // trans-5-O-(4-coumaroyl)shikimate // 1,2-di-O-sinapoyl-beta-D-glucose // O-sinapoylcholine // cinnamoyl-CoA // coumaryl acetate // 2-O-acetyl-3-O-trans-coutarate // methylcinnamate
Purine Riboucleotide De Novo Biosynthesis	8.07E-03	GDP // ADP // adenylo-succinate // 5-formamido-1-(5-phospho-D-ribosyl)-imidazole-4-carboxamide // 5-amino-1-(5-phospho-D-ribosyl)imidazole-4-carboxamide // 5'-phosphoribosyl-4-(N-succinocarboxamide)-5-aminoimidazole
cutin biosynthesis	9.63E-03	16-hydroxypalmitoyl-CoA // palmitoyl-CoA // oleoyl-CoA // 16-oxo-palmitate // (9R,10S)-dihydroxystearate // 10,16-dihydroxypalmitoyl-CoA
very long chain fatty acid biosynthesis II	1.02E-02	trans-cerot-2-enoyl-CoA // lignoceroyl-CoA // trans-lignocer-2-enoyl-CoA // icosanoyl-CoA // (3R)-3-hydroxylignoceroyl-CoA // (3R)-3-hydroxybehenoyl-CoA // (3R)-3-hydroxy-arachidoyl-CoA // 3-oxoicosanoyl-CoA // stearoyl-CoA
Jasmonate Biosynthesis	1.61E-02	L-phenylalanine // adenosine 3',5'-bisphosphate // cis-12-sulfojasmonate // (+)-7-epi-jasmonoyl-CoA // 3-oxo-2-(cis-2'-pentenyl)-cyclopentane-1-butanoyl-CoA // 3-oxo-2-(cis-2'-pentenyl)-cyclopentane-1-(E-buta-2-enoyl)-CoA // 3-oxo-2-(cis-2'-pentenyl)-cyclopentane-1-(E-octa-2-enoyl)-CoA // 3-oxo-2-(cis-2'-pentenyl)-cyclopentane-1-(3-oxohexanoyl)-CoA
Inosine-5'-phosphate Biosynthesis	1.72E-02	5-formamido-1-(5-phospho-D-ribosyl)-imidazole-4-carboxamide // 5-amino-1-(5-phospho-D-ribosyl)imidazole-4-carboxamide // 5'-phosphoribosyl-4-(N-succinocarboxamide)-5-aminoimidazole // ADP

Pathways	p-value	Matches
inosine-5'-phosphate biosynthesis II	1.72E-02	5-formamido-1-(5-phospho-D-ribosyl)-imidazole-4-carboxamide // 5-amino-1-(5-phospho-D-ribosyl)imidazole-4-carboxamide // 5'-phosphoribosyl-4-(N-succinocarboxamide)-5-aminoimidazole // ADP
superpathway of purine nucleotides de novo biosynthesis I	2.37E-02	ADP // GDP // adenylo-succinate // 5-formamido-1-(5-phospho-D-ribosyl)-imidazole-4-carboxamide // 5-amino-1-(5-phospho-D-ribosyl)imidazole-4-carboxamide // 5'-phosphoribosyl-4-(N-succinocarboxamide)-5-aminoimidazole
suberin monomers biosynthesis	3.05E-02	16-hydroxypalmitoyl-CoA // palmitoyl-CoA // oleoyl-CoA // 22-oxo-docosanoyl-CoA // N-feruloyltyramine // L-phenylalanine
adenosine ribonucleotides de novo biosynthesis	3.06E-02	ADP // adenylo-succinate // GDP
siroheme biosynthesis	3.06E-02	precorrin-1 // precorrin-2 // siroheme
Ellagitannin Biosynthesis	3.71E-02	tellimagrandin II // 1,2,3,4,6-pentagalloylglucose
Cell Structure Biosynthesis	3.84E-02	coniferyl alcohol // trans-5-O-(4-coumaroyl)-D-quinate // L-quinate // trans-5-O-(4-coumaroyl)shikimate // 7-hydroxylauroyl-CoA // 18-hydroxystearoyl-CoA // 16-hydroxypalmitoyl-CoA // oleoyl-CoA // stearoyl-CoA // palmitoyl-CoA // 16-oxo-palmitate // (9R,10S)-dihydroxystearate // 10,16-dihydroxypalmitoyl-CoA // 16-feruloyloxypalmitate // 22-oxo-docosanoyl-CoA // N-feruloyltyramine // L-phenylalanine // a xylogalacturonan // UDP-3-O-(3-hydroxymyristoyl)-alpha-D-glucosamine // ADP
alpha-solanine/alpha-chaconine biosynthesis	3.89E-02	UDP-beta-L-rhamnose // beta-solanine // alpha-chaconine
chlorogenic acid biosynthesis II	3.89E-02	trans-5-O-(4-coumaroyl)-D-quinate // L-quinate // trans-5-O-(4-coumaroyl)shikimate
Purine Nucleotide De Novo Biosynthesis	4.29E-02	GDP // ADP // adenylo-succinate // 5-formamido-1-(5-phospho-D-ribosyl)-imidazole-4-carboxamide // 5-amino-1-(5-phospho-D-ribosyl)imidazole-4-carboxamide // 5'-phosphoribosyl-4-(N-succinocarboxamide)-5-aminoimidazole
Epidermal Structures	4.76E-02	16-hydroxypalmitoyl-CoA // palmitoyl-CoA // oleoyl-CoA // 16-oxo-palmitate // (9R,10S)-dihydroxystearate // 10,16-dihydroxypalmitoyl-CoA
Purine Nucleotide Biosynthesis	4.98E-02	ADP // GDP // adenylo-succinate // 5-formamido-1-(5-phospho-D-ribosyl)-imidazole-4-carboxamide // 5-amino-1-(5-phospho-D-ribosyl)imidazole-4-carboxamide // 5'-phosphoribosyl-4-(N-succinocarboxamide)-5-aminoimidazole // 2'-deoxyadenosine
Nitrogen-Containing Glucoside Biosynthesis	5.17E-02	(E)-omega-(methylsulfanyl)hexyl-thiohydroximate // glutathione // 5-(methylsulfinyl)pentyl-glucosinolate // 5-(methylsulfanyl)pentyl-glucosinolate // adenosine 3',5'-bisphosphate // nicotinate // L-phenylalanine // 3,4-dihydroxymandelonitrile beta-D-glucoside // sinigrin // glucoiberverin // 3-(methylsulfanyl)propyl-desulfoglucosinolate // (E)-1-(L-cystein-S-yl)-N-hydroxy-omega-(methylsulfanyl)pentan-1-imine // 4-hydroxybutylglucosinolate // glucoraphanin // 4-(methylsulfanyl)butyl-desulfoglucosinolate // 7-(methylsulfanyl)-2-oxoheptanoate // 6-(methylsulfanyl)-2-oxohexanoate // 3-[(4'-methylsulfanyl)butyl]malate // 3-[(3'-methylsulfanyl)propyl]malate // 2-[(2'-methylsulfanyl)hexyl]maleate // glucobrassicin // N2,N2-dihydroxy-L-tryptophan // 4-hydroxyglucobrassicin // (E)-1-(L-cysteinylglycin-S-yl)-N-hydroxy-omega-(methylsulfanyl)heptan-1-imine // (E)-7-(methyltsulfanyl)heptanal oxime // 6-methylsulfinylhexyl-glucosinolate
Plant Cell Structures	8.88E-01	coniferyl alcohol // trans-5-O-(4-coumaroyl)-D-quinate // L-quinate // trans-5-O-(4-coumaroyl)shikimate // 7-hydroxylauroyl-CoA // 18-hydroxystearoyl-CoA // 16-hydroxypalmitoyl-CoA // oleoyl-CoA // stearoyl-CoA // palmitoyl-CoA // 16-oxo-palmitate // (9R,10S)-dihydroxystearate // 10,16-dihydroxypalmitoyl-CoA // 16-feruloyloxypalmitate // 22-oxo-docosanoyl-CoA // N-feruloyltyramine // L-phenylalanine // a xylogalacturonan

6. General Discussion

6.1. Constitutive differences in grafted pepper plants

Constitutive traits in plants do not need stress to be present, there is no mandatory induction by stress and, thus, the genotype x environment (G x E) interaction is lesser than in stress adaptive traits (Rizza et al., 2012). Several authors have pointed out that constitutive defenses can make a difference in the stress response. By way of example, Zandt (2007) proposes that plants that develop in abiotically stressful environments acquire constitutive defenses to herbivores (Zandt, 2007). When focusing on water stress, Rizza et al. (2012) stated constitutive differences in two wheat cultivars' water use efficiency (WUE), and this trait has also been studied by Fracasso et al. (2016) from a molecular point of view in two sorghum genotypes with contrasting tolerance to water stress. Under well-watered conditions, the sensitive sorghum genotype showed a down-regulation of the genes associated with "glutathione transferase activity" and "secondary metabolic process" GO Terms in relation to the tolerant sorghum genotype (Fracasso et al., 2016).

Chapter 2 indicates constitutive differences between the water stress-tolerant pepper rootstock NIBER® and the water stress-sensitive pepper accession A10 in roots gene expression. These differences under non water stress conditions comprised the expression of up to 3000 genes and were associated with GO Term categories, such as responses to stimulus, oxidative stress, chemical and inorganic substance and photosynthesis, which were overrepresented in NIBER® in relation to A10 roots. In other experiments with pepper rootstocks, the authors also found constitutive differences in gene expression under the control conditions between the salt stress-tolerant and salt stress-sensitive accessions, mostly related to the response to abiotic or biotic stimulus, response to stress and transport GO Terms (López-Serrano et al., 2021).

Therefore, the observed constitutive differences in Chapter 2 could be advantageous for the NIBER® response when stress comes into play. These differences in NIBER® *versus* A10 were found mainly for reactive oxygen species (ROS) detoxification-related genes, such as the up-regulation of formate and malate dehydrogenases, polyamine genes (*PAO*, *PUT4*) and a H_2O_2 and hydroxyl radicals scavenging dehydrin gene (*HIRD11*). Moreover, the superoxide anion production gene (*RbohB*) was down-regulated in NIBER® *vs.* A10 as well as five genes coding for the last enzyme on the ethylene biosynthesis pathway (ACO). Ethylene regulates *RbohB* gene transcription and, hence, plays a role in ROS production (Xia et al., 2015). Landi et al. (2017) found similar results in drought-tolerant and drought-sensitive tomato landraces, which suggests that the increased constitutive expression of ROS scavenging enzymes in tolerant landraces could establish the basal activation of the ROS detoxification system, and could result in better yields and fruit quality when water stress is applied. In fact in a recent study with the NIBER® rootstock (Gisbert-Mullor et al., 2023), the authors obtained higher yields in the variety grafted onto the NIBER® rootstock than in the ungrafted variety under non water stress conditions. These larger yields were associated with a bigger number of fruits, less blossom-end rot (BER), a higher root fresh weight and a bigger volume when using the NIBER® rootstock (Gisbert-Mullor et al., 2023).

BER is commonly known as a calcium-related disorder. However, some authors point out that Ca^{2+} deficiency is not a cause, but a consequence of BER, and abscisic acid (ABA) can be efficient in preventing BER, even with limited Ca^{2+} (Saure, 2014). Landi et al. (2017) proposed sustained ABA induction as a strategy to achieve a quick drought response because the *NCED* gene was up-regulated in drought-tolerant tomato in relation to drought-sensitive tomato under the non drought conditions. Moreover, this superiority was maintained under drought with no severe increase in *NCED* expression in the drought-tolerant plants (Landi et al., 2017). In the Chapter 2 experiment, *NCED1* was up-regulated in NIBER® *vs.* A10 under non water stress conditions, and there was no change in the gene expression of *NCED* under water stress conditions. However, the ABA receptor *PYL1* gene was down-regulated in NIBER® *vs.* A10 under the control conditions, which was linked with both the prevention of ABA accumulation detrimental effects and avoidance of ABA-dependent stomatal closure under optimal conditions to increase the photosynthesis rate (Gonzalez-Guzman et al., 2012; Ruiz-Partida et al., 2021).

Hence constitutive mechanisms under the control conditions could influence plants' response under water stress, particularly in grafted pepper plants, in which the strategies seemed to involve an enhanced ROS detoxification system and ABA induction. Nevertheless, further studies should be performed to unravel the additional molecules and pathways involved in constitutive mechanisms, which would allow better yields to be obtained when grafting onto water stress-tolerant peeper rootstocks like NIBER®.

6.2. Water stress responses in grafted pepper plants

NIBER® is a hybrid pepper rootstock that has been proven tolerant to water stress under long-term deficit irrigation conditions (Gisbert-Mullor et al., 2020, 2023). In previous experiments, the NIBER® rootstock was able to confer tolerance to the grafted variety under sustained water stress conditions (up to 115 days) in terms of less biomass and fruit yield decreases compared to the ungrafted variety (Gisbert-Mullor et al., 2020). The authors observed that the grafted variety was able to sustain photosynthesis under stress conditions, but information about tolerance mechanisms in the plants grafted onto NIBER® and the NIBER® rootstock itself was lacking. Thus the short-term mechanisms in the water stress response can provide useful information about plants' strategies that lead to tolerance. The relevance of a prompt response to water stress in pepper plants is reflected in Chapters 2, 3 and 4, and comprises a series of mechanisms at the transcriptomic, hormonal and metabolomic levels.

The first organs to sense osmotic stress under water stress conditions are roots, which produce a quick effect on leaves by leading to turgor losses and stomatal closure (Munns, 2002). In roots, the total number of differentially accumulated metabolites under water stress more than doubled that in leaves (Chapter 4). Roots' perception of water stress through rapid changes in the transcriptome (Chapter 2) evidenced a stronger impact of stress on the sensitive pepper accession A10 than on NIBER® because A10 showed more than double the amount of differentially expressed genes (DEGs) after 5 h under water stress. This effect has also been observed by Fracasso et al. (2016) in sorghum water-stressed plants. The sensitive genotype showed a markedly bigger number of differentially expressed genes (DEGs) than the tolerant genotype, and most were genes related to ROS detoxification. ROS overproduction is a consequence of water stress and there is usually excess H_2O_2 that can be scavenged by catalase or peroxidase enzymes (Hasanuzzaman et al., 2020). However, López-Serrano et al. (2020) found higher H_2O_2 content in the leaves of the variety grafted onto NIBER® under salt stress compared to the self-grafted and ungrafted variety, which did not result in higher lipid peroxidation. So these authors proposed that H_2O_2 could act as a signaling molecule instead of an oxidative damage generator (López-Serrano et al., 2020). In our experiment, catalase and glycolate oxidase genes were down-regulated in NIBER® roots under water stress, whereas several ROS detoxification genes were up-regulated in A10. These findings support the hypothesis of a lesser impact of water stress on NIBER® roots. Moreover, redox homeostasis involves the oxidation of reduced glutathione (GSH) to oxidized glutathione (GSSG) under stress conditions (Dorion et al., 2021), and GSSG content was lower in the NIBER® roots in relation to A10 at 24 h. Lower GSSG content is associated with less oxidative damage and water stress tolerance (Hasanuzzaman & Fujita, 2011). Regarding leaves, in Chapter 4 NIBER® was able to increase vitamin B6 synthesis in the grafted variety at 48 h under water stress, probably to benefit from its ROS scavenging ability as an antioxidant molecule (Mooney & Hellmann, 2010). This is why osmoprotectant sugars like galactinol and raffinose have been associated with photosynthetic apparatus protection from oxidative damage (Nishizawa et al., 2008). In Chapter 2, NIBER® promoted galactinol synthesis (*GolS2* up-regulation) and raffinose synthesis from galactinol (galactinol-sucrose galactosyltransferase gene up-regulation) in roots under water stress. Thus galactinol content lowered and raffinose content rose in NIBER® roots under water stress in relation to the control conditions at 24 h.

Photosynthesis is one of the first processes to be affected by water stress effects, including oxidative damage in the photosynthetic apparatus and photooxidative inhibition (Tognetti et al., 2012). Rivero et al. (2010) observed a reduction in the electron transfer between both photosystems and non photochemical quenching dissipation in sensitive plants under water stress, which resulted in less photosynthetic activity. Tolerant plants' photosynthesis was not altered (Rivero et al., 2010). Some authors suggest a role for proline in photoinhibition mitigation and photosynthetic apparatus protection under water stress for preserving the electron transfer (Ashraf & Foolad, 2007; Reddy et al., 2004; Szabados & Savouré, 2010). Proline accumulation under long-term water stress has been observed in plants grafted onto tolerant pepper hybrid H92 in Chapter 1, together with sustained photosynthesis and increased instantaneous WUE. In Chapter 2, proline transporter and proline dehydrogenase genes were up-regulated in the sensitive accession roots (A10) under short-term water stress, but no changes in proline-related genes were found in the NIBER® roots. However, higher proline content was noted in the leaves of both the variety grafted onto NIBER® and NIBER® grafted onto the variety under long-term salt stress (López-Serrano et al., 2020). These results show the ability of NIBER® to promote proline synthesis in leaves or to induce its synthesis on the grafted variety's leaves under long-term salt stress. Thus proline contribution to NIBER® water stress tolerance could depend on stress duration and must be further studied. Moreover, the chlorophyll a (Chl a) to chlorophyll b (Chl b) ratio commonly drops under water stress, and does so more rapidly in drought-sensitive genotypes (Majidi et al., 2015). In Chapter 2, the NIBER® roots showed the up-regulation of a chlorophyll synthesis gene (*ChlH*) at 5 h under water stress, which is consistent with the higher chlorophyll a (Chl a) content observed in Chapter 4 in the V/N roots at 48 h under water stress. In fact Chl a content also rose in the V/N leaves under water stress and NIBER® seemed to avoid Chl b synthesis to maintain the Chl a:Chl b ratio.

The chlorophyll synthesis gene (*ChlH*) is implicated in ABA signaling in guard cells and, thus, in stomatal movements (Tsuzuki et al., 2011). This gene and *WRKY70*, which negatively regulates stomatal closure (Li et al., 2013), were up-regulated in the NIBER® roots under water stress in Chapter 2. *PP2C72* was up-regulated in the NIBER® water stressed-roots at 24 h, and PP2C-type phosphatases avoided stomatal closure by ABA negative regulation (Lee et al., 2009). These results suggest in the very early response to water stress (up to 24 h) under our experimental conditions that NIBER® prevents stomatal closure. In Chapter 1, we observed a linear correlation between the photosynthetic rate (A_N) and stomatal conductance (g_s) during the water stress experiment, which suggests that the observed reduction in photosynthesis was provoked by stomatal closure. Sade et al. (2009) related sustained transpiration and stomatal opening under drought with higher growth and productivity in the tomato transgenic lines that overexpressed *SlTIP2-2* aquaporin. Aquaporins are water transport channels that have been proven to help in CO_2 homeostasis, which is affected by water starvation (Afzal et al., 2016). In Chapter 2, contrasting regulation of aquaporin genes under water stress occurred, i.e., NIBER® increased aquaporin *TIP-type RB7–5A* expression at 24 h and A10 decreased the expression of four aquaporin genes. Moreover, the sustained stomatal opening strategy was observed in NIBER® under salt stress (López-Serrano et al., 2020) to then decrease in both stomatal conductance and the photosynthetic rate started at 48 h. In Chapter 3, the increase in A_N/g_S in V/N than in V/V at 48 h was greater under water stress, which was associated with better stomatal closure management in the V/N plants. ABA is synthesized mainly in roots and transported to guard cells in leaves for stomatal closure regulation under short-term water stress (Allario et al., 2013; Sarwat & Tuteja, 2017; Wilkinson & Davies, 2002). Indeed at 4 h, under water stress the rise in the ABA concentration in roots was observed only in V/N. Then the ABA concentration in the V/N roots lowered at 48 h, which coincided with an increase in the V/N leaves. These results could indicate that NIBER® promotes stomatal closure as of 48 h under water stress *via* prior ABA synthesis in roots and transport to leaves under our experimental conditions. Stomatal movements' fine-tuning in the NIBER® early response to water stress (24 h opening *vs.* 48 h closure), and its implications in water stress tolerance, should be further studied.

Apart from ABA, salicylic acid (SA) and jasmonic acid (JA) are also implicated in stomatal regulation under water stress conditions (Müller & Munné-Bosch, 2021). SA has been mainly related to biotic stress, but has been recently linked with abiotic stress (Miura & Tada, 2014). In Chapter 3, SA content increased in roots under water stress at 24 h and was not plant type-dependent, which suggests a non specific water stress response. However, SA content increased immediately in the

V/N leaves under water stress to then be followed by a decreasing trend. The early increase in SA content could influence the V/N response under water stress. For this reason, the SA function in NIBER® water stress tolerance should be investigated. Unlike SA, the JA content in V/N did not immediately increase in leaves under water stress (4h), but it significantly increased in the V/N leaves at 48 h, and coincided with stomata closure and higher ABA content (Chapter 3). JA and its precursor 12-OPDA have been described as positive regulators of stomata closure and result in water stress tolerance (Savchenko & Dehesh, 2014). Moreover in Chapter 4, the biosynthesis pathways of JA and jasmonates (including precursors and derivatives) were enriched in the V/N leaves under water stress at 48 h. For the implication of JA in the water stress response on the NIBER® roots, we obtained contrasting results in Chapters 2, 3 and 4. On the one hand in Chapter 3, the JA concentration dropped in the V/N and V/V roots under water stress. On the other hand in Chapter 2, the JA content in the NIBER® roots increased at 5 h under water stress, and this content doubled at 24 h. Moreover in Chapter 4, the jasmonate biosynthesis pathway was enriched in the V/N roots. These results suggest that JA content in roots depends on its synthesis in leaves, which could be determined by root to leaf signaling under water stress. JA content increased in the NIBER® roots (Chapter 2), probably due to more efficient stress sensing in roots that promoted JA synthesis in leaves, which could be long-distance transported through vascular bundles toward roots and resynthesized (Ruan et al., 2019). In Chapter 2, the *MYC2* transcription factor was up-regulated in the NIBER® roots at 24 h under water stress, and *MYC2* activation was mediated by JA through a complex formation with JAZ repressors (Song et al., 2022). *MYC2* promotes the gene expression of many downstream genes *via* JA signaling, including dehydration-resistance genes (Li et al 2019). Similarly, the expression of dehydration-responsive element-binding transcription factors (*DREB*s) rapidly increases under water and osmotic stresses (Sakuma et al., 2002). In Chapter 2, three *DREB*s were up-regulated in the NIBER® roots under water stress. Hence *MYC2*, *DREB*s and JA play a role in NIBER® water stress tolerance, and reciprocal grafting can be performed to unravel JA signaling in the NIBER® stress response.

Although auxins and cytokinins are well-known growth and development-related phytohormones, they have been associated with drought response regulation (Devireddy et al., 2021; Raza et al., 2022). In Chapter 2, the IAA content increased in the NIBER® and A10 roots at 5 h under water stress, an auxin polar transporter gene (*ABCG37*) and an auxin homeostasis regulator (*MIZ1*) were down-regulated, and the "Hydrotropism" GO term was overrepresented. These results indicate a non specific rapid water stress response because both genotypes shared negative feedback and prevented auxin export from roots to favor movement and growth toward water. A common prompt response (5 h) to water stress was also found for cytokinins gene regulation in Chapter 2, and a CKs activation gene (*LOG1*) was up-regulated and a CKs synthesis gene (*IPT1*) was down-regulated in the NIBER® and A10 roots under water stress. Both genotypes promote CKs activation to the biologically active form, but avoid CKs biosynthesis, which could be a strategy to favor root growth over shoot growth in the very early phase of the water stress response, linked with the above-mentioned auxin increase and regulation. Later as reflected in Chapter 3, auxin content dropped in the V/V and V/N roots at 24 h under water stress, and CKs content increased only in the V/N roots, which could promote shoot growth. This shoot growth promotion at 24 h is the opposite to the root growth promotion observed at 5 h in Chapter 2, and is supported by sustained photosynthetic activity. Then in Chapter 3, from 24 h to 48 h IAA notably increased in both the V/N roots and V/V leaves under water stress, and CKs drastically decreased in the V/N roots. Moreover in Chapter 4, the cytokinin trans-zeatin biosynthesis pathway was enriched in V/V and V/N at 48 h under water stress with contrasting regulation. Intermediate metabolites were up-accumulated in the V/N leaves, while trans-zeatin and related-metabolites were down-regulated in the V/N roots under water stress. Once again, auxins/cytokinins increases in the V/N roots promoted root growth and restricted shoot growth (Kurepa and Smalle, 2022). The significance of root biomass in the water stress response is stated in Chapter 1 because the aerial biomass did not show differences in relation to the employed rootstock, but there was a differential response to water stress among plant combinations. The root biomass significantly increased in V/N under water stress at 48 h and the aerial biomass did not change in relation to the control conditions in V/N. In addition, major root length and root volume growth occurred in NIBER® under salt and water stress, respectively (López-Serrano et al., 2020; Gisbert-Mullor et al., 2023).

NIBER® influences the grafted variety under water stress, as reflected in the modulation of the variety's leaf metabolome. In Chapter 4, NIBER® was able to promote the synthesis of stearic acid in the leaves of the grafted variety, stearoyl-CoA was up-accumulated in the V/N leaves and the *stearate biosynthesis II (bacteria and plants)* pathway was enriched, but no differences were found in the V/V leaves. With peanut under water stress, stearic acid is up-accumulated in the leaves of the drought-tolerant genotype and in the roots of the drought-sensitive genotype (Guandaraniya et al., 2020), which suggests that the localization of stearate in leaves contributes to water stress tolerance. In Chapter 4, several of the metabolites implicated in the *suberin monomers biosynthesis* and *cutin biosynthesis* pathways were up-accumulated in the V/N leaves and roots, although these pathways were enriched in the V/N roots. In sorghum, cutin and its monomers increase in the drought-tolerant genotype under drought stress (Zhang et al., 2021). Cutin and suberin are cellular barrier constituents that protect plants under water stress by controlling non stomatal fluxes of gases, water and solutes (Pollard et al., 2008). Anthocyanins were another class of metabolites that were induced by NIBER® in the V/N leaves, where the *anthocyanin biosynthesis pathway* was enriched under water stress in Chapter 4. Anthocyanin increases in leaves because of combined drought and UV-B radiation has been observed in pea (Nogués et al., 1998). These compounds act in stress response as ROS scavengers mainly located in the vacuoles next to the main ROS production organs (i.e., chloroplasts and peroxisomes) (Naing & Kim, 2021). Another metabolite linked with oxidative damage mitigation under drought is chlorogenic acid (CGA). However, a recent study conducted with artichoke leaves and heads shows that decreases in chlorophyll, relative water content, growth and yield occur simultaneously with CGA increases (Nouraei et al., 2018). In Chapter 4, two intermediates of CGA synthesis were down-accumulated in the V/N roots and no changes were found in leaves. As chlorophyll increased, the aerial biomass was not affected and root biomass increased under water stress in V/N, a negative role for CGA is proposed and this role in pepper water stress should be investigated. Lastly, improved nitrogen assimilation is suggested in the NIBER® roots based on previous and present studies. NIBER® roots' nitrate reductase activity reduces to a lesser extent in relation to the ungrafted and self-grafted varieties under salt stress (López-Serrano et al., 2020). Five vacuolar iron transporter genes were down-regulated in the NIBER® roots under water stress, which may result in lesser iron compartmentation in vacuoles (Chapter 2). Siroheme is an iron-containing prosthetic group in nitrite reductases (Murphy & Siegel, 1973), which was up-accumulated in roots (Chapter 4) and could allow the better modulation of nitrate and nitrite reductase activity for improved nitrogen assimilation.

All these results reveal fast modulation at the physiological, transcriptomic and metabolomic levels in the NIBER® pepper rootstock under water stress conditions. The NIBER® rootstock is able to confer tolerance to the grafted variety under water stress by fine-tuning very early stress responses through hormonal signaling, gene expression regulation and the differential accumulation of metabolites.

6.3. References

Afzal, Z., Howton, T. C., Sun, Y., & Mukhtar, M. S. (2016). The roles of aquaporins in plant stress responses. *Journal of developmental biology*, *4*(1), 9.

Allario, T., Brumos, J., Colmenero-Flores, J. M., Iglesias, D. J., Pina, J. A., Navarro, L., ... & Morillon, R. (2013). Tetraploid Rangpur lime rootstock increases drought tolerance via enhanced constitutive root abscisic acid production. *Plant, cell & environment*, *36*(4), 856-868.

Dorion, S., Ouellet, J. C., & Rivoal, J. (2021). Glutathione metabolism in plants under stress: beyond reactive oxygen species detoxification. *Metabolites*, *11*(9), 641.

Fracasso, A., Trindade, L. M., & Amaducci, S. (2016). Drought stress tolerance strategies revealed by RNA-Seq in two sorghum genotypes with contrasting WUE. *BMC Plant Biology*, *16*(1), 1-18.

Gisbert-Mullor, R., Martín-García, R., Bažon Zidarić, I., Pascual-Seva, N., Pascual, B., Padilla, Y. G., ... & López-Galarza, S. (2023). A Water Stress–Tolerant Pepper Rootstock Improves the Behavior of Pepper Plants under Deficit Irrigation through Root Biomass Distribution and Physiological Adaptation. *Horticulturae*, *9*(3), 362.

Gisbert-Mullor, R., Pascual-Seva, N., Martínez-Gimeno, M. A., López-Serrano, L., Badal Marín, E., Pérez-Pérez, J. G., ... & López-Galarza, S. (2020). Grafting onto an appropriate rootstock reduces the impact on yield and quality of controlled deficit irrigated pepper crops. *Agronomy*, *10*(10), 1529.

Gonzalez-Guzman, M., Pizzio, G. A., Antoni, R., Vera-Sirera, F., Merilo, E., Bassel, G. W., ... & Rodriguez, P. L. (2012). Arabidopsis PYR/PYL/RCAR receptors play a major role in quantitative regulation of stomatal aperture and transcriptional response to abscisic acid. *The Plant Cell*, *24*(6), 2483-2496.

Hasanuzzaman, M., & Fujita, M. (2011). Selenium pretreatment upregulates the antioxidant defense and methylglyoxal detoxification system and confers enhanced tolerance to drought stress in rapeseed seedlings. *Biological Trace Element Research*, *143*, 1758-1776.

Hasanuzzaman, M., Bhuyan, M. B., Zulfiqar, F., Raza, A., Mohsin, S. M., Mahmud, J. A., ... & Fotopoulos, V. (2020). Reactive oxygen species and antioxidant defense in plants under abiotic stress: Revisiting the crucial role of a universal defense regulator. *Antioxidants*, *9*(8), 681.

Landi, S., De Lillo, A., Nurcato, R., Grillo, S., & Esposito, S. (2017). In-field study on traditional Italian tomato landraces: The constitutive activation of the ROS scavenging machinery reduces effects of drought stress. *Plant physiology and biochemistry*, *118*, 150-160.

Lee, S. C., Lan, W., Buchanan, B. B., & Luan, S. (2009). A protein kinase-phosphatase pair interacts with an ion channel to regulate ABA signaling in plant guard cells. *Proceedings of the National Academy of Sciences*, *106*(50), 21419-21424.

Li, J., Besseau, S., Törönen, P., Sipari, N., Kollist, H., Holm, L., & Palva, E. T. (2013). Defense-related transcription factors *WRKY 70* and *WRKY 54* modulate osmotic stress tolerance by regulating stomatal aperture in A rabidopsis. *New Phytologist*, *200*(2), 457-472.

Li, Y., Yang, X., & Li, X. (2019). Role of jasmonate signaling pathway in resistance to dehydration stress in Arabidopsis. *Acta Physiologiae Plantarum*, *41*, 1-12.

López-Serrano, L., Calatayud, Á., López-Galarza, S., Serrano, R., & Bueso, E. (2021). Uncovering salt tolerance mechanisms in pepper plants: a physiological and transcriptomic approach. *BMC Plant Biology*, *21*, 1-17.

López-Serrano, L., Canet-Sanchis, G., Selak, G. V., Penella, C., San Bautista, A., López-Galarza, S., & Calatayud, Á. (2020). Physiological characterization of a pepper hybrid rootstock designed to cope with salinity stress. *Plant Physiology and Biochemistry*, *148*, 207-219.

Majidi, M. M., Rashidi, F., & Sharafi, Y. (2015). Physiological traits related to drought tolerance in Brassica. *International Journal of Plant Production*, *9*(4).

Miura, K., & Tada, Y. (2014). Regulation of water, salinity, and cold stress responses by salicylic acid. *Frontiers in plant science*, *5*, 4.

Mooney, S., & Hellmann, H. (2010). Vitamin B6: Killing two birds with one stone?. *Phytochemistry*, *71*(5-6), 495-501.

Muchate, N. S., Nikalje, G. C., Rajurkar, N. S., Suprasanna, P., & Nikam, T. D. (2016). Plant salt stress: adaptive responses, tolerance mechanism and bioengineering for salt tolerance. *The Botanical Review*, *82*, 371-406.

Müller, M., & Munné-Bosch, S. (2021). Hormonal impact on photosynthesis and photoprotection in plants. *Plant Physiology*, *185*(4), 1500-1522.

Murphy, M. J., & Siegel, L. M. (1973). Siroheme and sirohydrochlorin: the basis for a new type of porphyrin-related prosthetic group common to both assimilatory and dissimilatory sulfite reductases. *Journal of Biological Chemistry*, *248*(19), 6911-6919.

Naing, A. H., & Kim, C. K. (2021). Abiotic stress-induced anthocyanins in plants: Their role in tolerance to abiotic stresses. *Physiologia Plantarum*, *172*(3), 1711-1723.

Nishizawa, A., Yabuta, Y., & Shigeoka, S. (2008). Galactinol and raffinose constitute a novel function to protect plants from oxidative damage. *Plant physiology*, *147*(3), 1251-1263.

Nogués, S., Allen, D. J., Morison, J. I., & Baker, N. R. (1998). Ultraviolet-B radiation effects on water relations, leaf development, and photosynthesis in droughted pea plants. *Plant physiology*, *117*(1), 173-181.

Nouraei, S., Rahimmalek, M., & Saeidi, G. (2018). Variation in polyphenolic composition, antioxidants and physiological characteristics of globe artichoke (*Cynara cardunculus* var. *scolymus* Hayek L.) as affected by drought stress. *Scientia Horticulturae*, *233*, 378-385.

Pollard, M., Beisson, F., Li, Y., & Ohlrogge, J. B. (2008). Building lipid barriers: biosynthesis of cutin and suberin. *Trends in plant science*, *13*(5), 236-246.

Raza, S. H., Athar, H. R., Ashraf, M., & Hameed, A. (2007). Glycinebetaine-induced modulation of antioxidant enzymes activities and ion accumulation in two wheat cultivars differing in salt tolerance. *Environmental and Experimental Botany*, *60*(3), 368-376.

Reddy, A. R., Chaitanya, K. V., & Vivekanandan, M. (2004). Drought-induced responses of photosynthesis and antioxidant metabolism in higher plants. *Journal of plant physiology*, *161*(11), 1189-1202.

Rivero, R. M., Gimeno, J., Van Deynze, A., Walia, H., & Blumwald, E. (2010). Enhanced cytokinin synthesis in tobacco plants expressing *PSARK::IPT* prevents the degradation of photosynthetic protein complexes during drought. *Plant and cell physiology*, *51*(11), 1929-1941.

Rizza, F., Ghashghaie, J., Meyer, S., Matteu, L., Mastrangelo, A. M., & Badeck, F. W. (2012). Constitutive differences in water use efficiency between two durum wheat cultivars. *Field Crops Research*, *125*, 49-60.

Ruan, J., Zhou, Y., Zhou, M., Yan, J., Khurshid, M., Weng, W., ... & Zhang, K. (2019). Jasmonic acid signaling pathway in plants. *International journal of molecular sciences*, *20*(10), 2479.

Ruiz-Partida, R., Rosario, S. M., & Lozano-Juste, J. (2021). An update on crop ABA receptors. *Plants*, *10*(6), 1087.

Sade, N., Vinocur, B. J., Diber, A., Shatil, A., Ronen, G., Nissan, H., ... & Moshelion, M. (2009). Improving plant stress tolerance and yield production: is the tonoplast aquaporin SlTIP2; 2 a key to isohydric to anisohydric conversion?. *New Phytologist*, *181*(3), 651-661.

Sakuma, Y., Liu, Q., Dubouzet, J. G., Abe, H., Shinozaki, K., & Yamaguchi-Shinozaki, K. (2002). DNA-binding specificity of the ERF/AP2 domain of Arabidopsis *DREB*s, transcription factors involved in dehydration-and cold-inducible gene expression. *Biochemical and biophysical research communications*, *290*(3), 998-1009.

Sarwat, M., & Tuteja, N. (2017). Hormonal signaling to control stomatal movement during drought stress. *Plant Gene*, *11*, 143-153.

Saure, M. C. (2014). Why calcium deficiency is not the cause of blossom-end rot in tomato and pepper fruit–a reappraisal. *Scientia Horticulturae*, *174*, 151-154.

Savchenko, T., Kolla, V. A., Wang, C. Q., Nasafi, Z., Hicks, D. R., Phadungchob, B., ... & Dehesh, K. (2014). Functional convergence of oxylipin and abscisic acid pathways controls stomatal closure in response to drought. *Plant Physiology*, *164*(3), 1151-1160.

Song, C., Cao, Y., Dai, J., Li, G., Manzoor, M. A., Chen, C., & Deng, H. (2022). The multifaceted roles of *MYC2* in plants: toward transcriptional reprogramming and stress tolerance by jasmonate signaling. *Frontiers in Plant Science*, *13*, 868874.

Szabados, L., & Savouré, A. (2010). Proline: a multifunctional amino acid. *Trends in plant science*, *15*(2), 89-97.

Tognetti, V. B., Mühlenbock, P. E. R., & Van Breusegem, F. (2012). Stress homeostasis–the redox and auxin perspective. *Plant, cell & environment*, *35*(2), 321-333.

Tsuzuki, T., Takahashi, K., Inoue, S. I., Okigaki, Y., Tomiyama, M., Hossain, M. A., ... & Kinoshita, T. (2011). Mg-chelatase H subunit affects ABA signaling in stomatal guard cells, but is not an ABA receptor in *Arabidopsis thaliana*. *Journal of Plant Research*, *124*, 527-538.

Wilkinson, S., & Davies, W. J. (2002). ABA-based chemical signalling: the co-ordination of responses to stress in plants. *Plant, cell & environment*, *25*(2), 195-210.

Xia, X. J., Zhou, Y. H., Shi, K., Zhou, J., Foyer, C. H., & Yu, J. Q. (2015). Interplay between reactive oxygen species and hormones in the control of plant development and stress tolerance. *Journal of experimental botany*, *66*(10), 2839-2856.

Zandt, P. A. V. (2007). Plant defense, growth, and habitat: a comparative assessment of constitutive and induced resistance. *Ecology*, *88*(8), 1984-1993.

7. Conclusions

1. Constitutive mechanisms under control conditions influence plants response under water stress in pepper grafted plants. Particularly, NIBER® rootstock mechanisms involve a basal activation of the ROS detoxification system and sustained ABA induction.

2. The water stress impact was lower in NIBER® roots compared to the pepper sensitive accession A10, supported by lower GSSG content associated with lower oxidative damage. NIBER® oxidative damage protection approaches include the synthesis of osmoprotectant sugars in roots and the synthesis of the antioxidant vitamin B6 in the grafted variety leaves.

3. Proline accumulation in plants grafted onto pepper hybrid H92 under long-term water stress contributes to sustained photosynthesis by photosynthetic apparatus protection to overcome water stress. This proline role was not observed in short-term water stress conditions and may be a late tolerance strategy in pepper plants.

4. NIBER® prevents stomatal closure in the very early response (up to 48 h) to water stress through gene expression changes that involve aquaporins and ABA negative regulators. Then, 48 h after water stress, NIBER® promotes stomatal closure by prior ABA synthesis in roots and transport from roots to shoots to maintain water status in the plant.

5. NIBER® increased JA content in the grafted variety leaves at 48 h under water stress, resulting in the activation of dehydration-responsive genes through JA signaling in roots. JA synthesis in leaves under water stress depends on long-distance signaling from roots, and it is later transported from leaves to roots and resynthesized. JA is a positive regulator of stomata closure, leading to increased drought stress tolerance.

6. NIBER® fine-tunes root/shoot biomass ratio during water stress response. At the early phase of water stress response (5 h), it favors root growth over shoot growth. At 24 h, auxin content decreases and CKs content increases in V/N roots to promote shoot growth. At 48 h, IAA increases and CKs decrease in V/N roots, coinciding with higher root biomass implicating a greater exploratory ability.

7. NIBER® modulates the variety leaves metabolome under water stress, increasing chlorophyll a, stearic acid, anthocyanins and metabolites involved in suberin and cutin biosynthesis, the latter increasing also in roots. These metabolites protect plants from water stress either for their antioxidant role or by controlling non-stomatal fluxes of gases, water and solutes. Moreover, siroheme increased in roots, which could be related to improved nitrogen assimilation.